

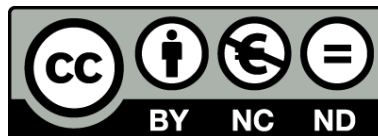


UNIVERSITAT DE
BARCELONA

Occurrence, Transport and Fate of Persistent Organic Pollutants in the Global Ocean

Presencia, Transporte y Destino de Contaminantes Orgánicos Persistentes en el Océano Global

Belén González-Gaya



Aquesta tesi doctoral està subjecta a la llicència **Reconeixement- NoComercial – SenseObraDerivada 3.0. Espanya de Creative Commons.**

Esta tesis doctoral está sujeta a la licencia **Reconocimiento - NoComercial – SinObraDerivada 3.0. España de Creative Commons.**

This doctoral thesis is licensed under the **Creative Commons Attribution-NonCommercial-NoDerivs 3.0. Spain License.**

Occurrence, Transport and Fate of Persistent Organic Pollutants in the Global Ocean

PhD Thesis
Occurrence, Transport and Fate of Persistent Organic Pollutants in the Global Ocean

Belén González Gaya
Programa de Doctorat en Ciències del Mar
Universitat de Barcelona
Barcelona, 2015



Belén González Gaya
Barcelona, 2015

Universitat de Barcelona
Programa de Doctorat en Ciències del Mar





CSIC
CONSEJO SUPERIOR DE INVESTIGACIONES CIENTÍFICAS

id \ae ^a



Occurrence, Transport and Fate of Persistent Organic Pollutants in the Global Ocean

Presencia, Transporte y Destino de
Contaminantes Orgánicos Persistentes en el Océano Global

Belén González-Gaya

Barcelona, 2015

Memòria presentada per Belén González Gaya per optar al grau de doctor

per la Universitat de Barcelona

Programa de Doctorat en Ciències del Mar

La Doctoranda

Belén González-Gaya

Los directores

Dr. Jordi Dachs

Dra. Begoña Jiménez

El Tutor

Dr. Miquel Canals

“Por diferentes motivos se marchan los hombres a los confines abandonados del mundo. A algunos les impele solamente el afán de aventuras, otros sienten una intensa sed de saber, los terceros obedecen a la seductora llamada de unas voces quedas, al encanto misterioso de lo desconocido que les aleja de los senderos rutinarios de la vida cotidiana.”

Ernest Shackleton, 1901.

“Water and air, the two essential fluids on which all life depends, have become global garbage cans.”

Jacques-Yves Cousteau, 1910.

Agradecimientos



Por fin, tras cientos de horas de muflar, pesar, limpiar, acondicionar, envolver, de no dormir, de mareos y risas, de viajes, de mal de tierra, de más viajes, del Atlántico y el Índico, de pescar, filtrar, subir y bajar escaleras oxidadas, de cambiar escobillas y fusibles, de baker, de extraer, purificar, reducir (sobretudo metanol) e inyectar, de cuantificar (de eso sí que han sido horas, mare de Deu de Monsterrat), de hacer excels (cuyo límite hemos llegado a rebasar), de escribir, corregir, escribir y volver a empezar, de difundir lo que hacemos (a grandes y chicos, desde las Ramblas al Pacífico, pasando por Móstoles), de recorrerme la A2, y, sobre todo, de aprender... por fin puedo enfrentarme a estas últimas líneas. Líneas para resumir lo que no caben en 5 años de vida, toda la gratitud y la emoción que se produce durante este “pequeño-gran” trabajo.

Por empezar por el principio, gracias a Jordi y a Begoña por confiar en mí para esta aventura. Nunca olvidaré mi primera conversación telefónica con una voz de fuerte acento Catalán, en los pasillos de mi antiguo trabajo, y la posterior reunión en el IQOG con una investigadora que me proponía medir la contaminación de los siete mares... Moltes gràcies, Jordi, por tu eficacia, tu apoyo incondicional y tus sabios consejos. No creo que pudiese encontrar un tutor en el mundo con más sustancia que exprimir que tú. Algún día yo también cumpliré nuestro sueño de “vespa blanca”. Gracias Bego por ponerme los pies en la tierra, por tus contactos, viajes y tu paciencia. Porque una caña sirve tanto para celebrar como para apaciguar. Creo haberme llevado lo mejor de vosotros y espero habérselo dado todo también.

En el IDAEA todo lo aprendí. De mis predecesores, Naiara, Ana y Cristóbal, tuve los ejemplos a seguir y las pautas de lo que funciona y lo que no funciona. Mil gracias por la paciencia y aguantar todas las preguntas de novata. Espero haber estado a la altura. De mis coetáneos me llevo lo mejor; horas de labo y despacho regadas de chistes malos, radio a todo trapo y comidas al solete. MariCarmen, te quiero siempre espalda contra espalda, porque todo el apoyo que nos hemos dado no se escribe en una línea, sino que se demuestra tras años de esfuerzo, trapillo, vestidos rojos y cereales. ¡Eres una campeona! Ha sido genial compartir el despacho con nuestro chileno preferido, ¿eh? Gracias también a mis niñas, Lauri y Gemma, sin vosotras esto no hubiera sido igual. ¡Porque haya mucho más fernet para brindar! Sin duda, gracias a Mari Jose, por la calidad de su trabajo dentro del labo y por su apoyo y creatividad fuera de él. Junto a MC, ¡habéis hecho que Barcelona tenga más colores para mí! Te deseo toda la suerte del mundo. De las nuevas generaciones mención especial a Paulo y a Mariana, por currar tanto, por crear un labo nuevo y porque todo ese buen rollo sea el motor de mil descubrimientos. Gracias por hacerme sentir que he aprendido cosas durante estos años y soy capaz de ayudar a los demás. No me olvido tampoco de los postdocs a los que pisar los talones: Javi, Maria, y en especial por su ayuda y consejos a Linda y a Elena. ¡Grazie i graciès! Agradecerle también a la gente de la quinta planta hacerme un huequito siempre a la hora del café; a Marta, a mis 3 adorables portus, a Eli, Maria, Denis, Mel y a los capos de la ecotoxicología. ¡Ya llevaré pastas cuando defienda! También gracias al combo hoquei-quimico por mezclar curro y deporte, y permitirme conocer a más gente dentro del IDAEA; Quique, Viky, Cayo, Oscar (you left my heart frozen), ¡espero encontraros en todas las SETACs y Dioxins del mundo para petarlo!

Mi segunda casa, que en realidad fue la primera, el IQOG, ha sido la “otra cara de la moneda” de mi doctorado. Gracias en genérico por darme siempre una nueva perspectiva, cada labo tiene sus misterios y sus trucos. Me siento afortunada por haber podido aprender de ambos. Gracias, gracias y mil gracias a Pepelu. Por nuestras conversaciones eternas y risas sin control, por ser mi colega en el curro, en los bares, en alta mar y en la montaña. Por todo lo que hemos compartido, y lo que nos queda. Por nuestra bohemian rapsody. Gracias a Juan, mi mejor profe de analítica, con el toque de ironía y sensibilidad perfecto. ¡Te debo mucho! Gracias a Miren por sus bailes, nuestros viajes y nuestras futuras colaboraciones. ¡Por el carbaZole symposium en Iruña! Gracias especiales también a María, que no es sólo mi compañera de trabajo, es mi colega. Por tu apoyo incondicional y nuestra conexión total (y gracias a Pitu por su asesoramiento!). Gracias a todos los demás por permitirme aprender siempre de vosotros. Porque todo aquel que haya conocido allí ha influido en mi aprendizaje, especialmente a Sagrario (artista!!!) y Lourdes por su cercanía.

Gracias a toda la gente que participó en ese gran proyecto llamado Malaspina. Tanto a la gente que muestreó conmigo como a los que lo hicieron por mí, o para cumplir sus propios objetivos, llegando todos juntos a un conocimiento más profundo de nuestro océano. No quiero poner nombres por temor a que me falte alguien, pero de todo corazón, gracias, porque este viaje cambió mi vida.

Nunca hubiera llegado hasta aquí sin mi formación previa en Mallorca, Buenos Aires, Napoles, Wageningen, y la Autonoma de Madrid. Gracias, por tanto, a la gente de la Roca, de capital, Mardel y Bariloche, a todos mis italianos (mi manchate!), a la Wage-people con la que descubrí la ciencia y la malegría, a mis ambientólogos locos. Sois todos parte de esto.

Gracias a la gente que nada tiene que ver con esta investigación pero que hace que quieras celebrar con ellos las cosas buenas de esta aventura y que penan contigo las cosas malas. A las seitonas y seitones en Barcelona, a mis amigas de toda la vida, a los isla planeros, a esas personas que te llaman y te preguntan sin tener muy claro lo que haces, pero se interesan por ti no obstante.

Gracias por encima de todo a mis padres porque siempre me han ayudado, animado y apoyado sin reticencias, aunque eso supusiera poner entre nosotros miles de kilómetros. Espero que estéis tan orgullosos de mí como lo estoy yo de vosotros. Eskerrik asko a mi “nueva” familia por cada momento, no he podido sentirme más cuidada en vuestra casa. Gracias a mi compañero, a mi colegui, a mi más mejor amigo, a la persona con la que lo he compartido todo durante estos años. Sin ti nada sería. Mundu propioa sortzeko gai izan garelako...

Belén

TABLE OF CONTENTS

List of Acronyms	5
Longhurst provinces	8
List of tables and figures	9
Abstracts	13
Chapter 1. General Introduction	19
<u>Pollution in the Open Ocean: Persistent Organic Pollutants and “not so Persistent” Pollutants</u>	21
<u>Environmental Fate and Dynamics of POPs</u>	23
<i>Atmospheric processes</i>	25
<i>Water column processes</i>	30
<u>Case studies in the Malaspina expedition: PAHs and PFASs</u>	32
<i>Polycyclic Aromatic Hydrocarbons (PAHs)</i>	34
<i>Perfluoroalkylated Substances (PFASs)</i>	38
<u>Aim and Outline of this thesis</u>	41
References	47
Chapter 2. Results	55
1. Field Measurements of the Atmospheric Dry Deposition Fluxes and Velocities of Polycyclic Aromatic Hydrocarbons to the Global Oceans	57
References	80
2. High Atmosphere-Ocean Exchange of Semivolatile Aromatic Hydrocarbons	85
References	105
3. Perfluoroalkylated Substances in the Global Tropical and Subtropical Surface Oceans	109
References	130
4. Oceanic Transport and Sinks of Perfluoroalkylated Substances	135
References	157

5. Cycling of Polycyclic Aromatic Hydrocarbons in the Surface Open Ocean	161
References	184
Summary of Results	187
Chapter 3. General Discussion	195
<u>Global Occurrence</u>	199
<i>PAHs</i>	199
<i>PFASs</i>	202
<u>Partitioning of PAHs and PFASs in the environmental compartments and Implications for their Global Fate</u>	203
<i>PAHs occurrence in atmospheric gas and aerosol phases</i>	203
<i>PAHs and PFASs occurrence in seawater's dissolved and particulate phases</i>	205
<u>Global fluxes and budgets of PAHs and PFASs in the Open Ocean</u>	208
<i>PAHs and SALCs</i>	209
<i>PFASs</i>	212
References	215
Chapter 4. General Conclusions	221
Annexes	227
Subchapter 1 Supporting Information	A1
Subchapter 2 Supporting Information	A35
Subchapter 3 Supporting Information	A47
Subchapter 4 Supporting Information	A78
Subchapter 5 Supporting Information	A110

List of Acronyms

List of the acronyms and abbreviations used in this thesis:

ΔH	Bond enthalpy
ΔS	Absolute entropy
ABL	Atmospheric boundary layer
B	Biomass
BCF	Bioconcentration factor
C	Carbon
C_A	Aerosol phase concentration
C_{DD}	Deposited aerosol phase concentration
C_G	Gas phase concentration
C_{Gf}	Final gas phase concentration
C_{Gi}	Initial gas phase concentration
Chl_s	Surface chlorophyll concentration
CLRTAP	Convention on Long-Range Transboundary Air Pollution
COP	Contaminantes orgánicos persistentes
C_p	Particulate phase concentration
$C_{Plankton}$	Plankton phase concentration
CTD	Conductivity, Temperature, Depth (device)
C_{TW}	Truly dissolved phase concentration
C_W	Dissolved phase concentration
D	Diffusivity
D_A	Diffusivity coefficient in the air
D_{atm}	Atmospheric degradation
DCM	Dichloromethane
DCM	Deep chlorophyll maximum
DDT	Dichlorodiphenyltrichloroethane
DL	Detection limit
DOC	Dissolved organic carbon
DP	Dechlorane Plus
EI	Electronic impact
EPA	Environmental Protection Agency
ESI	Electrospray ionization
f_A	Air fugacity
F_{AW}	Air-water exchange flux
F_{DD}	Dry deposition flux
$F_{DD\ coarse}$	Coarse aerosol dry deposition flux
$F_{DD\ fine}$	Fine aerosol dry deposition flux
F_{Eddy}	Eddy diffusive fluxes
F_{Fecal}	Fecal pellets sinking fluxes
F_{OC}	Organic carbon flux
F_{OM}	Organic matter flux
F_{Phyto}	Phytoplankton sinking flux
$F_{Settling}$	Biological pump sinking flux
f_W	Water fugacity

F _{WD}	Wet deposition flux
GC-MS	Gas chromatography Mass spectrometry
H'	Henry's law constant
HCB	Hexachlorobenzene
HCHs	Hexachlorocyclohexanes
HPLC	High Performance Liquid Chromatography
Hx	Hexane
IDL	Instrument detection limit
IQL	Instrument quantification limit
k	Inverse of e-folding time
k _A	Mass transfer coefficients in air
k _{AW}	Air-water mass transfer rate
k _{DOC}	Dissolved organic carbon partition coefficient
K _{OC}	Organic carbon partition coefficient
k _{OH}	Rate constant for OH radical reaction
K _{OW}	Octanol water partition coefficient
k _w	Mass transfer coefficients in water
K _p	Eddy diffusivity
LRET	Long range environmental transport
m	Slope (here used for <i>C_{Plankton} versus Biomass</i> relation)
MDL	Mixed deep layer
MeOH	Methanol
MQL	Method quantification level
MRM	Multiple reaction monitoring
N	Nitrogen
OC	Organic carbon
OCPs	Organochlorinated pesticides
OECD	Organization for Economic Co-operation and Development
p ₀	Precipitation rate
PAHs	Polycyclic aromatic hydrocarbons
PBDEs	Polybrominated diphenyl ethers
PCBs	Polychlorinated biphenyls
PCDD/Fs	Polychlorinated dibenzo-p-dioxins and furans
PFASAs	Perfluoroalkylated sulfonamides
PFASs	Perfluoroalkylated substances
PFCAs	Perfluoroalkylated carboxylic acids
PFCs	Perfluorinated compounds
PFSAAs	Perfluoroalkylated sulfonic acids
P _L	Vapor pressure
POC	Particulate organic carbon
POPs	Persistent organic pollutants
PP	Polypropylene
PUF	Polyurethane foam
PVC	Polyvinyl chloride
QA/QC	Quality Assurance/Quality Control
QL	Quantification limits
R	Gases constant

REACH	Registration, Evaluation, Authorization and restriction of Chemicals
SALCs	Semivolatile aromatic-like compounds
S_c	Schmidt number
SIM	Selected ion monitoring
SOA	Secondary organic aerosols
SOCs	Semivolatile organic compounds
SPE	Solid phase extraction
t	time
T	Temperature
TSP	Total solid phase
U_{10}	Wind speed at 10 meters height
UCM	Unresolved complex mixture
UNECE	United Nations Economic Commission for Europe
UNEP	United Nations Environment Programme
UPLC-MS/MS	Ultra performance liquid chromatography coupled to tandem mass spectrometry
v_D	Dry deposition velocity
v_{Dc}	Coarse aerosol dry deposition velocity
v_{Df}	Fine aerosol dry deposition velocity
VOCs	Volatile organic compounds
w_p	Washout ratio
z	Depth
Γ	Mixing efficiency
$\delta^{13}C$	‰ of ^{13}C isotope
$\delta^{15}N$	‰ of ^{15}N isotope
ϵ	Dissipation rate of turbulent kinetic energy

Longhurst provinces

Chronologically ordered provinces that *Malaspina 2010* cruise crossed correspond to:

N. Atlantic Subtropical Gyre Province East (NASE)
N. Atlantic Tropical Gyre Province (NATR)
Western Tropical Atlantic Province (WTRA)
South Atlantic Gyral Province (SATL)
Benguela Current Coastal Province (BENG)
E. Africa Coastal Province (EAFR)
Indian S. Subtropical Gyre Province (ISSG)
Australia-Indonesia Coastal Province (AUSW)
S. Subtropical Convergence Province (SSTC)
E. Australia Coastal Province (AUSE)
S. Pacific Subtropical Gyre Province (SPSG)
Pacific Equatorial Divergence Province (PEQD)
N. Pacific Equatorial Countercurrent Province (PNEC)
N. Pacific Tropical Gyre Province (NPTG)
Caribbean Province (CARB)

List of tables and figures

CHAPTER 1. General Introduction

Figure I.1. Schematic view of POPs processes in the global Ocean.

Figure I.2. Schematic draw of dry deposition.

Figure I.3. Schematic draw of wet deposition.

Figure I.4. Schematic draw of diffusive air-water exchange.

Figure I.5. Schematic draw of atmospheric degradation.

Figure I.6. Schematic draw of physical transport processes in the water column.

Figure I.7. Schematic draw of biological transport processes in the water column.

Figure I.8. Malaspina 2010 circumnavigation track.

Figure I.9. PAHs global production.

Figure I.10. National annual emissions rate of EPA's 16 regulated PAHs.

Table I.1. PAHs physicochemical properties.

Figure I.11. PFCs production and use timeline.

Figure I.12. PFO and related substances global production (tons y^{-1}).

Table I.2. PFASs physicochemical properties.

Figure I.13. Schematic view of processes reviewed in Chapter 1.

Figure I.14. Schematic view of processes reviewed in Chapter 2.

Figure I.15. Schematic view of processes reviewed in Chapter 3.

Figure I.16. Schematic view of processes reviewed in Chapter 4.

Figure I.17. Schematic view of processes reviewed in Chapter 5.

CHAPTER 2. Results

Graphical Abstract 1.

Figure 1.1. Maps of (a) PAHs concentration in suspended aerosols ($ng\ m^{-3}$), (b) dry deposition flux of PAHs measured for the coarse fraction of aerosols ($ng\ m^{-2}d^{-1}$), and (c) dry deposition flux of PAHs measured for the fine fraction of aerosols ($ng\ m^{-2}d^{-1}$).

Table 1.1. Comparison of the dry deposition fluxes ($ng\ m^{-2}d^{-1}$) measured in this work with those reported for marine and coastal sites.

Figure 1.2. PAHs distribution pattern of concentrations ($ng\ g^{-1}$) in suspended aerosols (upper panels), coarse (middle panels) and fine fraction (lower panels) of deposited aerosols.

Figure 1.3. Dry deposition velocity ($cm\ s^{-1}$) for Fluoranthene, Benzo (a) Pyrene and Benzo (ghi) Perylene determined from the measured dry deposition fluxes and concentrations in suspended aerosols.

Figure 1.4. Dry deposition velocity (cm s^{-1}) versus vapor pressure (Log(Pa)) for the target PAHs.

Figure 1.5. Concentrations in fine deposited aerosols (ng g^{-1}) versus wind velocity (m s^{-1}) for the target PAHs.

Graphical Abstract 2.

Figure 2.1. Concentration of PAHs in the gas phase (upper panel), aerosol phase (middle panel) and dissolved water phase (bottom panel).

Figure 2.2. Global measurements of the 2 more relevant processes affecting PAHs exchange in the open ocean: dry deposition fluxes for the 28 analyzed compounds (Top panel) and net diffusive fluxes for 3 representative compounds (bottom panel).

Figure 2.3. Dry deposition (F_{DD}) and net diffusive (F_{AW}) fluxes averaged per month for the Atlantic, Pacific and Indian Oceans.

Figure 2.4. Atmosphere-ocean exchange of carbon associated to semivolatile aromatic hydrocarbons (SALCs, figures in red), and $\Sigma 28\text{PAHs}$ (figures in black).

Figure 2.5. Overlaid chromatograms of a gas phase sample are shown in the top and dissolved phase sample in the bottom. In blue the total ion chromatogram (TIC) of the total aromatic fraction obtained by GC-MS in full scan mode and in red the TIC obtained by GC-MS in SIM mode of the analyzed ions.

Graphical Abstract 3.

Figure 3.1. Global distribution of PFASs in the tropical and subtropical oceans. Upper panel shows the PFSA concentrations, central panel shows the PFCA concentrations and lower panel shows the PFASA concentrations.

Figure 3.2. Relative contribution of the individual PFASs for each oceanic hemispherical sub basin.

Figure 3.3. Comparison of the surface seawater concentration ranges of PFOS and PFOA measured during the Malaspina 2010 expedition with those reported in previous studies.

Figure 3.4. Temporal trend of PFOA concentrations in the northern hemisphere in the Atlantic and Pacific oceans and the fitted linear temporal trend.

Graphical Abstract 4.

Figure 4.1. Global distribution of PFASs in the tropical and subtropical oceans at the DCM. Upper panel shows the PFSA concentrations, central panel shows the PFCA concentrations and lower panel shows the PFASA concentrations.

Figure 4.2. PFASs Log concentrations at the surface versus DCM (pg L^{-1}).

Figure 4.3. PFOS and PFOA modelled versus measured concentrations (pg L^{-1}) at the DCM depth.

Figure 4.4. Fluxes assessed for PFOS and PFOA; turbulent fluxes (F_{Eddy}) on the top and biological pump fluxes on the bottom (F_{Phyto} and F_{Fecal}).

Table 4.1. Annual mean export of PFASs due to turbulent fluxes (F_{Eddy}) and *biological pump fluxes* (F_{Settling}).

Graphical Abstract 5.

Figure 5.1. PAHs global concentration in the dissolved phase (pg L^{-1}) (upper panel), particulate phase (ng gC^{-1}) (middle panel) and plankton ($\text{ng g}_{\text{dw}}^{-1}$) (bottom panel).

Figure 5.2. Average concentrations and standard deviation of PAHs in the aerosol, gas, dissolved, particulate and plankton phase for the different oceanic basins.

Figure 5.3. Correlation between $\text{Log}K_{\text{OC}}$ (left) and $\text{Log}C_{\text{p}}$ (right) versus LogPOC .

Figure 5.4. Correlation between the theoretical C_{p}^* calculated from the reported C_{G} and real C_{p} measured.

Figure 5.5. PAH concentrations in plankton (C_{plankton}) versus plankton biomass (top panel). Slopes from the relationship between concentrations in plankton and biomass (m) versus the hydrophobicity of the compound (K_{OW}) (bottom panel).

Figure 5.6. Biological pump fluxes for the algal settling flux (F_{Phyto}) (top panel), and the fecal settling flux (F_{Fecal}) (bottom panel).

CHAPTER 3. General Discussion

Figure D.1. Global distribution of oceanic concentrations of PAHs in the gas, aerosol, dissolved, particulate and plankton phases.

Figure D.2. Global concentration of PFASs (blue colors) and PFCAs (red colors) in the surface seawater (5 m depth, top) and at the deep Chlorophyll maximum (DCM, bottom).

Figure D.3. $K_{\text{p-air}}$ (L kgTSP^{-1}) for four representative PAHs.

Figure D.4. PAHs profile for gas (C_{G}) and aerosol (C_{A}) phases.

Figure D.5. K_{OC} (L kgPOC^{-1}) for four representative PAHs.

Figure D.6. PAHs profile for dissolved (C_{W}) and particulate (C_{p}) phases.

Figure D.7. PAHs and SALCs global fluxes.

Figure D.8. PFASs global fluxes.

Abstract

The Open Ocean has been recognized as playing a key role on global dynamics of pollutants due to its large coverage of the planet surface, its high degradation potential and its sink and accumulation capacities towards anthropogenic chemicals. Nevertheless, there is a dearth of measurements of contaminants in the Open Ocean lower atmosphere, water column and trophic chain as a result of its remoteness and wide spatial reach. Persistent organic pollutants (POPs) are an important class of chemical contaminants due to their particular characteristics such as persistency, bioaccumulation potential, high toxicity and long range environmental transport capacity. Even though previous studies report their occurrence in the marine environment, the processes and magnitude of their fate, transport and sinks in the Open Ocean remain uncharacterized. In this Thesis two groups of organic contaminants have been selected in order to study POPs dynamics and fate in the oceanic environment. Polycyclic Aromatic Hydrocarbons (PAHs) are organic pollutants generated during incomplete combustion of fossil fuels and organic matter, but as well coming from petrogenic and biogenic natural sources. PAHs are semivolatile and highly mobile between the atmosphere and aqueous systems. Perfluoroalkylated substances (PFASs) are anthropogenic halogenated pollutants, recently developed for industrial and consumer goods usage. They are extremely persistent and exhibit higher solubility and lower hydrophobicity than most POPs, which makes them prone to be found in aqueous matrixes.

During the *Malaspina 2010* circumnavigation cruise across the Atlantic, Pacific and Indian oceans (35°N- 40°S), 64 PAHs were measured in the gas, aerosol, rainwater, dissolved, particulate and plankton matrixes, and 11 PFASs were quantified in dissolved phase at surface and deep chlorophyll maximum depth seawater. Degradation and atmospheric deposition of PAHs was assessed for dry deposition, wet deposition and diffusive air-water exchange, suggesting approaches for their global estimation, and proposing a global budget for PFAS, PAHs, and other semivolatile aromatic-like compounds, and their effect in the carbon global cycle. Dry deposition was obtained by direct measurements on board and parametrized for the whole tropical and subtropical Ocean; wet deposition was quantified from the precipitation

rainwater gathered during the cruise; and diffusive exchange was calculated from the measured PAHs concentrations in the gas and dissolved phases, concurrently with the environmental parameters affecting volatilization and absorption (temperature, wind speed, salinity, dissolved organic carbon among others). Moreover, vertical distribution processes and influencing parameters in the surface mixed layer of the water column were assessed for PAHs and PFASs. Processes evaluated for PAHs include the vertical fluxes associated to the organic matter sinking (biological pump), biomass dilution, planktonic degradation, and air-water-particle exchange. For PFASs, the biological pump and eddy diffusive fluxes (based on turbulence eddy diffusion coefficients measured concurrently to the PFASs sampling) were assessed empirically for the first time in literature. The analysis of the complex feedback established between atmospheric depositional fluxes and the diffusive, degradative and biological pumps fluxes in the marine water column at a global scale is also covered. Furthermore, a wide array of understudied environmental parameters are reviewed as plausible factors affecting POPs fate in the Open Ocean, and a proposal of the research directions to follow and missing gaps to be filled is done. Amongst the innovative outcomes of this study, it can be highlighted the comprehensive sampling covering the tropical and subtropical global oceans, and the large amount of experimentally determined processes and influencing factors in order to better understand the global fate of chemical organic pollutants in the Open Ocean.

Resumen

El Océano Abierto está reconocido como un ambiente clave en la dinámica global de la contaminación debido a que representa un gran porcentaje de la superficie terrestre, su alto potencial de degradación y su capacidad como sumidero de sustancias químicas antropogénicas. A pesar de ello, hay una carencia de medidas de contaminantes en la atmósfera, la columna de agua y el plancton oceánico como resultado de su difícil acceso y amplitud espacial. Los contaminantes orgánicos persistentes (COP) son un importante grupo de contaminantes químicos caracterizados por ser persistentes, bioacumulables, tóxicos y susceptibles de sufrir transporte a larga distancia. Aunque estudios previos documentan su existencia en el medio ambiente marino, los procesos y la magnitud de su comportamiento, capacidad de transporte y sumidero en el Océano abierto no están caracterizados. En esta Tesis dos grupos de contaminantes orgánicos han sido seleccionados para ilustrar la dinámica de los COP y su destino en el medio ambiente oceánico. Los hidrocarburos aromáticos policíclicos (PAHs, por sus siglas en inglés) son contaminantes orgánicos generados durante la combustión incompleta de combustibles fósiles y de materia orgánica, o provenientes de fuentes petrogénicas o biogénicas naturales. Son semivolátiles y altamente móviles entre la atmósfera y los sistemas acuosos debido a sus propiedades fisicoquímicas. Las sustancias perfluoroalquiladas (PFASs, por sus siglas en inglés) son contaminantes halogenados antropogénicos emergentes desarrollados recientemente para usos industriales y en productos de consumo. Son extremadamente persistentes y exhiben mayor solubilidad y menor hidrofobicidad que otros COP, lo que les hace susceptibles de hallarse en matrices acuosas.

Durante la campaña de circunnavegación Malaspina 2010 a través de los océanos Atlántico, Pacífico e Índico (35°N- 40°S), se midieron 64 PAHs en las matrices gas, aerosol, agua de lluvia, disuelto, particulado y en el plancton; y 11 PFAS se cuantificaron en la fase disuelta de agua marina superficial y de la profundidad del máximo de clorofila. La degradación y la deposición atmosférica de los PAHs se evaluaron mediante las medidas de deposición seca, deposición húmeda e intercambio difusivo aire-agua, sugiriéndose métodos para su cuantificación global y proponiéndose un cómputo global para estos contaminantes y otros compuestos

semivolátiles aromáticos, así como su efecto en el ciclo del carbono. La deposición seca se obtuvo directamente de medidas durante la campaña y fue parametrizada para todo el Océano tropical y subtropical; la deposición húmeda se cuantificó con agua de lluvia recogida durante la navegación; y el intercambio difusivo se estimó con las concentraciones de PAHs de las fases gas y disuelta, medidas simultáneamente con parámetros ambientales que afectan a la volatilización y la absorción de estos compuestos (temperatura, velocidad del viento, salinidad y carbono orgánico disuelto, entre otras). Asimismo, se midieron los procesos de distribución vertical y los parámetros que afectan a las concentraciones de PAHs y PFASs en la capa de mezcla superficial de la columna de agua. Los procesos examinados para PAHs incluyen los flujos verticales asociados con la sedimentación de materia orgánica (bomba biológica), la biodilución, la degradación planctónica, y el equilibrio aire-agua-partícula. Para las PFASs, la bomba biológica y los flujos difusivos turbulentos (basados en medidas de los coeficientes de difusión turbulenta simultáneas con el muestreo de PFASs) fueron medidos empíricamente por primera vez en la literatura. El análisis de los complejos efectos retroactivos establecidos entre los flujos de deposición y los procesos de degradación, difusión y la bomba biológica a escala global también ha sido abordado. De la misma forma, un amplio espectro de parámetros ambientales se ha revisado para dilucidar posibles factores que pudieran afectar al destino de los COP en el Océano Abierto, y se proponen una serie de líneas de investigación y necesidades prioritarias para su futura investigación. Entre los aspectos más innovadores de esta Tesis destacan la enorme cobertura espacial del Océano Global en sus zonas tropicales y subtropicales, y la gran cantidad de procesos de transporte determinados de manera empírica junto a sus factores determinantes, con el objeto de poder mejorar el conocimiento sobre el comportamiento y destino final de los contaminantes químicos orgánicos en el Océano Abierto.

Resum

L'Oceà Obert s'ha descrit com un ambient clau en la dinàmica global de la contaminació degut al seu gran percentatge de cobertura de la superfície terrestre, el seu alt potencial de degradació i la seva capacitat com a embornal i acumulador de substàncies químiques antropogèniques. Tot i això, hi ha una manca de mesures de contaminants a l'atmosfera, a la columna d'aigua i al plàncton oceànic com a resultat del seu difícil accés i de l'amplitud espacial. Els contaminants orgànics persistents (COP) són substàncies químiques no degradables, bioacumulatives, tòxiques per als humans i els ecosistemes, i susceptibles de patir transport a llarga distància. Encara que hi ha estudis previs que reporten la seva existència en el medi ambient marí, els processos i la magnitud del seu transport i embornal en l'Oceà Obert no està caracteritzada. En aquesta tesi dos exemples de grups de contaminants orgànics han estat seleccionats per il·lustrar la dinàmica dels COP i el seu destí en el medi ambient oceànic. Els hidrocarburs aromàtics policíclics (PAHs) són contaminants orgànics generats durant la combustió incompleta de combustibles fòssils i de matèria orgànica, o provinents de fonts petrogèniques o biogèniques naturals. Tot i que els PAHs no són considerats COP ja que són degradables en el medi, han estat descrits com nocius per als ecosistemes, es troben de manera ubiqua en el medi ambient i mostren nivells creixents en algunes regions a causa de l'augment de les seves fonts antropogèniques. Són compostos semivolàtils, altament mòbils entre l'aire i l'aigua com a resultat de les seves característiques fisicoquímiques. Les substàncies perfluoroalquilades (PFASs) són contaminants halogenats antropogènics de recent creació per al seu ús industrial i en productes de consum com aïllants i tensioactius. Són extremadament persistents i exhibeixen major solubilitat i menor hidrofobicitat que altres COP, fet que els fa susceptibles de trobar-se en matrius aquoses.

Durant la campanya de circumnavegació Malaspina 2010 a través dels oceans Atlàntic, Pacífic i Índic (35 ° N-40 ° S), 64 PAHs van ser mesurats en les matrius; gas, aerosol, aigua de pluja, fracció dissolta, fracció particulada i en el plàncton, i 11 PFASs van ser identificats en la fase dissolta d'aigua marina superficial i de la profunditat del màxim de clorofil·la. La degradació i la deposició atmosfèrica dels PAHs van ser avaluades mitjançant la mesura de la deposició seca, deposició humida i Intercanvi difusiu aire-

aigua, suggerint mètodes per a la seva quantificació global i proposant un còmput global per a aquests contaminants, i altres compostos semivolàtils aromàtics, així com el seu acoplament amb el cicle del carboni orgànic. La deposició seca es va obtenir directament de mesures durant la campanya i va ser parametritzada per tot l'Oceà tropical i subtropical; la deposició humida es va quantificar gràcies a l'aigua de pluja recollida durant la navegació; i l'Intercanvi difusiu va ser estimat amb les concentracions dels PAHs mesurades en les fases gas i dissolta, preses simultàniament amb paràmetres ambientals que afecten la volatilització i l'absorció d'aquests compostos (temperatura, velocitat del vent, salinitat, carboni orgànic dissolt, entre d'altres). A més a més, es van mesurar els processos de distribució vertical i els paràmetres que afectaven a la capa de mescla superficial de la columna d'aigua per als PAHs i PFASs. Els processos examinats per a PAHs inclouen els fluxos verticals associats amb la sedimentació de matèria orgànica (bomba biològica), la biodilució, degradació planctònica, i l'equilibri aire-aigua-partícula. Per a les PFASs, la bomba biològica i els fluxos difusius turbulents (basats en mesures dels coeficients de difusió turbulenta simultànies amb el mostreig de PFASs) van ser mesurats empíricament per primera vegada en la literatura. L'anàlisi dels complexos efectes retroactius establerts entre els fluxos de deposició i els processos de degradació, difusió i la bomba biològica a escala global també ha estat abordat. De la mateixa manera, un ampli espectre de paràmetres ambientals ha estat revisat per dilucidar possibles factors que puguin afectar al destí dels COP en l'Oceà Obert, i es proposen una sèrie de línies d'investigació i necessitats prioritàries per a la seva futura investigació. Entre els aspectes més innovadors d'aquesta tesi es poden destacar l'enorme cobertura espacial de l'Oceà Global a les seves zones tropicals i subtropicals, i la gran quantitat de processos de transport determinats de manera empírica juntament amb els seus factors determinants, per tal de poder identificar el destí final dels contaminants orgànics persistents en l'Oceà Obert.

Chapter 1

General Introduction

Pollution in the Open Ocean: Persistent Organic Pollutants and “not so Persistent” Pollutants

The Open Ocean remains as one the most fruitful and unexplored ecosystem on Earth yet if its extension covers more than three quarters of the Earth's surface. It provides the primary source of oxygen to our atmosphere and holds the first place as a sink for substances like CO₂, carbon, and of course, pollutants. Recent studies have dealt with the resilience capacity of the ocean, and if it would be possible to reach the tipping point from which its physico-chemical properties and natural biogeochemical cycles will not sustain life any more^{1,2}. Global change threatens in the Ocean are associated with i) ice melting in the poles and freshening of the oceanic waters, ii) oceanic currents modification with effects in the heat global transfer, iii) acidification, iv) ecosystems functioning and biodiversity alterations (both alien species proliferation and extinction of others) and v) pollution³.

The chemical alteration of the global Open Ocean has been recently considered for few emerging issues, like the plastic debris accumulation⁴⁻⁶ or acidification⁷, but other types of chemical pollution had not been assessed at a planetary scale, even if more than 2000 organic pollutants have been already reported in marine waters⁸. Moreover, this list is increasing exponentially nowadays with the production and release of new chemicals with still unknown effects in the environment. Indeed, chemical risk is one of the global dangers to which we are unaware, according to Rockstrom et al., who defines it as an *earth-system process yet to explore at a global scale*⁹.

In order to identify priority chemicals there is an established *Risk criteria* which includes i) production volume, ii) usage profile and iii) their physico-chemical properties¹⁰. Taking into account these premises, there is a particular group of pollutants that have been classified of major concern, as they fulfill all the requirements, the so called Persistent Organic Pollutants (POPs). Those are organic chemicals that:

- Are persistent since they do not degrade over long periods of time once released into the environment

General Introduction

- Bioaccumulate and biomagnify in the trophic chains
- Are toxic to both humans and wildlife
- Are prone to long-range environmental transport (LRET) and deposition

Consequently, POPs pose a threat to the environment and to human health all over the globe. Due to the international concern regarding these chemicals, the United Nations Environment Program (UNEP) promoted the adoption in 2001 of the Stockholm Convention to protect human health and the environment from POPs ¹¹. On it, 12 priority substances were initially regulated by controlling all their life cycle, from their production, use and consumption to their removal and waste disposal products. Nowadays, this list of pesticides, industrial chemicals and unintentional products has grown, nevertheless, it is still incomplete taking into account the myriads of toxics fulfilling those requirements released every year to our ecosystems. Other regional regulatory tools affecting POPs are the United States Environmental Protection Agency's (EPA) Toxic Release Inventory ¹², the Canadian Environmental Protection Act ¹³, and The European Union's regulation on Registration, Evaluation, Authorization, and Restriction of Chemicals (REACH) ¹⁴.

The legacy POPs more extensively studied in the literature are the polychlorinated biphenyls (PCBs), organochlorinated pesticides (OCPs) such as dichlorodiphenyltrichloroethane (DDT), hexachlorocyclohexanes (HCHs) and hexachlorobenzene (HCB) and other by-products of industrial processes or combustion, such as polychlorinated dibenzo-p-dioxins and dibenzofurans (PCDD/Fs). Among the new emerging contaminants, defined as chemicals that are not currently or have been only recently regulated, other halogenated contaminants are arising, like polybrominated compounds (such as polybrominated diphenyl ethers (PBDEs) and Dechlorane Plus (DP)) or perfluoroalkylated substances (PFASs). Traditionally, much attention has been paid as well to the polycyclic aromatic hydrocarbons (PAHs), which are not as recalcitrant as POPs, but because of their toxicity, bioaccumulation tendency in low trophic levels (e.g. in plankton), and susceptibility to undergo long-range atmospheric transport are of great concern globally ¹⁵. Indeed, PAHs are not listed in the Stockholm Convention but are included in the Aarhus Protocol of the United Nations Economic Commission for Europe (UNECE) ¹⁶ and the Convention on Long-

Range Transboundary Air Pollution (CLRTAP)¹⁷. Based on the previous considerations, in this thesis PAHs will be referred to as POPs in its most general sense.

Although the regulations on the use and production of those chemicals and the potentially new ones launched into the market, their continuous use and still unknown toxic effect for the ecosystem's health requires further research to understand their fate and behavior in the global environment. Most of the studies dealing with POPs in the last decades focus on ecotoxicological and health effects and assess their occurrence at limited regional scales. However, there is a big gap in the knowledge of POPs global fate¹⁸, even though in the last years some studies are emphasizing the significance of global dynamics and the role of the ocean on the global distribution and sink of these pollutants^{18,19}.

Environmental Fate and Dynamics of POPs

A combination of local, regional and long range transport is responsible of the POPs distribution in the global environment. The POPs potential to undergo LRET explains why they can be found in remote areas, which is even favored by their persistency. Already in the 60s, the dispersion of halogenated persistent contaminants was reported^{20, 21}, and also at that decade, popular concern for these pollutants caused the "Silent Spring" revolution²², starting a social movement towards chemical environmental awareness at global scale supported by the scientific community. Up to date several studies assessing global transport and accumulation processes to remote polar and oceanic regions have been undertaken^{18, 23-25}, suggesting all of them a need for further research on physico-chemical properties, good monitoring approaches and global understanding of processes^{18, 23, 26}.

The distribution of POPs in the environment may occur either in the atmosphere or in the water systems, or under a combination of both (soils and other environmental matrixes are considered as reservoirs²⁷). The presence of POPs in both environmental compartments is a matter of concern itself, as the uptake from atmosphere and the water are the two main paths of bioconcentration, and subsequent biomagnification

through the trophic chains, leading to a potential risk for wildlife and humans ²⁸. Moreover, the spread of pollution is accelerated and intensified in these highly dynamic media.

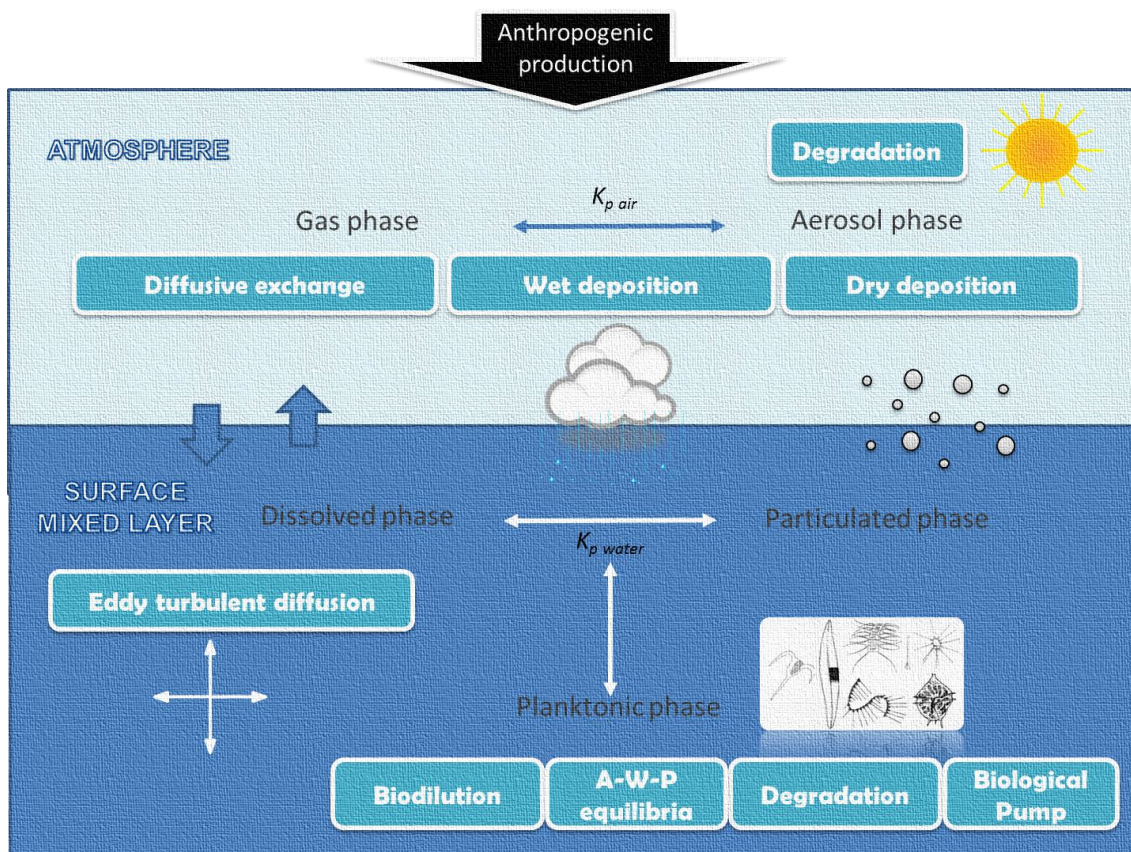


Figure I.1. Schematic view of POPs processes in the Global Ocean.

The potential fate and behavior of a given contaminant depends on their physico-chemical properties and environmental variables. It has been reported that mobilization occurs in pulses of deposition and volatilization, what is called the “grasshopper effect” ¹⁹. In each stage of the cycle, POPs may suffer from different degradation (like photolysis or OH reactions in the atmosphere, or biodegradation in soils or the water column) and/or accumulation processes (sequestration by soot in the atmosphere or bioaccumulation over a food web, for instance) that affects their occurrence, fate, toxicity and bioavailability. The grasshopper effect is mainly regulated by temperature and the biological pump, and it is a distillation global process towards the cold poles, where POPs have been reported to accumulate ²⁹⁻³¹. Nevertheless, other ambient factors like sources, precipitation, organic matter sorption, or the presence of secondary sources modify the global distribution of POPs.

Therefore, the total perspective of processes and their interrelations in the global Ocean is highly complex (Figure I.1) depending on many environmental factors and multi-media equilibria.

Atmospheric processes

Most POPs are semivolatile compounds which once released into the environment distribute over the atmosphere and spread at regional and global scale through a variety of deposition processes, chemical partition and interchanging fluxes with the ocean or soils^{19, 32, 33}. Atmospheric deposition of POPs has been assessed in remote areas like the Open Ocean and polar seas³⁴⁻⁴⁰ but not on a planetary scale except for few seminal works²⁵. The main entrance of POPs to the ocean is reported to be the atmosphere^{41, 42}, even if riverine inputs or run-off may be of particular relevance for some compounds like pesticides and PFASs in coastal areas^{43, 44}.

The atmospheric deposition processes considered are dry deposition, wet deposition and air-water diffusive fluxes (Figure I.1). These processes have different relative importance on pollution loading depending on environmental parameters (temperature, wind speed, aerosol abundance and organic matter content, precipitation rates, organic matter content of the surface water, salinity, density, etc.) and also on the physicochemical properties of the contaminant (volatility, solubility, hydrophobicity, shoot sorption, etc.). The gas-particle partition of the pollutant will determine which of the process will have a higher relevance in its total atmospheric deposition⁴⁵. POPs mainly partitioned to aerosols (like PAHs, the more toxic dioxins and furans, organophosphorus flame retardants and plasticizers, PBDEs and DPs) due to their low-medium volatility are prone to enter the open ocean via dry deposition. Contrarily, those POPs mainly found in the gas phase (like volatile PAHs, PCBs and HCHs) would be more affected by diffusive fluxes between the low atmosphere and the surface ocean.

Dry deposition in the open ocean consists in the direct load of pollutants adsorbed onto marine aerosols. The settling of these particles is a generalized process over the ocean surface, and even if the concentration of aerosols in the remote ocean

atmosphere is low there is a continuous production and renewal of these active elements⁴⁶ and their chemical characteristics (organic carbon content) makes them an effective attaching surface for low vapor pressure POPs. The dry deposition flux had been poorly described in the open ocean so far, being only characterized in the Mediterranean Sea⁴⁷⁻⁴⁹ and some parts of the Atlantic Ocean^{41, 50, 51}. Previous works described that dry deposition fluxes will depend on the concentration of contaminants in the aerosol fraction and the velocity of settling of that aerosol (Figure I.2), and may be affected by wind speed and other physico-chemical properties of the water that could enhance the aerosol affinity to the oceanic surface. Dry deposition fluxes (F_{DD}) can be calculated from

$$F_{DD} = v_D \cdot C_A \quad [I.1]$$

where C_A is the aerosol phase concentration and v_D is the deposition velocity of the specific aerosol-bound chemical⁵¹.

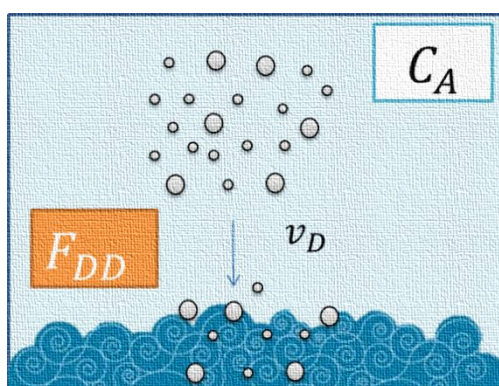


Figure I.2. Schematic draw of dry deposition.

Wet deposition is associated with the precipitation events that accelerate the entrance of pollution in the Open Ocean by a “washing process” of the atmosphere. In the tropical ocean, precipitation is mainly due to rain, but in higher latitudes or coastal areas fog, snow and hail should be considered as well. It consists on a double step equilibria: on the one hand each raindrop is chemically equilibrated with the gas phase concentration of organic pollutants through diffusion, and on the other, the rain sweeps the suspended particulate matter in the low atmosphere and enhances the entrance of hydrophobic compounds attached to the aerosol into the open ocean⁴⁵.

The wet deposition flux (F_{WD}) of POPs into the ocean can be calculated from a two terms equation,

$$F_{WD} = p_0 \left(\frac{C_G}{H'} + w_p C_A \right) \quad [1.2]$$

where p_0 is the precipitation rate, and multiplies a “gaseous equilibria” term, based on the concentration of the pollutant in the gas phase (C_G) and the Henry’s Law constant (H'), and a “scavenging” term, based on the washout ratio (w_p) and the concentration in the aerosol phase (Figure I.3).

Wet deposition is a very relevant entrance pathway of organic pollution to the ocean; nevertheless it is an episodic event very difficult to extrapolate spatially and temporally. It is also very intense during the first moments, but once that the fast removal of pollution has occurred it rapidly dilutes its strength as a transport vector since the atmosphere has become depleted in POPs. It has been assessed for compounds like PCBs^{42, 52, 53}, PAHs^{49, 54, 55} and PFASs⁵⁶⁻⁵⁸, but again limited to regional areas, and only modeled at a global scale⁴².

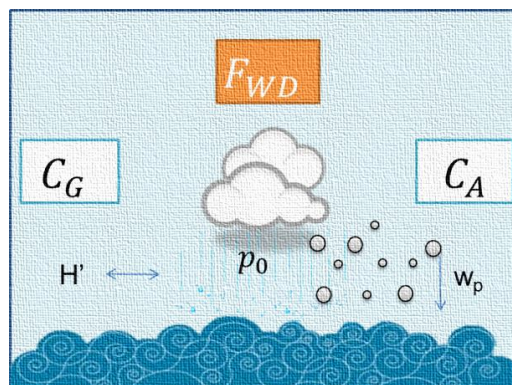


Figure I.3. Schematic draw of wet deposition.

Diffusive exchange between the atmosphere and the surface ocean appears to be the major diffuse entrance of POPs into the marine environment^{42, 59}. Among the interchanging processes it is the most reported one for many legacy halogenated pollutants^{39, 47, 53, 60} and hydrocarbons⁶¹⁻⁶⁴ and it is becoming a hot topic for the emerging contaminants, even if few information in the Open Ocean can be found yet⁶⁵⁻⁶⁷.

The direction of the air-water exchange depends on the fugacity of the chemical in air and water. Fugacity is the “the escaping tendency” of a substance from a media, and each POP will exhibit a particular fugacity from air and water according to its chemical properties and environmental conditions. Therefore the fugacity from the air (f_A) and the fugacity from the water (f_W) phases will be,

$$f_A = C_G R T \quad [1.3]$$

$$f_W = C_W H' R T \quad [1.4]$$

It is based on the concentration of the compound in the matrix (C_G in gas or C_W in water), the gases constant R , the dimensionless Henry’s Law constant H' , and on temperature (T). The net air-water diffusive flux is always from high to low fugacity, and there is a net equilibrium if air and water POP fugacities are similar in magnitude.

Diffusive fluxes are estimated from a fugacity gradient and a mass transfer coefficient, which depend on a wide array of environmental parameters. Air-water flux (F_{AW} , Figure 1.4) can be calculated from the concentration of the POP in the air and in the water as follows,

$$F_{AW} = k_{AW} \left(\frac{C_G}{H'} - C_W \right) \quad [1.5]$$

Where H' is the Henry’s Law constant of the compound (salinity and temperature corrected) and k_{AW} is the air-water mass transfer rate. In turn, this rate is estimated using the two film resistance model, and thus it is dependent on the mass transfer coefficients in each phase (k_A and k_W for the air and water, respectively),

$$\frac{1}{k_{AW}} = \frac{1}{k_A H'} + \frac{1}{k_W} \quad [1.6]$$

To calculate the particular k_A and k_W of a certain pollutant ($k_{A,POP}$ and $k_{W,POP}$), empirically determined coefficients for H_2O in the air ($k_{A,H2O}$) and CO_2 in the water ($k_{W,CO2}$) are used as comparison standards. Then in the air,

$$k_{A,POP} = k_{A,H2O} \left(\frac{D_{A,POP}}{D_{A,H2O}} \right)^{0.61} \quad [1.7]$$

being $k_{A,H_2O} = 0.2 U_{10} + 0.3$, where D_A is the diffusivity coefficient in the air and U_{10} is the wind speed at 10 m height of the air-ocean interphase.

The same way in the water,

$$k_{W,POP} = k_{W,CO_2} \left(\frac{S_{C,POP}}{S_{C,CO_2}} \right)^{-0.5} \quad [1.8]$$

being $k_{W,CO_2} = 0.24 U_{10}^2 + 0.061 U_{10}$ and S_{C,CO_2} the Schmidt number at 298 K, related with the diffusion of a substance in a liquid depending on the fluid viscosity, 600 for the CO_2 .

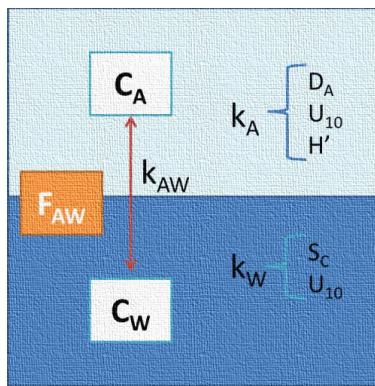


Figure I.4. Schematic draw of diffusive air-water exchange.

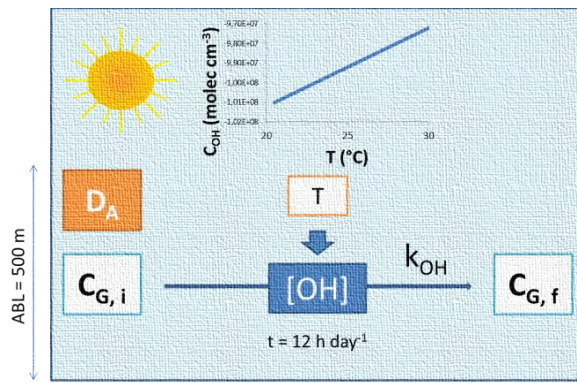


Figure I.5. Schematic draw of Atmospheric Degradation.

Nevertheless, the atmosphere holds also a high degradation capacity, and acts not only as an input vector of pollution to the remote ocean, but as a sink of released POPs, primarily originating in land. There are many reactions in the atmosphere that may affect POP concentrations, like photodegradation and interactions with oxidative substances or radicals, like ozone or OH ^{31, 68}. However, it is assumed that POPs degradation in the atmosphere is affecting mainly gas phase pollutants and it is dominated by the reaction with hydroxyl radical ³¹, and thus depend on the concentration of OH in the atmospheric boundary layer (ABL) (Figure I.5). OH production in the tropical and subtropical marine atmosphere is constant, and depends on temperature, being therefore a continuous and ubiquitous depletion process ³¹.

Water column processes

There are direct loads of POPs from inland waters via either run-off or through riverine discharges (Figure I.6). Run-off mainly depends on continental precipitation regimes (quite important in tropical and subtropical areas), temperature, vegetation cover and land use, and it has been recently turned into a research topic of interest due to the suggested future scenarios of climate change^{69, 70}. Riverine discharge has been more extensively studied in the past due to the habitual connection between rivers, harbors and human emplacements, with the consequent effects of POPs on human health and activities⁷¹⁻⁷³. Moreover, industrial activities and waste water treatment plants usually spill in riverine systems affecting as well pollution loading into the coastal marine environment⁷⁴⁻⁷⁶. However, POPs entrance through direct coastal inputs has a much lower effect on the open ocean concentrations when compared to atmospheric inputs and, thus, those processes are out of the scope of this thesis. Nevertheless, it should be taken into account that for some POP families, such as PFASs, it has been suggested that riverine inputs account for a main input to the marine environment^{77, 78}.

Ocean currents are an effective vector for transport of substances like oxygen⁷⁹, salts⁸⁰, nutrients⁸¹ and heat⁸² at a planetary scale. Equally, organic pollutants prone to be found in the dissolved water phase (like ionic PFASs) are reported to be affected by water masses transport^{44, 83-85}. Nevertheless, most POPs are highly hydrophobic and semivolatile and it can be assumed that they will not be affected directly by oceanic circulation, but mainly by atmospheric deposition and other processes, like phytoplankton blooms in upwelling areas, effects on air-water exchange due to ocean currents temperature, and organic matter cycling influence on air-water dis-equilibria. Moreover, the latitudinal area covered in this thesis (tropical and subtropical oceans) does not include the main marine subduction areas, placed in higher latitudinal strips⁸⁵, and therefore this process is out of the scope of this work (Figure I.6).

Dispersion in the deep ocean due to turbulent kinetics is another physical transport which has received little attention (Figure I.6). It is based on Fick's laws of diffusion, which explain diffusion caused by turbulent fluxes⁸⁶ by,

$$F_{Eddy} = -D \frac{\partial C_w}{\partial z} \quad [I.9]$$

where C_w is the seawater concentration of the target substance, z is depth, and D is the eddy diffusivity. Diffusivity has been estimated in literature from differences in the microscale temperature or density of the water^{87, 88}, being this coefficient is the main parameter to measure turbulence in the ocean. Turbulence, caused by macro and micro scale movement of the ocean and wind shear, has been used to explain diffusion of dissolved substances like nutrients and oxygen in the open ocean⁸⁹⁻⁹¹, but up to the moment has had very low application in POPs distribution⁸³ and thus it is a research field yet to explore⁸⁷.

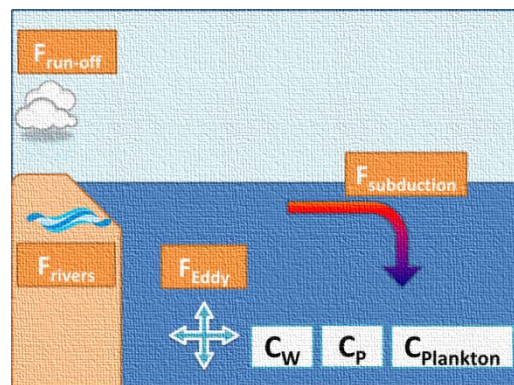


Figure 1.6. Schematic draw of physical transport processes in the water column.

Interactions of POPs with organic matter in the water column are relevant processes affecting their fate in the Open Ocean (Figure 1.7). POPs are rapidly sorpt onto particulate organic matter, if not entering the water directly attached to aerosols, and once there, they are susceptible to suffer physical or biological alteration. Among these processes; dilution, fast air-water-particle equilibrium, degradation, settling (biological pump), or bioaccumulation and biomagnification have been described to modify POPs concentrations in the marine water column and have a plausible effect on global fate of these compounds^{18, 23}. Studies regarding these processes have been conducted in lakes and coastal areas^{92, 93}, confined seas^{64, 94} and in polar regions^{37, 39, 95}, but for many of these processes there is a lack of a global assessments of their relevance.

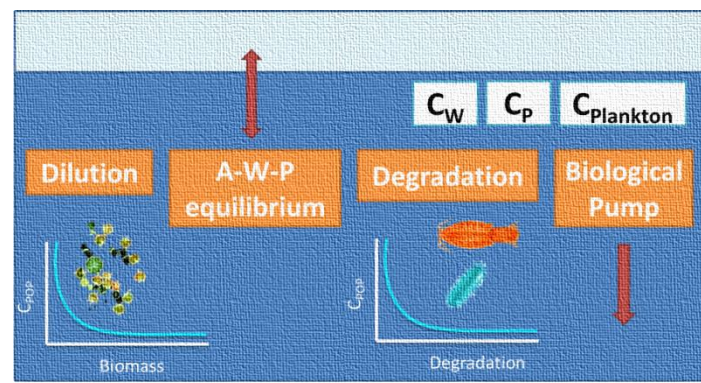


Figure I.7. Schematic draw of biological transport processes in the water column.

Case studies in the Malaspina expedition: PAHs and PFASs

The challenge to make a global study of POP's dynamics in the Open Ocean was difficult to consider taking into account the logistic and theoretical problems that could arise in such an effort. That is why most of the previous approaches have been formulated from non-empirical situations (like models or reviews of disperse datasets^{31, 59, 83}) or from new technologies like satellite imagery. Even if those serve as a very interesting base to infer the POPs dynamics in the Open Ocean, there was a lack of oceanic scale field studies comprehensively assessing processes affecting POP cycling and inputs.

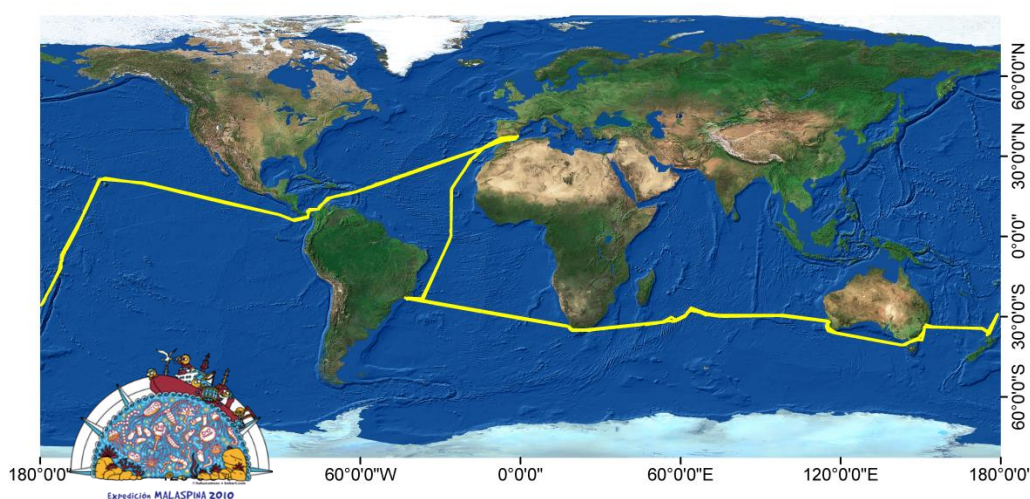


Figure I.8. Malaspina 2010 circumnavigation track.

The *Malaspina 2010* circumnavigation cruise (Figure I.8) was an optimal framework to hold such an ambitious objective. This interdisciplinary project linked many of the oceanographic sciences, like physical oceanography, biogeochemistry, chemical pollution, optics, phytoplankton science (production and metabolism), microbial biodiversity and functions and zooplankton science among others. This conjunction created myriads of measurements and data sets that could be interrelated in order to get a holistic view of the Global Ocean. It lasted 7 months and crossed all the tropical and subtropical oceans between 40° North and 30° South, making it possible to measure concentrations and fluxes of the pollutants of interest all around the globe with a daily resolution. By crossing this information with other measured parameters during the circumnavigation (like chemical properties or meteorological data) it is possible to infer the potential influence of some processes not evaluated so far in the field in terms of POP cycling.

The key processes of distribution and interchange between the atmosphere and the water surface were evaluated for the main POPs families during the development of this work, like dioxins, PCBs and some halogenated pesticides. Nevertheless, in this thesis, two particular groups of organic pollutants, PAHs and PFASs, were selected as target contaminants to assess POPs dynamics and fate in the open ocean. The first are semivolatile compounds (considered together with POPs even if they are susceptible to degradation) with a wide range of volatility and hydrophobicity, what makes them very interesting in order to assess atmosphere- seawater exchange. The second, PFASs, are ionic emerging POPs whose chemical characteristics (like much lower hydrophobicity compared with other POPs, and non-volatility) will serve as an example to show processes of mobility and diffusion within the water column in the Open sea.

Polycyclic Aromatic Hydrocarbons (PAHs)

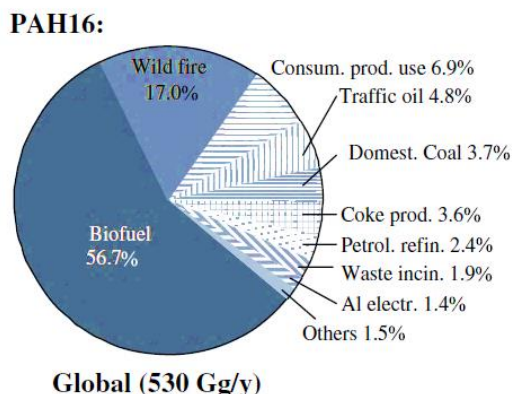


Figure I.9. PAHs global production (modified from Zang et al. 2009).

Polycyclic Aromatic Hydrocarbons are probably the more abundant and widely distributed carcinogens in the Earth⁹⁶, and they are present in our proximate environments^{15, 97} but also in remote areas like the open ocean and polar regions^{98 36, 99-101}. They come mainly from incomplete combustion of fossil fuels and organic matter and are related as well to petrogenic and biogenic processes. Even if

they have been described to be occurring naturally, due to wildfires, volcanoes¹⁰² and organic matter degradation in soils¹⁰³, the predominant view is that the main actual global emission is due to anthropogenic activities, being biofuel consumption the main global source and the principal producing countries China (114 Gg y⁻¹), India (90 Gg y⁻¹) and United States (32 Gg y⁻¹) (Figures I.9 and I.10)¹⁰⁴.

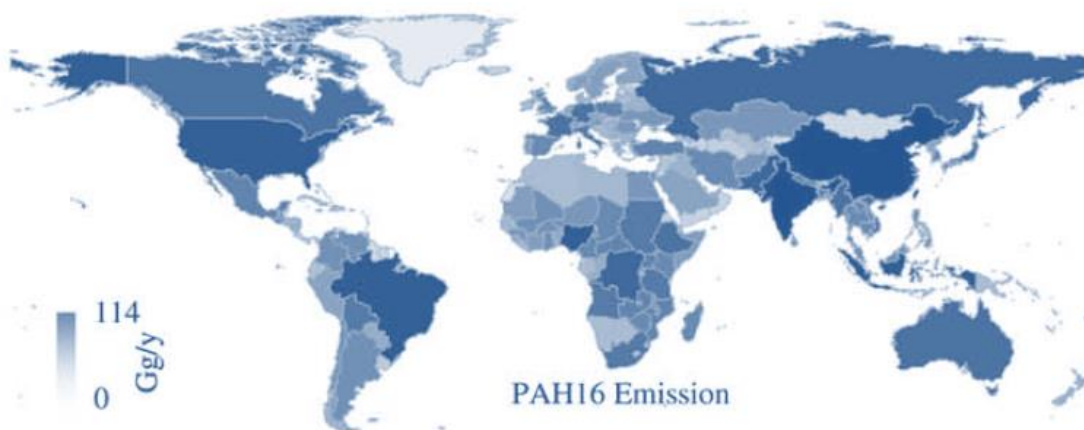
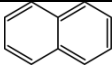
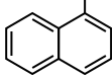
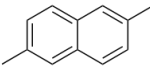
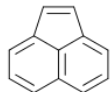
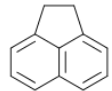
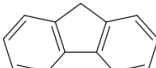
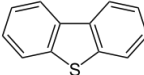
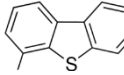
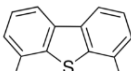
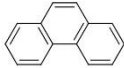
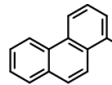
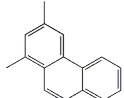
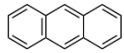
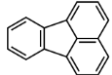
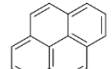


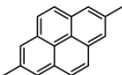
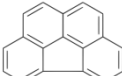
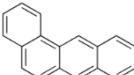
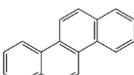
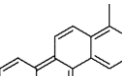
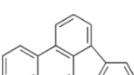
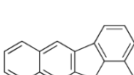
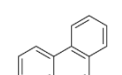
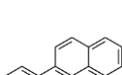
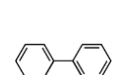
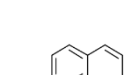
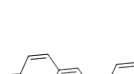
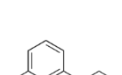
Figure I.10. National annual emissions rate of EPA's 16 regulated PAHs (modified from Zang et al 2009).

The EPA suggested a priority list of 16 compounds (those indicated in Figures I.9 and I.10 and Table I.1) as of particular toxicological and environmental concern. Among them, there are the seven PAH compounds classified as probable human carcinogens: benzo[*a*]anthracene, benzo[*a*]pyrene, benzo[*b*]fluoranthene, benzo[*k*]fluoranthene, chrysene, dibenz[*a,h*]anthracene, and indeno[1,2,3-*cd*]pyrene¹². The persistence and

toxicity of PAHs is related with the MW (Table I.1) and with the isomeric structure¹⁰⁵. However, the higher occurrence of other non-as-toxic compounds or those having a bigger LRET potential make other PAHs of high interest as well. The chemical properties of each considered PAH in this thesis are included in Table I.1 and show the wide range of volatility, hydrophobicity, and persistence these compounds may exhibit. Indeed, the reported array of their semi volatility and partitioning tendency to soot and organic carbon, makes PAHs as a good case study of organic pollutants being subject to a number of different biotic and abiotic processes, and for assessing global transport and exchange between air-water-biota in the open ocean.

Table I.1. PAHs physicochemical properties

		MW [g mol ⁻¹]	Log K _{OA}	Log K _{OW}	K _{OH} [cm ³ molec ⁻¹ s ⁻¹]	-ΔH [kJ mol ⁻¹]	ΔS [kJ mol ⁻¹ K ⁻¹]
Naphthalene*		128	5.1 ^a	3.33 ⁱ	1.9 10 ⁻¹¹	-19.29 ^d	0.054 ^d
Methyl-naphthalenes		142	5.79 ^b	3.87 ^j	4.1 10 ⁻¹¹	-42.4 ^m	0.11 ^m
Dimethyl-naphthalenes		156		4.42 ^j	6 10 ⁻¹¹	-48.69 ^d	
Acenaphthylene*		152	6.52 ^c	3.62 ⁱ	1.1 10 ⁻¹⁰	-52.2 ^m	0.131 ^m
Acenaphthene*		153	6.31 ^d	3.92 ⁱ	5.8 10 ⁻¹¹	-51.9 ^m	0.133 ^m
Fluorene*		166	6.83 ^d	4.21 ⁱ	1.3 10 ⁻¹¹	-48.8 ^m	0.118 ^m
Dibenzothiophene		184	7.24 ^e	4.38 ^k	1.4 10 ⁻¹¹	-21.6 ⁿ	0.056 ^o
Methyl-dibenzothiophenes		198			1.3 10 ⁻¹¹		
Dimethyl-dibenzothiophenes		212					
Phenanthrene*		178	7.22 ^e	4.57 ⁱ	1.3 10 ⁻¹¹	-47.3 ^m	0.106 ^m
Methyl-phenanthrenes		192	7.49 ^e	4.99 ⁱ	8 10 ⁻¹²	-35.4 ^m	0.067 ^m
Dimethyl-phenanthrenes		206	8.03 ^e		7.7 10 ⁻¹²		
Anthracene*		178	7.55 ^d	4.68 ⁱ	1.1 10 ⁻¹¹	-46.8 ^m	0.106 ^m
Fluoranthene*		202	8.61 ^d	5.23 ⁱ	9.1 10 ⁻¹²	-38.7 ^m	0.07 ^m
Pyrene*		202	8.75 ^d	5.11 ⁱ	8.6 10 ⁻¹²	-42.9 ^m	0.084 ^m
Methyl-pyrenes		216		5.45 ⁱ			

Dimethyl-pyrenes		230					
Benzo[ghi]fluoranthene		226				-5.35 ⁿ	
Benzo[a]anthracene*		228	9.5 ^a	5.91 ⁱ	6.9 10 ⁻¹²	-66.4 ^m	0.159 ^m
Chrysene*		228	10.4 ^a	5.81 ⁱ	7.7 10 ⁻¹²	-100.9 ^m	0.268 ^m
Methyl-chrysenes		242					
Benzo[b]fluoranthene*		252	11.19 ^f	6.2 ⁱ		-19.6 ⁿ	0.056 ^d
Benzo[k]fluoranthene*		252	11.19 ^f	6.2 ⁱ		-19.6 ⁿ	0.056 ^d
Benzo[e] pyrene		252	11.13 ^f	6.12 ⁱ		-16.57 ^d	0.036 ^d
Benzo[a] pyrene*		252	11.56 ^g	6.13 ⁱ		-25.61 ^d	0.032 ^d
Perylene		252	11.7 ^h	5.84 ⁱ		-31.88 ^d	0.057 ^d
Indeno[1,2,3-cd]pyrene*		276	12.43 ^g	6.65 ⁱ		-21.51 ^d	0.056 ^d
Dibenzo[a,h]anthracene*		278	12.59 ^g	6.86 ⁱ		-31.16 ^d	0.057 ^d
Benzo[ghi]perylene*		276	12.55 ^g	6.22 ⁱ		-17.37 ^d	0.031 ^d

^a Wania & Mackay 1996, ^b Hiatt 2014, ^c Ma et al 2010, ^d Mackay book 2006, ^e Lehndorff and Schwark 2009, ^f Finizio et al. 1997, ^g Odabasi 2006, ^h Mackay and Callcot 1998, ⁱ Bukhard EST 2000, ^j Mackay book 1992, ^k Blum et al 2011, ^l Keyte et al 2013, ^m Bamford 1999, ⁿ Acree and Chickos 2010, ^o Ramirez-Verduzco et al 2007. *included in the EPA priority list.

Perfluoroalkylated Substances (PFASs)

Perfluorinated compounds (PFCs) are anthropogenic halogenated chemicals recently developed for industrial and consumer goods usage. They were first produced by Dupont and 3M for isolation purposes and were included in daily products like plastics, food packages and clothes since the early sixties. The most produced and widely used compounds correspond to the perfluoroalkylated chains, the PFASs (Figure I.11 ¹⁰⁶).

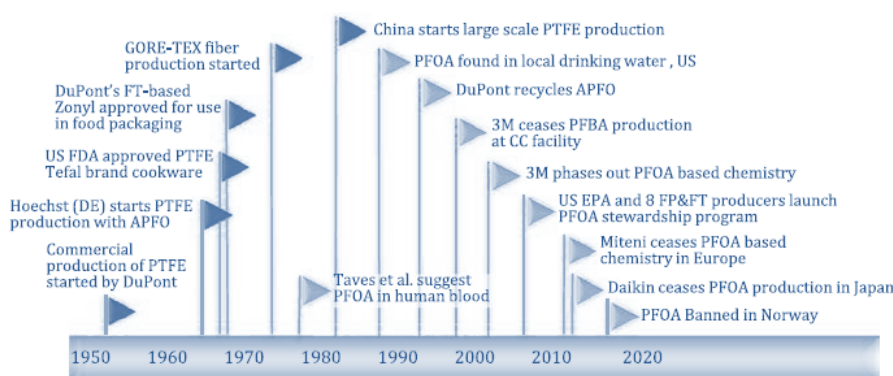


Figure I.11. PFCs production and use timeline.

They were first reported in human blood in 1968 ¹⁰⁷ and during last years they have been reported in all environmental matrixes from soils ⁷⁵, water ⁴⁴ and air ^{108, 109}, to biota ¹¹⁰, even in remote areas ^{35, 111, 112}. Because of this rising interest on their environmental distribution and little knowledge of their effects in the environment, coupled to a high pressure of the EPA in USA during the 90s, industry voluntarily

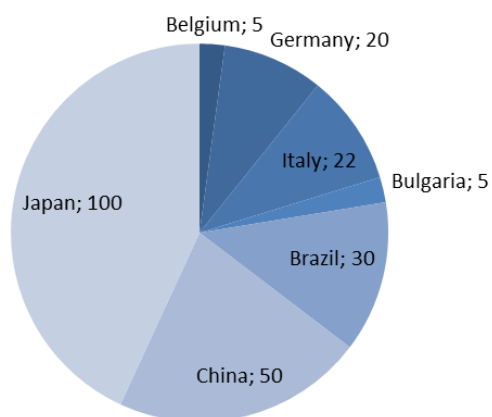


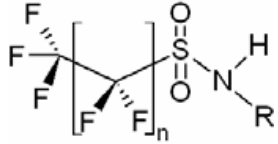
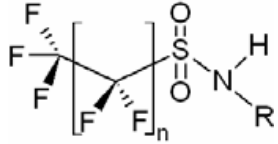
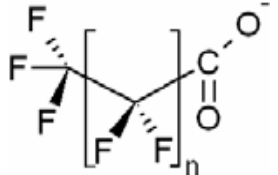
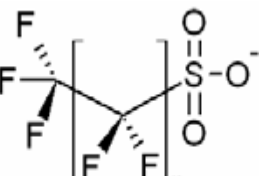
Figure I.12. PFOS and related substances global production (tons y⁻¹).

phased out perfluorooctane carboxylic acid (PFOA) and perfluorooctane sulfonic acid (PFOS) direct production in the 2000s ¹¹³. Nevertheless, electrochemical fluorination and telomerisation processes are still performed in industry, producing short chain PFASs and precursors of the more persistent PFASs even if some of them, like PFOS and its salts, were included in the Stockholm Convention in

2009¹¹⁴. There is little information about the generating volume of the producing countries and emplacement of the sources. The more complete studies found to date are the Organization for Economic Cooperation and Development (OECD) reports in which only direct production of PFOS is compulsory informed for some countries, but not for other fluorinated compounds extensively used in pesticides formulations, firefighting foams, photographic industry and aviation industry¹¹⁵. According to the report from 2009, the top annual producers in 2003 were Japan, China and Brazil (Figure I.12), even if previous to that year USA was by far the main producer and consumer reaching in year 2000 more than 3500 tons of annual production¹¹³.

PFASs consist on a fully fluorinated carbon chain, which makes them highly stable due to the strong fluoride-carbon bond, and an alkylated ionic “head” which gives them the amphipathic character. In particular PFOS and PFOA, the 8 carbons (C) sulphonic acid and carboxylic acid, respectively, have been reported all over the planet in all kind of environmental matrixes^{44, 110, 116-119}. These ionic families, perfluoroalkylated sulfonic and carboxylic acids (PFASs and PFCAs, respectively) are the more persistent and toxic among the PFASs, and even if long chain and 8C compounds are raising general concern, shorter chain compounds are still being used in the growing industry of surfactants⁴⁴. Among the neutral PFASs, fluorotelomer alcohols, sulfonamides (PFASAs) and fluorotelomer aldehydes are the more relevant precursors of PFASs and PFCAs¹¹⁴, and recently they have become also target pollutants in environmental research as they are more volatile and have high LRET potential^{74, 108, 120-122}. In this thesis, PFASs, PFCAs and PFASAs were selected for assessing their occurrence and cycling in the Open Ocean. Their properties affecting chemical dynamics are summarized in Table I.2. Of special interest is the fact that they have a particular organic matter affinity, as they are not as lipophilic as other POPs but they have been described as proteinophilic¹²³. There are few studies reporting their occurrence in the open ocean at big spatial scale^{35, 112, 124-126}, even less giving concentrations through the deep water column⁸⁴ and none to date assessing their fate in the open ocean relating them with organic matter cycling. Therefore the data provided in this thesis are novel and of high interest for the better understanding of these pollutants in the remote Oceanic environment.

Table I.2. PFASs physicochemical properties.

Compound	Acronym	Molecule	Chain length (n)	MW [g mol ⁻¹]	Log K _{OA} ¹²⁷	Log K _{OW} ¹²⁷	Log K _{PW} ¹²⁷	BAF ¹²⁸
Perfluoro-1-octanesulfonamide	PFOSA		7	498	8.4	6.3	-	
N-methylperfluoro-1-octanesulfonamide	N-MePFOSA		7	512				
Perfluoro-n-butanoic acid	PFBA		3					
Perfluoro-n-pentanoic acid	PFPA		4					
Perfluoro-n-hexanoic acid	PFHxA		5	312				
Perfluoro-n-heptanoic acid	PFHpA		6	363	5.9	3.8	2	
Perfluoro-n-octanoic acid	PFOA		7	413	6.3	4.6	2.5	292
Perfluoro-n-nonanoic acid	PFNA		8	463	6.6	5.5	3.1	1650
Perfluoro-n-decanoic acid	PFDA		9	512	6.8	6.4	3.8	765
Perfluoro-n-undecanoic acid	PFUnDA		10		7.1	7.4	4.5	
Perfluoro-n-dodecanoic acid	PFDoDA		11		7.4	8.1	5	
Perfluoro-n-tridecanoic acid	PFTTrDA		12		8.8	9	5.6	
Perfluoro-n-tetradecanoic acid	PFTeDA		13					
Perfluoro-n-hexadecanoic acid	PFHxDA		15					
Perfluoro-n-octadecanoic acid	PFODA		17					
Perfluoro-butanefulfonate	PFBS		3	298				
Perfluoro-hexanesulfonate	PFHxS		5	399				58
Perfluoro-heptanesulfonate	PFHpS		6	449				
Perfluoro-octanesulfonate	PFOS		7	499	7.8	5.3	3	169
Perfluoro-decanesulfonate	PFDS		9					
Perfluoro-dodecanesulfonate	PFDoDS		11					

Aim and Outline of this thesis

The general aim of this thesis is to assess the occurrence of POPs cycling in the global tropical and subtropical Open Oceans, focusing on PAHs and PFASs.

The specific objectives are

- To determine PAHs occurrence in gas, aerosol, dissolved, particulate and planktonic phases, and PFAS in dissolved phase from the global Open Ocean.
- To quantify POPs fluxes between the different environmental compartments.
- To study physical and trophic factors that affect POPs entrance in the plankton.
- To evaluate the relevance of semivolatile aromatic hydrocarbons (containing PAHs and other aromatic compounds) as a source of semivolatile organic carbon to the ocean.

The results obtained are presented in different chapters, depending on the contaminant family and the processes evaluated, as briefly described below:

Chapter 1: Field measurements of the Atmospheric Dry Deposition Fluxes and Velocities of Polycyclic Aromatic Hydrocarbons to the Global Oceans. Published in Environmental Science and Technology, 2014.

In the first chapter, as illustrated in Figure I.13, the empirical measurements of PAHs dry deposition done during the *Malaspina 2010* circumnavigation cruise are presented. PAHs velocities of deposition in coarse and fine aerosol are obtained separately and at a global scale resolution. Moreover, the directly quantified fluxes measured concurrently with other physicochemical and meteorological parameters, allowed to suggest an empirical parametrization of the velocity of deposition. The given equation allow to predict the dry depositional velocities of semivolatile organic compounds to the global Oceans by measuring the target compound concentration in the aerosol phase, its vapor pressure, the wind speed and the chlorophyll concentration of the water where the aerosol is depositing.

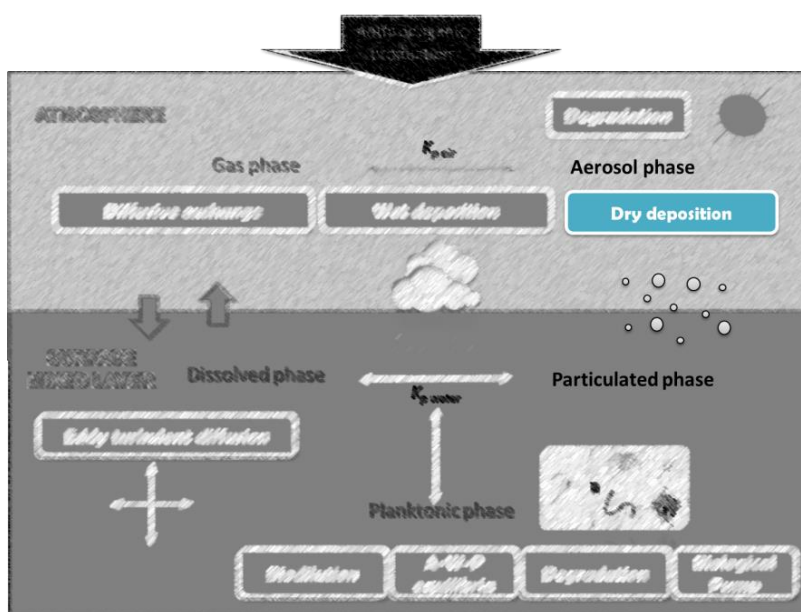


Figure I.13. Schematic view of processes evaluated in Chapter 1.

Chapter 2: High Atmosphere-Ocean Exchange of Semivolatile Aromatic Hydrocarbons. Submitted.

This Chapter describes all the measured and calculated depositional fluxes and fading processes in the atmospheric boundary layer over the tropical and subtropical global Oceans (Figure I.14). Diffusive exchange, wet deposition, dry deposition and atmospheric degradation (OH radical oxidation) are calculated from the measured 64 PAHs congener's concentrations in the gas, aerosol, rainwater and dissolved phases in the Open Ocean. Furthermore, an estimation of the semivolatile aromatic-like compounds (SALCs) concentration is done in the gaseous and dissolved phases and the diffusive exchange for them is calculated, as it appeared to be the highest magnitude flux affecting their fate. An estimation of the total carbon entrance to the Open Ocean due to these organic compounds, PAHs and SALCs, is also emphasized in order to suggest their account in the global carbon budgets calculations.

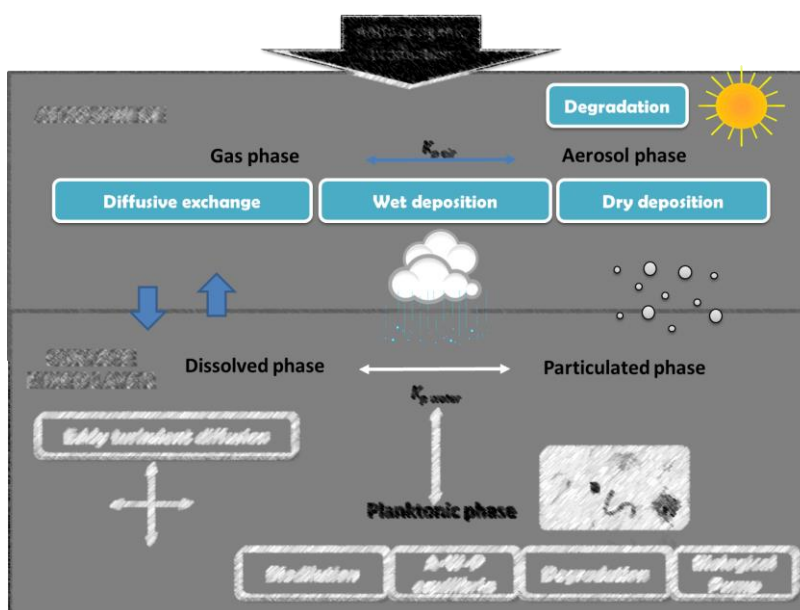


Figure I.14. Schematic view of processes evaluated in Chapter 2.

Chapter 3: Perfluoroalkylated Substances in the Global Tropical and Subtropical Surface Oceans. Published in Environmental Science and Technology, 2014.

PFASs occurrence in surface ocean waters is reported in this Chapter for the Atlantic, Indian and Pacific oceans. Eleven congeners of two ionic families (perfluoroalkyl carboxylic acids and perfluoroalkyl sulfonic acids) and two neutral precursors (perfluoroalkyl sulfonamides) were identified and quantified. Their global occurrence and the potential factors affecting their distribution patterns are discussed including the distance to coastal regions, oceanic subtropical gyres, currents and biogeochemical processes.

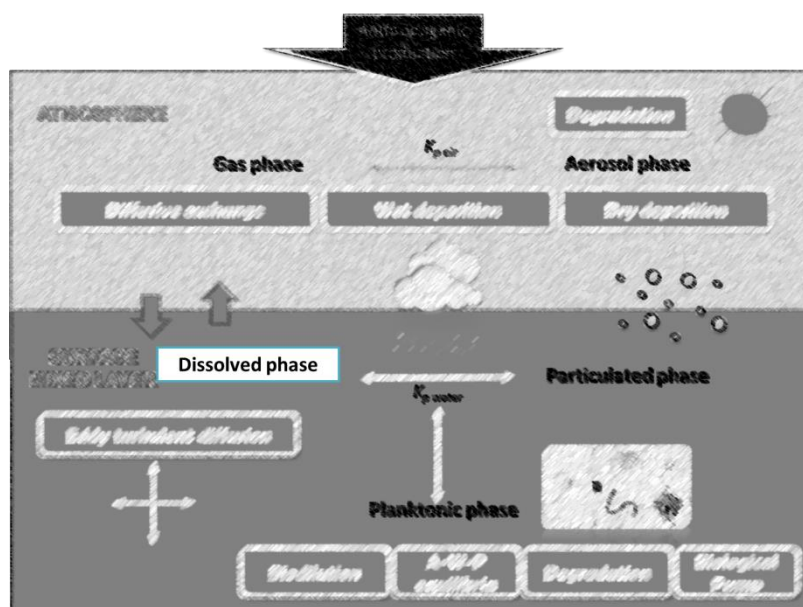


Figure 1.15. Schematic view of processes evaluated Chapter 3.

Chapter 4: Oceanic Transport and Sinks of Perfluoroalkylated Substances. To be submitted.

This Chapter goes a step further on the assessment of PFASs dynamics in the Open Ocean's water column. It provides paired concentration of PFASs at the deep chlorophyll maximum depth (around 100 m depth) to those presented for surface in the previous chapter, and affords the first calculations of eddy diffusion fluxes (F_{Eddy}) due to marine turbulence and settling fluxes ($F_{Settling}$) due to the biological pump at a global scale (Figure I.16). Moreover, F_{Eddy} was calculated from concurrent empirical measurements of turbulence in the water column with the PFASs sampling allowing the first reported estimations of diffusive fluxes of POPs from field data. $F_{Settling}$ was calculated separately for the phytoplankton and zooplankton fecal pellets contribution to total biological pump, which allows the characterization of $F_{Settling}$ magnitude depending on the biomass present, and enlightens the relevance of the biological pump in PFASs fate in the Open Ocean never assessed before.

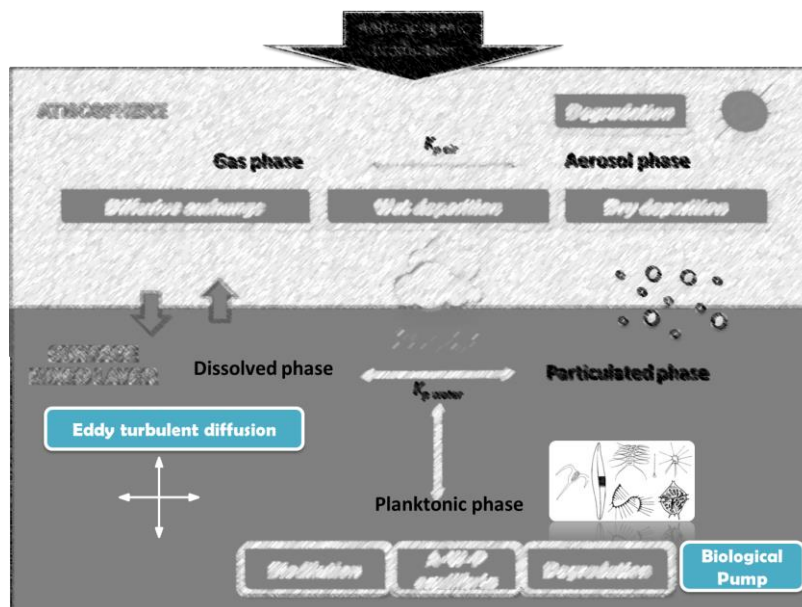


Figure I.16. Schematic view of processes evaluated in Chapter 4.

Chapter 5: Cycling of Polycyclic Aromatic Hydrocarbons in the Surface Open Ocean. In preparation.

The role of plankton and organic suspended particles in PAHs distribution and fate in the Open Ocean is an unresolved issue. In this Chapter it is described the measured PAHs concentration in the dissolved, particulate and plankton phases during the *Malaspina 2010* circumnavigation. Concentration dependence on organic carbon and physicochemical properties of the PAHs (particularly hydrophobicity) is evaluated. Furthermore, a review of the previously suggested processes regulating PAH concentrations in the water column is done, including biodilution, air-water-particle equilibria, and the degradative and biological pumps (Figure I.17). This last is calculated separately for the zooplankton and phytoplankton sinking matter, for the first time in literature, allowing an estimation of the sinking fluxes of PAHs in the Open Ocean and suggesting directions for future research.

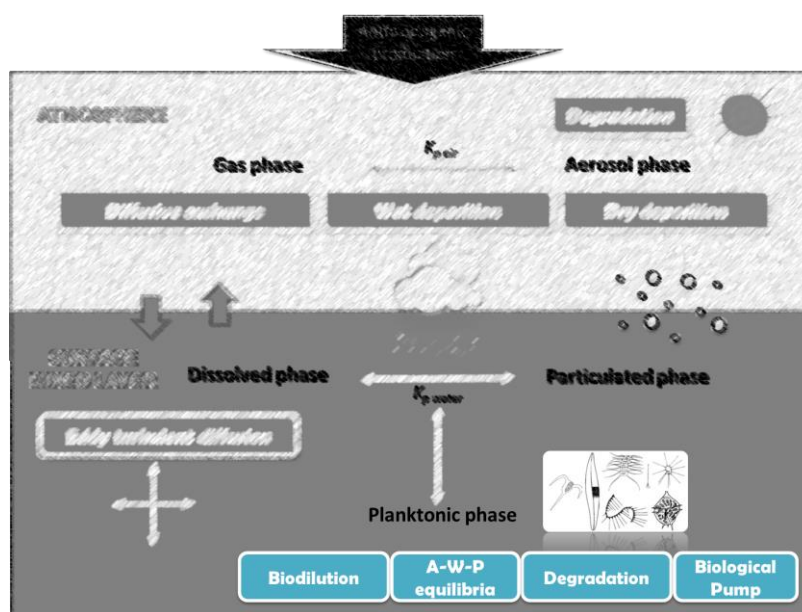


Figure I.17. Schematic view of processes reviewed in Chapter 5.

REFERENCES

1. Hughes, T. P.; Bellwood, D. R.; Folke, C.; Steneck, R. S.; Wilson, J., New paradigms for supporting the resilience of marine ecosystems. *Trends in Ecology & Evolution* **2005**, *20*, (7), 380-386.
2. Côté, I. M.; Darling, E. S., Rethinking ecosystem resilience in the face of climate change. *PLoS biology* **2010**, *8*, (7), e1000438.
3. Doney, S. C.; Ruckelshaus, M.; Emmett Duffy, J.; Barry, J. P.; Chan, F.; English, C. A.; Galindo, H. M.; Grebmeier, J. M.; Hollowed, A. B.; Knowlton, N.; Polovina, J.; Rabalais, N. N.; Sydeman, W. J.; Talley, L. D., Climate Change Impacts on Marine Ecosystems. *Annual Review of Marine Science* **2012**, *4*, (1), 11-37.
4. Cózar, A.; Echevarría, F.; González-Gordillo, J. I.; Irigoien, X.; Úbeda, B.; Hernández-León, S.; Palma, Á. T.; Navarro, S.; García-de-Lomas, J.; Ruiz, A.; Fernández-de-Puelles, M. L.; Duarte, C. M., Plastic debris in the open ocean. *Proceedings of the National Academy of Sciences of the United States of America* **2014**, *111*, (28), 10239-10244.
5. Andrady, A. L., Microplastics in the marine environment. *Marine Pollution Bulletin* **2011**, *62*, (8), 1596-1605.
6. Law, K. L.; Moret-Ferguson, S.; Maximenko, N. A.; Proskurowski, G.; Peacock, E. E.; Hafner, J.; Reddy, C. M., Plastic accumulation in the North Atlantic subtropical gyre. *Science* **2010**, *329*, (5996), 1185-8.
7. McCulloch, M.; Falter, J.; Trotter, J.; Montagna, P., Coral resilience to ocean acidification and global warming through pH up-regulation. *Nature Climate Change* **2012**, *2*, (8), 623-627.
8. Dachs, J.; Méjanelle, L., Organic Pollutants in Coastal Waters, Sediments, and Biota: A Relevant Driver for Ecosystems During the Anthropocene? *Estuaries and Coasts* **2010**, *33*, (1), 1-14.
9. Rockstrom, J.; Steffen, W.; Noone, K.; Persson, A.; Chapin, F. S.; Lambin, E. F.; Lenton, T. M.; Scheffer, M.; Folke, C.; Schellnhuber, H. J.; Nykvist, B.; de Wit, C. A.; Hughes, T.; van der Leeuw, S.; Rodhe, H.; Sorlin, S.; Snyder, P. K.; Costanza, R.; Svedin, U.; Falkenmark, M.; Karlberg, L.; Corell, R. W.; Fabry, V. J.; Hansen, J.; Walker, B.; Liverman, D.; Richardson, K.; Crutzen, P.; Foley, J. A., A safe operating space for humanity. *Nature* **2009**, *461*, (7263), 472-475.
10. (ECHA), E. C. A., EU criteria for risk assessment of persistence, bioaccumulation and toxicity of chemicals. In European Parliament and of the Council on the Registration, E., Authorisation and Restriction of Chemicals (REACH), Ed. Official Journal of the European Union, 2014.
11. UNEP, U. N. E. P., Report of the Conference of the Parties of the Stockholm Convention on Persistent Organic Pollutants on the work of its fourth meeting. In United Nations Environment Programme: Stockholm Convention on Persistent Organic Pollutants. Geneva, 2009; p p. 112.
12. EPA Toxic Release Inventory Program. (2015).
13. Canada, G. o. Canadian Environmental Protection Act.
14. Agency, E. C. Registration, Evaluation, Authorization, and Restriction of Chemicals (REACH) Program.
15. Menzie, C. A.; Potocki, B. B.; Santodonato, J., Exposure to carcinogenic PAHs in the environment. *Environmental science & technology* **1992**, *26*, (7), 1278-1284.
16. UNECE The 1998 Aarhus Protocol on Persistent Organic Pollutants (POPs).
17. UNECE, Protocol to the 1979 Convention on Long Range Transboundary Air Pollution on Persistent Organic Pollutants (POPs). In Europe, U. N. E. C. f., Ed. UN: http://www.unece.org/env/lrtap/pops_h1.html, 1998.

18. Lohmann, R.; Breivik, K.; Dachs, J.; Muir, D., Global fate of POPs: Current and future research directions. *Environmental Pollution* **2007**, *150*, (1), 150-165.
19. Wania, F.; MacKay, D., Peer Reviewed: Tracking the Distribution of Persistent Organic Pollutants. *Environmental Science & Technology* **1996**, *30*, (9), 390A-396A.
20. Risebrough, R.; Rieche, P., Polychlorinated biphenyls in the global ecosystem. *Nature* **1968**, *220*, 1098-1102.
21. Tatton, J.; Ruzicka, J., Organochlorine pesticides in Antarctica. *Nature* **1967**, *215*, 346-348.
22. Carson, R., *Silent spring*. Houghton Mifflin Harcourt: 2002.
23. Dachs, J.; Lohmann, R.; Ockenden, W. A.; Méjanelle, L.; Eisenreich, S. J.; Jones, K. C., Oceanic biogeochemical controls on global dynamics of persistent organic pollutants. *Environmental Science and Technology* **2002**, *36*, (20), 4229-4237.
24. Wania, F., Assessing the potential of persistent organic chemicals for long-range transport and accumulation in polar regions. *Environmental science & technology* **2003**, *37*, (7), 1344-1351.
25. Iwata, H.; Tanabe, S.; Sakai, N.; Tatsukawa, R., Distribution of persistent organochlorines in the oceanic air and surface seawater and the role of ocean on their global transport and fate. *Environmental Science & Technology* **1993**, *27*, (6), 1080-1098.
26. Kannan, K., Perfluoroalkyl and polyfluoroalkyl substances: current and future perspectives. *Environmental chemistry* **2011**, *8*, (4), 333-338.
27. Sweetman, A. J.; Valle, M. D.; Prevedouros, K.; Jones, K. C., The role of soil organic carbon in the global cycling of persistent organic pollutants (POPs): interpreting and modelling field data. *Chemosphere* **2005**, *60*, (7), 959-972.
28. Hageman, K. J.; Bogdal, C.; Scheringer, M., Chapter 11 - Long-Range and Regional Atmospheric Transport of POPs and Implications for Global Cycling. In *Comprehensive Analytical Chemistry*, Eddy, Y. Z., Ed. Elsevier: 2015; Vol. Volume 67, pp 363-387.
29. Gouin, T.; Mackay, D.; Jones, K. C.; Harner, T.; Meijer, S. N., Evidence for the "grasshopper" effect and fractionation during long-range atmospheric transport of organic contaminants. *Environmental Pollution* **2004**, *128*, (1-2), 139-148.
30. Beyer, A.; Wania, F.; Gouin, T.; Mackay, D.; Matthies, M., Temperature Dependence of the Characteristic Travel Distance. *Environmental Science & Technology* **2003**, *37*, (4), 766-771.
31. Jurado, E.; Dachs, J., Seasonality in the "grasshopping" and atmospheric residence times of persistent organic pollutants over the oceans. *Geophysical Research Letters* **2008**, *35*, (17).
32. Scheringer, M.; Salzmann, M.; Stroebe, M.; Wegmann, F.; Fenner, K.; Hungerbühler, K., Long-range transport and global fractionation of POPs: insights from multimedia modeling studies. *Environmental Pollution* **2004**, *128*, (1), 177-188.
33. Castro-Jiménez, J.; Dachs, J.; Eisenreich, S. J., Chapter 8 - Atmospheric Deposition of POPs: Implications for the Chemical Pollution of Aquatic Environments. In *Comprehensive Analytical Chemistry*, Eddy, Y. Z., Ed. Elsevier: 2015; Vol. Volume 67, pp 295-322.
34. Ahrens, L.; Shoeib, M.; Del Vento, S.; Codling, G.; Halsall, C., Polyfluoroalkyl compounds in the Canadian Arctic atmosphere. *Environmental Chemistry* **2011**, *8*, (4), 399-406.
35. Benskin, J. P.; Muir, D. C.; Scott, B. F.; Spencer, C.; De Silva, A. O.; Kylin, H.; Martin, J. W.; Morris, A.; Lohmann, R.; Tomy, G.; Rosenberg, B.; Taniyasu, S.; Yamashita, N., Perfluoroalkyl acids in the Atlantic and Canadian Arctic Oceans. *Environmental Science & Technology* **2012**, *46*, (11), 5815-23.
36. Friedman, C. L.; Zhang, Y.; Selin, N. E., Climate change and emissions impacts on atmospheric PAH transport to the arctic. *Environmental Science and Technology* **2014**, *48*, (1), 429-437.
37. Galbán-Malagón, C.; Berrojalbiz, N.; Ojeda, M. J.; Dachs, J., The oceanic biological pump modulates the atmospheric transport of persistent organic pollutants to the Arctic. *Nature communications* **2012**, *3*, 862.

38. Galbán-Malagón, C.; Cabrerizo, A.; Caballero, G.; Dachs, J., Atmospheric occurrence and deposition of hexachlorobenzene and hexachlorocyclohexanes in the Southern Ocean and Antarctic Peninsula. *Atmospheric Environment* **2013**, *47*, 41-49.
39. Galbán-Malagón, C. J.; Del Vento, S.; Cabrerizo, A.; Dachs, J., Factors affecting the atmospheric occurrence and deposition of polychlorinated biphenyls in the Southern Ocean. *Atmospheric Chemistry and Physics* **2013**, *13*, (23), 12029-12041.
40. Morales, L.; Dachs, J.; González-Gaya, B. n.; Hernán, G.; Ábalos, M.; Abad, E., Background Concentrations of Polychlorinated Dibenzo-p-Dioxins, Dibenzofurans, and Biphenyls in the Global Oceanic Atmosphere. *Environmental science & technology* **2014**, *48*, (17), 10198-10207.
41. Jurado, E.; Jaward, F. M.; Lohmann, R.; Jones, K. C.; Simó, R.; Dachs, J., Atmospheric dry deposition of persistent organic pollutants to the atlantic and inferences for the global oceans. *Environmental Science and Technology* **2004**, *38*, (21), 5505-5513.
42. Jurado, E.; Jaward, F.; Lohmann, R.; Jones, K. C.; Simó, R.; Dachs, J., Wet deposition of persistent organic pollutants to the global oceans. *Environmental Science and Technology* **2005**, *39*, (8), 2426-2435.
43. Bucheli, T. D.; Müller, S. R.; Heberle, S.; Schwarzenbach, R. P., Occurrence and behavior of pesticides in rainwater, roof runoff, and artificial stormwater infiltration. *Environmental Science & Technology* **1998**, *32*, (22), 3457-3464.
44. Ahrens, L.; Bundschuh, M., Fate and effects of poly- and perfluoroalkyl substances in the aquatic environment: A review. *Environmental Toxicology and Chemistry* **2014**, *33*, (9), 1921-1929.
45. Bidleman, T. F., Atmospheric processes. *Environmental Science and Technology* **1988**, *22*, (4), 361-367.
46. Fitzgerald, J. W., Marine aerosols: A review. *Atmospheric Environment. Part A. General Topics* **1991**, *25*, (3-4), 533-545.
47. Castro-Jiménez, J.; Eisenreich, S. J.; Ghiani, M.; Mariani, G.; Skejo, H.; Umlauf, G.; Wollgast, J.; Zaldívar, J. M.; Berrojalbiz, N.; Reuter, H. I.; Dachs, J., Atmospheric occurrence and deposition of polychlorinated dibenzo-p-dioxins and dibenzofurans (PCDD/Fs) in the open mediterranean sea. *Environmental Science and Technology* **2010**, *44*, (14), 5456-5463.
48. Demircioglu, E.; Sofuoglu, A.; Odabasi, M., Particle-phase dry deposition and air-soil gas exchange of polycyclic aromatic hydrocarbons (PAHs) in Izmir, Turkey. *Journal of Hazardous Materials* **2011**, *186*, (1), 328-335.
49. Birgül, A.; Tasdemir, Y.; Cindoruk, S. S., Atmospheric wet and dry deposition of polycyclic aromatic hydrocarbons (PAHs) determined using a modified sampler. *Atmospheric Research* **2011**, *101*, (1-2), 341-353.
50. Gigliotti, C. L.; Totten, L. A.; Offenber, J. H.; Dachs, J.; Reinfelder, J. R.; Nelson, E. D.; Glenn, T. R. t.; Eisenreich, S. J., Atmospheric concentrations and deposition of polycyclic aromatic hydrocarbons to the Mid-Atlantic East Coast region. *Environmental Science & Technology* **2005**, *39*, (15), 5550-9.
51. Del Vento, S.; Dachs, J., Atmospheric occurrence and deposition of polycyclic aromatic hydrocarbons in the northeast tropical and subtropical Atlantic Ocean. *Environmental Science and Technology* **2007**, *41*, (16), 5608-5613.
52. Günindi, M.; Tasdemir, Y., Wet and dry deposition fluxes of polychlorinated biphenyls (PCBs) in an urban area of Turkey. *Water, Air, and Soil Pollution* **2011**, *215*, (1-4), 427-439.
53. Park, J. S.; Wade, T. L.; Sweet, S. T., Atmospheric deposition of PAHs, PCBs, and organochlorine pesticides to Corpus Christi Bay, Texas. *Atmospheric Environment* **2002**, *36*, (10), 1707-1720.
54. Tsapakis, M.; Apostolaki, M.; Eisenreich, S.; Stephanou, E. G., Atmospheric deposition and marine sedimentation fluxes of polycyclic aromatic hydrocarbons in the eastern Mediterranean basin. *Environmental Science and Technology* **2006**, *40*, (16), 4922-4927.

55. Cavalcante, R. M.; Sousa, F. W.; Nascimento, R. F.; Silveira, E. R.; Viana, R. B., Influence of urban activities on polycyclic aromatic hydrocarbons in precipitation: Distribution, sources and depositional flux in a developing metropolis, Fortaleza, Brazil. *Science of the Total Environment* **2012**, *414*, 287-292.
56. Barton, C. A.; Kaiser, M. A.; Russell, M. H., Partitioning and removal of perfluorooctanoate during rain events: the importance of physical-chemical properties. *Journal of Environmental Monitoring* **2007**, *9*, (8), 839-46.
57. Kwok, K. Y.; Taniyasu, S.; Yeung, L. W.; Murphy, M. B.; Lam, P. K.; Horii, Y.; Kannan, K.; Petrick, G.; Sinha, R. K.; Yamashita, N., Flux of perfluorinated chemicals through wet deposition in Japan, the United States, and several other countries. *Environmental Science & Technology* **2010**, *44*, (18), 7043-9.
58. Taniyasu, S.; Yamashita, N.; Moon, H. B.; Kwok, K. Y.; Lam, P. K.; Horii, Y.; Petrick, G.; Kannan, K., Does wet precipitation represent local and regional atmospheric transportation by perfluorinated alkyl substances? *Environment International* **2013**, *55*, 25-32.
59. Jurado, E.; Lohmann, R.; Meijer, S.; Jones, K. C.; Dachs, J., Latitudinal and seasonal capacity of the surface oceans as a reservoir of polychlorinated biphenyls. *Environmental Pollution* **2004**, *128*, (1-2), 149-162.
60. Zhang, L.; Lohmann, R., Cycling of PCBs and HCB in the surface ocean-lower atmosphere of the open pacific. *Environmental Science and Technology* **2010**, *44*, (10), 3832-3838.
61. Gigliotti, C. L.; Brunciak, P. A.; Dachs, J.; Glenn Iv, T. R.; Nelson, E. D.; Totten, L. A.; Eisenreich, S. J., Air-water exchange of polycyclic aromatic hydrocarbons in the New York-New Jersey, USA, Harbor Estuary. *Environmental Toxicology and Chemistry* **2002**, *21*, (2), 235-244.
62. Lohmann, R.; Klanova, J.; Pribylova, P.; Liskova, H.; Yonis, S.; Bollinger, K., PAHs on a west-to-east transect across the tropical Atlantic Ocean. *Environmental Science and Technology* **2013**, *47*, (6), 2570-2578.
63. Nizzetto, L.; Lohmann, R.; Gioia, R.; Jahnke, A.; Temme, C.; Dachs, J.; Herckes, P.; Di Guardo, A.; Jones, K. C., PAHs in air and seawater along a North-South Atlantic transect: Trends, processes and possible sources. *Environmental Science and Technology* **2008**, *42*, (5), 1580-1585.
64. Castro-Jiménez, J.; Berrojalbiz, N.; Wollgast, J.; Dachs, J., Polycyclic aromatic hydrocarbons (PAHs) in the Mediterranean Sea: Atmospheric occurrence, deposition and decoupling with settling fluxes in the water column. *Environmental Pollution* **2012**, *166*, 40-47.
65. Möller, A.; Xie, Z.; Caba, A.; Sturm, R.; Ebinghaus, R., Occurrence and air-seawater exchange of brominated flame retardants and Dechlorane Plus in the North Sea. *Atmospheric Environment* **2012**, *46*, 346-353.
66. Cetin, B.; Odabasi, M., Air-water exchange and dry deposition of polybrominated diphenyl ethers at a coastal site in Izmir Bay, Turkey. *Environmental science & technology* **2007**, *41*, (3), 785-791.
67. Kim, S. K.; Kannan, K., Perfluorinated acids in air, rain, snow, surface runoff, and lakes: relative importance of pathways to contamination of urban lakes. *Environmental Science & Technology* **2007**, *41*, (24), 8328-34.
68. Keyte, I. J.; Harrison, R. M.; Lammel, G., Chemical reactivity and long-range transport potential of polycyclic aromatic hydrocarbons - a review. *Chemical Society Reviews* **2013**, *42*, (24), 9333-9391.
69. Paul, A. G.; Hammen, V. C.; Hickler, T.; Karlson, U. G.; Jones, K. C.; Sweetman, A. J., Potential implications of future climate and land-cover changes for the fate and distribution of persistent organic pollutants in Europe. *Global Ecology and Biogeography* **2012**, *21*, (1), 64-74.
70. Balbus, J. M.; Boxall, A.; Fenske, R. A.; McKone, T. E.; Zeise, L., Implications of global climate change for the assessment and management of human health risks of chemicals in the natural environment. *Environmental Toxicology and Chemistry* **2013**, *32*, (1), 62-78.

71. Guan, Y.-F.; Wang, J.-Z.; Ni, H.-G.; Zeng, E. Y., Organochlorine pesticides and polychlorinated biphenyls in riverine runoff of the Pearl River Delta, China: Assessment of mass loading, input source and environmental fate. *Environmental Pollution* **2009**, *157*, (2), 618-624.
72. Paul, A. G.; Scheringer, M.; Hungerbühler, K.; Loos, R.; Jones, K. C.; Sweetman, A. J., Estimating the aquatic emissions and fate of perfluorooctane sulfonate (PFOS) into the river Rhine. *Journal of Environmental Monitoring* **2012**, *14*, (2), 524-530.
73. Verhaert, V.; Covaci, A.; Bouillon, S.; Abrantes, K.; Musibono, D.; Bervoets, L.; Verheyen, E.; Blust, R., Baseline levels and trophic transfer of persistent organic pollutants in sediments and biota from the Congo River Basin (DR Congo). *Environment international* **2013**, *59*, 290-302.
74. Ahrens, L.; Shoeib, M.; Harner, T.; Lee, S. C.; Guo, R.; Reiner, E. J., Wastewater treatment plant and landfills as sources of polyfluoroalkyl compounds to the atmosphere. *Environmental Science & Technology* **2011**, *45*, (19), 8098-105.
75. Zareitalabad, P.; Siemens, J.; Hamer, M.; Amelung, W., Perfluorooctanoic acid (PFOA) and perfluorooctanesulfonic acid (PFOS) in surface waters, sediments, soils and wastewater - A review on concentrations and distribution coefficients. *Chemosphere* **2013**, *91*, (6), 725-32.
76. Hwang, I.-K.; Kang, H.-H.; Lee, I.-S.; Oh, J.-E., Assessment of characteristic distribution of PCDD/Fs and BFRs in sludge generated at municipal and industrial wastewater treatment plants. *Chemosphere* **2012**, *88*, (7), 888-894.
77. Ahrens, L.; Felizeter, S.; Ebinghaus, R., Spatial distribution of polyfluoroalkyl compounds in seawater of the German Bight. *Chemosphere* **2009**, *76*, (2), 179-84.
78. Ahrens, L.; Gerwinski, W.; Theobald, N.; Ebinghaus, R., Sources of polyfluoroalkyl compounds in the North Sea, Baltic Sea and Norwegian Sea: Evidence from their spatial distribution in surface water. *Marine Pollution Bulletin* **2010**, *60*, (2), 255-60.
79. Jaccard, S. L.; Galbraith, E. D., Large climate-driven changes of oceanic oxygen concentrations during the last deglaciation. *Nature Geosciences* **2012**, *5*, (2), 151-156.
80. Curry, R.; Dickson, B.; Yashayaev, I., A change in the freshwater balance of the Atlantic Ocean over the past four decades. *Nature* **2003**, *426*, (6968), 826-829.
81. Levitus, S.; Conkright, M. E.; Reid, J. L.; Najjar, R. G.; Mantyla, A., Distribution of nitrate, phosphate and silicate in the world oceans. *Progress in Oceanography* **1993**, *31*, (3), 245-273.
82. Stein, C. A.; Stein, S., A model for the global variation in oceanic depth and heat flow with lithospheric age. *Nature* **1992**, *359*, (6391), 123-129.
83. Lohmann, R.; Jurado, E.; Dijkstra, H. A.; Dachs, J., Vertical eddy diffusion as a key mechanism for removing perfluorooctanoic acid (PFOA) from the global surface oceans. *Environ Pollut* **2013**, *179*, 88-94.
84. Yamashita, N.; Taniyasu, S.; Petrick, G.; Wei, S.; Gamo, T.; Lam, P. K.; Kannan, K., Perfluorinated acids as novel chemical tracers of global circulation of ocean waters. *Chemosphere* **2008**, *70*, (7), 1247-55.
85. Lohmann, R.; Jurado, E.; Pilson, M. E. Q.; Dachs, J., Oceanic deep water formation as a sink of persistent organic pollutants. *Geophysical Research Letters* **2006**, *33*, (12).
86. Bramhall, G., Fick's laws and bound-water diffusion. *Wood science* **1976**, *8*, (3), 153-161.
87. Jurado, E.; Zaldívar, J.-M.; Marinov, D.; Dachs, J., Fate of persistent organic pollutants in the water column: Does turbulent mixing matter? *Marine pollution bulletin* **2007**, *54*, (4), 441-451.
88. Fernández-Castro, B.; Mouriño-Carballido, B.; Benítez-Barrios, V. M.; Chouciño, P.; Fraile-Nuez, E.; Graña, R.; Piedeleu, M.; Rodríguez-Santana, A., Microstructure turbulence and diffusivity parameterization in the tropical and subtropical Atlantic, Pacific and Indian Oceans during the Malaspina 2010 expedition. *Deep Sea Research Part I: Oceanographic Research Papers* **2014**, *94*, (0), 15-30.
89. Mouriño-Carballido, B., Eddy-driven pulses of respiration in the Sargasso Sea. *Deep Sea Research Part I: Oceanographic Research Papers* **2009**, *56*, (8), 1242-1250.

90. McGillicuddy Jr, D. J.; Anderson, L. A.; Bates, N. R.; Bibby, T.; Buesseler, K. O.; Carlson, C. A.; Davis, C. S.; Ewart, C.; Falkowski, P. G.; Goldthwait, S. A.; Hansell, D. A.; Jenkins, W. J.; Johnson, R.; Kosnyrev, V. K.; Ledwell, J. R.; Li, Q. P.; Siegel, D. A.; Steinberg, D. K., Eddy/Wind interactions stimulate extraordinary mid-ocean plankton blooms. *Science* **2007**, *316*, (5827), 1021-1026.
91. Riser, S. C.; Johnson, K. S., Net production of oxygen in the subtropical ocean. *Nature* **2008**, *451*, (7176), 323-325.
92. Nizzetto, L.; Gioia, R.; Li, J.; Borgå, K.; Pomati, F.; Bettinetti, R.; Dachs, J.; Jones, K. C., Biological pump control of the fate and distribution of hydrophobic organic pollutants in water and plankton. *Environmental science & technology* **2012**, *46*, (6), 3204-3211.
93. Hoepffner, N.; Dowell, M.; Schrimpf, W., Status and requirements for climate change research in European regional seas. *Climate Change Impacts on the Water Cycle, Resources and Quality* **2006**, *25*, 64.
94. Berrojalbiz, N.; Dachs, J.; Ojeda, M. J.; Valle, M. C.; Castro-Jiménez, J.; Wollgast, J.; Ghiani, M.; Hanke, G.; Zaldivar, J. M., Biogeochemical and physical controls on concentrations of polycyclic aromatic hydrocarbons in water and plankton of the Mediterranean and Black Seas. *Global Biogeochemical Cycles* **2011**, *25*, (4).
95. Galbán-Malagón, C. J.; Berrojalbiz, N.; Gioia, R.; Dachs, J., The "degradative" and "biological" pumps controls on the atmospheric deposition and sequestration of hexachlorocyclohexanes and hexachlorobenzene in the North Atlantic and Arctic Oceans. *Environmental Science and Technology* **2013**, *47*, (13), 7195-7203.
96. Harvey, R. G., *Polycyclic aromatic hydrocarbons: chemistry and carcinogenicity*. CUP Archive: 1991.
97. Harner, T.; Bidleman, T. F., Octanol-air partition coefficient for describing particle/gas partitioning of aromatic compounds in urban air. *Environmental Science & Technology* **1998**, *32*, (10), 1494-1502.
98. Gonzalez-Gaya, B.; Zuniga-Rival, J.; Ojeda, M. J.; Jimenez, B.; Dachs, J., Field measurements of the atmospheric dry deposition fluxes and velocities of polycyclic aromatic hydrocarbons to the global oceans. *Environmental Science & Technology* **2014**, *48*, (10), 5583-92.
99. Ma, Y.; Xie, Z.; Yang, H.; Möller, A.; Halsall, C.; Cai, M.; Sturm, R.; Ebinghaus, R., Deposition of polycyclic aromatic hydrocarbons in the North Pacific and the Arctic. *Journal of Geophysical Research: Atmospheres* **2013**, *118*, (11), 5822-5829.
100. Cabrerizo, A.; Galbán-Malagón, C.; Del Vento, S.; Dachs, J., Sources and fate of polycyclic aromatic hydrocarbons in the Antarctic and Southern Ocean atmosphere. *Global Biogeochemical Cycles* **2014**, *28*, (12), 1424-1436.
101. Lohmann, R.; Gioia, R.; Jones, K. C.; Nizzetto, L.; Temme, C.; Xie, Z.; Schulz-Bull, D.; Hand, I.; Morgan, E.; Jantunen, L., Organochlorine pesticides and PAHs in the surface water and atmosphere of the North Atlantic and Arctic Ocean. *Environmental science & technology* **2009**, *43*, (15), 5633-5639.
102. Blumer, M., Polycyclic aromatic compounds in nature. *Scientific American* **1976**, (234), 35-45.
103. Cabrerizo, A.; Dachs, J.; Moeckel, C.; Ojeda, M. J.; Caballero, G.; Barcelo, D.; Jones, K. C., Ubiquitous net volatilization of polycyclic aromatic hydrocarbons from soils and parameters influencing their soil-air partitioning. *Environmental Science & Technology* **2011**, *45*, (11), 4740-7.
104. Zhang, Y.; Tao, S., Global atmospheric emission inventory of polycyclic aromatic hydrocarbons (PAHs) for 2004. *Atmospheric Environment* **2009**, *43*, (4), 812-819.
105. Hylland, K., Polycyclic aromatic hydrocarbon (PAH) ecotoxicology in marine ecosystems. *Journal of Toxicology and Environmental Health A* **2006**, *69*, (1-2), 109-23.
106. Land, M.; de Wit, C. A.; Cousins, I. T.; Herzke, D.; Johansson, J.; Martin, J. W., What is the effect of phasing out long-chain per-and polyfluoroalkyl substances on the concentrations

- of perfluoroalkyl acids and their precursors in the environment? A systematic review protocol. *A systematic review protocol. Environmental Evidence* **2015**, *4*, 3.
107. Taves, D. R., Evidence that there are Two Forms of Fluoride in Human Serum. *Nature* **1968**, *217*, (5133), 1050-1051.
108. Barber, J. L.; Berger, U.; Chaemfa, C.; Huber, S.; Jahnke, A.; Temme, C.; Jones, K. C., Analysis of per- and polyfluorinated alkyl substances in air samples from Northwest Europe. *Journal of Environmental Monitoring* **2007**, *9*, (6), 530-541.
109. Jahnke, A.; Berger, U.; Ebinghaus, R.; Temme, C., Latitudinal gradient of airborne polyfluorinated alkyl substances in the marine atmosphere between Germany and South Africa (53 degrees N-33 degrees S). *Environmental Science & Technology* **2007**, *41*, (9), 3055-61.
110. Houde, M.; De Silva, A. O.; Muir, D. C.; Letcher, R. J., Monitoring of perfluorinated compounds in aquatic biota: an updated review. *Environmental Science & Technology* **2011**, *45*, (19), 7962-73.
111. González-Gaya, B.; Dachs, J.; Roscales, J. L.; Caballero, G.; Jiménez, B., Perfluoroalkylated Substances In The Global Tropical And Subtropical Surface Oceans. *Environmental Science & Technology* **2014**, *48*, (22), 13076-13084.
112. Zhao, Z.; Xie, Z.; Moller, A.; Sturm, R.; Tang, J.; Zhang, G.; Ebinghaus, R., Distribution and long-range transport of polyfluoroalkyl substances in the Arctic, Atlantic Ocean and Antarctic coast. *Environmental Pollution* **2012**, *170*, 71-7.
113. Carloni, D. *OECD Report Perfluorooctane Sulfonate (PFOS) Production and Use: Past and Current Evidence*; Report for UNIDO: 2009.
114. Buck, R. C.; Franklin, J.; Berger, U.; Conder, J. M.; Cousins, I. T.; de Voogt, P.; Jensen, A. A.; Kannan, K.; Mabury, S. A.; van Leeuwen, S. P., Perfluoroalkyl and polyfluoroalkyl substances in the environment: terminology, classification, and origins. *Integrated environmental assessment and management* **2011**, *7*, (4), 513-41.
115. *OECD Results of survey on Production and use of PFOS, PFAS and PFOA, related substances and products/mixtures containing these substances*; ORGANISATION FOR ECONOMIC CO-OPERATION AND DEVELOPMENT: Paris 2004, 2005.
116. Ahrens, L.; Yeung, L. W.; Taniyasu, S.; Lam, P. K.; Yamashita, N., Partitioning of perfluorooctanoate (PFOA), perfluorooctane sulfonate (PFOS) and perfluorooctane sulfonamide (PFOSA) between water and sediment. *Chemosphere* **2011**, *85*, (5), 731-7.
117. Armitage, J. M.; Schenker, U.; Scheringer, M.; Martin, J. W.; Macleod, M.; Cousins, I. T., Modeling the global fate and transport of perfluorooctane sulfonate (PFOS) and precursor compounds in relation to temporal trends in wildlife exposure. *Environmental science & technology* **2009**, *43*, (24), 9274-80.
118. Busch, J.; Ahrens, L.; Xie, Z.; Sturm, R.; Ebinghaus, R., Polyfluoroalkyl compounds in the East Greenland Arctic Ocean. *Journal of Environmental Monitoring* **2010**, *12*, (6), 1242-6.
119. Butt, C. M.; Berger, U.; Bossi, R.; Tomy, G. T., Levels and trends of poly- and perfluorinated compounds in the arctic environment. *Science of the Total Environment* **2010**, *408*, (15), 2936-65.
120. Benskin, J. P.; Ahrens, L.; Muir, D. C.; Scott, B. F.; Spencer, C.; Rosenberg, B.; Tomy, G.; Kylin, H.; Lohmann, R.; Martin, J. W., Manufacturing origin of perfluorooctanoate (PFOA) in Atlantic and Canadian Arctic seawater. *Environmental Science & Technology* **2012**, *46*, (2), 677-85.
121. Ellis, D. A.; Martin, J. W.; De Silva, A. O.; Mabury, S. A.; Hurley, M. D.; Sulbaek Andersen, M. P.; Wallington, T. J., Degradation of fluorotelomer alcohols: a likely atmospheric source of perfluorinated carboxylic acids. *Environ Sci Technol* **2004**, *38*, (12), 3316-21.
122. Taniyasu, S.; Kannan, K.; So, M. K.; Gulkowska, A.; Sinclair, E.; Okazawa, T.; Yamashita, N., Analysis of fluorotelomer alcohols, fluorotelomer acids, and short- and long-chain perfluorinated acids in water and biota. *Journal of chromatography. A* **2005**, *1093*, (1-2), 89-97.
123. Ng, C. A.; Hungerbühler, K., Bioaccumulation of Perfluorinated Alkyl Acids: Observations and Models. *Environmental Science & Technology* **2014**, *48*, (9), 4637-4648.

General Introduction

124. Ahrens, L.; Barber, J. L.; Xie, Z.; Ebinghaus, R., Longitudinal and latitudinal distribution of perfluoroalkyl compounds in the surface water of the Atlantic Ocean. *Environmental Science & Technology* **2009**, *43*, (9), 3122-7.
125. Cai, M.; Zhao, Z.; Yin, Z.; Ahrens, L.; Huang, P.; Cai, M.; Yang, H.; He, J.; Sturm, R.; Ebinghaus, R.; Xie, Z., Occurrence of perfluoroalkyl compounds in surface waters from the North Pacific to the Arctic Ocean. *Environmental Science & Technology* **2012**, *46*, (2), 661-8.
126. Wei, S.; Chen, L. Q.; Taniyasu, S.; So, M. K.; Murphy, M. B.; Yamashita, N.; Yeung, L. W.; Lam, P. K., Distribution of perfluorinated compounds in surface seawaters between Asia and Antarctica. *Marine Pollution Bulletin* **2007**, *54*, (11), 1813-8.
127. Kelly, B. C.; Ikonomou, M. G.; Blair, J. D.; SurrIDGE, B.; Hoover, D.; Grace, R.; Gobas, F. A. P. C., Perfluoroalkyl contaminants in an arctic marine food web: Trophic magnification and wildlife exposure. *Environmental Science and Technology* **2009**, *43*, (11), 4037-4043.
128. Loi, E. I.; Yeung, L. W.; Taniyasu, S.; Lam, P. K.; Kannan, K.; Yamashita, N., Trophic magnification of poly- and perfluorinated compounds in a subtropical food web. *Environmental Science & Technology* **2011**, *45*, (13), 5506-13.

Chapter 2

Chapter 2

Results

Results

1. Field Measurements of the Atmospheric Dry Deposition Fluxes and Velocities of Polycyclic Aromatic Hydrocarbons to the Global Oceans

**Belén González-Gaya^{1,2}, Javier Zúñiga-Rival¹, María José Ojeda¹, Begoña Jiménez²,
and Jordi Dachs^{1*}**

¹ Department of Environmental Chemistry, Institute of Environmental Assessment and Water Research, IDAEA-CSIC; Barcelona, Catalunya, Spain.

² Department of Instrumental Analysis and Environmental Chemistry, Institute of Organic Chemistry, IQOG-CSIC; Madrid, Spain.

Corresponding Author email: jordi.dachs@idaea.csic.es

Environ. Sci. Technol., 2014, 48 (10), pp 5583–5592

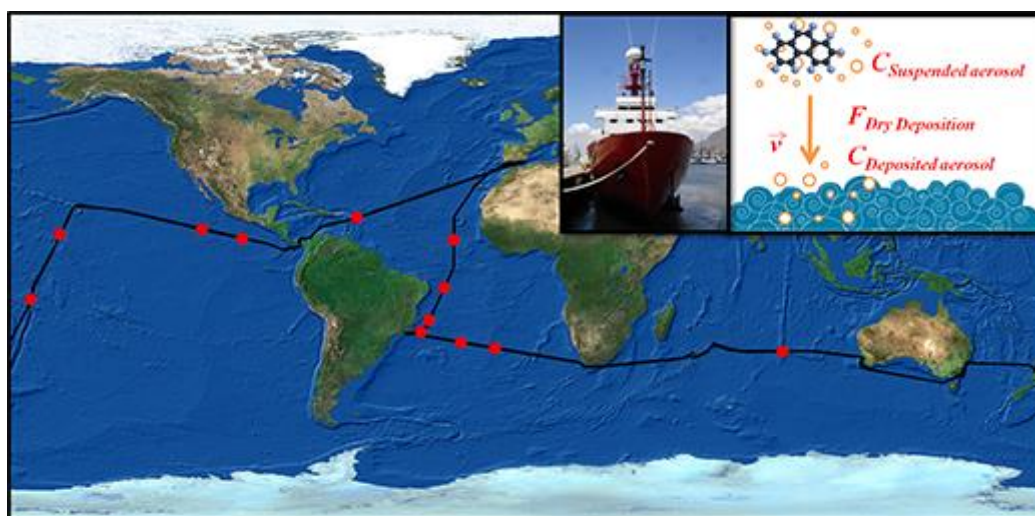
DOI: 10.1021/es500846p

Publication Date (Web): April 11, 2014

Copyright © 2014 American Chemical Society

ABSTRACT

The atmospheric dry deposition fluxes of 16 polycyclic aromatic hydrocarbons (PAHs) have been measured, for the first time, in the tropical and subtropical Atlantic, Pacific and Indian Oceans. Depositional fluxes for fine (0.7-2.7 μm) and coarse ($>2.7 \mu\text{m}$) aerosol fractions were simultaneously determined with the suspended aerosol phase concentrations, allowing the determination of PAH deposition velocities (v_D). PAHs dry deposition fluxes (F_{DD}) bound to coarse aerosols were higher than those of fine aerosols for 83% of the measurements. Average F_{DD} for total (fine + coarse) $\Sigma_{16}\text{PAHs}$ (sum of 16 individual PAHs) ranged from 8.33 $\text{ng m}^{-2}\text{d}^{-1}$ and 52.38 $\text{ng m}^{-2}\text{d}^{-1}$. Mean F_{DD} for coarse aerosol's individual PAHs ranged between 0.13 $\text{ng m}^{-2}\text{d}^{-1}$ (Perylene) and 1.96 $\text{ng m}^{-2}\text{d}^{-1}$ (Methyl Pyrene), and for the fine aerosol fraction these ranged between 0.06 $\text{ng m}^{-2}\text{d}^{-1}$ (Dimethyl Pyrene) and 1.25 $\text{ng m}^{-2}\text{d}^{-1}$ (Methyl Chrysene). The estimated deposition velocities went from the highest mean v_D for Methyl Chrysene (0.17-13.30 cm s^{-1}), followed by Dibenzo(ah)Anthracene (0.29-1.38 cm s^{-1}), and other high MW PAHs to minimum values of v_D for Dimethyl Pyrene (<0.00 -0.04 cm s^{-1}) and Pyrene (<0.00 -0.06 cm s^{-1}). Dry depositional processes depend on the concentration of PAHs in the suspended aerosol, but also on physicochemical properties and environmental variables (vapor pressure, wind speed and on the affinity of aerosols for depositing to the sea surface). Empirical parameterizations are proposed to predict the dry depositional velocities of semivolatile organic compounds in the global oceans.



Graphical Abstract 1.

INTRODUCTION

Atmospheric deposition is the main vector for the entrance of semivolatile organic compounds to the Global Oceans¹⁻⁴. The gas-particle partitioning of the chemical determines which of the different depositional processes dominates the overall atmospheric deposition⁵. Some persistent organic pollutants (POPs), such as polychlorinated biphenyls (PCBs) or hexachlorocyclohexanes, are mainly, but not only,^{6,7} found in the gas-phase, and therefore diffusive air-water exchange estimates support the idea that this is the main process driving their deposition to the surface ocean⁷⁻⁹. On the contrary, many polycyclic aromatic hydrocarbons (PAHs) and polychlorinated dibenzo-p-dioxins and furans (PCDD/Fs) are mainly found in the aerosol phase due to their low vapor pressure and strong sorption to aerosols¹⁰⁻¹³. Therefore, high MW PAHs, with more than four aromatic rings, and PCDD/Fs are mainly removed from the atmosphere by dry deposition^{1,11,12,14,15}. Similarly, dry deposition of aerosol bound POPs will be the dominant depositional process for other chemicals with analogous properties, such as organophosphorus flame retardants and plasticizers¹⁶, polybrominated diphenyl ethers and other brominated flame retardants^{17,18}, and dechlorane plus¹⁹⁻²¹. Wet deposition by rain and snow is another depositional process which is very efficient removing gas- and aerosol-phase organic compounds from the atmosphere, but its importance is limited to some specific oceanic regions and time periods².

To the best of our knowledge, there has been only one previous effort to measure the dry deposition fluxes (F_{DD} , $\text{ng m}^{-2}\text{d}^{-1}$) of semi-volatile organic compounds in the open ocean²², and very few at coastal sites²³⁻²⁷. Hence, the magnitude of F_{DD} is usually estimated from the measured aerosol phase concentrations (C_A , ng m^{-3}) by,

$$F_{DD} = 864v_D C_A \quad [1.1]$$

Where v_D (cm s^{-1}) is the deposition velocity of the specific aerosol-bound chemical, and 864 is a unit conversion factor. v_D is a function of wind speed, the size distribution of aerosols, atmospheric stability and relative humidity among other factors. In the case of the marine environment, the occurrence of a surface microlayer with reduced surface tension and higher hydrophobicity due to organic compounds and lipids

floating at surface also increases the values of v_D ²³. A number of early theoretical studies addressed the parameterization of v_D ^{28,29}, which have been used in many studies focusing on the deposition of semi-volatile organic compounds^{1,30,31}.

Field estimates of v_D can be obtained from the simultaneous determination of F_{DD} and C_A using equation [1.1]. There are few measures of v_D ^{22,32-36} with v_D ranging from 0.1 to 0.8 cm s⁻¹ in coastal or terrestrial areas. Higher values of v_D have been observed in urban/industrial areas due to the presence of large aerosols, with faster depositional velocities due to gravitational processes (sedimentation (settling by gravity) or impaction processes³⁷), coming from anthropogenic sources³³. However, there is only one study that experimentally studied v_D for the open marine environment, and it was carried out in the subtropical NE Atlantic²², with v_D ranging from 0.08 to 0.3 cm s⁻¹. These estimations have been used in the literature to estimate the dry deposition fluxes of PAHs and other POPs in various oceanic regions^{13,14,16-18,21}. Because of the scarcity of previous measures of dry deposition fluxes and v_D values for semivolatile organic compounds, there is a need for further field measurements in order to understand the factors affecting v_D over the ocean and to obtain a more precise range of v_D values in this environment.

PAHs are ubiquitous in the environment and have been included in the Convention on Long Range Transboundary Air Pollution Protocol on Persistent Organic Pollutants³⁸. Moreover, due to their chemical characteristics, PAHs are susceptible of partitioning between gas and particle phases in the atmosphere, their concentrations are higher than for other organic pollutants in the oceanic atmosphere, and can be used as surrogates of the depositional processes affecting aerosol-bound organic compounds. The objectives of this work are: i) to report a coherent dataset of field measurements of dry deposition fluxes of PAHs for the global oceans, ii) to estimate the v_D values for individual PAH compounds from the simultaneous determination of F_{DD} and C_A , iii) to assess the factors, such as the chemical vapor pressure, wind speed and aerosol size, influencing v_D values.

MATERIALS AND METHODS

Sampling strategy

Samples were collected during the *Malaspina 2010* cruise performed from December 14th, 2010 to July 14th, 2011 on board of RV Hespérides. The cruise completed a circumnavigation covering all the tropical and temperate oceans between 35°N and 40°S in seven consecutive transects: Cadiz (Spain) - Rio de Janeiro (Brazil) – Cape Town (South Africa) – Perth (Australia) – Sydney (Australia) – Auckland (New Zealand) – Honolulu (Hawaii, USA) – Cartagena de Indias (Colombia) – Cartagena (Spain) (Figure 1.1).

A total of 12 field experiments measuring the dry deposition fluxes of PAHs were carried out during the circumnavigation cruise (see Figure 1.1 and table S1.1 for positions and ancillary data) using the sampling methodology described elsewhere^{22,23}. Briefly, F_{DD} measures were obtained by exposing to the atmosphere stainless-steel trays (0.4m x 0.3 m x 0.1 m) filled with three liters of surface seawater collected at 4 m depth from the continuous pumping system of the ship. Seawater was previously pre-filtered with a GF/F filter (0.7 μm pore size, Whatman) and a sterile cellulose nitrate filter (0.2 μm pore size, Whatman) in order to remove marine particles (bacteria, phytoplankton, detritus, aerosols, etc.). The trays were previously cleaned with acetone and seawater. The dry deposition samplers were deployed on the upper deck, over the bridge of the ship, for a time period of 3-4 days, after which the final volume of water was measured and filtered consecutively over a pre combusted 2.7 μm pore size GF/D filter (Whatman) for the aerosol coarse size fraction, and over a 0.7 μm pore size GF/F filter (Whatman) for the fine size fraction. Filters were kept folded in aluminum foil and zip bags at -20°C during the cruise until their analysis in the laboratory.

Samples of suspended aerosol ($n = 29$) were taken using a high volume air sampler placed on the upper deck, over the bridge, in the top front part of the boat to minimize contamination from the ship exhaust. Furthermore, a wind vane was connected to the

Results 1

electric power system in order to allow sampling only when the wind was coming from the bow to avoid any perturbation of the sample by the ship emissions. The air sampling flux was set at $40 \text{ m}^3 \text{ hour}^{-1}$ and the volumes sampled ranged between 525 and 1982 m^3 of air per filter (Table S1.2). The suspended aerosols were collected on pre-combusted (450°C for 24 hours) quartz microfiber filters (QM/A, Whatman), which after sampling were kept folded in aluminum foil and zip bags at -20°C during the cruise until their analysis in the laboratory. The 29 air samples were taken simultaneously to the dry deposition measurements and in order to determine v_D values, the concentrations were weighted to the air volume sampled in order to obtain a mean value of suspended aerosol phase PAH concentration in the atmosphere per each measure of the dry deposition flux.

Sample extraction and instrumental analysis

All atmospheric samples for suspended aerosols and deposited coarse and fine particles were freeze-dried overnight, weighted and Soxhlet extracted with dichloromethane: methanol (DCM: MeOH) (2:1, v/v) for 24 hours. 25 ng of recovery standard (Semivolatile Internal Standard Mix©, Dr. Ehrenstorfer by Supelco), containing Chrysene- d_{12} and Perylene- d_{12} were added to each sample to estimate losses during the extraction and fractionation processes. After a solvent exchange to hexane (Hx), the extract was fractionated on 3 g of 3% chromatography grade quality water deactivated alumina on a chromatography column with a top layer of anhydrous sodium sulfate. A first fraction of 5 mL Hx was eluted (containing the more apolar compounds not analyzed here) and then a 12 mL DCM:Hx (2:1) fraction which contained the target PAHs. The second fraction was concentrated and solvent exchanged to isooctane in a rotavapor system and further concentrated under a gentle stream of nitrogen.

The instrumental analysis of PAHs was performed through an Agilent 6890 Series gas chromatographer coupled with a mass spectrometer Agilent 5973 (GS-MS) operating in selected ion monitoring (SIM) and electron impact mode (EI). The GC system used an Agilent DB-5MS column (30 m, 0.25 mm internal diameter, 0.25 μm film thickness).

2 μL of sample were injected in split less mode. The initial GC oven temperature was set at 90°C. It was risen up to 175°C at a rate of 6°C per minute and hold for 4 minutes. Then the temperature increasing rate slowed to 3°C per minute until 235°C. After, the heating rate was switched to 8°C per minute and hold for 8 minutes. At last, with the same rate, the temperature reached 315°C during 4 minutes. The quantification followed the internal standard procedure, using a mix of Pyrene-d₁₀ and Benzo-b-Fluoranthrene-d₁₂ (Dr. Ehrenstorfer, Supelco) added to the samples prior to injection.

Since dry deposition may not be the dominating depositional process for the low MW PAHs, and in order to avoid sampling artifacts of the lighter compounds due to gas diffusive exchange²², only PAHs with four or more aromatic rings were considered in this study. The target compounds were; Fluoranthrene (Flu), Pyrene (Pyr) , Methylpyrene (MePyr, as the sum of 5 isomers), Dimethylpyrene (DMePyr, as the sum of 8 isomers), Benzo(ghi)Fluoranthrene (B(ghi)Fluo), Benzo(a)Anthracene (B(a)Anthr), Chrysene (Chry), Methylchrysene (MeChry, as the sum of 2 isomers), Benzo(b)Fluoranthrene, Benzo(k)Fluoranthrene (both isomers are given together, B(b+k)Fluo), Benzo(e)Pyrene (B(e)Pyr), Benzo(a)Pyrene (B(a)Pyr), Perylene (Per), Indeno(1,2,3-cd)Pyrene (I(cd)Pyr), Dibenzo(a,h)Anthracene (DB(ah)Anthr) and Benzo(ghi)Perylene (B(ghi)Per). More information on their identification ions, retention times and MS method is given in the supplementary info (Table S1.3).

Organic Carbon (OC) was quantified in the settled particles during the dry deposition measurements. Filters were first lyophilized and a weighted portion of each of them was homogenized and acidified with hydrochloric acid at 7% to remove the carbonaceous inorganic fraction. Then it was vortexed repeatedly and pH adjusted with chromatography quality water. After a last lyophilization for 24 hours, OC was measured using a Pregl-Dumas (dynamic flash combustion) modified method, using helium as carrier gas, in an Elemental Microanalyzer (A7) model Flash 2000³⁹.

Quality assurance and control

The quality of the dry deposition measurements was assessed with 2 field blanks and 3 laboratory blanks. In the same manner, the extraction method for the suspended aerosols was assessed through 9 laboratory blanks and 6 field blanks. Field blanks were obtained from GF/F and GF/D filters placed in the filtration system during the sampling campaign (for settled aerosol) and clean QM/A filters placed in the high volume sampler for a minute (in the case of suspended aerosol), and processed in the laboratory together with the real samples. The laboratory blanks were extracted simultaneously to the processed aerosol filters to evaluate any contamination during sample treatment in the laboratory. The detection limit (DL) was set as the inferior limit of the calibration curve (0.02 ng for all compounds). Quantification limit (QL) corresponds to mean blank level of the sample class evaluated. The levels for all native PAHs in the blanks were under the measured levels for 100% of the samples of suspended and coarse deposited aerosols, and for 99.4% of fine fraction deposited aerosol samples (as a mean percentage of all individual compounds). Concentrations in aerosols samples were not subtracted for the concentration in the blanks. Mean surrogate recoveries in dry deposition samples were 78% for Chrysene-d₁₂ and 114% for Perylene-d₁₂. Recoveries of the Suspended Aerosol samples ranged between 92% for Chrysene-d₁₂ and 101% for Perylene-d₁₂. PAHs concentrations were corrected by the recoveries of Chrysene-d₁₂. Complete information on blank levels, DL and QL and recoveries is given through the tables of Annex 2.

Statistical analysis

Statistical analysis was performed using SPSS Statistics® version 21.0 (IBM Corp.©). Kolmogorov-Smirnov test were run to assure normality of the data, which was not encountered ($p < 0.05$). Non-Parametric statistics were thus applied for the comparisons and correlations within the data.

Back Trajectories

Back Trajectories were calculated using the NOAA Hysplit model online at 3 heights (30, 200 and 500 meters) using GDAS Meteorological data from the sampled period (Figure S1.1). In addition, back trajectories were also estimated for the upper boundary layer and above (800 and 2000 masl, Figure S1.2).

RESULTS AND DISCUSSION

Dry Deposition Fluxes of PAHs

Dry deposition fluxes ($\text{ng m}^{-2}\text{d}^{-1}$) were calculated from the measured mass of PAHs in the deposited aerosols and the time of exposure of the deposition samplers for each measurement per exposed area of the sampler. Figure 1.1b and figure 1.1c show the spatial variability of F_{DD} for the coarse (bigger than $2.7 \mu\text{m}$) and the fine (between 0.7 and $2.7 \mu\text{m}$) fraction of deposited aerosols, respectively, and compound and sample specific values are given in Table S1.8.

Overall, PAHs dry deposition was higher for the coarse than fine aerosols in the open ocean by a mean factor of 4. Only in two measurements in south and equatorial Pacific Ocean, the deposition fluxes of the fine fraction of aerosol-bound PAHs were higher than for larger aerosols. Average F_{DD} for total (fine + coarse) Σ_{16} PAHs ranged from $8.33 \text{ ng m}^{-2}\text{d}^{-1}$ to $52.38 \text{ ng m}^{-2}\text{d}^{-1}$. Mean F_{DD} for coarse aerosol's individual PAHs ranged between $0.13 \text{ ng m}^{-2} \text{ d}^{-1}$ (Per) and $1.96 \text{ ng m}^{-2} \text{ d}^{-1}$ (MePyr), while for the fine fraction, F_{DD} ranged between $0.06 \text{ ng m}^{-2} \text{ d}^{-1}$ (DMePyr) and $1.25 \text{ ng m}^{-2} \text{ d}^{-1}$ (MeChry) (Figure S1.3). Higher F_{DD} were observed in the southern tropical Atlantic which is associated to higher aerosol-phase PAH concentrations, presumably influenced by emissions from off-Africa and off-South America as indicated by the back trajectories. In addition, there is a relevant increase in the PAHs depositional fluxes in the fine fraction's PAHs in the central North Pacific sample due to a possible influence of the Hawaiian archipelago adjacent to the sampling area and an influence of air masses from East Asia in the upper boundary layer.

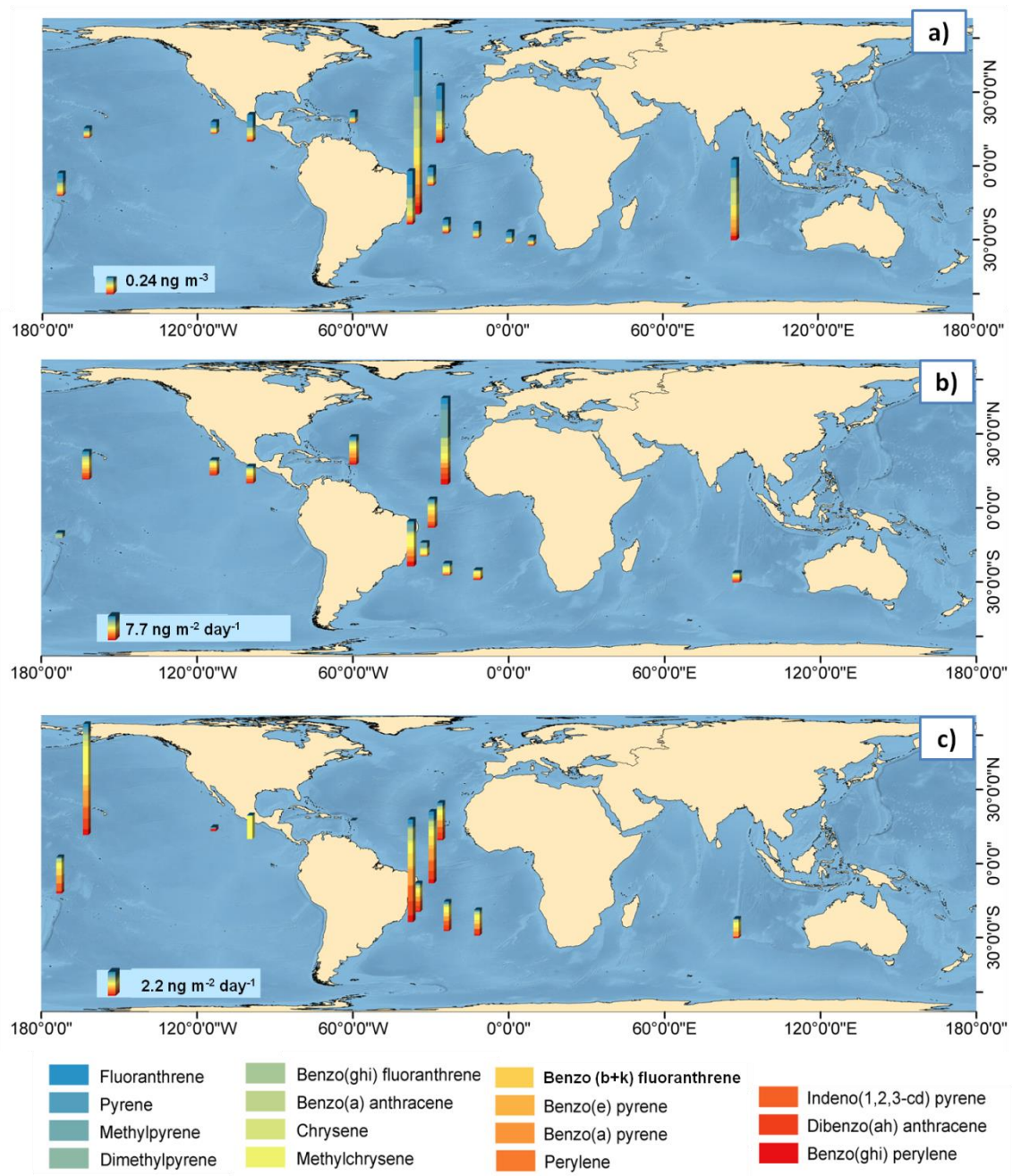


Figure 1.1. Maps of (a) PAHs concentration in suspended aerosols (ng m^{-3}), (b) dry deposition flux of PAHs measured for the coarse fraction of aerosols ($\text{ng m}^{-2} \text{ d}^{-1}$), and (c) dry deposition flux of PAHs measured for the fine fraction of aerosols ($\text{ng m}^{-2} \text{ d}^{-1}$).

Table 1.1 shows the comparison of the measured F_{DD} with those reported in the literature for marine sites (essentially coastal). The deposition fluxes reported here are significantly lower (factor of 2-8) than those reported for the NE Atlantic Ocean²², a region affected by high concentrations of PAHs and other POPs from west Africa⁴⁰ as well as those reported in coastal sites with predominantly maritime air masses affecting the depositional processes⁴¹. Unexpectedly, similar values have been reported in a terrestrial location in Toronto³⁶ and in the Corpus Christy Bay (FL, USA)⁴². The measured F_{DD} in the open ocean are more than an order of magnitude lower than those reported for the coastal NE Mediterranean sea²³, and other coastal sites^{25,43-47} (Table 1.1).

F_{DD} for aerosols (particles) ranged between 0.15 and 0.86 g m⁻²d⁻¹ in the fine fraction, and 0.28 and 1.25 g m⁻²d⁻¹ for the coarse particles (Figure S1.4). The depositional fluxes of individual PAHs were not correlated with the dry deposition of aerosols, which may indicate that dry deposition of PAHs is not determined by the amount of deposited matter, but by the origin and concentrations of the deposited aerosols, and presumably by the amount of carbonaceous aerosols due to the strong affinity of PAHs to organic matter and specially aerosol soot carbon¹⁰. Soot carbon could not be determined in the deposited aerosols, but OC concentrations ranged from <0.23% to 3.34% of the particle mass (Table S1.9). Nevertheless there is not a statistically significant correlation of PAH concentrations in settled aerosols with OC concentrations. PAHs with more than five rings are likely to be adsorbed to aerosol soot carbon. PAHs with 4 rings also show a strong association with soot carbon, but because they concentrations are higher in the gas phase²¹, they could dynamically partition to marine primary and secondary organic aerosols.

Table 1.1. Comparison of the dry deposition fluxes ($ng\ m^{-2}\ d^{-1}$) measured in this work with those reported for marine and coastal sites.

Sampling site	Sampling environment	Sampling period	Fluo	Pyr	B (a) Anthr	Chry	B (b) Fluo	B (k) Fluo	B (e) Pyr	B (a) Pyr	Per	I (123-cd) Pyr	DB(ah) Anthr	B (ghi) Per	total	Reference
<i>(ng m⁻² day⁻¹)</i>																
Miami, Florida, USA	coastal and mangrove area	Jun 1994 – Mar 1995	-	-	-	-	-	-	-	-	-	-	-	-	800,00	Lang et al 2002
Corpus Christi Bay, Texas, USA	industrialized bay and harbor	Ago 1998 - Sep 1999	0,014 (+Pyr)	-	0,01	0,04	0,05	0,03	0,03	0,03	0,02	0,04	0,01	0,04	0,13-2,95	Park et al 2002
Tampa, Florida, USA	coastal near urban area	May - Aug 2002	1870,00	650,00	10,00	60,00	30,00	10,00	-	10,00		10,00	10,00	20,00	11500,00	Poor et al 2004*
Finokalia, Creta Island Greece	coastal area	Sep 2001 - Jul 2002	6,60	3,30	4,00	9,50	5,10	2,90	2,90	1,80	1,50	0,70	0,40	0,70	58,00	Tsapakis et al 2006
Bursa, Turkey	industrial coastal city	Aug 2004 - May 2005	400,00	225,00	100,00	280,00	100,00	90,00	-	70,00	-	70,00	20,00	125,00	1480,00	Tasdemir&Esen 2007
NW Atlantic Ocean	open ocean	May - Jun 2003	5,75	8,24	2,44	4,31	12,31 (+B(k)Fluo)	-	6,63	3,84	0,00	5,90	0,00	8,94	58,55	Del Vento et al 2007a
NW Mediterranean	urban coastal area	Jul 2002 - Dec 2003	-	-	-	-	-	-	-	-	-	-	-	-	60-230	Del Vento et al 2007b
Guangzhou, Pearl River Delta, China	urban coastal area	Apr 2001- Mar 2002	215,49	152,32	39,63	143,32	93,15	69,52	-	37,99	-	82,65	-	104,51	938,57	Li et al 2009
Bursa, Turkey	suburban	Aug 2004 - May 2005	90,00	65,00	25,00	55,00	25,00	18,00	-	7,00	-	9,00	4,00	20,00	318,00	Esen et al 2010
Izmir, Turkey	suburban	May 2003 - May 2004	615,00	815,00	132,00	237,00	441,00	170,00	-	154,00	-	313,00	393,00	242,00	8160,00	Demircioglu et al 2011
Izmir, Turkey	urban	May 2003 - May 2004	732,00	428,00	78,00	350,00	162,00	94,00	-	66,00	-	90,00	34,00	113,00	4286,00	Demircioglu et al 2011
Bursa, Turkey	industrial coastal city	Sep 2008 - Jun 2009	1600,00	1100,00	100,00	300,00	100,00	100,00	-	<100	-	<100	<100	<100	3300,00	Birgul et al 2011
Toronto, Ontario, Canada	urban terrestrial area	Jun 2012 - Jan 2013	7,58	7,37	1,82	4,58	8,32	3,34	-	4,57	1,09	6,27	1,01	5,41	51,35	Eng et al 2014
Global ocean	open tropical ocean	Dec 2010 - Jun 2011	0,84	0,71	1,13	0,89	1,6067 (+B(k)Fluo)	-	0,52	2,04	0,17	1,55	1,36	1,00	16,93	This study

*Flux of gaseous phase is included in this study.

Concentrations of PAH in deposited and suspended aerosols

F_{DD} values depend on several factors, but primary on the chemical concentrations in the aerosol phase, and it is necessary to assess both suspended and deposited aerosol as different PAHs distributional patterns may occur (Figure 1.2). PAH concentrations were higher in the coarse than in the fine deposited aerosols. Concentrations (C_{DD}) of Σ_{16} PAHs in coarse particles ranged from 35.26 ng g⁻¹ to 1129.74 ng g⁻¹, while for fine aerosol these ranged between 14.23 ng g⁻¹ and 264.25 ng g⁻¹ Σ_{16} PAHs (Table S1.10 and Figure S1.5). The highest concentrations of all individual compounds were found in the Atlantic Ocean for the coarse fraction, in particular west of the Canary Islands, influenced by Saharan winds and air masses for which there are previous reports of high PAHs levels^{21,48}, followed by the Pacific and Indian Oceans consecutively. However, due to the large variability within oceanic basins, there are no statistically significant differences between the concentrations of individual compounds, nor for Σ_{16} PAHs, between the Atlantic, Indian and Pacific oceans. In the fine fraction, with less variability between basins, the higher PAHs levels were found in the Pacific Ocean followed by Atlantic and then Indian oceans, with no significant differences between oceans neither (Figures 1.1 and 1.2).

Figure 1.2 shows the PAHs congeners' profiles for the deposited coarse and fine fractions in the three oceanic basins (middle and inferior panels). In general, there is a higher abundance of the high MW PAHs than in suspended aerosols consistently for the Atlantic, Pacific and Indian oceans. This is probably due to the high affinity of soot aerosols to the marine surface microlayer, which is rich in hydrophobic organic compounds. Nevertheless, this different concentration of individual PAHs in fine and coarse aerosols according to molecular weight is less severe in large sized aerosols, due to the affinity of lower MW PAHs to the coarser fraction of particles^{24,25}. In addition, methylated PAHs are found predominantly in the coarse fraction for the Atlantic Ocean (51.15 ng g⁻¹ MePyr and 29.07 ng g⁻¹ MeChry), while in the fine fraction, B(a)Pyr, DB(ah)Ant, I(cd)Pyr and B(b+k)Flu register the highest concentrations (14.66 ng g⁻¹, 13.18 ng g⁻¹, 12.47 ng g⁻¹ and 12.09 ng g⁻¹, respectively). In the Pacific Ocean, the fine and coarse deposited aerosols show similar patterns with higher average concentrations of MeChry (27.09 ng g⁻¹) and B(a)Pyr (22.11 ng g⁻¹) followed by other

heavier compounds in the coarse fraction, as well as 32.82 ng g^{-1} and 21.36 ng g^{-1} for MeChry and B(a)Pyr, respectively, in the fine fraction. In the only sampling event for the Indian Ocean, there is a reverse trend in the PAH profile, being the unique dry deposition measurement where concentrations of some individual compounds in the fine aerosols are higher than in the coarse aerosols. The highest concentrations in the Indian ocean are for B(a)Pyr (12.94 ng g^{-1} and 23.55 ng g^{-1} in coarse and fine fractions) and for MeChry (11.98 ng g^{-1} and 22.37 ng g^{-1} in coarse and fine fractions).

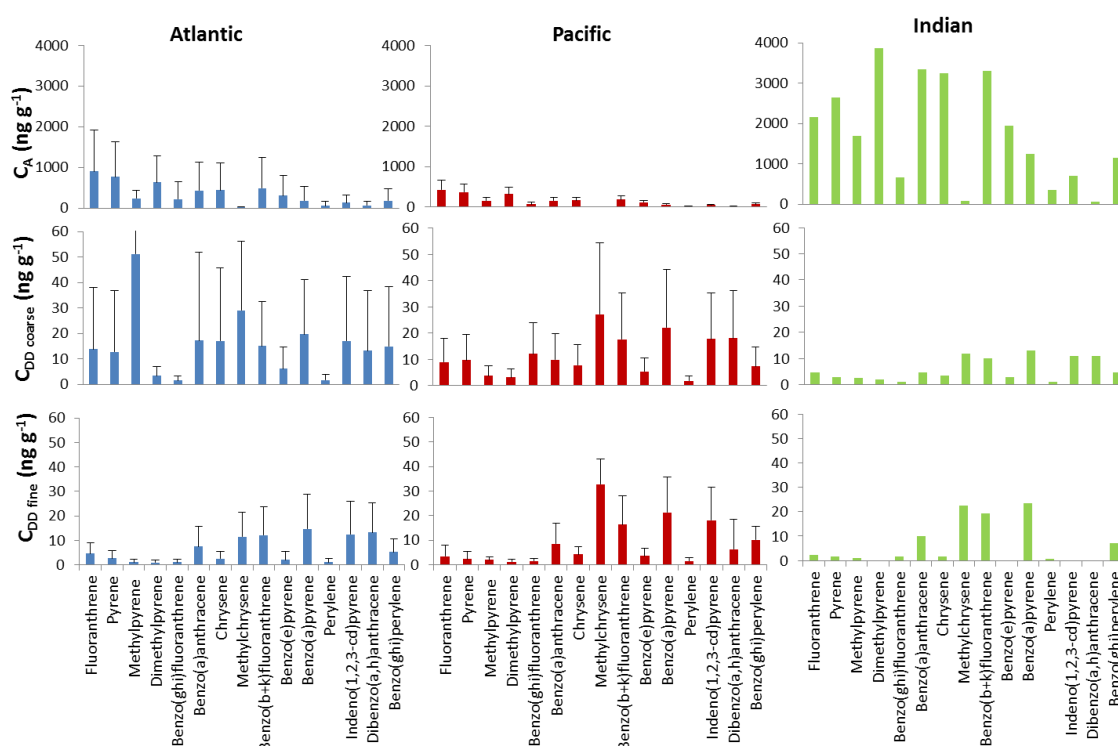


Figure 1.2. PAHs distribution pattern of concentrations (ng g^{-1}) in suspended aerosols (upper panels), coarse (middle panels) and fine fraction (lower panels) of deposited aerosols.

Generally, there were several measures of PAHs in suspended aerosols for each dry deposition measurement (Table S1.11 and Figure S1.6). Therefore, in order to obtain v_D from equation [1.1], PAHs concentrations in the aerosol phase gathered simultaneously to each dry deposition measurement were averaged depending on the sampled volume for each measurement. Figure 1a shows the suspended aerosol phase concentrations of PAHs corresponding to each dry deposition measurement. The mean C_A of individual PAHs in suspended aerosols are shown in Figure 1.2. $\Sigma_{16}\text{PAHs}$

Results 1

concentrations in suspended aerosols ranged between 0.06 ng m^{-3} and 6.52 ng m^{-3} . This high variability is particularly observed in the Atlantic Ocean, with the highest concentrations of PAHs found off-shore Brazil, whereas the lowest concentrations are observed in the central south Atlantic. High PAH concentrations were also described in the NE Atlantic in previous reports²² and in the measurements on this study. Unexpectedly, the sampling event for the Indian Ocean revealed the highest mean PAHs concentrations in the aerosol phase (given as ng g^{-1} , Figure 1.2). This is due to the first of the four suspended aerosols samples used to average the concentration during the time period when the dry deposition was measured, whose PAHs concentrations were anomalously high (Figure S1.6). It could have been caused by facilitated transport from distant sources due to the strong winds during this sampling period. Moreover, there is a particular switch of the direction of the wind during this sampling event since BT analysis showed that air masses were coming predominantly from Southeast Asia instead than from the south⁴⁹ (Figure S1.2). High levels of atmospheric PAHs have been reported in South and Southeast Asia. This region is responsible of half of the world PAHs emissions since 2007⁵⁰. Therefore, this abrupt change in wind direction could have affected the levels of the aerosol sampled, enhancing the PAHs content. Conversely, PAH concentrations and variability in the Atlantic are slightly greater than those measured in the Pacific atmosphere for all individual compounds.

Concerning the abundance of individual PAHs (Figure 1.2a), Flu, Pyr and methylated Pyr were the most abundant PAHs in the suspended aerosol; on average 17.8% and 16.0% of $\Sigma_{16}\text{PAHs}$ corresponds to Flu and Pyr, respectively, followed by Chry (7.8%), B(b+k)Flu (8.5%) and B(a)Anthr (6.9%) (see profile in Figure S1.7). Flu global maximal concentrations were found in the Atlantic Ocean, in particular near the South American coastal area. Even though the back trajectories in the low atmosphere (Figure S1.1) indicate that the air masses in that region were coming from the Central Atlantic, upper air masses show different origins, coming from the Brazilian coastal region, directly related with a heavier pollution with industrial and urban pollution uprising PAHs levels (Figure S1.2)^{51,52}. Pyr followed a very similar pattern, with slightly lower concentrations than Flu in all samples except for the measurement taken in the central Indian Ocean.

The measured concentrations in suspended aerosols reported here are in the same range of those reported previously in Atlantic^{22,48}, Pacific⁵³ and Indian⁴⁰ tropical and subtropical areas, but higher than the concentrations given in some studies^{54,55}. The PAHs concentrations in suspended aerosol were between one and two orders of magnitude higher than the deposited aerosol concentrations, suggesting there is a pool of aerosols with high PAH content that is not efficiently deposited to the ocean.

Dry Deposition Velocities

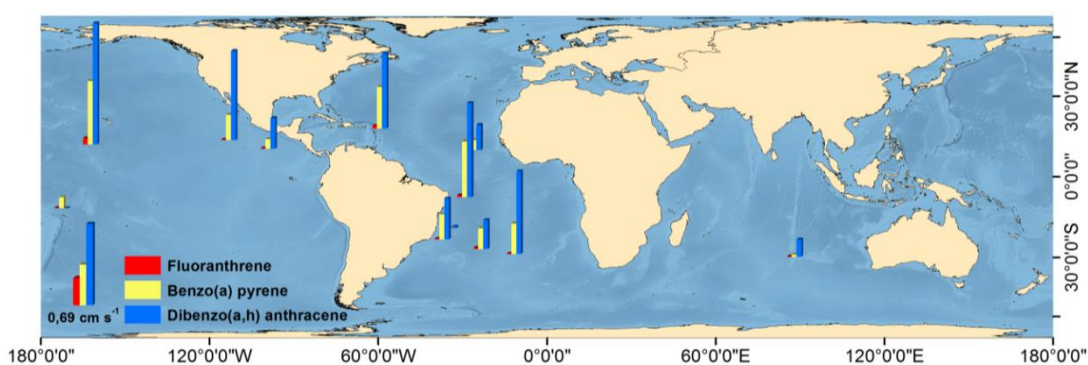


Figure 1.3. Dry deposition velocity (cm s^{-1}) for Fluoranthrene, Benzo (a) Pyrene and Benzo (ghi) Perylene determined from the measured dry deposition fluxes and concentrations in suspended aerosols.

Dry deposition velocities for all individual PAHs were calculated with the field measured F_{DD} and C_A using equation [1.1] (Table S1.12). Higher mean v_D corresponded to MeChry ($0.17\text{--}13.30 \text{ cm s}^{-1}$) followed by DB(ah)Anthr ($0.29\text{--}1.38 \text{ cm s}^{-1}$), and other high MW PAHs. Values reported in the few previous studies in the Atlantic Ocean²² (0.08 to 0.3 cm s^{-1}), coastal sites^{22,32-36} (0.01 and 0.8 cm s^{-1}) or in models¹ (0.01 and 0.8 cm s^{-1}) fall in the same range than those estimated here. Nevertheless, calculated velocities for large urban sites or industrial areas are far higher^{33,56}. Highest v_D were found in the North Pacific Ocean, followed by the Atlantic (showing no substantial statistical differences among north and south hemispheres). The lowest values of v_D are those from the South Pacific and Indian Oceans (Figure 1.3) and for lower MW compounds.

Previous studies have suggested that there is a direct relation between PAHs MW (and other MW dependent chemical properties, like vapor pressure, P_L) and v_D . For

example, higher MW PAHs were reported as more susceptible to attach to finer aerosols in polluted areas^{22,56}, but this trend is not always observed for coastal and marine atmospheres^{22,23} nor in this study. Figure 4 shows the correlations between P_L and v_D for individual PAHs (Table S1.13) for each sampling event. For 10 out of the 12 sampling events, v_D is inversely correlated with $\text{Log}(P_L)$, with higher values of v_D for the high MW PAHs ($p < 0.05$ or $p < 0.01$) (Table S1.14). Lower values of P_L are characteristic of the more hydrophobic PAHs. This suggests that higher MW PAHs are mainly deposited with either larger aerosols which have a faster v_D due to gravity, or attached to hydrophobic aerosols, for example soot carbon, that exhibit higher deposition velocity. Fine particles do not deposit due to gravity (they are suspended in air), but due to the collisions to the marine surface. At higher wind speed there is more turbulence and thus more collisions. In addition, the number of collisions that result in a deposited aerosol increase at lower surface tension and higher hydrophobicity of the surface microlayer²². This stickiness of the surface microlayer is due to organic substances with surfactant and hydrophobic properties that in the open oceans are mainly biogenic^{23,57,58}. Hydrophobic aerosols will be as well specially enriched with the more hydrophobic organic compounds such as high MW PAHs due to chemical affinity, and this sub-population of aerosols (presumably soot carbon) would be particularly prone to be deposited to the surface ocean. The abundance of high MW PAHs in suspended aerosols is generally small, suggesting that concentration of high MW PAHs is low in the accumulation mode aerosols (0.5-1.2 μm), which dominate the suspended aerosol population³⁷, also corroborated with the higher concentration of these compounds found in the coarse fraction (over 2.7 μm) of the dry deposited aerosol. In addition, the higher the P_L , the higher the fraction of the chemical in the gas phase. This means that for PAHs with higher P_L , gas-particle partitioning processes play a bigger role, and PAH may partition from the gas phase preferably to the fine particles, which dominate the number and surface size distribution of aerosols³⁷. Over the ocean, a large fraction of fine particles may be marine secondary organic aerosols. Contrariwise, high MW PAHs are unlikely to be present in the gas phase due to their strong association to aerosol soot carbon, and deposit faster as stated before. It is also possible that other processes specific of the marine environment, such as resuspension of marine aerosols, etc., may also affect the depositional velocities of PAHs.

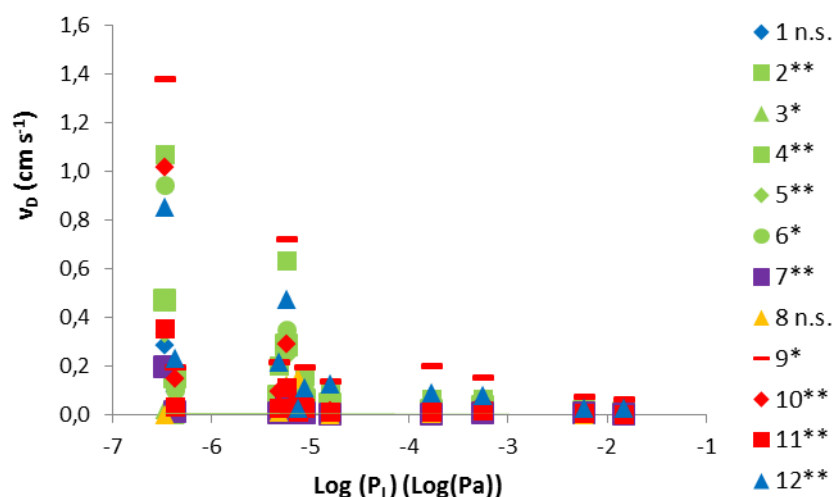


Figure 1.4. Dry deposition velocity (cm s^{-1}) versus vapor pressure (Log(Pa)) for the target PAHs. 1-12 Dry deposition samples code: blue in north Atlantic, green in south Atlantic, purple Indian, orange south Pacific and red north Pacific. Statistical significances are shown: ns means not significant, * means $p < 0.05$ (bilateral) and ** means $p < 0.01$ (bilateral).

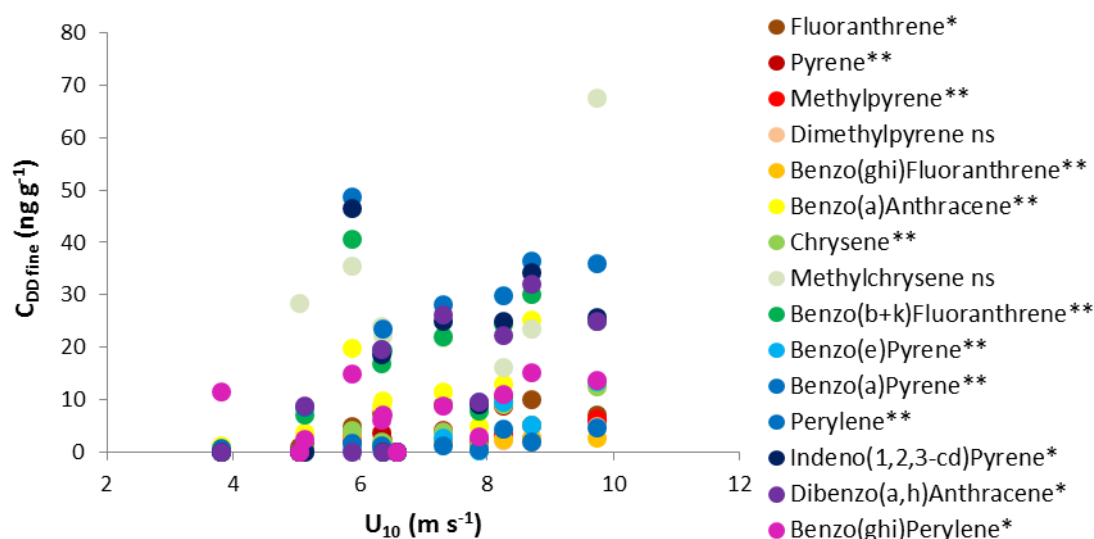


Figure 1.5. Concentrations in fine deposited aerosols (ng g^{-1}) versus wind velocity (m s^{-1}) for the target PAHs. Statistical significances are shown: ns means not significant, * means $p < 0.05$ (bilateral) and ** means $p < 0.01$ (bilateral).

Models predict that wind speed (U_{10}) also affects the values of v_D for fine aerosols because an increased turbulence close to the air-water interface enhances the efficiency of the depositional process by increasing the number of collisions of aerosols with the surface. Wind speed does influence to a lesser extent the deposition of coarse aerosols because dry deposition of large aerosols is mainly driven by gravity^{1,3}.

Results 1

Average U_{10} (Table S1.12) for the dry deposition sampling periods was positively correlated with aerosol concentration in the fine fraction for all the PAHs analyzed (except for DMePyr and MeChry) (Figure 1.5, Table S1.15), but not for the coarse fraction in any case. Additionally, by calculating the fine particles deposition velocity (v_{Df}) obtained from Equation [1.1] for the fine particles F_{DD} ($F_{DD\text{ fine}}$), it is found as well a positive correlation ($p < 0.05$) between v_{Df} and U_{10} for all target PAHs (but for MeChry and B(ghi)Per) (Table S1.16). These results support the theoretical predictions of higher deposition of fine aerosols at high wind speeds. Furthermore, the slope of v_D for the fine fraction when plotted against P_L is as well inversely correlated with U_{10} ($p < 0.05$) (Table S1.17); meaning that with fast wind speeds over the ocean there is a stronger gradient in v_D values between low and high MW PAHs, and therefore fast winds favors the relative deposition of high MW PAHs versus low MW PAHs.

Predicting Dry Deposition fluxes for semivolatile organic compounds to the oceans

Most field studies only measure the concentrations of organic compounds in suspended aerosols, but not the dry deposition fluxes. In addition environmental fate and transport models require of appropriate parameterization of v_D to predict the depositional fluxes. In order to formulate a parameterization for the 3 measured deposition velocities for PAHs (v_{Df} , v_{Dc} (coarse) and v_D) as a function of chemical and environmental factors (P_L , U_{10} and the existence of an hydrophobic microlayer over the sea surface), a multiple parameter least squares regression was applied to the data set (Table S1.18). As stated in the previous section, v_{Df} is correlated with P_L and wind speed for each of the measurements (Figure 1.5, Table S1.15). The stickiness of the surface due to biogenic organic compounds lowering the surface tension and increasing the surface hydrophobicity is accounted by using chlorophyll α concentrations as a surrogate of the biological source of these compounds (for example exudates from phytoplankton). The chlorophyll concentrations were measured in surface waters (Chl_s). The following equation is proposed for predicting v_{Df} values,

$$\text{Log}(v_{Df}) = -0.287(\pm 0.060)\text{Log}(P_L) + 0.442(\pm 0.115)U_{10} * Chl_s - 3.269(\pm 0.307) \quad [1.2]$$

with a significance of $p < 0.001$ for all parameters and $R^2 = 0.23$ (Table S1.18) (U_{10} [m s^{-1}] and Chl_s [mg m^{-3}]). Equation [1.2] reflects decreasing depositional velocities for compounds with higher P_L and with low U_{10} and Chl_s , as theoretically stated in models and previously discussed.

For the coarse particles deposition, v_{Dc} depends as well on the vapor pressure of the target compound and the interaction between wind speed and chlorophyll concentration in the ocean surface by ($R^2 = 0.50$, $p < 0.001$),

$$\text{Log}(v_{Dc}) = -0.253(\pm 0.047) \text{Log}(P_L) + 0.337(\pm 0.090) U_{10} * Chl_s - 2.973(\pm 0.240) \quad [1.3]$$

Regarding v_D , originated from fine and coarse aerosol depositional flux concurrently, it can be predicted by ,

$$\text{Log}(v_D) = -0.261(\pm 0.038) \text{Log}(P_L) + 0.387(\pm 0.074) U_{10} * Chl_s - 3.082(\pm 0.197) \quad [1.4]$$

Equation 1.4 ($R^2 = 0.37$ and $p < 0.001$) would be a good approximation for calculating dry depositional velocities for semi-volatile compounds over the open ocean surface from known parameters (P_L , U_{10} and Chl_s) and when atmospheric concentrations are measured using high volume samplers not discriminating aerosols of different size. U_{10} and Chl_s can be easily measured or estimated from satellite products, but in case that U_{10} or Chl_s were not available, the following parameterizations could be used,

$$\text{Log}(v_{Df}) = -0.287(\pm 0.063) \text{Log}(P_L) - 2.798(\pm 0.296) \quad [1.5]$$

$$\text{Log}(v_{Dc}) = -0.253(\pm 0.049) \text{Log}(P_L) - 2.614(\pm 0.231) \quad [1.6]$$

$$\text{Log}(v_D) = -0.261(\pm 0.042) \text{Log}(P_L) - 2.670(\pm 0.198) \quad [1.7]$$

which significances are all $p < 0.001$ and $R^2 = 0.139$, 0.172 and 0.229 respectively for equations [1.5], [1.6] and [1.7] (Table S1.19).

The usefulness of equations [1.2] to [1.7] can be observed if the error made when using a single value of v_D versus the measured v_D from this work is compared with the error made when using equation [1.4] for predicting v_D (or deposition fluxes). For instance, the mean v_D in this study is of 0.12 cm s^{-1} . If this value is used to predict the dry deposition fluxes of individual PAHs, there will be an average error of 1800%.

Results 1

Conversely, if equation [1.4] is used to predict the dry deposition velocities and fluxes from the suspended aerosol PAH concentrations, the mean error is of a factor of 3 (335%). Therefore, the error in estimating the dry deposition fluxes for individual PAHs at different locations is reduced by a factor of 5.

It is evident that the atmospheric input of PAHs and other organic pollutants to the Ocean need to be further studied, and that part of the variability of the measured dry deposition fluxes cannot be yet predicted from the empirical parameterizations. Further research should focus on a better characterization of the size distribution of aerosols, the chemical composition of the surface microlayer and aerosols, and other processes affecting the dry deposition of organic compounds to the ocean.

ACKNOWLEDGMENTS

We acknowledge the support of RV Hespérides staff and UTM technicians during the cruise. This work was funded by the Spanish Government through the Malaspina 2010 project. B.G and J.Z acknowledges a predoctoral fellowship from the BBVA Foundation and Chilean government, respectively. Thanks to Ana Maria Cabello, Pilar Rial, Prof. Marta Estrada, Prof. Mikel Latasa, Prof. Francisco Rodríguez and Prof. Patrizija Mozetič for the Chlorophyll measurements during Malaspina cruise.

REFERENCES

- 1 Jurado, E. *et al.* Atmospheric dry deposition of persistent organic pollutants to the atlantic and inferences for the global oceans. *Environmental Science and Technology* **38**, 5505-5513 (2004).
- 2 Jurado, E. *et al.* Wet deposition of persistent organic pollutants to the global oceans. *Environmental Science and Technology* **39**, 2426-2435 (2005).
- 3 Jurado, E., Dachs, J., Duarte, C. M. & Simó, R. Atmospheric deposition of organic and black carbon to the global oceans. *Atmospheric Environment* **42**, 7931-7939 (2008).
- 4 Farrington, J. W. & Takada, H. Persistent organic pollutants (POPs), polycyclic aromatic hydrocarbons (PAHs), and plastics: Examples of the status, trend, and cycling of organic chemicals of environmental concern in the ocean. *Oceanography* **27**, 196-213 (2014).
- 5 Bidleman, T. F. Atmospheric processes. *Environmental Science and Technology* **22**, 361-367 (1988).
- 6 Galbán-Malagón, C. J., Del Vento, S., Cabrerizo, A. & Dachs, J. Factors affecting the atmospheric occurrence and deposition of polychlorinated biphenyls in the Southern Ocean. *Atmospheric Chemistry and Physics* **13**, 12029-12041 (2013).
- 7 Galbán-Malagón, C., Cabrerizo, A., Caballero, G. & Dachs, J. Atmospheric occurrence and deposition of hexachlorobenzene and hexachlorocyclohexanes in the Southern Ocean and Antarctic Peninsula. *Atmospheric Environment* **80**, 41-49 (2013).
- 8 Jurado, E., Lohmann, R., Meijer, S., Jones, K. C. & Dachs, J. Latitudinal and seasonal capacity of the surface oceans as a reservoir of polychlorinated biphenyls. *Environmental Pollution* **128**, 149-162 (2004).
- 9 Galbán-Malagón, C., Berrojalbiz, N., Ojeda, M. J. & Dachs, J. The oceanic biological pump modulates the atmospheric transport of persistent organic pollutants to the Arctic. *Nature communications* **3**, 862 (2012).
- 10 Dachs, J. & Eisenreich, S. J. Adsorption onto aerosol soot carbon dominates gas-particle partitioning of polycyclic aromatic hydrocarbons. *Environmental Science and Technology* **34**, 3690-3697 (2000).
- 11 Gigliotti, C. L. *et al.* Air-water exchange of polycyclic aromatic hydrocarbons in the New York-New Jersey, USA, Harbor Estuary. *Environmental Toxicology and Chemistry* **21**, 235-244 (2002).
- 12 Gigliotti, C. L. *et al.* Atmospheric concentrations and deposition of polycyclic aromatic hydrocarbons to the Mid-Atlantic East Coast region. *Environmental Science & Technology* **39**, 5550-5559 (2005).
- 13 Lohmann, R., Gioia, R., Eisenreich, S. J. & Jones, K. C. Assessing the importance of ab- and adsorption to the gas-particle partitioning of PCDD/Fs. *Atmospheric Environment* **41**, 7767-7777 (2007).
- 14 Castro-Jiménez, J., Berrojalbiz, N., Wollgast, J. & Dachs, J. Polycyclic aromatic hydrocarbons (PAHs) in the Mediterranean Sea: Atmospheric occurrence, deposition and decoupling with settling fluxes in the water column. *Environmental Pollution* **166**, 40-47 (2012).
- 15 Castro-Jiménez, J. *et al.* Atmospheric occurrence and deposition of polychlorinated dibenzo-p-dioxins and dibenzofurans (PCDD/Fs) in the open mediterranean sea. *Environmental Science and Technology* **44**, 5456-5463 (2010).
- 16 Möller, A. *et al.* Organophosphorus flame retardants and plasticizers in airborne particles over the Northern Pacific and Indian Ocean toward the polar regions: Evidence for global occurrence. *Environmental Science and Technology* **46**, 3127-3134 (2012).

- 17 Xie, Z., Möller, A., Ahrens, L., Sturm, R. & Ebinghaus, R. Brominated flame retardants in seawater and atmosphere of the Atlantic and the southern ocean. *Environmental Science and Technology* **45**, 1820-1826 (2011).
- 18 Möller, A., Xie, Z., Sturm, R. & Ebinghaus, R. Polybrominated diphenyl ethers (PBDEs) and alternative brominated flame retardants in air and seawater of the European Arctic. *Environmental Pollution* **159**, 1577-1583 (2011).
- 19 Möller, A., Xie, Z., Caba, A., Sturm, R. & Ebinghaus, R. Occurrence and air-seawater exchange of brominated flame retardants and Dechlorane Plus in the North Sea. *Atmospheric Environment* **46**, 346-353 (2012).
- 20 Möller, A., Xie, Z., Cai, M., Sturm, R. & Ebinghaus, R. Brominated flame retardants and dechlorane plus in the marine atmosphere from Southeast Asia toward Antarctica. *Environmental Science and Technology* **46**, 3141-3148 (2012).
- 21 Möller, A., Xie, Z., Sturm, R. & Ebinghaus, R. Large-Scale Distribution of Dechlorane Plus in Air and Seawater from the Arctic to Antarctica. *Environmental Science & Technology* **44**, 8977-8982, doi:10.1021/es103047n (2010).
- 22 Del Vento, S. & Dachs, J. Atmospheric occurrence and deposition of polycyclic aromatic hydrocarbons in the northeast tropical and subtropical Atlantic Ocean. *Environmental Science and Technology* **41**, 5608-5613 (2007).
- 23 del Vento, S. & Dachs, J. Influence of the surface microlayer on atmospheric deposition of aerosols and polycyclic aromatic hydrocarbons. *Atmospheric Environment* **41**, 4920-4930 (2007).
- 24 Demircioglu, E., Sofuoglu, A. & Odabasi, M. Particle-phase dry deposition and air-soil gas exchange of polycyclic aromatic hydrocarbons (PAHs) in Izmir, Turkey. *Journal of Hazardous Materials* **186**, 328-335 (2011).
- 25 Birgül, A., Tasdemir, Y. & Cindoruk, S. S. Atmospheric wet and dry deposition of polycyclic aromatic hydrocarbons (PAHs) determined using a modified sampler. *Atmospheric Research* **101**, 341-353 (2011).
- 26 Günindi, M. & Tasdemir, Y. Wet and dry deposition fluxes of polychlorinated biphenyls (PCBs) in an urban area of Turkey. *Water, Air, and Soil Pollution* **215**, 427-439 (2011).
- 27 Esen, F., Tasdemir, Y. & Cindoruk, S. S. Dry deposition, concentration and gas/particle partitioning of atmospheric carbazole. *Atmospheric Research* **95**, 379-385 (2010).
- 28 Slinn, S. A. & Slinn, W. G. N. Predictions for particle deposition on natural waters. *Atmospheric Environment - Part A General Topics* **14**, 1013-1016 (1980).
- 29 Williams, M. M. R. On a generalization of the Telford equation for aerosols. *Annals of Nuclear Energy* **9**, 499-508 (1982).
- 30 Ondov, J. M. *Influence of temporal changes in relative humidity on size and dry depositional fluxes of aerosol particles bearing trace elements Atmospheric Deposition of Contaminants to the Great Lakes and Coastal Waters. Proceedings from a Session at the SETAC 15th Annual Meeting 30 October-4 November 1994.* (1994).
- 31 Chang, K. F., Fang, G. C., Lu, C. & Bai, H. Estimating PAH dry deposition by measuring gas and particle phase concentrations in ambient air. *Aerosol Air Quality Research* **3**, 41-51 (2003).
- 32 Holsen, T. M. & Noll, K. E. Dry deposition of atmospheric Particles: Application of current models to ambient data. *Environmental Science Technology* **26**, 1807-1815 (1992).
- 33 Bozlaker, A., Muezzinoglu, A. & Odabasi, M. Atmospheric concentrations, dry deposition and air-soil exchange of polycyclic aromatic hydrocarbons (PAHs) in an industrial region in Turkey. *Journal of Hazardous Materials* **153**, 1093-1102 (2008).
- 34 Bozlaker, A., Odabasi, M. & Muezzinoglu, A. Dry deposition and soil-air gas exchange of polychlorinated biphenyls (PCBs) in an industrial area. *Environmental Pollution* **156**, 784-793, doi:10.1016/j.envpol.2008.06.008 (2008).

- 35 Esen, F., Siddik Cindoruk, S. & Tasdemir, Y. Bulk deposition of polycyclic aromatic hydrocarbons (PAHs) in an industrial site of Turkey. *Environmental Pollution* **152**, 461-467, doi:10.1016/j.envpol.2007.05.031 (2008).
- 36 Eng, A., Harner, T. & Pozo, K. A Prototype Passive Air Sampler for Measuring Dry Deposition of Polycyclic Aromatic Hydrocarbons. *Environmental Science & Technology Letters*, doi:10.1021/ez400044z (2014).
- 37 Seinfeld, J. H. & Pandis, S. N. *Atmospheric Chemistry and Physics: From Air Pollution to Climate Change*. 2nd ed. edn, (Wiley-Interscience, 2006).
- 38 UNECE. (ed United Nations Economic Commission for Europe) (UN, http://www.unece.org/env/lrtap/pops_h1.html, 1998).
- 39 Cabrerizo, A., Dachs, J. & Barceló, D. Development of a soil fugacity sampler for determination of air - soil partitioning of persistent organic pollutants under field controlled conditions. *Environmental Science and Technology* **43**, 8257-8263 (2009).
- 40 Xu, Y. *et al.* The spatial distribution and potential sources of polycyclic aromatic hydrocarbons (PAHs) over the Asian marginal seas and the Indian and Atlantic Oceans. *Journal of Geophysical Research D: Atmospheres* **117** (2012).
- 41 Tsapakis, M., Apostolaki, M., Eisenreich, S. & Stephanou, E. G. Atmospheric deposition and marine sedimentation fluxes of polycyclic aromatic hydrocarbons in the eastern Mediterranean basin. *Environmental Science and Technology* **40**, 4922-4927 (2006).
- 42 Park, J. S., Wade, T. L. & Sweet, S. T. Atmospheric deposition of PAHs, PCBs, and organochlorine pesticides to Corpus Christi Bay, Texas. *Atmospheric Environment* **36**, 1707-1720 (2002).
- 43 Lang, Q., Zhang, Q. & Jaffé, R. Organic aerosols in the Miami area, USA: Temporal variability of atmospheric particles and wet/dry deposition. *Chemosphere* **47**, 427-441 (2002).
- 44 Poor, N. *et al.* Atmospheric concentrations and dry deposition rates of polycyclic aromatic hydrocarbons (PAHs) for Tampa Bay, Florida, USA. *Atmospheric Environment* **38**, 6005-6015 (2004).
- 45 Tasdemir, Y. & Esen, F. Dry deposition fluxes and deposition velocities of PAHs at an urban site in Turkey. *Atmospheric Environment* **41**, 1288-1301 (2007).
- 46 Li, J., Cheng, H., Zhang, G., Qi, S. & Li, X. Polycyclic aromatic hydrocarbon (PAH) deposition to and exchange at the air-water interface of Luhu, an urban lake in Guangzhou, China. *Environmental Pollution* **157**, 273-279, doi:10.1016/j.envpol.2008.06.039 (2009).
- 47 Esen, F., Tasdemir, Y. & Siddik Cindoruk, S. Determination of mass transfer rates and deposition levels of polycyclic aromatic hydrocarbons (PAHs) using a modified water surface sampler. *Atmospheric Pollution Research* **1**, 177-183 (2010).
- 48 Garrison, V. H. *et al.* Persistent organic contaminants in Saharan dust air masses in West Africa, Cape Verde and the eastern Caribbean. *Science of The Total Environment* **468-469**, 530-543, doi:10.1016/j.scitotenv.2013.08.076 (2014).
- 49 Draxler, R. R. a. R., G.D. (NOAA Air Resources Laboratory, College Park, MD, access via NOAA ARL READY Website (<http://www.arl.noaa.gov/HYSPLIT.php>), 2013).
- 50 Shen, H. *et al.* Global atmospheric emissions of polycyclic aromatic hydrocarbons from 1960 to 2008 and future predictions. *Environmental Science and Technology* **47**, 6415-6424 (2013).
- 51 Cavalcante, R. M., Sousa, F. W., Nascimento, R. F., Silveira, E. R. & Viana, R. B. Influence of urban activities on polycyclic aromatic hydrocarbons in precipitation: Distribution, sources and depositional flux in a developing metropolis, Fortaleza, Brazil. *Science of the Total Environment* **414**, 287-292 (2012).
- 52 Vasconcellos, P. C., Souza, D. Z., Magalhães, D. & Da Rocha, G. O. Seasonal variation of n-alkanes and polycyclic aromatic hydrocarbon concentrations in PM10 samples

- collected at urban sites of São Paulo State, Brazil. *Water, Air, and Soil Pollution* **222**, 325-336 (2011).
- 53 Inomata, Y. *et al.* Source contribution analysis of surface particulate polycyclic aromatic hydrocarbon concentrations in northeastern Asia by source–receptor relationships. *Environmental Pollution* **182**, 324-334, doi:10.1016/j.envpol.2013.07.020 (2013).
- 54 Jaward, F. M., Barber, J. L., Booij, K. & Jones, K. C. Spatial distribution of atmospheric PAHs and PCNs along a north–south Atlantic transect. *Environmental Pollution* **132**, 173-181, doi:10.1016/j.envpol.2004.03.029 (2004).
- 55 Lohmann, R. *et al.* PAHs on a west-to-east transect across the tropical Atlantic Ocean. *Environmental Science and Technology* **47**, 2570-2578 (2013).
- 56 Vardar, N., Odabasi, M. & Holsen, T. M. Particulate dry deposition and overall deposition velocities of polycyclic aromatic hydrocarbons. *Journal of Environmental Engineering* **128**, 269-274 (2002).
- 57 Kujawinski, E. B., Farrington, J. W. & Moffett, J. W. Evidence for grazing-mediated production of dissolved surface-active material by marine protists. *Marine Chemistry* **77**, 133-142 (2002).
- 58 Cunliffe, M. *et al.* Sea surface microlayers: A unified physicochemical and biological perspective of the air-ocean interface. *Progress in Oceanography* **109**, 104-116 (2013).

2. High Atmosphere-Ocean Exchange of Semivolatile Aromatic Hydrocarbons

Belén González-Gaya^{1,2}, María-Carmen Fernández-Pinos¹, Laura Morales¹, Esteban Abad¹, Benjamí Piña¹, Laurence Mejanelle³, Carlos Duarte^{4,5}, Begoña Jiménez², Jordi Dachs^{1*}

¹ Department of Environmental Chemistry, Institute of Environmental Assessment and Water Research (IDAEA-CSIC), Barcelona, Catalonia, Spain.

² Department of Instrumental Analysis and Environmental Chemistry, Institute of Organic Chemistry (IQOG-CSIC), Madrid, Spain.

³ Laboratory of Ecogeochemistry of Benthic Environments, Université Pierre et Marie Curie, Bagnuls sur Mer, France.

⁴ Department of Global Change Research, Mediterranean Institute for Advanced Studies (IMEDEA-CSIC), Esporles, Mallorca, Spain.

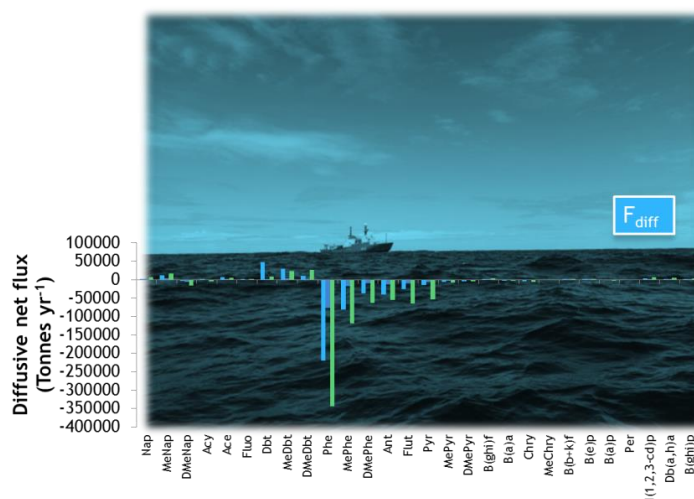
⁵ Division of Biological and Environmental Sciences and Engineering, Red Sea Research Center, King Abdullah University of Science and Technology, Thuwal, Saudi Arabia.

*Corresponding author email: jordi.dachs@idaea.csic.es

Submitted

ABSTRACT

Polycyclic aromatic hydrocarbons (PAHs), and other semivolatile aromatic-like compounds (SALCs), are an important and ubiquitous fraction of organic matter, with numerous sources such as incomplete combustion of fossil fuels, oil spills, and other anthropogenic and biogenic sources ¹⁻⁵. PAHs have been previously described in the oceanic atmosphere, seawater, sediments and biota, including remote regions ^{2,4,6,7}. However, their occurrence, fluxes and relevance at a planetary scale have been poorly assessed for the open ocean. Here we report the first global assessment of the occurrence and of the atmosphere-ocean fluxes of 64 PAHs and total SALCs. PAHs were ubiquitously found in the Atlantic, Pacific and Indian oceans, with gas phase concentrations of a few ng m^{-3} for the most abundant compounds (phenanthrene and alkylated phenanthrenes), and of hundreds of pg L^{-1} in surface seawater (with phenanthrene, pyrene and fluoranthene being the most abundant compounds). The global net diffusive atmospheric input and dry deposition of PAHs to the global ocean is estimated at $0.09 \text{ Tg month}^{-1}$, four folds the total PAH inputs from the Deep Horizon oil spill ¹. The resolved PAH input to the global ocean accounts for 1 Tg C yr^{-1} , comparable to ocean-atmosphere carbon fluxes of isoprene and other biogenic volatile organic compounds ⁸. SALC concentrations account for averaged $10000 \text{ ng C m}^{-3}$ in the gas phase and 870 ng C L^{-1} in the surface seawater, with a large contribution of an aromatic unresolved complex mixture (UCM). These large concentrations drive global inputs of carbon to the Atlantic, Pacific and Indian Oceans of 430 Tg C yr^{-1} , around 16% of the oceanic CO_2 uptake ⁹.



Graphical Abstract 2.

INTRODUCTION

There is a growing interest in the quantification of ocean-atmosphere and land-atmosphere exchange of organic compounds ^{8,10-15}, but besides some earlier efforts, this has been largely limited to volatile organic compounds (VOCs) such as methane, ethane, isoprene and other low molecular weight organic compounds with high volatility ^{8,11}. Atmospheric deposition is small for VOCs, for which the atmosphere is an ultimate sink. Conversely, semivolatile organic compounds (SOCs) tend to be deposited to oceans following atmospheric transport ¹⁶. Recent studies suggest a large contribution of SOCs in the overall air-sea and air-land exchanges of carbon ^{10,13-15}, but these remain uncharacterized.

PAHs, originated from incomplete combustion of biomass, fossil fuels, oil spills, diagenesis of organic matter and other biogenic sources ^{1,2,4,5}, are among the abundant known semivolatile organic compounds in the environment ^{4,17,18}. PAHs have raised significant concern due to their known toxic effects on biota and humans ³ coupled with their ubiquitous occurrence ¹⁹. PAHs are globally redistributed through cycles of atmospheric transport and deposition/volatilization due to their semivolatility ^{2,6,7,16,20}. Once deposited in the oceanic water column, PAHs enter the oceanic carbon biogeochemical cycle including accumulation in the marine food web, biotic and abiotic degradation and settling of the more refractory PAHs to deep waters and sediments ^{4,17,18}. However, the air-sea exchange of PAHs has only been assessed in limited marine regions, mainly coastal or semi-confined seas ^{18,20,21}. In addition, previous assessments quantified only a small fraction of the total PAHs present in the environment. Thus, we conducted a global assessment of air-sea exchange of a large number of PAHs and other SALCs in the open ocean to ascertain whether the resulting inputs represent a significant source of pollutants and semi-volatile organic carbon to the oceans.

MATERIALS AND METHODS

Sampling strategy

All samples were collected during the Malaspina 2010 circumnavigation cruise on board of the RV Hespérides from December 2010 until July 2011. The sampling campaign crossed the north and south basins of the Atlantic and Pacific oceans, as well as the Indian Ocean, between 35°N and 40°S, navigating all the tropical and subtropical oceanic gyres²². A total of 108 gas, 108 aerosols, 68 seawater samples and 11 wet deposition events were collected over the 3 oceanic basins.

Air samples (concurrent gas and aerosol phases) were taken as explained elsewhere^{2,6,18} with high volume samplers located above the bridge. The high volume samplers were connected to a wind vane in order to allow sampling only when the wind was coming from the bow to avoid any perturbation of the sample by the ship emissions. The mean air volume sampled was 824 m³ (525 - 1982 m³) per sample. The marine aerosols were first collected on precombusted quartz microfiber filters (QM/A, Whatman), and the gas phase compounds were retained over precleaned polyurethane foams (PUF). After sampling, all filters and PUFs were kept folded in aluminum foil and zip bags at -20 °C.

Water samples were taken from the continuous intake of surface (4 m) seawater of the research vessel and directly transferred to the sampling system, in which the water was filtered on precombusted GF/F filters (Whatman), and afterwards, the dissolved phase compounds were retained on XAD-2 sorbent kept in stainless-steel columns at a controlled flow. The average volume of water filtered was 239 L (69-391 L). XAD-2 columns were stored at 4°C until their extraction in the laboratory as described elsewhere²³.

Wet deposition samples were gathered exposing over the boat bridge a pre-cleaned stainless funnel attached to a Pyrex bottle during rain events. Rain water was solid phase extracted using HLB Oasis (3cc, 60mg) cartridges on board using a slightly modified protocol by Berrojalbiz et al²³. Briefly, cartridges were preconditioned with 3

mL Hexane (Hx), 3 mL Hx:Dichloromethane (DCIM) (1:2), 3 mL Methanol(MeOH):DCIM (1:2) and 3 mL of HPLC quality water. Then, the sample was loaded (previously spiked with a recovery standard) using a vacuum system until dryness. Then, it was eluted with 3 mL Hx, 6 mL Hx: DCIM (1:2) and 6 mL MeOH: DCIM (1:2) and the extracts were preserved frozen until their analysis in the laboratory.

PAHs analysis and quantification

Aerosol, gas and dissolved phase samples were analyzed as described elsewhere^{4,6,18,23}. HLB extracts from the rain water samples were further purified over 3 g of activated silica. All sample extracts were fractionated in three fractions (aliphatic, aromatic, polar), and PAHs and SALCs were determined in the aromatic fraction. 64 individual PAHs were quantified. These were: Naphthalene, Methylnaphthalenes (sum of 2 isomers), Dimethylnaphthalenes (sum of 6 isomers), Acenaphthylene, Acenaphthene, Fluorene, Dibenzothiophene, Methyl dibenzothiophenes (sum of 3 isomers), Dimethyldibenzothiophenes (sum of 5 isomers), Phenanthrene, Methylphenantrenes (sum of 4 isomers), Dimethylphenanthrenes (sum of 7 isomers), Anthracene, Fluoranthene, Pyrene, Methylpyrenes (sum of 5 isomers), Dimethylpyrenes (sum of 8 isomers), Benzo[ghi]fluoranthene, Benzo[a]Anthracene, Chrysene, Methylchrysenes (sum of 3 isomers), Benzo[b+k]fluoranthene (sum of 2 isomers), Benzo[e]Pyrene, Benzo[a]Pyrene, Perylene, Indeno[1,2,3-cd]Pyrene, Dibenzo[a,h]anthracene, Benzo[ghi]perylene. In the text and figures, we refer to 28 PAHs as we report the sum of concentrations of 64 alkylated and parental PAHs.

PAHs quantification was performed with an Agilent 6890 Series gas chromatograph coupled to a mass spectrometer Agilent 5973 (GC-MS) operating in selected ion monitoring (SIM) and electron impact mode (EI) as described elsewhere⁶. The quantification followed the internal standard procedure (using anthracene-d₁₀, pyrene-d₁₀, *p*-terphenyl-d₁₄, and benzo[*b*]fluoranthene-d₁₂) and measured concentrations were corrected with recovery of *perdeuterated* standards (acenaphthene-d₁₀, phenanthrene-d₁₀, chrysene-d₁₂, and perylene-d₁₂) added before the extraction of the samples.

Quantification of the total semivolatile aromatic-like compounds

A subset of ten pairs of gas and dissolved phase samples taken simultaneously were analyzed for the determination of SALCs. The aromatic fraction extracts were injected in the same GC-MS, using the same column and chromatographic conditions than for PAHs, but operating the mass detector in full scan mode (m/z from 50 to 500). The total ion current was integrated including resolved and unresolved compounds in the quantification; it is thus largely composed by the UCM. The chromatogram was divided in six retention time windows (Figure 2.5) around six individual PAHs which were used as quantification standard for the total SALCs in that chromatographic retention time window: 1) for more volatile compounds using Acenaphthene as reference standard, 2) for more semivolatile 3 ring aromatic hydrocarbons, using Phenanthrene, 3) lighter 4 ring hydrocarbons, using Pyrene, 4) heavier 4 rings, using Chrysene, 5) 5 aromatic ring hydrocarbons using Benzo[*a*]pyrene and 6) heavier 5 rings hydrocarbons, using Dibenzo[*a,h*]anthracene as reference standard. Concentrations were surrogate recovery corrected, such as in the PAHs quantification. Since it is possible that the response factors when using GC-MS may vary from chemical to chemical, the quantification of the SALCs has a higher uncertainty than the quantification of PAHs. However, the response factor for aromatic compounds, independently of their chemical structure, will not vary by more than a factor of 2, and the total uncertainty for the integration of the thousands compounds quantified as SALCs will likely be lower than a factor of 2.

The aromatic fraction of environmental samples is operationally defined as to ensure a good recovery of targeted PAHs during the analysis of these compounds. When abundant, the total lipid extract interferes with the purification (separation) of PAHs through matrix effects. In order to counteract these matrix effects, the aromatic fraction usually extends over a considerable range in polarity than strictly that of PAHs, and other neutral lipids than PAHs occur in the so called “aromatic fraction”, or “PAH fraction”. The extension in polarity used by various authors to isolate the PAHs and aromatic fraction is slightly variable. The mixture eluting the PAHs may vary from Hx:DCIM 30% (this work)^{2,6,18} to pure DCIM²⁴. In our samples, fatty acid methyl esters

(mostly C16 and C18) were identified in the second fraction of the gas and the marine dissolved phase. In the dissolved phase, slightly more polar compounds, such as aliphatic alcohols (primarily C14), were also identified. Aliphatic hydrocarbons were not present in neither the gas nor the dissolved phase as they eluted completely in the first, or aliphatic, fraction (see above). Therefore we refer to the sum of identified and non-identified resolved compounds, and non-resolved compounds of the second fraction as SALCs, and they might also include short-chain waxes, aldehydes and some alcohols. However, most of the SALC mass corresponds to the unresolved aromatic UCM.

In environmental samples, unresolved compounds are present in all fractions of different polarities ²⁴. In the aliphatic hydrocarbon fraction, this UCM is dominant in some sediment samples and have been extensively studied, quantified and qualified ²⁵. The UCM in the aliphatic hydrocarbon fraction is composed by alkyl substituted and/or cyclic hydrocarbons ^{26,27}. The UCM of the PAHs fraction is more seldom analyzed and include alkyl cyclic compounds (tertralin) and polycyclic hydrocarbons with a carbonyl substituent (indane) ²⁸. Lately, the UCM in polar fractions, eluted by mixtures including methanol, has been tentatively characterized and it is constituted by N, O and S-substituted branched PAHs ^{29,30}. The aliphatic and polar unresolved compounds were not quantified in this work.

Quality Assurance and Control

Laboratory and field blanks, recoveries and analytical limits were determined for each phase. Aerosol sample blanks and recoveries are included in González-Gaya et al ⁶. Breakthroughs of gas phase compounds were checked in 6 split PUFs samples (one per ocean basin). On average, 77% of total PAHs were present in the first half and 23% in the second half. The second half contained mainly 2-3 ring PAHs. For the gas phase 5 field blanks and 7 laboratory blanks were collected; dissolved phase blanks included 5 field blanks and 8 laboratory blanks, all extracted in batches with the rest of the samples to evaluate the analytical procedure. For the gas phase, mean Σ_{64} PAHs was 10 ng per sample in the field blanks and 10 ng per sample in the laboratory blanks.

Results 2

Equally, for the dissolved phase, mean Σ_{64} PAHs was 14 ng per sample and 4 ng per sample in the field and laboratory blanks respectively (Table S2.2). Measured PAHs in all analyzed field samples were above field and laboratory blanks concentrations, and thus, those were not subtracted from the quantified PAH amounts. Median recoveries of the perdeuterated PAHs used as surrogates in dissolved phase samples were: 52% Acenaphthene-d₁₀, 60% Phenanthrene-d₁₀, 69% Chrysene-d₁₂ and 93% of Perylene-d₁₂.

All concentrations in the different matrixes were surrogate recovery corrected. The detection limit (DL) was set as the inferior limit of the calibration curve (0.02 ng for all compounds). Quantification limit (QL) corresponds to the mean blank level of each sample phase.

Estimation of atmospheric deposition and degradation fluxes

Dry deposition fluxes (F_{DD} , ng m⁻²d⁻¹) were calculated per each individual compound from the measured aerosol phase concentrations (C_A , ng m⁻³) by,

$$F_{DD} = 864 \cdot v_D \cdot C_A \quad [2.1]$$

where v_D (cm s⁻¹) is the deposition velocity of the specific aerosol-bound chemical, and 864 is a unit conversion factor. The values of v_D were measured for 12 time periods in which deposited and suspended particles were collected simultaneously as reported in Gonzalez-Gaya et al ⁶. This allowed deriving an empirical equation for the prediction of v_D ,

$$\text{Log}(v_D) = -0.261 \text{Log}(P_L) + 0.387 U_{10} \cdot \text{Chl}_s - 3.082 \quad [2.2]$$

Where P_L is the subcooled liquid vapor pressure of the PAH, U_{10} is the wind speed at 10 m height, and Chl_s is the surface chlorophyll concentration. Equation [2.2] allowed estimating v_D for each compound and sampling period depending on the chemical vapor pressure of every compound and the environmental conditions. Based on the calculated v_D and the measured C_A , F_{DD} were obtained from equation [1.1] per each PAH and sampling period.

The wet deposition flux (F_{WD} , $\text{ng m}^{-2}\text{d}^{-1}$) of PAHs was estimated from the PAH concentrations quantified in the collected rainwater, and the precipitated water volume per time period and surface, for each one of the 11 rain events that occurred during the *Malaspina 2010* cruise.

The air-water diffusive fluxes (F_{AW} , $\text{ng m}^{-2}\text{d}^{-1}$) for PAHs were estimated in the traditional manner as,

$$F_{AW} = k_{AW} \left(\frac{C_G}{H'} - 1000 C_{TW} \right) \quad [2.3]$$

Where C_G and C_{TW} are the measured concentrations in the gas (ng m^{-3}) phase and the truly dissolved phase concentration (ng L^{-1}), respectively, H' is the temperature dependent dimensionless Henry's Law constant taken from elsewhere³¹ and corrected by salinity, and k_{AW} is the air-water mass transfer rate (m d^{-1}) estimated using the two film model and taking into account the non-linear influence of wind speed as described elsewhere²⁴.

Truly dissolved phase concentrations used in equation [2.3] were estimated from the measured dissolved phase concentrations (C_W , ng L^{-1}) by,

$$C_{TW} = \left(\frac{C_W}{1 + k_{DOC} DOC} \right) \quad [2.4]$$

where k_{DOC} is 10% the value of the octanol water partition coefficient (K_{OW}) and DOC is the dissolved organic carbon. Gross fluxes of absorption and volatilization correspond to the first and second term of equation [2.3]. Total accumulated fluxes for the Atlantic, Pacific and Indian oceans were obtained by multiplying the average basin flux by the surface area of the respective basin.

The diffusive air-water exchange fluxes of SALCs were estimated for each one of the six retention time windows quantified in the chromatogram (Figure 2.5) and using the physical-chemical properties of the major PAHs eluting in that time window. It is possible that H' values for some of the aromatic compounds contributing to SALCs are significantly different (different solubility in water rather than different vapor pressure) than those used for the diffusive fluxes calculations. Nevertheless, it is reasonable to assume that the average physical chemical properties of the aromatic

compounds contributing to SALCs are similar than those of PAHs since they were eluted in the same mid-polarity fraction during the fractionation of the extract (hydrophobicity), and moreover, because they show similar retention times on the GC-MS system (volatility). Uncertainty was calculated using values of H' one third and triple of those used for a representative PAH for each of the chromatographic intervals. Plausible maximum and minimum variation fluxes using those H' are pointed in Table S2.3. We do not provide the dry deposition fluxes of SALCs due to the minor role of dry deposition to the overall atmospheric deposition as demonstrated for individual PAHs. The fluxes reported as carbon assume an average 80% of carbon in the total mass of SALCs.

The atmospheric degradation fluxes (D_{atm}) of PAHs in the oceanic boundary atmosphere were estimated by,

$$D_{atm} = \frac{(C_{Gf} - C_{Gi})ABL}{t} \quad [2.5]$$

where C_{Gi} is the measured gas phase concentration at the initial time (ng m^{-3}), C_{Gf} is the final concentration (ng m^{-3}) after certain time in a supposed closed system, t is the time period considered (averaged 12 hours of light per day in tropical and subtropical areas), and ABL is the mean height of the atmospheric boundary layer (500 m). C_{Gf} was estimated from,

$$\ln \left(\frac{C_{Gi}}{C_{Gf}} \right) = k_{OH} [OH] t \quad [2.6]$$

where k_{OH} is the PAH dependent rate constant for reaction with OH radicals¹⁹, $[OH]$ is the concentration of hydroxyl radicals in the considered mixed layer, dependent on temperature (T , °C)³² and estimated from

$$[OH] = (0.5 + 4 (T - 273.15)) 10^5 \quad [2.7]$$

We do not provide the atmospheric degradation fluxes of SALCs due to major uncertainties in their k_{OH} values.

RESULTS AND DISCUSSION

108 gas, 108 aerosol, and 68 dissolved seawater phase samples from the lower atmosphere and surface waters were sampled in the Atlantic, Pacific and Indian Oceans during the *Malaspina 2010* circumnavigation expedition²² (Figure 2.1). 64 individual PAHs, corresponding to 28 parent and isomer groups of alkylated PAHs, were analyzed (mean concentrations of individual PAHs per ocean is showed in Table S2.1). Gas phase concentrations (ng m^{-3}) were highest in the North Atlantic Ocean, with mean Σ_{64} PAHs C_G (as the sum of all measured compounds) of 41 ng m^{-3} . The mean C_G did not differ significantly in the South Atlantic, Indian and Pacific oceans, but concentrations were higher in oceanic regions close to continents (Figure 2.1, top panel). Aerosol phase PAH concentrations (ng m^{-3}) were significantly higher in the Indian Ocean with a mean Σ_{64} PAHs of 10 ng m^{-3} (Figure 2.1 middle panel), associated with air mass back trajectories from Southern Asia. The global distribution of PAHs in the surface ocean shows a lower variability in concentrations than that in the atmosphere. Dissolved phase (ng L^{-1}) oceanic basin average concentrations of Σ_{64} PAHs ranged from 3.5 ng L^{-1} (North Atlantic) to 2 ng L^{-1} (Indian Ocean). Higher C_W was also observed close to continents than at the center of the oceanic basins, with the highest concentrations of PAHs found adjacent to the South American and South African coasts (Figure 2.1, bottom panel).

The relative abundance of individual PAHs in the gas, aerosol and dissolved seawater phases depends on the hydrophobicity and volatility of each chemical, as reflected in the PAH profiles measured (Figure S2.1). The gas and dissolved phase were dominated by low MW PAHs. In the gas phase, phenanthrene (global mean 6.1 ng m^{-3}), its methylated forms (methyl-phenanthrenes 5.7 ng m^{-3} , dimethyl-phenanthrenes 2.1 ng m^{-3}), and dibenzothiophene (DBT) and its methylated forms (0.7 ng m^{-3} for DBT, 2.5 ng m^{-3} methyl-DBTs, and 4.2 ng m^{-3} dimethyl-DBTs) accounted for more than 70% of Σ_{64} PAHs. There was a larger abundance of the high MW PAHs, such as chrysene (global mean 0.2 ng m^{-3}) and benzo[*a*]anthracene (global mean 0.2 ng m^{-3}) in the aerosol phase. In the seawater dissolved phase, fluoranthene and pyrene were the more abundant PAHs (global means of 0.3 and 0.4 ng L^{-1}).

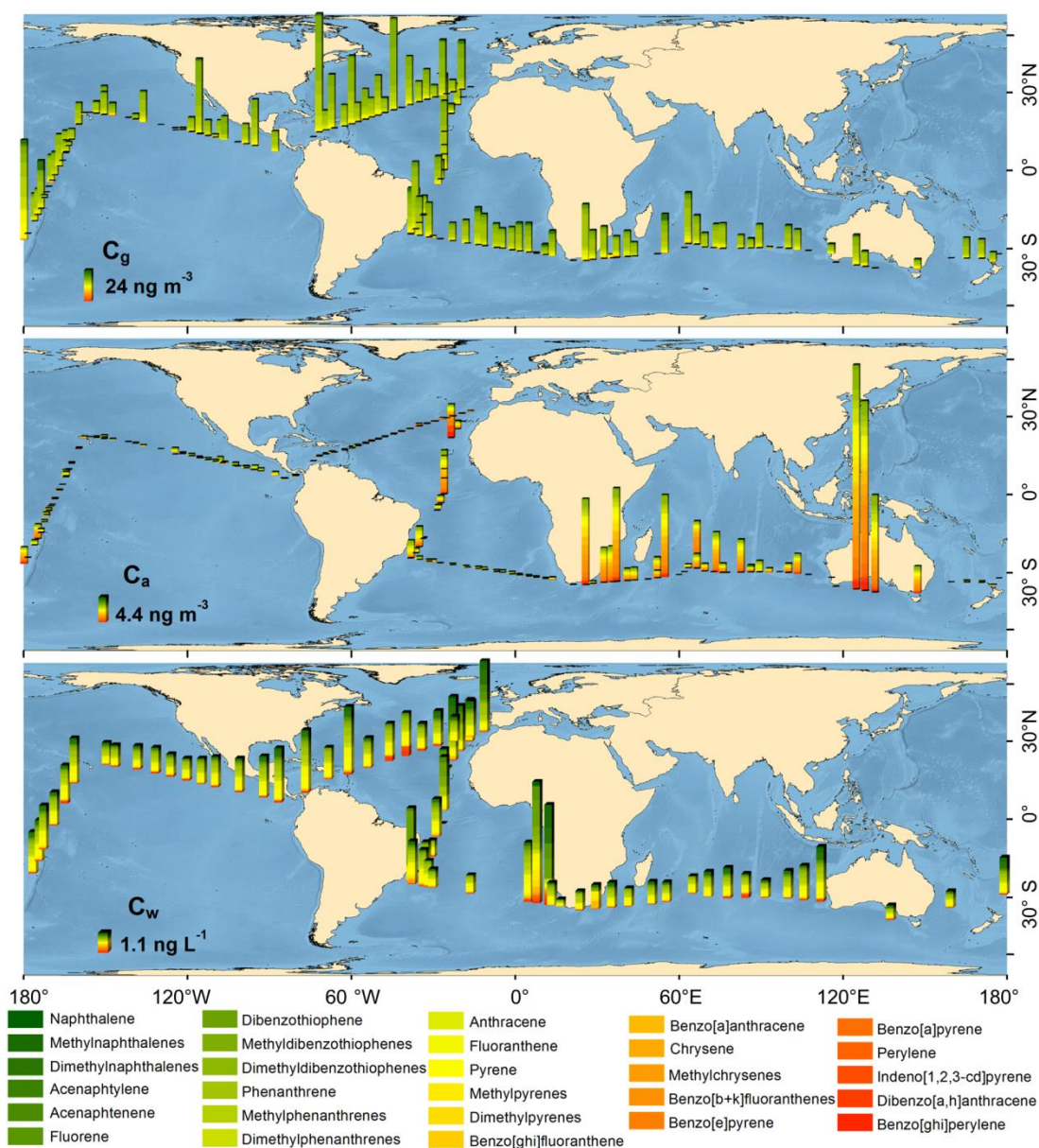


Figure 2.1. Concentration of PAHs in the gas phase (upper panel), aerosol phase (middle panel) and dissolved water phase (bottom panel). Colored bar represents the sum of the 28 quantified parent and alkylated PAHs, being each individual color noted in the bottom legend (from green, the lightest PAHs, to red, the heaviest PAHs).

The measured C_G , C_A and C_W fall within the range of previously reported concentrations for individual PAHs in the marine environment^{4,7,17,18}, but here we report the occurrence of a larger number of individual PAHs, and therefore, greater total concentrations.

Dry deposition of aerosol-bound PAHs ($\text{ng m}^{-2} \text{d}^{-1}$), is the main depositional process for PAHs with 5 or more aromatic rings²⁰. Average F_{DD} for Σ_{64} PAHs ranged from $1 \text{ ng m}^{-2} \text{d}^{-1}$ (in the open ocean) to almost $2500 \text{ ng m}^{-2} \text{d}^{-1}$ (near the coasts of South Africa and Australia, Figure 2.2), with this variability depending mainly on the concentration of PAHs in the suspended aerosol, but also on the variables affecting the deposition velocities such as the chemical vapor pressure and wind speed.

Wet deposition fluxes ($\mu\text{g m}^{-2} \text{d}^{-1}$) of Σ_{64} PAHs for the 11 rain events that occurred during the Malaspina Circumnavigation were in the order of hundreds to $5000 \mu\text{g m}^{-2} \text{d}^{-1}$ (Figure S2.2). Wet deposition is an efficient scavenging process of atmospheric gas and aerosol phase semivolatile organic compounds. However, rain events are sporadic, and of lower global relevance than the other depositional processes³³.

Diffusive air-water fluxes are the main process driving the exchange of the lighter SALCs present in marine samples, such as 2-4 aromatic ring PAHs²⁰. We estimated the net diffusive air-water exchange ($\text{ng m}^{-2} \text{d}^{-1}$) by applying the two-film resistance model¹³ to the measured gas and dissolved phase concentrations. There was a net input from the atmosphere to the ocean for most PAHs, except for the more volatile compounds such as parent and alkylated naphthalenes and DBTs which represent between 27 to 46% of Σ_{64} PAHs (Figure 2.2 and S2.3).

The integrated monthly F_{AW} fluxes (Tg month^{-1}) of the 5-6 ring PAHs were in the same order of magnitude than F_{DD} fluxes in all sampled basins, except in the Indian Ocean where dry deposition fluxes were higher (Figure 2.3). For the other 3-4 rings PAHs, F_{AW} was up to 3 orders of magnitude greater than F_{DD} in all oceans. The global gross volatilization and gross absorption of Σ_{64} PAHs were $0.042 \text{ Tg month}^{-1}$, $0.132 \text{ Tg month}^{-1}$, respectively, resulting in a net input of atmospheric Σ_{64} PAHs to the ocean of $0.090 \text{ Tg month}^{-1}$ (Figure S2.3), 90 times larger than the global dry deposition of aerosol-bound PAHs estimated at $0.001 \text{ Tg month}^{-1}$.

Results 2

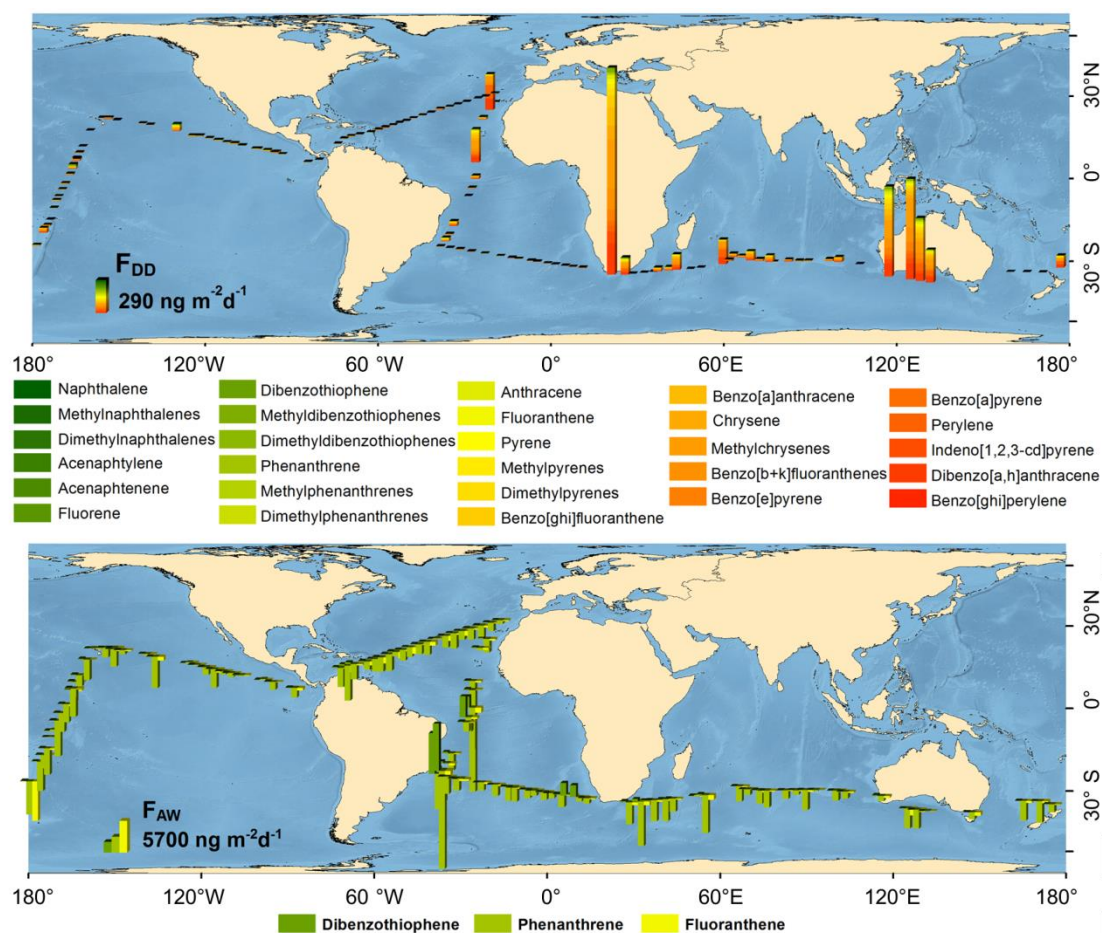


Figure 2.2. Global measurements of the 2 more relevant processes affecting PAHs exchange in the open ocean: Dry deposition fluxes for the 28 analyzed compounds (Top panel) and net diffusive fluxes for 3 representative compounds (bottom panel). In upper panel, colored bar represents the sum of the 28 quantified compounds, being each individual color noted in the bottom legend (from green, the lightest PAHs, to red, the heaviest PAHs). In bottom panel downwards bars indicate net deposition into the ocean, and upwards bars net volatilization of the compounds.

For comparison, the collapse of the Deepwater Horizon drilling rig in the Gulf of Mexico in 2010, the largest accidental oil spill to the ocean, delivered an estimated input of $2.1 \cdot 10^{10} \text{ g}$ of PAHs to the ocean¹. The monthly net diffuse input of PAHs to the ocean estimated here is 4-fold larger than the reported Deepwater Horizon PAHs release to the ocean, thus indicating that the annual atmospheric input of PAHs to the ocean amounts to about 50 Deepwater Horizon accidents. This comparison confirms the important role that diffuse fluxes play at a global scale on the overall atmosphere-ocean exchange of semivolatile organic compounds.

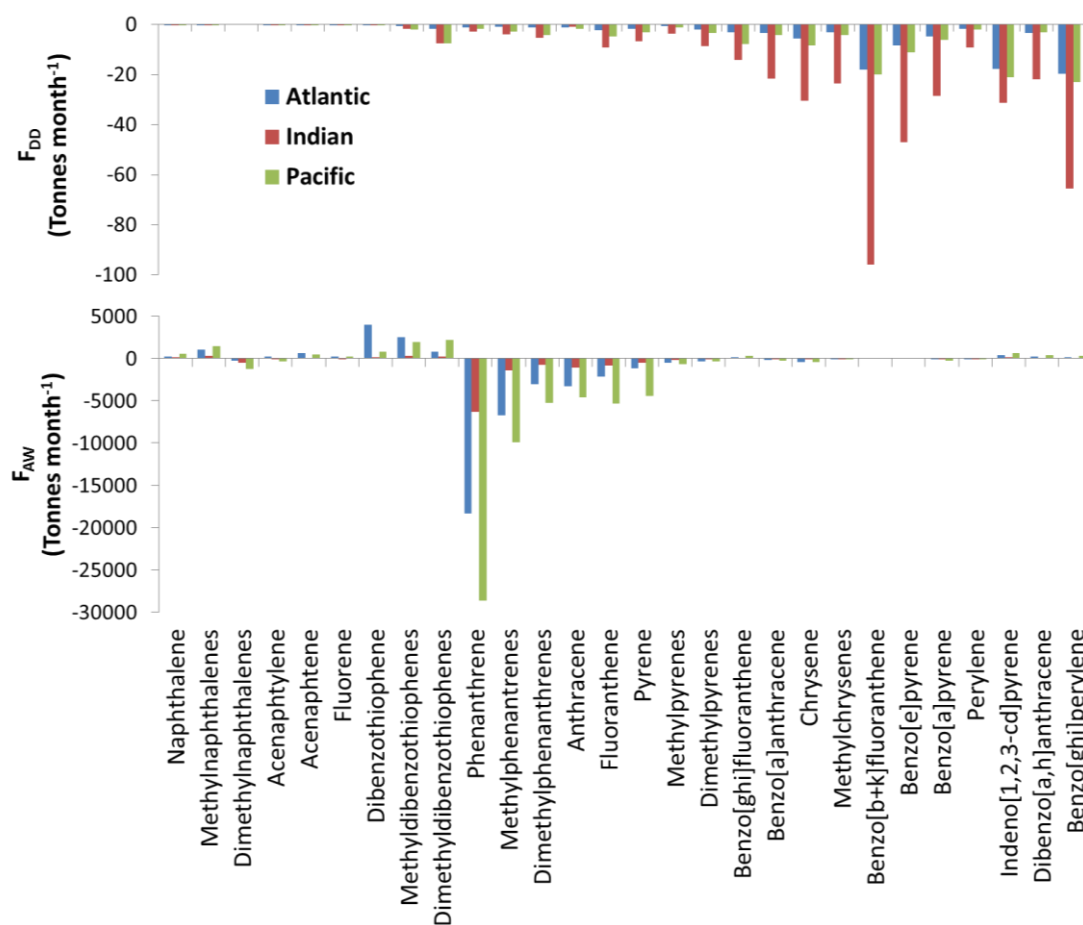


Figure 2.3. Dry deposition (F_{DD}) and net diffusive (F_{AW}) fluxes averaged per month for the Atlantic, Pacific and Indian Oceans.

In addition to the amount of PAHs transferred to the ocean, PAHs are also degraded during their atmospheric transport due to reaction with OH radicals¹⁹. The estimated degradation fluxes ($\text{ng m}^{-2} \text{d}^{-1}$) over the oceanic atmosphere (Figure S2.4) account for an additional sink of $0.18 \text{ Tg month}^{-1}$ of Σ_{64} PAHs. The large PAHs net deposition to the ocean and atmospheric sink must be supported by large global PAH sources, mainly from continental origin. The increase of total global atmospheric emissions has been reported for the last century, mainly due to the use of fossil and bio fuels, and wildfires⁵. Potential biogenic sources may also be ubiquitous from land².

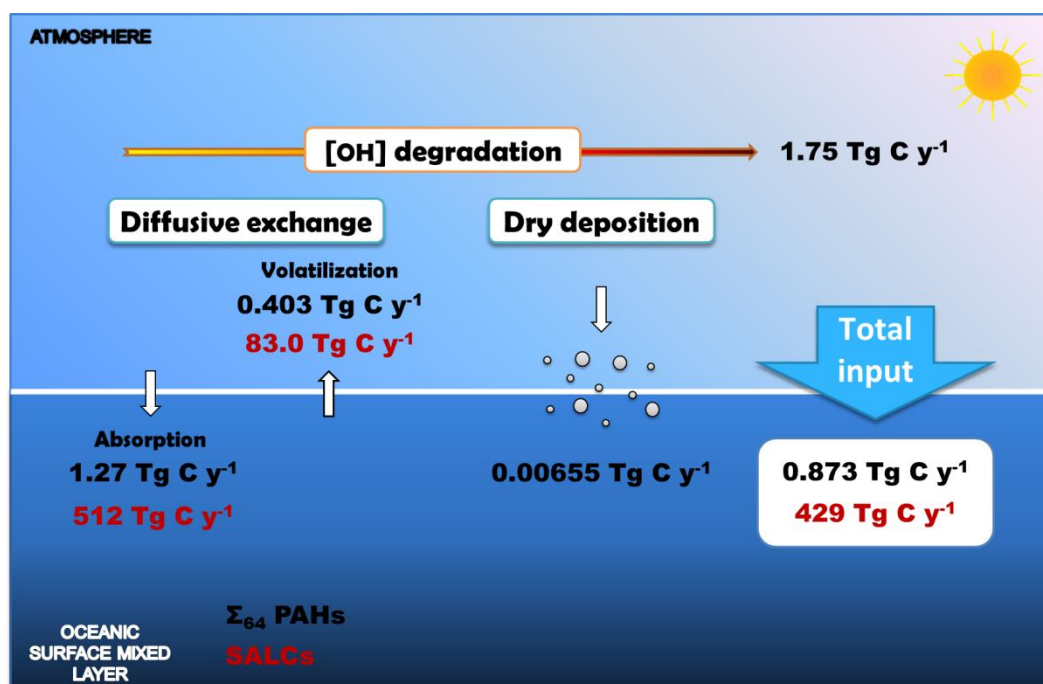


Figure 2.4. Atmosphere-ocean exchange of carbon associated to semivolatile aromatic hydrocarbons (SALCs, figures in red), and Σ_{64} PAHs (figures in black).

When extrapolated annually, and expressed as carbon fluxes, the global annual input of Σ_{64} PAHs to the ocean is estimated to be 0.87 Tg C y^{-1} (Figure 2.4). This flux is of comparable magnitude to the estimated oceanic volatilization flux of some VOCs such as isoprene (1.1 to 1.29 Tg C y^{-1}), or dimethyl sulfur (2.8 Tg C y^{-1}), but still lower than most estimates of the oceanic sink of oxygenated VOCs such as methanol (0.3 to 101 Tg C y^{-1}) and acetone (0.7 to 67 Tg C y^{-1})^{8,11}. However, the measured fluxes of Σ_{64} PAHs only account for a small fraction of the total SALCs present in the gas and dissolved phases. There are hundreds, if not thousands, of other SALCs, including oxygenated PAHs, Nitro-PAHs, halogenated-PAHs, and even the not yet resolved and identified aromatic compounds^{24,29}. When analyzed by gas chromatography coupled to mass spectrometry, the aromatic fraction of a gas or dissolved water sample comprises hundreds of other compounds than targeted PAHs. These semivolatile compounds of similar polarity as aromatic hydrocarbons, appear on chromatograms as resolved compounds over a large hump referred to as unresolved complex mixture^{24,29} which includes the majority of SALCs (Figure 2.5). The SALCs are semi volatile organic compounds of middle polarity, thus propitious to exchange between air and water.

We quantified the total gas and dissolved phase SALC concentrations and estimated their fluxes for a representative subset of paired samples. Dissolved and gas phase concentrations of SALCs ranged between 360 and 1900 ng C L⁻¹ and between 2000 and 47000 ng C m⁻³, respectively. The SALC concentrations in the dissolved and gas phase are between 100 and 7000 times larger than the Σ_{64} PAH concentrations, with this difference being highest for the gas samples (Figure S2.5). The estimated average net diffusive flux of SALCs from the atmosphere to the ocean is of 4.3 mg C m⁻² d⁻¹ (0.36 mmol C m⁻² d⁻¹), which is of comparable magnitude to the reported air-sea CO₂ fluxes⁹. The global diffusive gross absorption and volatilization fluxes of SALCs are of 512 Tg C y⁻¹ and 83 Tg C y⁻¹ respectively, resulting in a net input of organic carbon to the Atlantic, Pacific and Indian oceans of 429 Tg C y⁻¹ (Figure 2.4). This input is larger than the reported 244 Tg C y⁻¹ for dry and wet deposition of organic carbon to the global oceans³⁴. The global net uptake of atmospheric CO₂ by the ocean is of 2700 Tg C y⁻¹⁹, seven fold higher than the estimated SALC net fluxes. Furthermore, there are other fractions of semivolatile organic matter (aliphatic UCM, polar UCM)²⁹ with yet unquantified inventories and fluxes which may be playing a role in the global biogeochemical cycles. This work supports previous claims from studies using alternative approaches¹³⁻¹⁵ suggesting an important role of atmospheric fluxes of SOCs to the ocean as a component of the marine organic carbon budget.

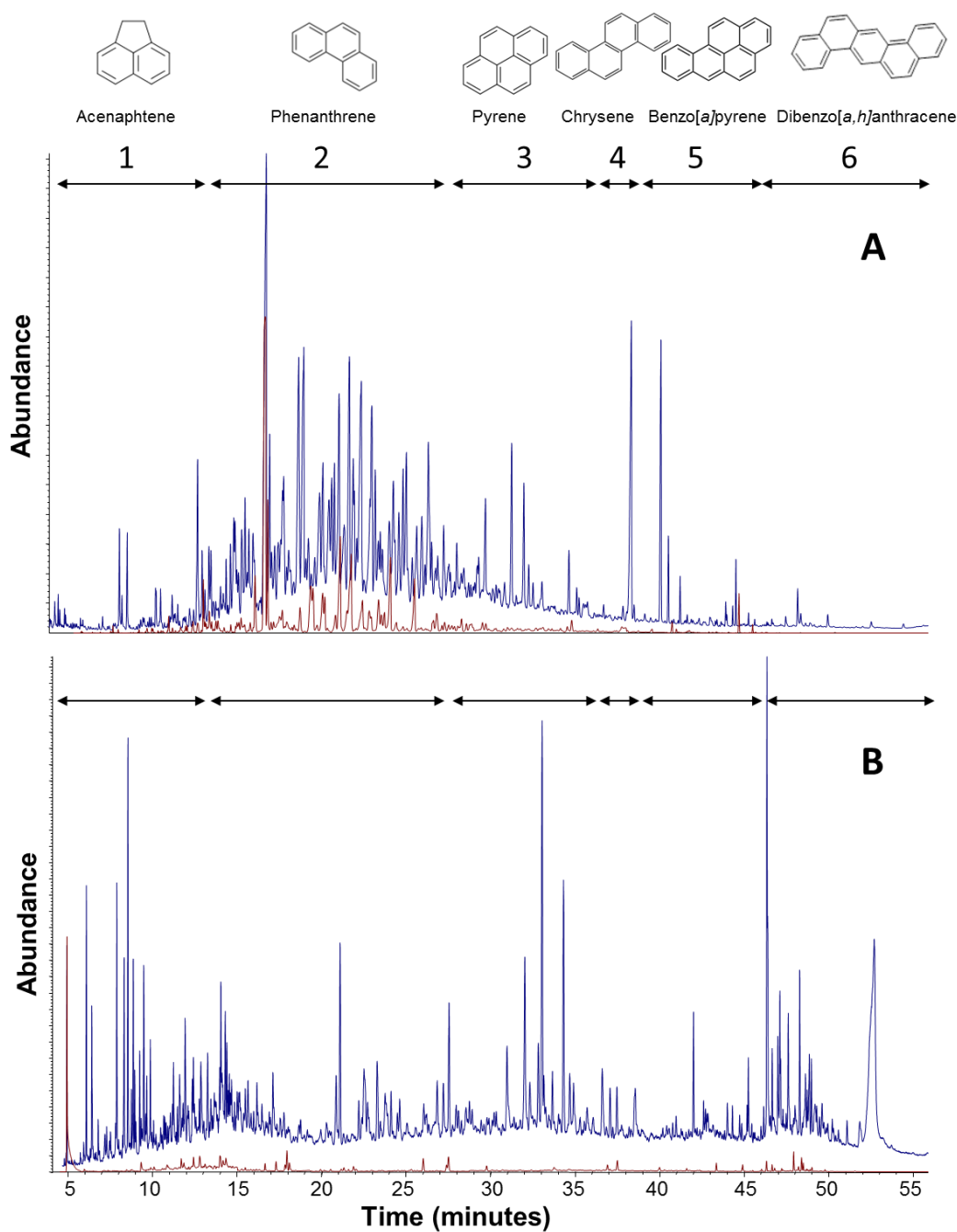


Figure 2.5. Overlaid chromatograms of a gas phase sample (A) and dissolved phase sample (B). In blue the total ion chromatogram (TIC) of the total aromatic fraction obtained by GC-MS in full scan mode and in red the TIC obtained by GC-MS in SIM mode of the analyzed ions. Quantification groups and standards are 1) from retention time 6 to 12.38 minutes using Acenaphthene, 2) from 12.38 to 28 minutes using Phenanthrene, 3) from 28 to 37.5 minutes using Pyrene, 4) from 37.5 to 39 minutes using Chrysene, 5) from 39 to 46.5 minutes using Benzo[a]pyrene and 6) from 46.5 to 56 minutes using Dibenzo[a,h]anthracene as reference standard..

These large inputs and outputs of SALCs in the open ocean have important implications in the Earth Sciences which have not hitherto been accounted for³⁵. Many PAHs are known to be efficiently degraded by bacteria in marine waters⁴, and thus, atmospheric inputs of PAHs and other SALCs could fuel ocean respiration¹³. Furthermore, the presence of a sustained and sizable diffusive input of SALCs and PAHs to the ocean could condition marine microbial communities for the capacity to degrade these compounds, thereby allowing rapid degradation of these compounds when introduced from point sources, such as oil spills³⁶. In addition, some PAHs have been described as precursors of secondary organic aerosols (SOA)³⁷, and the large volatilization fluxes of some SALCs could play an important role on SOA formation and other atmospheric chemistry processes. Conversely, some PAHs and the UCM can also have toxic effects on the oceanic food webs^{3,29}.

Whereas PAHs are natural components of the environment, increasing fossil fuel use have led to a major growth in PAH inputs during the anthropocene⁵. The results presented here show that diffusive PAH and SALC contributions from the atmosphere to the ocean represent a key perturbation of the oceanic carbon cycle and potentially marine food webs, which remains largely unexplored and requires urgent research efforts.

ACKNOWLEDGEMENTS

This work was funded by the Spanish Government through the Malaspina 2010 project. We acknowledge the support of RV Hespérides staff and UTM technicians during the cruise. B.G-G. and M-C. F-P. acknowledge predoctoral fellowships from the BBVA Foundation and CSIC. Diana García, Gemma Caballero and María J. Ojeda are acknowledged for collaborating in the laboratory work.

REFERENCES

- 1 Reddy, C. M. *et al.* Composition and fate of gas and oil released to the water column during the Deepwater Horizon oil spill. *Proceedings of the National Academy of Sciences* **109**, 20229-20234, doi:10.1073/pnas.1101242108 (2012).
- 2 Cabrerizo, A. *et al.* Ubiquitous net volatilization of polycyclic aromatic hydrocarbons from soils and parameters influencing their soil-air partitioning. *Environmental Science & Technology* **45**, 4740-4747, doi:10.1021/es104131f (2011).
- 3 Hylland, K. Polycyclic aromatic hydrocarbon (PAH) ecotoxicology in marine ecosystems. *Journal of Toxicology and Environmental Health A* **69**, 109-123, doi:10.1080/15287390500259327 (2006).
- 4 Berrojalbiz, N. *et al.* Biogeochemical and physical controls on concentrations of polycyclic aromatic hydrocarbons in water and plankton of the Mediterranean and Black Seas. *Global Biogeochemical Cycles* **25** (2011).
- 5 Zhang, Y. & Tao, S. Global atmospheric emission inventory of polycyclic aromatic hydrocarbons (PAHs) for 2004. *Atmospheric Environment* **43**, 812-819, doi:10.1016/j.atmosenv.2008.10.050 (2009).
- 6 Gonzalez-Gaya, B., Zuniga-Rival, J., Ojeda, M. J., Jimenez, B. & Dachs, J. Field measurements of the atmospheric dry deposition fluxes and velocities of polycyclic aromatic hydrocarbons to the global oceans. *Environmental Science & Technology* **48**, 5583-5592, doi:10.1021/es500846p (2014).
- 7 Ma, Y. *et al.* Deposition of polycyclic aromatic hydrocarbons in the North Pacific and the Arctic. *Journal of Geophysical Research: Atmospheres* **118**, 5822-5829, doi:10.1002/jgrd.50473 (2013).
- 8 Carpenter, L. J., Archer, S. D. & Beale, R. Ocean-atmosphere trace gas exchange. *Chemical Society Reviews* **41**, 6473-6506, doi:10.1039/c2cs35121h (2012).
- 9 Le Quéré, C. *et al.* Global carbon budget 2013. *Earth System Science Data* **6**, 235-263, doi:10.5194/essd-6-235-2014 (2014).
- 10 Park, J.-H. *et al.* Active Atmosphere-Ecosystem Exchange of the Vast Majority of Detected Volatile Organic Compounds. *Science* **341**, 643-647, doi:10.1126/science.1235053 (2013).
- 11 Yang, M. *et al.* Air-sea fluxes of oxygenated volatile organic compounds across the Atlantic Ocean. *Atmospheric Chemistry and Physics* **14**, 7499-7517, doi:10.5194/acp-14-7499-2014 (2014).
- 12 Goldstein, A. H. & Galbally, I. E. Known and unexplored organic constituents in the earth's atmosphere. *Environmental Science & Technology* **41**, 1514-1521 (2007).
- 13 Dachs, J. *et al.* High atmosphere-ocean exchange of organic carbon in the NE subtropical Atlantic. *Geophysical research letters* **32** (2005).
- 14 Hauser, E. J., Dickhut, R. M., Falconer, R. & Wozniak, A. S. Improved method for quantifying the air-sea flux of volatile and semi-volatile organic carbon. *Limnology and Oceanography: Methods* **11**, 287-297 (2013).
- 15 Ruiz-Halpern, S. *et al.* Ocean-atmosphere exchange of organic carbon and CO₂ surrounding the Antarctic Peninsula. *Biogeosciences* **11**, 2755-2770 (2014).
- 16 Lohmann, R., Breivik, K., Dachs, J. & Muir, D. Global fate of POPs: Current and future research directions. *Environmental Pollution* **150**, 150-165 (2007).
- 17 Cabrerizo, A., Galbán-Malagón, C., Del Vento, S. & Dachs, J. Sources and fate of polycyclic aromatic hydrocarbons in the Antarctic and Southern Ocean atmosphere. *Global Biogeochemical Cycles* **28**, 1424-1436 (2014).
- 18 Castro-Jiménez, J., Berrojalbiz, N., Wollgast, J. & Dachs, J. Polycyclic aromatic hydrocarbons (PAHs) in the Mediterranean Sea: Atmospheric occurrence, deposition

- and decoupling with settling fluxes in the water column. *Environmental Pollution* **166**, 40-47 (2012).
- 19 Keyte, I. J., Harrison, R. M. & Lammel, G. Chemical reactivity and long-range transport potential of polycyclic aromatic hydrocarbons - a review. *Chemical Society Reviews* **42**, 9333-9391, doi:10.1039/C3CS60147A (2013).
- 20 Gigliotti, C. L. *et al.* Air-water exchange of polycyclic aromatic hydrocarbons in the New York-New Jersey, USA, Harbor Estuary. *Environmental Toxicology and Chemistry* **21**, 235-244 (2002).
- 21 Nizzetto, L. *et al.* PAHs in air and seawater along a North-South Atlantic transect: Trends, processes and possible sources. *Environmental Science and Technology* **42**, 1580-1585 (2008).
- 22 Duarte, C. M. Seafaring in the 21st Century: The Malaspina 2010 Circumnavigation Expedition. *Limnology and Oceanography Bulletin* **24**, 11-14, doi:10.1002/lob.10008 (2015).
- 23 Berrojalbiz, N. *et al.* Accumulation and Cycling of Polycyclic Aromatic Hydrocarbons in Zooplankton. *Environmental Science & Technology* **43**, 2295-2301, doi:10.1021/es8018226 (2009).
- 24 White, H. K., Xu, L., Hartmann, P., Quinn, J. G. & Reddy, C. M. Unresolved complex mixture (UCM) in coastal environments is derived from fossil sources. *Environmental science & technology* **47**, 726-731 (2013).
- 25 Farrington, J. W. & Quinn, J. G. "Unresolved Complex Mixture" (UCM): A brief history of the term and moving beyond it. *Marine Pollution Bulletin* **96**, 29-31, doi:10.1016/j.marpolbul.2015.04.039 (2015).
- 26 Sutton, P. A., Lewis, C. A. & Rowland, S. J. Isolation of individual hydrocarbons from the unresolved complex hydrocarbon mixture of a biodegraded crude oil using preparative capillary gas chromatography. *Organic Geochemistry* **36**, 963-970, doi:10.1016/j.orggeochem.2004.11.007 (2005).
- 27 Ventura, G. T. *et al.* Analysis of unresolved complex mixtures of hydrocarbons extracted from Late Archean sediments by comprehensive two-dimensional gas chromatography (GC×GC). *Organic Geochemistry* **39**, 846-867, doi:10.1016/j.orggeochem.2008.03.006 (2008).
- 28 Booth, A. M., Scarlett, A. G., Lewis, C. A., Belt, S. T. & Rowland, S. J. Unresolved Complex Mixtures (UCMs) of Aromatic Hydrocarbons: Branched Alkyl Indanes and Branched Alkyl Tetralins are present in UCMs and accumulated by and toxic to, the mussel *Mytilus edulis*. *Environmental Science & Technology* **42**, 8122-8126, doi:10.1021/es801601x (2008).
- 29 Melbye, A. G. *et al.* Chemical and toxicological characterization of an unresolved complex mixture-rich biodegraded crude oil. *Environmental Toxicology and Chemistry* **28**, 1815-1824 (2009).
- 30 Donkin, P., Smith, E. L. & Rowland, S. J. Toxic Effects of Unresolved Complex Mixtures of Aromatic Hydrocarbons Accumulated by Mussels, *Mytilus edulis*, from Contaminated Field Sites. *Environmental Science & Technology* **37**, 4825-4830, doi:10.1021/es021053e (2003).
- 31 Bamford, H. A., Poster, D. L. & Baker, J. E. Temperature dependence of Henry's law constants of thirteen polycyclic aromatic hydrocarbons between 4°C and 31°C. *Environmental Toxicology and Chemistry* **18**, 1905-1912 (1999).
- 32 Jurado, E. & Dachs, J. Seasonality in the "grasshopping" and atmospheric residence times of persistent organic pollutants over the oceans. *Geophysical Research Letters* **35** (2008).
- 33 Jurado, E. *et al.* Wet deposition of persistent organic pollutants to the global oceans. *Environmental Science and Technology* **39**, 2426-2435 (2005).

- 34 Jurado, E., Dachs, J., Duarte, C. M. & Simó, R. Atmospheric deposition of organic and black carbon to the global oceans. *Atmospheric Environment* **42**, 7931-7939 (2008).
- 35 Sarmiento, J. L. *Ocean biogeochemical dynamics*. (Princeton University Press, 2013).
- 36 King, G. M., Kostka, J. E., Hazen, T. C. & Sobecky, P. A. Microbial Responses to the Deepwater Horizon Oil Spill: From Coastal Wetlands to the Deep Sea. *Annual Review of Marine Science* **7**, 377-401, doi:doi:10.1146/annurev-marine-010814-015543 (2015).
- 37 Chan, A. W. H. *et al.* Secondary organic aerosol formation from photooxidation of naphthalene and alkylnaphthalenes: implications for oxidation of intermediate volatility organic compounds (IVOCs). *Atmospheric Chemistry and Physics* **9**, 3049-3060 (2009).

3. Perfluoroalkylated Substances in the Global Tropical and Subtropical Surface Oceans

Belén González-Gaya^{1,2}, Jordi Dachs², Jose L. Roscales¹, Gemma Caballero², Begoña Jiménez^{1*}

¹Department of Instrumental Analysis and Environmental Chemistry, Institute of Organic Chemistry, Spanish National Research Council (IQOG-CSIC), Juan de la Cierva 3, 28006 Madrid, Spain.

²Department of Environmental Chemistry, Institute of Environmental Assessment and Water Research (IDAEA-CSIC), Jordi Girona 18-26, 08034 Barcelona, Catalunya, Spain.

*Corresponding author. Email: bjimenez@iqog.csic.es

Environ. Sci. Technol., 2014, 48 (22), pp 13076–13084

DOI: 10.1021/es503490z

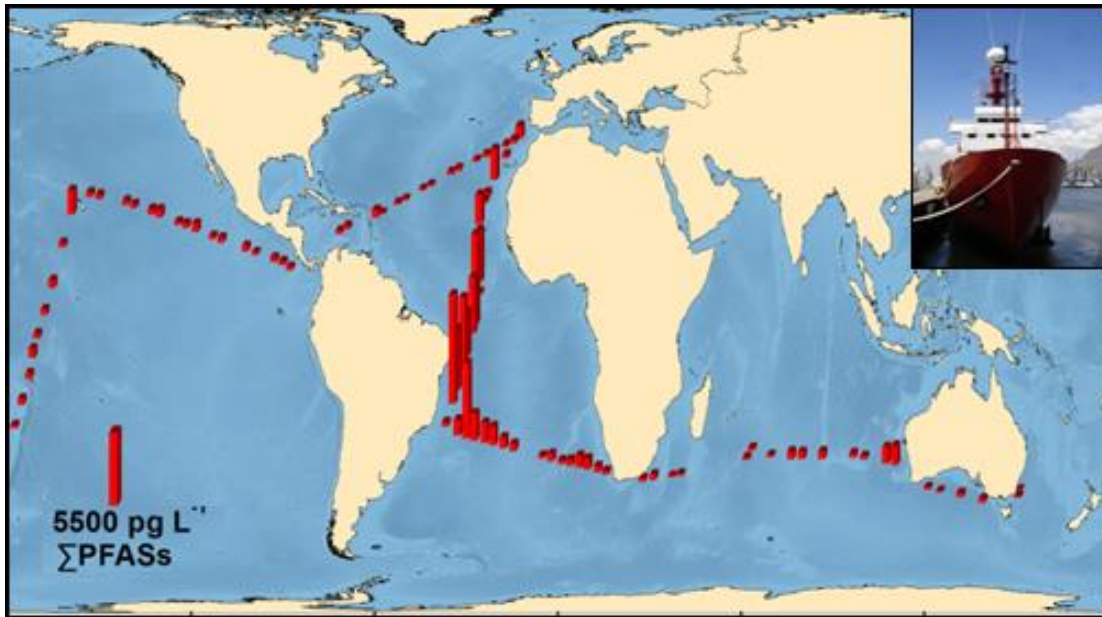
Publication Date (Web): October 17, 2014

Copyright © 2014 American Chemical Society

ABSTRACT

In this study, perfluoroalkylated substances (PFASs) were analyzed in 92 surface seawater samples taken during the *Malaspina 2010* expedition which covered all the tropical and subtropical Atlantic, Pacific and Indian oceans. Nine ionic PFASs including C6-C10 perfluoroalkyl carboxylic acids (PFCAs), C4 and C6-C8 perfluoroalkyl sulfonic acids (PFSA) and two neutral precursors perfluoroalkyl sulfonamides (PFASAs), were identified and quantified. The Atlantic Ocean presented the broader range in concentrations of total PFASs (131-10900 pg L⁻¹, median 645 pg L⁻¹, n=45) compared to the other oceanic basins, probably due to a better spatial coverage. Total concentrations in the Pacific ranged from 344 to 2500 pg L⁻¹ (median=527 pg L⁻¹, n=27) and in the Indian Ocean from 176 to 1976 pg L⁻¹ (median=329, n=18). Perfluorooctane sulfonic acid (PFOS) was the most abundant compound, accounting for 33% of the total PFASs globally, followed by perfluorodecanoic acid (PFDA, 22%) and perfluorohexanoic acid (PFHxA, 12%), being the rest of the individual congeners under 10% of total PFASs, even for perfluorooctane carboxylic acid (PFOA, 6%). PFASAs accounted for less than 1% of the total PFASs concentration. This study reports the ubiquitous occurrence of PFCAs, PFSA and PFASAs in the global ocean, being the first attempt, to our knowledge, to show a comprehensive assessment in surface water samples collected in a single oceanic expedition covering tropical and subtropical oceans for the first time.

The potential factors affecting their distribution patterns were assessed including the distance to coastal regions, oceanic subtropical gyres, currents and biogeochemical processes. Field evidence of biogeochemical controls on the occurrence of PFASs was tentatively assessed considering environmental variables (solar radiation, temperature, chlorophyll *a* concentrations among others), and these showed significant correlations with some PFASs, but explaining small to moderate percentages of variability. This suggests that a number of physical and biogeochemical processes collectively drive the oceanic occurrence and fate of PFASs in a complex manner.



Graphical Abstract 3.

INTRODUCTION

PFASs, such as PFCAs and PFASs have received increasing worldwide attention due to their global distribution and toxic properties¹. PFASs are ubiquitous, being found in densely populated areas² or the remote poles^{3,4}, in a huge variety of environmental compartments and ecosystems⁵⁻⁷. Many PFASs have also been stated as bioaccumulative and susceptible to biomagnification⁸⁻¹⁰, thus meeting the criteria of persistent organic pollutants (POPs). PFOS, its salts and perfluorooctane sulfonyl fluoride were added in 2009 by the Fourth Conference of Parties to the Stockholm Convention on POPs¹¹. In spite of this, many PFASs and volatile precursors are still being produced¹².

The high stability of the Fluorine-Carbon bond makes PFASs extremely persistent in the environment. In addition, PFASs have higher water solubility and lower lipophilicity when compared to other legacy POPs, thus the processes driving the long range transport and cycling of ionic PFASs are different than those described for more hydrophobic pollutants, for instance the polychlorinated biphenyls^{13,14}. The neutral and more volatile PFASs like the fluorotelomer alcohols and PFASAs undergo atmospheric transport^{15,16}, which after oxidation in the atmosphere reach remote oceanic and continental regions through dry/wet deposition¹⁷⁻¹⁹. However, direct transport by oceanic water masses is thought to be the main vector for the global transport of the ionic PFASs from source regions, as suggested for PFOA and PFOS²⁰⁻²³. Besides, the open-ocean is presumably the main final global sink for the most persistent ionic species^{20,24}. Nevertheless, many uncertainties exist on the main drivers of their global distribution, including the influence of source regions, currents and biogeochemical cycles, such as the biological pump and degradative processes.

There are a number of previous studies on the occurrence of PFASs in the oceans²⁵⁻²⁷, focusing primarily on long-chain PFCAs and PFASAs, especially PFOA and PFOS, and recently other non-ionic species, for instance PFASAs^{28,29}. Any potential comparison of levels between oceanic basins or subregions can be strongly biased due to differences in the analytical and sampling procedures of the different assessments. For this reason, a global comprehensive data set of measurements on surface water samples collected in a single oceanic expedition, for the different oceanic regions, can provide a unique

data set to identify the major known or still unknown biogeochemical and physical processes driving the PFASs occurrence in the global ocean.

Therefore, the objectives of this study were i) to provide, for the first time, an assessment of the occurrence of PFCAs, PFSAAs and PFASAs in the surface water of all the tropical and subtropical oceans sampled during the *Malaspina 2010* expedition and analyzed using the same protocols, and ii) to assess the relative influence of coastal regions, subtropical oceanic gyres and the physical and biogeochemical controls affecting the occurrence of PFASs in the global tropical and subtropical oceans.

MATERIAL AND METHODS

Sampling

A total of 92 surface seawater samples were collected during the *Malaspina 2010* expedition performed from December 14th, 2010 to July 14th, 2011 on board of the research vessel Hespérides. The cruise completed a circumnavigation covering all the tropical and temperate oceans between 35°N and 40°S in eight consecutive transects: Cadiz (Spain) - Rio de Janeiro (Brazil) – Cape Town (South Africa) – Perth (Australia) – Sydney (Australia) – Auckland (New Zealand) – Honolulu (Hawaii, USA) – Cartagena de Indias (Colombia) – Cartagena (Spain). During the cruise, all the oceanic gyres (north and south Atlantic and Pacific, and south Indian oceans), and the coastal regions out of territorial waters were sampled (SI, Table S3.1).

Surface seawater at 3 m depth was sampled with a polyvinyl chloride (PVC) 30 L *Niskin* bottle and 1 L was collected in a polypropylene (PP) bottle, previously rinsed with methanol and washed 3 times with seawater from the *Niskin* bottle immediately before sample collection. The PP bottle was fully filled in order to avoid the loss of volatile species to the trapped air³⁰.

Sample treatment and instrumental analysis

The extraction method was based on a previously reported procedure³¹ with minor modifications. Briefly, samples were extracted on board by solid phase extraction using OASIS WAX cartridges and kept during the cruise at -20 °C until their further treatment in the laboratory (Details in SI, Text S3.1).

The instrumental analysis was performed using a Waters Acquity Ultra Performance Liquid Chromatography system coupled with a Waters XEVO TQS, triple-quadrupole mass spectrometer (UPLC-MS/MS). To further reduce instrumental contamination, a C18 hold-up column available as a PFC kit analysis from Waters®, was installed on the aqueous solvent line just before the mixing chamber.

A 10 μL aliquot of each sample was injected onto an Acquity UPLC BEH C18 column (1.7 μm , 2.1 x 50 mm; Waters®) maintained at 50 °C. Separation was achieved by the use of a gradient mobile phase of water and methanol with a constant 1% of acetonitrile buffer at a flow rate of 400 $\mu\text{L}/\text{min}$. Electrospray negative ionization (ESI) was used with the mass spectrometer operating in the multiple-reaction-monitoring (MRM) mode. Ionization and collision cell parameters were optimized for each individual analyte (SI, Table S3.2). Each sample was injected in triplicate. A calibration curve was made with 10 points from 0.001 pg to 100 pg injected on column. The quantification followed the internal standard procedure, using the labeled compounds indicated in Table S3.2. Of the 21 target analytes, 9 ionic PFASs (C_6 - C_{10} PFCAs and C_4 , C_6 - C_8 PFASs) and two neutral PFASs precursor compounds, perfluorooctane sulfonamide (PFOSA) and N-methyl perfluorooctane sulfonamide (N-MePFOSA) were identified and quantified.

Quality assurance and quality control

Fluorinated materials (e.g. Teflon®, Gore-Tex®, etc.) were avoided during the sampling and analysis. Field blank samples of the *Niskin* bottle were carried out with chromatography-grade water after washing the *Niskin* bottle with methanol and chromatography-grade water. Then, the *Niskin* field blanks were obtained subtracting the levels of PFASs present in the chromatographic-grade water not in contact with the bottle. Laboratory blanks consisted on a) chromatographic-grade water (accounted for field blanks), b) SPE-extracted chromatographic-grade water and c) the reagents used for analysis. There were no substantial differences among field and laboratory blanks *b* and *c*, showing a negligible contamination effect by neither the *Niskin* bottle nor the sample treatment method (details in SI, Table S3.3).

The method detection limit (MDL) and method quantification limit (MQL) were calculated as the mean of instrument detection limit (IDL) and instrumental quantification limit (IQL) (automatically calculated through iteration of all the analyzed samples and standards by *MassLynx* software package, Waters®) of 20 random samples plus the standard deviation. MDL ranged from 0.01 to 4.89 pg L^{-1} and MQL

Results 3

ranged from 0.01 to 10.25 $\mu\text{g L}^{-1}$. The mean recovery of the labeled surrogates ranged between 72% for PFNA- $^{13}\text{C}_5$ and 149% for PFHxA- $^{13}\text{C}_4$. Concentrations were not corrected by surrogate recoveries. Matrix spikes tests with PFHxA- $^{2}\text{C}_{13}$, PFHxS- $^{2}\text{O}_{18}$, PFOA- $^{4}\text{C}_{13}$, PFNA- $^{5}\text{C}_{13}$, PFOS- $^{4}\text{C}_{13}$, PFDA- $^{2}\text{C}_{13}$, following the same extraction and analysis procedures, resulted in recoveries of $96\pm 24\%$. See SI, Table S3.3 for details on MDL, MQL, and recoveries.

Back Trajectories and statistical analysis.

Atmospheric back trajectories were calculated with the NOAA Hysplit model online at 3 different heights (30, 200 and 500 meters) using GDAS Meteorological data from the sampling dates (SI, Figure S3.1). SPSS Statistics version 21.0 (IBM Corp.®) was used for non-parametric statistical analysis (see normality test results in Table S3.4, SI).

RESULTS AND DISCUSSION

Hemispheric and oceanic-basin occurrence of PFASs

The global median surface seawater concentration for the sum of all the analyzed compounds (Σ PFAS) was $1180 \pm 1860 \text{ pg L}^{-1}$. In the northern hemisphere the median concentration was $708 \pm 831 \text{ pg L}^{-1}$, while in the southern hemisphere the median concentration was $1620 \pm 488 \text{ pg L}^{-1}$. The Atlantic Ocean presented the broader concentrations range of Σ PFAS ($131\text{-}10900 \text{ pg L}^{-1}$, median 645 pg L^{-1} , $n=45$) compared to the other ocean basins. Total concentrations in the Pacific ranged from 344 to 2500 pg L^{-1} (median= 527 pg L^{-1} , $n=27$), and in the Indian Ocean from 176 to 1980 pg L^{-1} (median= 329 , $n=18$). Therefore, the Atlantic Ocean shows the highest concentrations globally, presenting as well a higher variability in concentrations, in accordance with previous studies (SI, Tables S3.5 and S3.6). This may be due to the fact that the sampling coverage of the Atlantic included a larger latitudinal and coastal transects versus open ocean gradients. Nevertheless, the *Malaspina* cruise did not cover the north west Pacific, where PFASs concentrations have been reported in the same range or even higher²⁰ than the maximum found in this study.

Figure 3.1 shows the global distribution of PFCAs, PFSAAs and PFASAs in surface seawater in all the tropical and subtropical oceans. There are significant differences in the relative contribution and concentrations of the three PFAS families in the different oceanic basins. Ionic PFASs were present in all the samples analyzed, while PFOSA and N-Me-PFOSA were only found in 49.4% and 61.8% of the samples, respectively. The median concentration of Σ PFASAs was 0.38 pg L^{-1} , thus significantly lower (T-test, $p<0.05$) than ionic PFASs concentrations. The global median concentrations for the two ionic groups were 595 pg L^{-1} and 189 pg L^{-1} for Σ PFCAs and Σ PFSAAs, respectively, with a different global distribution (Figure 3.1).

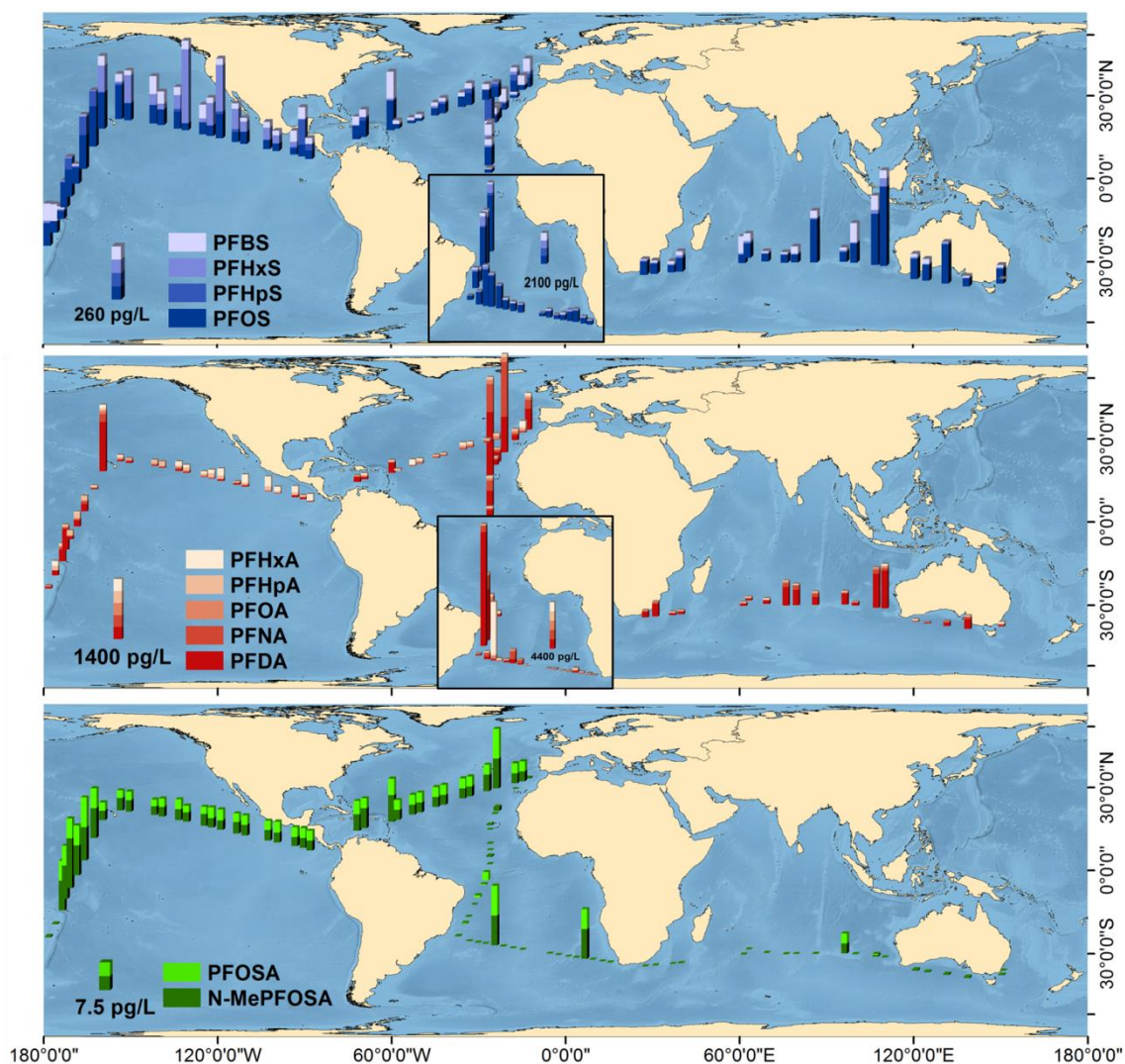


Figure 3.1. Global distribution of PFASs in the tropical and subtropical oceans. Upper panel shows the PFSA concentrations, central panel shows the PFCA concentrations and lower panel shows the PFASA concentrations. Note that the concentrations of PFSA and PFCA in the South Atlantic Ocean are shown with a different scale in the separated square sub-panels.

The inter-oceanic comparison showed no significant differences for Σ PFCA, while Σ PFSA showed statistically higher concentrations in the South Atlantic Ocean (Kruskal-Wallis, $p < 0.01$), and PFASA were significantly more abundant in the Pacific (Kruskal-Wallis, $p < 0.01$). The higher abundance in the South Atlantic may be influenced by a better coverage of continent-influenced regions, such as the area in front of Brazil, in comparison to the Pacific Ocean where more remote regions from potential sources were sampled. The fact that PFASAs, presumably airborne, have mainly been found in the northern hemisphere, would be consistent with the described direct release to the atmosphere by the fluoropolymer manufacturing sites, which are largely located in

USA, Belgium, France, Italy, Japan and into a lesser extent in China, Russia and India^{24,32,33}. The low levels of PFASAs, suggest that these are either degraded before they are deposited to seawater, and/or they are volatilized/degraded during oceanic transport³⁴.

Figure 3.2 shows the relative contribution of PFCAs, PFSA and PFASAs depending on hemispheres and oceanic basins. On average, PFOS contributed a 33% of the total PFASs (from 64% in South Atlantic to 16% in North Atlantic), followed by PFDA (22%), and PFHxA (12%), being the rest of the individual congeners under 10%, with PFOA contributing 6% and PFASAs accounting for less than 1% of the total PFASs concentration. There was a significantly higher concentration of PFSA (Kruskal-Wallis, $p < 0.004$) in the southern hemisphere, a higher concentration of PFASAs in the northern hemisphere (Kruskal-Wallis, $p < 0.01$) and no hemispheric differences for PFCAs. The most often reported PFASs, such as PFOA and PFOS, show a concentration variability of several orders of magnitude depending on the ocean basin. PFOA and PFOS concentrations in the North Atlantic (PFOA with a median of 44 $\mu\text{g L}^{-1}$ and PFOS with a median of 59 $\mu\text{g L}^{-1}$; the South Atlantic medians were 58 $\mu\text{g L}^{-1}$ and 742 $\mu\text{g L}^{-1}$ respectively), Pacific (median 25 $\mu\text{g L}^{-1}$ of PFOA; 101 $\mu\text{g L}^{-1}$ PFOS) and Indian oceans (median 23 $\mu\text{g L}^{-1}$ of PFOA; and 89 $\mu\text{g L}^{-1}$ of PFOS) were not substantially different than those previously reported (Figure 3.3 and SI, Table S3.5)^{4,26,35-37}. However, most surveys of PFASs in the Pacific Ocean correspond to coastal waters from east Asian countries^{20,31,36,38,39}. Since China and other south east Asian countries are the major consumers of many fluorinated products³², there is a huge range of concentrations between few nanograms per liter of PFOS and PFOA reported in coastal Japanese and Chinese waters,^{31,39,40} to the picograms per liter concentrations in the center of the Pacific oceanic gyres. There are few previous reports of PFAS concentrations for the southern Indian Ocean, and these are limited to coastal surveys in Australia⁴¹, or further north in the South East Asia^{42,43} with seawater concentrations similar to those measured during the *Malaspina 2010* expedition. Concentrations of other individual PFASs measured in this work are also in agreement with those reported in previous studies (SI, Table S3.6).

Results 3

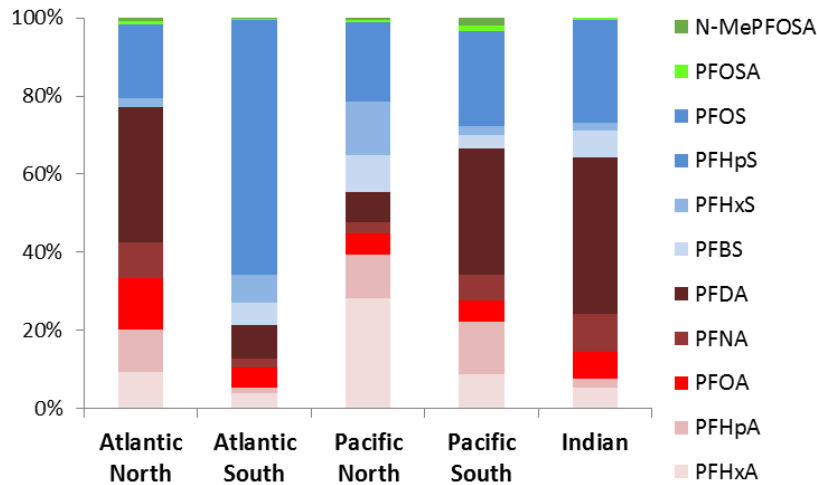


Figure 3.2. Relative contribution of the individual PFASs for each oceanic hemispherical sub basin. Sample sizes correspond to: north Atlantic n=25, south Atlantic n=22, north Pacific n=19, south Pacific n=8 and Indian Ocean n=18.

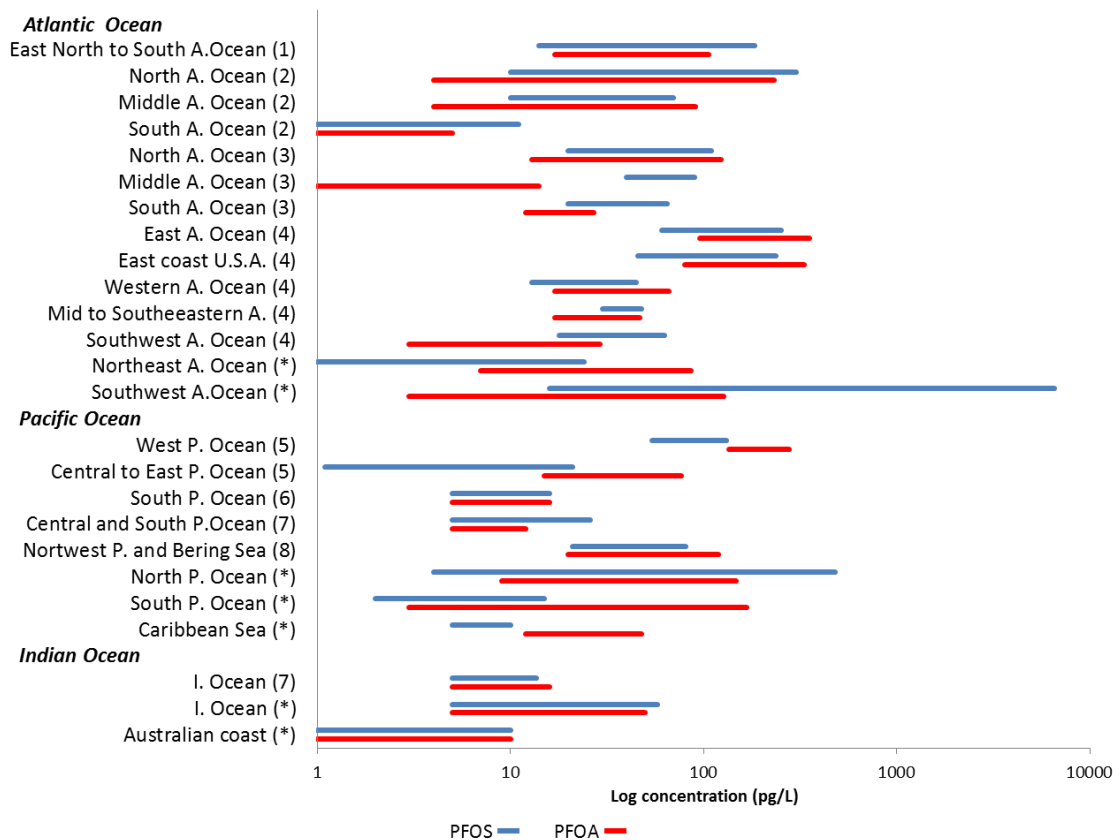


Figure 3.3. Comparison of the surface seawater concentration ranges of PFOS and PFOA measured during the Malaspina 2010 expedition with those reported in previous studies. 1) Theobald et al.(2007a)⁴⁴, 2) Ahrens et al. (2009a)²⁷, 3) Zhao et al (2012)⁴, 4) Benskin et al (2012)²⁶, 5) Yamashita et al.(2005)³¹, 6) Yamashita et al.(2008)²⁰, 7) Wei et al.(2007)⁴², 8) Cai et al. (2012b)³⁷, *) this study. The bars extend from the minimum to the maximum reported values on a logarithmic scale.

Coastal versus open ocean occurrence of PFASs in the global ocean

PFAS concentrations in coastal waters have been reported to be 1–2 orders of magnitude higher than in open-ocean waters^{12,45,46}. Moreover, their sources in the marine environment have been identified to be mostly terrestrial through wastewaters and riverine inputs, and directly linked to population density^{12,29,47}. This is consistent with decreasing concentrations from the coasts towards the open ocean (Figure 3.1). None of the sampling sites was located within the 12 miles of territorial waters, so we refer as coastal sites those that are at a distance that can range from tens of miles to more than 200 miles from the coast.

Of special interest are the high levels of PFOS found along the Brazilian coast compared with much lower concentrations in the North Atlantic Ocean, or the center of the sub-Atlantic gyre (Figure 3.1 and SI, Table S3.5). The particularly high PFOS concentrations ranging from 3240 to 6560 pg L⁻¹ found near Brazil have not been reported before in this region (Figure 3.1). Nevertheless, previous studies have reported higher levels of PFOS in the south Atlantic compared to the north Atlantic²⁶. *Sulfluramid* (N-ethyl perfluorooctane sulfonamide) is extensively used as a pesticide in Brazil, which can be transformed to PFOS via different degradation pathways^{26,48}. The declared consumption of *Sulfluramid* in 2004 was of 20.58 tons, increasing up to about 30 tons year⁻¹ in 2007³². Nonetheless, the high concentration plume detected covering a large oceanic region gives a calculated total mass of PFASs superior to the reported pesticide use in Brazil. In addition, PFAS surface concentrations were not correlated with the surface salinity during the *Malaspina* cruise, thus, without a direct apparent riverine influence. Therefore, other contributions, including atmospheric contributions of PFOS may need to be considered. The air mass backtrajectories (SI, Figure S3.1) for the lower troposphere had an oceanic origin (from the East), however, in the upper boundary layer (800 m), air masses were coming from the coastal zone of Espírito Santo and Rio de Janeiro states, among the more populated and developed in Brazil⁴⁹. Additionally, January coincides with the rainfall period⁵⁰ and before and during the sampling activities, several extreme rain events occurred, facilitating scavenging of gas phase fluorinated precursors and aerosol bound ionic PFASs by wet deposition¹⁷. Dry deposition of aerosol bound PFASs could also be a source to surface waters from the

upper boundary layer, which cannot be quantified here, even if it has been reported to be of major relevance for other pollutants in the Open Ocean⁵¹. Nevertheless, the great amount of PFASs quantified in the south Atlantic is still a surprising novelty which would deserve further research based on a more comprehensive sampling approach in the area which was out of the scope of this work.

In the Indian Ocean, there was a clear coastal-open ocean gradient of concentrations, with concentrations of PFASs, mainly PFOS and PFDA, of more than 1500 pg L⁻¹ in the Australian coast to 200 pg L⁻¹ in open seawater. The influence of Hawaii and the Caribbean islands and continents was also noticeable in the Pacific and Atlantic oceans concentrations, mainly regarding PFCAs and PFASs (Figure 3.1 and SI, Table S3.5).

Potential influence of the oceanic currents and gyres and biogeochemical processes on PFASs occurrence in the global ocean

Despite the coastal influence on PFAS concentrations in the open ocean, sometimes the maximum concentrations are not found in the sampling site closest to the continental shelf. In the regions affected by the Benguela and Brazilian currents along the South African and Brazilian coasts (SI, Figure S3.2), the maximum concentrations, especially for PFCAs and PFOS, are observed in the sampling points strongly affected by the currents, but not in the sites closest to the continental shelf (Figure 3.1). It is possible that these well delimited currents transport PFASs from other source regions, contributing more than the adjacent continental shelf, and/or that there is lower dilution within the currents.

The influence of oceanic currents driving an important variability in concentrations, especially of PFCAs, is also observed around the equator, where for both the Pacific and Atlantic oceans there are South, North and Counter Equatorial currents (SI, Figure S3.2). For instance, total PFAS levels are higher in the Atlantic Equator (due to the counter current flowing from South American coast) compared with contiguous sampling stations. In the southern hemisphere, the decrease of PFAS concentrations at higher latitudes may be influenced by the adjacent Antarctic Circumpolar Current with

low concentration of these pollutants^{20,26}. In addition, primary emissions of fluorinated compounds from south African countries are generally low^{7,26}.

The central areas of the subtropical oceanic gyres are known to accumulate “swimmer” pollutants, like plastic debris, driven by the oceanic currents transporting the contaminants⁵²⁻⁵⁵. Ionic PFASs, behaving as swimmers, show a slight increase in concentrations, especially for PFCAs, in the central areas of the Indian, north Pacific and north and south Atlantic oceans, which is consistent with oceanic currents accumulating PFASs in the center of the oceanic gyres. This accumulation is not observed for semivolatile POPs which can be volatilized driven by the higher temperatures⁵⁶. Therefore, more research should be done to analyze the gyres’ relative influence on PFASs accumulation depending on the compound volatility and environmental drivers.

Biogeochemical processes, such as sinking of organic matter and biodegradation, are known to control the occurrence of hydrophobic POPs in the water column^{57 58}, but its influence is presumably of lower importance for the less hydrophobic PFASs. Nevertheless, PFASs have been reported to enter food webs in aquatic environments from the Poles⁵⁹⁻⁶¹ to the subtropical regions^{10,62} and therefore organic matter and biota may influence their global distribution. *Longhurst provinces*⁶³, account for the geographical variability of biogeochemical and physical processes (SI, Table S3.1 and Table S3.7). Figure S3.3 (SI) shows the concentration of PFOA, PFOS, and the ratio PFOA/PFOS in the Longhurst oceanic provinces sampled during the *Malaspina 2010 Expedition*. There is an important and significant variability in the PFOA/PFOS ratio (Figure S3.3 middle panel) among the Longhurst provinces (ANOVA, $p < 0.001$). The highest PFOS concentrations and lowest PFOA/PFOS ratios are observed in the Benguela (BENG) and South Atlantic gyre (SATL) provinces, followed by the North Pacific Equatorial Countercurrent (PNEC). The highest PFOA/PFOS ratios were found in the northern hemisphere provinces, with a particular relevance of the North Atlantic Subtropical Gyre Province East (NASE) and North Atlantic Tropical Gyre Province (NATR). Generally, the variability of PFOA and PFOS and their ratio seems most probably related to proximity to source regions and currents, in addition to the intrinsic biogeochemical characteristics considered by the Longhurst provinces. The

PFOA/PFOS ratios were generally lower than 1 when averaged per biogeochemical province (Figure S3.3, SI), or averaged per oceanic subbasin (Figure 3.2). Other recent studies have described higher concentrations of PFOS than PFOA in some oceanic regions, as shown in Figure 3.3. Higher median concentration of PFOS were found in the north and south Atlantic by Theobald et al.⁶⁴ and by Ahrens et al.²⁷, respectively. Ahrens et al. also described higher PFOS than PFOA concentrations in the South Atlantic and Southern Ocean³⁵. Zhao et al.⁴ reported higher PFOS than PFOA medians in the middle and south Atlantic. Yamashita²⁰ reported higher PFOS than PFOA concentrations in the Equatorial Pacific ocean, while Benskin et al.²⁶ did not encounter a higher PFOS median in their north-south transects in 2008 and 2009, but PFOS concentrations were higher than PFOA in some regions, especially where PFOS was maximum, as observed for the South Atlantic. Wei et al.⁴² reported as well higher PFOS concentrations compared to PFOA in remote areas, particularly in the south east Indian and Southern Oceans. The overall trend is that most observations of higher PFOS than PFOA are in the southern hemisphere and equatorial oceans, and also for the remote locations. This contrasts with higher PFOA/PFOS ratios usually observed in many studies of PFAS in the northern hemisphere^{20,26,27} and other regions. In our study, the sampling sites showing PFOA/PFOS higher than 1 were also from the Northern hemisphere. It is possible that the source regional variability plays an important role explaining the relative predominance of PFOS *versus* PFOA. Nevertheless, the specific processes affecting their fate and transport once released in the environment may be of particular interest regarding their presence and relative abundance in the remote areas.

The physico-chemical and biological processes affecting the fate of PFASs have been poorly described, especially for the open ocean. However, biodegradation, adsorption to settling organic matter (biological pump), and photodegradation have shown to be relevant for other organic pollutants⁶⁵. PFASAs and other ionic PFASs precursors can degrade through photolysis and/or biotransformation processes^{34,60}. On the contrary, no biodegradation has been described for most ionic PFASs under aerobic or anaerobic conditions⁶⁶⁻⁶⁹. Nevertheless, PFOS and PFOA have been reported to degrade anaerobically in sewage sludge⁶⁶, having PFOS a fastest removal rate than PFOA⁷⁰. In

any case, defluorination of a perfluorinated compound has only appeared to occur within explicit chemical conditions (molecule conformation, pH and sulfur limiting conditions being the most relevant) which cannot be extrapolated to the open ocean⁶⁸. Nevertheless, due to the huge marine bacterial and functional diversity, the relevance of biodegradation cannot be disregarded and should be further studied.

The biological pump is an effective process to remove organic pollutants^{58,65}, but PFOS, PFOA and other PFASs have low hydrophobicities, even though it could be relevant for the longer chain substances. There are potential non-hydrophobicity driven bioconcentration processes in phytoplankton and other organic matter pools for ionic compounds^{9,71,72}. PFASs have been recently stated as proteinophilic compounds in biological tissues^{61, 73}. The partition coefficient of PFASs depends on carbon chain length, pH and organic carbon fraction^{74,75}. PFASs and PFASAs have a higher tendency to partition to organic matter than PFCAs, and indeed, PFCAs with shorter chains (less than seven carbons) have been found only in the dissolved phase, but not in suspended matter⁷⁶. Significant non-parametric correlations were found between concentrations of individual or total PFASs versus chlorophyll *a* concentrations and bacterial biomass measured at each sampling station, but generally explaining a small fraction of the variability (SI, Table S3.8). For instance PFOS and PFOA do correlate ($p < 0.05$) with chlorophyll *a* concentrations and bacterial biomass, suggesting a potential role of the biological pump and/or unknown degradative pathways decreasing their dissolved phase concentrations, processes that require further research.

The concentrations of some PFASs showed a significant correlation with the measured light intensity during the sampling periods (Σ PFASs, $p < 0.05$ and Σ PFASAs $p < 0.01$, SI, Table S3.9). A large variability of PFAS concentrations, including the sampling stations with the maximum concentrations of some PFASs, was observed at the low solar radiated areas (SI, Figure S3.4), suggesting a potential role of photodegradation. PFOS photodegradation in water has been experimentally confirmed and it depends on UV wavelength and pH. Laboratory experiments showed that 68% of PFOS is lost after 10 days of UV exposition under certain conditions,⁷⁷ even though these loss rates cannot be extrapolated to the field conditions⁷⁸. Alternatively, the recent study from Taniyasu

et al.⁷⁹ shows that photolytic degradation of perfluorinated compounds may occur in the natural environment under high solar radiation intensities. Photodegradation reduces mainly the concentration of long chain fluorochemicals, but also of PFOS, thus the amount of short PFBS and PFBA could increase due to their formation. This may cause that radiation is not directly correlated with the total amount of PFASs, even if it is influencing the marine surface concentrations as reported. Indeed, the positive correlation found between PFOS and radiation may arise from the fact that long chain PFASs are degrading and forming more PFOS.

Temperature can affect the degradation processes, but also the partitioning, and it is related to the water mass. PFCAs and PFASAs are significantly positively correlated with surface water temperature ($p < 0.01$, Kendall-Tau non-parametric coefficients, SI, Table S3.8). PFOS is also significantly correlated with water temperature ($p < 0.01$) using non-parametric coefficients to avoid a bias by source locations overprint (SI, Figure S3.5 and Table S3.8). This suggests that temperature is an important environmental variable of the processes affecting the fate of PFASs in surface water. However the relative importance of the specific processes driving these correlations cannot be elucidated here.

Time-trends of PFASs in the surface global ocean

Even though field studies dealing with PFASs in the open ocean only expand for one decade, the assessment of potential temporal trends of PFASs in surface oceanic water could be attempted for the Atlantic Ocean (SI, Table S3.6). Nevertheless, a high variability of the sampled areas, seasonal variations, sampling and analytical techniques, among other factors, introduce a non-negligible uncertainty in this assessment. In the north Atlantic, a decreasing tendency in surface seawater concentrations has been described for total PFASAs⁴. Conversely, the shorter chain PFASAs have increased in the north Atlantic^{27,31}. On the contrary, the concentration range of total PFCAs have remained constant during the last decade in the north Atlantic, excluding long chain compounds which show higher values for the field studies performed since 2008^{4,26} (SI, Table S3.6).

Figure 3.4 shows a decreasing tendency of PFOA concentrations in the northern hemisphere (both in Atlantic and Pacific oceans) for the last decade. Fitting this data set to,

$$\ln\left(\frac{C_t}{C_0}\right) = -k t + \text{constant} \quad [3.1]$$

Where t is the year, we obtain that k (inverse of e-folding time) equals 0.12, and thus the time needed to reduce the concentration to half of the initial value is of 5.8 years. This decrease, only observed for the Northern Atlantic, suggests that dilution by homogenization of the concentrations in this basin, removal to deeper waters, or biotic or abiotic degradation, may have become important drivers once primary emissions have been reduced. The lower decrease in PFOA concentrations observed in the Pacific ocean may be due to a different evolution of the potential sources directly affecting the Pacific basin (like increasing instead of decreasing production in Asian countries), or to a higher uncertainty due to a fewer number of measurements in the open Pacific ocean.

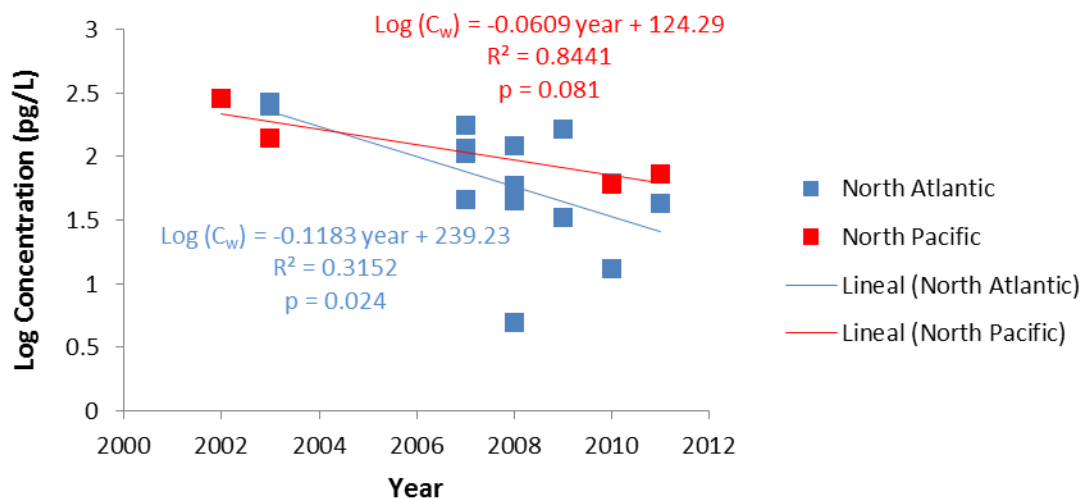


Figure 3.4. Temporal trend of PFOA concentrations in the northern hemisphere in the Atlantic and Pacific oceans and the fitted linear temporal trend. Data from Yamashita et al.(2005)³¹, Ahrens et al. (2009a)²⁷, Ahrens et al. (2010), Zhao et al (2012)⁴, and Benskin et al (2012)²⁶.

PFASs can undergo photo- and maybe bacterial degradation in seawater^{68, 77,79,80}, therefore, the lower concentrations of PFOS in the north Atlantic, the Canary Island region, and the westerly current north of equator, reported here in comparison to other studies, may reflect the phasing out of its peak in production and use in the northern hemisphere regions after 2009, when it was banned¹¹. This would indicate that once primary emissions are reduced; there are significant losses of PFOS either by eddy diffusion and the biological or degradative pumps; which is not appreciated in other short chain compounds with higher recent emissions.

This study shows the ubiquitous occurrence of PFCAs, PFASs and PFASAs in the global ocean, being the first attempt, to our knowledge, to show a comprehensive assessment in surface water samples collected in a single oceanic expedition covering tropical and subtropical oceans and using consistently the same sampling and analytical procedures. Nevertheless, more and new fluorinated products are being added to the market¹² and the main processes affecting their fate remain largely unknown, even though, presumably, it is a complex interaction of many factors and processes what drives their global distribution. Therefore, more research is needed to explain PFASs fate and behavior in the global ocean, which is presumably their main sink.

ACKNOWLEDGEMENTS

This work was funded by the Spanish Ministry of Economy and Competitiveness (Circumnavigation Expedition Malaspina 2010: Global Change and Biodiversity Exploration of the Global Ocean. CSD2008-00077). BBVA Foundation is acknowledged for its economic support of the PhD fellow granted to B. González-Gaya. CSIC and MAGRAMA are also acknowledged for additional financial support. Thanks to Ana Maria Cabello, Pilar Rial, Prof. Marta Estrada, Prof. Mikel Latasa, Prof. Francisco Rodríguez and Prof. Patrizija Mozetič for the surface Chlorophyll measurements. Ana Gomes, Prof. Josep M. Gasol (ICM-CSIC), and the rest of the people on board measuring bacterial abundances are also acknowledged, as well Dr. Pepe Salgado (IIM-CSIC) for discussions on water masses.

REFERENCES

- 1 Lindstrom, A. B., Strynar, M. J. & Libelo, E. L. Polyfluorinated compounds: past, present, and future. *Environmental Science & Technology* **45**, 7954-7961, doi:10.1021/es2011622 (2011).
- 2 Sakurai, T. *et al.* Spatial, phase, and temporal distributions of perfluorooctane sulfonate (PFOS) and perfluorooctanoate (PFOA) in Tokyo Bay, Japan. *Environmental Science & Technology* **44**, 4110-4115, doi:10.1021/es1007609 (2010).
- 3 Butt, C. M., Berger, U., Bossi, R. & Tomy, G. T. Levels and trends of poly- and perfluorinated compounds in the arctic environment. *Science of the Total Environment* **408**, 2936-2965, doi:10.1016/j.scitotenv.2010.03.015 (2010).
- 4 Zhao, Z. *et al.* Distribution and long-range transport of polyfluoroalkyl substances in the Arctic, Atlantic Ocean and Antarctic coast. *Environmental Pollution* **170**, 71-77, doi:10.1016/j.envpol.2012.06.004 (2012).
- 5 Martin, J. W. *et al.* Collection of airborne fluorinated organics and analysis by gas chromatography/chemical ionization mass spectrometry. *Analytical chemistry* **74**, 584-590 (2002).
- 6 Stock, N. L., Furdui, V. I., Muir, D. C. & Mabury, S. A. Perfluoroalkyl contaminants in the Canadian Arctic: evidence of atmospheric transport and local contamination. *Environmental Science & Technology* **41**, 3529-3536 (2007).
- 7 Jahnke, A., Berger, U., Ebinghaus, R. & Temme, C. Latitudinal gradient of airborne polyfluorinated alkyl substances in the marine atmosphere between Germany and South Africa (53 degrees N-33 degrees S). *Environmental Science & Technology* **41**, 3055-3061 (2007).
- 8 Fernandez-Sanjuan, M. *et al.* Screening of perfluorinated chemicals (PFCs) in various aquatic organisms. *Analytical and bioanalytical chemistry* **398**, 1447-1456, doi:10.1007/s00216-010-4024-x (2010).
- 9 Houde, M., De Silva, A. O., Muir, D. C. & Letcher, R. J. Monitoring of perfluorinated compounds in aquatic biota: an updated review. *Environmental Science & Technology* **45**, 7962-7973, doi:10.1021/es104326w (2011).
- 10 Loi, E. I. *et al.* Trophic magnification of poly- and perfluorinated compounds in a subtropical food web. *Environmental Science & Technology* **45**, 5506-5513, doi:10.1021/es200432n (2011).
- 11 UNEP, U. N. E. P. p. 112 (United Nations Environment Programme, Stockholm Convention on Persistent Organic Pollutants. Geneva, 2009).
- 12 Ahrens, L. Polyfluoroalkyl compounds in the aquatic environment: a review of their occurrence and fate. *Journal of Environmental Monitoring* **13**, 20-31, doi:10.1039/c0em00373e (2011).
- 13 Lohmann, R., Breivik, K., Dachs, J. & Muir, D. Global fate of POPs: Current and future research directions. *Environmental Pollution* **150**, 150-165 (2007).
- 14 Nizzetto, L. *et al.* Past, present, and future controls on levels of persistent organic pollutants in the global environment. *Environmental Science and Technology* **44**, 6526-6531 (2010).
- 15 Li, J. *et al.* Perfluorinated compounds in the asian atmosphere. *Environmental Science and Technology* **45**, 7241-7248 (2011).
- 16 Ahrens, L., Shoeib, M., Del Vento, S., Codling, G. & Halsall, C. Polyfluoroalkyl compounds in the Canadian Arctic atmosphere. *Environmental Chemistry* **8**, 399-406 (2011).
- 17 Barton, C. A., Kaiser, M. A. & Russell, M. H. Partitioning and removal of perfluorooctanoate during rain events: the importance of physical-chemical

- properties. *Journal of Environmental Monitoring* **9**, 839-846, doi:10.1039/b703510a (2007).
- 18 Kwok, K. Y. *et al.* Flux of perfluorinated chemicals through wet deposition in Japan, the United States, and several other countries. *Environmental Science & Technology* **44**, 7043-7049, doi:10.1021/es101170c (2010).
- 19 Taniyasu, S. *et al.* Does wet precipitation represent local and regional atmospheric transportation by perfluorinated alkyl substances? *Environment International* **55**, 25-32, doi:10.1016/j.envint.2013.02.005 (2013).
- 20 Yamashita, N. *et al.* Perfluorinated acids as novel chemical tracers of global circulation of ocean waters. *Chemosphere* **70**, 1247-1255, doi:10.1016/j.chemosphere.2007.07.079 (2008).
- 21 Armitage, J. M., MacLeod, M. & Cousins, I. T. Modeling the global fate and transport of perfluorooctanoic acid (PFOA) and perfluorooctanoate (PFO) emitted from direct sources using a multispecies mass balance model. *Environmental Science & Technology* **43**, 1134-1140 (2009).
- 22 Stemmler, I. & Lammel, G. Pathways of PFOA to the Arctic: variabilities and contributions of oceanic currents and atmospheric transport and chemistry sources. *Atmospheric Chemistry and Physics* **10**, 9965-9980, doi:10.5194/acp-10-9965-2010 (2010).
- 23 Lohmann, R., Jurado, E., Dijkstra, H. A. & Dachs, J. Vertical eddy diffusion as a key mechanism for removing perfluorooctanoic acid (PFOA) from the global surface oceans. *Environ Pollut* **179**, 88-94, doi:10.1016/j.envpol.2013.04.006 (2013).
- 24 Prevedouros, K., Cousins, I. T., Buck, R. C. & Korzeniowski, S. H. Sources, fate and transport of perfluorocarboxylates. *Environmental Science & Technology* **40**, 32-44 (2006).
- 25 Benskin, J. P. *et al.* Perfluorinated acid isomer profiling in water and quantitative assessment of manufacturing source. *Environmental Science & Technology* **44**, 9049-9054, doi:10.1021/es102582x (2010).
- 26 Benskin, J. P. *et al.* Perfluoroalkyl acids in the Atlantic and Canadian Arctic Oceans. *Environmental Science & Technology* **46**, 5815-5823, doi:10.1021/es300578x (2012).
- 27 Ahrens, L., Barber, J. L., Xie, Z. & Ebinghaus, R. Longitudinal and latitudinal distribution of perfluoroalkyl compounds in the surface water of the Atlantic Ocean. *Environmental Science & Technology* **43**, 3122-3127 (2009).
- 28 Ahrens, L., Felizeter, S. & Ebinghaus, R. Spatial distribution of polyfluoroalkyl compounds in seawater of the German Bight. *Chemosphere* **76**, 179-184, doi:10.1016/j.chemosphere.2009.03.052 (2009).
- 29 Benskin, J. P. *et al.* Manufacturing origin of perfluorooctanoate (PFOA) in Atlantic and Canadian Arctic seawater. *Environmental Science & Technology* **46**, 677-685, doi:10.1021/es202958p (2012).
- 30 van Leeuwen, S. P. & de Boer, J. Extraction and clean-up strategies for the analysis of poly- and perfluoroalkyl substances in environmental and human matrices. *Journal of chromatography. A* **1153**, 172-185, doi:10.1016/j.chroma.2007.02.069 (2007).
- 31 Yamashita, N. *et al.* A global survey of perfluorinated acids in oceans. *Marine Pollution Bulletin* **51**, 658-668, doi:10.1016/j.marpolbul.2005.04.026 (2005).
- 32 Carloni, D. OECD Report Perfluorooctane Sulfonate (PFOS) Production and Use: Past and Current Evidence. (Report for UNIDO, 2009).
- 33 Ring, K., Kalin, T. & Kishi, A. Fluoropolymers. (CEH Marketing Research Report 2002, Menlo Park CA, 2002).
- 34 Ellis, D. A. *et al.* Degradation of fluorotelomer alcohols: a likely atmospheric source of perfluorinated carboxylic acids. *Environ Sci Technol* **38**, 3316-3321 (2004).

- 35 Ahrens, L., Xie, Z. & Ebinghaus, R. Distribution of perfluoroalkyl compounds in seawater from northern Europe, Atlantic Ocean, and Southern Ocean. *Chemosphere* **78**, 1011-1016, doi:10.1016/j.chemosphere.2009.11.038 (2010).
- 36 Cai, M. *et al.* Spatial distribution of per- and polyfluoroalkyl compounds in coastal waters from the East to South China Sea. *Environmental Pollution* **161**, 162-169, doi:10.1016/j.envpol.2011.09.045 (2012).
- 37 Cai, M. *et al.* Occurrence of perfluoroalkyl compounds in surface waters from the North Pacific to the Arctic Ocean. *Environmental Science & Technology* **46**, 661-668, doi:10.1021/es2026278 (2012).
- 38 Taniyasu, S. *et al.* Analysis of fluorotelomer alcohols, fluorotelomer acids, and short- and long-chain perfluorinated acids in water and biota. *Journal of chromatography. A* **1093**, 89-97, doi:10.1016/j.chroma.2005.07.053 (2005).
- 39 So, M. K. *et al.* Perfluorinated compounds in coastal waters of Hong Kong, South China, and Korea. *Environmental Science & Technology* **38**, 4056-4063 (2004).
- 40 Taniyasu, S., Kannan, K., Horii, Y., Hanari, N. & Yamashita, N. A survey of perfluorooctane sulfonate and related perfluorinated organic compounds in water, fish, birds, and humans from Japan. *Environmental Science and Technology* **37**, 2634-2639 (2003).
- 41 Thompson, J. *et al.* Perfluorinated alkyl acids in water, sediment and wildlife from Sydney Harbour and surroundings. *Marine Pollution Bulletin* **62**, 2869-2875, doi:10.1016/j.marpolbul.2011.09.002 (2011).
- 42 Wei, S. *et al.* Distribution of perfluorinated compounds in surface seawaters between Asia and Antarctica. *Marine Pollution Bulletin* **54**, 1813-1818, doi:10.1016/j.marpolbul.2007.08.002 (2007).
- 43 Guruge, K. S., Taniyasu, S., Yamashita, N. & Manage, P. M. Occurrence of perfluorinated acids and fluorotelomers in waters from Sri Lanka. *Marine Pollution Bulletin* **54**, 1667-1672, doi:10.1016/j.marpolbul.2007.05.021 (2007).
- 44 Theobald, N., Gerwinski, W., Caliebe, C. & Haarich, M. Vol. Project 202 22 213 (Federal Environmental Agency, Germany, 2007).
- 45 Ahrens, L., Gerwinski, W., Theobald, N. & Ebinghaus, R. Sources of polyfluoroalkyl compounds in the North Sea, Baltic Sea and Norwegian Sea: Evidence from their spatial distribution in surface water. *Marine Pollution Bulletin* **60**, 255-260, doi:10.1016/j.marpolbul.2009.09.013 (2010).
- 46 Kim, S. K. & Kannan, K. Perfluorinated acids in air, rain, snow, surface runoff, and lakes: relative importance of pathways to contamination of urban lakes. *Environmental Science & Technology* **41**, 8328-8334 (2007).
- 47 Pistocchi, A. & Loos, R. A map of European emissions and concentrations of PFOS and PFOA. *Environmental Science & Technology* **43**, 9237-9244, doi:10.1021/es901246d (2009).
- 48 Armitage, J. M. *et al.* Modeling the global fate and transport of perfluorooctane sulfonate (PFOS) and precursor compounds in relation to temporal trends in wildlife exposure. *Environmental science & technology* **43**, 9274-9280, doi:10.1021/es901448p (2009).
- 49 *Instituto Brasileiro de Geografia e Estatística*, 2014).
- 50 BBC. *Weather Average Conditions: Rio de Janeiro, Brazil*, 2012).
- 51 Gonzalez-Gaya, B., Zuniga-Rival, J., Ojeda, M. J., Jimenez, B. & Dachs, J. Field measurements of the atmospheric dry deposition fluxes and velocities of polycyclic aromatic hydrocarbons to the global oceans. *Environmental Science & Technology* **48**, 5583-5592, doi:10.1021/es500846p (2014).
- 52 Andrady, A. L. Microplastics in the marine environment. *Marine Pollution Bulletin* **62**, 1596-1605, doi:10.1016/j.marpolbul.2011.05.030 (2011).

- 53 Engler, R. E. The Complex Interaction between Marine Debris and Toxic Chemicals in the Ocean. *Environmental Science & Technology* **46**, 12302-12315, doi:10.1021/es3027105 (2012).
- 54 Law, K. L. *et al.* Plastic accumulation in the North Atlantic subtropical gyre. *Science* **329**, 1185-1188, doi:10.1126/science.1192321 (2010).
- 55 Cózar, A. *et al.* Plastic debris in the open ocean. *Proceedings of the National Academy of Sciences of the United States of America* **111**, 10239-10244 (2014).
- 56 Nizzetto, L., Lohmann, R., Gioia, R., Dachs, J. & Jones, K. C. Atlantic ocean surface waters buffer declining atmospheric concentrations of persistent organic pollutants. *Environmental Science and Technology* **44**, 6978-6984 (2010).
- 57 Galbán-Malagón, C. J., Berrojalbiz, N., Gioia, R. & Dachs, J. The "degradative" and "biological" pumps controls on the atmospheric deposition and sequestration of hexachlorocyclohexanes and hexachlorobenzene in the North Atlantic and Arctic Oceans. *Environmental Science and Technology* **47**, 7195-7203 (2013).
- 58 Galbán-Malagón, C., Berrojalbiz, N., Ojeda, M. J. & Dachs, J. The oceanic biological pump modulates the atmospheric transport of persistent organic pollutants to the Arctic. *Nature communications* **3**, 862 (2012).
- 59 Martin, J. W. *et al.* Identification of Long-Chain Perfluorinated Acids in Biota from the Canadian Arctic. *Environmental Science and Technology* **38**, 373-380 (2004).
- 60 Tomy, G. T. *et al.* Fluorinated organic compounds in an Eastern arctic marine food web. *Environmental Science and Technology* **38**, 6475-6481 (2004).
- 61 Kelly, B. C. *et al.* Perfluoroalkyl contaminants in an arctic marine food web: Trophic magnification and wildlife exposure. *Environmental Science and Technology* **43**, 4037-4043 (2009).
- 62 Xu, J., Guo, C. S., Zhang, Y. & Meng, W. Bioaccumulation and trophic transfer of perfluorinated compounds in a eutrophic freshwater food web. *Environmental Pollution* **184**, 254-261 (2014).
- 63 Longhurst, A. R. in *Ecological Geography of the Sea (Second Edition)* 103-114 (Academic Press, 2007).
- 64 Theobald, N., Gerwinski, W. & Jahnke, A. Occurrence of perfluorinated organic acids in surface sea-water of the East Atlantic Ocean between 53° north and 30° south. *SETAC Europe Annual Meeting* (2007).
- 65 Dachs, J. *et al.* Oceanic Biogeochemical Controls on Global Dynamics of Persistent Organic Pollutants. *Environmental Science & Technology* **36**, 4229-4237, doi:10.1021/es025724k (2002).
- 66 Schröder, H. F. Determination of fluorinated surfactants and their metabolites in sewage sludge samples by liquid chromatography with mass spectrometry and tandem mass spectrometry after pressurised liquid extraction and separation on fluorine-modified reversed-phase sorbents. *Journal of chromatography. A* **1020**, 131-151 (2003).
- 67 Sáez, M., De Voogt, P. & Parsons, J. R. Persistence of perfluoroalkylated substances in closed bottle tests with municipal sewage sludge. *Environmental Science and Pollution Research* **15**, 472-477 (2008).
- 68 Fromel, T. & Knepper, T. P. Biodegradation of fluorinated alkyl substances. *Reviews of environmental contamination and toxicology* **208**, 161-177, doi:10.1007/978-1-4419-6880-7_3 (2010).
- 69 Parsons, J. R., Sáez, M., Dolfig, J. & de Voogt, P. Vol. 196 53-71 (2008).
- 70 Meesters, R. J. W. & Schröder, H. F. Perfluorooctane sulfonate - A quite mobile anionic anthropogenic surfactant, ubiquitously found in the environment. *Water Science and Technology* **50**, 235-242 (2004).

- 71 Kannan, K. *et al.* Perfluorinated compounds in aquatic organisms at various trophic levels in a Great Lakes food chain. *Arch Environ Contam Toxicol* **48**, 559-566, doi:10.1007/s00244-004-0133-x (2005).
- 72 Haukas, M., Berger, U., Hop, H., Gulliksen, B. & Gabrielsen, G. W. Bioaccumulation of per- and polyfluorinated alkyl substances (PFAS) in selected species from the Barents Sea food web. *Environmental Pollution* **148**, 360-371, doi:10.1016/j.envpol.2006.09.021 (2007).
- 73 Xia, X., Rabearisoa, A. H., Jiang, X. & Dai, Z. Bioaccumulation of perfluoroalkyl substances by daphnia magna in water with different types and concentrations of protein. *Environmental Science and Technology* **47**, 10955-10963 (2013).
- 74 Higgins, C. P. & Luthy, R. G. Sorption of perfluorinated surfactants on sediments. *Environmental Science & Technology* **40**, 7251-7256 (2006).
- 75 Ahrens, L., Yeung, L. W., Taniyasu, S., Lam, P. K. & Yamashita, N. Partitioning of perfluorooctanoate (PFOA), perfluorooctane sulfonate (PFOS) and perfluorooctane sulfonamide (PFOSA) between water and sediment. *Chemosphere* **85**, 731-737, doi:10.1016/j.chemosphere.2011.06.046 (2011).
- 76 Ahrens, L. *et al.* Distribution of polyfluoroalkyl compounds in water, suspended particulate matter and sediment from Tokyo Bay, Japan. *Chemosphere* **79**, 266-272, doi:10.1016/j.chemosphere.2010.01.045 (2010).
- 77 Yamamoto, T., Noma, Y., Sakai, S. & Shibata, Y. Photodegradation of perfluorooctane sulfonate by UV irradiation in water and alkaline 2-propanol. *Environmental Science & Technology* **41**, 5660-5665 (2007).
- 78 Giri, R. R., Ozaki, H., Okada, T., Taniguchi, S. & Takanami, R. Factors influencing UV photodecomposition of perfluorooctanoic acid in water. *Chemical Engineering Journal* **180**, 197-203 (2012).
- 79 Taniyasu, S., Yamashita, N., Yamazaki, E., Petrick, G. & Kannan, K. The environmental photolysis of perfluorooctanesulfonate, perfluorooctanoate, and related fluorochemicals. *Chemosphere* **90**, 1686-1692 (2013).
- 80 Buck, R. C. *et al.* Perfluoroalkyl and polyfluoroalkyl substances in the environment: terminology, classification, and origins. *Integrated environmental assessment and management* **7**, 513-541, doi:10.1002/ieam.258 (2011).

4. Oceanic Transport and Sinks of Perfluoroalkylated Substances

**González-Gaya B^{1,2*}, Jurado E.², Fernández-Castro B.³, Mouriño-Carballido B.³,
Siegel D.A.⁴, Dachs J², Jiménez B¹**

¹ Department of Instrumental Analysis and Environmental Chemistry, Institute of Organic Chemistry of the Spanish National Research Council (IQOG-CSIC), Juan de la Cierva 3, 28006 Madrid, Spain.

² Department of Environmental Chemistry, Institute of Environmental Assessment and Water Research of the Spanish National Research Council (IDAEA-CSIC), Jordi Girona 18-26, 08034 Barcelona, Catalonia, Spain.

³ Vigo University, Vigo, Pontevedra, Spain.

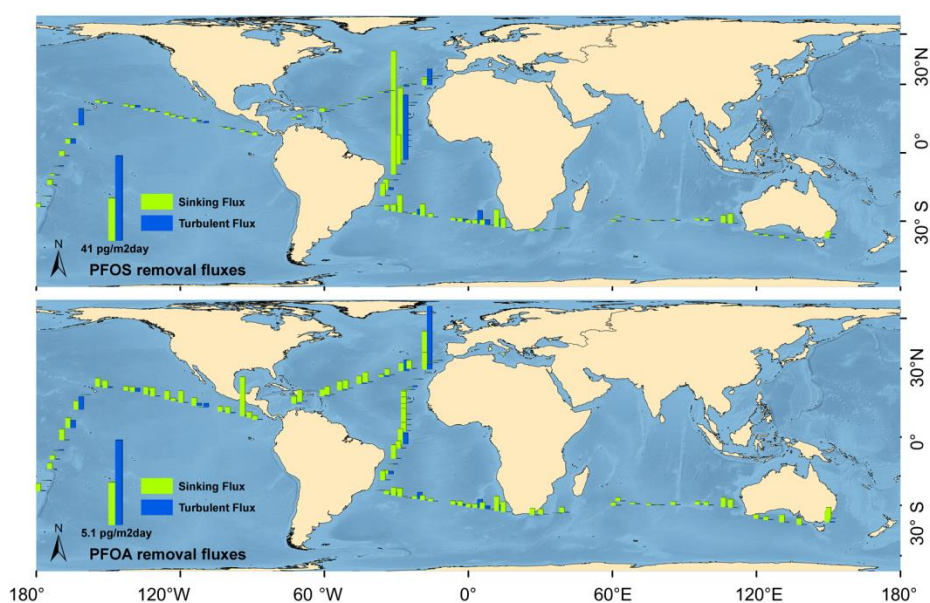
⁴ Earth Research Institute and Department of Geography, University of California, Santa Barbara, California, USA.

* Corresponding author email b.gonzalez@iqog.csic.es

To be submitted

ABSTRACT

Perfluoroalkylated substances (PFASs) dynamics at the open ocean is an unresolved issue at a global scale. At the *Malaspina 2010* circumnavigation cruise, 21 PFASs were measured at the deep chlorophyll maximum (around 100 m depth) alongside physical and biological parameters influencing their chemistry, in order to elucidate their vertical transport along the water column. The samples were taken at the Atlantic, Pacific and Indian Oceans between 35°N and 40°S, providing the first synoptic global sampling and allowing a direct comparison between oceanic basins at surface and subsurface in the mixed layer. The vertical transport of PFASs was assessed empirically for eddy Diffusion and settling fluxes of organic matter bound PFASs (Biological pump). The eddy diffusion coefficients in the photic water column were measured concurrently with the PFASs concentrations, allowing the first reported estimation of PFASs diffusive fluxes from field data. The biological pump fluxes were calculated based on bioconcentration factors of the selected PFASs and organic carbon export from the mixed layer. The phytoplankton and zooplankton contribution to the biological pump fluxes were estimated separately; zooplankton influence dominates over the phytoplankton, according to our measurements. Moreover, the biological pump vertical transport of PFASs is of higher magnitude than turbulent diffusion, except in regions with strong water column eddy diffusion.

*Graphical Abstract 4.*

INTRODUCTION

Perfluoroalkylated substances (PFASs) are persistent synthetic compounds, receiving rising concern worldwide due to their increasing use and therefore widespread occurrence as environmental contaminants. PFASs are ubiquitous and can reach remote regions, including the open oceans¹⁻⁵. Although earlier studies reported PFASs occurrence in the marine environment, including assessments at oceanic scale⁶⁻⁸, and inter oceanic comparisons^{1,5,9,10}, the understanding of their fate still represent an important scientific challenge¹¹. Neutral PFASs can be atmospherically transported and deposited globally¹²⁻¹⁴, while for ionic PFASs, such as perfluorooctane carboxylic acids (PFCAs) and perfluorooctane sulfonic acids (PFASs), marine currents are thought to be the main transport vector to remote areas¹⁵. Among those, perfluorooctane carboxylic acid (PFOA) and perfluorooctane sulfonic acid (PFOS) are frequently assessed⁴. Moreover, atmospheric deposition of ionic PFASs is feasible after their neutral precursors are degraded in the atmosphere^{14,16,17}, but the relevance of this input to the ocean has been poorly constrained. Once in the oceanic water column their residence times and their global fate is still uncertain due to their particular chemical properties (e.g high water solubility and lipophobicity) compared to other Persistent Organic Pollutants (POPs)¹¹.

Most previous assessments of PFAS in the marine environment report concentrations for surface waters^{6,18}, while the transport routes (horizontally and vertically) as well as the potential biogeochemical controls on their occurrence have received little attention. In addition, the magnitude of the oceanic sinks of PFASs remain largely uncharacterized^{15,19,20}. Nevertheless, the potential relevance of the ocean as an ultimate sink of PFASs has been suggested⁴. To date, a limited number of studies focus on the PFASs vertical transport and their water column distributions in the marine environment. A remarkable attempt was published by Yamashita and coworkers.¹⁵, who reported the concentrations' vertical profiles, from the surface down to several thousand meters depth, at 9 locations from North Atlantic, South Pacific and offshore Japan. Their study showed PFOA and PFOS concentrations generally higher at surface compared to deep waters, consistent with these chemicals being introduced at surface through riverine inputs and atmospheric deposition. Nevertheless, the database was

based on PFOS and PFOA measured during several independent research cruises between 2002 and 2006, which may enhance variability due to sampling methodologies. Subsequently, this database was used to test the relevance of vertical transport by eddy Diffusion as a process affecting PFOA depletion from surface marine waters and driving their transport to the deep ocean ²¹. The study suggested that vertical eddy diffusion was an oceanic sink with a magnitude three fold larger than subduction of water masses, previously suggested to be important as a sink for other organic pollutants ²² and PFASs ². Both, vertical transport by eddy diffusion and subduction of water masses, are part of the “physical pump”. Lohmann and coworkers also noted the scarce information on the efficiency of vertical mixing due to the limited field derived data sets of eddy diffusion coefficients, as well the limited knowledge on the occurrence of PFASs for many oceanic regions, especially in the Indian and Pacific Oceans.

On the other hand, the Biological pump may be taking part in the removal processes of PFASs in surface tropical oceans as it has been described as a key factor driving POP concentrations in remote areas, being able to trap the pollutants and change water and even air concentrations in the Arctic ^{23,24}, the Antarctica ^{25,26} and in other marine environments ²⁷. As pollutants with high octanol- water partition coefficient (K_{ow}) tend to accumulate in the organic matter in the water column, the vertical settling of these particles drives a sinking flux of hydrophobic POPs. PFASs sorb onto particulate matter in aquatic systems, ^{8,28} even if to a lower extend, and may be affected by this settling process. There are some studies about bioaccumulation of PFASs in biota, including planktonic organisms ²⁹⁻³¹, but attention has been given mainly to their toxicity or transfer through food webs. The potential role of the biological pump on the removal of PFAS from surface waters has not been assessed so far.

Based on the previous considerations, the removal fluxes caused by turbulent diffusion in the water column (physical pump) and by sorption to biomass with subsequent sinking (biological pump), as it occurs for other POPs, are the two main processes potentially affecting the superficial depletion of PFASs, which deserve further evaluation. For this purpose, our study is based on the *Malaspina 2010* circumnavigation cruise, which allowed field measurements of 21 PFAS, including

PFCAs, PFASs and perfluoroalkyl sulfonamides (PFASAs), at surface and at the deep chlorophyll maximum (DCM) depth, concurrently with in-situ measurements of the eddy diffusion coefficients in the photic zone of the water column³². To our knowledge, this research represents the first synoptic estimation of PFASs eddy diffusive fluxes and settling fluxes derived from field measurements and climatologies at a global scale.

Therefore, the objective of this work is to assess for a wide range PFASs the removal fluxes from the superficial ocean through i) the evaluation of their spatial and vertical concentrations in the global tropical and subtropical Open Ocean and ii) the quantification of vertical turbulent diffusion and the biological pump affecting PFASs, as the main settling mechanism for oceanic POPs.

MATERIAL AND METHODS

Sampling

PFASs and eddy diffusivities were measured during the *Malaspina 2010* circumnavigation cruise with RV Hespérides from December 14, 2010 to July 14, 2011, providing the first global sampling of PFASs in the tropical and subtropical Atlantic, Pacific and Indian Oceans. The surface seawater concentrations of PFASs have been discussed in a companion work ¹. In addition, 89 water samples at the DCM depth were taken in the north and south basins of the Atlantic and Pacific Oceans and in the Indian Ocean between 35°N and 40°S (Figure 4.1), allowing to assess the vertical distribution of PFASs globally. The DCM depth oscillated between 20 and 160 m during the circumnavigation cruise, depending on the transparency and nutrients content in the water column ³³. The DCM was chosen because it is where the concentration of phytoplanktonic biomass is at its maximum, and it has been reported to be an area of special interest regarding biological processes ³⁴⁻³⁶. One liter of seawater from the DCM depth was sampled in 30 L *Niskin* bottles attached to an oceanographic rosette coupled with a CTD device (conductivity, temperature, depth), which allowed the detection of the DCM depth precisely. The water was then transferred to 1L polypropylene bottles for its subsequent concentration in the laboratory. All the sampling stations, localizations and depths for DCM samples are included in the Supplementary Info (SI, Table S4.1).

Sample treatment & Instrumental Analysis

The samples were analyzed following the same protocols used for surface water samples as described in Gonzalez-Gaya et al. and its supplementary info ¹. Briefly, after collection, water samples were filtered using glass fiber filters (GF/F, 0.7 µm) and spiked with a mixture of ¹³C labeled C_{4,6,8-12} PFCAs and ¹⁸O C₆ and ¹³C C₈ PFASs. The filtrate was concentrated on solid phase extraction OASIS WAX cartridges and kept at -20°C during the cruise until their further treatment in the laboratory.

After the elution and concentration of the extract, the instrumental analysis was performed using a Waters Acquity Ultraperformance Liquid Chromatography system coupled with a Waters XEVO TQS, triple-quadrupole mass spectrometer (UPLC-MS/MS) with the mass spectrometer operating in the multiple-reaction-monitoring (MRM) mode. Separation was achieved on an Acquity UPLC BEH C18 Column (1.7 μm , 1.0 x 50 mm; Waters Corp.). Electrospray negative ionization (ESI) was used. Three labeled (^{13}C) PFASs and PFCAs, and one deuterated (D) PFASA were used as injection standard for an internal standard quantification. Of the 21 target PFASs analyzed, 9 ionic PFASs (C_6 - C_{10} PFCAs and C_4 , C_6 - C_8 PFASs) and 2 neutral PFASAs precursor compounds (perfluorooctane sulfonamide (PFOSA) and N-methyl perfluorooctane sulfonamide (N-MePFOSA)) were consistently identified. Therefore, the present study is focused on these 11 compounds.

Quality Assurance/Quality Control

Each sample was injected in triplicate and all the detection and quantification limits (DL, QL) were calculated as explained elsewhere ¹. *Niskin* field blanks and laboratory blanks (chromatographic-grade water, SPE-extracted chromatographic-grade water and of the reagents used for analysis) were analyzed simultaneously with the sample batches, and give no significant signals of the target compounds in both blanks types, being the concentrations found of few pg per sample ¹. Recoveries for the DCM water samples ranged from 76% for perfluorononane carboxylic acid PFNA $^{13}\text{C}_5$ to 142% for perfluorohexane sulfonic acid PFHxS $^{18}\text{O}_2$ (SI, table S4.2). Additional details on QA/QC are reported in González-Gaya et al 2014 ¹.

Estimation of Eddy vertical Diffusion of PFASs

The oceanic sink due to vertical eddy diffusion was calculated for individual PFASs with a one dimension diffusion model as described elsewhere ²¹. Briefly, the estimation of the turbulent flux (F_{Eddy} , $\text{ng m}^{-2}\text{d}^{-1}$) is based on the Fick's first law,

$$F_{Eddy} = -K_{\rho} \frac{\partial C_w}{\partial z} \quad [4.1]$$

where C_w (ng m^{-3}) is the PFASs seawater concentration, z is depth, and K_{ρ} is the eddy diffusivity ($\text{m}^2 \text{d}^{-1}$). In the model, it is assumed that no PFASs pollution was present in the marine surface in the initial time step ($C_{w0} = 0$, $t_0 = 1970$) and that the flux is unidirectional coming from the surface towards the deep ocean, driven uniquely by eddy diffusion. T_0 was selected as the moment when the production of perfluorochemicals started to be relevant, but the oceanic concentrations were still likely to be negligible³⁷. The concentrations are allowed to increase until reaching the C_w values measured for the surface ocean in 2011. Time steps are lapsed in $\Delta t = 0.5$ years and the resolution of the water column is of 1 m depth. Details on the integration method are given by Lohmann et al.²¹, except that for the K_{ρ} values. K_{ρ} was calculated from in-situ measurements during the Malaspina cruise³² by,

$$K_{\rho} = \Gamma \frac{\varepsilon}{N^2} \quad [4.2]$$

where N^2 (s^{-2}) is the squared buoyancy frequency, Γ is the mixing efficiency described by Osborn³⁸ and modified as described in Fernandez-Castro et al.³², and ε (W kg^{-1}) is the dissipation rate of turbulent kinetic energy measured by a microstructure turbulence profiler launched during the sampling campaign. It was deployed, immediately after the water sampling for PFASs analysis, at 50 stations with a profile resolution of one ε measurement per meter between 0 to 300 m depth. From 2 to 6 profiles were obtained in each station, being the ε used here an averaged value. When the ε records were not available, K_{ρ} was obtained from hydrographic and meteorological data by using the K-profile parameterization described by Fernandez-Castro et al.³². The estimated F_{Eddy} are based on the surface concentrations recorded during the sampling cruise¹ and the K_{ρ} averaged per meter over the water column of each sampling point. Fluxes are given for 9 ionic species (C_{6-10} PFCAs and $\text{C}_{4, 6-8}$ PFASs) as their detection in the global sampling campaign was consistent, allowing their comparison in all the tropical and subtropical oceans.

Settling fluxes of PFAS due to the Biological pump

The settling flux ($F_{Settling}$) associated with the settling of organic matter bound PFASs (biological pump) was estimated by,

$$F_{Settling} = -F_{OM} BCF C_W = -(F_{Phyto} + F_{Fecal}) BCF C_W \quad [4.3]$$

where F_{OM} ($\text{ng m}^{-2} \text{s}^{-1}$) is the flux of organic matter that settles out of the mixed layer to the deep ocean with an algal matter flux component (F_{Phyto}) and a zooplankton related matter flux component (F_{Fecal}), C_W (ng L^{-1}) is the concentration of PFASs measured in the DCM during the *Malaspina 2010* sampling cruise, and BCF is the bioconcentration factor of the given PFASs in plankton (phytoplankton and fecal).

We assume that F_{OM} is 1.8 times the flux of organic carbon (F_{OC} , $\text{ng m}^{-2} \text{s}^{-1}$) exported from the mixed layer³⁹. F_{OC} is taken from the recently described climatology of export fluxes of organic carbon in the global oceans by Siegel and coworkers⁴⁰. This climatology separates the contribution to F_{OC} from phytoplankton from those derived from zooplankton fecal pellets of organic matter (last term of equation [4.3]). Therefore, both, the phytoplankton and zooplankton contribution to the biological pump fluxes were estimated separately for the first time, as previous estimates of POPs fluxes due to the biological pump considered one unique settling flux of organic matter. Even if there is no available data for PFASs, fecal pellets have been reported to accumulate persistent organic pollutants^{41 42,43}.

The BCF values for PFASs accumulation in plankton were taken from the literature³⁰. In order to estimate the two components of the settling flux of PFAS, we assume that the PFAS's BCFs of phytoplankton is of equal magnitude than the fecal pellet-water partition coefficient for PFASs (Equation [4.3]).

Statistical analysis

SPSS Statistics version 21.0 (IBM Corp.) was used for nonparametric statistical analysis as the measured concentration of individual PFASs were not normally distributed (see normality test results in SI, Table S4.3).

RESULTS AND DISCUSSION

Global occurrence of PFASs in the deep chlorophyll maximum depth

The Atlantic Ocean showed the highest average concentrations (as the sum of all the measured compounds, Σ PFASs) at DCM; followed by the Pacific and the Indian Ocean. Average concentrations found in the Northern hemisphere were lower than values found in the Southern hemisphere (Figure 4.1, and SI, Table S4.4), mainly due to the high concentrations found near Brazil, South Africa and West Australia. It is remarkable the high abundance of PFOS, as 39% of the total average PFASs concentration, perfluorodecanoic acid (PFDA) 17%, and perfluorohexanoic acid (PFHxA) 12%. The relative contribution of the remaining compounds was under 10%, with PFOA, contributing 5% to Σ PFASs measured at the DCM (SI, Figure S4.1). The PFASs pattern found at the DCM depth resembles that described previously for the corresponding surface waters ¹ for most oceans basins with the exception of the North Atlantic Ocean. In this case, PFCAs were predominant at the surface, meanwhile PFCAs and PFASs had similar occurrence at the DCM depth, as PFOA and PFDA were highly reduced with depth.

Regarding global occurrence for the three PFAS families, PFASs showed a clear coastal gradient, with the highest concentrations in the South Atlantic Ocean, near the Brazilian coast as observed previously at surface ¹ (Figure 4.1, top panel). PFCAs followed a similar spatial occurrence pattern, even if the highest concentrations were not found in the Brazilian coasts, but near West Africa in the North Atlantic gyre, and close to the East and West coasts of the Indian Ocean transect (Figure 4.1, middle panel). PFASAs concentrations (Figure 4.1, bottom panel) were 2 or 3 orders of magnitude lower than the other two ionic families and very close to the analytical method DL. Neutral compounds have been reported here for the first time in deep waters, although their detection was possible in 60% of the samples and mostly in the Northern hemisphere. Their chemical characteristics, such as high volatility and lower persistence, and lower abundances in the southern hemisphere could be influencing these results ⁶.

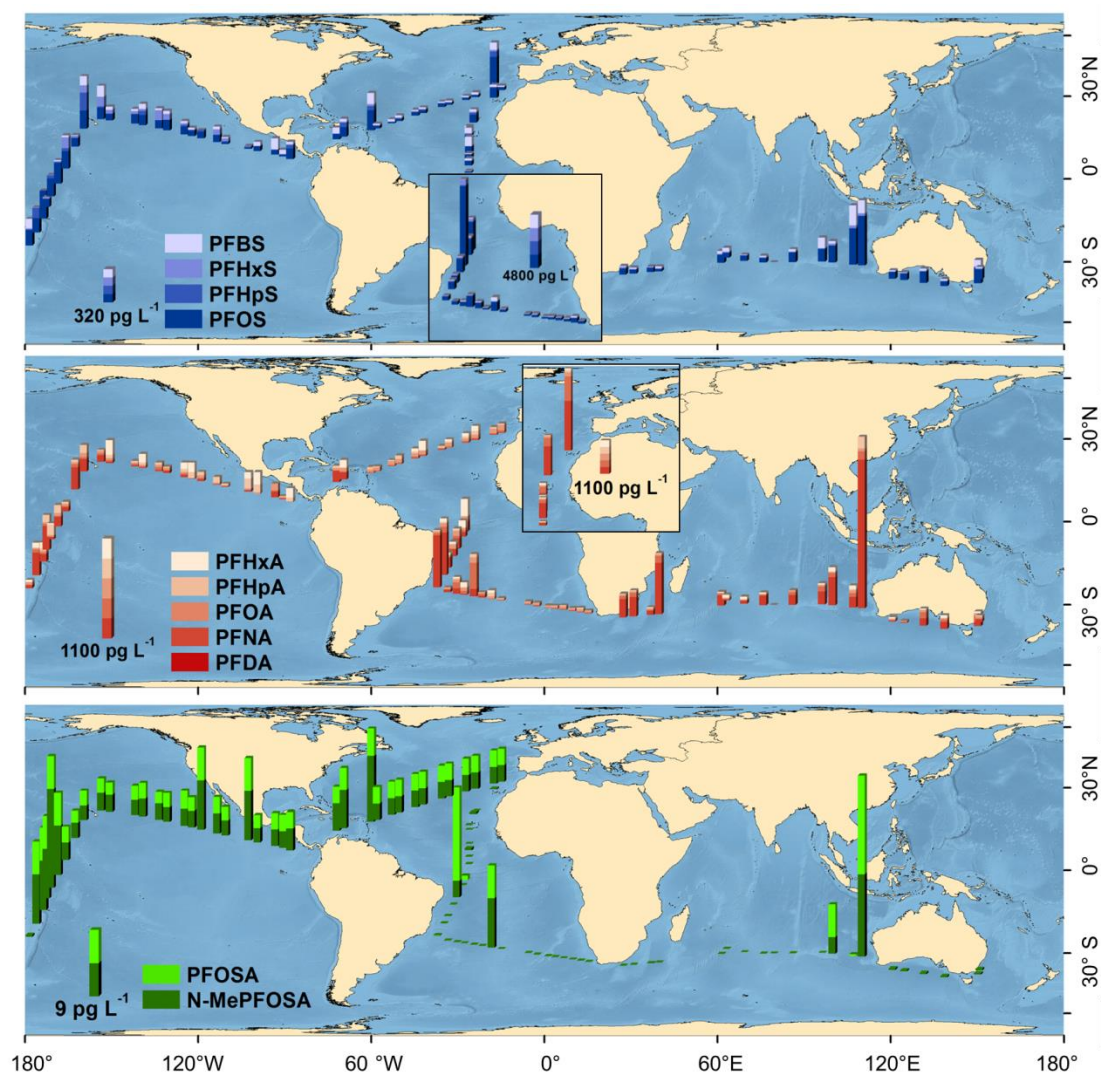


Figure 4.1. Global distribution of PFASs in the tropical and subtropical oceans at the DCM. Upper panel shows the PFSA concentrations, central panel shows the PFCA concentrations and lower panel shows the PFASA concentrations. Note that the concentrations of PFSA and PFCA in the South Atlantic Ocean are shown with a different scale in the separated square sub-panels.

The concentration spatial patterns of PFASs at DCM were similar to those found at surface previously¹, even though the concentration ranges at DCM were much smaller than that of surface samples. Indeed, PFAS concentrations at DCM are positively correlated with those at surface, being significant this correlation for all analyzed compounds, except for the PFHxA (Figure 4.2 and SI, Table S4.5). Surface concentrations of individual PFASs were generally higher than at the DCM for most samples (surface/DCM ratio was over 0.8 in 75 out of 92 samples, and between 0.8 and 1.2 in 26 out of 92 samples), (SI, Figure S4.2 and Table S4.4) likely due to different factors (e.g. regional strength of removal processes, influence of oceanic circulation,

and different historical/ongoing emissions). Assuming a main superficial income of PFASs pollution, it seems that in some areas the factors affecting surface depletion are more intense than in others. Also the amount of pollution seems to be relevant; for instance, in areas with a very low surface PFASs concentration, like the central Pacific Ocean, there are many stations where PFAS concentrations at DCM are higher than at surface or in the same range, most likely due to a similar level of the individual contaminants in both layers, close to the baseline concentrations. Conversely, DCM total concentration is also higher than at surface in areas with extremely high concentrations combined with intense removal fluxes (as described later in this paper), like in the Central America, South African and Australian coasts (SI, Figure S4.2). Therefore, it is relevant to assess the magnitude and spatial distribution of the eddy diffusion and settling fluxes due to the biological pump on PFAS in order to understand their vertical distribution.

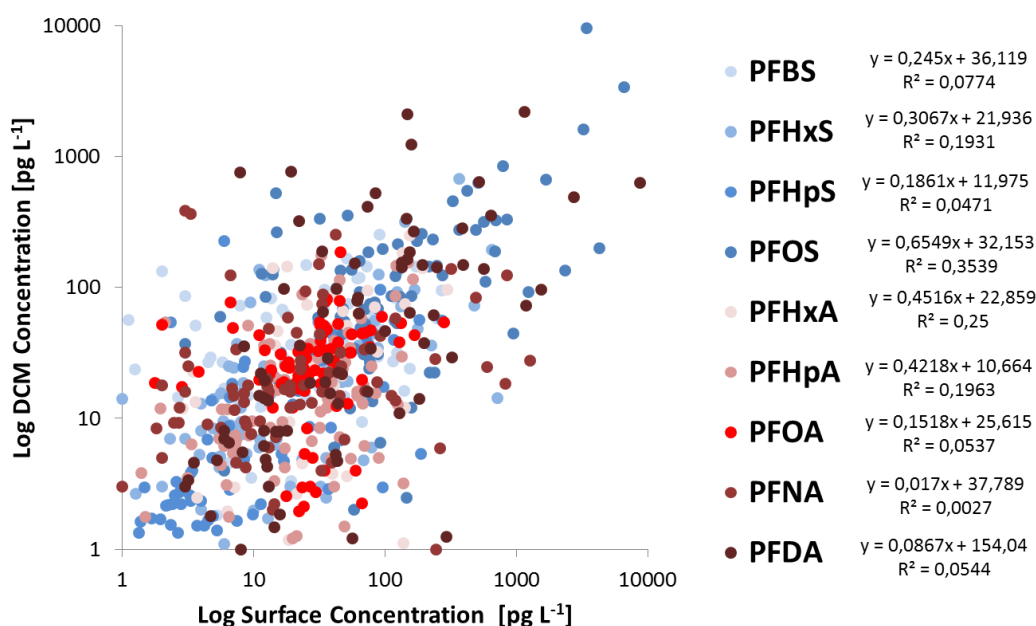


Figure 4.2. PFASs Log concentrations at the surface versus DCM (pg L^{-1}).

Vertical eddy diffusion fluxes of PFASs

K_p ranged from $5.07 \text{ m}^2\text{s}^{-1}$ in surface areas of the North Atlantic (with strong turbulent events, like a storm, which enhanced diffusion) to $3.53 \cdot 10^{-7} \text{ m}^2\text{s}^{-1}$ in the deepest areas of the measured mixed layer, causing the latter a very slow diffusion typical from the inner parts of the ocean³² (SI, Figure S4.3).

The application of the one dimensional model using the measured eddy diffusion coefficients allowed predicting the vertical profile of C_W in the water column, and therefore, it was possible to calculate a theoretical value of C_W at the DCM depth. To test the *model's goodness-of-fit* we compared the measured field concentration of PFASs at the DCM with those obtained from the model at the same depth (Figure 4.3). In general, there was a good agreement in the order of magnitude between the model and the measured field concentration at DCM. However, the model usually underestimated the measured concentrations (ranging the mean absolute error from 13 pg L^{-1} for perfluoroheptane acid (PFHpS) to 324 pg L^{-1} for PFOS) (SI, Table S4.6). In the South Atlantic Ocean, where maximal concentrations were found at surface ¹, there is more dissimilarity between modeled and measured concentrations (SI, Figure S4.4). This may be also a consequence of different past or ongoing PFASs loadings from the surrounding areas and potential unknown vertical transport mechanisms. Therefore, extreme PFASs concentrations seem to be a factor influencing the model predictive potential. Likewise, the chemical properties of each individual PFAS may be a matter of interest, as the fit of every congener is different (SI, Table S4.6 and Figure S4.4).

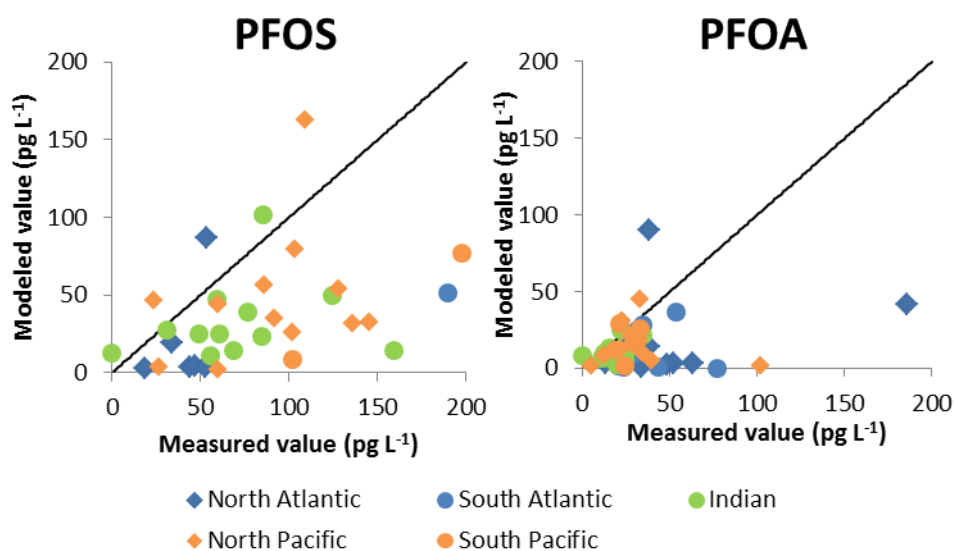


Figure 4.3. PFOS and PFOA modelled versus measured concentrations (pg L^{-1}) at the DCM depth.

The calculated turbulent fluxes were obtained computing the modeled concentrations in the water column. F_{Eddy} generally decreased with depth because microstructure turbulence is 1-3 orders of magnitude lower in the deep ocean than in the mixing layer of the open ocean at tropical and subtropical latitudes³². F_{Eddy} at the surface were generally higher, up to 4 orders of magnitude, than at the DCM. An inversion of turbulence fluxes intensity (higher at the DCM) only occurred consistently for all analyzed compounds at 5 sampling stations (placed in the Brazilian coast, in the Pacific Equatorial Countercurrent and near the Caribbean sea) corresponding to areas where situations like to coastal vicinity, lateral water mass intrusion, internal waves or salt-fingers occur, causing increased interior shear areas as reported by Fernandez-Castro et al.³².

F_{Eddy} at surface oscillated between $2.92 \cdot 10^{-8}$ and $5.42 \cdot 10^{-2}$ ng m⁻²day⁻¹ for PFOS and between $3.24 \cdot 10^{-8}$ and $9.11 \cdot 10^{-4}$ ng m⁻²day⁻¹ for PFOA (SI, Table S4.7 and Figure S4.5). F_{Eddy} at DCM depth ranged between $1.53 \cdot 10^{-5}$ and $1.96 \cdot 10^{-2}$ for PFOS and between $1.28 \cdot 10^{-3}$ and $1.08 \cdot 10^{-6}$ ng m⁻²day⁻¹ for PFOA (Figure 4.4 and SI, Table S4.7). The turbulent fluxes calculated by Lohmann et al. for PFOA are in the same order of magnitude and exhibit as well those broad ranges depending on the location²¹. F_{Eddy} calculated for other PFASs are displayed in Table S4.7 at the SI, and were logically lower for the less abundant PFASs (e.g. PFHpS and PFNA). The PFOS eddy diffusion flux was one order of magnitude superior to PFOA due to the higher concentrations of PFOS. Even at the maximal measured K_p for PFOS, eddy diffusion will disperse 7 ng m⁻²y⁻¹ of PFOS from the oceanic surface, being thus a flux of small magnitude.

The PFOS and PFOA annual removal fluxes for the global tropical and subtropical surface oceans are of 2.3 and 0.2 tons per year, respectively. Yamasita et al. reported a rate of 620 Kg year⁻¹ for PFOS and 1460 Kg year⁻¹ for PFOA due to deep water formation globally, which is of comparable magnitude taking into account the few areas where deep water subduction occurs. Likewise, Lohmann and coauthors estimated a total amount of PFOA removed from the top 100 m of the global ocean by turbulence as 664 tons from 1970 to 2009, which attends for a mean of 17 tons per year, 85 times our calculated values for this compound. Nevertheless, they assume an error of their estimations of eddy diffusivity of several orders of magnitude, as they

were not field derived. Therefore, they provide a range of the estimated PFOA export from 1.5 tons to 4818 tons since 1970, being then our values within their estimations. Moreover, they also estimated the mean deep water formation flux for PFOA as 220 tons (80-360 tons). The mean annual sinking according to these calculations would be 5.6 tons, being our calculations of F_{Eddy} in the range of the minimum fluxes due to subduction according to Lohmann²¹.

Eddy diffusion is not constant over the open ocean at a fixed depth. For instance, at the DCM depth very high F_{Eddy} was recorded for PFOS at the east South Atlantic, probably due to elevated concentrations of the pollutant coupled with an intense internal turbulence caused by upwelling waters. Besides, high F_{Eddy} peaks for PFOA in selected points of West African coasts in the North Atlantic Ocean were found, probably associated with a significant occurrence of PFOA (Figure 4.4). Shallower areas (like Tasmanian straight), upwelling water (near South African west coast) and natural stratification of the mixed layer (for instance due to riverine discharge or cold water intrusions) among other processes, affect the intensity of the turbulence³² as reflected in our measurements.

At surface, turbulence is even more variable (SI, Figure S4.4) depending mostly on meteorological events (rain, wind, etc.) that may be episodic and thus difficult to generalize. Indeed, the extremely high variability of instantaneous turbulent fluxes at the surface ocean have already been reported²¹. Therefore, the turbulent fluxes obtained correspond to a snapshot of the diffusion occurred during the *Malaspina* 2010 circumnavigation. Moreover, the influence of turbulence alone does not fully explain the concentrations found at depth, being other sinking processes able to have an important influence on PFASs behavior.

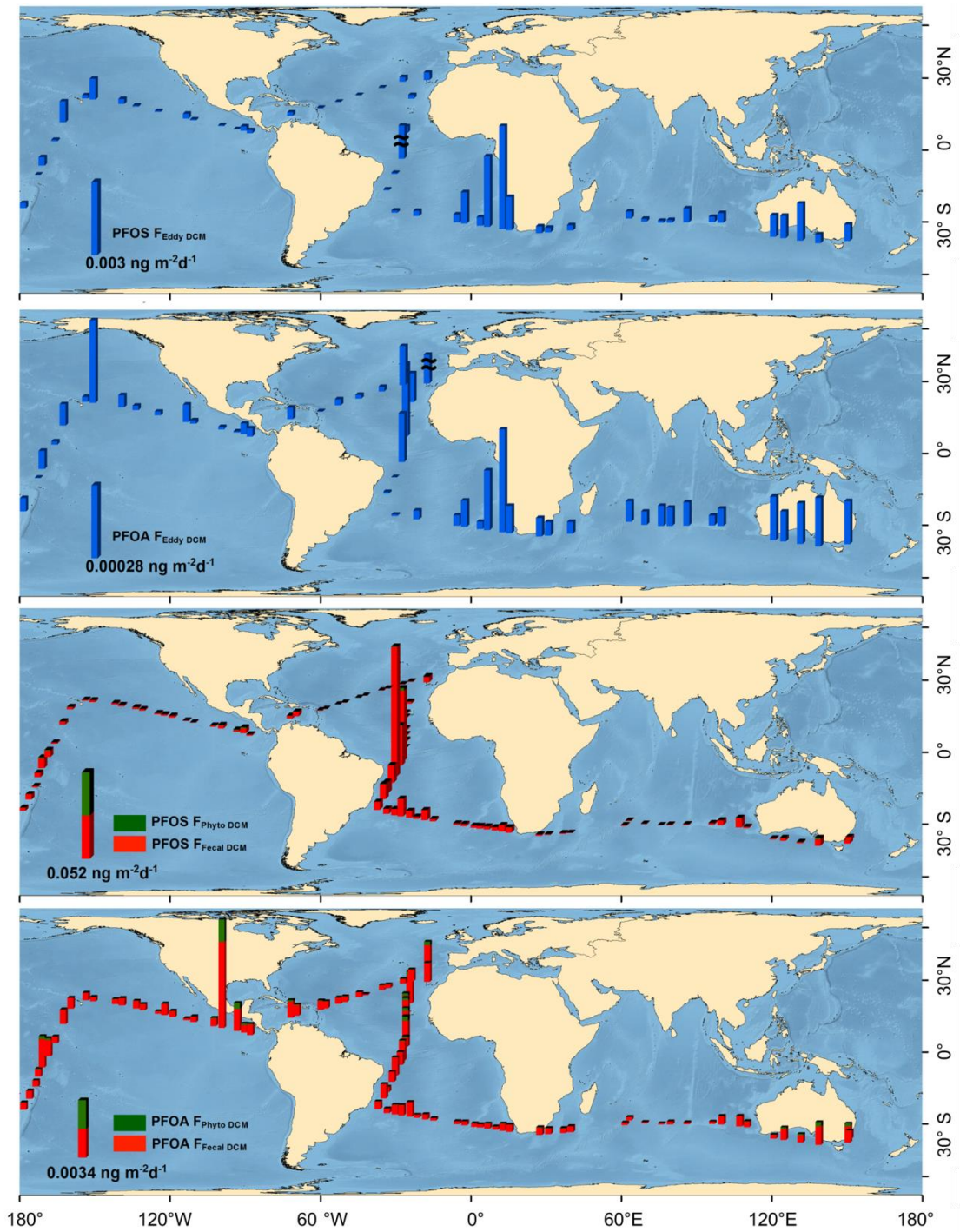


Figure 4.4. Fluxes assessed for PFOS and PFOA; turbulent fluxes (F_{Eddy}) on the top and biological pump fluxes on the bottom (F_{Phyto} and F_{Fecal}). Bars with \sim symbol have been manually diminished by a factor of 10 in order to ease the global comparison of all the measurements.

Settling Fluxes due to the Biological Pump

Settling fluxes due to the biological pump were calculated for the 5 ionic PFASs (C_{8-10} PFCAs and $C_{6,8}$ PFSA) for which their BCF data in the marine phytoplankton were available³⁰. Bioconcentration onto organic matter will deplete PFASs from the dissolved water phase and export them out from the surface mixed layer. The magnitude of these fluxes is related to the chemical BCF, the concentration at the DCM, and the magnitude of F_{OC} . The BCF is positively correlated with the $F_{Settling}$ (Equation 4.3, Figure S4.6); consequently, PFASs with high BCF, such as PFNA and PFDA, will be more affected by the removal through the biological pump. The global organic carbon sinking fluxes have been poorly described due to a high variability on a temporal and regional scale, coupled to a not clear definition of what kind of organic matter should be taken into account to quantify the sinking processes and the difficulties to empirically measure it⁴⁴⁻⁴⁶. Traditionally, the biological pump effect on POPs has been calculated based on estimation of F_{OC} from chlorophyll a concentrations³⁹, however it is now possible to quantify organic carbon fluxes associated to plankton through different methods and parametrizations^{46,47}. Siegel et al.⁴⁰ modeled global oceanic carbon export from the euphotic layer individually for algae ($F_{OC\ Phyto}$) and zooplankton fecal matter ($F_{OC\ Fecal}$) on a monthly basis in a one by one degree global grid. Based on these estimations, we used the corresponding monthly average export for the sampled positions to obtain the F_{OC} to calculate the sinking fluxes (SI, Table S4.8).

The global export of organic carbon is correlated with the concentrations of PFASs at the surface, at DCM depth and with the ratio between them in a complex manner. For instance, the surface PFOA concentration is significantly reduced with increased F_{OC} by phytoplankton ($p < 0.05$), by fecal matter ($p < 0.05$) and as a total OC flux ($p < 0.05$). Also PFOS concentrations at surface and DCM were negatively correlated with phytoplankton F_{OC} ($p < 0.01$). Moreover, the phytoplanktonic fraction of export of organic carbon was negatively correlated with the ratio of surface/DCM concentrations for PFOS and for 3 PFCAs ($p < 0.05$), including PFOA, meaning that for those compounds the concentration decrease with depth was correlated with the biological pump strength.

Results 4

Algal sinking fluxes ranged from 10^{-8} ng m⁻² day⁻¹ for PFHxS, with a low K_{OW} , up to 10^{-2} ng m⁻² day⁻¹ for PFNA and PFDA, long chain PFCAs that have much higher K_{OW} ⁴⁸. Sinking fluxes attributed to zooplankton fecal pellets ranged between 10^{-6} ng m⁻² day⁻¹ for PFHxS and 10^{-1} ng m⁻² day⁻¹ for PFOS, PFNA and PFDA. Even if hydrophobicity is positively correlated with the perfluoroalkyl chain length, PFASs exhibit a higher partition to organic matter than PFCAs, showing PFOS a similar K_{OW} than larger carboxylate chains^{4,49} and therefore comparable sinking fluxes by the biological pump (SI, Table S4.9).

Fluxes associated with the zooplankton fecal matter were found to be higher than those associated only with phytoplankton for the measured concentrations of PFASs at DCM depth (Figure 4.4 and SI, Table S4.9). The settling fluxes of fecal pellets are thus relevant for PFASs, as previously described for other POPs. Conversely, the zooplankton eggs production, included in some studies as a contribution to total planktonic export of POPs^{43,50}, may enhance the $F_{Settling}$ particularly due to the tendency of PFASs to bind to albumin⁵¹. Moreover, as zooplankton undergoes a vertical daily migration, it could be playing an additional role as well. For other hydrophobic POPs, such as polychlorinated biphenyls, their bioconcentration in zooplankton is driven by water-lipid partitioning, whereas for PFASs, it is possible that water-protein partitioning gets more influence⁵¹. During its vertical migration, PFASs will partition at surface and at depth, and since the concentrations are lower at deeper waters, this could induce an additional flux as suggested for other organic pollutants^{43,52,53} which cannot be estimated here as we have no information on the kinetics of these partitioning processes for PFASs in the open deep ocean.

PFOS adsorption to organic carbon is higher than PFOA's, Log K_{OW} 5.3 and 4.6, respectively⁵⁴ and thus its sinking fluxes due to the biological pump were found to be at least one order of magnitude greater, even if a higher concentration of PFOS is affecting as well. Total median $F_{Settling}$ (algal and zooplankton) at the DCM depth for PFOS was $4.54 \cdot 10^{-3}$ and for PFOA $8.25 \cdot 10^{-4}$ ng m⁻² day⁻¹. They differed not only on their rates of export from the surface, but on the global patterns (Figure 4.4). PFOS' higher $F_{Settling}$ was recorded in the South Atlantic Ocean basin, principally near the Brazilian coast, where the concentration of this compound has been reported to be extremely

high^{1,20}. PFOA's $F_{Settling}$ was also intense in the Atlantic Ocean, even if the maximum level of export was found near Central America West coast. Indeed in that area, high concentrations of PFOA coincide with significant phytoplankton abundances⁵⁵ which made the biological pump to be especially relevant. Moreover, the relative importance of the algal sinking fluxes is remarkable at that zone.

Hence, in general zooplankton contribution to the biological pump is highly significant, but the particular case of each PFASs and well as the algal abundance should be taken into account when calculating the export of PFASs from the mixed layer associated with biomass sinking.

Global sinking and PFASs fate

Vertical turbulent diffusion fluxes are generally low, being the maximum values generally associated to extraordinary events of mixing. Sinking fluxes due to the biological pump, several orders of magnitude higher than the turbulent fluxes, seem to dominate the removal processes in the water column according to our estimations (Figure 4.4 and SI, Tables S4.7 and S4.9). Nevertheless, both removal processes are slow, in spite of the considerable uncertainty in their estimation, resulting in long residence times of PFASs in the surface ocean. A mean PFASs concentration in the mixed layer (between surface and DCM) can be calculated to obtain an averaged inventory of PFASs in the global marine euphotic zone of the water column. With the calculated turbulent and sinking fluxes and the averaged inventory, we can estimate a mean residence time for the analyzed compounds; PFOS mean residence time in the mixed layer would be of 27000 years, more than the 17000 years calculated for PFOA, before they are removed from the surface by eddy diffusion and the biological pump. The estimated mean F_{Eddy} plus $F_{Settling}$ for the individual compounds would range from 0.1 ng m⁻² per year for PFHxS to 4 ng m⁻² of annual export for PFDA (Table 4.1).

The more complete assessment on production rates of PFASs is the OECD survey from 2005, reporting almost 100 tons of PFOS and related substances produced in Japan in 2003, followed by China and Brazil with 50 and 30 tons respectively during the same

year⁵⁶. More recent studies endorse China a total production of more than 200 tons of PFASs in 2006⁵⁷. Hence, the production seems to be growing on a much higher rate than rate at which the environment is able to receive and transfer PFASs to the inner areas of the deep ocean. Therefore, unless there are other still unidentified relevant removal processes, the surface ocean will remain as a key reservoir of PFASs for millennia.

Table 4.1. Annual mean export of PFASs due to turbulent fluxes (F_{Eddy}) and biological pump fluxes ($F_{Settling}$).

	PFHxS	PFOS	PFOA	PFNA	PFDA
	$(ng\ m^{-2}\ year^{-1})$				
Mean F_{Eddy}	0.07	0.36	0.05	0.07	0.22
Mean $F_{Settling}$	0.06	1.66	0.30	2.32	3.82
Total	0.13	2.02	0.35	2.39	4.04

Assuming both processes accounted here, the turbulent fluxes and the biological pump, the decay of PFASs from ocean's surface is still not fully described. Firstly, the regions where a higher biological pump export occurs, like Northern Atlantic and Pacific Oceans, Southern Ocean and upwelling areas, like near the western coast of South America⁵⁸, have not been assessed. Therefore, the global means of $F_{Settling}$ could be much higher than those here reported.

Conversely, export of organic matter and particles from the continental shelves towards the Open Ocean, through dense shelf water cascading, has been recently reported to transfer PFASs to deep-sea ecosystems⁵⁹. Therefore, the fluxes of organic and inorganic material in the inner parts of the water column should be assessed further to obtain a total budget of PFASs entrances to the marine environment. Eventually, the formation of deep oceanic water will also deplete PFASs from the global ocean surface. The latter is only relevant at certain regions of the North Atlantic and Southern oceans not sampled during the Malaspina cruise, where the thermohaline circulation provokes the sinking of cooled and less saline water masses.⁶⁰ Other plausible process affecting environmental removal of PFASs from the marine surface is photodegradation, recently reported for a few compounds, but only under precise conditions difficult to reach in the oceanic environment⁶¹ and called into question by Wang and

collaborators⁶². Likewise, biodegradation has not been reported yet for these chemicals⁶³⁻⁶⁶. Nevertheless, surface/DCM concentrations ratio for PFOA, for PFCAs, ($p < 0.01$) and for the total PFASs ($p < 0.05$) correlated with some bacterial activity concurrently measured during the sampling (Pep Gasol, direct communication). Also some correlations were found with other microbiological parameters, like bacterial size or total bacteria carbon content ($p < 0.05$), which supports the idea that the biological activity of the mixed layer of the global ocean could be playing a still unknown but maybe important role in PFASs fate, which needs further research.

More extensive field data of marine turbulence would be needed to confirm F_{Eddy} of PFASs in yet unexplored parts of the ocean. Conversely, even if this study provides the first synoptic approach to the topic at a global scale and with a strong empirical base, more development of the biological pump effects studies is also required. Moreover, the role of marine biota in the biological pump and other processes should be characterized further. Considering the new fluorinated compounds being created as substitutes², the full understanding of PFASs fate in the open Global Ocean, is a complex issue that needs further research.

ACKNOWLEDGEMENTS

This work was funded by the Spanish Ministry of Economy and Competitiveness (Circumnavigation Expedition Malaspina 2010: Global Change and Biodiversity Exploration of the Global Ocean. CSD2008-00077). BBVA Foundation is acknowledged for its economic support of the PhD fellow granted to B. González-Gaya. CSIC and MAGRAMA are also acknowledged for additional financial support. Thanks to the staff from the Physics Block in the Malaspina 2010 circumnavigation for the water turbulence measurements. Ana Gomes, Prof. Josep M. Gasol (ICM-CSIC), and the rest of the people on board measuring bacterial abundances are also acknowledged. Sagrario Calvarro is acknowledged for the instrumental help with UPLC-MS/MS.

REFERENCES

- 1 González-Gaya, B., Dachs, J., Roscales, J. L., Caballero, G. & Jiménez, B. Perfluoroalkylated Substances In The Global Tropical And Subtropical Surface Oceans. *Environmental Science & Technology* **48**, 13076-13084, doi:10.1021/es503490z (2014).
- 2 Ahrens, L. Polyfluoroalkyl compounds in the aquatic environment: a review of their occurrence and fate. *Journal of Environmental Monitoring* **13**, 20-31, doi:10.1039/c0em00373e (2011).
- 3 Lindstrom, A. B., Strynar, M. J. & Libelo, E. L. Polyfluorinated compounds: past, present, and future. *Environmental Science & Technology* **45**, 7954-7961, doi:10.1021/es2011622 (2011).
- 4 Ahrens, L. & Bundschuh, M. Fate and effects of poly- and perfluoroalkyl substances in the aquatic environment: A review. *Environmental Toxicology and Chemistry* **33**, 1921-1929 (2014).
- 5 Yamashita, N. *et al.* A global survey of perfluorinated acids in oceans. *Marine Pollution Bulletin* **51**, 658-668, doi:10.1016/j.marpolbul.2005.04.026 (2005).
- 6 Ahrens, L., Barber, J. L., Xie, Z. & Ebinghaus, R. Longitudinal and latitudinal distribution of perfluoroalkyl compounds in the surface water of the Atlantic Ocean. *Environmental Science & Technology* **43**, 3122-3127 (2009).
- 7 Ahrens, L., Gerwinski, W., Theobald, N. & Ebinghaus, R. Sources of polyfluoroalkyl compounds in the North Sea, Baltic Sea and Norwegian Sea: Evidence from their spatial distribution in surface water. *Marine Pollution Bulletin* **60**, 255-260, doi:10.1016/j.marpolbul.2009.09.013 (2010).
- 8 Ahrens, L. *et al.* Distribution of polyfluoroalkyl compounds in water, suspended particulate matter and sediment from Tokyo Bay, Japan. *Chemosphere* **79**, 266-272, doi:10.1016/j.chemosphere.2010.01.045 (2010).
- 9 Wei, S. *et al.* Distribution of perfluorinated compounds in surface seawaters between Asia and Antarctica. *Marine Pollution Bulletin* **54**, 1813-1818, doi:10.1016/j.marpolbul.2007.08.002 (2007).
- 10 Zhao, Z. *et al.* Distribution and long-range transport of polyfluoroalkyl substances in the Arctic, Atlantic Ocean and Antarctic coast. *Environmental Pollution* **170**, 71-77, doi:10.1016/j.envpol.2012.06.004 (2012).
- 11 Buck, R. C. *et al.* Perfluoroalkyl and polyfluoroalkyl substances in the environment: terminology, classification, and origins. *Integrated environmental assessment and management* **7**, 513-541, doi:10.1002/ieam.258 (2011).
- 12 Jahnke, A., Berger, U., Ebinghaus, R. & Temme, C. Latitudinal gradient of airborne polyfluorinated alkyl substances in the marine atmosphere between Germany and South Africa (53 degrees N-33 degrees S). *Environmental Science & Technology* **41**, 3055-3061 (2007).
- 13 Ahrens, L., Shoeib, M., Del Vento, S., Codling, G. & Halsall, C. Polyfluoroalkyl compounds in the Canadian Arctic atmosphere. *Environmental Chemistry* **8**, 399-406 (2011).
- 14 Del Vento, S., Halsall, C., Gioia, R., Jones, K. & Dachs, J. Volatile per- and polyfluoroalkyl compounds in the remote atmosphere of the western Antarctic Peninsula: an indirect source of perfluoroalkyl acids to Antarctic waters. *Atmospheric Pollution Research* **3**, 450-455 (2012).
- 15 Yamashita, N. *et al.* Perfluorinated acids as novel chemical tracers of global circulation of ocean waters. *Chemosphere* **70**, 1247-1255, doi:10.1016/j.chemosphere.2007.07.079 (2008).

- 16 Benskin, J. P. *et al.* Manufacturing origin of perfluorooctanoate (PFOA) in Atlantic and Canadian Arctic seawater. *Environmental Science & Technology* **46**, 677-685, doi:10.1021/es202958p (2012).
- 17 Kwok, K. Y. *et al.* Flux of perfluorinated chemicals through wet deposition in Japan, the United States, and several other countries. *Environmental Science & Technology* **44**, 7043-7049, doi:10.1021/es101170c (2010).
- 18 Cai, M. *et al.* Occurrence of perfluoroalkyl compounds in surface waters from the North Pacific to the Arctic Ocean. *Environmental Science & Technology* **46**, 661-668, doi:10.1021/es2026278 (2012).
- 19 Prevedouros, K., Cousins, I. T., Buck, R. C. & Korzeniowski, S. H. Sources, fate and transport of perfluorocarboxylates. *Environmental Science & Technology* **40**, 32-44 (2006).
- 20 Benskin, J. P. *et al.* Perfluoroalkyl acids in the Atlantic and Canadian Arctic Oceans. *Environmental Science & Technology* **46**, 5815-5823, doi:10.1021/es300578x (2012).
- 21 Lohmann, R., Jurado, E., Dijkstra, H. A. & Dachs, J. Vertical eddy diffusion as a key mechanism for removing perfluorooctanoic acid (PFOA) from the global surface oceans. *Environ Pollut* **179**, 88-94, doi:10.1016/j.envpol.2013.04.006 (2013).
- 22 Lohmann, R., Jurado, E., Pilson, M. E. Q. & Dachs, J. Oceanic deep water formation as a sink of persistent organic pollutants. *Geophysical Research Letters* **33**, doi:10.1029/2006gl025953 (2006).
- 23 Galbán-Malagón, C., Berrojalbiz, N., Ojeda, M. J. & Dachs, J. The oceanic biological pump modulates the atmospheric transport of persistent organic pollutants to the Arctic. *Nature communications* **3**, 862 (2012).
- 24 Galbán-Malagón, C. J., Berrojalbiz, N., Gioia, R. & Dachs, J. The "degradative" and "biological" pumps controls on the atmospheric deposition and sequestration of hexachlorocyclohexanes and hexachlorobenzene in the North Atlantic and Arctic Oceans. *Environmental Science and Technology* **47**, 7195-7203 (2013).
- 25 Galbán-Malagón, C., Cabrerizo, A., Caballero, G. & Dachs, J. Atmospheric occurrence and deposition of hexachlorobenzene and hexachlorocyclohexanes in the Southern Ocean and Antarctic Peninsula. *Atmospheric Environment* **80**, 41-49 (2013).
- 26 Galbán-Malagón, C. J., Del Vento, S., Cabrerizo, A. & Dachs, J. Factors affecting the atmospheric occurrence and deposition of polychlorinated biphenyls in the Southern Ocean. *Atmospheric Chemistry and Physics* **13**, 12029-12041 (2013).
- 27 Berrojalbiz, N. *et al.* Biogeochemical and physical controls on concentrations of polycyclic aromatic hydrocarbons in water and plankton of the Mediterranean and Black Seas. *Global Biogeochemical Cycles* **25** (2011).
- 28 Boulanger, B., Peck, A. M., Schnoor, J. L. & Hornbuckle, K. C. Mass budget of perfluorooctane surfactants in Lake Ontario. *Environmental Science and Technology* **39**, 74-79 (2005).
- 29 Houde, M. *et al.* Fractionation and bioaccumulation of perfluorooctane sulfonate (PFOS) isomers in a Lake Ontario food web. *Environmental Science & Technology* **42**, 9397-9403 (2008).
- 30 Loi, E. I. *et al.* Trophic magnification of poly- and perfluorinated compounds in a subtropical food web. *Environmental Science & Technology* **45**, 5506-5513, doi:10.1021/es200432n (2011).
- 31 Powley, C. R., George, S. W., Russell, M. H., Hoke, R. A. & Buck, R. C. Polyfluorinated chemicals in a spatially and temporally integrated food web in the Western Arctic. *Chemosphere* **70**, 664-672, doi:10.1016/j.chemosphere.2007.06.067 (2008).
- 32 Fernández-Castro, B. *et al.* Microstructure turbulence and diffusivity parameterization in the tropical and subtropical Atlantic, Pacific and Indian Oceans during the Malaspina 2010 expedition. *Deep Sea Research Part I: Oceanographic Research Papers* **94**, 15-30, doi:10.1016/j.dsr.2014.08.006 (2014).

- 33 Huisman, J., Thi, N. N. P., Karl, D. M. & Sommeijer, B. Reduced mixing generates oscillations and chaos in the oceanic deep chlorophyll maximum. *Nature* **439**, 322-325 (2006).
- 34 Cullen, J. J. The deep chlorophyll maximum: comparing vertical profiles of chlorophyll a. *Canadian Journal of Fisheries and Aquatic Sciences* **39**, 791-803 (1982).
- 35 Longhurst, A. R. & Harrison, W. G. The biological pump: profiles of plankton production and consumption in the upper ocean. *Progress in Oceanography* **22**, 47-123 (1989).
- 36 Weinbauer, M. G. Ecology of prokaryotic viruses. *FEMS microbiology reviews* **28**, 127-181 (2004).
- 37 Paul, A. G., Jones, K. C. & Sweetman, A. J. A First Global Production, Emission, And Environmental Inventory For Perfluorooctane Sulfonate. *Environmental Science & Technology* **43**, 386-392, doi:10.1021/es802216n (2009).
- 38 Osborn, T. R. Estimates of the Local Rate of Vertical Diffusion from Dissipation Measurements. *Journal of Physical Oceanography* **10**, 83-89, doi:10.1175/1520-0485(1980)010<0083:EOTLRO>2.0.CO;2 (1980).
- 39 Dachs, J. *et al.* Oceanic Biogeochemical Controls on Global Dynamics of Persistent Organic Pollutants. *Environmental Science & Technology* **36**, 4229-4237, doi:10.1021/es025724k (2002).
- 40 Siegel, D. A. *et al.* Global assessment of ocean carbon export by combining satellite observations and food-web models. *Global Biogeochemical Cycles* **28**, 2013GB004743, doi:10.1002/2013GB004743 (2014).
- 41 Lipiatou, E., Marty, J.-C. & Saliot, A. Sediment trap fluxes of polycyclic aromatic hydrocarbons in the Mediterranean Sea. *Marine Chemistry* **44**, 43-54, doi:10.1016/0304-4203(93)90005-9 (1993).
- 42 Dachs, J., Bayona, J. M., Fowler, S. W., Miquel, J. C. & Albaigés, J. Vertical fluxes of polycyclic aromatic hydrocarbons and organochlorine compounds in the western Alboran Sea (southwestern Mediterranean). *Marine Chemistry* **52**, 75-86 (1996).
- 43 Berrojalbiz, N. *et al.* Accumulation and Cycling of Polycyclic Aromatic Hydrocarbons in Zooplankton. *Environmental Science & Technology* **43**, 2295-2301, doi:10.1021/es8018226 (2009).
- 44 Boyd, P. *et al.* Measuring biogenic carbon flux in the ocean. *Science* **275**, 554-555 (1997).
- 45 Boyd, P. & Trull, T. Understanding the export of biogenic particles in oceanic waters: is there consensus? *Progress in Oceanography* **72**, 276-312 (2007).
- 46 Henson, S. A., Sanders, R. & Madsen, E. Global patterns in efficiency of particulate organic carbon export and transfer to the deep ocean. *Global Biogeochemical Cycles* **26** (2012).
- 47 Lima, I. D., Lam, P. J. & Doney, S. C. Dynamics of particulate organic carbon flux in a global ocean model. *Biogeosciences* **11**, 1177-1198, doi:10.5194/bg-11-1177-2014 (2014).
- 48 Armitage, J. M., Macleod, M. & Cousins, I. T. Comparative assessment of the global fate and transport pathways of long-chain perfluorocarboxylic acids (PFCAs) and perfluorocarboxylates (PFCs) emitted from direct sources. *Environmental science & technology* **43**, 5830-5836 (2009).
- 49 Wang, Z., MacLeod, M., Cousins, I. T., Scheringer, M. & Hungerbühler, K. Using COSMOtherm to predict physicochemical properties of poly- and perfluorinated alkyl substances (PFASs). *Environmental Chemistry* **8**, 389-398, doi:10.1071/EN10143 (2011).
- 50 Nizzetto, L. *et al.* Biological pump control of the fate and distribution of hydrophobic organic pollutants in water and plankton. *Environmental science & technology* **46**, 3204-3211 (2012).

- 51 Ng, C. A. & Hungerbühler, K. Bioaccumulation of Perfluorinated Alkyl Acids: Observations and Models. *Environmental Science & Technology* **48**, 4637-4648, doi:10.1021/es404008g (2014).
- 52 Frouin, H. *et al.* Partitioning and bioaccumulation of PCBs and PBDEs in marine plankton from the Strait of Georgia, British Columbia, Canada. *Progress in Oceanography* **115**, 65-75 (2013).
- 53 Pućko, M. *et al.* Importance of Arctic zooplankton seasonal migrations for α -hexachlorocyclohexane bioaccumulation dynamics. *Environmental Science and Technology* **47**, 4155-4163, doi:10.1021/es304472d (2013).
- 54 Kelly, B. C. *et al.* Perfluoroalkyl contaminants in an arctic marine food web: Trophic magnification and wildlife exposure. *Environmental Science and Technology* **43**, 4037-4043 (2009).
- 55 Royer, S. J., Mahajan, A. S., Galí, M., Saltzman, E. & Simó, R. Small-scale variability patterns of DMS and phytoplankton in surface waters of the tropical and subtropical Atlantic, Indian, and Pacific Oceans. *Geophysical Research Letters* **42**, 475-483, doi:10.1002/2014GL062543 (2015).
- 56 OECD. Results of survey on Production and use of PFOS, PFAS and PFOA, related substances and products/mixtures containing these substances. (ORGANISATION FOR ECONOMIC CO-OPERATION AND DEVELOPMENT, Paris 2004, 2005).
- 57 Carloni, D. OECD Report Perfluorooctane Sulfonate (PFOS) Production and Use: Past and Current Evidence. (Report for UNIDO, 2009).
- 58 Honjo, S., Manganini, S. J., Krishfield, R. A. & Francois, R. Particulate organic carbon fluxes to the ocean interior and factors controlling the biological pump: A synthesis of global sediment trap programs since 1983. *Progress in Oceanography* **76**, 217-285 (2008).
- 59 Sanchez-Vidal, A. *et al.* Delivery of unprecedented amounts of perfluoroalkyl substances towards the deep-sea. *Science of The Total Environment* **526**, 41-48, doi:10.1016/j.scitotenv.2015.04.080 (2015).
- 60 Rahmstorf, S. Ocean circulation and climate during the past 120,000 years. *Nature* **419**, 207-214 (2002).
- 61 Taniyasu, S., Yamashita, N., Yamazaki, E., Petrick, G. & Kannan, K. The environmental photolysis of perfluorooctanesulfonate, perfluorooctanoate, and related fluorochemicals. *Chemosphere* **90**, 1686-1692 (2013).
- 62 Wang, Z., Cousins, I. T. & Scheringer, M. Comment on "The environmental photolysis of perfluorooctanesulfonate, perfluorooctanoate, and related fluorochemicals". *Chemosphere* **122**, 301-303 (2015).
- 63 Fromel, T. & Knepper, T. P. Biodegradation of fluorinated alkyl substances. *Reviews of environmental contamination and toxicology* **208**, 161-177, doi:10.1007/978-1-4419-6880-7_3 (2010).
- 64 Zhang, X. J., Lai, T. B. & Kong, R. Y. Biology of fluoro-organic compounds. *Topics in current chemistry* **308**, 365-404, doi:10.1007/128_2011_270 (2012).
- 65 Liou, J.-C., Szostek, B., DeRito, C. & Madsen, E. Investigating the biodegradability of perfluorooctanoic acid. *Chemosphere* **80**, 176-183 (2010).
- 66 Liu, J. & Avendaño, S. M. Microbial degradation of polyfluoroalkyl chemicals in the environment: a review. *Environment international* **61**, 98-114 (2013).

5. Cycling of Polycyclic Aromatic Hydrocarbons in the Surface Open Ocean

Belén González-Gaya^{1,2*}, María-Carmen Fernández-Pinos¹, Cristóbal Galbán-Malagón¹, Antonio Bode³, Montserrat Vidal⁴, Begoña Jiménez², and Jordi Dachs¹

¹ Department of Environmental Chemistry, Institute of Environmental Assessment and Water Research, IDAEA-CSIC; Barcelona, Catalunya, Spain.

² Department of Instrumental Analysis and Environmental Chemistry, Institute of Organic Chemistry, IQOG-CSIC; Madrid, Spain.

³ Spanish Oceanography Institute; A Coruña, Spain.

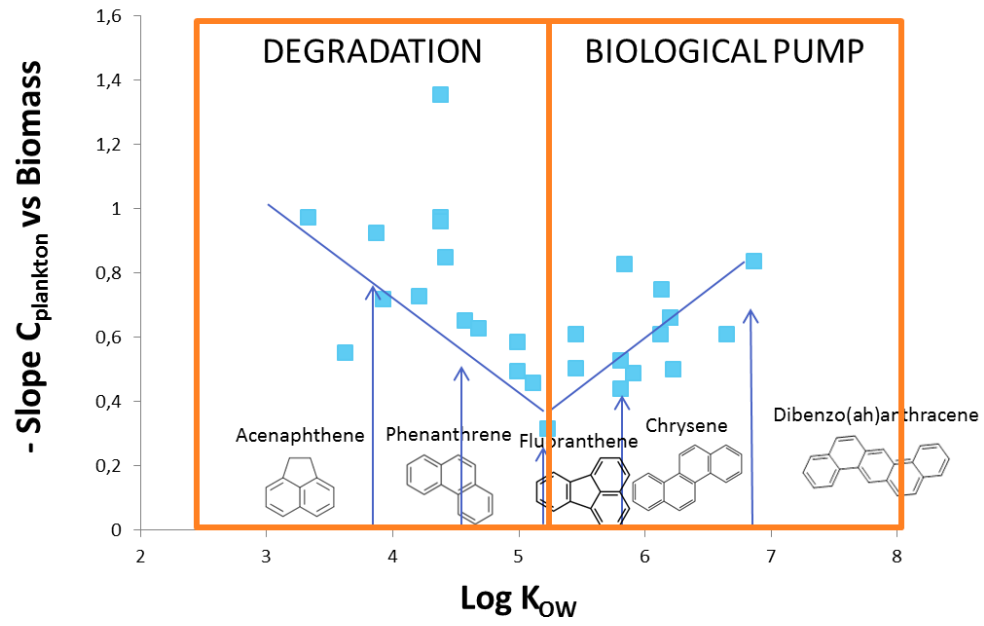
⁴ Department of Ecology, Barcelona University; Barcelona, Catalunya, Spain.

*Corresponding Author email: bgggam@idaea.csic.es

In preparation

ABSTRACT

Polycyclic Aromatic Hydrocarbons (PAHs) are organic pollutants coming from anthropogenic origins (incomplete combustion and fossil fuels) but also from natural sources. Their occurrence in marine environments has been widely reported but most studies focused to the effects that such substances may have in wildlife or ecosystems health. Conversely, some reports have been conducted about their dynamics, mainly originated in continental areas and reaching remote areas due to their long range transport potential, being the Open Ocean a relevant sink at a global scale. Moreover, PAHs degradation in the water column and the oceanic sink through the sequestration of pollutants by biomass and particles, and subsequent settling (biological pump), have been pointed to strongly affect PAHs occurrence in some marine environments. The assessment of these processes and the identification of the key parameters affecting them at a global scale is the purpose of this work. During the *Malaspina 2010* circumnavigation cruise, which sailed the Atlantic, Pacific and Indian oceans between 35°N and 40°S simultaneous water and plankton samples were taken. PAHs occurrence was analyzed for 64 individual congeners; in surface dissolved water phase concentration ranged from 0.2 to 11.0 ng L⁻¹, in particulate surface phase from 8.0 to 4700 ng g_{dw}⁻¹ and in plankton phase from 11.0 to 7700 ng g_{dw}⁻¹. Correlations versus total suspended particles and biomass showed a relevant influence of the air-water-particles equilibria for surface samples, and an effective removal by degradation and the biological pump in the mixed layer. Biological pump fluxes were estimated separately for the phytoplankton and zooplanktonic fecal sinking matter, being the last 1 order of magnitude higher. Total biological pump fluxes showed to remove an annual amount of 0.008 Tg of PAHs at a planetary scale. Therefore, it is a very relevant process in the global budget of these pollutants even if the complexity of their governing mechanisms needs still to be fully understood.



Graphical Abstract 5.

INTRODUCTION

Polycyclic Aromatic Hydrocarbons (PAHs) are generated during incomplete combustion of fossil fuels and organic matter, in addition to accidental oil spills and biogenic sources¹⁻³. They cause carcinogenic and toxic effects in biota, and have been proved to be harmful for ecosystems⁴. Moreover, PAHs are ubiquitous in the environment. Due to their physicochemical properties, PAHs partition to all environmental matrixes and are found at proximate and remote sites from primary anthropogenic sources^{3,5,6}.

Earlier assessments of PAHs in the marine environment have focused on their occurrence in sediments⁷⁻¹⁰ and in surface waters¹¹⁻¹⁴, with few reports of the PAH occurrence and cycling in different matrixes in the surface (top 200 m) of the marine environment^{13,15,16}. PAHs reach the Open Ocean by atmospheric deposition^{5,17} (Chapter 2). Once PAHs enter the water column by diffusive air-water exchange and dry/wet deposition, they move into the organic matter cycle by partitioning to particulate organic carbon (POC), accounting bacteria, phytoplankton and zooplankton as important pools. In addition, part of this particulate matter, mainly aggregates of organic matter, fecal pellets, and dead cells, will settle to the deep ocean (biological pump), favoring an oceanic sink of PAHs^{7,8,10,17-19}. However, it has been observed that atmospheric inputs of PAHs are two orders of magnitude higher than their sinking fluxes^{17,20}, thus pointing out to important degradation processes in the water column. This degradation is mostly due to bacteria and zooplankton^{16,21}. Even though these earlier works were performed at the Mediterranean and Black Sea, it is possible that a similar scenario occurs for the global ocean. As the atmosphere-ocean exchange of PAHs is remarkable, the cycling/degradation in the water column and how they partition to particles and plankton are important processes for understanding the regional and global environmental fate and sinks of this family of organic pollutants. These degradative processes, together with the biological pump will be responsible for the oceanic sink of PAHs.

Previously, the degradative potential in surface waters has been determined by comparison of settling fluxes and atmospheric inputs of PAHs^{17,20}, and by the patterns of PAHs in plankton samples. Accumulation of PAHs and other organic pollutants in phyto- and zooplankton is important as an introduction vector of pollution into oceanic

food webs, and also as supporting contaminants levels in sinking particles (Biological pump). Nevertheless, there is a dearth of measurements of PAHs in oceanic plankton and particulate matter, and of the assessment of their role in the oceanic cycling of these pollutants. In general, previous studies have been undertaken from an ecotoxicological point of view and report effects of PAHs in marine wildlife ²²⁻²⁴ and plankton ²⁵⁻²⁷. Earlier works on PAHs and other persistent organic pollutants (POPs) have described a complex interaction between plankton and contaminants which includes the influence of biomass dilution, air-water-biomass exchange and the biological pump ^{16,28-31}. All these processes drive the occurrence of organic pollutants in water and biota from proximate and remote marine regions ³¹⁻³⁵ (Chapter 4). Biomass dilution is explained by the lower concentrations in plankton depleted into large amounts of plankton biomass, largely in very productive areas ³⁶⁻³⁸. Also trophic dilution through marine food webs has been described ³⁹. Air-water exchange can counteract this biomass dilution by supplying POPs to surface waters, when they are depleted of pollutants. Nevertheless, this exchange plays a relevant role at a global scale mostly in the ocean surface, being not that significant along the whole water column ¹⁶. The biological pump fluxes are significant modifying plankton phase concentrations when the sinking fluxes due to organic matter settling are higher than the air-water-plankton exchange, mainly for highly hydrophobic POPs that strongly attach to organic matter and at deeper depths than surface ¹⁶.

The objectives of this work are therefore, i) to report the largest dataset available for PAHs in the dissolved phase, particulate phase and plankton from the Atlantic, Pacific and Indian oceans, and ii) to elucidate the biogeochemical and physical controls that drive their occurrence in the water column, as well their accumulation in surface particles and photic zone plankton in the Open Ocean.

MATERIALS AND METHODS

Sampling strategy

All samples were gathered during the *Malaspina 2010* circumnavigation cruise between December 2010 and July 2011 on board of the Hesperides research vessel. The sampling campaign crossed the north and south basins of the Atlantic and Pacific oceans as well as the Indian Ocean, between 35°N and 40°S, covering all the tropical and subtropical oceanic gyres (Figure 5.1). Water samples (n = 69) were taken from the subsurface (4 m) using the continuous water sampling systems of the boat, during one-day transects in alternate days. Particles were retained over precombusted GF/F filters (0.7 µm pore size, Whatman) and the dissolved pollutants were concentrated in XAD-2 resin placed on stainless columns after the filtration. Mean filtration volume was 239 L (ranging from 69 to 391 L). Columns and filters were kept at 4°C and -20°C respectively until their further treatment in the laboratory after the cruise. Concurrently, plankton samples (n = 71) were gathered in 50 µm mesh size vertical trawl, from 20 m deeper than the deep chlorophyll maximum depth (DCM; see Chapter 4 SI for a detailed list of the DCM depths), and were immediately filtered (GF/D, 1.7 µm pore size, Whatman) and kept at -20°C, as done in other studies¹⁶, until their analysis in the laboratory after the circumnavigation. Emplacement and time of sampling for water sampling transects and for plankton trawls are noted in Table S5.1, and in Table S5.2, respectively in the supplementary information (SI).

PAH analysis and quantification

Dissolved phase, particulate phase, and plankton samples were analyzed following a slightly modified protocol previously reported^{16,17} (Chapter 2). Prior to the extraction, a mix of deuterated PAHs (Acenaphthene D10, Phenanthrene D10, Chrysene D12, and Perylene D12) was added as a recovery standard. Briefly, the XAD-2 resin was washed sequentially with methanol (MeOH) and dichloromethane (DCM), which were liquid-

liquid extracted with hexane (Hx) and further purified on a sulfate column and fractionated on an alumina column.

Filters containing the particulate and plankton samples were freeze dried and soxhlet extracted overnight with DCIM/MeOH (2:1) and DCl/Hx (1:1), respectively. Particulate phase samples were further purified and fractionated over an alumina column. Plankton samples were purified and fractionated over a combined silica and alumina column. Further details are provided in the SI (Text S5.1).

The aromatic fractions underwent the instrumental analysis for 64 individual PAHs, that was carried out on an Agilent 6890 Series gas chromatograph coupled with a mass spectrometer Agilent 5973 (GS-MS) operating in selected ion monitoring (SIM) and electron impact mode (EI) as described elsewhere ⁵ (Chapter 2). The quantification followed the internal standard procedure, using a mix of Anthracene-d₁₀, Pyrene-d₁₀, P-terphenyl-d₁₄ and Benzo[*b*]fluoranthene-d₁₂ added to the samples prior to injection.

The 64 PAHs identified and quantified were grouped in 28 parent and isomer clusters.

Quality Assurance and Quality Control

Laboratory and field blanks, recoveries and analytical limits were controlled and fulfilled standard QA/QC constraints. The detection limit (DL) was set as the inferior limit of the calibration curve (0.02 ng for all compounds). The quantification limit (QL) corresponds to the mean blank level of each sample phase.

Dissolved phase blanks and recoveries are reported elsewhere (Chapter 2). Particulate phase blanks (4 field blanks and 7 laboratory blanks) were concurrently extracted and analyzed with the field samples. The average total pg found per blank was one order of magnitude lower than the PAHs measured at the samples. Average recoveries were 76% for Perylene D12, for which all given concentrations have been surrogate recovery corrected. See Table S5.3 in the SI for complete QA/QC information. 4 field blanks and 7 laboratory blanks were concurrently extracted and analyzed with plankton samples. The average total pg found per blank was as well one order of magnitude lower than the measured samples. Moreover, plankton samples breakthrough was evaluated by

doing a second extraction of five random samples and between 81% and 100% of each single PAHs was extracted in the first batch. Recoveries of the deuterated PAHs ranged between 25% for Acenaphthene D10 and 102% for Perylene D12. All concentrations have been surrogate recovery corrected with the proper standard (Table S5.4 in the SI).

Organic Carbon in particles and plankton

POC has been reported to affect binding and therefore occurrence and bioavailability of PAHs in marine environments ³⁵. POC was measured during *Malaspina 2010* circumnavigation concurrently with the water phase sampling. Total suspended matter was trapped onto GF/F filters (0.7 µm pore size, Whatman), dried overnight (60°C) and exposed to HCl (35%) vapors to remove carbonates. Combustion catalyzed with V₂O₅ was performed with an elemental analyzer (Carlo Erba 1108) and quantification of OC was done through gas chromatography coupled with a thermic conductivity detector ⁴⁰ (complete data set in Table S5.5).

The spatial variability of biomass and stable isotopes in plankton size fractions was studied in concurrent samples to the plankton phase to determine nitrogen and carbon sources. Samples for isotopes analysis were collected by 40 mm mesh size vertical tows along the upper 200 m of the water column. Sampling was always performed right after the plankton phase collection, during the local early morning time. Filtrate was separated into five size fractions (40 - 200, 200 - 500, 500 - 1000, 1000 - 2000 and over 2000 mm mesh size) by filtration over nylon sieves and removing the large gelatinous organisms found. Aliquots for each size fraction were collected on glass-fiber filters, dried (60°C, 48 h) and stored in a desiccator. The determination of biomass (dry weight), carbon and nitrogen content and natural abundance of stable carbon and nitrogen isotopes was performed after the circumnavigation. Isotope analysis was accomplished with an elemental analyzer (Carlo Erba CHNSO 1108) coupled to an isotope-ratio mass spectrometer (Finnigan Mat Delta Plus). Further analytical details can be consulted elsewhere ⁴¹. Total carbon and nitrogen data is included in Table S5.6.

The biological pump

The contribution of the export of PAHs from the ocean surface due to sorption to organic matter and subsequent sinking (biological pump) was evaluated from the plankton phase samples taken during the *Malaspina 2010* circumnavigation. Biological pump calculations follow the same procedure than those in Chapter 4, by using Siegel and coworker's global climatology of organic carbon export from the surface mixed layer (F_{OC})⁴². The reported monthly averaged F_{OC} during the sampling was used to estimate the organic matter flux (F_{OM} , assuming that it is 1.8 times F_{OC} ³²) due to phytoplankton (F_{Phyto} , $\text{gC m}^{-2}\text{day}^{-1}$) and to zooplankton associated pellets (F_{Fecal} , $\text{gC m}^{-2}\text{day}^{-1}$) separately (Table S5.7, SI). Therefore, the biological pump fluxes ($F_{Settling}$, $\text{ng m}^{-2}\text{day}^{-1}$) is given by,

$$F_{Settling} = -F_{OM} C_{Plankton} = -(F_{Phyto} + F_{Fecal})C_{Plank} \quad [5.1]$$

where $C_{Plankton}$ (ng gC^{-1}) is the concentration of PAHs measured in plankton normalized by organic carbon content. We assume that the concentrations in plankton are representative of the concentrations in phytoplankton and fecal pellets. The calculated biological pump fluxes shape the biggest database reported for PAHs at a global scale and moreover, this is the first time that phytoplankton and fecal contribution are estimated individually at such spatial resolution.

Statistical analysis

Statistical analysis was performed using SPSS Statistics (21.0 IBM Corp.). Kolmogorov-Smirnov test were run to assure normality of the data, which was found for most compounds (24 and 20 out of 28 in dissolved and particulate phases, respectively) ($p > 0.05$). PAH concentrations in plankton were not normally distributed though. Nevertheless, logarithmic transformation of the data gave a statistically normalized distribution ($p > 0.05$). Parametric statistics were thus applied for the comparisons and correlations within the data.

RESULTS AND DISCUSSION

PAH concentrations in oceanic water

Dissolved phase concentrations (C_w) for all measured PAHs have been briefly reported in Chapter 2 (concentrations can be found in Table S5.8 in the SI). Total Σ_{64} PAHs concentration ranged between 0.2 and 10.6 ng L⁻¹, with an average value of 2.7 ng L⁻¹ in the open ocean. The more abundant individual PAHs were fluoranthene and pyrene (average 0.3 and 0.4 ng L⁻¹ respectively) (Figure 5.2). C_w is relatively homogeneous globally when compared to atmospheric concentrations (Chapter 2), with no significant differences of Σ_{64} PAHs concentrations for the sampled oceanic subbasins. Nevertheless, decreasing concentration gradients were found from continents towards central tropical gyres, especially in the South Atlantic and Indian Oceans (Figure 5.1). Concentrations of PAHs in remote oceanic areas have been rarely described. In the North Atlantic and Arctic oceans, Lohmann and collaborators¹² showed values ranging from tens to hundreds pg L⁻¹ for individual measured PAHs, which are in the lowest values of our concentrations, corresponding with the decreasing latitudinal gradient that they report. Similar low values are reported in the same area by Schulz-Bull⁴³. Another study by Lohmann¹³ in the tropical western area of Atlantic Ocean provided values for phenanthrene (Phe), fluoranthene and pyrene between 32 to 1400 pg L⁻¹, 13 to 190 pg L⁻¹ and 25 to 240 pg L⁻¹, respectively, which are in the range of our measurements for the same oceanic basin. Besides, the western Atlantic covered by Nizzetto¹¹, reported also values in the same order of magnitude for individual PAHs, even if they provide lower total concentrations as they considered only 10 individual PAHs. Conversely, given upper ranges of this work coincide with those reported in the Mediterranean by Berrojalbiz et al¹⁶.

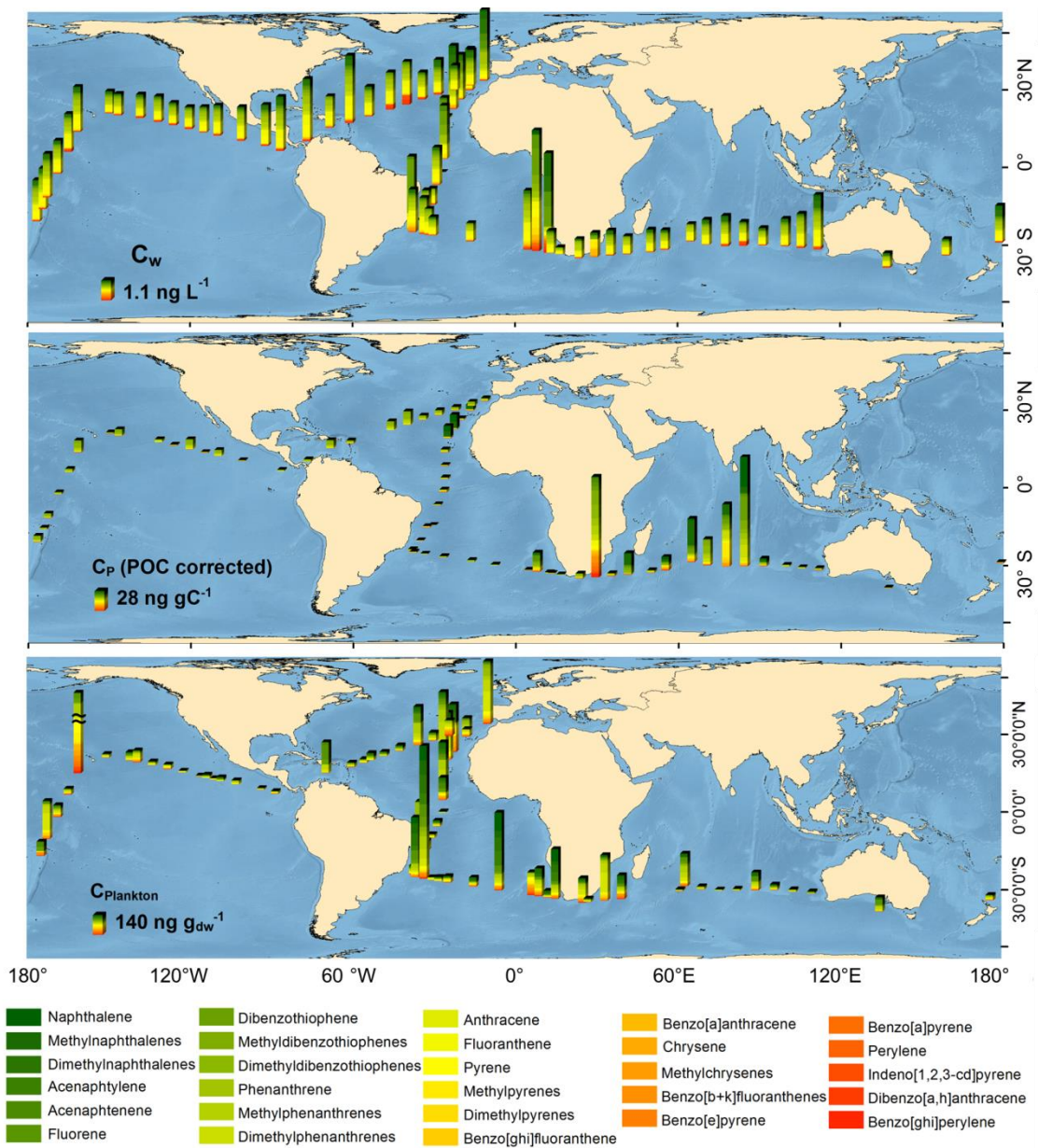


Figure 5.1. PAHs global concentration in the dissolved phase (ng L^{-1}) (upper panel), particulate phase (ng gC^{-1}) (middle panel) and plankton (ng g_{dw}^{-1}) (bottom panel). Marked sample (\approx) has been reduced by 10 fold to adjust the bars size.

Particulate phase total concentrations (C_p) ranged between 7.7 and 4700 ng g_{dw}^{-1} (global mean 270 ng g_{dw}^{-1}). The more abundant compounds were found to be dibenzothiophene (DBT, 14 ng g_{dw}^{-1}) and its methylated forms (dimethyl-DBT and methyl-DBT at 42 and 31 mean ng g_{dw}^{-1} respectively), naphthalenes (Naph) (25 and 15 ng g_{dw}^{-1} for methyl-Naph and Naph) and phenanthrenes (22 and 19 ng g_{dw}^{-1} methyl-Phe and Phe), being always the methylated forms more abundant (Figure 5.2, Table S5.9, SI). The relative abundance of individual congeners in the subbasins sampled was comparable (Figure S5.1, SI). However, total concentrations were significantly higher ($p < 0.05$) in the Indian Ocean than in the rest of the subbasins. This is even more patent when the obtained concentrations are corrected by measured POC in the water column, as this correction modulates the higher presence of PAHs for sampling periods with higher particulate organic matter concentrations (Figure 5.1). Highest POC was recorded near continental areas, reaching maximal concentrations near Central America's west coast and near South Africa, contrasting with the particularly oligotrophic center of the oceanic subtropical gyres, with low POC concentrations. Therefore, after normalizing C_p by POC, a high PAHs contamination arises, for instance, in the central Indian Ocean (Figure 5.1). High concentrations of PAHs have been reported in the Indian Ocean in the marine aerosol⁵, which may act as the main entry vector to the open ocean for some PAHs as suggested in previous works⁴⁴. Similar concentrations in particulate phase in the Atlantic Ocean (particularly those of high MW PAHs) were reported as well by Nizzetto et al¹¹, even if slightly lower volumetric concentrations are given by Lohmann in the western part of the North and South Atlantic Ocean¹³, in the range of few $pg L^{-1}$, when the mean values for individual compounds reported in this work are from few to tens $pg L^{-1}$. On the other hand, the concentrations reported in the Mediterranean Sea¹⁶ are between the same range and one order of magnitude higher than the concentrations found in the open ocean for individual PAHs.

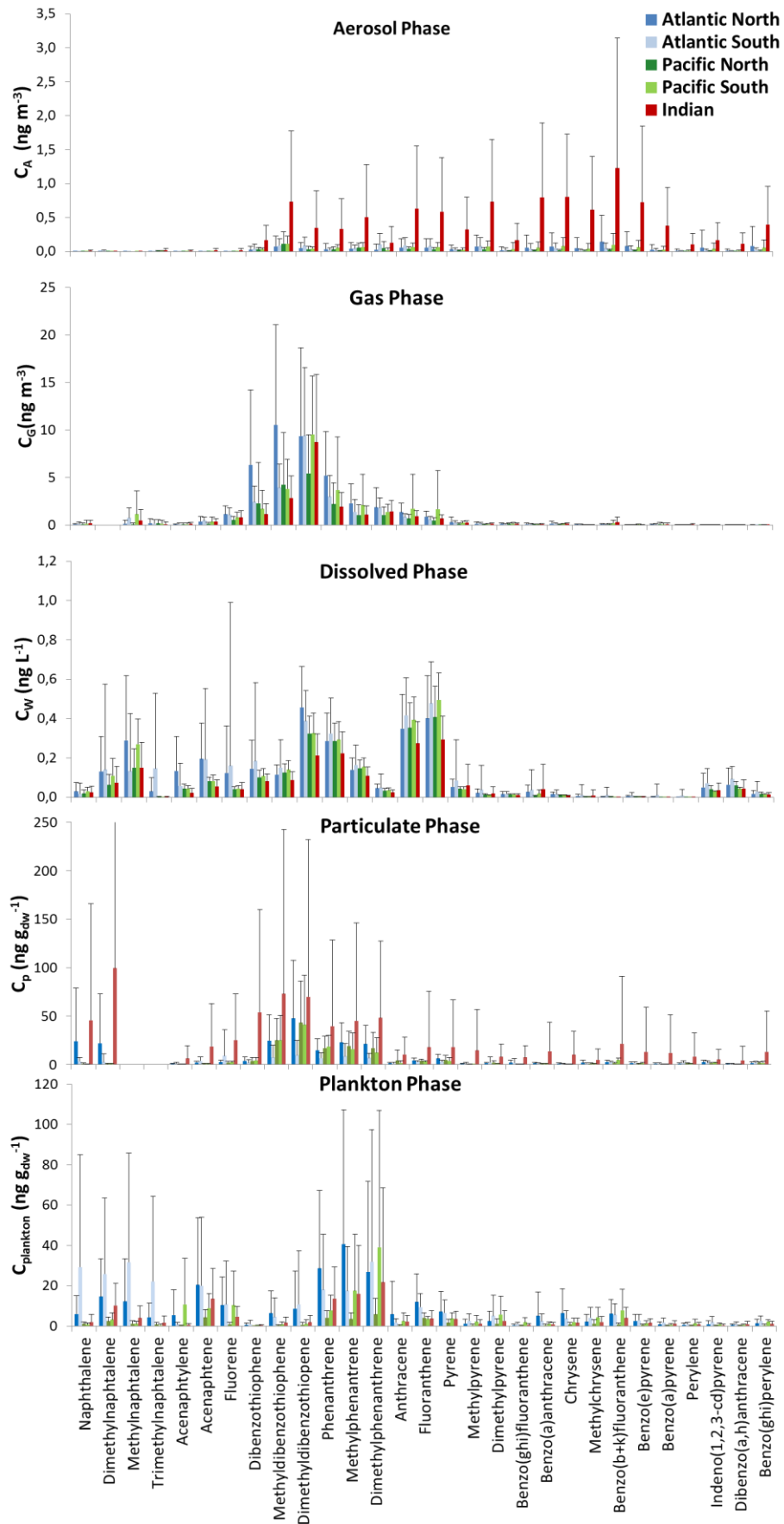


Figure 5.2. Average concentrations and standard deviation of PAHs in the aerosol, gas, dissolved, particulate and plankton phase for the different oceanic basins.

PAHs occurrence in oceanic plankton

All 64 selected PAHs were found ubiquitously in plankton (Table S5.10, SI), being the Phe and its methylated forms (methyl-Phe, dimethyl-Phe) the most abundant congeners (1000 ng g_{dw}⁻¹, 260 ng g_{dw}⁻¹ and 280 ng g_{dw}⁻¹ respective medians) (Figure 5.2). Relevant concentrations of lighter PAHs were also found, being the profiles similar to the dissolved phase profile (Figure 5.2). The relative abundance of the individual PAHs was not significantly different among the oceanic sub basins (Figure S5.2, SI). Only in South Atlantic Ocean, a lower percentage of Phe and methyl-Phe and higher occurrence of 2-ring and volatile PAHs was observed. Concurrently, the PAHs plankton phase concentrations ($C_{Plankton}$) was higher in the South Atlantic Ocean (median $\sum_{64}PAHs$ 140 ng g_{dw}⁻¹) followed by North Atlantic Ocean (median $\sum_{64}PAHs$ 130 ng g_{dw}⁻¹), with particularly high $C_{Plankton}$ in the Brazilian and West African coasts proximities (Figure 5.1). Lowest concentrations were found in the Indian Ocean (median $\sum_{64}PAHs$ 100 ng g_{dw}⁻¹) and large regions of the Pacific Ocean. The $C_{Plankton}$ found are between one and two orders of magnitude lower than the average values in the Mediterranean Sea for individual compounds, even if the maximum records reported here, in coastal Atlantic areas, are of the same order of magnitude¹⁶.

Particle-water partition of PAHs and controls on surface particle phase concentrations

The coefficient of partition (K_{OC}) between the dissolved and the particulate phases of the surface water was calculated by,

$$K_{OC} = \frac{C_P}{C_W} \quad [5.2]$$

where C_P is the PAH concentration in the particulate phase corrected by POC (ng kg_{POC}⁻¹) and C_W is the concentration in the dissolved phase (ng L⁻¹). K_{OC} ranged from 10⁴ to 10⁸ L Kg⁻¹ and its values were larger for the higher MW PAHs (Figure S5.3, SI). The particular chemical properties of a PAH, namely hydrophobicity as measured by the octanol-water partition coefficient (K_{OW}) and the environmental conditions (like temperature) influence the partition in the water phase^{32,45}.

K_{OC} and C_p are affected by the amount of present particles (total suspended particles, TSP , or organic matter as measured by the POC in the water column). The dependence between the obtained K_{OC} values and POC during the *Malaspina 2010* cruise exhibits a potential decreasing correlation (statistically significant for 17 out of 28 congeners, $p < 0.05$) (Figure 5.3, left). In general, for the more hydrophobic compounds (higher K_{OW}) K_{OC} decreased faster with growing POC than for the lighter compounds, confirming a decrease of the C_p/C_w ratio if the particles are enriched in organic carbon. This trend follows the pattern described before for POPs in plankton, where higher concentrations are observed at sites with lower organic matter, and lower concentrations are observed at sites with higher POC. This is probably due to a biomass (or organic carbon) dilution, but since the more hydrophobic compounds show a stronger dependence, it may indicate that this biomass dilution is modulated by air-water exchange and settling fluxes of POC^{16,31}. Likewise, C_p is also negatively correlated with POC (Figure 5.3, right) (statistically significant for 4 out of 28 congeners, $p < 0.05$).

Both the dissolved and particulate samples were taken close to the surface, and thus it is reasonable to consider that the PAH concentrations in the particulate phase are influenced by the levels of PAHs in the gas phase (C_G). By assuming air-water-particle equilibria, it is possible to predict a C_p^* value (concentrations in particles equilibrated with the gas phase) from the measured C_G (Chapter 2) by,

$$C_p^* = \frac{C_G K_{OC}}{H'} \quad [5.3]$$

where K_{OC} values were estimated as described above, and H' is Henry's Law constant temperature and salinity corrected as explained elsewhere (Chapter 2). Figure 5.4 shows the predicted C_p^* versus the measured C_p where it can be observed that there is a significant positive correlation ($p < 0.01$) for 25 out of 28 compounds. It is not significant for the heavy PAHs Dibenzo[*a,h*]anthracene and Benzo[*ghi*]perylene, which enter the ocean mainly by dry deposition and not by diffusive exchange⁵. Even though there are correlations between predicted and measured C_p , the predicted values are a factor between 2 and 10 higher than the measured C_p . This indicated that generally, the surface water was undersaturated respect to atmospheric PAHs, which is consistent

Results 5

with the net air to water diffusive flux measured for most sampling periods and individual compounds during the *Malaspina 2010* circumnavigation (Chapter 2). Thus, the accumulation of PAHs in surface particulates reflects the levels found in the atmosphere, even if they are not equilibrated, but other processes may modulate their concentrations, such as dilution with POC. Overall, it is remarkable that even though C_W and C_P were measured close to the surface, these are not equilibrated with the atmosphere, which suggests a fast kinetics of the partitioning, maybe degradation and other controls of water column concentrations.

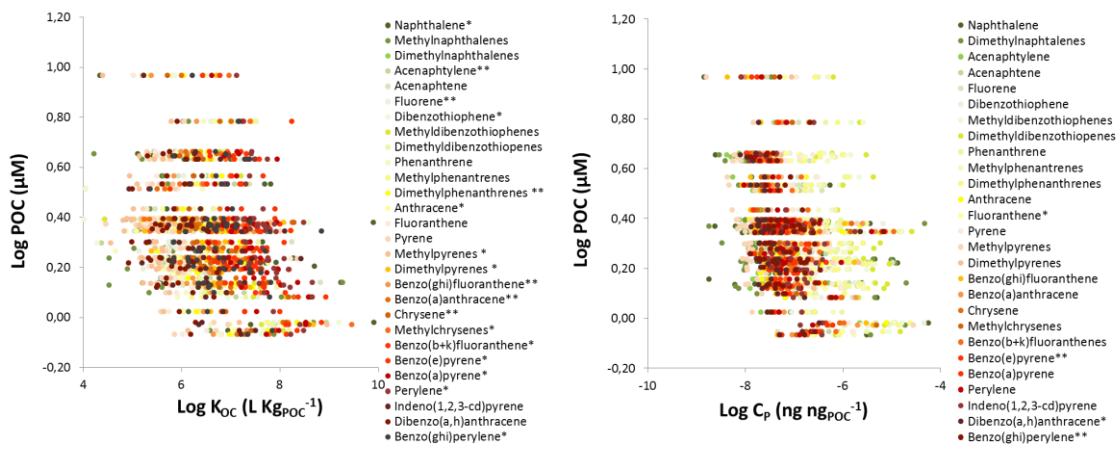


Figure 5.3. Correlation between $\text{Log}K_{OC}$ (left) and $\text{Log}C_p$ (right) versus $\text{Log}POC$. Statistical significance is noted per each PAH by * ($p < 0.05$) and ** ($p < 0.01$).

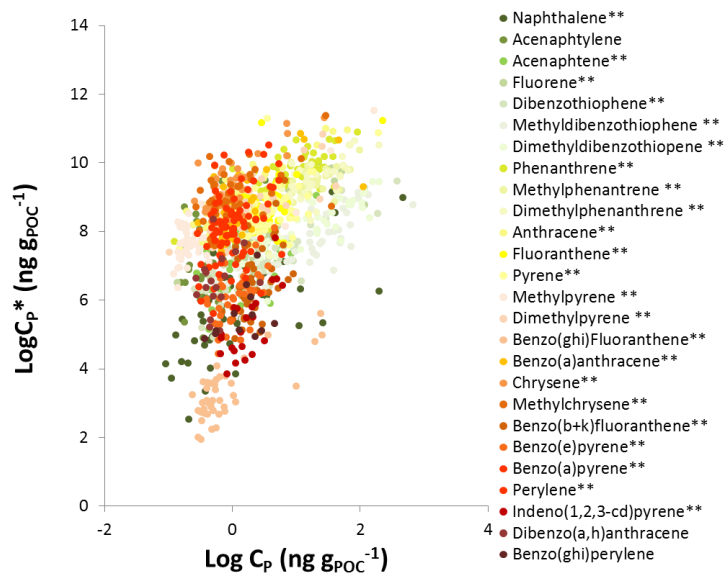


Figure 5.4. Correlation between the theoretical C_p^* calculated from the reported C_G and real C_p measured. Statistical significance is noted per each PAH ** ($p < 0.01$).

Biomass as a descriptor of plankton phase concentrations of PAHs

The spatial distribution of PAHs in plankton shows a large variability, and even though high levels are sometimes found close to the continents (such as off-shore Brazil), high concentrations are also found in the middle of the Pacific, Atlantic and Indian oceans (Figure 5.1). Therefore, there is not a significant correlation between PAH concentrations and distance to continents, as previously reported for other POPs¹⁶{Morales, 2015 #586.

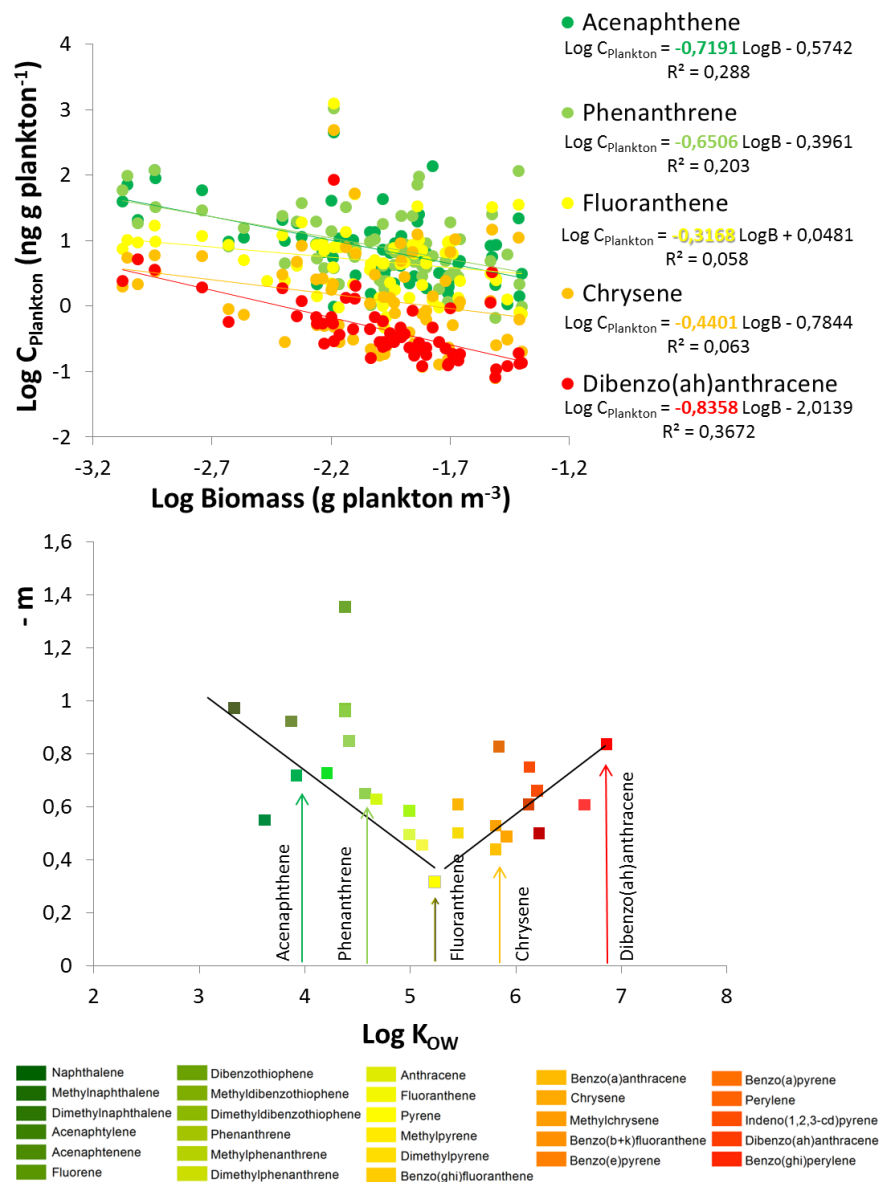


Figure 5.5. PAH concentrations in plankton ($C_{plankton}$) versus plankton biomass (top panel). Slopes from the relationship between concentrations in plankton and biomass (m) versus the hydrophobicity of the compound (K_{OW}) (bottom panel).

Similarly to the influence of POC on surface particle phase PAH concentrations (see above), previous works have identified that biomass is a key descriptor of the spatial and temporal variability of organic pollutants in the marine environment^{16,28,29}{Morales, 2015 #586}. For the photic zone, which comprises waters directly influenced by atmospheric inputs, and deeper ones, which are isolated from atmospheric inputs by the thermocline, the concentration dilution at high biomass abundance is an important process driving the occurrence of PAHs¹⁶. There is a decrease of the concentrations at higher biomass, especially for the more hydrophobic compounds as they partition to the organic matter and are faster removed from the water column by settling particles. This trend is also observed for PAHs from the global oceans (Figure 5.5, top panel). Berrojalbiz and coworkers¹⁶ described the effects that plankton abundance may have on pollutants concentration by

$$C_{Plankton} = a B^{-m} \quad [5.4]$$

where $C_{Plankton}$ ($\text{ng g}_{\text{dw}}^{-1}$) is the concentration of the pollutant in the planktonic phase and B is the plankton biomass (mg m^{-3}). The negative correlations between $C_{Plankton}$ and B were significant for all PAHs ($p < 0.05$, see Figure 5.5, top panel, for 5 examples). However, the slope (m) of this relationship is different for each individual compound (Table S5.11, SI). Figure 5.5 (bottom panel) shows that m values are lowest for PAHs with middle hydrophobicities ($\log K_{OW}$ around 5-6). Conversely, m values are larger for the least and most hydrophobic PAHs. Indeed, m values are significantly correlated with K_{OW} ($p < 0.05$).

The dependence of $C_{Plankton}$ on biomass reflects the different processes driving PAH concentrations in the water column, and the conceptual framework for the interpretations of these complex trends has been introduced elsewhere¹⁶. One key process is biomass dilution. This is especially important below the thermocline since it is isolated from the atmosphere. Biomass dilution results in lower concentrations at high biomass, but this effect is independent of the chemical hydrophobicity¹⁶. Therefore, even though biomass dilution may be affecting the concentrations of PAHs, there are other processes driving the trends depicted in Figure 5.5 as they appeared to be somehow related to K_{OW} . The biological pump is the main process regulating the

PAH concentrations in the water column if the sinking fluxes of PAHs are higher than their air-water exchange. If PAHs are adsorbed to organic matter and those particles rapidly settle to the deep ocean, the surface ocean is depleted of PAHs. This process is responsible for the high m values of the more hydrophobic PAHs, but the less hydrophobic compounds are scarcer affected by this process. It can be said that the increasing tendency of the right part of the $-m$ versus K_{OW} plot, is therefore due to the biological pump effects (Figure 5.5, bottom). Conversely, air-water exchange tends to replenish the water column due to chemical equilibria, and this flux is faster for the lighter PAHs in the Open Ocean (Chapter 2). This would lead to lower values of m for the lower MW PAHs. However, PAHs with low MW show large m values (Figure 5.5). Probably, air-water exchange is not able to counterbalance PAH depletion in the entire photic zone, down to DCM. Degradation of PAHs is another plausible process affecting depletion in the water column, being a relevant process for low MW PAHs, which have been described to be metabolized by bacteria and plankton in the ocean²¹. Therefore, the m values for the lowest MW PAHs are consistent with efficient degradation in the water column. Probably, large biomass indicates a large zooplankton community, and maybe also a larger bacterial population, which efficiently degrade some of the PAHs. A higher amount of biomass may induce biotransformation of the lower MW PAHs, but will not affect the intermediate and high MW compounds as they are not so susceptible to be degraded²¹. Therefore, the decreasing tendency of $-m$ for the low K_{OW} PAHs (Figure 5.5, bottom) can be explained by degradative processes affecting the lower MW compounds.

No statistical correlation was found between $C_{Plankton}$ and δN^{15} , suggesting that the trophic level did not influence significantly the occurrence of PAHs. This is consistent with the narrow range of trophic positions for the plankton samples (from 1.2 to 1.9), and the equilibrium partitioning between the dissolved phase and both phytoplankton and zooplankton (concentrations are independent of the relative proportion of phytoplankton and zooplankton).

Oceanic sink of PAHs due to the biological pump

As the biological pump appeared to be a relevant removal path of PAHs from the surface mixed layer, the biological pump settling fluxes were calculated for all the sampled areas and analyzed PAHs (Figure 5.6, Table S5.12, SI).

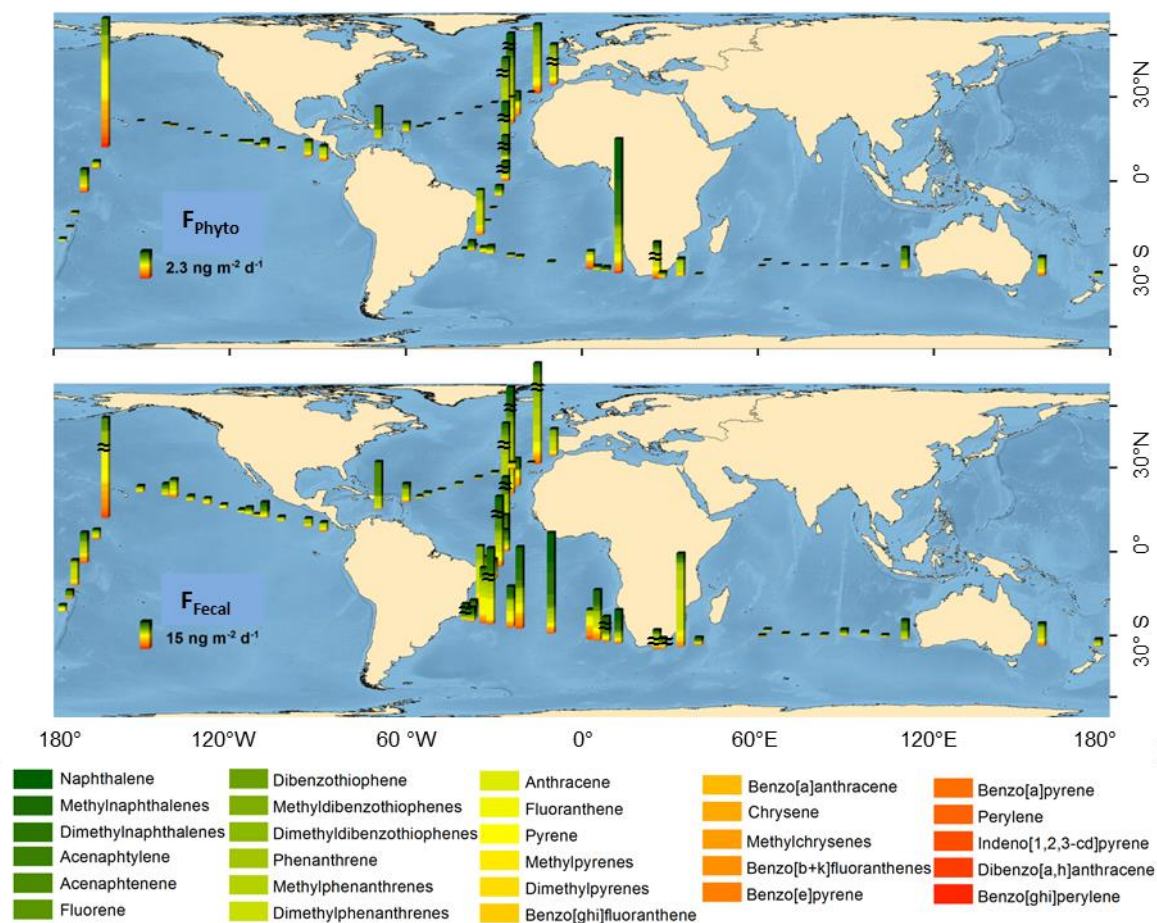


Figure 5.6. Biological pump fluxes for the algal settling flux (F_{phyto}) (top panel), and the fecal settling flux (F_{fecal}) (bottom panel). Marked bars (\approx) have been reduced by a factor of 10 in order to ease the global comparison of all the measurements.

Export of total measured PAHs due to the phytoplankton sinking fluxes are in the order of tens $\text{ng m}^{-2} \text{ day}^{-1}$, and maximal fluxes are found in the eastern part of the North Atlantic basin and near South African coasts (Figure 5.6, top). Fecal sinking fluxes for total PAHs were in the order of magnitude of hundreds of $\text{ng m}^{-2} \text{ day}^{-1}$, and the largest export rates were found as well in the Atlantic Ocean, but with higher fluxes in the southern basin (Figure 5.6, bottom). Therefore, the sinking fluxes due to fecal pellets

export are one order of magnitude higher than those due to algae communities, as reported elsewhere for other organic compounds in the Open Ocean (Chapter 4).

Previous measurements and estimations of the sinking fluxes for PAHs in marine areas have been undertaken. In the Mediterranean Sea, reported as a highly polluted basin due to the surrounding developed countries, and to its semi-enclosed character, Lipiatou⁷, Dachs⁸, Raoux⁴⁶, Tsapakis²⁰, Deyme¹⁰ and Castro¹⁷ described sinking fluxes in the range of the higher rates here obtained for the open ocean (hundreds of $\text{ng m}^{-2}\text{day}^{-1}$), even if they generally considered less PAH congeners. Probably, in the Mediterranean Sea, the individual PAHs sinking rates are higher than in the open ocean due to the higher PAH concentrations reported in particles and plankton^{16,17}. Other studies near North American coasts (at heavily polluted areas)^{47,48} reported sinking rates even in the order of $\mu\text{g m}^{-2}\text{day}^{-1}$, which were not found in this study as the remote open ocean does not hold such great concentrations. Moreover, the biological pump has been described as an effective removal process also for other POPs in remote areas; for instance in the Arctic, α and γ HCHs biological pump fluxes were between 10^{-1} and 10^{-2} $\text{ng m}^{-2}\text{day}^{-1}$ ²⁸, in the range of the fluxes detected for individual PAHs in the middle of the oligotrophic open ocean (Table S5.12, SI). Conversely, perfluoroalkylated substances sinking fluxes have been estimated to range between 10^{-8} and 10^{-1} $\text{ng m}^{-2}\text{day}^{-1}$, due to the low hydrophobicity of these compounds, and thus their low tendency to partition to settling particles, and considerable lower environmental concentrations (Chapter 4).

The average estimated flux for the Σ_{64} PAHs was of $82.5 \text{ ng m}^{-2}\text{day}^{-1}$, standing for a total of 0.008 Tg of PAHs per year sinking out the tropical and subtropical surface oceans. Moreover, the more productive oceanic areas, like northern and southern oceans and upwelling zones near continental margins, have not been accounted in this work, and thus, total global means of the biological pump settling fluxes may be even higher than those reported here (Chapter 4). This sinking flux is of the same magnitude than the estimated global dry deposition flux of PAHs in the Open Ocean⁵, but still, there are 2 orders of magnitude higher entrance fluxes of PAHs through diffusive exchange (Chapter 2). Also previous reports in the Mediterranean Sea estimate that total atmospheric entrance of PAHs is far higher than what its accounted to sink due to the

Results 5

Biological pump^{17,20}, pointing to unrevealed rates of degradation on the water column which need to be further assessed.

There is strong evidence that the plankton does influence PAHs cycling at a global scale, and that the open ocean is an important sink for PAHs. Both, the biological pump and degradation are process affecting PAHs removal, availability and fate. The complexity of the results demonstrates that the characterization of the planktonic food webs, the organic matter and the parameters influencing the kinetics needs further research in order to fully understand the role of biomass in POPs global cycling.

ACKNOWLEDGEMENTS

The authors thank the support of RV Hespérides staff and UTM technicians during the cruise. This work was funded by the Spanish Government through the *Malaspina 2010* project Consolider-Ingenio 2010 program (CSD2008-00077). B.G-G. and M-C.-F-P. acknowledge pre-doctoral fellowships from the BBVA Foundation and Spanish National Research Council (CSIC), respectively. Staff from the Biogeochemical Block from the Malaspina 2010 circumnavigation is acknowledged for the organic carbon measurements. Staff from the Plankton Block from the Malaspina 2010 circumnavigation is acknowledged for the plankton carbon and nitrogen measurements.

REFERENCES

- 1 Zhang, Y. & Tao, S. Global atmospheric emission inventory of polycyclic aromatic hydrocarbons (PAHs) for 2004. *Atmospheric Environment* **43**, 812-819, doi:10.1016/j.atmosenv.2008.10.050 (2009).
- 2 Reddy, C. M. *et al.* Composition and fate of gas and oil released to the water column during the Deepwater Horizon oil spill. *Proceedings of the National Academy of Sciences* **109**, 20229-20234, doi:10.1073/pnas.1101242108 (2012).
- 3 Cabrerizo, A. *et al.* Ubiquitous net volatilization of polycyclic aromatic hydrocarbons from soils and parameters influencing their soil-air partitioning. *Environmental Science & Technology* **45**, 4740-4747, doi:10.1021/es104131f (2011).
- 4 Harvey, R. G. *Polycyclic aromatic hydrocarbons: chemistry and carcinogenicity*. (CUP Archive, 1991).
- 5 Gonzalez-Gaya, B., Zuniga-Rival, J., Ojeda, M. J., Jimenez, B. & Dachs, J. Field measurements of the atmospheric dry deposition fluxes and velocities of polycyclic aromatic hydrocarbons to the global oceans. *Environmental Science & Technology* **48**, 5583-5592, doi:10.1021/es500846p (2014).
- 6 Ma, Y. *et al.* Deposition of polycyclic aromatic hydrocarbons in the North Pacific and the Arctic. *Journal of Geophysical Research: Atmospheres* **118**, 5822-5829, doi:10.1002/jgrd.50473 (2013).
- 7 Lipiatou, E., Marty, J.-C. & Saliot, A. Sediment trap fluxes of polycyclic aromatic hydrocarbons in the Mediterranean Sea. *Marine Chemistry* **44**, 43-54, doi:10.1016/0304-4203(93)90005-9 (1993).
- 8 Dachs, J., Bayona, J. M., Fowler, S. W., Miquel, J. C. & Albaigés, J. Vertical fluxes of polycyclic aromatic hydrocarbons and organochlorine compounds in the western Alboran Sea (southwestern Mediterranean). *Marine Chemistry* **52**, 75-86 (1996).
- 9 Dachs, J. & Méjanelle, L. Organic Pollutants in Coastal Waters, Sediments, and Biota: A Relevant Driver for Ecosystems During the Anthropocene? *Estuaries and Coasts* **33**, 1-14, doi:10.1007/s12237-009-9255-8 (2010).
- 10 Deyme, R. *et al.* Vertical fluxes of aromatic and aliphatic hydrocarbons in the Northwestern Mediterranean Sea. *Environmental Pollution* **159**, 3681-3691, doi:10.1016/j.envpol.2011.07.017 (2011).
- 11 Nizzetto, L. *et al.* PAHs in air and seawater along a North-South Atlantic transect: Trends, processes and possible sources. *Environmental Science and Technology* **42**, 1580-1585 (2008).
- 12 Lohmann, R. *et al.* Organochlorine pesticides and PAHs in the surface water and atmosphere of the North Atlantic and Arctic Ocean. *Environmental science & technology* **43**, 5633-5639 (2009).
- 13 Lohmann, R. *et al.* PAHs on a west-to-east transect across the tropical Atlantic Ocean. *Environmental Science and Technology* **47**, 2570-2578 (2013).
- 14 Farrington, J. W. & Takada, H. Persistent organic pollutants (POPs), polycyclic aromatic hydrocarbons (PAHs), and plastics: Examples of the status, trend, and cycling of organic chemicals of environmental concern in the ocean. *Oceanography* **27**, 196-213 (2014).
- 15 Dachs, J., Bayona, J. M., Raoux, C. & Albaigés, J. Spatial, Vertical Distribution and Budget of Polycyclic Aromatic Hydrocarbons in the Western Mediterranean Seawater. *Environmental Science & Technology* **31**, 682-688, doi:10.1021/es960233j (1997).
- 16 Berrojalbiz, N. *et al.* Biogeochemical and physical controls on concentrations of polycyclic aromatic hydrocarbons in water and plankton of the Mediterranean and Black Seas. *Global Biogeochemical Cycles* **25** (2011).
- 17 Castro-Jiménez, J., Berrojalbiz, N., Wollgast, J. & Dachs, J. Polycyclic aromatic hydrocarbons (PAHs) in the Mediterranean Sea: Atmospheric occurrence, deposition

- and decoupling with settling fluxes in the water column. *Environmental Pollution* **166**, 40-47 (2012).
- 18 Gustafsson, Ö., Gschwend, P. M. & Buesseler, K. O. Using ²³⁴Th disequilibria to estimate the vertical removal rates of polycyclic aromatic hydrocarbons from the surface ocean. *Marine Chemistry* **57**, 11-23, doi:10.1016/S0304-4203(97)00011-X (1997).
- 19 Bouloubassi, I. *et al.* PAH transport by sinking particles in the open Mediterranean Sea: A 1 year sediment trap study. *Marine Pollution Bulletin* **52**, 560-571, doi:10.1016/j.marpolbul.2005.10.003 (2006).
- 20 Tsapakis, M., Apostolaki, M., Eisenreich, S. & Stephanou, E. G. Atmospheric deposition and marine sedimentation fluxes of polycyclic aromatic hydrocarbons in the eastern Mediterranean basin. *Environmental Science and Technology* **40**, 4922-4927 (2006).
- 21 Berrojalbiz, N. *et al.* Accumulation and Cycling of Polycyclic Aromatic Hydrocarbons in Zooplankton. *Environmental Science & Technology* **43**, 2295-2301, doi:10.1021/es8018226 (2009).
- 22 Douben, P. E. *PAHs: an ecotoxicological perspective*. (John Wiley & Sons, 2003).
- 23 Meador, J., Stein, J., Reichert, W. & Varanasi, U. in *Reviews of environmental contamination and toxicology* 79-165 (Springer, 1995).
- 24 Hylland, K. Polycyclic aromatic hydrocarbon (PAH) ecotoxicology in marine ecosystems. *Journal of Toxicology and Environmental Health A* **69**, 109-123, doi:10.1080/15287390500259327 (2006).
- 25 Echeveste, P., Agustí, S. & Dachs, J. Cell size dependent toxicity thresholds of polycyclic aromatic hydrocarbons to natural and cultured phytoplankton populations. *Environmental Pollution* **158**, 299-307, doi:10.1016/j.envpol.2009.07.006 (2010).
- 26 Echeveste, P., Agustí, S. & Dachs, J. Cell size dependence of additive versus synergetic effects of UV radiation and PAHs on oceanic phytoplankton. *Environmental Pollution* **159**, 1307-1316 (2011).
- 27 Barata, C., Calbet, A., Saiz, E., Ortiz, L. & Bayona, J. M. Predicting single and mixture toxicity of petrogenic polycyclic aromatic hydrocarbons to the copepod *Oithona davisae*. *Environmental Toxicology and Chemistry* **24**, 2992-2999 (2005).
- 28 Galbán-Malagón, C. J., Berrojalbiz, N., Gioia, R. & Dachs, J. The "degradative" and "biological" pumps controls on the atmospheric deposition and sequestration of hexachlorocyclohexanes and hexachlorobenzene in the North Atlantic and Arctic Oceans. *Environmental Science and Technology* **47**, 7195-7203 (2013).
- 29 Frouin, H. *et al.* Partitioning and bioaccumulation of PCBs and PBDEs in marine plankton from the Strait of Georgia, British Columbia, Canada. *Progress in Oceanography* **115**, 65-75 (2013).
- 30 Morales, L. *et al.* Background Concentrations of Polychlorinated Dibenzo-p-Dioxins, Dibenzofurans, and Biphenyls in the Global Oceanic Atmosphere. *Environmental science & technology* **48**, 10198-10207 (2014).
- 31 Morales, L. *et al.* Oceanic Sink and Biogeochemical controls on the Accumulation of Polychlorinated dibenzo-p-Dioxins, Dibenzofurans, and Biphenyls in Plankton. *Environmental Science & Technology*, doi:10.1021/acs.est.5b01360 (2015).
- 32 Dachs, J. *et al.* Oceanic Biogeochemical Controls on Global Dynamics of Persistent Organic Pollutants. *Environmental Science & Technology* **36**, 4229-4237, doi:10.1021/es025724k (2002).
- 33 Galbán-Malagón, C., Berrojalbiz, N., Ojeda, M. J. & Dachs, J. The oceanic biological pump modulates the atmospheric transport of persistent organic pollutants to the Arctic. *Nature communications* **3**, 862 (2012).
- 34 Galbán-Malagón, C. J., Del Vento, S., Cabrerizo, A. & Dachs, J. Factors affecting the atmospheric occurrence and deposition of polychlorinated biphenyls in the Southern Ocean. *Atmospheric Chemistry and Physics* **13**, 12029-12041 (2013).

- 35 Gioia, R. *et al.* in *Persistent Pollution – Past, Present and Future* (eds Markus Quante, Ralf Ebinghaus, & Götz Flöser) Ch. 8, 111-139 (Springer Berlin Heidelberg, 2011).
- 36 Chiuchiolo, A. L., Dickhut, R. M., Cochran, M. A. & Ducklow, H. W. Persistent Organic Pollutants at the Base of the Antarctic Marine Food Web. *Environmental Science & Technology* **38**, 3551-3557, doi:10.1021/es0351793 (2004).
- 37 Del Vento, S. & Dachs, J. Prediction of uptake dynamics of persistent organic pollutants by bacteria and phytoplankton. *Environmental Toxicology and Chemistry* **21**, 2099-2107, doi:10.1002/etc.5620211013 (2002).
- 38 Dachs, J., Eisenreich, S. J. & Hoff, R. M. Influence of eutrophication on air-water exchange, vertical fluxes, and phytoplankton concentrations of persistent organic pollutants. *Environmental Science and Technology* **34**, 1095-1102 (2000).
- 39 Wan, Y., Jin, X., Hu, J. & Jin, F. Trophic dilution of polycyclic aromatic hydrocarbons (PAHs) in a marine food web from Bohai Bay, North China. *Environmental science & technology* **41**, 3109-3114 (2007).
- 40 Moreno-Ostos, E. *Expedición de circunnavegación Malaspina 2010. Cambio global y exploración de la biodiversidad del océano. Libro blanco de métodos y técnicas de trabajo oceanográfico* (Consejo Superior de Investigaciones Científicas 2012).
- 41 Mompeán, C. *et al.* Spatial patterns of plankton biomass and stable isotopes reflect the influence of the nitrogen-fixer *Trichodesmium* along the subtropical North Atlantic. *Journal of Plankton Research* **35**, 513-525, doi:10.1093/plankt/fbt011 (2013).
- 42 Siegel, D. A. *et al.* Global assessment of ocean carbon export by combining satellite observations and food-web models. *Global Biogeochemical Cycles* **28**, 2013GB004743, doi:10.1002/2013GB004743 (2014).
- 43 Schulz-Bull, D. E., Petrick, G., Bruhn, R. & Duinker, J. C. Chlorobiphenyls (PCB) and PAHs in water masses of the northern North Atlantic. *Marine Chemistry* **61**, 101-114, doi:10.1016/S0304-4203(98)00010-3 (1998).
- 44 Del Vento, S. & Dachs, J. Atmospheric occurrence and deposition of polycyclic aromatic hydrocarbons in the northeast tropical and subtropical Atlantic Ocean. *Environmental Science and Technology* **41**, 5608-5613 (2007).
- 45 Berrojalbiz, N. *et al.* Persistent organic pollutants in Mediterranean seawater and processes affecting their accumulation in plankton. *Environmental science & technology* **45**, 4315-4322 (2011).
- 46 Raoux, C. *et al.* Particulate Fluxes of Aliphatic and Aromatic Hydrocarbons in Near-shore Waters to the Northwestern Mediterranean Sea, and the Effect of Continental Runoff. *Estuarine, Coastal and Shelf Science* **48**, 605-616, doi:10.1006/ecss.1998.0458 (1999).
- 47 Ko, F.-C., Sanford, L. P. & Baker, J. E. Internal recycling of particle reactive organic chemicals in the Chesapeake Bay water column. *Marine Chemistry* **81**, 163-176, doi:10.1016/S0304-4203(03)00027-6 (2003).
- 48 Adhikari, P. L., Maiti, K. & Overton, E. B. Vertical fluxes of polycyclic aromatic hydrocarbons in the northern Gulf of Mexico. *Marine Chemistry* **168**, 60-68, doi:10.1016/j.marchem.2014.11.001 (2015).

Summary of Results

Through chapters 1-5 presented in this Thesis, the fate and dynamics of two families of organic pollutants, polycyclic aromatic hydrocarbons (PAHs) and perfluoroalkylated substances (PFASs), have been studied in the global Open Ocean. The assessed processes include atmospheric deposition to the remote ocean, distribution along the water column horizontally and vertically, and interactions with the plankton as the first link to the oceanic food chain. The present research is circumscribed to the *Malaspina 2010* circumnavigation, and covers the tropical and subtropical regions (35°N - 40°S) of the Atlantic, Pacific and Indian Oceans.

In **Chapter 1** the direct input of PAHs to the Open Ocean via dry deposition is assessed. The study provides a collection of 12 direct measurements of dry deposition fluxes (F_{DD}) in the Atlantic, Indian and Pacific oceans. The assortment of coarse (>2.7 μm) and fine (0.7 – 2.7 μm) deposited marine aerosol collected allowed to quantify the F_{DD} to the Open Ocean surface for 16 individual PAHs. Average F_{DD} for total (fine + coarse) $\Sigma_{16}\text{PAHs}$ (sum of 16 individual PAHs) ranged from few $\text{ng m}^{-2}\text{d}^{-1}$ to around 50 $\text{ng m}^{-2}\text{d}^{-1}$. PAHs F_{DD} bound to coarse aerosols were higher than those of fine aerosols for the 80% of the measurements and compounds. Coarse aerosol's F_{DD} for individual PAHs ranged between an average of $10^{-1} \text{ ng m}^{-2}\text{d}^{-1}$ to 2 $\text{ng m}^{-2}\text{d}^{-1}$. Fine aerosol fraction's F_{DD} ranged between an average of $10^{-2} \text{ ng m}^{-2}\text{d}^{-1}$ to 1 $\text{ng m}^{-2}\text{d}^{-1}$, being in all cases the fluxes for high MW PAHs of higher magnitude than those for the more volatile compounds. Concentrations of PAHs were measured in the suspended aerosol (C_A) concurrently with the F_{DD} . $\Sigma_{16}\text{PAHs}$ concentrations in suspended aerosols ranged between $10^{-2} \text{ ng m}^{-3}$ and few ng m^{-3} and were maximal in the Indian Ocean, where highly polluted marine aerosols were found. The PAHs velocity of deposition (v_D) was calculated from the measured F_{DD} and the C_A , ranging from 10^{-3} to 1 cm s^{-1} , being faster the deposition of high MW PAHs. The empirical v_D was found to be significantly affected by the chemical properties of the PAHs, like the vapor pressure (P_L) of the congener, and the environmental conditions, like wind speed (U_{10} , which enhances turbulence and favors aerosol collisions with the marine surface) and chlorophyll concentration in the surface water (Chl_s , which increases stickiness of the ocean by lowering the surface tension and increasing hydrophobicity). According to these 3 factors, a parametrized equation

is proposed to predict v_D in the coarse and fine fractions as well as the deposition velocity for the total aerosols. This empirical equation reduces by a factor of 5 the error of calculating F_{DD} with fixed v_D values, as traditionally reported in the literature. Moreover, this equation would be a good approximation for calculating dry depositional velocities for other semi-volatile compounds over the open ocean surface from known parameters (P_L , U_{10} and ChI_s) when atmospheric concentrations are measured.

The other main atmospheric input fluxes of chemical pollutants into the Open Ocean, wet deposition and diffusive exchange, are assessed for PAHs in **Chapter 2**. In this chapter it is also evaluated the extent of all the measured deposition fluxes and the implication of the total entrance of PAHs and other semivolatile aromatic-like compounds (SALCs) to the ocean on the carbon cycle. 64 PAHs and total SALCs were identified and ubiquitously found in the Atlantic, Pacific and Indian oceans, with gas phase concentrations (C_G) of a few ng m^{-3} for the most abundant compounds, aerosol concentration of tens of pg m^{-3} , and of hundreds of pg L^{-1} in surface seawater (C_W). C_G was maximal in the North Atlantic and revealed a dominance of the more volatile PAHs in the gas phase. Contrarily, C_A highest records were found in the Indian Ocean with a higher occurrence of PAHs with 4 or more aromatic rings. Total PAHs C_W was less variable in all the sampled oceans, compared with the atmosphere, being in the range of hundreds of pg L^{-1} in surface seawater. Nevertheless, in the 3 environmental phases, a decreasing concentration gradient was observed from continental margins to the open ocean. Dry deposition fluxes for the Open Ocean were calculated from the C_A measured and the v_D estimated from the parametrization explained in Chapter 1. Average F_{DD} for $\Sigma_{64}\text{PAHs}$ ranged from $1 \text{ ng m}^{-2}\text{d}^{-1}$ (in the Open Ocean) to almost $2500 \text{ ng m}^{-2}\text{d}^{-1}$ (in the west and east margins of the Indian Ocean). Rain water was gathered during the 11 precipitation events that occurred during the *Malaspina 2010* cruise, and showed concentrations of hundreds to ten thousands ng L^{-1} of $\Sigma_{64}\text{PAHs}$. The associated wet deposition fluxes (F_{WD}) were calculated to be in the order of hundreds to $5000 \mu\text{g m}^{-2} \text{d}^{-1}$. Net diffusive air-water exchange (F_{AW}) was estimated from the measured C_G and C_W by applying a two-film resistance model. F_{AW} showed a net input of most PAHs to the ocean, except for some of the more volatile compounds, ranging from hundreds

of $\text{ng m}^{-2}\text{d}^{-1}$ $\Sigma_{64}\text{PAHs}$ volatilizing from the surface ocean to tens of thousands of $\text{ng m}^{-2}\text{d}^{-1}$ being absorbed. The global wet deposition is difficult to extrapolate spatially and temporally, due to its episodic character. Conversely, the comparison between total F_{AW} and F_{DD} integrated monthly for all the tropical and subtropical oceans revealed that the global gross volatilization and gross absorption of $\Sigma_{64}\text{PAHs}$ were $0.042 \text{ Tg month}^{-1}$ and $0.132 \text{ Tg month}^{-1}$, respectively, resulting in a net input of atmospheric $\Sigma_{64}\text{PAHs}$ to the ocean of $0.090 \text{ Tg month}^{-1}$, 90 times larger than the global F_{DD} of aerosol-bound PAHs estimated at $0.001 \text{ Tg month}^{-1}$. When extrapolated annually, and expressed as carbon fluxes, the global annual input of $\Sigma_{64}\text{PAHs}$ to the ocean is estimated to be $0.873 \text{ Tg C y}^{-1}$. Moreover, by accounting not only PAHs, but the whole unresolved complex mixture of SALCs (whose concentrations in the dissolved and gas phase are between 100 and 7000 times larger than the $\Sigma_{64}\text{PAH}$ concentrations) the input of organic carbon to the Open Ocean is even greater. According to our estimations, the global diffusive gross absorption and volatilization fluxes of SALCs are of 512 Tg C y^{-1} and 83 Tg C y^{-1} , respectively, resulting in a net input of organic carbon to the Atlantic, Pacific and Indian oceans of 429 Tg C y^{-1} . Therefore, this first and unique report of global fluxes input of PAHs, SALCs and associated carbon to the Open Ocean suggests that atmospheric diffuse deposition of those organic pollutants is a key process influencing the global carbon cycle.

Once in the water column, the pollutants suffer as well from other horizontal and vertical transport processes. **Chapters 3 and 4** cope with the occurrence and dynamics of PFASs within the water column. **Chapter 3** reports the occurrence of 11 PFASs congeners including ionic perfluoroalkyl carboxylic acids (PFCAs), perfluoroalkyl sulfonic acids (PFASAs) and neutral perfluoroalkyl sulfonamides (PFASAs) in surface waters. The global mean C_W of $\Sigma_{11}\text{PFASs}$ was in the order of hundreds to thousands of pg L^{-1} , even if the single concentrations for individual congeners showed broad ranges (from thousand pg L^{-1} for the more abundant compounds like perfluorooctane sulfonic acid (PFOS), to concentrations very close to the detection limit of $10^{-2} \text{ pg L}^{-1}$). The Atlantic Ocean exhibited the highest concentrations, found in southern basin for most compounds, but for the neutral precursors, which occurred mostly in the northern hemisphere and at very low concentrations. On average, PFOS contributed a 33% to

total PFASs (ranging from 64% in the South Atlantic to 16% in the North Atlantic), followed by perfluorodecanoic acid (22%), and perfluorohexanoic acid (12%). The mean concentrations for the remaining congeners was under 10%, with even perfluorooctane carboxylic acid (PFOA) contributing 6% and PFASAs accounting for less than 1% to total PFASs concentration. C_w in coastal waters was higher than those found in the center of the subtropical gyres, suggesting a continental origin of the pollutants. Of special interest is the high abundance of PFOS found in surface waters near Brazil, never reported previously at such concentrations in that region, for which riverine and atmospheric inputs (probably wet deposition) are suggested. The high concentrations found in other areas (like nearby the equator in the Pacific and Atlantic oceans) are attributed to global distribution by oceanic currents, which may transport and accumulate ionic PFASs in certain locations of the Global Ocean. The influence of biogeochemical and physicochemical processes, like adsorption to organic matter, biodegradation, or photodegradation is evaluated as well. According to our results and previous studies, biological pump fluxes could significantly affect PFASs concentrations, even if they had not been assessed previously to this Thesis. Time trends for some PFAS congeners are evaluated for the Northern Hemisphere, through a comparison of a reviewed dataset of PFAS concentrations in the oceanic environment. For instance, a general decrease of PFOA is observed in the North Atlantic and Pacific Oceans, with an estimated e-fold time (the time needed to reduce the concentration to $1/e$ of the initial value) of 5.8 years. However, the main processes affecting PFASs fate remain largely unknown, even though, presumably, it is a complex interaction of many factors and processes driving their global distribution. Therefore, PFASs fate and behavior in the Open Ocean, as their presumably main sink, merit further research.

Chapter 4 intends to further understand PFASs fate in the Open Ocean by evaluating their sinking processes and vertical distribution. For that purpose, a global database of concentrations in the mixed layer at the deep chlorophyll maximum depth (DCM, around 100 m) is given. The DCM is an area of special interest regarding biological processes. Concentrations at DCM were concurrently measured with other physical and biological parameters influencing their occurrence and discussed. To our

knowledge, the vertical transport of PFASs has been assessed empirically for eddy diffusion fluxes and for settling fluxes of organic matter bound PFASs (biological pump) here for the first time. As found for surface C_W , concentrations measured at the DCM showed maximal values in the South Atlantic basin with a very similar contribution of individual compounds to total PFASs concentration. PFOS accounted for 39% to the total PFASs concentration followed by perfluorodecanoic acid (17%) and perfluorohexanoic acid (12%), being the contribution of the remaining compounds under 10% (including PFOA, which mean contribution was 5%). A clear coast - Open Ocean decreasing concentrations was found as well for all the PFASs analyzed, as occurred for surface seawater. DCM C_W showed less variability between oceanic basins than PFAS concentrations measures at surface seawater. However, they were significantly positively correlated. Vertical eddy diffusion fluxes (F_{Eddy}) were calculated from measured eddy diffusivity parameters (K_ρ) concurrently with the PFAS concentrations along the *Malaspina 2010* circumnavigation, and modelled on the mixed layer of the Open Ocean. The application of this one dimensional model predicted the vertical profile of C_W in the water column, and therefore, it was possible to calculate a theoretical value of C_W at the DCM depth. The modeled C_W was generally of the same order of magnitude than the real measured value. The calculated F_{Eddy} at the surface were between 4 orders of magnitude higher and of comparable values than at the DCM. F_{Eddy} at surface oscillated between 10^{-8} and 10^{-2} $\text{ng m}^{-2}\text{day}^{-1}$ for PFOS and between 10^{-8} and 10^{-3} $\text{ng m}^{-2}\text{day}^{-1}$ for PFOA. F_{Eddy} at DCM depth ranged between 10^{-5} and 10^{-2} for PFOS and between 10^{-3} and 10^{-6} $\text{ng m}^{-2}\text{day}^{-1}$ for PFOA. At the maximal measured K_ρ , eddy diffusion will only disperse around 7 ng m^{-2} of PFOS per year, being thus a flux of small magnitude. Nevertheless, as turbulent diffusion is a continuous and ubiquitous process it should be accounted at a global scale. For instance, PFOS and PFOA annual removal fluxes for the global tropical and subtropical surface Oceans would be of 2.3 and 0.2 tons per year, respectively. Settling fluxes due to the biological pump ($F_{Settling}$) were calculated for 5 ionic PFASs (C_{8-10} PFCAs and $C_{6,8}$ PFSAs) using the measured surface C_W , bioconcentration factors (BCF) from literature and a database of global export of organic matter (F_{OC}) from the mixed layer. Fluxes were calculated for organic matter sinking related to phytoplankton (F_{Phyto}) and to zooplankton fecal pellets export (F_{Fecal}). F_{Phyto} ranged from an order of magnitude of 10^{-8} $\text{ng m}^{-2} \text{day}^{-1}$ up

Summary of Results

to 10^{-2} ng m⁻² day⁻¹ per individual congener. Individual PFASs F_{Fecal} oscillated between 10^{-6} ng m⁻² day⁻¹ and 10^{-1} ng m⁻² day⁻¹. The magnitude of the flux was positively correlated with the hydrophobicity of the particular compound. F_{Fecal} were found to be about one order of magnitude higher than those associated only with phytoplankton. Moreover, $F_{Settling}$ seem to dominate the removal processes in the water column according to our calculations, several orders of magnitude higher than the turbulent fluxes calculated for all the analyzed compounds. The mean residence time of PFASs in the surface Open Ocean was calculated with the measured inventory in the mixed layer and considering the both removal processes quantified; being 27000 years for PFOS and 17000 years for PFOA. According to the actual production rates of PFASs and the estimated fluxes affecting their occurrence, the surface Open Ocean will remain a reservoir of these pollutants for millenniums. Nevertheless, other biological unrevealed processes not considered in the present study may be occurring in remote or deep areas of the ocean, and further research is needed to fully understand PFASs global behavior at the long-term.

The interactions of POPs with organic matter in the water column and the effects of their accumulation in marine food webs are among the unstudied processes occurring in the global oceanic environment. **Chapter 5** reviews the role of organic carbon and plankton on PAHs cycling in the Open Ocean and particularly focuses on the effects that total suspended particles (*TSP*) and biomass (*B*) may have on PAHs concentration in the surface mixed layer. 64 PAHs were simultaneously measured in dissolved and particulate phases (C_p) of surface water, and in plankton pools of the total mixed layer ($C_{Plankton}$). $\Sigma_{64}PAHs$ ranged between 10^{-1} and 10 ng L⁻¹ in the dissolved water phase, between 10 and 10^3 ng g_{dw}⁻¹ in the particulate phase and between 10 and 10^4 ng g_{dw}⁻¹ in the plankton phase. The PAHs congeners occurrence profile was not significantly different between the 3 matrixes, even if intermediate volatility PAHs were more abundant in the particulate phase. Contrarily, total concentrations differed in their global occurrence; maximal C_w were recorded in south Atlantic coastal areas (with no significant differences among basins even though), C_p was maximal in the Indian Ocean and $C_{Plankton}$ was the highest in different sampling spots along the Atlantic Ocean, near the European and Brazilian coasts. Partition coefficients (K_{OC}) at the oceanic surface

were obtained for the water phase from C_W and C_p , and ranged from 10^4 to 10^8 L Kg⁻¹, with bigger ratios for higher MW PAHs. K_{OC} and C_p negatively correlated with particulate organic carbon (POC) found in the TSP, at different rates for the individual PAHs, thus, the partition and occurrence in the particles are affected by a POC dilution, but also modulated by other processes depending on hydrophobicity (like air-water exchange or the biological pump). Similarly, PAHs concentration in the surface particulate phase appeared to be influenced by the PAHs found in the gas phase. Indeed, the suggested situation occurring at surface waters is that there is a fast air-water-particle exchange governing PAHs occurrence at surface waters (dissolved and particulate phases). This equilibrium/exchange depends on C_G , K_{OC} and the Henry's Law constant. Theoretical C_p calculated assuming air-water-particle equilibrium, positively correlated with measured C_p confirming the plausibility of this situation. Conversely at deeper depths of the mixed photic layer, $C_{Plankton}$ was significantly affected by the B present in the water column; higher amounts of biomass resulted in decreased concentrations of PAHs. The slope (m) of this correlation was characteristic for each individual PAH, and turned to be dependent on their hydrophobicity (K_{OW}). For less hydrophobic compounds there is a decrease of the slope with increasing K_{OW} ; thus, the low hydrophobic congeners are more affected by B than intermediate PAHs. These results attend for degradative processes, as the low K_{OW} are faster and easier degraded than the intermediate MW PAHs by bacteria, detoxifying phytoplankton processes and zooplankton metabolization. From medium to high K_{OW} PAHs, m increased with higher hydrophobicity, and therefore, the more hydrophobic PAHs are further affected by B abundance. In this case, the governing process is the biological pump, as the more hydrophobic PAHs are faster and stronger adsorbed onto organic matter. Thus, their concentration and removal from surface water is driven by the settling of these particles. Biological pump fluxes were calculated for PAHs from $C_{Plankton}$ and literature reported organic carbon export fluxes, separately for algae (F_{Phyto}) and zooplankton fecal pellets (F_{Fecal}). Export of total measured PAHs due to F_{Phyto} are in the order of tens ng m⁻²day⁻¹, and maximal fluxes are found in the eastern part of the North Atlantic basin and near South African coasts. F_{Fecal} for total PAHs were in the order of magnitude of hundreds of ng m⁻²day⁻¹, and the largest export rates were found as well in the Atlantic Ocean, but in the southern basin. The average calculated total fluxes for

Summary of Results

the Σ_{64} PAHs was of $82.5 \text{ ng m}^{-2}\text{day}^{-1}$, standing for a total of 0.008 Tg of PAHs per year sinking out the tropical and subtropical surface oceans, which may be even greater taking into account the highly productive marine areas not assessed in this thesis (e.g. higher latitudinal and upwelling areas). Also the degradative processes seem to be of interest, especially for the lower MW PAHs, and should be fully characterized and quantified in the Open Ocean in the future. Therefore, there is evidence that the plankton does influence PAHs cycling at a global scale, and that the role of the Open Ocean as a pollutants sink depends on an extraordinary manner on the organic matter and plankton cycling in the water column.

Chapter 3

CHAPTER 3

General Discussion

GENERAL DISCUSSION

General Discussion

This Thesis evaluates the occurrence of two families of organic pollutants, polycyclic aromatic hydrocarbons (PAHs) and perfluoroalkylated substances (PFASs) in the Global tropical and subtropical Oceans. In addition, we have evaluated the role that atmospheric deposition and biogeochemical cycling has on the occurrence and fate of PAHs and PFAS. The processes influencing these Persistent Organic Pollutants (POPs) fate and distribution in the marine environment were assessed taking into account the contrasting physicochemical properties of PAHs and PFASs. The empirical description and characterization of the processes affecting these two examples of POP's fate in the Global Ocean aims to help to elucidate as well global dynamics of other pollutants with similar properties. For instance, the parametrization proposed to calculate dry deposition velocity ¹ has been successfully applied to dioxins and furans (PCDD/Fs), dioxin-like polychlorinated biphenyls (PCBs) ², and organophosphorus flame retardants ³. As well, it is noteworthy that it has been verified the relevance of the biological pump as a key regulator of PAHs and PFASs distribution in the Open Ocean, as already suggested for other POPs in earlier works ⁴⁻⁷.

This discussion will integrate all the measurements performed in the Atlantic, Indian and Pacific Oceans, and will assess the status of the sampled areas regarding PAHs and PFASs pollution. We aim to integrate in this discussion the processes evaluated in the several chapters of the thesis, and thus compare the occurrence, transport and fate of the two families of POPs. In 1988 Bidleman showed that the gas-particle partition of organic semivolatile compounds controls their behavior and deposition process in the atmosphere ⁸. Likewise, in the water column, transport and fate will depend on the phase where the target compound is predominantly found ⁹. Therefore, the discussion Chapter will review as well the obtained partition coefficients found in the atmosphere for PAHs and in the water for PAHs and PFASs, in order to assess which are the governing processes affecting their fate in the Open Ocean. As a final point, a global budget of the quantified PAHs, SALCs and PFASs including all the reported processes is done; highlighting not only what has been assessed in this Thesis but the missing gaps in the global fate of PAHs and PFAS, which provide information for other POPs.

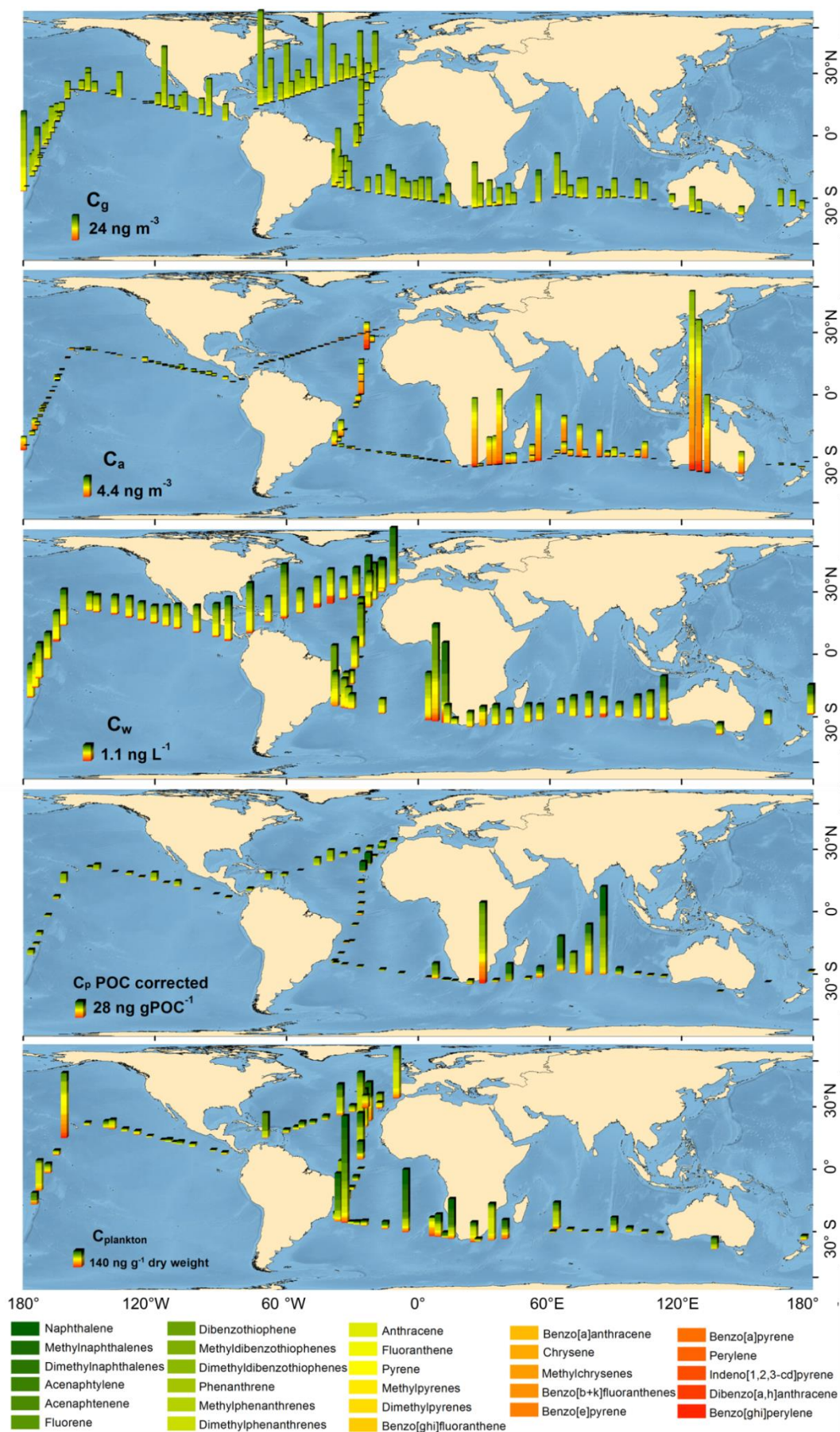


Figure D.1. Global distribution of oceanic concentrations of PAHs in the gas, aerosol, dissolved, particulate and plankton phases.

Global Occurrence

PAHs

Figure D.1 presents Σ_{64} PAHs concentrations measured in the 5 environmental compartments studied in the global Ocean. The relative abundance of the different PAHs in the gas, aerosol, dissolved, particulate and planktonic phases depends on the hydrophobicity and volatility of each chemical, and is also affected by the sources and magnitude of transport and degradation processes. Therefore, the resulting global occurrence is a combination of physicochemical properties of PAHs and the environmental cycling of these compounds.

Gas phase concentrations were within the same range in all the sampled oceans. No significant differences were found between Oceans, even if the North Atlantic exhibited the highest concentrations, and generally PAHs stand out near continental shelf margins. Contrarily, aerosol phase PAH concentrations were maximal in the Indian Ocean and statistically different from the rest of the oceanic basins. Also high concentrations were found in the NE Atlantic. Few previous records of PAHs in the Open Ocean atmosphere can be found; on the one hand because they are mostly related with human activity and some PAHs can be degraded during transport and once in the water column. Therefore, most studies on PAHs are performed in urban and coastal areas¹⁰⁻¹³. On the other hand, self-contamination of samples has been frequently detected by boat fumes, and make difficult their sampling in remote oceanic areas¹⁴. Nevertheless, the previous available measurements exhibit individual PAHs concentrations within the range of our study in the Atlantic Northern basin¹⁵⁻¹⁷, showing as well the peaks near North African coasts. Regarding the Indian Ocean, no previous sampling campaigns covered the longitudinal transect at $\sim 30^\circ\text{S}$, and the comparison stands with data sets from much northern and coastal regions¹⁸. However, those indicate a large PAHs load from Asian margins and support the high concentrations measured during the *Malaspina 2010* circumnavigation, which presumably are due to air masses in the upper troposphere originating in Southern East Asia.

Likewise, dissolved phase PAHs concentrations were not statistically different between the sampled Oceans. The highest concentrations were measured in the Atlantic continental margins, both in the North and South basins, being particularly high in the southern Atlantic. The particulate phase significant larger concentrations were found in the Indian Ocean, with some remarkable peaks as well in NE Atlantic. This seems consistent with the higher aerosol phase concentrations in these basins. Conversely, PAH concentrations in the plankton phase showed very variable concentrations, with the highest occurrence in the Atlantic Ocean, reflecting the dynamic character of this environmental compartment. Concentrations in the plankton phase, with samples integrating the photic zone do not reflect the proximity to continents, but biogeochemical controls such as biomass dilution and settling fluxes, as discussed in Chapter 5. Water (dissolved phase) concentrations are correlated with those in the atmosphere, confirming the effective transfer of PAHs through diffuse air-water exchange. Most of previous studies about PAHs in seawater have focused in coastal regions and semi enclosed bays or seas ^{13,19-22}, as occurred with atmospheric assessments. The few existing reports in open waters ^{14,15,17}, are in the range of our measurements both for the dissolved phase and the particulate, as reviewed in Chapter 5. Studies of PAHs in plankton are even scarcer. The available data set from the Mediterranean basin ¹⁹ ranges from the same level (our maximal $C_{plankton}$ measured in the Atlantic Ocean) to 3 orders of magnitude higher (the lowest records recorded in Indian and South Pacific Oceans) than our Open Ocean concentrations, as this semi-closed sea is reported to be further polluted with PAHs due to proximate land sources ¹³.

PFASs

Figure D.2 shows the total concentrations measured for ionic PFASs and PFCAs ubiquitously found at surface and DCM depth of the Open Ocean.

PFCAs total abundance in all sampled oceans was superior to PFASs at marine surface, but in the South Atlantic basin, and their global distribution showed remarkable different patterns. In surface seawater, the interoceanic comparison revealed no significant differences for Σ PFCAs, while Σ PFASs showed statistically higher concentrations in the South Atlantic Ocean. However, the maximal concentrations for PFCAs were as well recorded in the South Atlantic basin. Similarly to the PAHs distribution, high concentration peaks occurred in NE Atlantic, near African coasts, particularly high for PFCAs. Data from previous studies for individual PFASs are in the same order of magnitude than those measured in the Atlantic Ocean during the *Malaspina 2010* circumnavigation²³⁻²⁶. Nevertheless, the range of our measurements is wider than those previously described, probably due to a higher sampling coverage of the oceanic basin. Contrarily, the comparison with earlier reports in the Indian and Pacific Oceans²⁷⁻³⁰ shows that our measurements are in the lower concentration ranges, as those studies focus mainly in coastal regions from Asian countries, which exponentially increase the PFASs loads³¹.

PFAS concentration patterns found in surface and DCM depth seawater were quite similar in terms of the range of concentrations, even though concentrations were higher at surface at most of the sampling sites. Nevertheless, there is a general increase of PFASs concentrations at the subsurface and thus, their contribution to total PFASs is of similar magnitude than PFCAs at depth, with the exception of the South Atlantic Ocean, where the PFASs relative concentration is larger, as observed at the surface. Only two studies were found dealing with PFAS concentrations in seawater at depths different than surface^{28,32}, and using the same global data set. The lower concentrations reported for PFOS and PFOA are in the range of the individual PFASs found in the Open Ocean in this Thesis. Conversely, their registers for Labrador Sea,

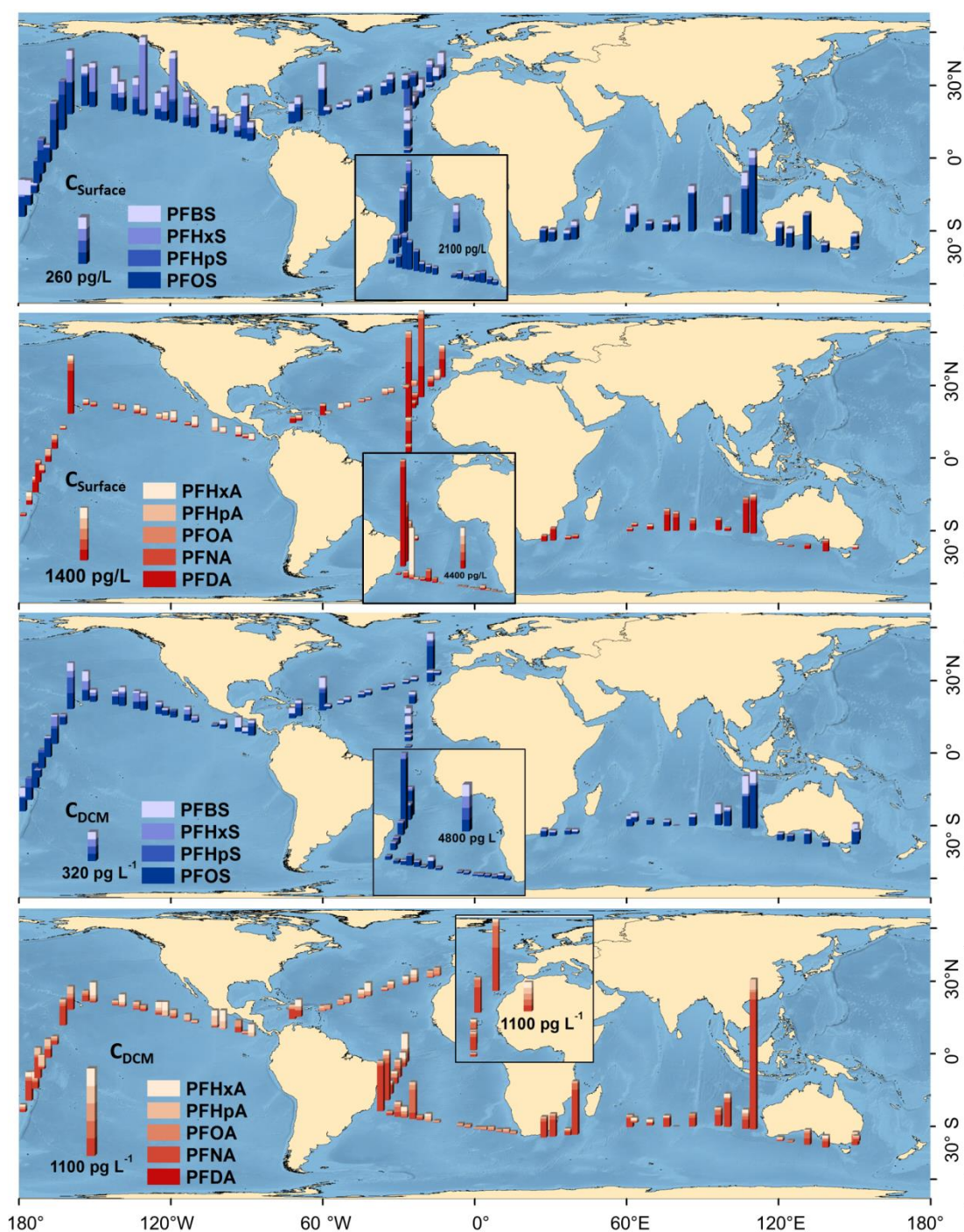


Figure D.2. Global concentration of PFSA (blue colors) and PFCA (red colors) in the surface seawater (5 m depth, top) and at the deep Chlorophyll maximum (DCM, bottom).

Middle Atlantic Ocean and Japan Sea come near the mid-high concentrations found in DCM samples in the present study, even if those do not exceed the concentrations found near Brazilian and West African coasts in this study.

Partitioning of PAHs and PFASs in the environmental compartments and implications for their Global Fate

PAHs occurrence in atmospheric gas and aerosol phases

The considered atmospheric processes affecting PAHs (dry and wet deposition, air-water diffusive exchange and degradation) are universal vectors of transport, transfer and transformation of POPs in the Open Ocean's lower atmosphere which depend on the chemical properties of the substances and environmental parameters^{8,9}. The partition (K_{P-air}) of a contaminant between the aerosol and the gaseous phase will determine the key process affecting its transference to the ocean; dry deposition will predominate if the pollutant is prone to be attached to aerosols while diffusive exchange will dominate if the pollutant is found mainly on the gaseous phase. Wet deposition will affect concentrations in both matrixes as the rain water is equilibrated with the gas concentration, and precipitation will scavenge aerosols affecting atmospheric gas and aerosol phase organic compounds occurrence⁸. Moreover, the susceptibility to be photo chemically degraded in the atmosphere is also dependent on the phase where the POP is found³³⁻³⁶. Therefore, the atmospheric fate of organic pollutants is exceptionally reliant on the aerosol-gas equilibria.

According to our measurements for PAHs, K_{P-air} obtained as the ratio between the aerosol concentration (C_A) and the gas concentration (C_G) is shown in Figure D.3 for some representative compounds at the Global Oceans. It can be observed that the more volatile compounds (like phenanthrene) reflect low K_{P-air} and therefore, they are mainly present in the gas phase and will be more susceptible to atmospheric degradation, as there is a higher rate of reaction with OH radical in the gaseous form³³. Meanwhile, heavier compounds exhibit a greater partition to marine aerosol and will be degraded on a lesser extent but preferably transferred to the ocean through dry deposition. The highest partition to the aerosol fraction for all PAHs was found in the central Indian basin and near the Australian southern coast. Besides, the high Σ PAHs C_A found in the Indian Ocean and the large dry deposition fluxes measured there¹

facilitate the entrance of high MW PAHs (like perylene) in this particular ocean (Figure D.3), not previously assessed in the literature.

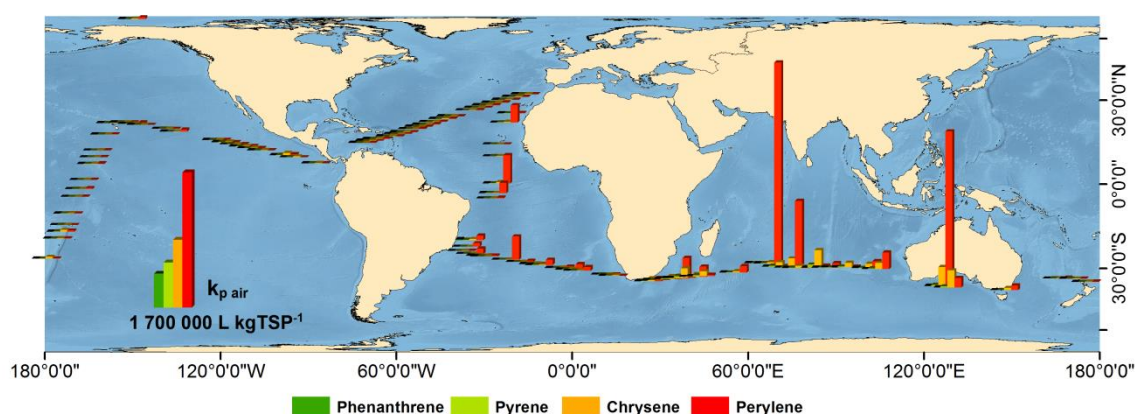


Figure D.3. K_{p-air} (L kgTSP⁻¹) for four representative PAHs.

The partition is the reflection of the concentrations of the different PAHs measured in the gas and aerosol phases, whose profiles (as mean abundances of individual PAHs in each matrix) are displayed in Figure D.4.

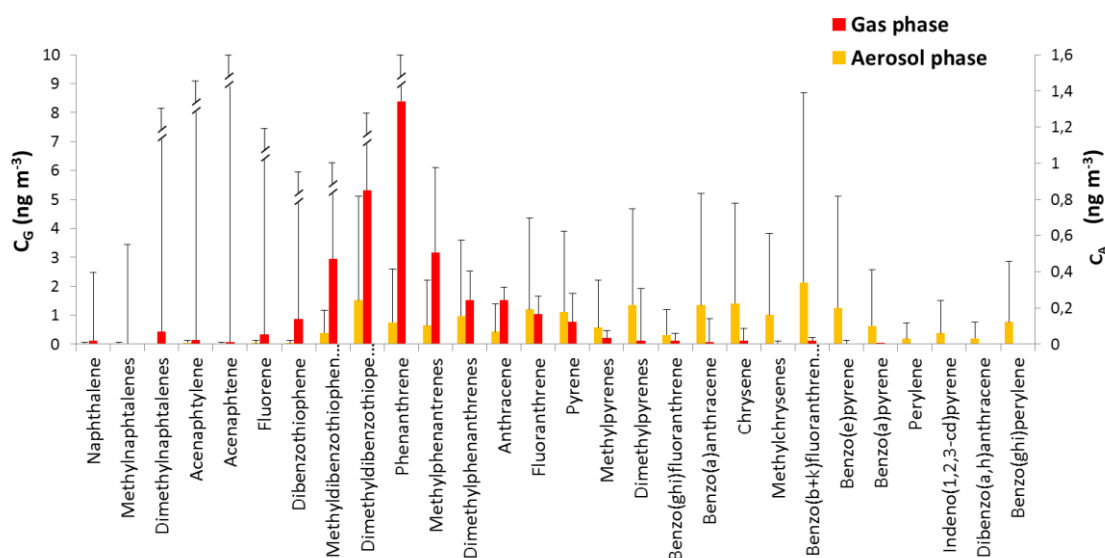


Figure D.4. PAHs profile for gas (C_g) and aerosol (C_a) phases.

PAHs pollution in the aerosol accounted for only 9.8% of total PAHs found in the atmosphere, even if the relative presence of higher MW compounds is larger in this phase than on the gas phase. On the contrary, the intermediate to high volatile compounds were largely present in the gas phase, holding more than 90% of the total PAHs measured in the oceanic atmosphere. The dominance of the atmospheric

concentrations in the gas phase has been reported previously in the Open Ocean ¹⁵, and moreover, in some studies the aerosol pollution is even neglected in the total atmospheric occurrence of PAHs ¹⁷. Therefore, the majority of PAHs will be affected by transport processes occurring mainly in the gas phase (diffusive exchange, degradation); meanwhile the more recalcitrant PAHs attached to the marine aerosol will be prone to be carried over the ocean with suspended atmospheric particles and affected by different processes (dry deposition). This is confirmed by the magnitude of the calculated fluxes presented in Chapter 2; diffusive exchange accounts for 99% of the total PAHs entrance to the Open Ocean, while dry deposition only stands for less than 1% of the PAHs input to the Global Oceans.

PAHs and PFASs occurrence in seawater's dissolved and particulate phases

The presence of POPs either in the dissolved or particulate phase of the Open Ocean seawater will be affected by different factors leading their distribution and fate. For PAHs, several processes have been reviewed and calculated in Chapter 5; like biomass dilution, degradation, biological pump, effects of the air-water diffusive exchange, etc. Regarding PFASs, even if here there is a lack of direct measurements of concentrations in the particulate phase, an estimation of the particulate fraction fate has been conducted in Chapter 4. Effectively, as reported here and in other works, the biological pump is a key regulator of POPs occurrence in remote areas ^{4,5}, affecting pollutants in the particulate phase fate. On the other hand distribution of POPs in the dissolved phase will be more affected by other processes in the Open Ocean, like water masses subduction or turbulent diffusion ^{32,37}.

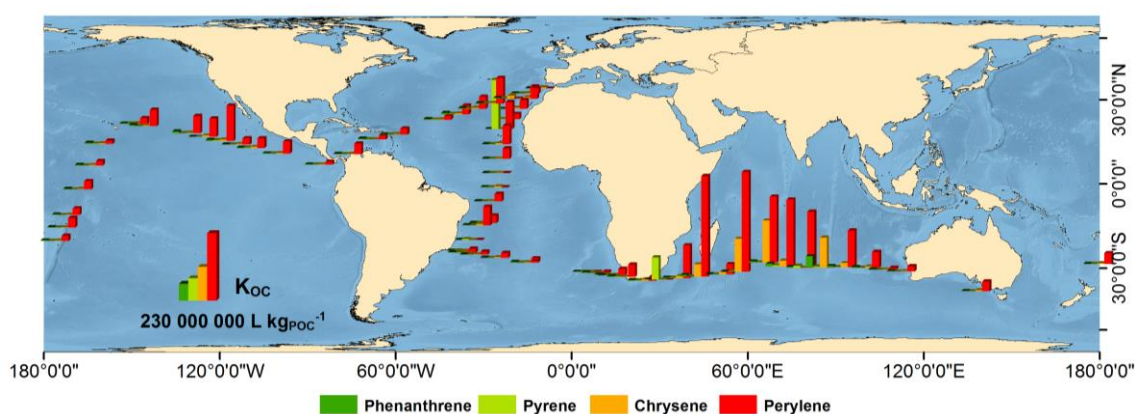


Figure D.5. K_{oc} (L kg_{POC}⁻¹) for four representative PAHs.

PAH's organic carbon-water partition as given by K_{OC} in the water phase is discussed in Chapter 5. The main drivers of partition act on a complex manner; the chemical equilibrium between particulate organic matter and water is affected by a wide array of variables like gas-water exchange, temperature, the composition of the particulate organic matter and several others that will modify the final concentration of PAHs. According to our measurements of dissolved (C_w) and particulate concentrations (C_p) in surface waters for four representative PAHs (Figure D.5), there is a higher ratio of pollutants in the particulate phase in the Indian Ocean, as found in the atmosphere, and in the North Atlantic eastern margins. The Northeast Atlantic highest concentrations, and higher partition to particles of the more hydrophobic compounds, were previously discussed by Nizzetto and coworkers¹⁷, concluding that African emissions would explain such occurrence of PAHs at high concentrations. Moreover, other POPs, such as brominated flame retardants³⁸ and polychlorinated naphthalenes³⁹ were also highly abundant in that area. Conversely, PAHs occurrence in the Indian Ocean seawaters, with high partition to the particulate phase and high concentrations reported in Chapter 5, would be explained by the high concentrations measured as well in the atmosphere and intense depositional fluxes¹ for that area. Besides, likewise in the atmosphere, higher partition coefficients correspond for the more hydrophobic compounds (like perylene) in all the sampled Oceans. Nevertheless, the differences between the individual PAHs K_{OC} in the water are much lower than in the atmosphere, showing narrower ranges.

Due to a low concentration of total particles in the oligotrophic ocean⁴⁰, PAHs are more abundant in the dissolved than on the particulate phase, as found in the atmosphere. Nevertheless, the proportion of PAHs in the water column particles is slightly higher than in the aerosol, as 11% of total measured PAHs are found on the particles versus the 89% found dissolved in the water. This is probably due to the stronger binding forces in an aqueous solution that attach PAHs to organic matter more than those in the air⁴¹, and to the degradation of low MW PAHs in the water column. The dissolved phase contained a higher relative concentration of the intermediate and more volatile congeners, whereas the particulate fraction holds a higher proportion of the more hydrophobic compounds (Figure D.6). Therefore,

biomass dilution and the biological pump, processes ruling the concentration of PAHs in the organic matter will mainly affect the more hydrophobic congeners. Contrarily, dissolved pollutants (like low MW PAHs and most ionic PFASs) will undergo other distribution processes within the water column.

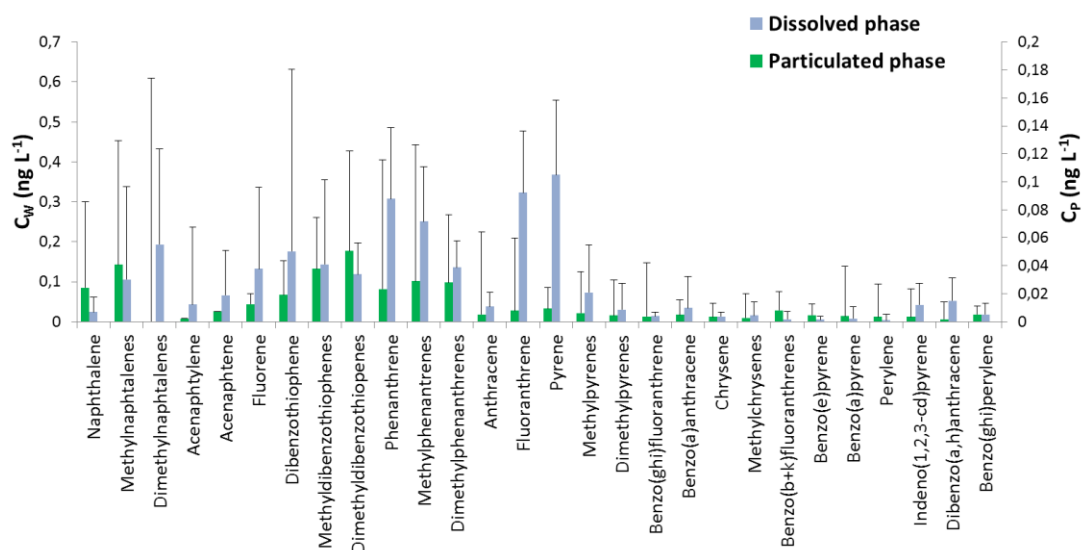


Figure D.6. PAHs profile for dissolved (C_w) and particulate (C_p) phases.

PFASs have been reported to be present in both dissolved and particulate phases in aquatic environments, depending on the partition on the amount of suspended solids, and the density and organic content of those (analogously as for PAHs)⁴². Due to the low concentrations of suspended solids in the Open Ocean and their lesser hydrophobicity compared with other POPs, PFASs like PFOS, PFOA and PFOSA have been reported to be found mainly in the dissolved phase⁴². Indeed, the calculated turbulent fluxes presented in Chapter 4 proved to successfully explain part of the occurrence of dissolved PFASs at depth in the water column. Nevertheless, according to our measurements and calculations, the biological pump is also a relevant removal process in the tropical and subtropical Open Ocean, playing even a larger role than eddy diffusion at a global scale for PFASs removal from the Open Ocean surface. This means that the occurrence of PFASs in the particulate phase deserves further research, as there is a need of more empirical measurements in the Open Ocean. A recent work has reported the occurrence of PFASs in settling particles in the NE Mediterranean sea, in this case, high fluxes were found due to dense shelf water cascading⁴³, a mechanism different than the biological pump estimated for the Open Ocean.

In addition, the occurrence of pollutants trapped onto organic matter influences their bioavailability to marine biota. PAHs are typically metabolized within the planktonic food web⁴⁴, and bioaccumulation is not so relevant, but degradation dominates in the Open Ocean. The length and complexity of the food web and the persistence of the particular PAHs⁴⁴ are factors influencing this process⁴⁵. Lighter compounds are easily degraded, meanwhile the more recalcitrant PAHs are prone to be accumulated in the organic matter and therefore redistributed in the water column by the biological pump, as explained in Chapter 5. Conversely, Higgins described that the sediment-associated PFASs can be easier accumulated in aquatic food chains⁴⁶ and also Martin reported further accumulation of those pollutants when they are found on sediments and particles of the water column, as they are then bioavailable to benthic and filtering organisms, than in the dissolved phase⁴⁷. The degradation of those POPs has not been reported to date, but bioaccumulation and biomagnification⁴⁸⁻⁵⁰ turn as an additional process (and risk) to the PFASs fate in the Open Ocean yet to be fully characterized.

Global fluxes and budgets of PAHs and PFASs in the Open Ocean

At a global scale, all the processes and factors evaluated are interconnected within a dynamic coupling of various processes. The partitioning among the different phases (gas, aerosol, water, particles) strive to put the concentrations at equilibrium. On the other hand, there are a number of processes such as dry/wet deposition, biological pump, biomass dilution, advection, etc, that can drive the concentrations away from equilibrium. For instance, a biomass growth on a certain area may drive a decrease of pollution into the water column and a consequent enhanced diffusive flux from the atmosphere towards the Ocean. All the feedbacks and side-effects involved are not fully quantified, and even to a lesser extent at an oceanic global scale. Nevertheless, the data and discussion provided here enlightens the magnitude of the processes affecting PAHs and PFASs distribution and the balance among them which may provide new insights about the total budgets and governing parameters for the POPs distribution and fate in the global Open Ocean.

An important challenge for this Thesis was to have a first understanding on the global budget for PAHs in the marine lower atmosphere and surface mixed layer, and even an estimation of the occurrence and fate of other aromatic-like compounds (Chapter 2). These results highlight a potential yet unknown perturbation of the global biogeochemical cycling of organic matter which could influence the balance of the oceanic carbon cycle. Moreover, regarding the emerging PFASs in the mixed layer, their fate in the Global Ocean was analyzed for the first time based on direct field measurements (Chapter 4).

PAHs and SALCs

The annual global balance for PAHs and SALCs considering all the analyzed transport and transformation processes is shown in Figure D.7. Among all the PAHs present in the atmosphere, a high fraction of them is directly degraded via oxidative reactions with OH radical³³, as discussed in Chapter 2. In the oceanic lower atmosphere, accounting the mean inventory measured over the Atlantic, Pacific and Indian oceans, there is a degradation of near 2.2 Tg y^{-1} of the 64 PAHs identified and quantified. This atmospheric sink is approximately two times bigger than the global Open Ocean entrance through diffuse fluxes (F_{AW} and F_{DD}), but it only affects the lighter and degradable compounds. The preferential degradation of the low MW compounds may account for a distillation process towards remote areas, even if this was not observed in our measurements, probably due to the volatilization registered from marine surface in the central areas of the oceanic tropical basins (Chapter 2). Contrarily, this differential degradation and consequent distillation effect is evident for other non-biogenic POPs, like PCBs. The lower hydrophobic PCBs show shorter residence times in intertropical regions due to the OH radical attack, and as they are not produced in the Open Ocean, the remote areas exhibit lower concentrations of lighter PCBs⁵¹ even if they are potentially more mobile⁵². The degradation rates for PCBs are estimated to be 0.008 Tg y^{-1} , 3 orders of magnitude lower than those calculated here for PAHs, but also much larger than the calculated sinks for the Open Global Ocean for PCBs, 240 tons y^{-1} ⁵³. Assuming the higher persistence of PCBs and the much lower environmental

concentrations (3 orders of magnitude lower than PAHs in the Open Ocean ^{54,55}), the ranges of the fluxes are in agreement with those calculated here for PAHs, highlighting the degradative potential of the Earth's atmosphere.

The atmospheric measurements of PAHs in the gas phase and the aerosol, in the rainwater and the depositing aerosols over the marine surface, allowed us to calculate the diffusive, wet and dry depositional processes during the *Malaspina 2010* circumnavigation cruise. Their calculation and extrapolation to the global ocean, taking into account the varying environmental conditions and assuming a certain degree of uncertainty, provided the total fluxes of PAHs deposition per year in the Open Ocean (Figure D.7).

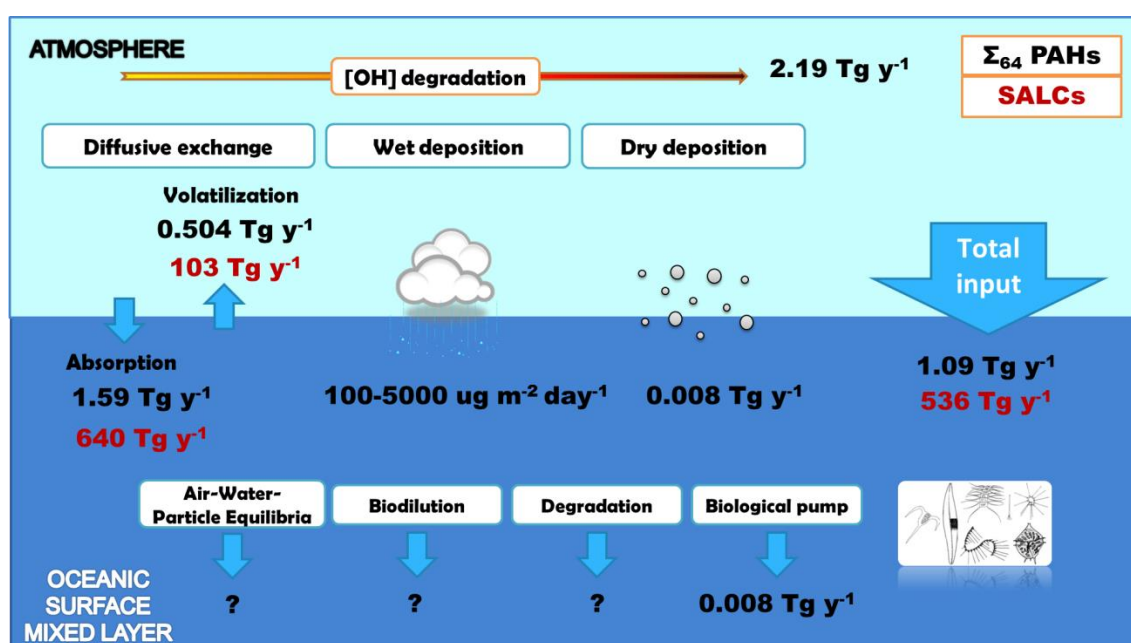


Figure D.7. PAHs and SALCs global fluxes.

Regarding diffusive exchange of PAHs, 1.6 Tg y⁻¹ are absorbed through direct diffusion, counterbalanced by 0.5 Tg y⁻¹ volatilizing from the seas surface. Wet deposition is very difficult to extrapolate spatially and temporally, and thus only an approximation of the measured rates can be showed, of hundreds to thousands μg m⁻²d⁻¹ of Σ₆₄PAHs entering the ocean through precipitations. This value, though, is highly variable depending on the atmospheric concentrations, the interval of the precipitation, and other physical parameters ⁵⁶, and may vary between few tons and half Mg of PAHs depositing onto the Global Ocean per year. Dry deposition, directly measured for the

first time with such a resolution, appeared to be as well a relevant process influencing PAHs input onto the marine surface for the high MW PAHs. Even if the calculated global fluxes are 3 orders of magnitude lower than the diffusion exchange, the 0.008 Tg y⁻¹ of PAHs entering the Open Ocean with settling aerosols are twice the European's year 2000 emission of the 16 EPA's regulated PAHs⁵⁷, thus an unneglectable quantity.

As stated previously, the magnitude of each depositional process depends on each POPs family class, specifically on their physical-chemical properties. For instance, PCBs are mainly affected by diffusive exchange fluxes as PAHs do, while for PCDD/Fs, those are in the range of wet deposition fluxes. Indeed, wet deposition accounts for 40-75% of the total deposition of PCDD/Fs to the Open Ocean, inducing particularly the entrance of the hepta- and octa- congeners, but for PCBs it does not represent more than 35% of total input⁵⁶. Dry deposition fluxes for PCBs and PCDD/Fs stand for an estimated 15% of total flux, and reported to be significant in areas with high wind speeds and high concentrations of marine aerosols⁵⁶. Nevertheless, in a recent study of PCDD/Fs and dioxin-like-PCBs in the open global ocean conducted as well during the *Malaspina 2010* cruise, it is calculated a dry deposition global input of 360 Kg y⁻¹ and 900 Kg y⁻¹ respectively², much lower than previous estimates⁵⁸ and thus, pointing to diffusive fluxes as the main vector of entrance of POPs into the Open Ocean², as occurs for PAHs according to our measurements.

The processes causing the sequestration of PAHs and their transfer to the deep ocean by the biological pump are of the same range of their dry deposition fluxes (Figure D.7). Virtually, the same amount of PAHs that enter to the ocean with settling aerosol will continue their sinking to the deep ocean (0.008 Tg y⁻¹). Other studies show the evidence of the correlation between biological pump fluxes and atmospheric inputs in temperate and polar oceans for PCBs, PCDD/Fs and halogenated pesticides^{4,5,59,60}. Moreover, in mid to high latitudes air-to-water fluxes are enhanced by the high settling fluxes of the abundant primary producers in these rich areas, as described for PCBs and hydrophobic dioxins⁹. Those fluxes range within several orders of magnitude and depend on the amount of suspended biomass, POP concentrations, chemical affinities and other key environmental factors. Settling fluxes have been described to regulate pollutants dynamics between the atmosphere and the water oceanic ecosystem, down

to the deep ocean. There and even in shallower areas of the water column, dilution, degradation and other transformation processes will take part at an uncertain rates (at least at a global scale and for the myriads of pollutants present in the ocean⁶¹), leaving the Open Ocean as a global sink of pollutants with many open questions about the global risk for the marine ecosystems.

In 2004 there was a global estimated production of 530 Gg y⁻¹ of the 16 EPA's regulated PAHs by anthropogenic sources⁵⁷. The concentrations and fluxes here calculated are far larger, of 900 Gg yr⁻¹ entering into the Open Ocean through dry deposition and diffusive exchange. This could be explained by an underestimation of the global anthropogenic production, to a large biogenic production of PAHs not accounted, and also to the fact that the more recalcitrant PAHs do accumulate and cycle in the Open Ocean for long time once they have been produced and released into the environment. Nevertheless, it is obvious that the resilience of the Open Ocean and its degradative and sink potential for PAHs is enormous, even if it seems that the real total loads of PAHs to the environment are poorly constrained.

PFASs

The global budget for the emerging fluorinated pollutants assessed in this Thesis, the PFASs, is still more uncertain to date than that of PAHs (Figure D.8). No degradation of those compounds has been reported neither in the atmosphere, nor by any organism in the ocean (in other aerobic or anaerobic ecosystems)⁶². Moreover, the atmospheric inputs to the Ocean have largely being omitted in earlier studies, and are just starting to be considered in the literature. These remained out of the scope of this thesis. Some approaches attempted to estimate the relevance of the deposition process and origin of the PFASs in remote marine areas and lakes through a characterization of the ratios and isomer profiles of the congeners measured in water⁶³⁻⁶⁵. Only few studies suggest a temperature dependent occurrence of some volatile compounds, like perfluoroalkylated sulfonamides, in the remote Arctic indicating a plausible diffusive exchange with ocean or ice, and mentioning partition to aerosol^{66,67}. Further, others correlated the presence of PFASs and their precursors in air, water and sediments in

Arctic lakes assuming atmospheric transport ⁶⁸. But a precise description and quantification of their fluxes has not been conducted to date in the Open Ocean. Wet deposition has been tentatively assessed by Taniyasu et al. in Japan and North Pacific rain and snow ⁶⁹ and by coworkers based on land measurements ⁷⁰ and showed an effective flux of PFASs deposition which should be studied further and characterized for the Open Ocean. Riverine and run-off contributions have been estimated for some specific regions ⁷¹⁻⁷³, but there is a lack of total inputs measurements at a global scale, which may vary exceptionally depending on the river basin and the sources, riverine discharges and seasonal fluxes ⁷⁴.

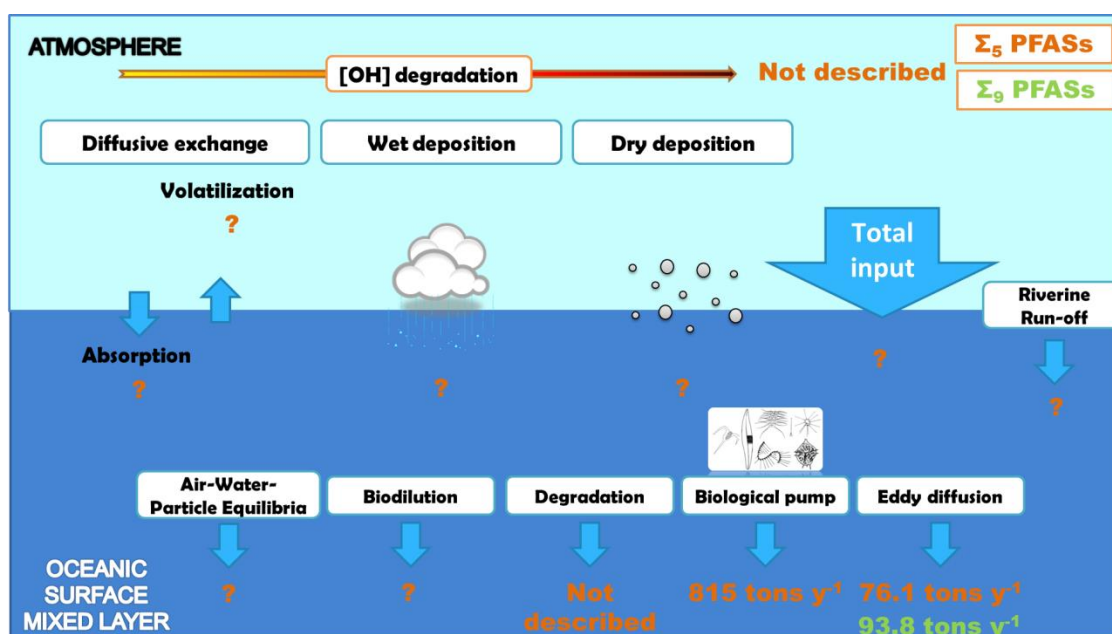


Figure D.8. PFASs global fluxes.

Nonetheless, the inventory provided here for the tropical and subtropical surface ocean for the target PFASs and the calculated sinking fluxes to the mesopelagic ocean are examples of the most updated research on this topic. The previously reported eddy diffusion transport for PFOA by Lohmann et al ³² has been completed and recalculated here by using direct turbulence measurements concurrently with the PFASs concentrations along the 3 sampled oceans in the *Malaspina 2010* circumnavigation. It was calculated also for 9 PFASs other than PFOA, with a total contribution of 93.8 tons of the 9 selected PFASs diffusing out of the surface mixed layer annually (76.1 tons y⁻¹ attend for the 5 PFASs for which also biological pump export was calculated, Figure

D.8). No much attention has been paid previously to turbulence affecting POPs transport in the Ocean; only Jurado et al ⁷⁵ explicitly assessed the relevance of this process by modeling PCBs fate in the costal marine water column. Likewise in our results for PFASs, they concluded that turbulent mixing helps to predict real concentration of POPs in the water column, where may be other processes playing a role depending on the particular environmental conditions.

Biological pump estimations were done for the first time for the 5 more abundant PFASs found in the open ocean during the *Malaspina 2010* expedition. The settling flux turned to be 100 times higher than the eddy diffusion flux calculated for those 5 PFASs (Figure D.8). The almost 900 tons of PFASs sinking per year into the ocean in aggregates of organic matter or by turbulent diffusion, may have unknown effects in the deep marine ecosystems, as the deep ocean will remain as a reservoir for millenniums due to PFASs persistence. However other processes occurring in the open ocean may also play a key role, like biomass dilution, equilibration with the atmosphere (for neutral PFASs), ejection with sea spray aerosol, and thus with a potential reemission of the PFASs if the concentrations in the water are large enough, or even the non-yet discovered degradation in the deep ocean. Therefore, more research is still needed to fully understand the behavior of all the emerging perfluorinated pollutants in the Global Ocean, considering the relevant processes proposed here.

The significance that anthropogenic POPs pollution, considering the huge amounts of compounds constantly produced and their coupling with global biogeochemical cycles can only be better understood if the processes affecting POPs fate in the Global Ocean are comprehensively studied.

REFERENCES

- 1 Gonzalez-Gaya, B., Zuniga-Rival, J., Ojeda, M. J., Jimenez, B. & Dachs, J. Field measurements of the atmospheric dry deposition fluxes and velocities of polycyclic aromatic hydrocarbons to the global oceans. *Environmental Science & Technology* **48**, 5583-5592, doi:10.1021/es500846p (2014).
- 2 Morales, L. *et al.* Background Concentrations of Polychlorinated Dibenzo-p-Dioxins, Dibenzofurans, and Biphenyls in the Global Oceanic Atmosphere. *Environmental science & technology* **48**, 10198-10207 (2014).
- 3 Castro Jiménez, J., Casal, P., González Gaya, B., Pizarro, M. & Dachs, J. Organophosphate ester (OPE) flame retardants and plasticizers in the atmosphere over the Global Oceans. *Organohalogen Compounds* **76**, 364-367 (2014).
- 4 Galbán-Malagón, C., Berrojalbiz, N., Ojeda, M. J. & Dachs, J. The oceanic biological pump modulates the atmospheric transport of persistent organic pollutants to the Arctic. *Nature communications* **3**, 862 (2012).
- 5 Galbán-Malagón, C. J., Berrojalbiz, N., Gioia, R. & Dachs, J. The "degradative" and "biological" pumps controls on the atmospheric deposition and sequestration of hexachlorocyclohexanes and hexachlorobenzene in the North Atlantic and Arctic Oceans. *Environmental Science and Technology* **47**, 7195-7203 (2013).
- 6 Galbán-Malagón, C. J., Del Vento, S., Cabrerizo, A. & Dachs, J. Factors affecting the atmospheric occurrence and deposition of polychlorinated biphenyls in the Southern Ocean. *Atmospheric Chemistry and Physics* **13**, 12029-12041 (2013).
- 7 Nizzetto, L. *et al.* Biological pump control of the fate and distribution of hydrophobic organic pollutants in water and plankton. *Environmental science & technology* **46**, 3204-3211 (2012).
- 8 Bidleman, T. F. Atmospheric processes. *Environmental Science and Technology* **22**, 361-367 (1988).
- 9 Dachs, J. *et al.* Oceanic Biogeochemical Controls on Global Dynamics of Persistent Organic Pollutants. *Environmental Science & Technology* **36**, 4229-4237, doi:10.1021/es025724k (2002).
- 10 Bozlaker, A., Muezzinoglu, A. & Odabasi, M. Atmospheric concentrations, dry deposition and air-soil exchange of polycyclic aromatic hydrocarbons (PAHs) in an industrial region in Turkey. *Journal of Hazardous Materials* **153**, 1093-1102 (2008).
- 11 Demircioglu, E., Sofuoglu, A. & Odabasi, M. Particle-phase dry deposition and air-soil gas exchange of polycyclic aromatic hydrocarbons (PAHs) in Izmir, Turkey. *Journal of Hazardous Materials* **186**, 328-335 (2011).
- 12 Vardar, N., Odabasi, M. & Holsen, T. M. Particulate dry deposition and overall deposition velocities of polycyclic aromatic hydrocarbons. *Journal of Environmental Engineering* **128**, 269-274 (2002).
- 13 Castro-Jiménez, J., Berrojalbiz, N., Wollgast, J. & Dachs, J. Polycyclic aromatic hydrocarbons (PAHs) in the Mediterranean Sea: Atmospheric occurrence, deposition and decoupling with settling fluxes in the water column. *Environmental Pollution* **166**, 40-47 (2012).
- 14 Lohmann, R. *et al.* Organochlorine pesticides and PAHs in the surface water and atmosphere of the North Atlantic and Arctic Ocean. *Environmental science & technology* **43**, 5633-5639 (2009).
- 15 Lohmann, R. *et al.* PAHs on a west-to-east transect across the tropical Atlantic Ocean. *Environmental Science and Technology* **47**, 2570-2578 (2013).
- 16 Del Vento, S. & Dachs, J. Atmospheric occurrence and deposition of polycyclic aromatic hydrocarbons in the northeast tropical and subtropical Atlantic Ocean. *Environmental Science and Technology* **41**, 5608-5613 (2007).

- 17 Nizzetto, L. *et al.* PAHs in air and seawater along a North-South Atlantic transect: Trends, processes and possible sources. *Environmental Science and Technology* **42**, 1580-1585 (2008).
- 18 Xu, Y. *et al.* The spatial distribution and potential sources of polycyclic aromatic hydrocarbons (PAHs) over the Asian marginal seas and the Indian and Atlantic Oceans. *Journal of Geophysical Research D: Atmospheres* **117** (2012).
- 19 Berrojalbiz, N. *et al.* Biogeochemical and physical controls on concentrations of polycyclic aromatic hydrocarbons in water and plankton of the Mediterranean and Black Seas. *Global Biogeochemical Cycles* **25** (2011).
- 20 Dachs, J., Bayona, J. M., Fowler, S. W., Miquel, J. C. & Albaigés, J. Vertical fluxes of polycyclic aromatic hydrocarbons and organochlorine compounds in the western Alboran Sea (southwestern Mediterranean). *Marine Chemistry* **52**, 75-86 (1996).
- 21 Gigliotti, C. L. *et al.* Air-water exchange of polycyclic aromatic hydrocarbons in the New York-New Jersey, USA, Harbor Estuary. *Environmental Toxicology and Chemistry* **21**, 235-244 (2002).
- 22 Law, R., Dawes, V., Woodhead, R. & Matthiessen, P. Polycyclic aromatic hydrocarbons (PAH) in seawater around England and Wales. *Marine pollution bulletin* **34**, 306-322 (1997).
- 23 Theobald, N., Gerwinski, W. & Jahnke, A. Occurrence of perfluorinated organic acids in surface sea-water of the East Atlantic Ocean between 53° north and 30° south. *SETAC Europe Annual Meeting* (2007).
- 24 Ahrens, L., Barber, J. L., Xie, Z. & Ebinghaus, R. Longitudinal and latitudinal distribution of perfluoroalkyl compounds in the surface water of the Atlantic Ocean. *Environmental Science & Technology* **43**, 3122-3127 (2009).
- 25 Zhao, Z. *et al.* Distribution and long-range transport of polyfluoroalkyl substances in the Arctic, Atlantic Ocean and Antarctic coast. *Environmental Pollution* **170**, 71-77, doi:10.1016/j.envpol.2012.06.004 (2012).
- 26 Benskin, J. P. *et al.* Perfluoroalkyl acids in the Atlantic and Canadian Arctic Oceans. *Environmental Science & Technology* **46**, 5815-5823, doi:10.1021/es300578x (2012).
- 27 Yamashita, N. *et al.* A global survey of perfluorinated acids in oceans. *Marine Pollution Bulletin* **51**, 658-668, doi:10.1016/j.marpolbul.2005.04.026 (2005).
- 28 Yamashita, N. *et al.* Perfluorinated acids as novel chemical tracers of global circulation of ocean waters. *Chemosphere* **70**, 1247-1255, doi:10.1016/j.chemosphere.2007.07.079 (2008).
- 29 Wei, S. *et al.* Distribution of perfluorinated compounds in surface seawaters between Asia and Antarctica. *Marine Pollution Bulletin* **54**, 1813-1818, doi:10.1016/j.marpolbul.2007.08.002 (2007).
- 30 Cai, M. *et al.* Occurrence of perfluoroalkyl compounds in surface waters from the North Pacific to the Arctic Ocean. *Environmental Science & Technology* **46**, 661-668, doi:10.1021/es2026278 (2012).
- 31 González-Gaya, B., Dachs, J., Roscales, J. L., Caballero, G. & Jiménez, B. Perfluoroalkylated Substances In The Global Tropical And Subtropical Surface Oceans. *Environmental Science & Technology* **48**, 13076-13084, doi:10.1021/es503490z (2014).
- 32 Lohmann, R., Jurado, E., Dijkstra, H. A. & Dachs, J. Vertical eddy diffusion as a key mechanism for removing perfluorooctanoic acid (PFOA) from the global surface oceans. *Environ Pollut* **179**, 88-94, doi:10.1016/j.envpol.2013.04.006 (2013).
- 33 Keyte, I. J., Harrison, R. M. & Lammel, G. Chemical reactivity and long-range transport potential of polycyclic aromatic hydrocarbons - a review. *Chemical Society Reviews* **42**, 9333-9391, doi:10.1039/C3CS60147A (2013).
- 34 Koester, C. J. & Hites, R. A. Photodegradation of polychlorinated dioxins and dibenzofurans adsorbed to fly ash. *Environmental Science & Technology* **26**, 502-507, doi:10.1021/es00027a008 (1992).

- 35 Wania, F. & Daly, G. L. Estimating the contribution of degradation in air and deposition to the deep sea to the global loss of PCBs. *Atmospheric Environment* **36**, 5581-5593, doi:10.1016/S1352-2310(02)00693-3 (2002).
- 36 Raff, J. D. & Hites, R. A. Deposition versus Photochemical Removal of PBDEs from Lake Superior Air. *Environmental Science & Technology* **41**, 6725-6731, doi:10.1021/es070789e (2007).
- 37 Lohmann, R., Jurado, E., Pilson, M. E. Q. & Dachs, J. Oceanic deep water formation as a sink of persistent organic pollutants. *Geophysical Research Letters* **33**, doi:10.1029/2006gl025953 (2006).
- 38 Xie, Z., Möller, A., Ahrens, L., Sturm, R. & Ebinghaus, R. Brominated flame retardants in seawater and atmosphere of the Atlantic and the southern ocean. *Environmental Science and Technology* **45**, 1820-1826 (2011).
- 39 Jaward, F. M., Barber, J. L., Booij, K. & Jones, K. C. Spatial distribution of atmospheric PAHs and PCNs along a north-south Atlantic transect. *Environmental Pollution* **132**, 173-181, doi:10.1016/j.envpol.2004.03.029 (2004).
- 40 Siegel, D. A., Dickey, T. D., Washburn, L., Hamilton, M. K. & Mitchell, B. G. Optical determination of particulate abundance and production variations in the oligotrophic ocean. *Deep Sea Research Part A. Oceanographic Research Papers* **36**, 211-222, doi:10.1016/0198-0149(89)90134-9 (1989).
- 41 Mackay, D. & Callcott, D. in *PAHs and Related Compounds Vol. 3 / 31 The Handbook of Environmental Chemistry* (ed AlasdairH Neilson) Ch. 8, 325-345 (Springer Berlin Heidelberg, 1998).
- 42 Ahrens, L., Yeung, L. W., Taniyasu, S., Lam, P. K. & Yamashita, N. Partitioning of perfluorooctanoate (PFOA), perfluorooctane sulfonate (PFOS) and perfluorooctane sulfonamide (PFOSA) between water and sediment. *Chemosphere* **85**, 731-737, doi:10.1016/j.chemosphere.2011.06.046 (2011).
- 43 Sanchez-Vidal, A. *et al.* Delivery of unprecedented amounts of perfluoroalkyl substances towards the deep-sea. *Science of The Total Environment* **526**, 41-48, doi:10.1016/j.scitotenv.2015.04.080 (2015).
- 44 Berrojalbiz, N. *et al.* Accumulation and Cycling of Polycyclic Aromatic Hydrocarbons in Zooplankton. *Environmental Science & Technology* **43**, 2295-2301, doi:10.1021/es8018226 (2009).
- 45 D'Adamo, R., Pelosi, S., Trotta, P. & Sansone, G. Bioaccumulation and biomagnification of polycyclic aromatic hydrocarbons in aquatic organisms. *Marine Chemistry* **56**, 45-49, doi:10.1016/S0304-4203(96)00042-4 (1997).
- 46 Higgins, C. P., McLeod, P. B., MacManus-Spencer, L. A. & Luthy, R. G. Bioaccumulation of Perfluorochemicals in Sediments by the Aquatic Oligochaete *Lumbriculus variegatus*. *Environmental Science & Technology* **41**, 4600-4606, doi:10.1021/es062792o (2007).
- 47 Martin, J. W., Whittle, D. M., Muir, D. C. G. & Mabury, S. A. Perfluoroalkyl Contaminants in a Food Web from Lake Ontario. *Environmental Science & Technology* **38**, 5379-5385, doi:10.1021/es049331s (2004).
- 48 Haukas, M., Berger, U., Hop, H., Gulliksen, B. & Gabrielsen, G. W. Bioaccumulation of per- and polyfluorinated alkyl substances (PFAS) in selected species from the Barents Sea food web. *Environmental Pollution* **148**, 360-371, doi:10.1016/j.envpol.2006.09.021 (2007).
- 49 Houde, M. *et al.* Fractionation and bioaccumulation of perfluorooctane sulfonate (PFOS) isomers in a Lake Ontario food web. *Environmental Science & Technology* **42**, 9397-9403 (2008).
- 50 Houde, M., De Silva, A. O., Muir, D. C. & Letcher, R. J. Monitoring of perfluorinated compounds in aquatic biota: an updated review. *Environmental Science & Technology* **45**, 7962-7973, doi:10.1021/es104326w (2011).

General Discussion

- 51 Jurado, E. & Dachs, J. Seasonality in the "grasshopping" and atmospheric residence times of persistent organic pollutants over the oceans. *Geophysical Research Letters* **35** (2008).
- 52 Wania, F. & MacKay, D. Peer Reviewed: Tracking the Distribution of Persistent Organic Pollutants. *Environmental Science & Technology* **30**, 390A-396A, doi:10.1021/es962399q (1996).
- 53 Anderson, P. N. & Hites, R. A. OH Radical Reactions: The Major Removal Pathway for Polychlorinated Biphenyls from the Atmosphere. *Environmental Science & Technology* **30**, 1756-1763, doi:10.1021/es950765k (1996).
- 54 Gioia, R. *et al.* Factors Affecting the Occurrence and Transport of Atmospheric Organochlorines in the China Sea and the Northern Indian and South East Atlantic Oceans. *Environmental Science & Technology* **46**, 10012-10021, doi:10.1021/es302037t (2012).
- 55 Lohmann, R., Klanova, J., Kukucka, P., Yonis, S. & Bollinger, K. PCBs and OCPs on a East-to-West Transect: The Importance of Major Currents and Net Volatilization for PCBs in the Atlantic Ocean. *Environmental Science & Technology* **46**, 10471-10479, doi:10.1021/es203459e (2012).
- 56 Jurado, E. *et al.* Wet deposition of persistent organic pollutants to the global oceans. *Environmental Science and Technology* **39**, 2426-2435 (2005).
- 57 Zhang, Y. & Tao, S. Global atmospheric emission inventory of polycyclic aromatic hydrocarbons (PAHs) for 2004. *Atmospheric Environment* **43**, 812-819, doi:10.1016/j.atmosenv.2008.10.050 (2009).
- 58 Lohmann, R., Jurado, E., Dachs, J., Lohmann, U. & Jones, K. C. Quantifying the importance of the atmospheric sink for polychlorinated dioxins and furans relative to other global loss processes. *Journal of Geophysical Research: Atmospheres* **111**, n/a-n/a, doi:10.1029/2005JD006923 (2006).
- 59 Berrojalbiz, N. *et al.* Persistent organic pollutants in Mediterranean seawater and processes affecting their accumulation in plankton. *Environmental science & technology* **45**, 4315-4322 (2011).
- 60 Castro-Jiménez, J. *et al.* Atmospheric occurrence and deposition of polychlorinated dibenzo-p-dioxins and dibenzofurans (PCDD/Fs) in the open mediterranean sea. *Environmental Science and Technology* **44**, 5456-5463 (2010).
- 61 Lohmann, R., Breivik, K., Dachs, J. & Muir, D. Global fate of POPs: Current and future research directions. *Environmental Pollution* **150**, 150-165 (2007).
- 62 Fromel, T. & Knepper, T. P. Biodegradation of fluorinated alkyl substances. *Reviews of environmental contamination and toxicology* **208**, 161-177, doi:10.1007/978-1-4419-6880-7_3 (2010).
- 63 Simcik, M. F. & Dorweiler, K. J. Ratio of perfluorochemical concentrations as a tracer of atmospheric deposition to surface waters. *Environmental Science & Technology* **39**, 8678-8683 (2005).
- 64 Benskin, J. P. *et al.* Perfluorinated acid isomer profiling in water and quantitative assessment of manufacturing source. *Environmental Science & Technology* **44**, 9049-9054, doi:10.1021/es102582x (2010).
- 65 Benskin, J. P. *et al.* Manufacturing origin of perfluorooctanoate (PFOA) in Atlantic and Canadian Arctic seawater. *Environmental Science & Technology* **46**, 677-685, doi:10.1021/es202958p (2012).
- 66 Ahrens, L., Shoeib, M., Del Vento, S., Codling, G. & Halsall, C. Polyfluoroalkyl compounds in the Canadian Arctic atmosphere. *Environmental Chemistry* **8**, 399-406 (2011).
- 67 Shoeib, M., Harner, T. & Vlahos, P. Perfluorinated Chemicals in the Arctic Atmosphere. *Environmental Science & Technology* **40**, 7577-7583, doi:10.1021/es0618999 (2006).

- 68 Stock, N. L., Furdui, V. I., Muir, D. C. & Mabury, S. A. Perfluoroalkyl contaminants in the Canadian Arctic: evidence of atmospheric transport and local contamination. *Environmental Science & Technology* **41**, 3529-3536 (2007).
- 69 Taniyasu, S. *et al.* Does wet precipitation represent local and regional atmospheric transportation by perfluorinated alkyl substances? *Environment International* **55**, 25-32, doi:10.1016/j.envint.2013.02.005 (2013).
- 70 Kwok, K. Y. *et al.* Flux of perfluorinated chemicals through wet deposition in Japan, the United States, and several other countries. *Environmental Science & Technology* **44**, 7043-7049, doi:10.1021/es101170c (2010).
- 71 Ahrens, L., Felizeter, S. & Ebinghaus, R. Spatial distribution of polyfluoroalkyl compounds in seawater of the German Bight. *Chemosphere* **76**, 179-184, doi:10.1016/j.chemosphere.2009.03.052 (2009).
- 72 Ahrens, L., Gerwinski, W., Theobald, N. & Ebinghaus, R. Sources of polyfluoroalkyl compounds in the North Sea, Baltic Sea and Norwegian Sea: Evidence from their spatial distribution in surface water. *Marine Pollution Bulletin* **60**, 255-260, doi:10.1016/j.marpolbul.2009.09.013 (2010).
- 73 Cai, M. *et al.* Spatial distribution of per- and polyfluoroalkyl compounds in coastal waters from the East to South China Sea. *Environmental Pollution* **161**, 162-169, doi:10.1016/j.envpol.2011.09.045 (2012).
- 74 Ahrens, L. & Bundschuh, M. Fate and effects of poly- and perfluoroalkyl substances in the aquatic environment: A review. *Environmental Toxicology and Chemistry* **33**, 1921-1929 (2014).
- 75 Jurado, E., Zaldívar, J.-M., Marinov, D. & Dachs, J. Fate of persistent organic pollutants in the water column: Does turbulent mixing matter? *Marine pollution bulletin* **54**, 441-451 (2007).

Chapter 4

General Conclusions

General Conclusions

The general aim of this work, as stated in the introductory chapter, was *to assess the occurrence of POPs cycling in the global tropical and subtropical oceans, focusing on PAHs and PFASs*. The results obtained in this Thesis, according to the specific objectives, contribute to the further advance in the knowledge on this issue, and a summary of the main conclusions per each objective are presented below.

- *To determine the occurrence of PAHs in gas, aerosol, dissolved, particulate and planktonic phases, and PFAS in the dissolved phase from the global Open Ocean.*

Both POPs families were detected worldwide in the tropical and subtropical Open Ocean, with different total concentrations and distribution patterns depending on their production sources, governing transport processes, chemical properties and decaying rates.

- In general, PAHs were homogeneously distributed in gas and dissolved phases; meanwhile Indian Ocean revealed very high concentrations of PAHs in the aerosol and particulate phases. The highest PAHs concentration in the plankton phase was detected in the Atlantic Ocean.
 - PFASs were dominated by PFCAs at the surface, and more balanced between the PFCAs and PFSAAs at DCM depth, even if concentrations at both depths are correlated. PFOSAs were rarely detected, mainly in the northern hemisphere. The highest concentration of PFASs by far was found in the Atlantic Ocean, particularly near Brazilian coasts followed by North East Atlantic margins.
- *To quantify the POPs fluxes between the different environmental compartments.*

Depositional fluxes of PAHs in the Open Ocean were dominated by diffusive exchange, followed by wet deposition and dry deposition. This last, even if of lower magnitude, is relevant for the heavier PAHs at global scale. Atmospheric

degradation accounted for a large sink for the more volatile PAHs.

- PAHs dry deposition fluxes bound to coarse aerosols were higher than those of fine aerosols in the Open Ocean.
- Dry deposition velocities (v_D) were higher for higher MW PAHs, due to their chemical affinities to aerosol organic matter.
- The chemical properties of the compound and environmental factors (aerosol size, wind speed, phytoplankton presence in the water column, among others) have a great impact on dry deposition. Through a parameterization of those is possible to predict v_D with an error 5 times smaller than that obtained when using a fixed v_D value from the literature, as it accounts for environmental conditions.
- Dry deposition was especially relevant in the Indian Ocean.
- Wet deposition is very intense but limited to certain periods and areas in the Open Ocean for PAHs.
- Diffusive atmospheric deposition of PAHs and other semivolatile aromatic-like compounds to the global oceans is much larger than expected, and account for a significant source of carbon to the Open Ocean that should be further studied.
- Diffusive global exchange occurred on a higher extent in the Pacific Ocean due to its large surface.

In the water column, the biological pump resulted to be the main sinking process governing PAHs and PFASs fate in the Open Ocean. Degradation was also important for low MW PAHs, and other processes like dilution for PAHs and eddy diffusive fluxes for PFAS are also relevant and should be further studied.

- Eddy diffusive fluxes allow an estimation of the subsurface concentrations of some PFASs, even if other processes may be affecting the pollutants transport and their sinking in the Open Ocean.
- The biological pump is an oceanic sink flux not previously reported for PFASs, showing an effective removal of pollutants from the surface. Fecal pellets associated fluxes were of higher magnitude than those associated with phytoplankton.

- The biological pump fluxes, several orders of magnitude higher than eddy diffusion fluxes, dominated the removal processes for PFASs, dependent on the physicochemical properties of the compound, the turbulence in the water column and the biomass abundance and sinking rates.
 - According to the temporal trends observed and the estimated residence times of PFASs, the Open Ocean will act as a reservoir of these pollutants for extremely long periods. Nevertheless, other processes of deposition and transport in the water phase may take part and need to be as well assessed to elucidate PFASs fate at a global scale in the Open Ocean.
 - Water-particle partition was higher for the high MW PAHs and turned to be dependent on particulate organic carbon with a negative correlation, at a higher extent for the more hydrophobic compounds. Also particulate phase concentration was correlated with the particulate organic carbon. This air-water-particle exchange governs the occurrence and transport/degradation of PAHs in the surface ocean.
 - Air-water-particle transfer of PAHs was confirmed for superficial particulate phase concentrations, even if the phases were not in equilibria, causing a net diffusive flux towards the Ocean.
 - Zooplankton fecal pellet settling was one order of magnitude higher than the biological pump due to settling phytoplankton. This process is a very effective sink for PAHs from the euphotic surface ocean, and should be further characterized according to sinking matter composition.
 - The reported atmospheric deposition is not totally counterbalanced by the settling fluxes for PAHs, thus, the degradative pump and other sink processes in the Open Ocean should be further assessed.
- *To study physical and trophic factors that affect POPs entrance in the plankton.*

Hydrophobicity and the biomass concentration resulted to be the governing parameters for PAHs occurrence in the oceanic plankton. The amount of plankton biomass in the water column negatively correlated with the measured PAHs concentrations, modulated by the hydrophobicity of each particular compound.

- For the lighter PAHs there was a decreasing rate of biomass influence with increasing hydrophobicity. As their occurrence is governed by degradation, the lightest are more affected than the intermediate PAHs, which are less

General Conclusions

prone to be biotransformed.

- For the intermediate and heavier compounds, there was an increasing rate of biomass dependence with higher hydrophobicity. The biological pump drives these PAHs occurrence in the plankton, and therefore, the heavier compounds (more hydrophobic) are more intensively affected at higher biomass occurrence.
 - Biomass dilution, air-water-particle exchange, degradation, and the biological pump are playing a role in the PAHs occurrence in plankton, and thus governing the POPs entrance in the lower levels of the trophic chains in the Open Ocean.
 - Following the trends suggested here, degradation rates and in-situ sinking fluxes should be assessed further in order to fully understand the entrance of pollution into marine food webs.
- *To evaluate the relevance of semivolatile aromatic hydrocarbons (containing PAHs and other aromatic compounds) as a source of semivolatile organic carbon to the Open Ocean.*

PAHs and other semivolatile aromatic-like compounds (SALCs) present in the Open Ocean lower atmosphere and surface water account for a significant portion of the total Organic Carbon at global scale.

- Their transport and deposition fluxes to the Open Ocean are vectors of carbon cycling of the same order of magnitude than other's organic substances already accounted in the global budgets.
- Future work should focus on alternative approach of Organic Carbon measurements and characterization in order to add PAHs and SALCs, and probably other fractions of semivolatile organic compounds to better understand the processes governing the occurrence and fluxes of semivolatile organic compounds in the marine carbon cycle.

Annexes
Annexes

**1. FIELD MEASUREMENTS OF THE ATMOSPHERIC DRY
DEPOSITION FLUXES AND VELOCITIES OF POLYCYCLIC
AROMATIC HYDROCARBONS TO THE GLOBAL OCEANS**

Supporting Information

**Belén González-Gaya^{1,2}, Javier Zúñiga-Rival¹, María José Ojeda¹, Begoña
Jiménez², and Jordi Dachs^{1*}**

*Corresponding Author email: jordi.dachs@idaea.csic.es

INDEX

Table S1.1, Ancillary and meteorological information for the dry deposition measurements.

Table S1.2, Ancillary and meteorological information for the suspended aerosols samples.

Figure S1.1, Air mass back trajectories for the low atmosphere.

Figure S1.2, Air mass back trajectories for the upper atmospheric boundary layer. Back trajectories are shown for two characteristic dry deposition samples (Samples 4 and 7).

Table S1.3, Information on the Mass Spectrometer method.

Table S1.4, Field blanks for the dry deposited aerosols samples.

Table S1.5, Field blanks for the suspended aerosol samples.

Table S1.6, Surrogate recoveries for the dry deposited aerosol samples.

Table S1.7, Surrogate recoveries for the suspended aerosol samples.

Table S1.8, Dry deposition fluxes (F_{DD}) measured for aerosols ($\text{g m}^{-2}\text{d}^{-1}$) and PAHs ($\text{ng m}^{-2}\text{d}^{-1}$).

Figure S1.3, Mean dry deposition fluxes (F_{DD}) for individual PAHs in the coarse and fine deposited fractions ($\text{ng m}^{-2}\text{d}^{-1}$).

Figure S1.4, Aerosol dry deposition fluxes (F_{DD}) in the Global Oceans ($\text{g m}^{-2}\text{d}^{-1}$).

Table S1.9, Organic Carbon concentrations in the deposited particles (OC%) and their dry deposition fluxes ($F_{DD\text{ OC}}$; $\text{mg m}^{-2}\text{day}^{-1}$).

Table S1.10, Concentrations of PAHs in dry deposited fine and coarse aerosols (C_{DD} , ng g^{-1}).

Figure S1.5, PAHs Concentration in dry deposited aerosol (C_{DD} , ng g^{-1}) for the a) fine fraction and b) coarse fraction.

Table S1.11, Concentrations of individual PAHs in the suspended aerosols (C_A , ng m^{-3}).

Figure S1.6, Concentrations of PAHs in suspended aerosol (C_A , ng m^{-3}) in the Global Oceans.

Figure S1.7, Individual PAHs profile in suspended aerosols (C_A , ng m^{-3}).

Table S1.12, Estimated dry deposition velocity (v_D , cm s^{-1}) of suspended aerosol-bound PAHs.

Table S1.13, Vapor pressures (P_L) for individual PAHs used in this work.

Table S1.14, Spearman correlation data between PAHs dry deposition velocity (v_D , cm s^{-1}) for each sampling period versus compound specific vapor pressure (P_L).

Table S1.15, Spearman correlations between PAHs concentration in the fine fraction of the dry deposited aerosols (C_{DDfine}) and wind speed (U_{10}).

Table S1.16, Spearman correlations between PAHs dry deposition flux associated to fine particles (F_{Dfine}) and wind speed (U_{10}).

Table S1.17, Pearson's correlation between PAHs dry deposition velocity slopes when plotted against vapor pressure (slope V_{Dfine}) versus wind speed (U_{10}).

Table S1.18. Parameterization of the deposition velocity (v_D) versus physic and biochemical parameters using least squares multiple parametric linear regression.

Table S1.19, Parameterization of the deposition velocity (v_D) versus specific vapor pressure (P_L) using least squares multiple parametric linear regression.

Table S1.1, Ancillary and meteorological information for the dry deposition measurements.

Station	Sample	Transect	Day	Hour	Longitude	Latitude	Coarse particles >2.7 μm	Fine particles 2.7-0.7 μm	Mean Wind Velocity	Instant Wind Velocity	Air Temp.	Humidity	Solar Radiation	Atmospheric Pressure
				(UTC)	(°E)	(°N)	(g day ⁻¹)	(g day ⁻¹)	(m s ⁻¹)	(m s ⁻¹)	(°C)	(%)	(W m ⁻²)	(mmHg)
10	1	initial	26/12/2010	12:00	-26.040	14.494	0	0						
12	1	final	28/12/2010	12:05	-26.014	9.565	0.0597	0.0430	7.31	8.71	25.30	67.54	214.65	1003.15
17	2	initial	02/01/2011	21:00	-27.544	-3.464	0	0						
19	2	final	04/01/2011	13:00	-29.356	-7.200	0.2432	0.1349	8.26	9.33	26.40	74.62	220.35	1000.30
22	3	initial	07/01/2011	12:00	-32.382	-13.704	0	0						
24	3	final	09/01/2011	18:00	-34.714	-18.607	0.1101	0.0891	7.87	9.08	25.81	69.47	404.71	1004.80
25	4	initial	10/01/2011	11:13	-35.800	-19.900	0	0						
26	4	final	11/01/2011	14:26	-37.400	-22.800	0.0407	0.0355	8.71	11.57	26.64	71.21	380.68	1001.69
29	5	initial	21/01/2011	18:00	-29.995	-25.448	0	0						
31	5	final	23/01/2011	19:00	-23.584	-26.583	0.1499	0.1036	6.34	7.00	24.14	73.99	427.01	1011.01
33	6	initial	25/01/2011	19:45	-17.205	-27.706	0	0						
35	6	final	27/01/2011	16:45	-11.792	-28.598	0.1029	0.0649	5.13	5.83	22.58	68.15	472.62	1013.86
58	7	initial	02/03/2011	09:15	79.775	-29.827	0	0						
60	7	final	04/03/2011	16:28	87.907	-29.717	0.0483	0.0279	6.36	6.98	21.48	69.41	271.52	1011.08
85	8	initial	23/04/2011	18:55	-174.489	-15.902	0	0						
87	8	final	25/04/2011	18:59	-172.659	-11.209	0.0453	0.0257	5.88	6.57	27.92	73.94	220.35	1003.28
95	9	initial	03/05/2011	18:40	-164.425	6.980	0	0						
97	9	final	05/05/2011	18:19	-162.413	11.593	0.0818	0.0707	9.73	10.78	26.30	77.84	340.11	1000.98
115	10	initial	28/05/2011	14:00	-115.773	13.765	0	0						
116	10	final	29/05/2011	19:00	-113.264	13.185	0.0517	0.0326	3.81	4.81	25.04	63.99	452.94	1001.37
120	11	initial	02/06/2011	16:10	-102.462	10.761	0	0						
121	11	final	03/06/2011	20:00	-99.224	10.034	0.0340	0.1269	5.03	5.75	27.08	75.43	306.89	1002.51
0	12	initial	24/06/2011	14:00	-62.958	16.483	0	0						
0	12	final	25/06/2011	21:00	-59.580	17.508	0.2175	0.0413	6.58	7.245	28.12	72.32	353.86	1007.59

* Meteorological data is used for calculations; therefore it is averaged for the measurement (whole exposition event) with data steps of second to minutes depending on the attribute.

Table S1.2, Ancillary and meteorological information for the suspended aerosols samples.

The correspondence of these samples with the simultaneous measurements of dry deposition is also indicated.

Station	Dry Dep sample corresp.	Transect	Date	Time	Longitude	Latitude	Sampled Volume	Aerosol Concentration	Mean Wind velocity	Instant Wind velocity	Air Temp .	Humidity	Solar Radiation	Atmospheric Pressure
				(UTC)	(° E)	(° N)	(m ³)	(mg m ⁻³)	(m s ⁻¹)	(m s ⁻¹)	(°C)	(%)	(W m ⁻²)	(mmHg)
11	1	initial	26/12/2010	13:30	-26.031	14.504			6.92	9.09	22.80	66.20	276.17	1005.53
		final	28/12/2010	13:00	-26.025	9.567	945	0.087	7.94	9.69	25.58	65.18	865.98	1005.16
12	1	initial	28/12/2010	13:15	-26.027	9.565			5.41	6.04	21.94	65.18	1160.88	1012.91
		final	29/12/2010	21:55	-25.994	6.405	767	0.244	8.44	9.99	26.35	61.1	599.16	1001.83
17	2	initial	02/01/2011	12:00	-27.331	-3.028			5.70	6.07	21.94	67.42	1179.60	1012.73
		final	03/01/2011	13:15	-28.181	-4.823	945	0.073	7.29	8.31	26.44	62.12	786.40	1001.83
18	2 and 3	initial	08/01/2011	19:02	-33.755	-16.559			2.68	3.72	20.61	75.89	351.07	1012.18
		final	08/01/2011	12:30	-33.429	-15.809	960	0.163	10.26	11.51	26.64	74.87	0.00	1000.72
23	3	initial	08/01/2011	17:30	-33.623	-16.283			6.72	7.38	20.80	74.56	79.57	1012.36
		final	09/01/2011	22:30	-35.142	-19.424	632	0.067	8.32	10.12	27.12	72.52	950.23	1000.72
24	4	initial	09/01/2011	23:00	-35.189	-19.514			9.08	11.32	21.56	61.20	636.61	1012.36
		final	10/01/2011	20:45	-36.353	-21.835	525	0.133	8.39	9.20	27.41	72.52	1146.84	1000.72
25	4	initial	10/01/2011	21:15	-36.385	-21.904			6.52	7.17	27.02	76.71	0.00	1004.42
		final	11/01/2011	20:45	-38.077	-23.382	275	0.331	5.42	7.20	27.12	64.67	383.83	1004.42
30	5	initial	20/01/2011	22:40	-31.479	-25.191			7.60	8.15	27.89	75.00	0.00	1002.02
		final	21/01/2011	13:10	-30.167	-25.402	1339	0.086	4.22	4.86	26.54	63.85	1029.81	1005.71
31	5	initial	22/01/2011	13:35	-27.528	-25.877			7.73	8.53	27.89	74.05	0.00	1001.28
		final	23/01/2011	22:00	-22.978	-26.684	1149	0.050	2.83	3.32	26.73	67.32	865.98	1004.42
33	6	initial	25/01/2011	18:40	-17.441	-27.666			6.16	6.71	26.64	81.40	0.00	1001.28
		final	26/01/2011	20:30	-13.636	-28.328	940	0.028	5.27	6.17	25.19	71.81	0.00	1005.16
34	6	initial	26/01/2011	21:10	-13.487	-28.353			9.86	10.86	26.64	79.36	0.00	1000.72
		final	27/01/2011	18:20	-11.452	-28.707	617	0.056	5.54	6.76	25.19	70.28	0.00	1005.34
57	7	initial	01/03/2011	13:15	77.418	-29.883			6.87	7.99	24.62	64.47	800.44	1004.79
		final	03/03/2011	6:05	82.625	-29.799	1982	0.018	8.79	9.47	25.10	69.57	1245.14	1012.18

Station	Dry Dep sample corresp.	Tran sect	Date	Time	Longitude	Latitude	Sampled Volume	Aerosol Concen tration	Mean Wind velocity	Instant Wind velocity	Air Temp .	Humidity	Solar Radiation	Atmospheric Pressure
				(UTC)	(° E)	(° N)	(m ³)	(mg m ⁻³)	(m s ⁻¹)	(m s ⁻¹)	(°C)	(%)	(W m ⁻²)	(mmHg)
58	7	initial	01/03/2011	6:00	76.061	-29.886			5.99	7.32	25.00	62.53	500.86	1000.54
		final	03/03/2011	5:35	82.618	-29.800	927	0.035	6.38	7.05	22.80	76.50	0.00	1013.10
59	7	initial	03/03/2011	6:10	82.628	-29.801			4.69	5.44	24.81	62.73	285.53	1000.72
		final	04/03/2011	6:20	86.256	-29.748	889	0.037	5.53	6.20	23.18	64.06	346.39	1013.65
60	7	initial	04/03/2011	5:58	86.252	-29.746			8.05	9.97	26.16	66.61	215.32	999.06
		final	05/03/2011	5:00	89.433	-29.671	871	0.039	5.95	6.46	22.04	74.77	0.00	1012.84
85	8	initial	23/04/2011	13:15	-174.731	-16.341			2.96	3.35	26.06	79.87	248.08	1002.57
		final	24/04/2011	12:30	-173.616	-14.028	672	0.047	5.81	6.18	22.23	73.95	0.00	1014.02
86	8	initial	24/04/2011	12:45	-173.598	-13.990			5.95	6.53	28.57	70.38	547.67	100.17
		final	26/04/2011	12:15	-172.420	-10.069	582	0.071	3.70	4.02	22.80	63.14	294.89	1011.99
95	9	initial	03/05/2011	11:00	-164.578	6.515			5.87	6.65	28.28	71.50	809.80	1004.23
		final	03/05/2011	20:15	-164.431	6.976	618	0.106	4.26	4.59	21.66	69.67	0.00	1013.28
95	9	initial	03/05/2011	20:20	-164.430	6.978			6.35	7.94	28.08	72.12	0.00	1000.54
		final	04/05/2011	20:15	-163.581	9.227	902	0.118	2.63	2.92	21.75	65.38	4.67	1012.54
96	9	initial	04/05/2011	20:30	-163.582	9.227			5.76	6.71	28.28	69.87	60.84	999.99
		final	05/05/2011	18:00	-162.411	11.592	1088	0.112	2.41	2.61	21.66	65.08	0.00	1012.73
114	10	initial	27/05/2011	21:45	-118.426	14.449			6.12	7.30	27.70	78.54	276.17	100.72
		final	28/05/2011	22:50	-115.712	13.765	857	0.074	3.36	3.56	20.80	67.53	0.00	1012.54
115	10	initial	28/05/2011	23:15	-115.627	13.762			6.12	7.30	27.70	78.54	276.17	100.72
		final	30/05/2011	0:05	-112.528	13.008	800	0.046	3.85	4.16	20.80	68.04	0.00	1012.36
120	11	initial	02/06/2011	21:48	-101.628	10.610			5.68	6.14	26.93	82.52	1305.99	1004.79
		final	03/06/2011	22:30	-98.714	9.951	853	0.035	1.36	1.51	20.04	83.13	23.40	1013.47
120	11	initial	02/06/2011	16:45	-102.468	10.761			6.77	7.39	27.79	79.05	393.20	100.72
		final	04/06/2011	0:20	-98.328	9.878	916	0.065	6.00	6.53	20.33	78.95	0.00	1013.84
121	11	initial	03/06/2011	23:50	-98.433	9.898			5.37	6.26	27.60	80.28	781.72	1003.86
		final	04/06/2011	23:00	-95.274	9.216	883	0.030	7.82	8.74	19.95	78.24	0.00	1010.33
122	11	initial	04/06/2011	23:00	-95.274	9.216			4.01	4.37	29.73	66.61	1118.75	1007
		final	05/06/2011	15:40	-93.139	8.792	551	0.090	5.33	7.06	20.23	89.56	0.00	999.80

Station	Dry Dep sample corresp.	Tran sect	Date	Time	Longitude	Latitude	Sampled Volume	Aerosol Concentration	Mean Wind velocity	Instant Wind velocity	Air Temp .	Humidity	Solar Radiation	Atmospheric Pressure
				(UTC)	(° E)	(° N)	(m ³)	(mg m ⁻³)	(m s ⁻¹)	(m s ⁻¹)	(°C)	(%)	(W m ⁻²)	(mmHg)
122	11	initial	04/06/2011	20:20	-95.796	9.330			7.35	7.95	27.99	73.54	177.87	1009.59
		final	07/06/2011	17:30	-87.839	7.174	789	0.024	7.29	8.05	20.14	74.97	0.00	1010.14
0**	12	initial	24/06/2011	16:25	-62.491	16.577			7.69	8.52	27.41	72.93	60.84	1008.3
		final	25/06/2011	13:00	-59.831	17.427	818	0.075	4.34	4.94	21.85	68.24	0.00	1004.60
131	12	initial	25/06/2011	10:20	-59.829	17.427			11.05	12.25	27.5	72.52	332.34	1009.77
		final	26/06/2011	11:00	-57.812	18.064	820	0.069	5.56	6.24	22.04	66.71	1179.60	1012.73

* Meteorological data is not used for calculations, therefore only starting and ending values are included.

** No station (no stop) was done when this sample was gathered.

Figure S1.1, Air mass back trajectories for the low atmosphere.

The back trajectories were calculated using the NOAA Hysplit model for the 12 end locations of the Dry Deposition measures. Blue lines correspond to the 48 hours backwards trajectories of the air masses at 30, 200 and 500 meters above sea level.

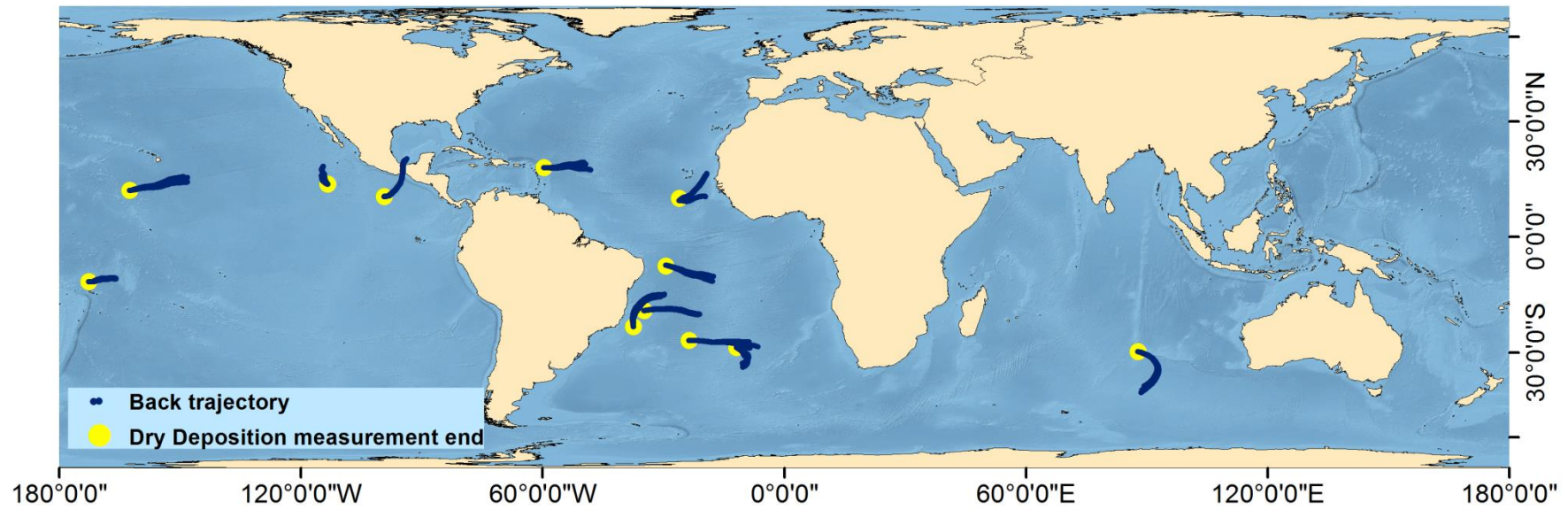


Figure S1.2, Air mass back trajectories for the upper atmospheric boundary layer. Back trajectories are shown for two characteristic dry deposition samples (Samples 4 and 7).

In sample 4 (located in east south Atlantic, offshore Brazil), some of upper air masses are originated in Brazilian inland and coastal zone, facilitating then the distribution of industrial and urban (particularly heavily populated in this area) aerosols along the entire air column by deposition. Left panel shows the air masses during the sampling at 800 m above sea level for this sample.

Sample 7 (located in the central Indian Ocean) was affected by a previous strong storm and wind coming from Southern East Asia, especially in the upper layers of the lower atmosphere above the boundary layer (2000 m). The central panel shows the 96 hours back trajectories and it can be observed starting points of the trajectories coming from the south and southwest. Right panel shows the evolution of the air masses during two previous days of the sampling at 800 m, showing as well upper intrusion of South East originated air masses, particularly at the heights of low clouds formation and from the North East.

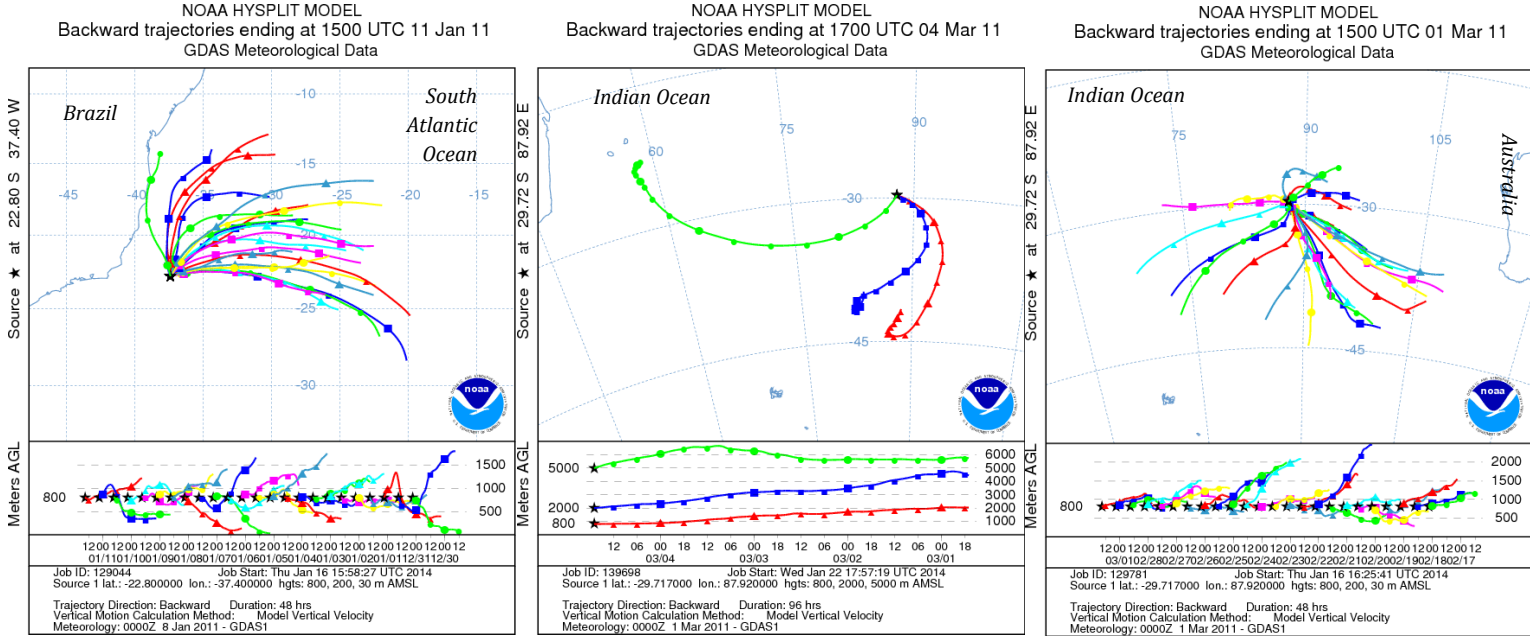


Table S1.3, Information on the Mass Spectrometer method.

PAH Species	Type	Molecular ion	Confirmation ion	RT	Calibration reference
Fluoranthrene	nat	202	-	25.12	
Pyrene D10	is	212	-	26.51	
Pyrene	nat	202	-	26.60	
Trimethylphenanthrene (12 isom)	ni	220	205	29.30	Phenanthrene
Methylpyrene (1)	ni	216	215	28.92	Pyrene
Methylpyrene (2)	ni	216	215	29.53	Pyrene
Methylpyrene (3)	ni	216	215	29.97	Pyrene
Methylpyrene (4+5)	ni	216	215	30.90	Pyrene
P-terphenyl D14	is	244	-	28.90	
Dimethylpyrene (1+2+3+4)	ni	230	215	32.79	Pyrene
Dimethylpyrene (5+6)	ni	230	215	34.40	Pyrene
Dimethylpyrene (7+8)	ni	230	215	35.01	Pyrene
Benzo(ghi)Fluoranthrene	ni	226	113	34.32	Benzo(a)Anthracene
Benzo(a)Anthracene	nat	228	226	35.92	
Chrysene D12	surr	240	-	36.06	
Chrysene	nat	228	226	36.18	
Methylchrysene (1+2)	ni	242	119	39.57	Chrysene
Benzo(b)Fluoranthrene D12	is	264	-	42.68	
Benzo(b+k)Fluoranthrene	nat	252	250	42.80	
Benzo(e)Pyrene	ni	252	126	43.85	Benzo(a)Pyrene
Benzo(a)Pyrene	nat	252	250	43.98	
Perylene D12	surr	264	264	44.22	Benzo(a)Pyrene
Perylene	ni	252	250	44.33	
Indeno (1,2,3-cd)Pyrene	nat	276	277	47.52	
Dibenzo(a,h)Anthracene	nat	278	276	47.67	
Benzo(ghi)perylene	nat	276	277	48.18	

Type column identifies recovery standards (surr), internal standards (is), native species with standard in the calibration curve (nat) and native without self-calibration standard (ni). For those last, calibration curve reference is pointed in the table. RT means retention time.

Table S1.4, Field blanks for the dry deposited aerosols samples.

	DL	Blank coarse	Blank fine	Samples over QL coarse	Samples over QL fine
	<i>(ng/sample)</i>	<i>(ng/sample)</i>	<i>(ng/sample)</i>	<i>(%)</i>	<i>(%)</i>
Fluoranthene	0.02	0.02	0.05	94	100
Pyrene	0.02	0.01	0.05	100	91
Methylpyrene	0.02	0.00	0.00	100	100
Dimethylpyrene	0.02	0.00	0.00	100	100
Benzo(ghi)Fluoranthene	0.02	0.00	0.00	100	100
Benzo(a)Anthracene	0.02	0.10	0.14	100	100
Chrysene	0.02	0.02	0.06	100	100
Methylchrysene	0.02	0.36	1.88	100	100
Benzo(b+k)Fluoranthene	0.02	0.28	0.00	100	100
Benzo(e)Pyrene	0.02	0.00	0.00	100	100
Benzo(a)Pyrene	0.02	0.35	0.54	100	100
Perylene	0.02	0.00	0.00	100	100
Indeno(1,2,3-cd)Pyrene	0.02	0.00	0.00	100	100
Dibenzo(a,h)Anthracene	0.02	0.00	0.00	100	100
Benzo(ghi)perylene	0.02	0.00	0.00	100	100

Table S1.5, Field blanks for the suspended aerosol samples.

	DL	Lab Blank	Field Blank	Samples over QL
	<i>(ng/sample)</i>	<i>(ng/sample)</i>	<i>(ng/sample)</i>	<i>(%)</i>
Fluoranthene	0.02	nd	0.02	100
Pyrene	0.02	nd	0.05	100
Methylpyrene	0.02	nd	nd	100
Dimethylpyrene	0.02	nd	0.23	100
Benzo(ghi)Fluoranthene	0.02	nd	nd	100
Benzo(a)Anthracene	0.02	nd	0.25	100
Chrysene	0.02	nd	0.02	100
Methylchrysene	0.02	nd	0.12	97
Benzo(b+k)Fluoranthene	0.02	nd	1.16	100
Benzo(e)Pyrene	0.02	nd	nd	100
Benzo(a)Pyrene	0.02	nd	nd	100
Perylene	0.02	nd	nd	100
Indeno(1,2,3-cd)Pyrene	0.02	nd	nd	100
Dibenzo(a,h)Anthracene	0.02	nd	nd	100
Benzo(ghi)Perylene	0.02	nd	nd	100

Table S1.6, Surrogate recoveries for the dry deposited aerosol samples.

	Station	Aerosol fraction	Chrysene D12	Perylene D12
	<i>(initial-final)</i>		<i>% recovery</i>	<i>% recovery</i>
1	10-12	<i>coarse</i>	112.5	121.0
		<i>fine</i>	59.0	104.9
2	17-19	<i>coarse</i>	63.0	112.1
		<i>fine</i>	51.0	89.2
3	22-24	<i>coarse</i>	521.3*	340.7*
		<i>fine</i>	64.2	118.4
4	25-26	<i>coarse</i>	120.8	203.0
		<i>fine</i>	42.9	77.7
5	29-31	<i>coarse</i>	184.7	147.0
		<i>fine</i>	78.3	124.3
6	33-35	<i>coarse</i>	70.0	128.3
		<i>fine</i>	70.8	124.7
7	58-60	<i>coarse</i>	69.7	112.8
		<i>fine</i>	56.2	65.7
8	85-87	<i>coarse</i>	21.2	28.2
		<i>fine</i>	41.9	78.6
9	95-97	<i>coarse</i>	79.8	129.4
		<i>fine</i>	69.2	120.3
10	115-116	<i>coarse</i>	75.1	128.1
		<i>fine</i>	0.0**	0.0**
11	120-121	<i>coarse</i>	84.6	140.0
		<i>fine</i>	139.1	114.7
12	0-0	<i>coarse</i>	81.8	136.3
		<i>fine</i>	0.0*	0.0*

* 13 coarse sample was spiked wrongly due to an error during the extraction process

**fine aerosol 10 and 12 samples were not surrogate marked

Both anomalies did not account for the mean calculations.

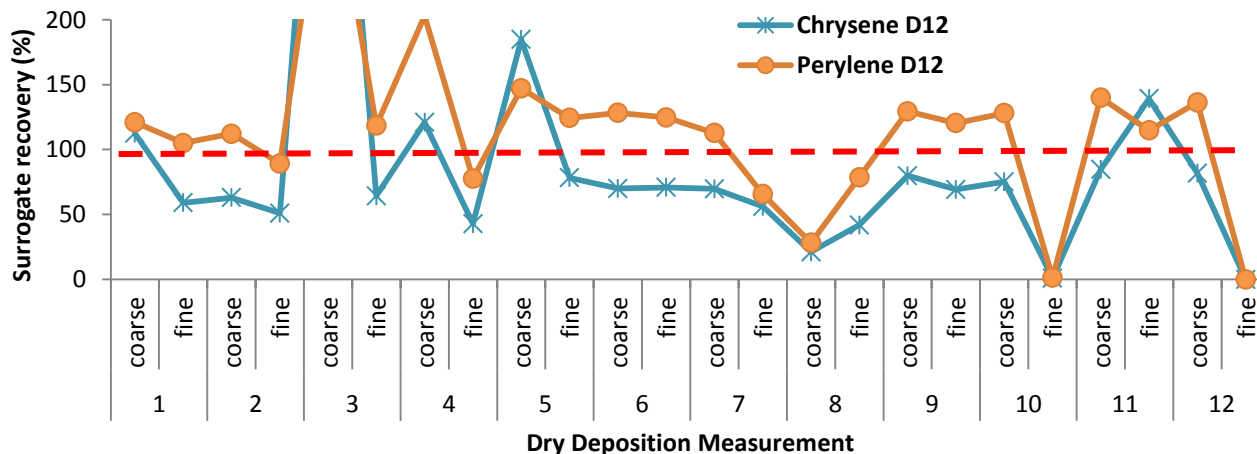


Table S1.7, Surrogate recoveries for the suspended aerosol samples.

Dry Deposition correspondence	Station	Sample	Chrysene D12 % recovery	Perylene D12 % recovery
1	11	MH013K011FPOP	95.20	101.14
2	17	MH019K017FPOP	109.73	110.93
3	23	MH025K023FPOP	87.90	88.84
4	24	MH026K024FPOP	119.17	114.29
4	25	MH027K025FPOP	102.86	100.03
5	30	MH039K030FPOP	119.03	123.68
5	31	MH040K031FPOP	122.74	129.47
6	33	MH042K033FPOP	102.86	105.31
6	34	MH043K034FPOP	127.75	134.19
7	36	MH045K036FPOP	71.82	75.50
7	37	MH046K037FPOP	102.38	95.45
7	38	MH047K038FPOP	114.25	132.73
8	40	MH049K040FPOP	107.08	132.29
8	41	MH050K041FPOP	40.16	48.45
9	57	MH077K057FPOP	93.91	112.13
9	58	MH078K058FPOP	67.06	64.05
9	59	MH079K059FPXX	97.96	105.01
9	60	MH080K060FPOP	120.16	130.47
10	85	MH129K085FPOP	94.37	112.47
10	86	MH130K086FPOP1	97.45	109.26
11	95	MH139K095FPOP1	88.44	116.07
11	95	MH139K095FPOP3	95.10	109.89
11	96	MH140K096FPOP2	91.45	108.27
12	114	MH163K114FPOP1	100.18	110.34
12	115	MH164K115FPOP1	96.83	104.74
13	120	MH169K120FPOP1	72.50	82.58
13	120	MH169K120FPOP2	92.60	119.51
13	121	MH170K121FPOP1	91.98	104.60
13	122	MH171K122FPOP1	90.17	103.18
13	122	MH171K122FPOP2	93.32	121.11
14	000	MH192K000FPOP1	104.25	117.28
14	131	MH193K131FPOP1	102.59	115.35

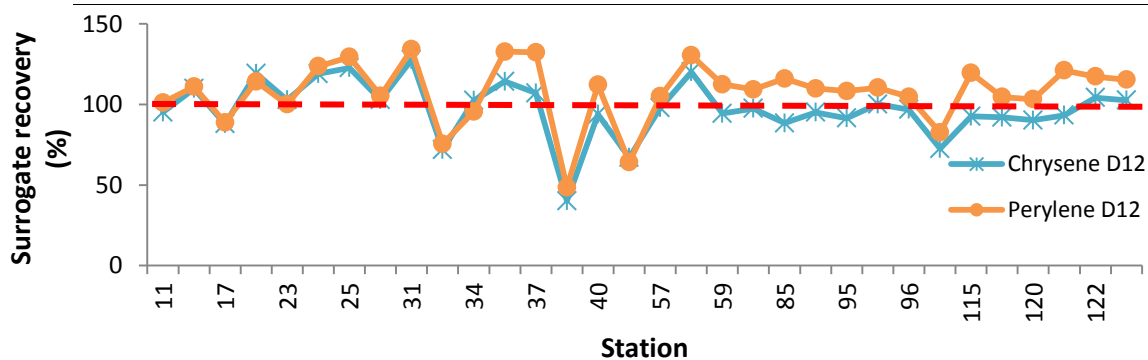


Table S1.8, Dry deposition fluxes (F_{DD}) measured for aerosols ($\text{g m}^{-2}\text{d}^{-1}$) and PAHs ($\text{ng m}^{-2}\text{d}^{-1}$).

Sample	Aerosol fraction	Particles	$(\text{ng m}^{-2}\text{day}^{-1})$														$\Sigma 16\text{PAHs}$	
			Fluo	Pyr	MePyr	DMePyr	B(ghi) Fluo	B (a) Anthr	Chry	MeChry	B (b+k) Fluo	B(e)Pyr	B (a)Pyr	Per	I(1,2,3-cd) Pyr	DiB(a,h) Anthr		B(ghi) Per
		$(\text{g m}^{-2}\text{day}^{-1})$																
1	coarse	2.22	5.90	15.00	19.29	3.35	0.00	0.00	0.00	0.00	3.11	3.08	15.33	0.00	0.00	4.46	3.76	3.08
	fine	0.07	0.00	0.19	0.21	1.12	0.43	0.23	0.21	0.11	0.30	0.14	0.07	0.09	0.07	0.39	0.14	0.73
2	coarse	0.29	0.04	0.25	0.60	0.62	0.44	0.55	0.39	0.12	0.67	0.62	0.60	0.66	0.34	0.66	0.87	1.45
	fine	0.16	0.00	0.14	0.19	0.70	0.29	0.23	0.19	0.09	0.60	0.50	0.21	0.13	0.14	0.74	0.52	0.92
3	coarse	0.03	1.03	0.09	0.17	0.14	0.16	0.06	0.16	0.02	0.18	0.07	2.28	0.49	0.02	0.34	0.62	2.07
	fine	0.08	0.00	0.07	0.10	0.37	0.15	0.12	0.09	0.04	0.19	0.10	0.04	0.02	0.05	0.37	0.07	0.63
4	coarse	0.21	1.04	1.59	2.10	0.92	0.02	0.31	0.32	0.07	0.92	0.73	3.50	0.36	0.44	0.71	1.06	6.00
	fine	0.16	0.00	0.29	0.33	1.67	0.66	0.42	0.33	0.16	0.69	0.35	0.16	0.15	0.19	1.72	0.35	1.60
5	coarse	0.06	0.18	0.25	0.46	0.48	0.14	0.13	0.18	0.05	0.32	0.38	0.58	0.28	0.08	0.38	0.58	2.07
	fine	0.04	0.00	0.12	0.14	0.72	0.26	0.15	0.10	0.07	0.25	0.13	0.04	0.01	0.05	0.31	0.07	0.83
6	coarse	0.05	0.06	0.14	0.25	0.23	0.17	0.09	0.09	0.04	0.19	0.10	0.03	0.03	0.20	0.34	0.06	1.36
	fine	0.13	0.13	0.13	0.13	0.57	0.21	0.11	0.09	0.06	0.14	0.08	0.04	0.03	0.06	0.33	0.07	0.79
7	coarse	0.05	0.20	0.15	0.24	0.45	0.32	0.29	0.22	0.05	0.29	0.17	0.15	0.13	0.06	0.28	0.22	0.74
	fine	0.03	0.00	0.04	0.07	0.14	0.09	0.08	0.07	0.04	0.08	0.05	0.03	-0.01	0.05	0.33	0.06	0.73
8	coarse	0.98	9.47	0.00	7.26	2.01	0.00	0.00	0.00	0.00	0.00	0.87	0.00	0.00	1.94	0.00	0.00	0.00
	fine	0.04	0.00	0.08	0.10	0.22	0.13	0.10	0.07	0.05	0.12	0.09	0.05	0.00	0.09	0.49	0.11	0.88
9	coarse	0.04	0.18	0.15	0.21	0.27	0.37	0.94	1.97	0.07	1.14	0.89	0.41	0.45	0.24	1.07	1.42	1.70
	fine	0.04	0.00	0.15	0.26	0.71	0.40	0.47	0.44	0.09	0.47	0.39	0.41	0.32	0.17	0.86	0.82	4.37
10	coarse	0.07	0.12	0.11	0.15	0.54	0.30	0.22	0.16	0.07	0.30	0.19	0.17	0.12	0.09	0.54	0.24	1.43
	fine	0.00	0.00	0.00	0.00	0.02	0.00	0.00	0.02	0.15	0.02	0.00	0.00	0.00	0.00	0.04	0.00	0.00
11	coarse	0.09	1.42	0.18	0.25	0.93	0.38	0.29	0.28	0.09	0.54	0.22	0.22	0.16	0.12	0.51	0.31	1.96
	fine	0.27	4.55	0.39	0.56	0.35	0.00	0.00	0.00	0.00	0.12	0.00	0.00	0.00	0.00	0.00	0.00	3.57
12	coarse	0.09	0.00	0.14	0.26	0.75	0.40	0.46	0.37	0.09	1.09	0.82	0.36	0.45	0.18	0.93	1.09	1.57
	fine	0.00	0.00	0.00	0.00	0.00	0.00	0.00	0.00	0.00	0.00	0.00	0.00	0.00	0.00	0.00	0.00	0.00

Figure S1.3, Mean dry deposition fluxes (F_{DD}) for individual PAHs in the coarse and fine deposited fractions ($\text{ng m}^{-2}\text{d}^{-1}$).

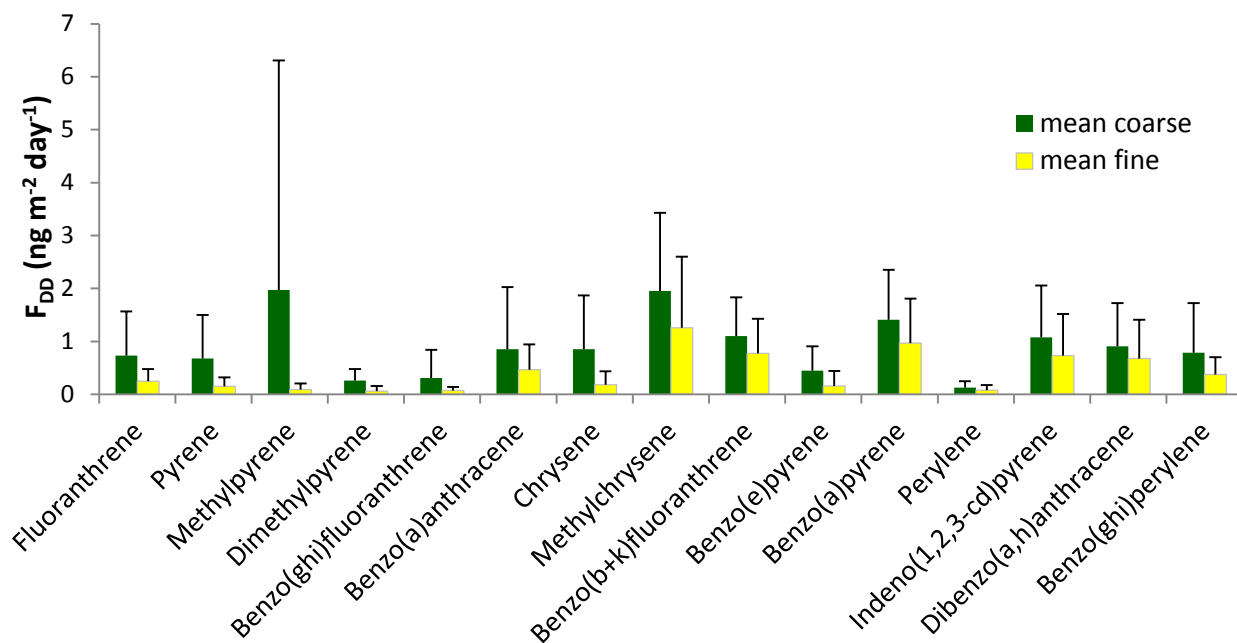


Figure S1.4, Aerosol dry deposition fluxes (F_{DD}) in the Global Oceans ($\text{g m}^{-2}\text{d}^{-1}$).

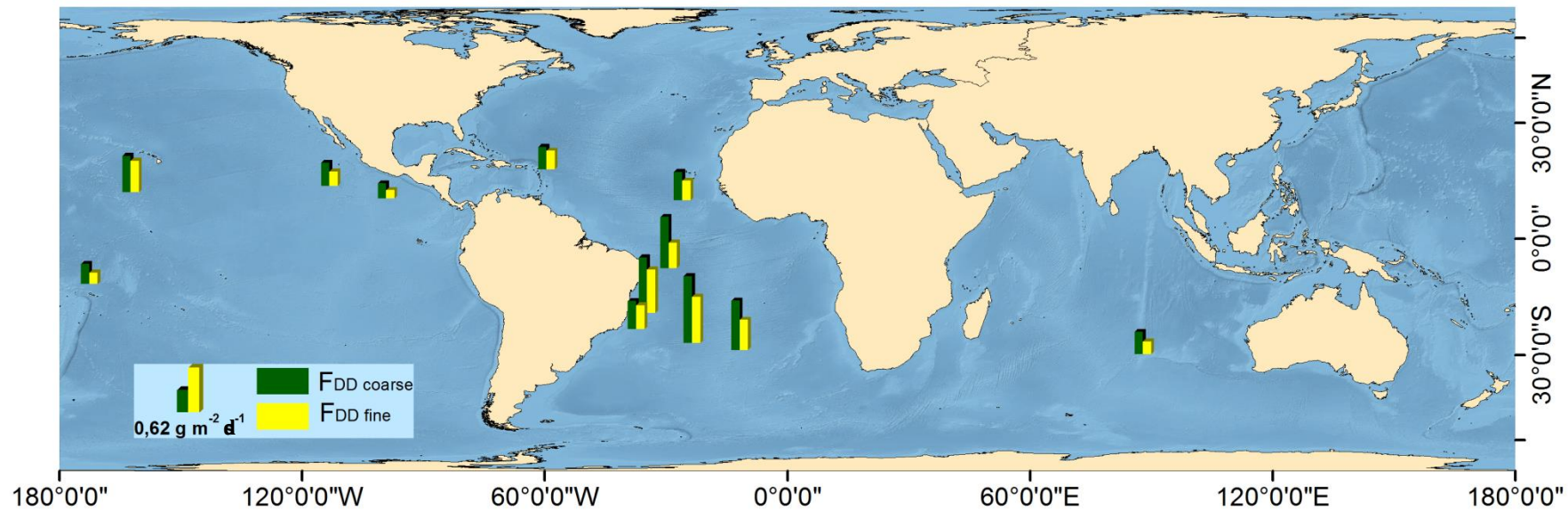


Table S1.9, Organic Carbon concentrations in the deposited particles (OC%) and their dry deposition fluxes ($F_{DD\ OC}$; $mg\ m^{-2}d^{-1}$)

Sample	OC (% mass in sample)	
	<i>coarse</i>	<i>fine</i>
1	0.56	0.37
2	0.00*	0.00*
3	0.56	0.23
4	3.34	0.95
5	0.00*	0.00*
6	0.68	0.69
7	0.64	0.48
8	1.53	0.97
9	0.00*	0.60*
10	1.74	2.11
11	1.19	0.79
12	1.19	0.38

* The value is set to 0.00% when the value was detection limit (<0.10%)

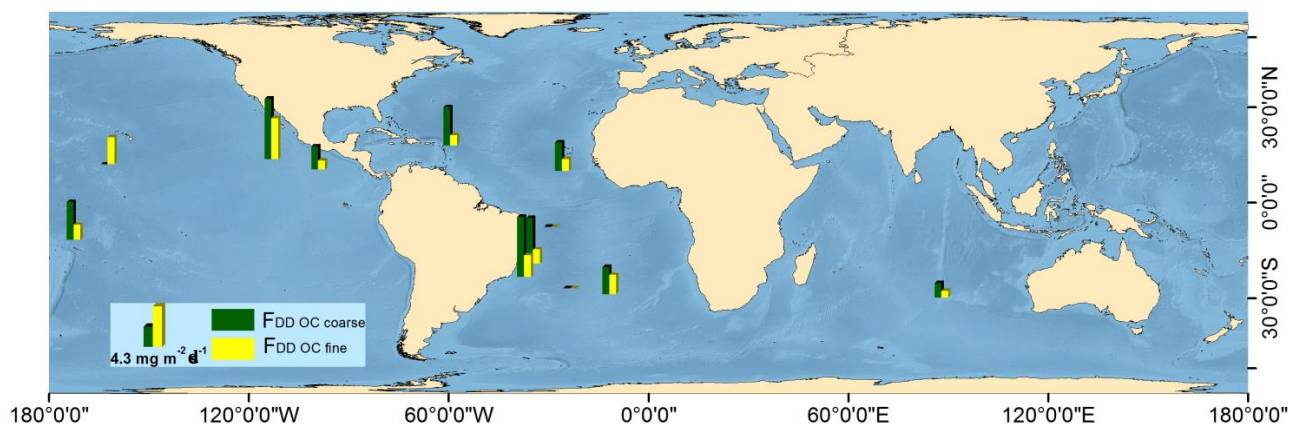


Table S1.10, Concentrations of PAHs in dry deposited fine and coarse aerosols (C_{DD}, ng g⁻¹)

Sample	Aerosol Fraction	Particle	Fluo	Pyr	MePyr	DMePyr	B (ghi) Fluo	B (a) Anthr	Chry	MeChry	B (b+k) Fluo	B (e) Pyr	B (a) Pyr	Per	I (1,2,3-cd)Pyr	DB (a,h) Anthr	B (ghi) Per	Σ ₁₆ PAHs
		(g)	(ng g ⁻¹)															
1	coarse	0.0825	75.390	74.709	371.537	nd	nd	108.113	91.053	74.722	53.025	nd	60.375	nd	76.489	72.567	71.763	1129.74
	fine	0.0674	9.037	4.178	1.992	2.558	2.018	11.486	4.047	21.700	22.160	2.861	28.068	1.250	25.033	26.271	8.941	171.601
2	coarse	0.1915	5.844	5.380	5.235	5.746	2.967	5.735	7.580	12.579	20.017	9.028	25.194	2.665	10.437	9.647	5.896	133.951
	fine	0.0956	10.528	8.775	3.576	2.208	2.479	12.914	9.039	16.069	24.603	9.514	29.929	4.349	25.071	22.374	11.157	192.584
3	coarse	0.1948	2.092	0.830	26.332	5.698	0.238	3.878	7.106	23.920	2.298	3.002	5.013	0.464	1.470	1.376	1.272	84.989
	fine	0.1681	2.550	1.311	0.493	0.282	0.684	4.892	0.986	8.488	7.998	0.252	9.538	0.443	9.064	9.551	2.994	59.525
4	coarse	0.1061	9.668	7.726	36.835	3.734	4.665	7.421	11.138	63.074	13.662	12.796	25.229	3.192	26.039	5.212	25.722	256.114
	fine	0.0760	10.101	5.097	2.398	2.132	2.839	25.278	5.209	23.483	30.016	5.179	36.399	2.147	34.376	32.086	15.093	231.832
5	coarse	0.0924	6.851	7.974	12.331	5.862	1.608	8.034	12.389	43.820	6.958	5.505	11.028	1.924	6.943	nd	6.768	137.994
	fine	0.0674	7.315	3.654	1.203	0.251	1.560	8.978	2.073	24.076	16.995	0.491	19.516	1.241	18.709	19.581	6.244	131.886
6	coarse	0.2883	1.223	0.650	0.207	0.175	1.319	2.202	0.391	8.841	8.222	0.049	5.026	0.290	nd	5.143	1.523	35.262
	fine	0.1660	1.610	0.960	0.503	0.318	0.621	3.731	0.762	8.931	7.034	nd	8.499	0.362	nd	8.813	2.600	44.702
7	coarse	0.1422	4.748	2.826	2.465	2.036	0.968	4.552	3.544	11.982	9.959	3.007	12.941	1.093	10.823	10.817	4.680	86.442
	fine	0.0755	2.338	1.647	0.992	nd	1.673	9.932	1.812	22.373	19.406	nd	23.553	0.540	nd	nd	7.161	90.993
8	coarse	0.0977	nd	17.738	nd	nd	39.736	nd	nd	nd	nd	nd	nd	nd	nd	nd	nd	57.474
	fine	0.0498	4.855	3.487	1.909	nd	3.532	19.741	4.328	35.437	40.503	0.659	48.707	1.703	46.476	nd	15.071	226.362
9	coarse	0.0824	13.655	10.698	4.897	5.385	2.915	12.784	16.983	20.323	18.577	8.945	23.894	1.526	16.707	16.416	6.669	180.374
	fine	0.0638	7.222	5.999	6.369	4.982	2.641	13.214	12.602	67.565	25.025	13.380	36.010	4.661	25.666	25.068	13.844	264.248
10	coarse	0.0545	6.655	4.210	3.783	2.736	2.070	12.015	5.327	31.678	23.290	3.701	28.473	3.052	24.716	25.676	8.953	186.335
	fine	0.0389	0.689	nd	nd	nd	nd	1.210	nd	nd	nd	nd	0.728	nd	nd	nd	11.600	14.228
11	coarse	0.0423	15.419	6.324	6.453	4.574	3.385	14.725	8.853	56.381	28.402	8.565	36.093	2.812	29.367	30.161	13.844	265.358
	fine	0.1534	0.969	nd	nd	nd	nd	nd	nd	28.293	nd	nd	nd	nd	nd	nd	nd	29.263
12	coarse	0.0587	23.897	17.948	7.902	9.827	3.941	20.398	24.007	34.639	31.650	25.605	45.955	7.180	32.201	25.380	21.500	332.031
	fine	0.0485	nd	nd	nd	nd	nd	nd	nd	nd	nd	nd	nd	nd	nd	nd	nd	nd

Figure S1.5, PAHs concentration in dry deposited aerosol (C_{DD} , $ng\ g^{-1}$) for the a) fine fraction and b) coarse fraction.

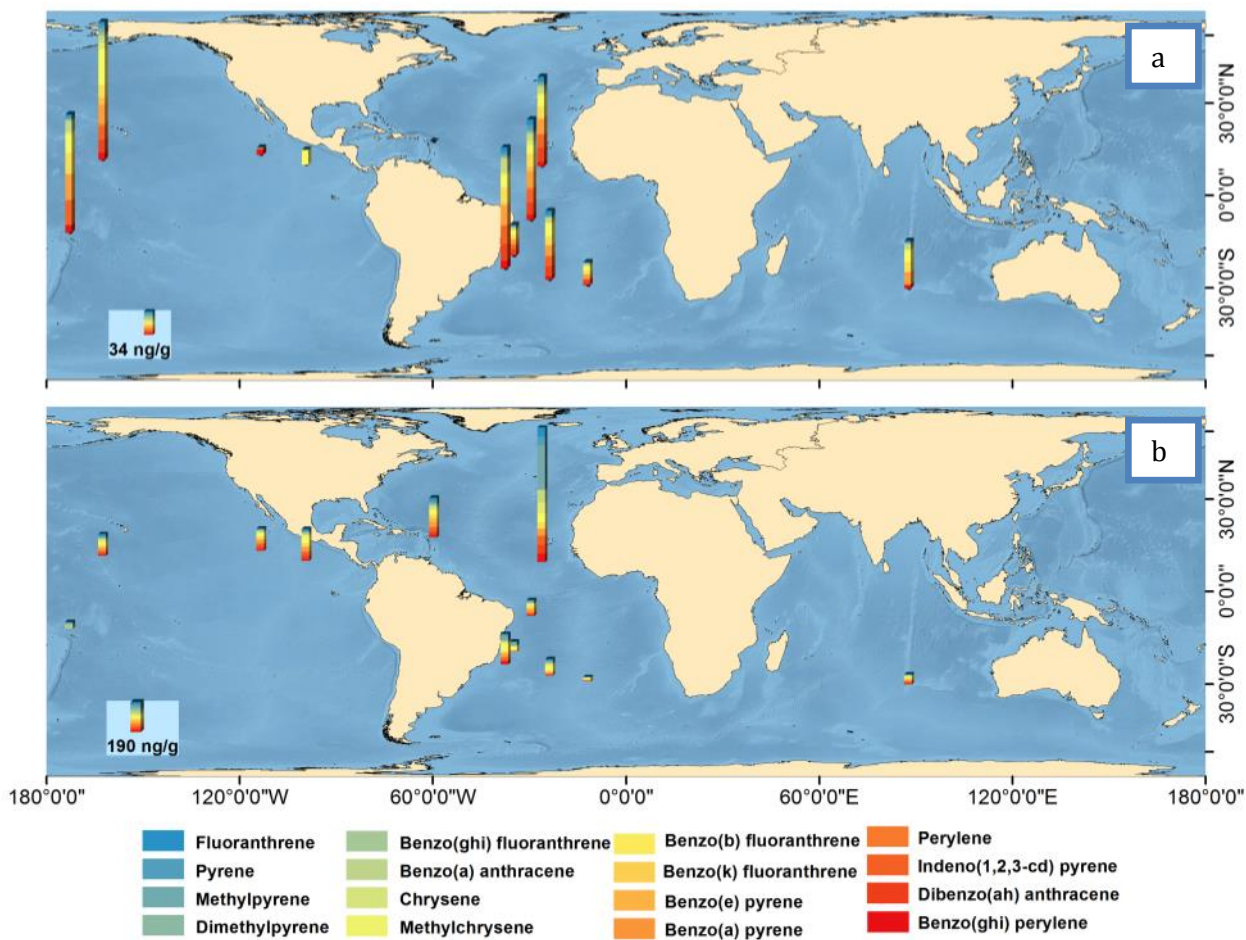


Table S1.11, Concentrations of individual PAHs in the suspended aerosols (C_A, ng m⁻³)

Dry Dep measure	Station	Vol sampled (m ³)	Aerosol (mg m ⁻³)	Fluo	Pyr	MetPyr	DMe Pyr	B (ghi) Fluo	B (a) Anthr	Chry	MeChry	(ng m ⁻³)								Σ ₁₆ PAHS
												B (b) Fluo	B (k) Fluo	B (e) Pyr	B (a) Pyr	Per	I (1,2,3-cd)Pyr	DB(a,h) Anthr	B (ghi) Per	
1	11	945	0.087	0.207	0.185	0.077	0.116	0.034	0.085	0.083	0.001	0.074	0.024	0.057	0.035	0.010	0.027	0.016	0.039	1.069
2	17	945	0.073	0.071	0.062	0.014	0.045	0.017	0.025	0.026	0.001	0.021	0.006	0.020	0.008	0.003	0.007	0.003	0.011	0.339
3	23	632	0.067	0.474	0.404	0.090	0.311	0.181	0.305	0.294	0.005	0.256	0.080	0.218	0.148	0.044	0.087	0.048	0.129	3.073
4	24	525	0.133	0.126	0.111	0.022	0.086	0.027	0.043	0.045	0.002	0.034	0.010	0.026	0.014	0.005	0.019	0.005	0.022	0.596
4	25	275	0.331	0.365	0.381	0.102	0.532	0.004	0.155	0.227	0.005	0.094	0.023	0.079	0.032	0.011	0.021	0.009	0.035	2.077
5	30	1339	0.086	0.059	0.047	0.011	0.038	0.014	0.019	0.022	0.001	0.026	0.007	0.021	0.007	0.003	0.015	0.003	0.021	0.313
5	31	1149	0.050	0.040	0.031	0.015	0.031	nd	0.015	0.015	0.001	0.012	0.003	0.009	0.005	0.001	0.004	0.002	0.005	0.189
6	33	940	0.028	0.052	0.040	0.017	0.039	0.017	0.016	0.019	0.001	0.014	0.004	0.011	0.005	0.003	0.004	0.002	0.005	0.249
6	34	617	0.056	0.072	0.057	0.026	0.066	0.001	0.026	0.029	0.001	0.021	0.006	0.016	0.005	0.002	0.005	0.002	0.006	0.342
7	33	1982	0.018	0.010	0.012	0.003	0.025	0.001	0.002	0.004	0.001	0.003	0.001	0.004	0.001	nd	0.001	nd	0.003	0.071
7	37	927	0.035	0.501	0.613	0.448	0.834	0.131	0.907	0.858	0.013	0.662	0.194	0.481	0.335	0.092	0.174	0.007	0.272	6.524
7	59	889	0.037	0.114	0.114	0.001	0.002	nd	0.120	0.115	nd	0.116	0.106	0.001	0.111	nd	0.116	0.120	0.109	1.145
7	60	871	0.039	0.061	0.092	0.028	0.191	0.066	0.018	0.028	0.007	0.021	0.004	0.027	0.010	0.003	0.007	0.003	0.024	0.592
8	85	672	0.047	0.067	0.059	0.016	0.075	0.001	0.060	0.066	0.002	0.078	0.021	0.072	0.021	0.009	0.026	0.012	0.041	0.625
8	86	582	0.071	0.059	0.050	0.022	0.042	0.001	0.025	0.023	0.001	0.022	0.007	0.016	0.009	0.003	0.005	0.002	0.008	0.295
9	95	618	0.106	0.105	0.089	0.037	0.062	0.032	0.039	0.037	0.001	0.033	0.009	0.028	0.015	0.005	0.011	0.005	0.015	0.522
9	96	902	0.118	0.016	0.016	0.008	0.013	nd	0.010	0.008	nd	0.010	0.002	0.009	0.003	0.002	0.004	0.001	0.005	0.108
9	114	1088	0.112	0.026	0.024	0.012	0.022	0.011	0.016	0.015	nd	0.016	0.005	0.015	0.010	0.003	0.006	0.003	0.010	0.194
10	114	857	0.074	0.028	0.024	0.012	0.021	0.011	0.014	0.012	0.001	0.014	0.004	0.012	0.005	0.002	0.005	0.002	0.007	0.173
10	115	800	0.046	0.051	0.043	0.016	0.034	nd	0.016	0.020	0.001	0.014	0.003	0.011	0.005	0.001	0.003	0.001	0.004	0.224
11	120	853	0.035	0.050	0.042	0.016	0.035	0.011	0.014	0.019	0.001	0.016	0.005	0.012	0.006	0.002	0.006	0.002	0.008	0.243
11	120	916	0.065	0.046	0.040	0.017	0.028	nd	0.015	0.017	0.001	0.013	0.004	0.011	0.006	0.002	0.004	0.002	0.005	0.211
11	121	883	0.030	0.023	0.031	0.010	0.065	0.001	0.005	0.008	0.002	0.007	0.002	0.009	0.003	0.001	0.003	0.001	0.008	0.181

Dry Dep measure	Station	Vol sampled	Aerosol	Fluo	Pyr	MetPyr	DMe Pyr	B (ghi) Fluo	B (a) Anthr	Chry	MeChry	B(b) Fluo	B(k) Fluo	B (e) Pyr	B (a) Pyr	Per	I (1,2,3-cd)Pyr	DB(a,h) Anthr	B (ghi) Per	Σ_{16} PAHS
11	122	551	0.090	0.100	0.086	0.033	0.063	0.001	0.034	0.040	0.001	0.034	0.009	0.028	0.010	0.002	0.014	0.003	0.021	0.477
11	122	789	0.024	0.071	0.065	0.028	0.049	0.027	0.024	0.030	nd	0.022	0.007	0.018	0.011	0.003	0.007	0.003	0.010	0.375
12	0	818	0.075	0.007	0.010	0.004	0.020	0.001	0.002	0.002	0.001	0.002	0.001	0.002	0.001	nd	0.001	nd	0.002	0.055
12	131	820	0.069	0.048	0.042	0.018	0.028	nd	0.013	0.014	0.001	0.011	0.003	0.010	0.005	0.002	0.004	0.002	0.005	0.205

Figure S1.6, Concentrations of PAHs in suspended aerosol (C_A , ng m^{-3}) in the Global Oceans

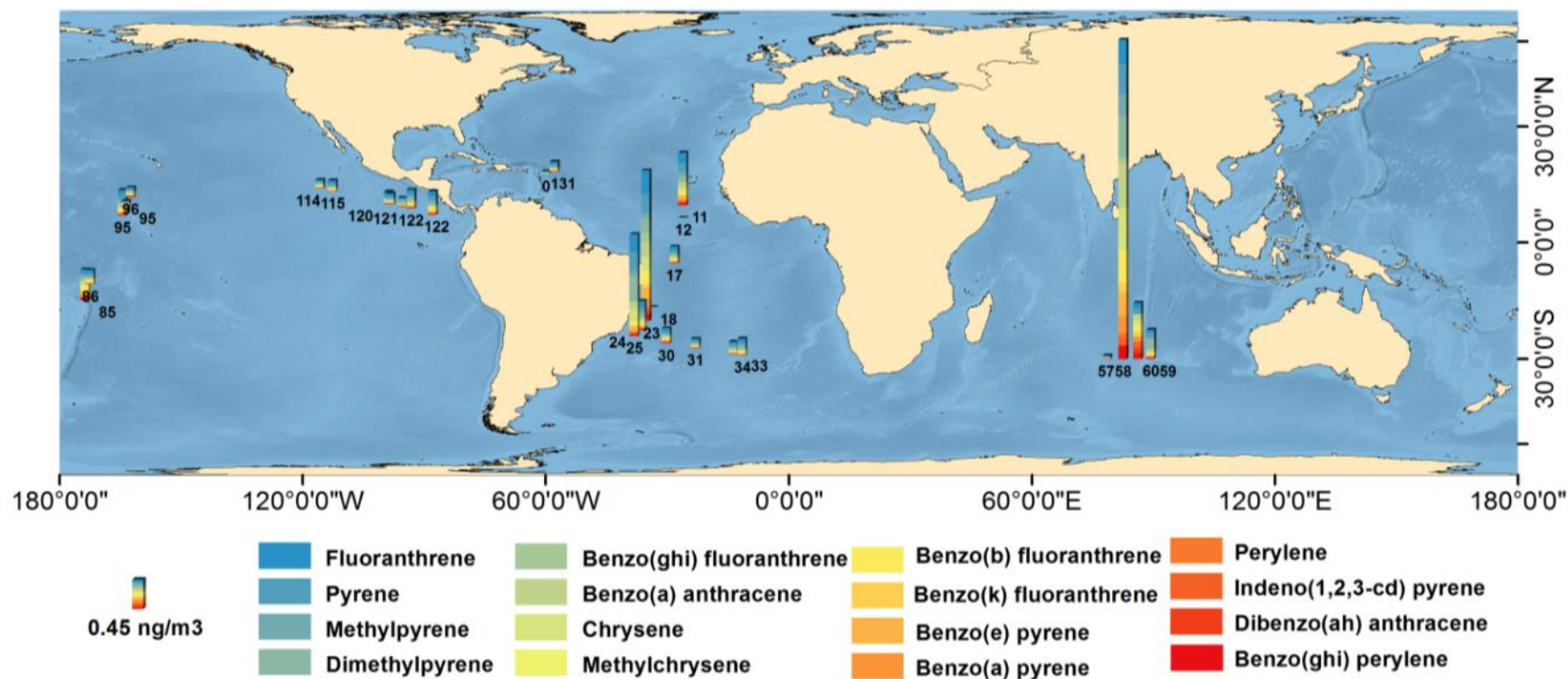


Figure S1.7, Individual PAHs profile in suspended aerosols (C_A , ng m^{-3}).

Bars show the standard deviation (SD) of the deposition measures in the signed ocean. Indian Ocean only holds one measurement, thus with no SD bar.

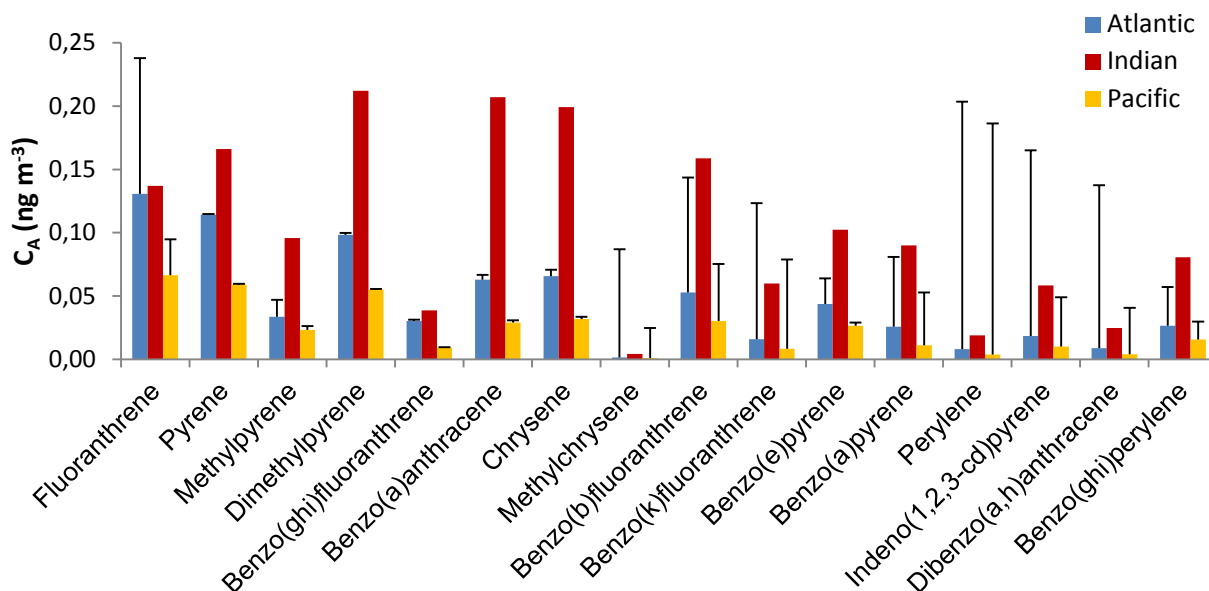


Table S1.12, Estimated dry deposition velocity (v_D , cm s^{-1}) of suspended aerosol-bound PAHs

Sample	Fluo	Pyr	MePyr	DMePyr	B (ghi) Fluo	B (a) Anthr	Chry	MetChry	B (b+k) Fluo	B (e) Pyr	B (a) Pyr	Per	I (1,2,3- cd)Pyr	DB(a,h) Anthr	B (ghi) Per	
								(cm s^{-1})								
1	0.019	0.020	0.232	0.001	0.002	0.066	0.054	3.016	0.035	0.002	0.114	0.005	0.170	0.287	0.097	
2	0.021	0.021	0.068	0.020	0.033	0.065	0.063	2.860	0.159	0.094	0.630	0.199	0.425	1.069	0.142	
3	0.001	0.000	0.030	0.002	0.000	0.003	0.003	0.634	0.003	0.001	0.009	0.002	0.011	0.020	0.003	
4	0.009	0.006	0.086	0.002	0.039	0.034	0.015	2.941	0.056	0.041	0.283	0.073	0.286	0.467	0.151	
5	0.013	0.015	0.056	0.010	0.019	0.047	0.041	5.315	0.042	0.020	0.236	0.077	0.113	0.330	0.046	
6	0.006	0.005	0.004	0.001	0.028	0.038	0.006	2.831	0.101	0.000	0.347	0.035	0.000	0.940	0.099	
9	0.003	0.002	0.002	0.001	0.003	0.004	0.002	0.368	0.008	0.002	0.025	0.005	0.019	0.197	0.009	
10	0.002	0.016	0.002	0.000	0.146	0.018	0.004	1.095	0.034	0.001	0.124	0.014	0.171	0.000	0.039	
11	0.073	0.063	0.084	0.043	0.060	0.151	0.200	13.301	0.197	0.138	0.722	0.214	0.642	1.378	0.198	
12	0.007	0.005	0.012	0.004	0.018	0.045	0.014	2.701	0.064	0.017	0.288	0.097	0.264	1.015	0.148	
13	0.008	0.003	0.007	0.002	0.010	0.018	0.009	2.632	0.029	0.012	0.111	0.029	0.106	0.351	0.030	
14	0.029	0.024	0.025	0.019	0.028	0.078	0.089	0.177	0.110	0.126	0.472	0.214	0.448	0.852	0.234	

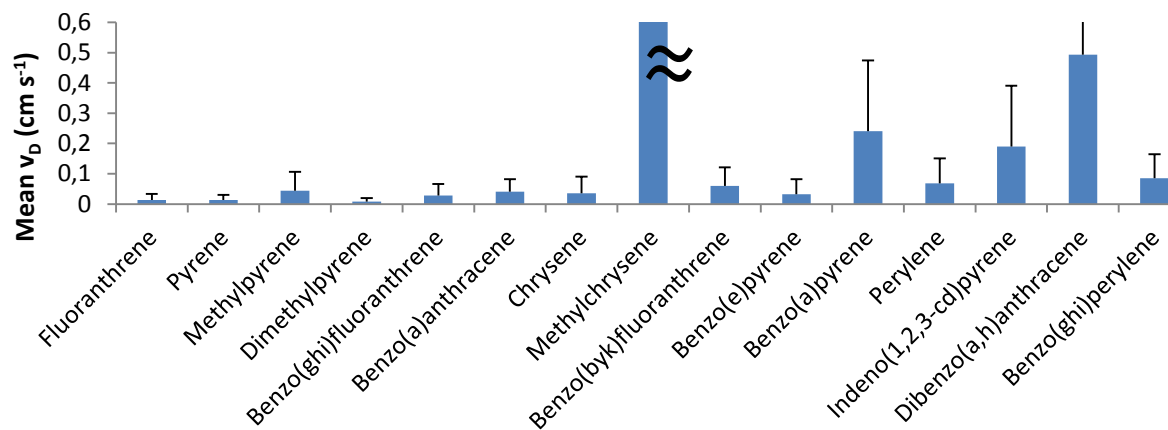


Table S1.13, Vapor pressures (P_L) for individual PAHs used in this work.

Compound	P_L [Pa]
Fluoranthrene	0.00598
Pyrene	
Benzo(g,h,i)fluoranthrene	0.00000755
Benzo(a)anthracene	
Chrysene	0.00017
Benzo(b+k)fluoranthrene	0.00000896
Benzo(e)pyrene	
Benzo(a)pyrene	0.0000059
Perylene	0.00000488
Dibenzo(a,h)anthracene	0.000000344
Benzo(g,h,i)perylene	0.000000428

Adapted from Lei et al. 2002¹, Super-cooled Liquid vapor Pressure at 25°C.

¹ Lei, Y. D.; Chankalal, R.; Chan, A.; Wania, F., Supercooled liquid vapor pressures of the polycyclic aromatic hydrocarbons. *Journal of Chemical and Engineering Data* **2002**, *47*, (4), 801-806.

Table S1.14, Spearman correlation data between PAHs dry deposition velocity (v_D) for each sampling period versus compound specific vapor pressure (P_L)

Rho Spearman test		Log(P_L)
v_D 1	P	-.382
	Sig. (two-tailed)	.247
	N	11
v_D 2	P	-.827**
	Sig. (two-tailed)	.002
	N	11
v_D 3	P	-.627*
	Sig. (two-tailed)	.039
	N	11
v_D 4	P	-.936**
	Sig. (two-tailed)	.000
	N	11
v_D 5	P	-.736**
	Sig. (two-tailed)	.010
	N	11
v_D 6	P	-.709*
	Sig. (two-tailed)	.015
	N	11
v_D 7	P	-.755**
	Sig. (two-tailed)	.007
	N	11
v_D 8	P	-.127
	Sig. (two-tailed)	.709
	N	11
v_D 9	P	-.673*
	Sig. (two-tailed)	.023
	N	11
v_D 10	P	-.900**
	Sig. (two-tailed)	.000
	N	11
v_D 11	P	-.882**
	Sig. (two-tailed)	.000
	N	11
v_D 12	P	-.827**
	Sig. (two-tailed)	.002
	N	11

** . Correlation is significant at level 0.01 (two-tailed).

*. Correlation is significant at level 0.05 (two-tailed).

Table S1.15, Spearman correlations between PAHs concentration in the fine fraction of the dry deposited aerosols (C_{DDfine}) and wind speed (U_{10})

Rho Spearman		Mean U_{10}
Fluoranthrene_ C_{DDfine}	P	.692*
	Sig. (bilateral)	.013
	N	12
Pyrene_ C_{DDfine}	P	.803**
	Sig. (bilateral)	.002
	N	12
Methylpyrene_ C_{DDfine}	P	.796**
	Sig. (bilateral)	.002
	N	12
Dimethylpyrene_ C_{DDfine}	P	.542
	Sig. (bilateral)	.069
	N	12
Benzo(ghi)Fluoranthrene_ C_{DDfine}	P	.746**
	Sig. (bilateral)	.005
	N	12
Benzo(a)Anthracene_ C_{DDfine}	P	.774**
	Sig. (bilateral)	.003
	N	12
Chrysene_ C_{DDfine}	P	.810**
	Sig. (bilateral)	.001
	N	12
Methylchrysene_ C_{DDfine}	P	.315
	Sig. (bilateral)	.318
	N	12
Benzo(b+k)Fluoranthrene_ C_{DDfine}	P	.746**
	Sig. (bilateral)	.005
	N	12
Benzo(e)Pyrene_ C_{DDfine}	P	.732**
	Sig. (bilateral)	.007
	N	12
Benzo(a)Pyrene_ C_{DDfine}	P	.739**
	Sig. (bilateral)	.006
	N	12
Perylene_ C_{DDfine}	P	.810**
	Sig. (bilateral)	.001
	N	12
Indeno(123-cd)Pyrene_ C_{DDfine}	P	.682*
	Sig. (bilateral)	.015

Rho Spearman		Mean U ₁₀
	N	12
Dibenzo(ah)Anthracene_ C _{DDfine}	P	.689*
	Sig. (bilateral)	.013
	N	12
Benzo(ghi)Perylene_ C _{DDfine}	P	.627*
	Sig. (bilateral)	.029
	N	12

** . Correlation is significant at level 0.01 (two-tailed).

* . Correlation is significant at level 0.05 (two-tailed).

Table S1.16, Spearman correlations between PAHs dry deposition flux associated to fine particles (F_{DDfine}) and wind speed (U_{10})

Rho Spearman		Mean U_{10}
	P	.657*
Fluoranthrene_ F_{DDfine}	Sig. (bilateral)	.020
	N	12
	P	.657*
Pyrene_ F_{DDfine}	Sig. (bilateral)	.020
	N	12
	P	.664*
Methylpyrene_ F_{DDfine}	Sig. (bilateral)	.019
	N	12
	P	.618*
Dimethylpyrene_ F_{DDfine}	Sig. (bilateral)	.032
	N	12
	P	.695*
Benzo(ghi)Fluoranthrene_ F_{DDfine}	Sig. (bilateral)	.012
	N	12
	P	.649*
Benzo(a)Anthracene_ F_{DDfine}	Sig. (bilateral)	.022
	N	12
	P	.638*
Chrysene_ F_{DDfine}	Sig. (bilateral)	.026
	N	12
	P	.523
Methylchrysene_ F_{DDfine}	Sig. (bilateral)	.081
	N	12
	P	.644*
Benzo(b+k)Fluoranthrene_ F_{DDfine}	Sig. (bilateral)	.024
	N	12
	P	.692*
Benzo(e)Pyrene_ F_{DDfine}	Sig. (bilateral)	.013
	N	12
	P	.601*
Benzo(a)Pyrene_ F_{DDfine}	Sig. (bilateral)	.039
	N	12
	P	.678*
Perylene_ F_{DDfine}	Sig. (bilateral)	.015
	N	12
	P	.702*
Indeno123cdpyrene_ F_{DDfine}	Sig. (bilateral)	.011
	N	12
	P	.591*
Dibenzoanthracene_ F_{DDfine}	Sig. (bilateral)	.043
	N	12

Rho Spearman		Mean U ₁₀
	P	.326
Benzoghiperylene_ F _{DDfine}	Sig. (bilateral)	.301
	N	12

*. Correlation is significant at level 0.05 (two-tailed).

Table S1.17, Pearson's correlation between PAHs dry deposition velocity slopes when plotted against vapor pressure (slope V_{DDfine}) versus wind speed (U_{10})

Slopes are obtained from S14 per each measurement. In this case parametric statistics are applied as the slope is already normalized within the logarithmic plotting in S14.

Pearson correlation		Mean U_{10}
P		-.638*
Slope	Sig. (bilateral)	.026
	N	12

*. Correlation is significant at level 0.05 (two-tailed).

Table S1.18, Parameterization of the deposition velocity versus physic and biochemical parameters using least squares multiple parametric linear regression.

Parameters include: vapor pressure ($\text{Log}P_L$), wind speed (U_{10}) and chlorophyll a concentrations at the sea surface (Chl_s). The term $U_{10} \times \text{Chl}_s$ accounts for the interaction of wind speed and chlorophyll a concentration at surface.

Coefficient^s

Model	Not standardized Coefficients		Standardized Coefficients	t	Sig.	R square
	B	Typical Error	β			
1 (Constant)	-3.082	.197		-15.656	.000	.365 ^a
Log P_L	-.261	.038	-.479	-6.826	.000	
$U_{10} \times \text{Chl}_s$.387	.074	.368	5.243	.000	

a. Dependent Variable: $\text{log}v_D$

Coefficient^s

Model	Not standardized Coefficients		Standardized Coefficients	t	Sig.	R square
	B	Typical Error	β			
1 (Constant)	-3.269	.307		-10.645	.000	.227 ^b
Log P_L	-.287	.060	-.373	-4.819	.000	
$U_{10} \times \text{Chl}_s$.442	.115	.297	3.840	.000	

b. Dependent Variable: $\text{log}v_{Dfine}$

Coefficient^s

Model	Not standardized Coefficients		Standardized Coefficients	t	Sig.	R square
	B	Typical Error	β			
1 (Constant)	-2.973	.240		-12.402	.000	.503 ^c
Log P_L	-.253	.047	-.415	-5.450	.000	

U10xChl _s	.337	.090	.285	3.749	.000
----------------------	------	------	------	-------	------

c. Dependent Variable: $\log v_{D\text{coarse}}$

Table S1.19, Parameterization of the deposition velocity (v_D) versus vapor pressure (P_L) using least squares multiple parametric linear regression.

Coefficient^a

Model	Not standardized Coefficients		Standardized Coefficients	t	Sig.	R square
	B	Typical Error	β			
1 (Constant)	-2.670	.198		-13.483	.000	.229
LogP _L	-.261	.042	-.479	-6.222	.000	

a. Dependent Variable: $\log v_D$

Coefficient^b

Model	Not standardized Coefficients		Standardized Coefficients	t	Sig.	R square
	B	Typical Error	β			
1 (Constant)	-2.798	.296		-9.452	.000	.139
LogP _L	-.287	.063	-.373	-4.583	.000	

b. Dependent Variable: $\log v_{D\text{fine}}$

Coefficient^c

Model	Not standardized Coefficients		Standardized Coefficients	t	Sig.	R square
	B	Typical Error	β			
1 (Constant)	-2.614	.231		-11.339	.000	.172
LogP _L	-.253	.049	-.415	-5.196	.000	

c. Dependent Variable: $\log v_{D\text{coarse}}$

2. HIGH ATMOSPHERE-OCEAN EXCHANGE OF SEMIVOLATILE AROMATIC HYDROCARBONS

Supporting Information

**Belén González-Gaya^{1,2}, María-Carmen Fernández-Pinos¹, Laura Morales¹,
Esteban Abad¹, Benjamí Piña¹, Laurence Mejanelle³, Carlos Duarte^{4,5},
Begoña Jiménez², Jordi Dachs^{1*}**

*Corresponding author email: jordi.dachs@idaea.csic.es

Index

Table S2.1. Mean concentrations of PAHs per ocean in each analyzed matrix

Table S2.2. Mean concentrations of PAHs in dissolved and gas phase blanks

Table S2.3. Calculated uncertainty for SALCs Diffusive fluxes according to Henry's constant (H')

Figure S2.1. Mean PAHs profile in each matrix analyzed; gas, aerosol and dissolved phase

Figure S2.2. Wet deposition fluxes

Figure S2.3. Ocean basin averaged gross volatilization and absorption fluxes, and net diffusive fluxes

Figure S2.4. Degradation of PAHs in the atmosphere by reaction with OH radical

Figure S2.5. Mean concentrations of total aromatics and the quantified fraction of PAHs in gas and water samples for the six retention time intervals quantified

Table S2.1. Mean concentrations of PAHs per ocean in each analyzed matrix

	Gas Phase (ng m ⁻³)					Aerosol Phase (ng m ⁻³)					Dissolved Phase (ng L ⁻¹)				
	Atlantic North	Atlantic South	Pacific North	Pacific South	Indian	Atlantic North	Atlantic South	Pacific North	Pacific South	Indian	Atlantic North	Atlantic South	Pacific North	Pacific South	Indian
Naphthalene	0.072	0.105	0.080	0.144	0.179	0.001	0.001	0.000	0.001	0.004	0.029	0.018	0.019	0.031	0.024
Methylnaphthalenes	0.000	0.000	0.000	0.000	0.000	0.001	0.009	0.000	0.001	0.001	0.131	0.140	0.062	0.110	0.074
Dimethylnaphthalenes	0.146	0.730	0.041	1.120	0.470	0.001	0.001	0.000	0.001	0.001	0.289	0.133	0.150	0.270	0.150
Acenaphthylene	0.198	0.144	0.176	0.135	0.086	0.003	0.004	0.005	0.007	0.020	0.030	0.146	0.004	0.001	0.001
Acenaphtene	0.048	0.085	0.059	0.076	0.112	0.000	0.001	0.000	0.001	0.005	0.135	0.058	0.043	0.043	0.022
Fluorene	0.368	0.434	0.132	0.329	0.366	0.003	0.004	0.002	0.003	0.017	0.195	0.192	0.083	0.083	0.056
Dibenzothiophene	1.130	1.060	0.489	0.784	0.779	0.003	0.003	0.002	0.002	0.018	0.123	0.160	0.042	0.044	0.040
Methyldibenzothiophenes	6.330	2.410	2.260	1.670	1.120	0.024	0.042	0.029	0.030	0.167	0.145	0.185	0.101	0.109	0.081
Dimethyldibenzothiopenes	10.500	3.930	4.230	3.780	2.840	0.074	0.088	0.112	0.114	0.729	0.115	0.151	0.125	0.140	0.088
Phenanthrene	9.360	9.380	5.400	9.510	8.710	0.051	0.084	0.036	0.042	0.348	0.458	0.387	0.325	0.326	0.212
Methylphenantrenes	5.180	2.960	2.200	3.660	1.910	0.036	0.024	0.030	0.053	0.333	0.287	0.324	0.285	0.293	0.223
Dimethylphenanthrenes	2.260	1.380	1.050	2.070	1.060	0.043	0.045	0.053	0.067	0.507	0.139	0.164	0.147	0.154	0.108
Anthracene	1.860	1.780	1.050	1.370	1.420	0.028	0.101	0.047	0.020	0.130	0.045	0.049	0.033	0.035	0.025
Fluoranthene	1.340	0.828	0.674	1.700	0.908	0.058	0.090	0.041	0.067	0.631	0.349	0.417	0.353	0.393	0.274
Pyrene	0.862	0.565	0.476	1.640	0.662	0.059	0.078	0.035	0.065	0.587	0.401	0.477	0.407	0.495	0.295
Methylpyrenes	0.278	0.226	0.102	0.208	0.244	0.029	0.023	0.013	0.024	0.320	0.052	0.085	0.043	0.042	0.061
Dimethylpyrenes	0.127	0.162	0.052	0.092	0.127	0.072	0.079	0.035	0.075	0.730	0.022	0.037	0.014	0.011	0.020
Benzo[ghi]fluoranthene	0.122	0.081	0.109	0.120	0.114	0.019	0.015	0.007	0.035	0.165	0.016	0.018	0.015	0.015	0.012
Benzo[a]anthracene	0.079	0.073	0.048	0.061	0.082	0.059	0.041	0.014	0.055	0.799	0.026	0.038	0.008	0.019	0.041
Chrysene	0.141	0.126	0.063	0.104	0.121	0.076	0.048	0.020	0.077	0.806	0.016	0.016	0.010	0.011	0.007
Methylchrysenes	0.037	0.043	0.025	0.021	0.027	0.049	0.012	0.010	0.039	0.612	0.007	0.011	0.003	0.003	0.010
Benzo[b+k]fluoranthenes	0.051	0.026	0.056	0.190	0.283	0.142	0.048	0.022	0.097	1.227	0.003	0.010	0.002	0.002	0.002
Benzo[e]pyrene	0.014	0.022	0.018	0.035	0.024	0.078	0.032	0.014	0.061	0.725	0.006	0.008	0.004	0.004	0.003

	Gas Phase (ng m⁻³)					Aerosol Phase (ng m⁻³)					Dissolved Phase (ng L⁻¹)				
	Atlantic North	Atlantic South	Pacific North	Pacific South	Indian	Atlantic North	Atlantic South	Pacific North	Pacific South	Indian	Atlantic North	Atlantic South	Pacific North	Pacific South	Indian
Benzo[<i>a</i>]pyrene	0.033	0.045	0.070	0.063	0.071	0.028	0.016	0.006	0.026	0.377	0.002	0.011	0.002	0.002	0.002
Perylene	0.010	0.007	0.020	0.026	0.040	0.009	0.005	0.002	0.008	0.107	0.001	0.007	0.001	0.001	0.001
Indeno[1,2,3- <i>cd</i>]pyrene	0.005	0.016	0.005	0.007	0.004	0.060	0.014	0.007	0.037	0.167	0.050	0.072	0.042	0.030	0.036
Dibenzo[<i>a,h</i>]anthracene	0.004	0.014	0.007	0.010	0.006	0.010	0.005	0.001	0.007	0.115	0.064	0.093	0.060	0.043	0.045
Benzo[<i>ghi</i>]perylene	0.004	0.003	0.002	0.010	0.001	0.084	0.019	0.011	0.053	0.396	0.017	0.028	0.016	0.014	0.014
Σ64 PAHS	40.589	26.635	18.887	28.961	21.750	1.103	0.933	0.556	1.067	10.044	3.151	3.433	2.400	2.722	1.927

Table S2.2. Mean concentrations of PAHs in the gas and dissolved phase blanks

	Gas Phase		Dissolved Phase	
	Field blank mean (total ng)	Laboratory blank mean (total ng)	Field blank mean (total ng)	Laboratory blank mean (total ng)
Naphthalene	0.82	0.98	0.91	0.96
Methylnaphthalenes	0.00	0.00	0.35	0.32
Dimethylnaphthalenes	0.40	0.00	0.49	0.38
Acenaphthylene	0.15	0.09	0.08	0.05
Acenaphthene	0.09	0.47	0.04	0.03
Fluorene	0.05	0.41	0.12	0.08
Dibenzothiophene	0.04	0.09	0.09	0.04
Methyldibenzothiophenes	0.41	0.23	0.48	0.20
Dimethyldibenzothiophenes	0.13	1.91	0.56	0.19
Phenanthrene	0.14	0.18	0.72	0.58
Methylphenantrenes	0.16	0.47	0.69	0.22
Dimethylphenanthrenes	0.12	0.32	0.49	0.16
Anthracene	0.14	0.33	0.31	0.02
Fluoranthene	0.22	0.44	0.28	0.18
Pyrene	0.21	0.35	0.33	0.22
Methylpyrenes	0.01	0.00	0.26	0.13
Dimethylpyrenes	0.03	0.00	0.13	0.04
Benzo[ghi]fluoranthene	0.35	0.75	0.64	0.02
Benzo[a]anthracene	0.08	0.26	0.15	0.13
Chrysene	0.07	0.12	0.09	0.08
Methylchrysenes	0.13	0.00	0.04	0.02
Benzo[b+k]fluoranthenes	0.02	1.98	0.03	0.04
Benzo[e]pyrene	0.65	0.32	0.01	0.04
Benzo[a]pyrene	3.06	0.00	0.08	0.03
Perylene	1.27	0.00	0.11	0.05
Indeno[1,2,3-cd]pyrene	1.01	0.00	1.83	0.07
Dibenzo[a,h]anthracene	0.32	0.00	3.88	0.26
Benzo[ghi]perylene	0.00	0.00	0.80	0.02
Σ₆₄PAHs	10.09	9.72	14.01	4.55

Table S2.3. Calculated uncertainty for SALCs Diffusive fluxes according to Henry's constant (H')

The results are for H' values 3 times higher and 3 times lower than the H' values corresponding to the individual PAH selected for each analysis time window and used to quantify SALCs.

	Mean total SALCs flux (ng m⁻²d⁻¹)	
	H' _{1/3}	H' _{x3}
Absorption flux	-8,13 10 ⁶	-4,02 10 ⁶
Volatilization flux	4,61 10 ⁵	1,84 10 ⁶
Net flux	-7,67 10 ⁶	-2,18 10 ⁶

Figure S2.1. Mean PAH profile in each matrix analyzed; gas (top), aerosol (middle) and dissolved phase (bottom panel)

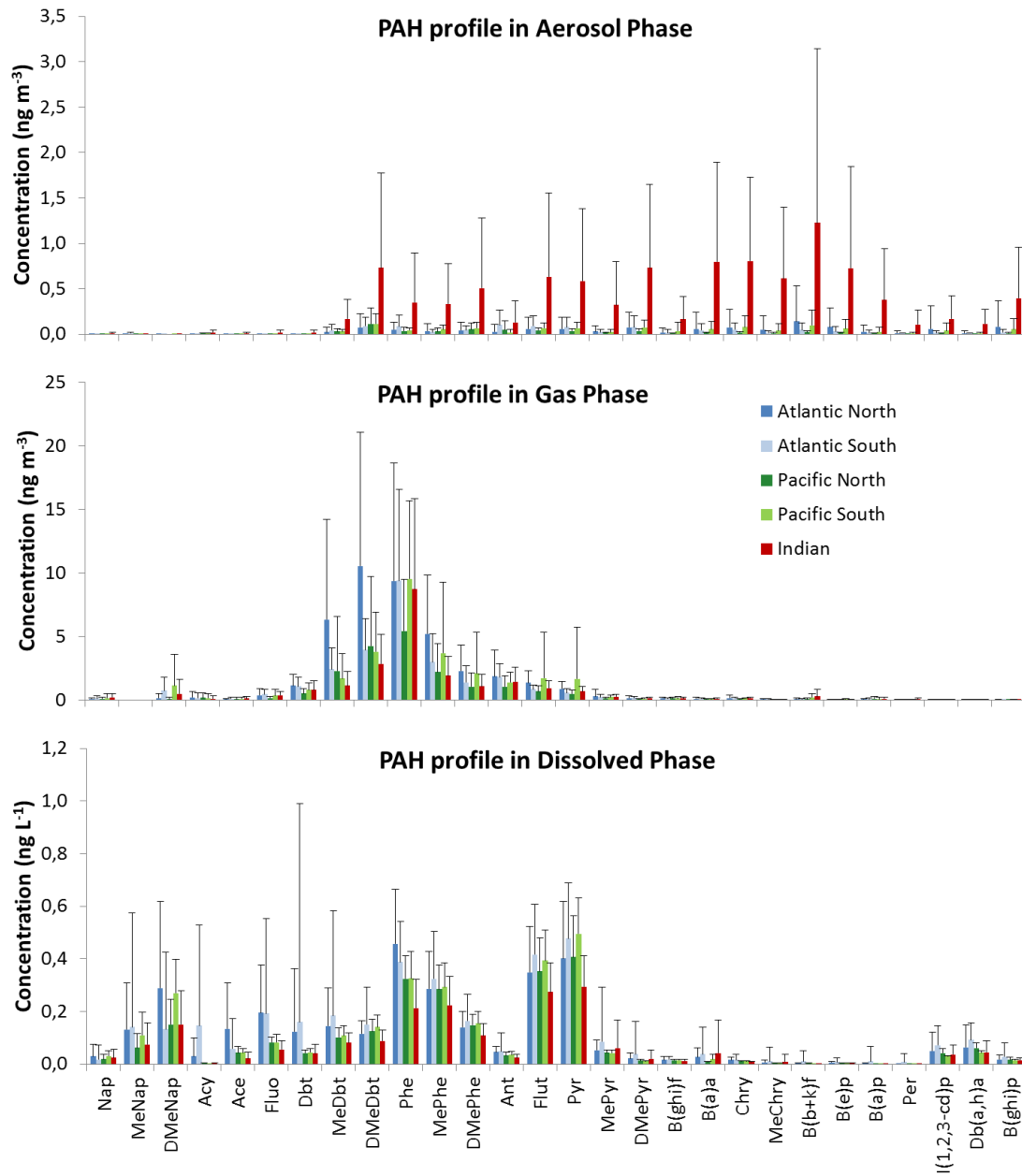


Figure S2.2. Wet deposition fluxes measured during the 11 rain events that occurred during the Malaspina cruise

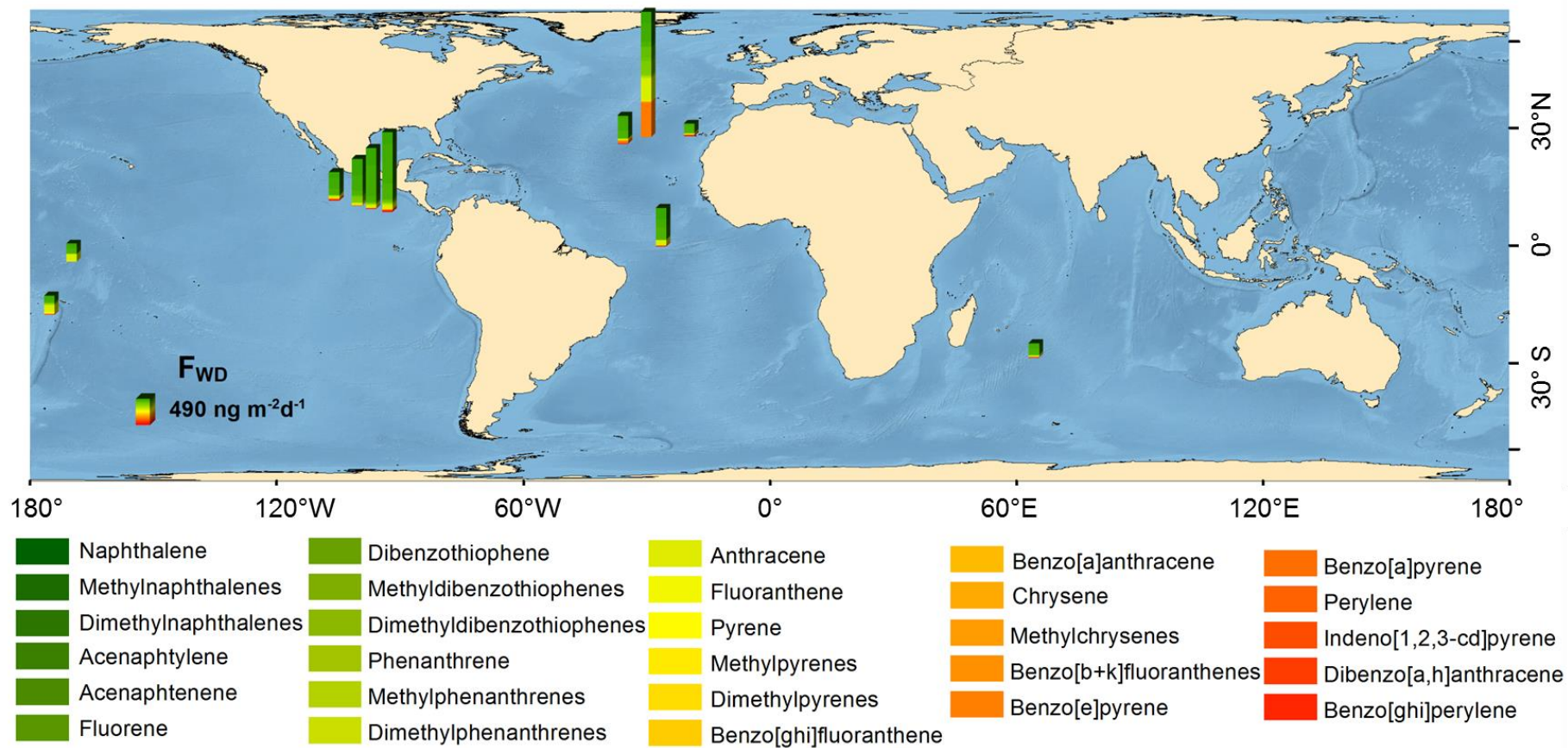


Figure S2.3. Ocean basin averaged gross volatilization (top) and absorption (middle) fluxes, and net diffusive fluxes (bottom) of PAHs

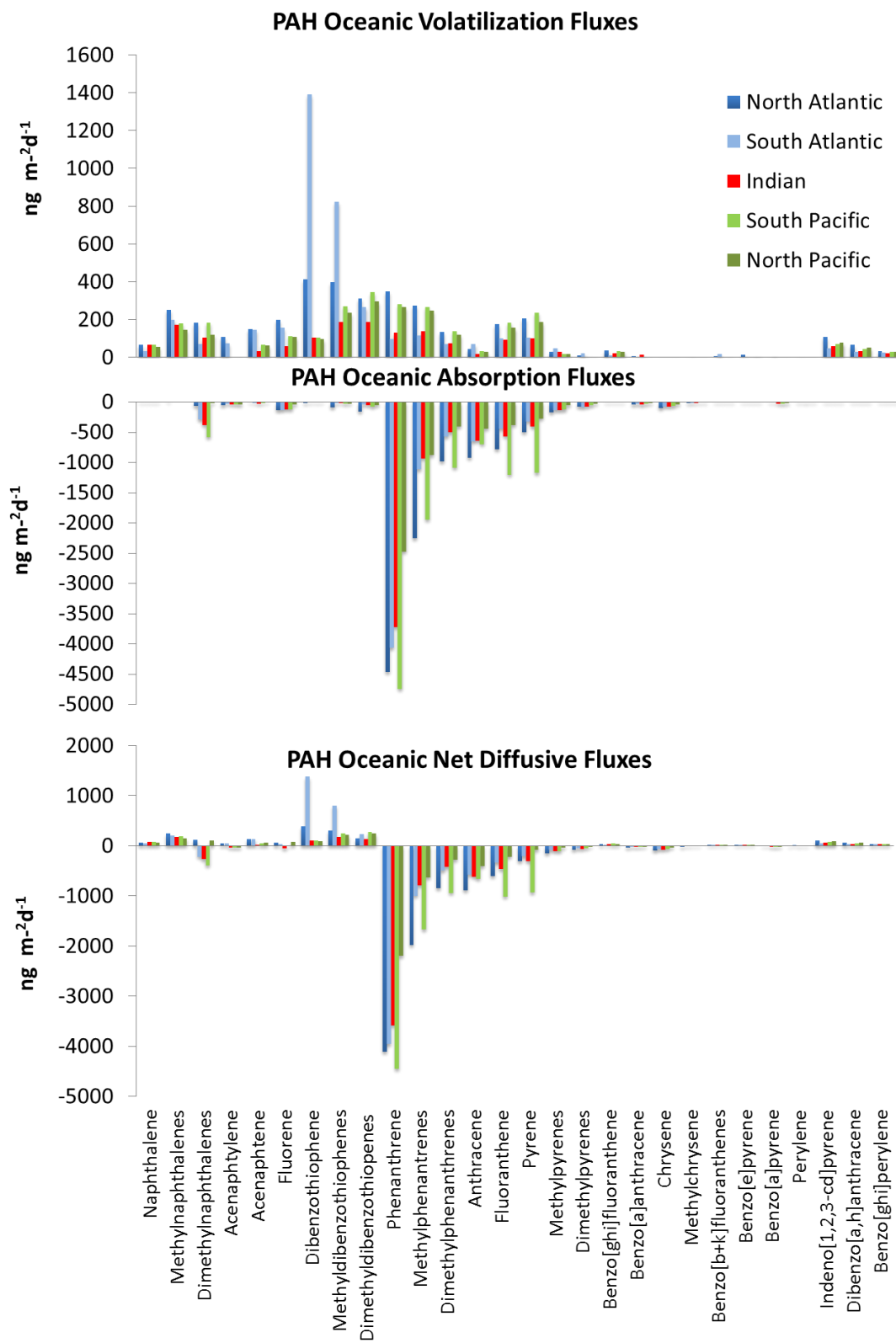


Figure S2.4. Degradation of PAHs in the atmosphere by reaction with OH radicals

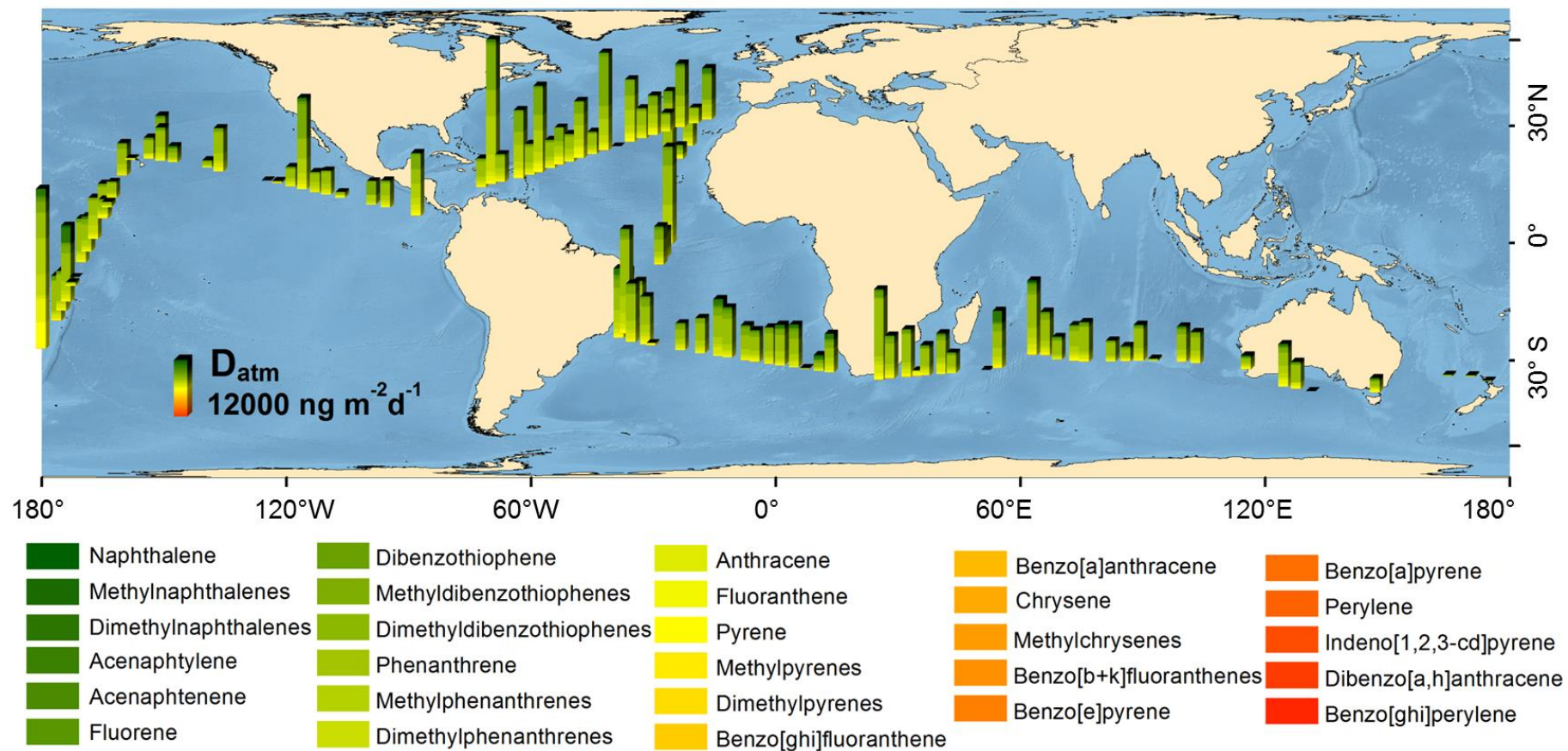
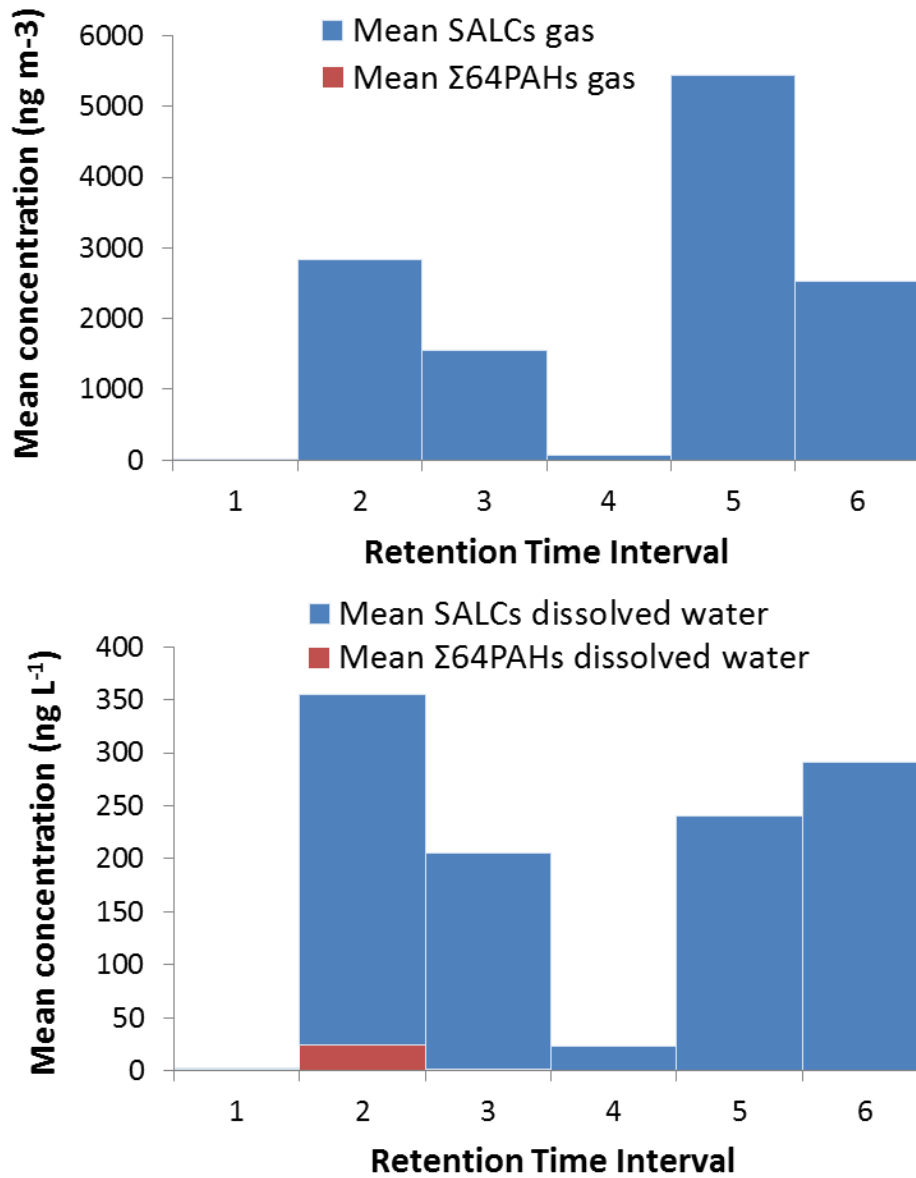


Figure S2.5. Mean concentrations of total aromatics, id SALCs (blue) and of targeted PAHs (red) in gas (top) and dissolved water (bottom) samples for the six retention time intervals quantified



3. PERFLUOROALKYLATED SUBSTANCES IN THE GLOBAL TROPICAL AND SUBTROPICAL SURFACE OCEANS

Supporting Information

**Belén González-Gaya^{1,2}, Jordi Dachs², Jose L. Roscales¹, Gemma
Caballero², Begoña Jiménez^{1*}**

*Corresponding author. Email: bjimenez@iqog.csic.es

INDEX

Table S3.1. Stations and positional information of the sampling points

Text S3.1. Details of sample treatment

Table S3.2. MS/MS parameters for the target compounds

Table S3.3. Details of laboratory and field blanks, MDLs, MQLs (pg/L) and % recoveries of the 9 target compounds

Figure S3.1. Air mass back trajectories for the upper atmospheric boundary layer in the South Atlantic coastal sites

Table S3.4. Concentration Normality test

Table S3.5. Individual and \sum PFAS concentration (pg/L) in surface ocean water samples obtained for the Malaspina 2010 expedition

Table S3.6. Comparison of PFAS concentrations (pg/L) in surface seawaters from different ocean basins including values from the present study

Figure S3.2. Schematics of the global oceanic currents and the *Malaspina 2010* cruise track

Table S3.7. Biogeochemical parameters measured at each sampling station retrieved from the meteorological station or from the continuous surface seawater measurement system

Figure S3.3. PFOA and PFOS in the different oceanic biogeochemical provinces

Table S3.8. Non parametric statistical correlations between PFAS concentrations and biological parameters (chlorophyll a concentrations and bacterial biomass)

Figure S3.4. Solar radiation influence on PFASs concentration

Figure S3.5. Temperature influence on PFASs concentration

Table S3.9. Non parametric statistical correlations between PFAS concentrations and solar radiation and water and air temperature

References

Table S3.1. Stations and positional information of the sampling points

Leg*	Station	Ocean	Longhurst Province**	Day	UTC time	Longitude	Latitude
1	2	Atlantic	NASE	17/12/2010	8:17	-12.782	34.003
1	3	Atlantic	NASE	19/12/2010	7:15	-17.285	29.686
1	5	Atlantic	NASE	21/12/2010	13:00	-21.028	25.005
1	7	Atlantic	NATR	23/12/2010	12:10	-23.453	21.447
1	8	Atlantic	NATR	24/12/2010	10:30	-24.304	20.26
1	9	Atlantic	NATR	25/12/2010	11:30	-26.01	16.143
1	11	Atlantic	NATR	27/12/2010	8:19	-26.005	14.519
1	12	Atlantic	WTRA	28/12/2010	8:44	-25.994	9.564
1	13	Atlantic	WTRA	29/12/2010	8:12	-25.996	7.326
1	14	Atlantic	WTRA	30/12/2010	8:15	-26.033	5.011
1	15	Atlantic	WTRA	31/12/2010	8:55	-26.032	2.472
1	17	Atlantic	WTRA	02/01/2011	8:05	-27.327	-3.03
1	18	Atlantic	WTRA	03/01/2011	11:30	-28.174	-4.773
1	20	Atlantic	SATL	05/01/2011	9:20	-30.189	-9.11
1	21	Atlantic	SATL	06/01/2011	9:15	-31.412	-11.568
1	23	Atlantic	SATL	08/01/2011	9:18	-33.412	-15.824
1	24	Atlantic	SATL	09/01/2011	9:34	-34.675	-18.399
1	26	Atlantic	SATL	11/01/2011	9:20	-36.987	-23.021
2	28	Atlantic	SATL	20/01/2011	9:00	-33.095	-24.852
2	29	Atlantic	SATL	21/01/2011	9:00	-30.131	-25.4
2	30	Atlantic	SATL	22/01/2011	9:00	-27.589	-25.863
2	31	Atlantic	SATL	23/01/2011	9:00	-24.243	-26.424
2	32	Atlantic	SATL	24/01/2011	9:00	-21.431	-26.901
2	33	Atlantic	SATL	25/01/2011	9:00	-18.091	-27.55
2	34	Atlantic	SATL	26/01/2011	9:00	-14.789	-28.101
2	37	Atlantic	SATL	29/01/2011	9:00	-5.401	-29.687
2	38	Atlantic	SATL	30/01/2011	9:00	-2.448	-30.239
2	39	Atlantic	SATL	31/01/2011	8:30	0.956	-30.879
2	40	Atlantic	SATL	01/02/2011	7:30	3.727	-31.296
2	41	Atlantic	SATL	02/02/2011	9:00	6.786	-31.772
2	42	Atlantic	BENG	03/02/2011	8:45	9.417	-32.104
2	43	Atlantic	BENG	04/02/2011	8:35	12.749	-32.791
2	44	Atlantic	BENG	05/02/2011	8:40	15.474	-33.297
3	46	Indian	EAFR	14/02/2011	5:11	27.546	-34.837
3	47	Indian	EAFR	15/02/2011	5:32	31.083	-34.446
3	49	Indian	ISSG	17/02/2011	5:10	37.001	-33.881
3	50	Indian	ISSG	18/02/2011	5:20	39.88	-33.532
3	52	Indian	ISSG	24/02/2011	3:30	61.458	-30.053
3	53	Indian	ISSG	25/02/2011	3:40	63.248	-27.976
3	55	Indian	ISSG	27/02/2011	3:00	69.414	-29.363
3	57	Indian	ISSG	01/03/2011	2:00	76.086	-29.906

Leg*	Station	Ocean	Longhurst Province**	Day	UTC time	Longitude	Latitude
3	58	Indian	ISSG	02/03/2011	2:00	79.607	-29.834
3	60	Indian	ISSG	04/03/2011	2:15	86.262	-29.756
3	63	Indian	ISSG	07/03/2011	1:00	96.395	-29.582
3	64	Indian	ISSG	08/03/2011	1:05	99.998	-29.907
3	66	Indian	AUSW	10/03/2011	1:20	107.211	-30.812
3	67	Indian	AUSW	11/03/2011	1:15	110.18	-31.154
4	70	Indian	SSTC	20/03/2011	22:30	120.846	-36.644
4	71	Indian	SSTC	21/03/2011	22:55	124.874	-37.345
4	73	Indian	SSTC	24/03/2011	22:15	131.541	-38.548
4	75	Indian	SSTC	25/03/2011	21:00	138.768	-39.86
4	77	Pacific	AUSE	28/03/2011	19:50	150.426	-38.671
4	78	Pacific	AUSE	29/03/2011	19:52	150.991	-36.685
5	82	Pacific	SPSG	20/04/2011	17:20	-178.212	-23.376
5	84	Pacific	SPSG	22/04/2011	16:55	-175.848	-18.554
5	86	Pacific	SPSG	24/04/2011	18:23	-173.397	-13.533
5	88	Pacific	SPSG	26/04/2011	19:15	-172.323	-9.46
5	90	Pacific	PEQD	28/04/2011	17:05	-170.781	-5.733
5	92	Pacific	PEQD	30/04/2011	17:07	-168.357	-1.304
5	94	Pacific	PEQD	02/05/2011	15:40	-165.805	3.821
5	97	Pacific	PNEC	05/05/2011	17:06	-162.422	11.6
5	99	Pacific	NPTG	07/05/2011	16:30	-159.442	17.977
6	102	Pacific	NPTG	15/05/2011	16:16	-153.42	21.571
6	103	Pacific	NPTG	16/05/2011	13:12	-150.366	21.067
6	106	Pacific	NPTG	19/05/2011	16:15	-141.617	19.902
6	107	Pacific	NPTG	20/05/2011	16:10	-138.966	19.279
6	109	Pacific	NPTG	22/05/2011	15:05	-133.262	18.057
6	110	Pacific	NPTG	23/05/2011	15:18	-130.595	17.404
6	112	Pacific	NPTG	25/05/2011	15:10	-124.508	15.914
6	113	Pacific	NPTG	26/05/2011	15:10	-121.995	15.311
6	114	Pacific	NPTG	27/05/2011	14:15	-118.773	14.529
6	116	Pacific	PNEC	29/05/2011	14:15	-113.27	13.195
6	117	Pacific	PNEC	30/05/2011	14:15	-110.392	12.493
6	120	Pacific	PNEC	02/06/2011	14:15	-102.448	10.757
6	121	Pacific	PNEC	03/06/2011	13:15	-99.251	10.083
6	123	Pacific	PNEC	05/06/2011	13:10	-93.148	8.764
6	124	Pacific	PNEC	06/06/2011	12:35	-90.362	8.142
6	125	Pacific	PNEC	07/06/2011	13:10	-87.947	7.221
7	128	Atlantic	CARB	21/06/2011	11:07	-71.703	14.184
7	129	Atlantic	CARB	22/06/2011	11:05	-69.289	15.073
7	131	Atlantic	NATR	25/06/2011	10:10	-59.829	17.428
7	132	Atlantic	NATR	26/06/2011	10:20	-57.81	18.065
7	134	Atlantic	NATR	28/06/2011	9:05	-52.629	20.013
7	135	Atlantic	NATR	29/06/2011	9:35	-50.143	20.805

Leg*	Station	Ocean	Longhurst Province**	Day	UTC time	Longitude	Latitude
7	137	Atlantic	NATR	01/07/2011	14:03	-44.539	22.869
7	138	Atlantic	NATR	02/07/2011	8:15	-41.912	23.736
7	140	Atlantic	NASE	04/07/2011	8:11	-35.274	26.111
7	141	Atlantic	NASE	05/07/2011	8:05	-32.89	26.918
7	143	Atlantic	NASE	07/07/2011	7:25	-26.952	28.875
7	144	Atlantic	NASE	08/07/2011	7:14	-23.693	29.966
7	146	Atlantic	NASE	10/07/2011	6:00	-17.26	32.088
7	147	Atlantic	NASE	11/07/2011	6:10	-14.65	32.875

**"Leg" term corresponds with transects: (1) Cadiz (Spain) – Rio de Janeiro (Brazil), (2) Rio de Janeiro (Brazil) – Cape Town (Republic of South Africa), (3) Cape Town (Republic of South Africa) – Perth (Australia), (4) Perth (Australia) – Sydney (Australia), (5) Sydney (Australia) – Honolulu (Hawaii, USA), (6) Honolulu (Hawaii, USA) – Cartagena de Indias (Colombia), (7) Cartagena de Indias (Colombia) – Cartagena (Spain).

**Longhurst Provinces acronyms corresponds to: North Atlantic Subtropical Gyral Province East (NASE), North Atlantic Tropical Gyral Province (NATR), Western Tropical Atlantic Province (WTRA), South Atlantic Gyral Province (SATL), Benguela Current Coastal Province (BENG), East Africa Coastal Province (EAFR), Indian South Subtropical Gyre Province (ISSG), Australia-Indonesia Coastal Province (AUSW), South Subtropical Convergence Province (SSTC), East Australia Coastal Province (AUSE), South Pacific Subtropical Gyre Province (SPSG), Pacific Equatorial Divergence Province (PEQD), North Pacific Equatorial Countercurrent Province (PNEC), North Pacific Tropical Gyre Province (NPTG), Caribbean Province (CARB).

Text S3.1. Details of sample treatment

Reagents and standards

All the solvents and solutions used were of analytical grade. Methanol, acetone and water (LiChrosolv) were purchased from Merk. Acetonitrile was purchased from Fluka and acetic acid (HPLC) from Scharlab. Ammonia (30% for analysis) and Ammonium acetate (solid PRS) were provided by Panreac. Glass fiber filters (GF/F, 0.7 μm pore size) were supplied by Whatman. OASIS WAX cartridges (150 mg, 6 cc, 30 μm) were supplied by Waters.

The native standard solution used was made of C₄-C₁₄, C₁₆ and C₁₈ PFCAs and C₄, C₆-C₈, C₁₀ and C₁₂ PFSAs acquired as a mix solution (PFAC-MXB commercial solution), plus the perfluorooctane sulfonamide (PFOSA) and N-methyl perfluorooctane sulfonamide (N-MePFOSA). The recovery standard solution contained ¹³C labeled C_{4,6,8-12} PFCAs, ¹⁸O C₆ and ¹³C C₈ PFSAs (MPFAC-MXA commercial solution). The injection standard consisted of a mixture of PFOA ¹³C₈, PFOS ¹³C₈, ³D-N-MePFOSA and PFUnDA ¹³C₇. All standards were supplied by Wellington Laboratories (Ontario, Canada).

Sample treatment

Immediately after sampling, seawater samples were filtered through pre-combusted glass fiber filters. Samples were spiked with a solution containing seven ¹³C labelled PFCAs, and two ¹⁸O and ¹³C labelled PFSAs. Samples were extracted on board by solid phase extraction using OASIS WAX cartridges. The cartridges were conditioned with 4 mL methanol, 4 mL ammonia 0.1% in methanol and 4 mL of chromatographic-grade water. Then, the sample was loaded and vacuum extracted at a constant slow flow. The cartridges were then washed with 4 mL of chromatographic-grade water to remove salts and matrix impurities, dried under vacuum aspiration for 30 minutes and kept at -20 °C during the cruise folded in aluminum foil and zip PP bags, until their elution in the laboratory. After unfreezing, each cartridge was pH conditioned with 4 mL of ammonium acetate buffer 25 mM at pH 4 and vacuum dried to remove all aqueous phase. The target compounds were eluted with 4 mL methanol and 4 mL ammonia 0.1% in methanol, concentrated under a gentle nitrogen flux down to ~0.3 mL and then, transferred to self-filtration PP vials (Mini-UniPrep Syringeless Filters vials, Whatman).

Table S3.2. MS/MS parameters for the target compounds

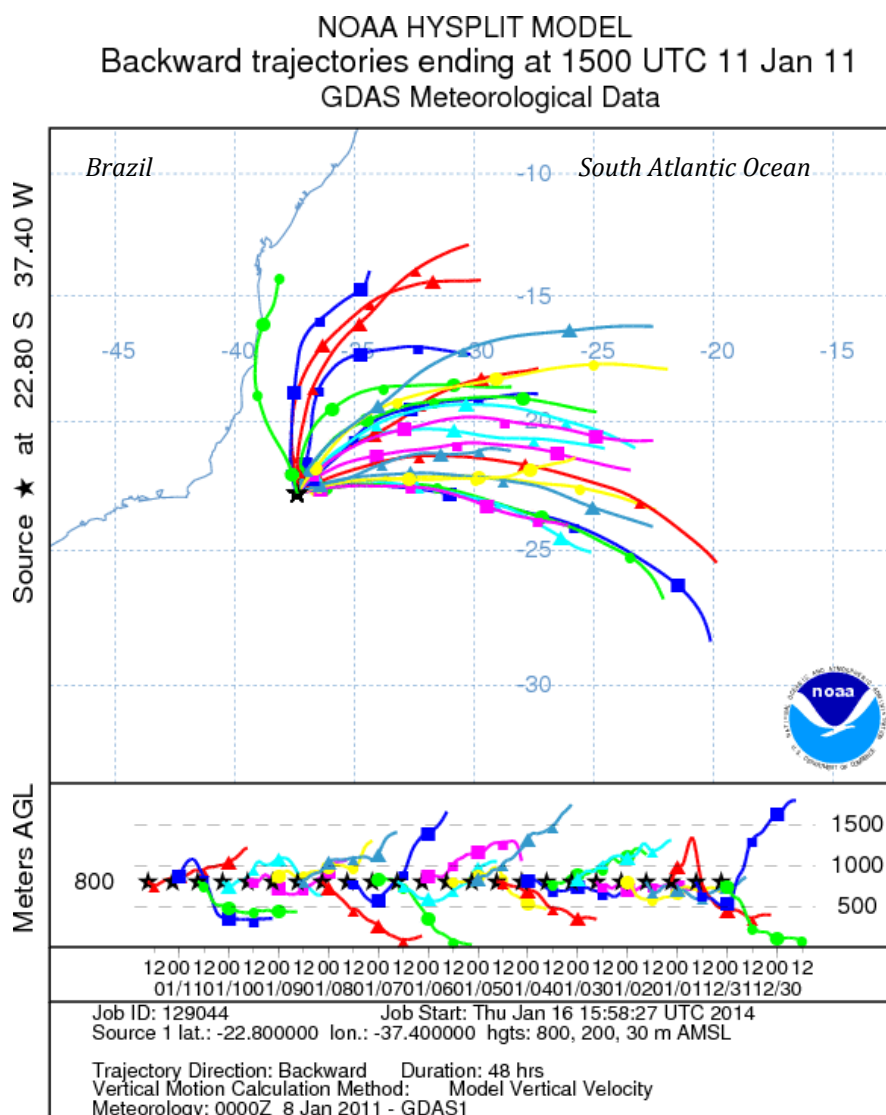
Compound	Acronym	RT	Parent Ion	Quan Ion	Conf Ion	Cone Voltage	Collision Energy Q1	Collision Energy Q2	Dwell time
Perfluoro-butanesulfonate	PFBS	2.33	298	79	98.8	40	30	28	0.110
Perfluoro-n-hexanoic acid	PFHxA	3.09	312	268	118.9	10	8	19	0.023
Perfluoro-n-[1,2-¹³C₂]hexanoic acid	*PFHxA ¹³ C ₂	3.1	314	269	119	10	9	14	0.023
Perfluoro-n-heptanoic acid	PFHpA	3.8	362.9	318.8	169	10	10	16	0.023
Perfluoro-hexanesulfonate	PFHxS	3.87	398.9	79.7	98.9	45	33	33	0.020
Perfluoro-1-hexane[¹⁸O₂]sulfonate	*PFHxS ¹⁸ O ₂	3.88	402.9	102.9	83.8	45	33	35	1.000
Perfluoro-n-octanoic acid	PFOA	4.32	412.9	368.8	168.9	10	10	17	0.030
Perfluoro-n-[1,2,3,4-¹³C₄]octanoic acid	*PFOA ¹³ C ₄	4.32	416.9	371.8	172	10	9	16	0.030
Perfluoro-n-[¹³C₈]octanoic acid	# PFOA ¹³ C ₈	4.32	420.8	375.8	172	10	10	18	0.030
Perfluoro-heptanesulfonate	PFHpS	4.34	448.8	79.8	98.8	55	40	42	2.000
Perfluoro-n-nonanoic acid	PFNA	4.72	462.8	418.9	218.9	10	10	15	2.000
Perfluoro-n-[1,2,3,4,5-¹³C₅]nonanoic acid	*PFNA ¹³ C ₅	4.75	467.9	422.7	219	10	10	14	1.000
Perfluoro-1-octanesulfonamide	PFOSA	5.24	497.9	77.8	168.7	42	40	24	1.000
Perfluoro-octanesulfonate	PFOS	4.75	498.8	79.8	98.9	25	40	39	0.020
Perfluoro-1-[1,2,3,4-¹³C₄]octanesulfonate	*PFOS ¹³ C ₄	4.76	502.8	79.8	98.8	25	42	36	1.000
Perfluoro-[¹³C₈]octanesulfonate	#PFOS ¹³ C ₈	4.76	506.8	79.8	98.8	25	40	34	0.016
Perfluoro-n-decanoic acid	PFDA	5	512	468.8	269	15	10	21	0.050
Perfluoro-n-[1,2-¹³C₂]decanoic acid	*PFDA ¹³ C ₂	5.08	514	469.8	219	15	8	18	0.050
N-methylperfluoro-1-octanesulfonamide	N-MePFOSA	5.56	511.9	168.9	219	35	26	23	8.000
N-methyl-d₃-perfluoro-1-octanesulfonamide	#d ₃ -N-MePFOSA	5.58	514	169	218.9	35	27	25	5.000
Perfluoro-n-[1,2-¹³C₂]undecanoic acid	*PFUnDA ¹³ C ₂	5.28	564	519	269	15	10	18	1.000
Perfluoro-n-[1,2,3,4,5,6,7-¹³C₇]undecanoic acid	#PFUnDA ¹³ C ₇	5.24	569	524	219	15	12	18	8.000

*recovery standards, # injection standards.

Table S3.3. Details of laboratory and field blanks, MDLs, MQLs (pg/L) and % recoveries of the 9 target compounds

	<i>n</i>	PFBS	PFHxA	PFHpA	PFHxS	PFOA	PFHpS	PFNA	FOSA	PFOS	N-MeFOSA	PFDA
Laboratory blanks												
Chromatography water	3	8.33	3.67	7.00	0.50	5.67	18.1	28.7	nd	4.33	2.74	12.7
SPE- extracted Chromatography water	4	12.0	3.00	8.00	0.37	13.0	3.16	14.0	nd	4.75	3.25	25.0
Reagents	4	6.00	2.75	7.37	0.00	5.25	1.96	8.12	nd	3.25	2.62	8.50
Field blanks												
Niskin bottle	3	7.00	4.00	1.33	3.00	14.7	0.00	58.7	0.00	3.00	0.00	1.33
MDL AND MQL												
MDL		0.32	2.75	1.75	0.59	0.01	0.49	0.01	0.01	0.06	0.02	0.659
MQL		1.17	10.2	5.31	1.90	0.80	1.70	0.29	0.01	0.42	0.02	1.07
Recoveries												
Standard		PFHxA - ¹³ C ₂		PFHxS - ¹⁸ O ₂		PFOA - ¹³ C ₄		PFNA - ¹³ C ₅		PFOS - ¹³ C ₄		PFDA - ¹³ C ₂
Average Recovery %		149		137		96		72		79		97

Figure S3.1 Air mass back trajectories for the upper atmospheric boundary layer in the South Atlantic coastal sites



At the sampling locations in east south Atlantic, offshore Brazil, some of upper air masses are originated in Brazilian inland and coastal zone according to the GDAS Meteorological data provided by NOAA¹, facilitating then the distribution of industrial and urban (particularly heavily populated in this area²) air masses and possible increase of PFASs precursors over the ocean.

Left panel shows the air masses during the sampling at 800 m above sea level for this area at the time the sampling campaign was ongoing. Left upper coastline corresponds to Brazilian coast.

Table S3.4. Concentration Normality test

Normality Test						
	Kolmogorov-Smirnov ^a			Shapiro-Wilk		
	Statistic	df	Sig.	Statistic	df	Sig.
PFBS	,168	92	,000	,817	92	,000
PFHxA	,236	92	,000	,736	92	,000
PFHpA	,158	92	,000	,829	92	,000
PFHxS	,348	92	,000	,391	92	,000
PFOA	,220	92	,000	,666	92	,000
PFHpS	,328	92	,000	,472	92	,000
PFNA	,366	92	,000	,434	92	,000
FOSA	,286	92	,000	,750	92	,000
PFOS	,337	92	,000	,413	92	,000
NMeFOSA	,262	92	,000	,719	92	,000
PFDA	,372	92	,000	,319	92	,000
∑PFCAAs	,352	92	,000	,393	92	,000
∑PFSAAs	,322	92	,000	,409	92	,000
∑PFOSAAs	,268	92	,000	,739	92	,000
∑allPFASs	,320	92	,000	,509	92	,000

a. Significance Lilliefors corrected

Since all distributions were not normal, non-parametric statistics was applied.

Table S3.5. Individual and Σ PFAS concentration (pg/L) in surface ocean water samples obtained for the *Malaspina 2010* expedition

Station	PFBS	PFHxA	PFHpA	PFHxS	PFOA	PFHpS	PFNA	PFOSA	PFOS	N-MePFOSA	PFDA	Σ PFAS
2	81.7	68.3	50.1	18.2	82.1	23.1	274	nd	61.4	0.255	633	1290
3	34.5	47.7	23.3	8.39	45.8	0.572	31.2	nd	14.8	nd	148	354
5	80.2	33.4	67.1	10.8	145	0.664	1670	nd	43.6	nd	1080	3130
7	26.4	10.8	18.0	7.30	41.7	4.18	53.8	nd	56.3	1.25	296	516
8	36.2	20.9	13.2	6.44	35.2	8.54	30.0	nd	43.0	nd	159	353
9	46.9	38.4	32.3	6.59	102	188	1270	nd	74.9	0.270	1190	2940
11	68.4	15.0	11.0	5.45	21.7	8.35	46.1	nd	29.0	nd	80.2	285
12	64.3	18.7	13.4	5.54	32.2	3.33	42.0	nd	76.2	0.030	84.7	340
13	67.1	18.3	63.4	23.3	129	6.54	847	nd	124	nd	2720	4000
14	38.5	32.0	36.4	11.2	66.5	2.80	318	nd	118	0.390	519.	1140
15	6.59	28.2	7.27	1.27	33.9	1.34	37.4	nd	22.0	nd	161	299
17	269	154	32.0	1420	132	308	30.2	2.47	6560	nd	1330	9040
18	139	138	16.5	652	77.0	183	22.1	0.300	4250	nd	154	5630
20	154	142	14.3	366	60.7	96.9	32.8	0.740	3420	nd	193	4480
21	249	87.1	125	717	282	91.8	825	nd	3240	nd	1540	7150
23	100	40.0	69.8	125	131	18.0	1010	nd	793	nd	3940	6230
24	118	51.2	17.3	140	60.9	33.4	494	0.210	1240	0.090	8750	10900
26	5.29	6.27	5.46	31.1	18.5	6.57	7.36	nd	310	0.150	109	500
28	18.6	52.7	17.1	46.5	66.6	16.2	263	nd	952	nd	200	1630
29	67.0	nd	106	226	167	45.8	110	nd	2730	nd	61.3	3510
30	36.0	83.5	21.4	123	77.4	37.2	21.1	nd	2340	nd	12.0	2750
31	nd	nd	55.0	84.0	36.0	26.6	nd	9.00	1680	9.00	129	2080
32	107	nd	38.9	67.4	106	9.90	600	nd	689	nd	322	1940
33	91.7	nd	20.1	35.1	54.2	6.88	245	nd	584	nd	89.6	1130
35	39.6	5.07	13.4	51.7	32.2	8.50	8.71	nd	569	nd	5.03	733

Station	PFBS	PFHxA	PFHpA	PFHxS	PFOA	PFHpS	PFNA	PFOSA	PFOS	N-MePFOSA	PFDA	ΣPFAS
37	nd	nd	6.50	15.5	29.3	2.25	5.65	nd	239	nd	6.41	305
38	70.9	nd	17.1	69.0	38.8	7.76	20.7	nd	492	nd	15.9	732
39	12.6	0.840	3.36	46.9	24.0	2.07	9.57	nd	305	nd	4.72	409
40	106	0.060	19.1	79.9	29.6	4.41	8.58	nd	368	nd	3.50	620
41	48.0	51.0	101	82.0	55.0	40.4	45.0	6.00	692	9.00	nd	1250
42	34.3	7.11	14.3	88.7	66.7	11.3	22.0	nd	845	nd	12.3	1100
43	25.2	3.60	27.8	90.4	39.2	6.52	20.5	nd	419	nd	12.6	645
44	41.9	1.65	6.02	35.7	23.4	2.07	8.45	nd	302	nd	3.20	424
46	7.32	3.69	5.71	5.60	21.1	3.67	31.6	nd	83.8	nd	166	329
47	11.9	6.77	6.28	6.65	17.6	2.50	48.8	nd	64.7	nd	386	551
49	19.3	18.5	5.99	6.00	10.8	1.96	8.51	nd	46.8	nd	62.8	181
50	26.1	12.1	9.71	14.2	18.7	2.33	20.7	nd	88.5	nd	70.9	263
52	109	17.4	5.60	7.94	16.4	1.47	14.3	nd	53.9	nd	58.9	285
53	49.3	23.5	7.36	12.9	24.4	3.25	8.83	nd	91.9	nd	56.5	278
55	9.63	29.9	6.95	6.46	22.2	1.38	14.8	nd	48.0	nd	99.7	239
57	10.8	21.3	10.4	5.90	42.1	2.42	119	nd	48.8	nd	562	823
58	45.0	20.7	9.66	6.36	33.5	1.56	118	nd	51.0	nd	471	757
60	46.5	17.7	7.29	4.90	43.0	7.44	91.1	nd	274	nd	249	742
63	nd	nd	45.0	1nd	11.0	0.138	33.0	3.00	64.0	3.00	nd	519
64	124	nd	4.75	6.46	21.2	0.828	18.0	nd	126	nd	73.5	374
66	91.3	nd	19.1	22.8	55.8	4.92	120	0.300	328	0.480	1030	1680
67	51.3	51.0	33.0	52.7	59.8	nd	60.7	nd	511	nd	1160	1980
70	20.7	30.4	4.05	8.78	24.2	3.98	10.8	nd	129	0.360	12.9	245
71	31.6	nd	nd	5.50	12.9	1.67	7.35	nd	102	0.260	14.3	176
74	4.71	nd	nd	8.60	25.7	4.19	33.5	nd	250	0.350	102	429
75	10.2	14.7	9.20	3.89	26.2	3.07	69.6	nd	50.5	0.350	292	480

Station	PFBS	PFHxA	PFHpA	PFHxS	PFOA	PFHpS	PFNA	PFOSA	PFOS	N-MePFOSA	PFDA	ΣPFAS
77	13.7	47.0	6.90	8.35	23.2	2.58	24.7	nd	95.6	0.180	33.6	256
78	nd	nd	nd	nd	nd	nd	nd	nd	nd	nd	nd	0.00
82	110	nd	3.12	13.4	35.1	3.33	17.3	nd	146	0.400	43.2	372
84	109	143	132	2.31	17.0	nd	nd	nd	74.1	0.300	145	622
86	15.0	39.0	54.0	nd	16.0	2.16	87.0	6.00	52.0	9.00	nd	640
88	nd	9.00	61.0	nd	24.0	4.82	46.0	6.00	159	1nd	637	967
90	nd	nd	149	11.0	35.0	71.2	13.0	6.00	174	15.0	78.0	552
92	9.00	nd	164	8.00	33.0	4.80	33.0	6.00	105	9.00	183	585
94	4.50	nd	134	11.0	45.0	117	71.0	9.00	218	nd	233	852
97	nd	24.0	27.0	7.00	25.0	96.2	13.0	6.00	nd	9.00	22.0	489
99	61.5	121	68.1	169	94.0	5.90	243	2.51	232	2.84	1500	2500
102	49.4	55.8	44.3	12.4	32.0	12.4	22.1	2.33	216	3.71	42.9	493
103	31.1	nd	35.4	178	41.2	nd	22.7	2.61	112	3.49	44.1	470
106	115	nd	107	70.0	34.8	nd	18.8	2.07	119	2.58	26.8	497
107	79.6	nd	138	36.2	23.3	nd	12.7	2.47	101	2.95	15.9	413
109	50.8	134	37.7	89.5	42.4	16.9	39.0	3.01	110	3.22	47.0	573
110	56.0	75.2	84.2	476	31.0	nd	27.9	2.01	46.0	2.87	22.5	824
112	88.0	73.9	52.5	24.6	30.8	nd	12.6	2.25	79.5	3.55	8.48	376
113	34.2	104	120	144	25.4	nd	9.38	3.24	69.6	2.85	14.8	527
114	41.3	208	90.0	300	34.4	15.6	6.90	3.29	158	2.83	36.6	896
116	34.2	nd	34.6	132	20.9	18.0	7.11	2.60	64.2	3.46	42.0	359
117	23.7	257	49.6	63.5	24.6	5.27	3.91	2.84	76.3	3.25	38.0	548
120	36.6	296	122	79.2	21.9	nd	4.47	2.75	58.2	3.16	11.3	636
121	30.6	136	45.0	50.7	13.0	3.03	nd	3.30	45.8	2.97	13.3	344
123	72.5	184	77.7	32.4	19.9	9.44	nd	2.97	41.1	2.75	62.5	505
124	74.0	nd	49.0	7.00	17.0	161	nd	3.00	76.0	3.00	44.0	444

Station	PFBS	PFHxA	PFHpA	PFHxS	PFOA	PFHpS	PFNA	PFOSA	PFOS	N-MePFOSA	PFDA	ΣPFAS
125	38.0	193	9.00	4.00	14.0	39.1	1.50	3.00	56.0	3.00	14.0	375
128	53.0	nd	12.0	5.00	27.0	0.201	19.0	4.00	88.0	5.00	147	360
129	47.0	41.0	36.0	5.00	28.0	20.3	7.00	3.00	104	6.00	74.0	371
131	174	9.00	41.0	12.0	24.0	0.201	9.00	5.00	191	8.00	307	780
132	23.0	nd	61.5	2.00	11.0	0.201	nd	3.00	27.0	3.00	nd	131
134	17.0	155	15.0	4.00	nd	0.201	nd	3.00	16.0	3.00	3.00	236
135	23.0	61.5	32.0	4.00	34.0	0.201	nd	3.00	16.0	3.00	nd	207
137	23.0	nd	31.0	15.0	36.0	0.201	19.0	3.00	47.0	3.00	12.0	189
138	22.0	18.0	7.50	8.00	32.0	9.03	13.0	3.00	nd	3.00	8.00	184
140	25.0	82.0	48.0	3.00	52.0	nd	nd	3.00	66.0	3.00	11.0	313
141	35.0	51.0	39.0	nd	44.0	28.0	19.0	3.00	76.0	3.00	13.0	311
143	32.0	nd	41.0	3.00	44.0	6.91	14.0	3.00	59.0	5.00	18.0	226
144	nd	25.5	66.0	13.0	71.0	15.5	24.0	9.00	69.0	9.00	nd	302
146	27.0	nd	79.0	19.0	63.0	38.9	nd	3.00	71.0	3.00	6.00	330
147	nd	192	69.0	3.00	45.0	nd	nd	3.00	nd	3.00	6.00	441
Ocean [median]												
<i>Atlantic</i>	39.6	33.4	27.8	21.1	45.0	8.35	30.0	3.00	191	3.00	99.5	645
<i>Indian</i>	45.4	121	61.0	32.4	25.4	12.4	15.2	3.00	101	3.16	42.9	527
<i>Pacific</i>	20.0	14.7	6.90	6.65	23.2	2.42	24.7	0.000	88.5	0.000	99.7	329
Hemisphere [median]												
<i>North</i>	38.2	55.8	42.6	11.2	33.9	8.35	21.1	3.00	69.3	3.00	42.9	708
<i>South</i>	40.8	22.4	16.5	15.5	33.0	4.80	30.1	4.50	274	0.400	109	1620
[median]												
Total	39.1	38.4	32.0	12.9	33.5	6.21	23.3	3.00	101	3.00	73.8	1180

nd: non-detected

Table S3.6. Comparison of PFAS concentrations (pg/L) in surface seawaters from different ocean basins including values from the present study

Location	Position	Year	PFBS	PFHxS	PFOS	PFBA	PFPA	PFHxA	PFHpA	PFOA	PFNA	PFDA	PFOUnDA	PFOSA	N-Me FOSA
ARTIC AND GREENLAND															
Labrador Sea (deep water) ³	56°N-52° W	2004-06	na	na	9-12	na	na	na	na	55-75	na	na	na	na	na
Labrador Sea (coastal) ⁴		2008	na	2.3-10	24-73	na	na	na	na	8-182	<mdl	na	na	na	na
North Sea ⁵	60°N-7°E	2004	na	na	25	na	na	na	na	300	na	na	na	na	na
Greenland Sea ⁶	75-80°N	2004	na	<2-20	12-32	na	na	na	na	25-80	na	na	na	na	na
Norwegian Sea ⁶	72-75°N	2005	na	5-16	25-80	na	na	na	na	45-60	na	na	na	na	na
Northwest Atlantic (east of Newfoundland) ⁷		2007	na	na	<10	na	na	<5.7	na	40-81	<5.1	na	na	na	na
East Greenland Arctic Ocean ⁸	67.5–80.4°N	2009	nd	nd-14.5	nd-38.0	nd	nd	nd-22.0	nd-26.9	nd-120	nd	na	na	nd-300	na
Labrador sea/ Davis strait/ North Baffin Bay ⁹	59-77° N	2008	na	nd-15	nd-39	na	na	0.4-26	na	21-41	nd-13	na	na	na	na
Canadian Artic Archipelago ⁹	87-124° N	2005	na	nd-19	nd-32	na	na	3-65	na	6-54	2-47	na	na	na	na
Beaufort Sea/ Chukchi Sea/ Bering Strait ⁹	137-169° N	2005	na	nd15	9-27	na	na	11-45	na	26-39	5-13	na	na	na	na
Chukchi Sea and Artic Ocean ¹⁰	39-76°N	2010	na	<66	<21-53	na	na	<27-28	na	<20-67	<22-51	na	na	na	na
ATLANTIC															
North Atlantic Ocean ¹¹	>40° N	2002-03	na	4.1-6.1	8.6-36	na	na	na	na	160-338	15-36	na	na	na	na
Middle Atlantic Ocean ¹¹	40-0°N	2002-03	na	2.6-12	37-73	na	na	na	na	100-439	na	na	na	na	na
German Bight ⁵		2004	na	na	250-7000	na	na	na	na	3000-13000	na	na	na	na	na
German Bight ¹²		2003-05	na	na	280-3100	na	na	na	na	540-5900	na	na	na	na	na
West Baltic Sea ¹²		2003-05	na	na	330-900	na	na	na	na	470-1100	na	na	na	na	na
East North to South Atlantic Ocean ¹³	53°N-30°S	2007	na	na	<14-170	na	na	na	na	<17-90	na	na	na	na	na
North Atlantic Ocean ⁷		2007	<1.6-60	nd	<10-291	na	na	<5.7-127	<5.9-104	<4.0-229	<5.1-107	na	na	<17-307	na
Middle Atlantic Ocean ⁷		2007	<1.6	nd	<10-60	na	na	<5.7	<5.9-9.7	<4.0-87	<5.1-35	na	na	<17-60	na

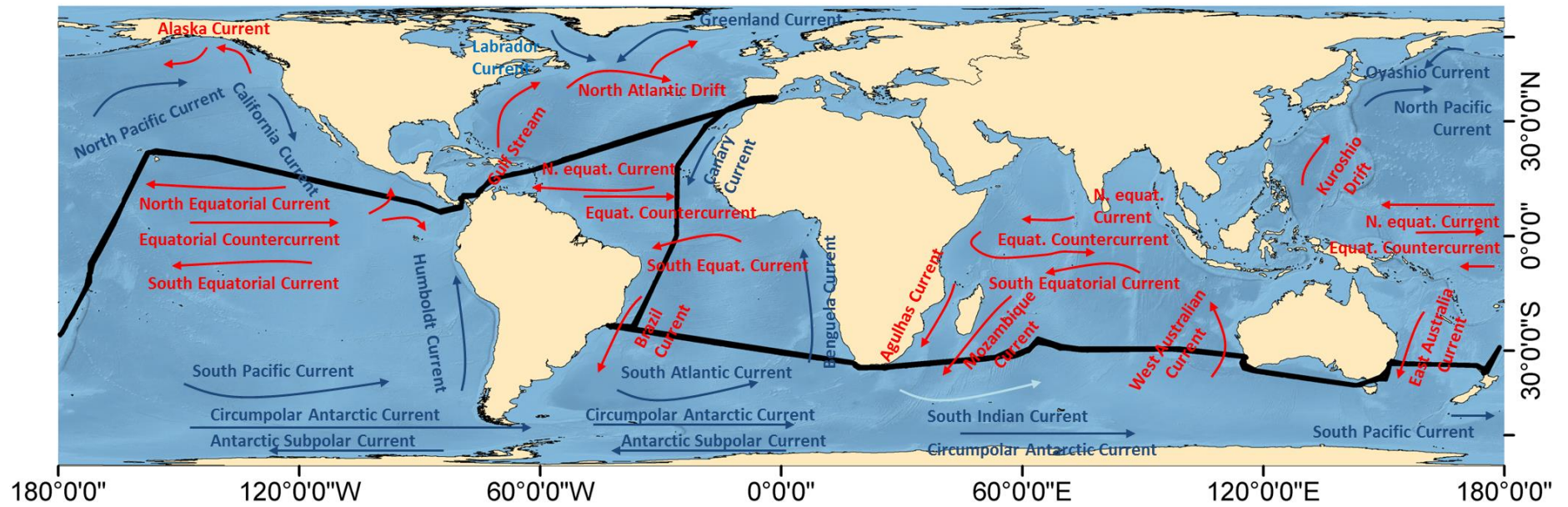
Location	Position	Year	PFBS	PFHxS	PFOS	PFBA	PFPA	PFHxA	PFHpA	PFOA	PFNA	PFDA	PFUnDA	PFOSA	N-Me FOSA
South Atlantic Ocean ¹⁴		2007	<1.6	nd	<10	na	na	<5.7	<5.9	<4.0	<5.1	na	na	<17-53	na
German Bight ¹⁴		2007	na	na	699-3950	na	na	na	na	2670-7830	na	na	na	na	na
Norwegian Sea ¹⁵		2008	nd	nd	nd	nd	nd	nd	nd	10-nd	nd	nd	na	nd	na
Norwegian Coast ¹⁵		2008	nd-90	nd-30	nd	nd	nd	200-310	nd-210	70-350	10-40	nd	na	120-280	na
Open North sea ¹⁵		2008	nd-70	nd	nd-70	nd	nd	nd	nd	20-70	40-50	nd	na	nd-70	na
German Coast ¹⁵		2008	10-6510	nd-280	nd-2260	nd-4730	nd-380	nd-1180	nd-580	80-3020	50-370	nd-170	na	nd-380	na
Riber Elbe ¹⁵		2008	3490-5270	320-500	4090-6160	nd-400	370-470	1660-2560	700-940	4360-4810	690-1160	240-850	na	500-780	na
Baltic Sea ¹⁵		2008	260-880	nd-610	nd-350	nd-440	nd-120	120-270	60-260	250-4550	100-420	nd	na	nd-460	na
North Atlantic Ocean ¹⁶		2007	<1.6-45	nd	<10-114	na	nd	<5.7-88	na	<4.0-209	<5.1-100	nd	nd	na	na
North Atlantic Ocean ¹⁶		2008	<4.4-20	13-27	54-116	na	30-74	38-54	na	87-154	24-39	12-37	20-39	na	na
North Atlantic Ocean ¹⁶		2010	<51	<6.5-39	<20-90	na	16-77	40-79	na	<13-110	13-38	<21	<13	na	na
Middle Atlantic Ocean ¹⁶		2007	<1.6	nd	<10-60	na	nd	<5.7	na	<4.0-87	<5.1-35	nd	nd	na	na
Middle Atlantic Ocean ¹⁶		2008	<4.4-17	8.1-14	62-77	na	21-35	20-31	na	49-70	4.4-25	19-35	26-30	na	na
Middle Atlantic Ocean ¹⁶		2010	<51	<6.5-12	40-50	na	<13-32	33-38	na	<13	<12-16	<21	<1	na	na
South Atlantic Ocean ¹⁶		2007	<1.6	nd	<10	na	nd	<5.7	na	<4.0	<5.1	nd	nd	na	na
South Atlantic Ocean ¹⁶		2008	<4.4-13	<4.1-17	<11-72	na	<14-24	<3.0-26	na	<5.2-62	<3.0	<5.5-27	<11-28	na	na
South Atlantic Ocean ¹⁶		2010	<51	<6.5	<20-45	na	<13	<5.9	na	<13-15	<12	<21	<13	na	na
East Atlantic ⁹	27-46° N	2009	na	11-36	61-192	na	na	47-110	na	96-259	26-70	na	na	na	na
East coast U.S.A. ⁹	38-41° N	2009	na	13-51	46-191	na	na	53-150	na	80-252	48-131	na	na	na	na
Western Atlantic ⁹	3-37° N	2007	na	1-7	13-32	na	na	14-75	na	17-49	4-27	na	na	na	na
Mid to Southeastern Atlantic ⁹	3-21° S	2009	na	2-5	18-30	na	na	18-75	na	17-30	5-19	na	na	na	na
Southwest Atlantic (not including Rio de la Plata) ⁹	5-52° S	2007	na	nd-8	18-45	na	na	3-17	na	3-26	2-15	na	na	na	na
Northeast Atlantic Ocean (this study)	35-0° N	2011	0-174	0-188	0-23	15-191	nd	nd	0-192	7-79	11-145	0-1669	0-2722	0-9	0-9
Southwest Atlantic Ocean (this study)	0-40° S	2011	0-269	2-308	16-1420	239-6558	nd	nd	0-154	3-125	19-282	6-1013	3-8751	0-9	0-9

Location	Position	Year	PFBS	PFHxS	PFOS	PFBA	PFPA	PFHxA	PFHpA	PFOA	PFNA	PFDA	PFUnDA	PFOSA	N-Me FOSA
PACIFIC															
Tokyo Bay, Japan ¹¹		2002	na	na	340-58000	na	na	na	na	1800-192000	na	na	na	na	na
Coastal Hong Kong, China ¹¹		2002	na	na	70-2600	na	na	na	na	670-5500	na	na	na	na	na
Coastal South Korea ¹¹		2002	na	na	40-2500	na	na	na	na	240-11000	na	na	na	na	na
South China Sea ¹¹		2002	na	na	8-110	na	na	na	na	160-420	na	na	na	na	na
Coastal area of Japan ¹⁷		2002	na	na	<2500-59000	na	na	na	na	na	na	na	na	na	na
West Pacific Ocean ¹¹		2002-03	na	2.2-2.8	54-78	na	na	na	na	136-142	na	na	na	na	na
Central to East Pacific Ocean ¹¹		2002-03	na	0.1-1.6	1.1-20	na	na	na	na	15-62	1.0-16	na	na	na	na
Central to East Pacific Ocean (deep water 4000m) ¹¹		2002-03	na	0.4-0.6	3.2-3.4	na	na	na	na	45-56	na	na	na	na	na
Coastal South Korea ¹⁸		2003-04	na	na	40-730000	na	na	na	na	240-320000	na	na	na	na	na
Perl River Delta, China ¹⁸		2003-04	na	na	20-1200	na	na	na	na	240-16000	na	na	na	na	na
Hong Kong, China ¹⁸		2003-04	na	na	90-3100	na	na	na	na	730-5500	na	na	na	na	na
South Pacific Ocean ³		2004	na	na	<5-11	na	na	na	na	<5-11	na	na	na	na	na
Dalian coast, China ¹⁹		2006	na	na	<100-2300	na	na	na	na	170-38000	na	na	na	na	na
Central and South Pacific Ocean ²⁰		2007	<25	<5	<5-21	na	na	<5	<5	<5-7.0	<5	na	na	<5	na
East to South China Sea ²¹		2010	23.0-941.0	na	<20.7-70.3	na	<20.3-439.0	<27.2-304	<11.3-422.0	37.5-1542.0	<22.5-37.9	na	na	na	na
Northwest Pacific and Bering Sea ²²	39-79°N	2010	na	<66	<21-60	na	na	<27	na	<20-100	<22-70	na	na	na	na
North Pacific Ocean (this study)	35-0° N	2011	0-115	0-161	4-476	41-260	nd	nd	0-296	9-138	13-94	0-243	8-1503	2-9	3-10
South Pacific Ocean (this study)	0-40° S	2011	0-110	0-71	2-13	52-174	nd	nd	0-143	3-164	16-35	0-87	43-637	0-6	0-15
Caribbean Sea (this study)		2011	47-53	0-20	5-5	88-104	nd	nd	0-41	12-36	27-28	7-19	74-147	3-4	5-6
INDIAN															
Sri Lanka (coastal lakes) ²³		2005	<16-1180	<16-1140	650-44000	na	na	330-2170	260-2030	1070-12400	230-610	110-500	18-130	<16-7500	na
Indian Ocean ²⁰		2007?	<5	<5	<5-8.6	na	na	<5	<5	<5-11	<5	na	na	na	na
Indian Ocean (this study)	0-40° S	2011	7-124	0-7	5-53	47-511	nd	nd	0-51	5-45	11-60	9-120	57-1156	0-3	0-3
Australian coast (this study)	0-40° S	2011	0-32	0-4	0-9	0-250	nd	nd	0-47	0-9	0-26	0-70	0-292	0-0	0-0

Location	Position	Year	PFBS	PFHxS	PFOS	PFBA	PFPA	PFHxA	PFHpA	PFOA	PFNA	PFDA	PFUnDA	PFOSA	N-Me FOSA
ANTARCTIC															
Antarctic region ²⁰		2007	<1(5)-2.9	<1(5)	5.1-22.6	na	na	<5	<5	<5	<5	na	na	na	na
Fildes and King George ²²	62°S	2011	<8.3-11.3	na	na	<64.1-79.7	25.1-82.2	56.6-360	<5.6-28.1	81-15096	na	na	<10.5-43.2	<40.3-46.4	na

na: not analyzed; nd: not detected

Figure S3.2. Schematics of the global oceanic currents and the *Malaspina 2010* cruise track



Warm currents are displayed in red. Cold currents correspond to the blue ones. Black line is the cruise track during the *Malaspina 2010* expedition.

Table S3.7. Biogeochemical parameters measured at each sampling station retrieved from the meteorological station or from the continuous surface seawater measurement system

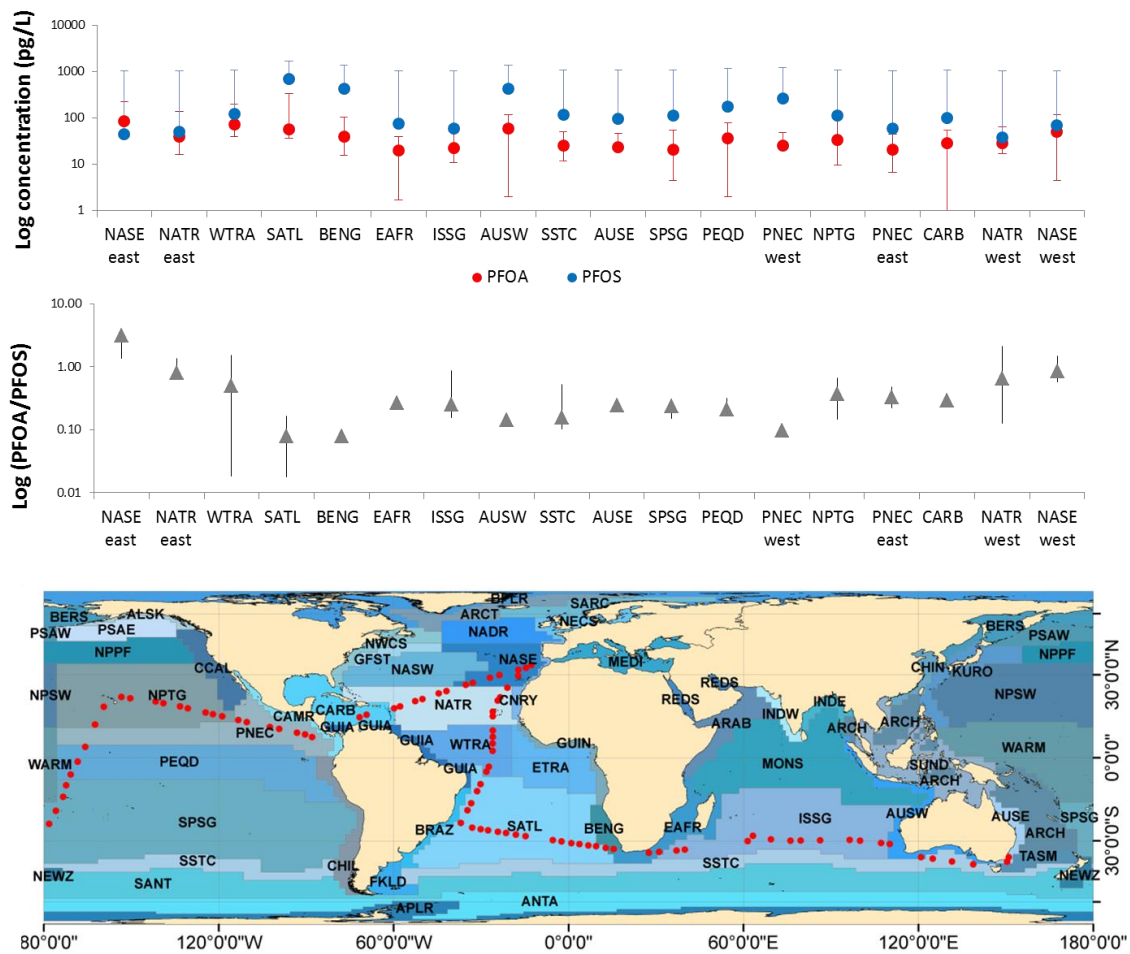
Station	Air temperature (°C)	Humidity- (%)	Solar radiation (w/ m ²)	Salinity (PSU)	Water Temperature (°C)	Fluorescence (adim)	Conductivity (S/m)	Water density (Kg/m ³)
2	17.96	87.72	0	36.3827	19.3434	0.0488	48.9349	25.9908
3	19.28	70.48	46.8	36.9057	21.1895	0.0391	51.5265	25.8947
5	22.99	64.77	767.68	36.9370	23.1915	0.0415	53.7231	25.3493
7	23.18	64.36	341.7	36.9783	25.0572	0.0391	55.8105	24.8215
8	23.47	51.51	276.17	36.6332	25.5721	0.0366	55.9087	24.4016
9	24.62	63.55	322.98	36.3869	26.9941	0.0366	57.1210	23.7669
11	24.72	70.08	0	35.7813	27.4287	0.0366	56.7450	23.1705
12	25.29	65.89	42.12	35.4439	27.8767	0.0366	56.7493	22.7710
13	26.06	69.97	0	35.4009	28.3027	0.0391	57.1442	22.5990
14	26.44	76.6	14.03	35.5171	28.5429	0.0440	57.5688	22.6070
15	26.35	74.05	196.59	35.6446	27.9858	0.0440	57.1516	22.8864
17	25.96	73.95	4.67	36.0982	27.9917	0.0415	57.8022	23.2257
18	27.21	70.69	940.87	36.3231	27.7474	0.0391	57.8540	23.4749
20	25.58	78.75	117.02	36.5988	27.8583	0.0000	58.3649	23.6463
21	26.54	68.24	355.75	36.8678	27.6718	0.0000	58.5380	23.9098
23	26.06	64.98	271.49	37.2380	27.8186	0.0000	59.2219	24.1406
24	23.09	78.34	79.57	37.2265	27.7199	0.0000	59.0955	24.1643
26	25.96	76.71	98.29	36.6801	26.9831	0.0000	57.5165	23.9914
28	25.1	82.11	102.97	36.6345	27.1598	0.0000	57.6471	23.9002
29	24.33	71.61	135.74	36.5812	26.0425	0.0000	56.3508	24.2155
30	22.42	89.15	70.21	36.4865	25.6802	0.0000	55.8275	24.2571
31	23.18	77.73	402.56	36.4102	24.6138	0.0000	54.5709	24.5268

Station	Air temperature (°C)	Humidity- (%)	Solar radiation (w/ m ²)	Salinity (PSU)	Water Temperature (°C)	Fluorescence (adim)	Conductivity (S/m)	Water density (Kg/m ³)
32	22.71	69.06	440.01	36.2004	23.9521	0.0000	53.5829	24.5665
33	22.61	67.22	117.02	36.2058	23.7886	0.0000	53.4153	24.6191
35	22.52	67.73	472.77	36.5073	23.8035	0.0000	53.8259	24.8432
37	22.04	68.14	496.18	36.1066	22.6482	0.0000	52.0732	24.8762
38	21.56	62.43	828.53	35.9812	22.8164	0.0000	52.0902	24.7326
39	21.94	65.79	365.11	35.9319	21.7726	0.0000	50.9276	24.9914
40	20.33	81.4	538.31	35.7931	21.5748	0.0000	50.5458	24.9409
41	20.8	74.67	1240.46	35.7748	21.3115	0.0000	50.2478	24.9998
42	19.76	93.54	365.11	35.8058	21.315	0.0000	50.2903	25.0225
43	20.71	88.64	449.37	35.4656	20.9058	0.0000	49.4419	24.8755
44	20.9	77.52	1006.41	35.5409	21.0717	0.0000	49.7070	24.8875
46	25.1	79.56	243.4	35.2933	26.3909	0.0073	54.9561	23.1340
47	23.28	77.73	397.88	35.5106	23.7084	0.0073	52.4190	24.1159
49	22.61	56.61	145.1	35.6274	23.8482	2.0000	52.7195	24.1631
50	20.99	57.02	196.59	35.5671	24.4647	2.0024	53.2903	23.9337
52	22.04	61.3	177.87	0.0000	0.0000	0.0000	0.0000	0.0000
53	22.42	87.52	145.1	35.2860	26.3192	1.7314	54.8700	23.1511
55	21.75	92.52	159.15	35.4577	25.6305	1.7436	54.3761	23.4955
57	21.85	66.91	46.8	35.6690	24.9659	1.7900	53.9571	23.8592
58	21.56	67.53	276.17	36.0047	23.5609	1.8462	52.9098	24.5338
60	21.56	72.63	552.35	35.9466	22.8594	1.8828	52.0912	24.6940
63	20.8	56.71	60.84	35.7717	22.1645	1.9267	51.1361	24.7595
64	20.04	57.94	407.24	35.5304	22.1143	1.9683	50.7770	24.5903
66	20.9	55.39	173.19	35.5737	23.4565	2.0317	52.2369	24.2377
67	20.99	61.92	711.5	35.4728	23.3919	2.1001	52.0376	24.1801

Station	Air temperature (°C)	Humidity- (%)	Solar radiation (w/ m ²)	Salinity (PSU)	Water Temperature (°C)	Fluorescence (adim)	Conductivity (S/m)	Water density (Kg/m ³)
70	14.19	74.87	42.12	35.3687	18.4103	2.4542	46.7689	25.4535
71	14.19	81.09	60.84	35.4493	18.6765	2.3687	47.1349	25.4481
74	13.53	61.1	84.25	35.2497	16.9175	2.4176	45.1250	25.7265
75	12.88	83.74	4.67	35.1478	16.4225	3.2063	44.5144	25.7647
77	20.33	75.38	0	35.5502	22.0825	3.0965	50.7689	24.6143
78	20.33	73.14	0	0.0000	0.0000	0.0000	0.0000	0.0000
82	23.57	62.12	0	35.2816	27.0522	1.5507	55.6413	22.9153
84	26.16	82.52	0	34.5453	28.9403	1.5897	56.5867	21.7449
86	28.66	72.93	617.88	34.9384	29.6889	1.6313	57.9544	21.7883
88	27.79	76.81	14.03	35.2433	29.542	1.8071	58.2450	22.0668
90	27.5	78.34	28.08	35.3715	28.7436	3.1209	57.5748	22.4309
92	27.41	80.17	524.26	35.4516	27.9378	3.8266	56.8256	22.7568
94	26.83	76.3	0	34.9893	27.996	5.3309	56.2294	22.3901
97	23.66	83.03	93.61	34.5525	26.7716	3.8486	54.3265	22.4554
99	20.71	87.62	0	0.0000	0.0000	0.0000	0.0000	0.0000
102	22.04	75.69	32.76	34.9421	24.9412	2.2662	52.9533	23.3171
103	21.66	71.81	0	34.5712	24.4214	2.2271	51.9172	23.1932
106	19.95	84.15	37.44	34.6146	23.8118	2.1050	51.3476	23.4068
107	21.47	77.83	159.15	34.7804	22.762	2.1978	50.4856	23.8369
109	20.04	69.46	9.35	34.8413	22.3751	2.2637	50.1670	23.9932
110	20.14	63.14	65.53	34.8462	22.058	2.3175	49.8484	24.0862
112	21.85	68.44	107.65	34.6703	23.8151	2.5128	51.4245	23.4480
113	22.32	71.3	42.12	34.5075	24.5749	2.4908	51.9900	23.0991
114	22.61	71.91	131.06	34.4197	25.2931	2.4542	52.6113	22.8153
116	24.72	65.59	201.27	34.0548	28.4774	2.7082	55.3923	21.5299

Station	Air temperature (°C)	Humidity- (%)	Solar radiation (w/ m ²)	Salinity (PSU)	Water Temperature (°C)	Fluorescence (adim)	Conductivity (S/m)	Water density (Kg/m ³)
117	26.25	67.93	98.29	34.1531	29.1432	2.8278	56.2274	21.3828
120	27.41	73.24	46.8	33.4412	29.6864	3.2869	55.7415	20.6667
121	27.21	77.73	149.78	33.8554	29.4574	3.3895	56.1170	21.0543
123	26.83	83.85	98.29	34.3193	28.1317	8.0244	55.4135	21.8420
124	25.19	85.07	23.4	34.2250	28.5718	5.2625	55.7364	21.6266
125	26.54	82.52	177.87	34.1586	28.1704	8.4737	55.2233	21.7087
128	27.89	79.36	23.4	35.5559	29.2159	1.8510	58.3503	22.4115
129	28.18	78.75	65.53	35.5043	29.2817	1.7460	58.3463	22.3506
131	27.5	72.52	32.76	35.5153	29.4255	1.8217	58.5174	22.3103
132	27.21	73.24	60.84	35.5783	29.031	1.7314	58.1833	22.4903
134	26.25	74.77	0	36.7524	28.1236	1.8095	58.8748	23.6747
135	25.58	78.13	42.12	37.0479	27.5184	1.8388	58.6207	24.0955
137	26.73	65.18	1128.11	37.0533	27.0288	1.9585	58.0851	24.2581
138	23.95	66.71	0	37.4466	26.4516	1.9805	57.9858	24.7396
140	23.09	75.58	42.12	37.6315	24.8824	2.0977	56.4885	25.3695
141	22.71	68.65	9.35	37.4785	24.3872	2.1758	55.7374	25.4043
143	20.14	88.44	23.4	37.3438	22.9963	2.4127	54.0341	25.7152
144	20.23	64.36	0	36.9525	21.6126	2.5324	52.0386	25.8127
146	20.14	80.99	0	36.7039	21.8145	2.8987	51.9435	25.5669
147	19.66	84.66	0	36.7783	21.6044	3.2332	51.8120	25.6824

Figure S3.3. PFOA and PFOS in the different oceanic biogeochemical provinces



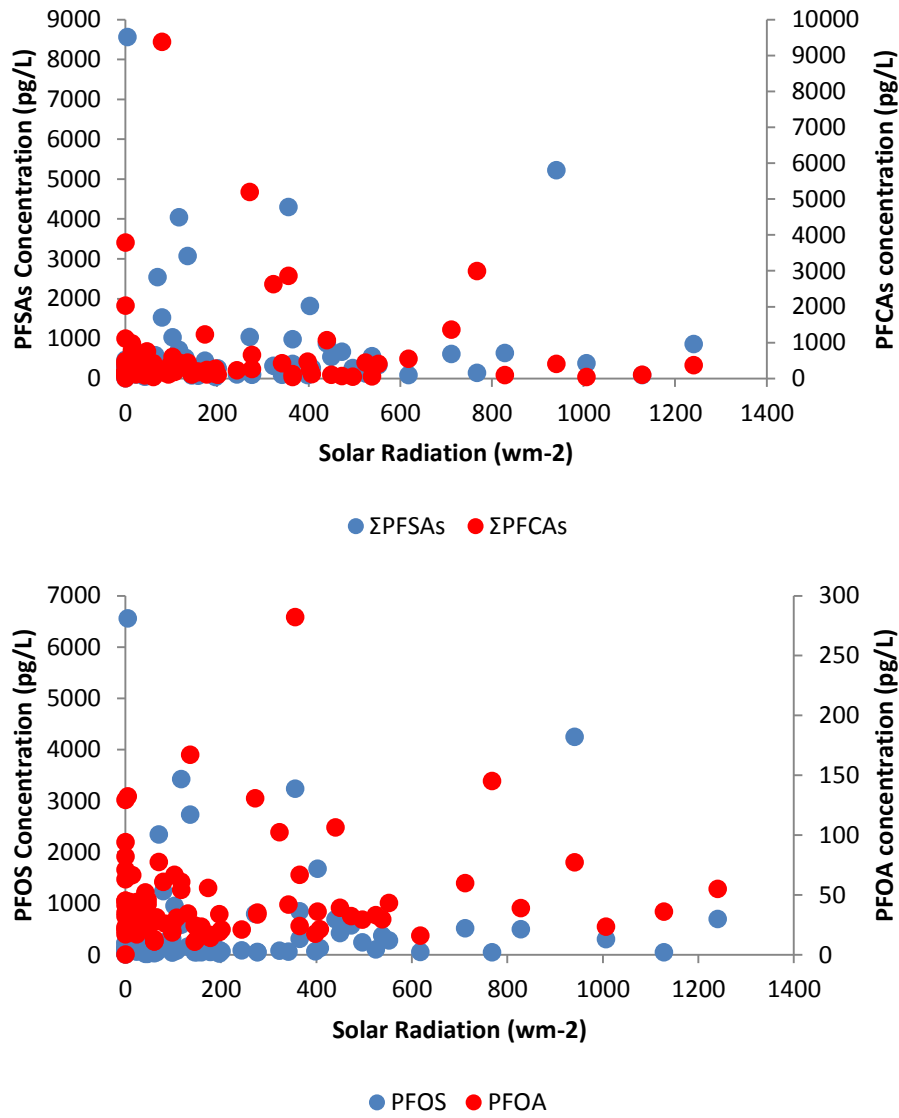
Upper panel shows mean and minimum and maximum records of PFOA and PFOS (pg/L) and medium panel PFOA/PFOS ratio mean, minimum and maximum records per Longhurst province. Map draws Longhurst 2010 biogeochemical provinces and sampling points in red dots. Chronologically ordered provinces Malaspina cruise crossed correspond to: N. Atlantic Subtropical Gyre Province East (NASE), N. Atlantic Tropical Gyre Province (NATR), Western Tropical Atlantic Province (WTRA), South Atlantic Gyral Province (SATL), Benguela Current Coastal Province (BENG), E. Africa Coastal Province (EAFR), Indian S. Subtropical Gyre Province (ISSG), Australia-Indonesia Coastal Province (AUSW), S. Subtropical Convergence Province (SSTC), E. Australia Coastal Province (AUSE), S. Pacific Subtropical Gyre Province (SPSG), Pacific Equatorial Divergence Province (PEQD), N. Pacific Equatorial Countercurrent Province (PNEC), N. Pacific Tropical Gyre Province (NPTG), Caribbean Province (CARB). NASE, NATR and PNEC have been divided into west and east as they were crossed in different areas and periods during the campaign.

Table S3.8. Non parametric statistical correlations between PFAS concentrations and biological parameters (chlorophyll a concentrations and bacterial biomass)

Non Parametric Correlations			CHLTotal (mgm ⁻³)	BacterialBiomass(µgCl1)
Tau_b Kendall	ΣPFASs	Correlation	-,077	-,100
		Sig. (bilateral)	,319	,194
		N	78	79
	ΣPFCAs	Correlation	,057	-,104
		Sig. (bilateral)	,461	,177
		N	78	79
	ΣPFASAs	Correlation	,203 [*]	,125
		Sig. (bilateral)	,013	,120
		N	78	79
	ΣPFASs	Correlation	-,041	-,126
		Sig. (bilateral)	,596	,100
		N	78	79
	PFOS	Correlation	-,151	-,163 [*]
		Sig. (bilateral)	,051	,034
		N	78	79
PFOA	Correlation	-,195 [*]	-,206 ^{**}	
	Sig. (bilateral)	,012	,007	
	N	78	79	
Rho Spearman	ΣPFASs	Correlation	-,114	-,140
		Sig. (bilateral)	,319	,219
		N	78	79
	ΣPFCAs	Correlation	,076	-,149
		Sig. (bilateral)	,507	,190
		N	78	79
	ΣPFASAs	Correlation	,279 [*]	,181
		Sig. (bilateral)	,013	,110
		N	78	79
	ΣPFASs	Correlation	-,063	-,173
		Sig. (bilateral)	,587	,127
		N	78	79
	PFOS	Correlation	-,228 [*]	-,242 [*]
		Sig. (bilateral)	,044	,031
		N	78	79
PFOA	Correlation	-,294 ^{**}	-,276 [*]	
	Sig. (bilateral)	,009	,014	
	N	78	79	

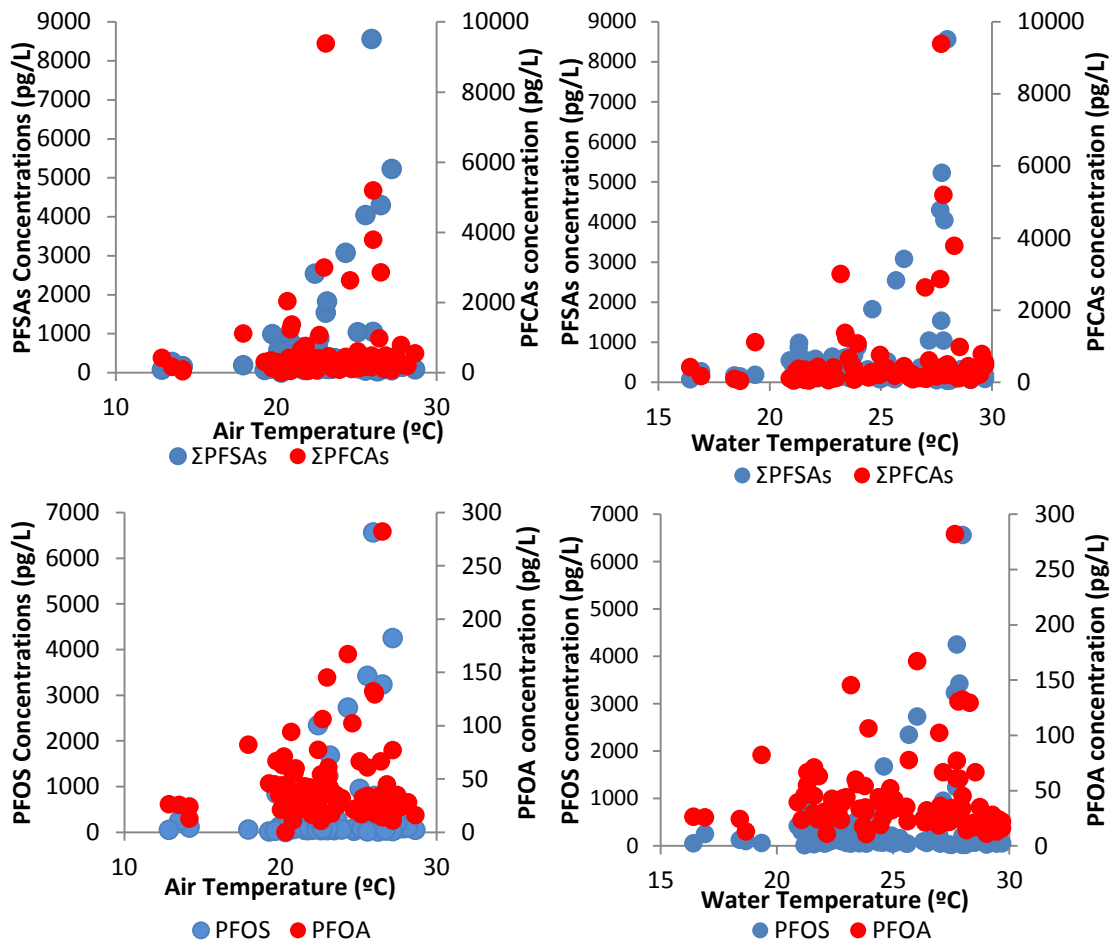
** p < 0,01 (bilateral). * p < 0,05 (bilateral).

Figure S3.4. Solar radiation influence on PFASs concentration



Total PFASs and PFCAs in the upper panel and PFOS and PFOA in the bottom panel.

Figure S3.5. Temperature influence on PFASs concentration



Total PFASs and PFCAs in the upper panels and PFOS and PFOA in the bottom panels; air temperature on the left and water temperature on the right.

Table S3.9. Non parametric statistical correlations between PFAS concentrations and solar radiation and water and air temperature

Non parametric Correlations			Solar Radiation Wm ⁻²	Air temp. °C	Water temp °C
Tau_b Kendall	ΣPFCAAs	Correlation	-,037	,182*	,196**
		Sig. (bilateral)	,610	,011	,006
		N	92	92	89
	ΣPFSAAs	Correlation	,165*	-,016	-,035
		Sig. (bilateral)	,021	,821	,630
		N	92	92	89
	ΣPFOSAAs	Correlation	-,262**	,217**	,243**
		Sig. (bilateral)	,001	,004	,001
		N	92	92	89
	PFOA	Correlation	-.031	-.079	-.101
		Sig. (bilateral)	,663	,270	,160
		N	92	92	89
	PFOS	Correlation	,179*	-.017	,345**
		Sig. (bilateral)	,013	,881	,000
		N	92	92	92
Rho Spearman	ΣPFCAAs	Correlation	-,044	,269**	,294**
		Sig. (bilateral)	,675	,010	,005
		N	92	92	89
	ΣPFSAAs	Correlation	,253*	-,030	-,062
		Sig. (bilateral)	,015	,773	,566
		N	92	92	89
	ΣPFOSAAs	Correlation	-,357**	,297**	,338**
		Sig. (bilateral)	,000	,004	,001
		N	92	92	89
	PFOA	Correlation	-.039	-.112	-.138
		Sig. (bilateral)	,712	,287	,198
		N	92	92	89
	PFOS	Correlation	,272**	-.030	-.101
		Sig. (bilateral)	,009	,778	,346
		N	92	92	89

*. p< 0,05 (bilateral).
 **. p< 0,01 (bilateral).

REFERENCES

1. Draxler, R. R. a. R., G.D., HYSPLIT (HYbrid Single-Particle Lagrangian Integrated Trajectory) Model. In NOAA Air Resources Laboratory, College Park, MD: access via NOAA ARL READY Website (<http://www.arl.noaa.gov/HYSPLIT.php>), 2013.
2. Carloni, D., *Perfluorooctane Sulfonate (PFOS) Production and Use: Past and Current Evidence*. 2009.
3. Yamashita, N.; Taniyasu, S.; Petrick, G.; Wei, S.; Gamo, T.; Lam, P. K.; Kannan, K., Perfluorinated acids as novel chemical tracers of global circulation of ocean waters. *Chemosphere* **2008**, *70*, (7), 1247-55.
4. Rosenberg, B.; DeLaronde, J.; MacHutchon, A.; Stern, G.; Spencer, C.; Scott, B.; Lopez, E.; Muir, D.; Gregg, T., Spatial and vertical distribution of perfluorinated compounds in Canadian Arctic and sub-Arctic ocean water. *Organohalogen Compounds* **2008**, *70*, 386– 389.
5. Caliebe, C.; Gerwinski, W.; Hühnerfuss, H.; Theobald, N., Occurrence of perfluorinated organic acids in the water of the North Sea. *Organohalogen Compd.* **2004**, *66*, 4074-4078.
6. Caliebe, C.; Gerwinski, W.; Theobald, N.; Hühnerfuss, H., Occurrence of perfluorinated 465 organic acids in the water of the North Sea and Arctic North Atlantic. In *Poster presented at Fluoros, Toronto, Canada.*, 2005.
7. Ahrens, L.; Barber, J. L.; Xie, Z.; Ebinghaus, R., Longitudinal and latitudinal distribution of perfluoroalkyl compounds in the surface water of the Atlantic Ocean. *Environ Sci Technol* **2009**, *43*, (9), 3122-7.
8. Busch, J.; Ahrens, L.; Xie, Z.; Sturm, R.; Ebinghaus, R., Polyfluoroalkyl compounds in the East Greenland Arctic Ocean. *J Environ Monit* **2010**, *12*, (6), 1242-6.
9. Benskin, J. P.; Muir, D. C.; Scott, B. F.; Spencer, C.; De Silva, A. O.; Kylin, H.; Martin, J. W.; Morris, A.; Lohmann, R.; Tomy, G.; Rosenberg, B.; Taniyasu, S.; Yamashita, N., Perfluoroalkyl acids in the Atlantic and Canadian Arctic Oceans. *Environ Sci Technol* **2012**, *46*, (11), 5815-23.
10. Cai, M.; Zhao, Z.; Yin, Z.; Ahrens, L.; Huang, P.; Cai, M.; Yang, H.; He, J.; Sturm, R.; Ebinghaus, R.; Xie, Z., Occurrence of perfluoroalkyl compounds in surface waters from the North Pacific to the Arctic Ocean. *Environ Sci Technol* **2012**, *46*, (2), 661-8.
11. Yamashita, N.; Kannan, K.; Taniyasu, S.; Horii, Y.; Petrick, G.; Gamo, T., A global survey of perfluorinated acids in oceans. *Mar Pollut Bull* **2005**, *51*, (8-12), 658-68.
12. Theobald, N.; Gerwinski, W.; Caliebe, C.; Haarich, M., Validation meth PFCs in water sediments and biota. In Federal Environmental Agency: Germany, 2007; Vol. Project 202 22 213.
13. Theobald, N.; Gerwinski, W.; Jahnke, A. In *Occurrence of perfluorinated organic acids in surface sea-water of the East Atlantic Ocean between 53° north and 30°south.*, Poster presentation at the SETAC Europe Annual Meeting 20–24 May 2007 in Porto, Portugal., 2007; 2007.
14. Ahrens, L.; Felizeter, S.; Ebinghaus, R., Spatial distribution of polyfluoroalkyl compounds in seawater of the German Bight. *Chemosphere* **2009**, *76*, (2), 179-84.
15. Ahrens, L.; Gerwinski, W.; Theobald, N.; Ebinghaus, R., Sources of polyfluoroalkyl compounds in the North Sea, Baltic Sea and Norwegian Sea: Evidence from their spatial distribution in surface water. *Mar Pollut Bull* **2010**, *60*, (2), 255-60.
16. Zhao, Z.; Xie, Z.; Moller, A.; Sturm, R.; Tang, J.; Zhang, G.; Ebinghaus, R., Distribution and long-range transport of polyfluoroalkyl substances in the Arctic, Atlantic Ocean and Antarctic coast. *Environ Pollut* **2012**, *170*, 71-7.
17. Taniyasu, S.; Kannan, K.; Horii, Y.; Hanari, N.; Yamashita, N., A survey of perfluorooctane sulfonate and related perfluorinated organic compounds in water, fish, birds, and humans from Japan. *Environmental Science and Technology* **2003**, *37*, (12), 2634-2639.

18. So, M. K.; Taniyasu, S.; Yamashita, N.; Giesy, J. P.; Zheng, J.; Fang, Z.; Im, S. H.; Lam, P. K., Perfluorinated compounds in coastal waters of Hong Kong, South China, and Korea. *Environ Sci Technol* **2004**, *38*, (15), 4056-63.
19. Ju, X.; Jin, Y.; Sasaki, K.; Saito, N., Perfluorinated Surfactants in Surface, Subsurface Water and Microlayer from Dalian Coastal Waters in China. *Environmental Science & Technology* **2008**, *42*, (10), 3538-3542.
20. Wei, S.; Chen, L. Q.; Taniyasu, S.; So, M. K.; Murphy, M. B.; Yamashita, N.; Yeung, L. W.; Lam, P. K., Distribution of perfluorinated compounds in surface seawaters between Asia and Antarctica. *Mar Pollut Bull* **2007**, *54*, (11), 1813-8.
21. Cai, M.; Zhao, Z.; Yang, H.; Yin, Z.; Hong, Q.; Sturm, R.; Ebinghaus, R.; Ahrens, L.; Cai, M.; He, J.; Xie, Z., Spatial distribution of per- and polyfluoroalkyl compounds in coastal waters from the East to South China Sea. *Environ Pollut* **2012**, *161*, 162-9.
22. Cai, M.; Yang, H.; Xie, Z.; Zhao, Z.; Wang, F.; Lu, Z.; Sturm, R.; Ebinghaus, R., Per- and polyfluoroalkyl substances in snow, lake, surface runoff water and coastal seawater in Fildes Peninsula, King George Island, Antarctica. *J Hazard Mater* **2012**, *209-210*, 335-42.
23. Guruge, K. S.; Taniyasu, S.; Yamashita, N.; Manage, P. M., Occurrence of perfluorinated acids and fluorotelomers in waters from Sri Lanka. *Mar Pollut Bull* **2007**, *54*, (10), 1667-72.

4. OCEANIC TRANSPORT AND SINKS OF PERFLUOROALKYLATED SUBSTANCES

Supporting Information

González-Gaya B ^{1,2*}, Jurado E. ², Fernández-Castro B. ³, Mouriño-
Carballido B. ³, Siegel D.A. ⁴, Dachs J ², Jiménez B ¹

* Corresponding author b.gonzalez@iqog.csic.es

INDEX

Table S4.1. Stations, positional information and sampling dates of the DCM water samples

Table S4.2. Surrogate recoveries of the DCM samples

Table S4.3. Normality test for the individual PFASs concentrations

Table S4.4. Individual and total concentration (pg L⁻¹) in DCM ocean water samples and total concentration (pg L⁻¹) of surface water samples 1

Figure S4.1. Relative contribution of the individual PFASs at the DCM for each oceanic sub basin

Table S4.5. Non parametric correlation coefficients and significances for individual PFASs between surface and DCM concentrations

Figure S4.2. Comparison of PFASs concentration at surface and DCM water samples

Figure S4.3. Eddy diffusion coefficients (K_p , m²s⁻¹) at the surface and DCM depth

Table S4.6. Mean relative error of modeled DCM concentration (pg L⁻¹)

Figure S4.4. Relative error of modelled DCM concentration per sub basin

Table S4.7. Turbulent fluxes (F_{Eddy} , ng m⁻²day⁻¹)

Figure S4.5. Turbulent fluxes at Surface for PFOS and PFOA (F_{Eddy} , ng m⁻²day⁻¹)

Figure S4.6. Relation between DCM concentrations and $F_{Settling}$ on a logarithmic scale for PFASs with different BCF

Table S4.8. Organic Carbon Sinking fluxes (F_{OC} , mg C m⁻²day⁻¹)

Table S4.9. Biological pump fluxes ($F_{Settling}$, ng m⁻²day⁻¹)

Table S4.1. Stations, positional information and sampling dates of the DCM water samples

Leg*	Station	Ocean	Day	UTC Time	Longitude	Latitude	DCM Depth (m)
1	3	Atlantic	12/19/2010	10:30	-17.285	29.686	98
1	7	Atlantic	12/23/2010	12:40	-23.456	21.456	88
1	8	Atlantic	12/24/2010	10:30	-24.36	20.275	45
1	9	Atlantic	12/25/2010	12:40	-26.018	16.165	75
1	11	Atlantic	12/27/2010	11:53	-26.021	14.514	65
1	12	Atlantic	12/28/2010	10:25	-26.001	9.563	88
1	13	Atlantic	12/29/2010	10:20	-26.011	7.33	55
1	14	Atlantic	12/30/2010	10:35	-26.035	5.021	120
1	15	Atlantic	12/31/2010	10:55	-26.071	2.503	80
1	17	Atlantic	1/2/2011	11:17	-27.348	-3.024	75
1	18	Atlantic	1/3/2011	11:25	-28.167	-4.785	110
1	20	Atlantic	1/5/2011	11:19	-30.191	-9.069	150
1	21	Atlantic	1/6/2011	12:45	-31.465	-11.647	150
1	23	Atlantic	1/8/2011	11:50	-33.435	-15.801	152
1	24	Atlantic	1/9/2011	12:50	-34.669	-18.411	130
1	26	Atlantic	1/11/2011	11:48	-37.001	-23.054	125
2	28	Atlantic	1/20/2011	11:11	-33.366	-24.795	120
2	29	Atlantic	1/21/2011	10:50	-30.151	-25.402	120
2	30	Atlantic	1/22/2011	11:30	-27.591	-25.847	130
2	31	Atlantic	1/23/2011	11:00	-24.257	-26.409	140
2	32	Atlantic	1/24/2011	11:00	-21.433	-26.892	125
2	33	Atlantic	1/25/2011	11:05	-18.084	-27.556	120
2	34	Atlantic	1/26/2011	10:35	-14.792	-28.079	150
2	37	Atlantic	1/29/2011	10:30	-5.424	-29.675	110
2	38	Atlantic	1/30/2011	10:30	-2.441	-30.256	105
2	39	Atlantic	1/31/2011	16:00	1.475	-30.949	110
2	40	Atlantic	2/1/2011	10:40	3.841	-31.317	70
2	41	Atlantic	2/2/2011	10:45	6.752	-31.771	85
2	42	Atlantic	2/3/2011	10:40	9.92	-32.274	72
2	43	Atlantic	2/4/2011	10:35	12.734	-32.771	48
2	44	Atlantic	2/5/2011	10:50	15.479	-33.307	55
3	46	Indian	2/14/2011	8:52	27.494	-34.863	93
3	47	Indian	2/15/2011	7:03	31.05	-34.464	80
3	49	Indian	2/17/2011	8:52	36.981	-33.868	87
3	50	Indian	2/18/2011	6:42	39.872	-33.526	125
3	52	Indian	2/24/2011	5:30	61.483	-30.053	130
3	53	Indian	2/25/2011	6:00	63.259	-27.972	130
3	55	Indian	2/27/2011	5:00	69.424	-29.355	130
3	57	Indian	3/1/2011	5:00	76.066	-29.892	140
3	58	Indian	3/2/2011	4:30	79.612	-29.824	130
3	60	Indian	3/4/2011	4:57	86.252	-29.747	150

3	63	Indian	3/7/2011	3:20	96.416	-29.571	114
3	64	Indian	3/8/2011	3:15	99.999	-29.897	113
3	66	Indian	3/10/2011	3:50	107.25	-30.81	100
3	67	Indian	3/11/2011	2:20	110.22	-31.12	130
4a	70	Indian	3/20/2011	0:55	120.866	-36.634	100
4a	71	Indian	3/21/2011	1:50	124.878	-37.281	75
4a	73	Indian	3/24/2011	0:20	131.592	-38.515	70
4a	75	Indian	3/25/2011	22:21	138.791	-39.853	60
4a	77	Pacific	3/28/2011	23:54	150.436	-38.699	60
4a	78	Pacific	3/29/2011	22:16	150.949	-36.779	80
5	82	Pacific	4/20/2011		-178.24	-23.346	110
5	84	Pacific	4/22/2011		-175.864	-18.562	89
5	86	Pacific	4/24/2011		-173.397	-13.533	105
5	88	Pacific	4/26/2011		-172.367	-9.455	115
5	90	Pacific	4/28/2011		-170.816	-5.732	100
5	92	Pacific	4/30/2011		-168.385	-1.289	65
5	94	Pacific	5/2/2011		-165.734	3.943	80
5	97	Pacific	5/5/2011		-162.398	11.657	89
5	99	Pacific	5/7/2011		-159.443	17.982	140
6	102	Pacific	5/15/2011	19:56	-153.43	21.577	140
6	103	Pacific	5/16/2011	19:56	-150.442	21.063	105
6	106	Pacific	5/19/2011	18:47	-141.635	19.917	125
6	107	Pacific	5/20/2011	19:40	-138.977	19.287	130
6	109	Pacific	5/22/2011	18:30	-133.324	18.075	125
6	110	Pacific	5/23/2011	18:20	-130.634	17.39	110
6	112	Pacific	5/25/2011	17:48	-124.523	15.916	40
6	113	Pacific	5/26/2011	15:10	-121.998	15.31	137
6	114	Pacific	5/27/2011	15:35	-118.776	14.528	88
6	116	Pacific	5/29/2011	18:10	-113.267	13.187	70
6	117	Pacific	5/30/2011	18:50	-110.373	12.475	124
6	120	Pacific	6/2/2011	15:54	-102.459	10.76	37
6	121	Pacific	6/3/2011	15:25	-99.253	10.07	43
6	123	Pacific	6/5/2011	17:20	-93.143	8.809	24
6	124	Pacific	6/6/2011	15:10	-90.341	8.153	23
6	125	Pacific	6/7/2011	15:10	-87.9	7.207	20
7	128	Atlantic	6/21/2011	14:15	-71.772	14.226	97
7	129	Atlantic	6/22/2011	14:52	-69.384	15.068	95
7	131	Atlantic	6/25/2011	13:50	-59.833	17.427	90
7	132	Atlantic	6/26/2011	13:20	-57.845	18.094	160
7	134	Atlantic	6/28/2011	12:30	-52.691	20.014	130
7	135	Atlantic	6/29/2011	12:45	-50.178	20.79	135
7	137	Atlantic	7/1/2011	12:36	-44.531	22.862	137
7	138	Atlantic	7/2/2011	11:05	-41.918	23.766	130
7	140	Atlantic	7/4/2011	11:07	-35.324	26.111	140
7	141	Atlantic	7/5/2011	10:40	-32.924	26.925	150
7	143	Atlantic	7/7/2011	9:50	-26.97	28.874	120

7	144	Atlantic	7/8/2011	10:33	-23.71	29.978	100
7	146	Atlantic	7/10/2011	9:20	-17.286	32.084	110
7	147	Atlantic	7/11/2011	9:30	-14.678	32.846	90

*"Leg" term corresponds with transects: (1) Cadiz (Spain) – Rio de Janeiro (Brazil), (2) Rio de Janeiro (Brazil) – Cape Town (Republic of South Africa), (3) Cape Town (Republic of South Africa) – Perth (Australia), (4) Perth (Australia) – Sydney (Australia), (5) Sydney (Australia) – Honolulu (Hawaii, USA), (6) Honolulu (Hawaii, USA) – Cartagena de Indias (Colombia), (7) Cartagena de Indias (Colombia) – Cartagena (Spain).

Table S4.2. Surrogate recovery data in DCM samples

Standard	PFH _x A - ¹³ C ₂	PFH _x S - ¹⁸ O ₂	PFOA - ¹³ C ₄	PFNA - ¹³ C ₅	PFOS - ¹³ C ₄	PFDA - ¹³ C ₂
Average Recovery %	140	142	96	76	82	87

Table S4.3. Normality test for the individual PFASs concentrations

	Normality Test					
	Kolmogorov-Smirnov ^a			Shapiro-Wilk		
	Statistic	gf	Sig.	Statistic	gf	Sig.
S_PFBs	,168	92	,000	,817	92	,000
S_PFHxA	,236	92	,000	,736	92	,000
S_PFHpA	,158	92	,000	,829	92	,000
S_PFHxS	,348	92	,000	,391	92	,000
S_PFOA	,220	92	,000	,666	92	,000
S_PFHpS	,328	92	,000	,472	92	,000
S_PFNA	,366	92	,000	,434	92	,000
S_FOSA	,286	92	,000	,750	92	,000
S_PFOS	,337	92	,000	,413	92	,000
S_NMeFOSA	,262	92	,000	,719	92	,000
S_PFDA	,372	92	,000	,319	92	,000
S_∑PFCAs	,352	92	,000	,393	92	,000
S_∑PFSA s	,322	92	,000	,409	92	,000
S_∑PFOSA s	,268	92	,000	,739	92	,000
S_∑PFAS s	,320	92	,000	,509	92	,000
DCM_PFBs	,216	92	,000	,651	92	,000
DCM_PFHxA	,258	92	,000	,697	92	,000
DCM_PFHpA	,225	92	,000	,700	92	,000
DCM_PFHxS	,324	92	,000	,428	92	,000
DCM_PFOA	,155	92	,000	,772	92	,000
DCM_PFHpS	,314	92	,000	,519	92	,000
DCM_PFNA	,347	92	,000	,333	92	,000
DCM_FOSA	,261	92	,000	,631	92	,000
DCM_PFOS	,367	92	,000	,290	92	,000
DCM_NMeFOSA	,253	92	,000	,683	92	,000
DCM_PFDA	,326	92	,000	,468	92	,000
DCM_∑PFCAs	,281	92	,000	,503	92	,000
DCM_∑PFSA s	,345	92	,000	,326	92	,000
DCM_∑PFOSA s	,269	92	,000	,713	92	,000
DCM_∑PFAS s	,289	92	,000	,458	92	,000

a. Significance Lilliefors corrected

S attends for Surface samples concentrations and DCM for the DCM ones.

Since all distributions were not normal, non-parametric statistics was applied.

Table S4.4. Individual and total PFAS concentrations ($\mu\text{g L}^{-1}$) in DCM ocean water samples and total PFAS concentrations ($\mu\text{g L}^{-1}$) in surface water samples ¹

station	PFBS	PFHxS	PFHpS	PFOS	PFHxA	PFHpA	PFOA	PFNA	PFDA	PFOSA	N-MePFOSA	Σ PFASs DCM	Σ PFASs surface
2												No sample	1290
3	95.9	18.8	67.6	524	66.2	89.0	186	1050	2120	nd	0.18	4220	355
5												No sample	3130
7												No sample	516
8	32.5	8.54	27.4	99.0	11.9	37.4	78.5	363	1230	nd	0.36	1890	353
9	50.0	6.88	5.36	37.2	19.0	11.3	33.1	27.7	72.9	nd	nd	263	2940
11	68.0	7.14	24.6	34.2	46.4	11.9	32.0	24.9	50.5	nd	nd	300	285
12	119	5.10	2.34	74.3	90.4	25.3	51.4	254	525	nd	nd	1150	340
13	9.40	4.88	2.86	53.2	26.8	15.7	38.1	123	489	nd	0.39	763	4000
14	25.8	6.88	2.22	55.1	45.1	14.1	44.0	139	643	nd	nd	975	1140
15	4.62	2.65	1.34	16.2	26.4	6.33	22.2	22.4	97.9	nd	nd	200	300
17	95.3	316	85.4	3400	249	8.47	53.2	25.0	144	0.82	nd	4370	9040
18	106	193	56.3	1910	100	9.37	34.9	27.7	64.5	nd	nd	2500	5630
20	24.0	681	108	9580	12.0	21.0	77.0	40.0	149	17.0	3.00	10700	4480

station	PFBS	PFHxS	PFHpS	PFOS	PFHxA	PFHpA	PFOA	PFNA	PFDA	PFOSA	N-MePFOSA	ΣPFASs DCM	ΣPFASs surface
21	57.8	140	96.4	1620	32.3	12.8	54.0	18.4	96.6	nd	nd	2130	7150
23	56.3	134	25.7	844	30.8	6.15	23.4	15.0	148	nd	0.03	1280	6230
24	83.9	138	27.7	902	51.5	19.7	49.2	84.3	629	nd	0.03	1990	10900
26	10.8	53.9	14.5	509	11.0	6.99	26.9	33.7	769	0.03	0.11	1440	500
28	26.9	21.3	5.34	404	nd	4.02	20.3	5.91	37.7	nd	nd	526	1630
29	103	36.2	6.83	506	17.7	16.1	43.2	90.5	78.9	nd	nd	898	3510
30	40.2	92.5	20.9	1340	71.0	10.3	46.1	45.1	14.4	nd	nd	1680	2750
31	85.6	55.6	8.63	667	6.03	40.9	81.4	384	110	nd	nd	1440	2090
32	62.76	14.58	1.835	189.6	nd	4.900	18.47	24.57	29.35	nd	nd	346.1	1941
33	480.0	50.00	18.40	1101	39.00	54.00	32.00	10.00	nd	6.000	9.000	1799	1127
35	46.14	19.22	4.083	319.0	nd	8.490	18.38	4.240	4.770	nd	nd	424.3	733.2
37	32.18	19.76	2.172	220.2	nd	10.76	23.28	8.460	6.560	nd	nd	323.4	304.9
38	72.33	40.81	4.583	275.2	nd	5.930	27.82	9.320	7.960	nd	nd	443.9	732.3
39	59.33	18.89	2.729	209.2	nd	6.380	19.78	7.610	1.080	nd	nd	325.0	409.2
40	67.80	31.98	1.068	277.0	nd	10.21	20.75	9.580	4.590	nd	nd	422.9	619.6
41	39.49	44.08	6.870	325.0	3.060	10.78	31.59	14.99	6.160	nd	nd	482.0	1249
42	68.67	34.57	2.199	332.0	2.970	3.340	19.76	12.80	4.840	nd	nd	480.7	1102

station	PFBS	PFHxS	PFHpS	PFOS	PFHxA	PFHpA	PFOA	PFNA	PFDA	PFOSA	N-MePFOSA	ΣPFASs DCM	ΣPFASs surface
43	148.7	77.36	8.695	547.0	13.29	6.720	34.35	9.200	4.250	nd	nd	849.4	644.6
44	14.07	20.48	1.330	337.2	nd	3.120	25.52	13.28	3.380	nd	nd	418.5	424.2
46	14.33	15.47	2.449	76.82	2.490	11.70	21.32	43.86	268.9	nd	nd	457.3	328.8
47	15.31	8.890	2.571	49.36	6.260	11.69	20.53	60.87	285.4	nd	nd	460.9	551.4
49	3.340	10.10	1.686	55.65	10.17	6.180	18.71	15.46	63.36	nd	0.060	184.7	180.6
50	24.03	6.240	1.535	31.13	8.145	9.550	24.33	102.2	757.0	nd	nd	964.1	263.2
52	36.72	9.330	2.971	102.0	8.895	4.040	18.34	20.20	152.1	nd	nd	354.6	285.3
53	51.03	10.72	2.059	60.54	40.50	6.830	16.18	8.850	10.21	nd	nd	206.9	278.0
55	3.540	7.600	1.623	68.77	36.45	5.400	10.95	7.170	46.71	nd	nd	188.2	239.0
57	18.33	9.480	2.201	55.33	20.64	3.800	12.38	13.76	138.3	nd	nd	274.3	823.3
58												No sample	757.5
60	29.08	8.040	1.652	124.5	nd	7.040	24.17	42.63	143.1	nd	nd	380.2	741.8
63	133.7	10.98	2.193	159.4	22.51	7.190	19.64	74.68	189.5	nd	nd	619.7	519.1
64	32.00	25.00	0.138	215.0	69.00	nd	19.00	59.00	415.0	6.000	3.000	843.1	373.8
66	255.0	32.97	10.80	458.0	51.52	16.93	43.72	58.40	154.1	0.300	nd	1082	1676
67	167.0	33.00	nd	631.0	nd	175.0	40.00	124.0	2193	18.00	15.00	3396	1976
70	14.47	5.340	2.340	84.61	22.59	0.900	20.11	8.340	13.75	nd	0.290	172.7	245.3

station	PFBS	PFHxS	PFHpS	PFOS	PFHxA	PFHpA	PFOA	PFNA	PFDA	PFOSA	N-MePFOSA	ΣPFASs DCM	ΣPFASs surface
71	8.360	4.210	1.711	85.48	nd	nd	14.94	4.570	10.48	nd	0.230	130.0	176.0
74	29.30	8.570	1.524	146.1	13.95	8.540	34.29	88.21	109.5	nd	0.255	440.2	429.0
75	23.68	5.270	1.519	59.37	36.33	7.350	21.54	33.46	100.3	nd	0.230	289.0	479.7
77	82.54	16.32	3.206	197.6	21.24	6.405	31.64	94.02	64.67	nd	0.240	517.9	255.6
78	14.17	11.02	5.759	121.9	7.8	nd	34.56	14.38	34.90	nd	0.250	244.8	No sample
82	120.3	15.03	3.835	200.5	30.47	3.540	33.26	16.59	40.71	nd	0.350	464.5	372.2
84	nd	7.000	130.62	185.0	75.00	nd	25.00	47.00	335.0	6.000	9.000	819.6	622.2
86	nd	nd	2.155	357.0	85.50	34.50	31.00	19.00	109.0	6.000	9.000	653.2	640.2
88	3.000	14.00	4.978	102.0	nd	106.0	24.00	32.00	353.0	6.000	9.000	654.0	966.8
90	nd	6.000	42.24	227.0	18.0	156.0	21.00	6.000	34.00	6.000	18.00	534.3	552.2
92	15.00	7.500	13.70	264.0	nd	116.0	44.00	16.00	140.0	6.000	9.000	631.2	584.8
94	26.07	137.2	39.97	220.4	nd	29.63	32.68	16.27	61.81	2.890	3.160	570.1	852.2
97	8.770	24.21	2.960	108.9	nd	37.10	28.81	48.33	323.6	2.230	2.750	587.7	489.6
99	116.4	96.30	226.0	232.9	nd	120.1	59.43	28.49	185.3	2.690	2.710	1070	2503
102	140.8	124.2	14.50	145.5	nd	13.35	39.20	24.88	98.19	2.610	3.250	606.5	493.1
103	41.75	48.43	nd	85.89	217.0	49.70	27.79	23.75	22.53	2.220	3.140	522.2	470.4
106	27.43	37.15	nd	121.8	nd	25.85	18.52	16.78	18.67	2.540	2.790	271.6	496.8

station	PFBS	PFHxS	PFHpS	PFOS	PFHxA	PFHpA	PFOA	PFNA	PFDA	PFOSA	N-MePFOSA	ΣPFASs DCM	ΣPFASs surface
107	66.29	22.56	55.36	128.3	129.2	30.19	20.96	17.69	10.84	2.850	3.310	487.5	412.6
109	26.84	125.8	4.713	102.1	nd	33.66	34.66	40.59	21.74	2.100	3.030	395.2	572.7
110	43.84	72.91	nd	134.4	nd	15.51	32.76	13.02	35.85	2.630	2.660	353.6	823.7
112	29.52	19.05	19.71	103.4	94.42	44.96	22.80	19.93	35.73	3.290	3.150	396.0	376.3
113	25.57	nd	13.91	68.24	139.1	86.41	8.380	nd	7.940	2.510	3.050	355.1	526.5
114	nd	nd	19.02	86.00	nd	50.00	40.00	17.00	29.00	6.000	9.000	256.0	895.9
116	34.94	71.91	nd	91.88	nd	84.09	17.28	11.61	5.250	3.045	3.630	323.6	359.4
117	17.99	36.32	10.39	26.53	nd	26.90	5.330	nd	15.46	2.500	2.740	144.2	548.3
120	nd	6.000	12.29	20.00	96.00	147.0	17.00	9.000	22.00	6.000	9.000	344.3	635.6
121	51.17	nd	3.991	59.80	182.6	114.4	21.92	0.450	nd	2.360	2.610	439.3	344.1
123	145.3	3.000	0.201	60.00	nd	nd	102.0	18.00	84.00	3.000	3.000	418.5	505.4
124	54.00	8.000	0.201	24.00	nd	10.50	19.00	3.000	13.00	3.000	3.000	137.7	443.7
125	34.00	8.000	44.10	136.00	141.0	51.00	12.00	nd	nd	3.000	4.000	433.1	374.5
128	75.00	5.000	0.201	69.00	nd	36.00	30.00	12.00	164.1	3.000	5.000	399.3	360.1
129	36.00	14.00	54.06	126.0	108.0	12.00	50.00	15.00	106.0	4.000	7.000	532.1	371.3
131	144.1	25.00	51.21	257.6	nd	39.00	34.00	18.00	nd	5.000	12.00	586.0	780.0
132	19.00	3.000	6.425	33.00	nd	15.00	43.00	15.00	nd	3.000	3.000	140.4	130.7

station	PFBS	PFHxS	PFHpS	PFOS	PFHxA	PFHpA	PFOA	PFNA	PFDA	PFOSA	N-MePFOSA	ΣPFASs DCM	ΣPFASs surface
134	29.00	2.000	0.201	19.00	nd	16.50	52.00	15.00	3.000	3.000	3.000	142.7	235.9
135	28.00	13.00	0.201	32.00	nd	52.00	51.00	16.00	6.000	3.000	3.000	204.2	206.7
137	18.00	7.000	5.033	44.00	43.50	29.00	48.00	18.00	8.000	3.000	3.000	226.5	189.2
138	21.00	12.00	0.201	40.00	144.0	nd	54.00	16.00	10.00	3.000	3.000	303.2	183.5
140	14.00	7.000	0.201	47.00	nd	24.00	13.00	5.000	15.00	3.000	3.000	131.2	313.0
141	21.00	6.000	nd	29.00	33.00	19.00	53.00	16.00	3.000	3.000	3.000	186.0	311.0
143	17.00	nd	nd	34.00	43.50	30.00	38.00	20.00	8.000	3.000	3.000	196.5	226.0
144	28.00	3.000	nd	31.00	73.50	58.00	45.00	18.00	13.00	3.000	3.000	275.5	302.0
146	28.00	3.000	8.046	53.00	nd	25.00	63.00	18.00	7.000	3.000	3.000	211.1	330.0
147	17.00	3.000	nd	37.00	nd	18.00	79.00	32.00	8.000	3.000	3.000	200.0	441.0

nd: non detected

Figure S4.1. Relative contribution of the individual PFASs at the DCM for each oceanic sub basin

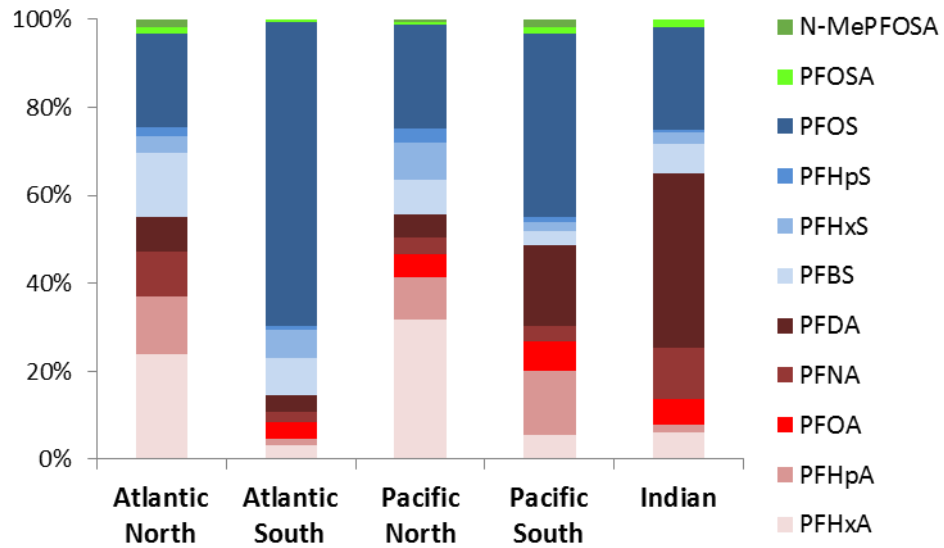


Table S4.5. Non parametric correlation coefficients and significances for individual PFASs between surface and DCM concentrations

Compound	Correl. Coeff.	Sig.
PFBS	.332	.000**
PFHxS	.445	.000**
PFHpS	.245	.001**
PFOS	.588	.000**
PFHxA	.113	.124
PFHpA	.393	.000**
PFOA	.261	.000**
PFNA	.271	.000**
PFDA	.435	.000**
FOSA	.577	.000**
NMeFOSA	.572	.000**

Non-parametric Kendall's Tau

** . P < 0,01 (bilateral).

* . P < 0,05 (bilateral).

Figure S4.2. Comparison of PFASs concentration at surface and DCM water samples

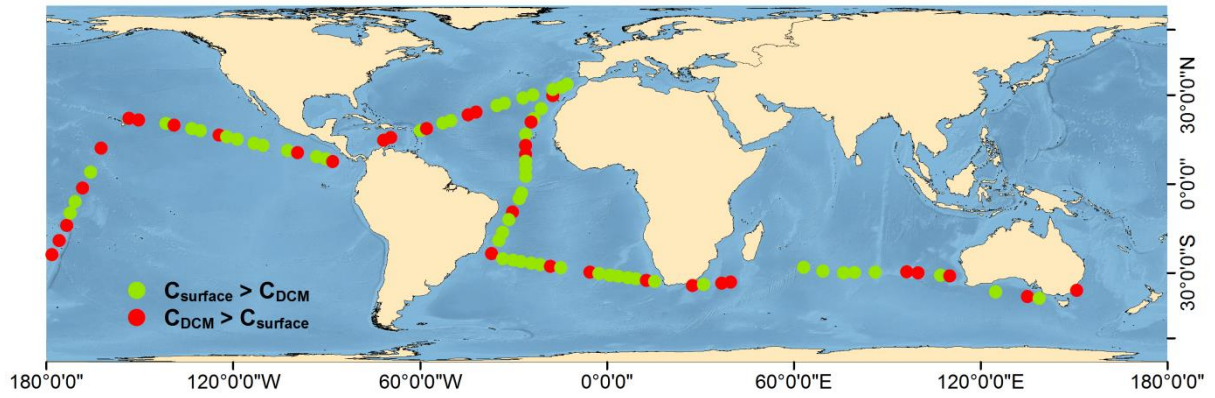
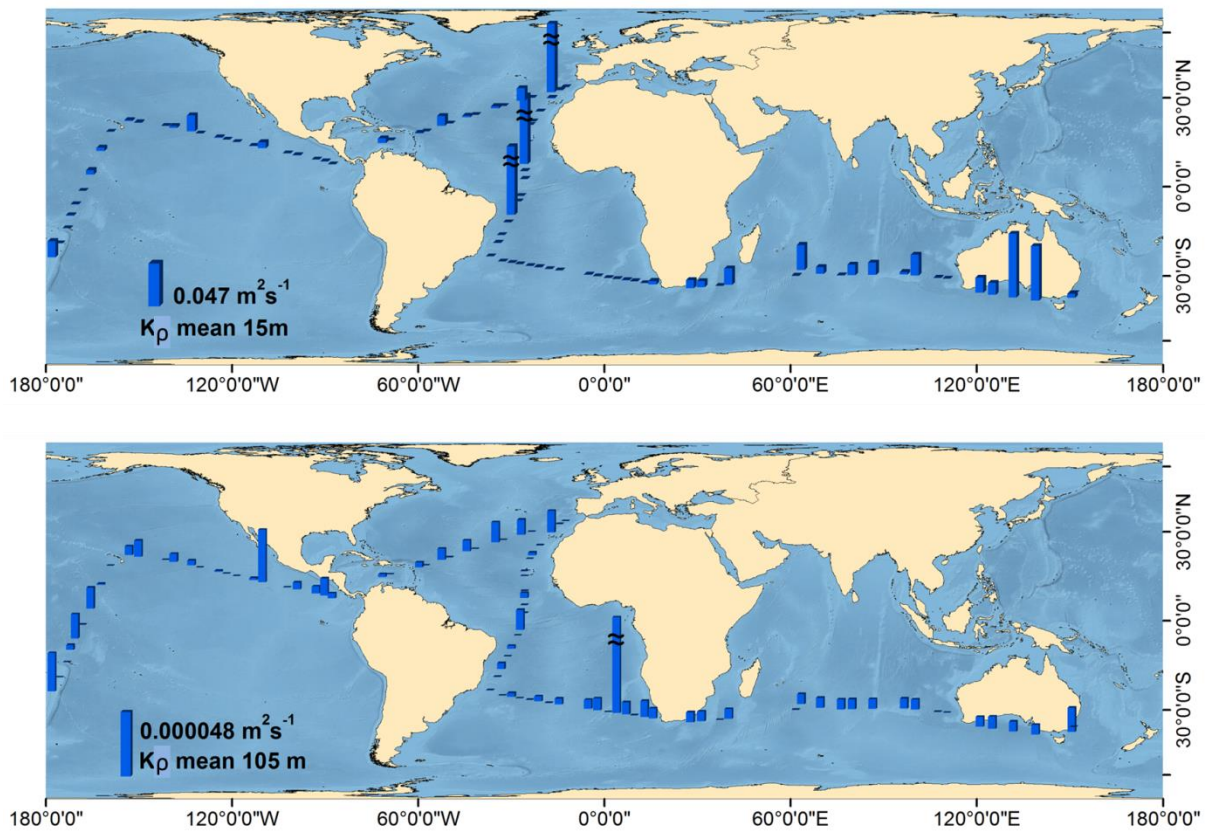


Figure S4.3. Eddy diffusion coefficients (K_ρ , m^2s^{-1}) at the surface and DCM depth



Top panel shows the value of K_ρ at 15 m, corresponding to the surface diffusivity (shallower diffusivity is not considered due to variability induced by non-diffusion processes like waves and wind shear). Bottom panel shows the value of K_ρ at 105 m, close to the mean DCM depth during Malaspina 2010 campaign.

Bars with \approx symbol have been diminished by a factor of 10 in order to ease the global comparison of all the measurements.

Table S4.6. Mean relative error of modeled DCM concentration (pg L^{-1})

	Mean error
PFBS	38.37
PFHxS	39.01
PFHpS	13.66
PFOS	323.51
PFHxA	13.91
PFHpA	21.53
PFOA	23.11
PFNA	51.69
PFDA	145.95
PFOSA	1.96
N-MePFOSA	2.24

Figure S4.4. Relative error of modelled DCM concentration per sub basin

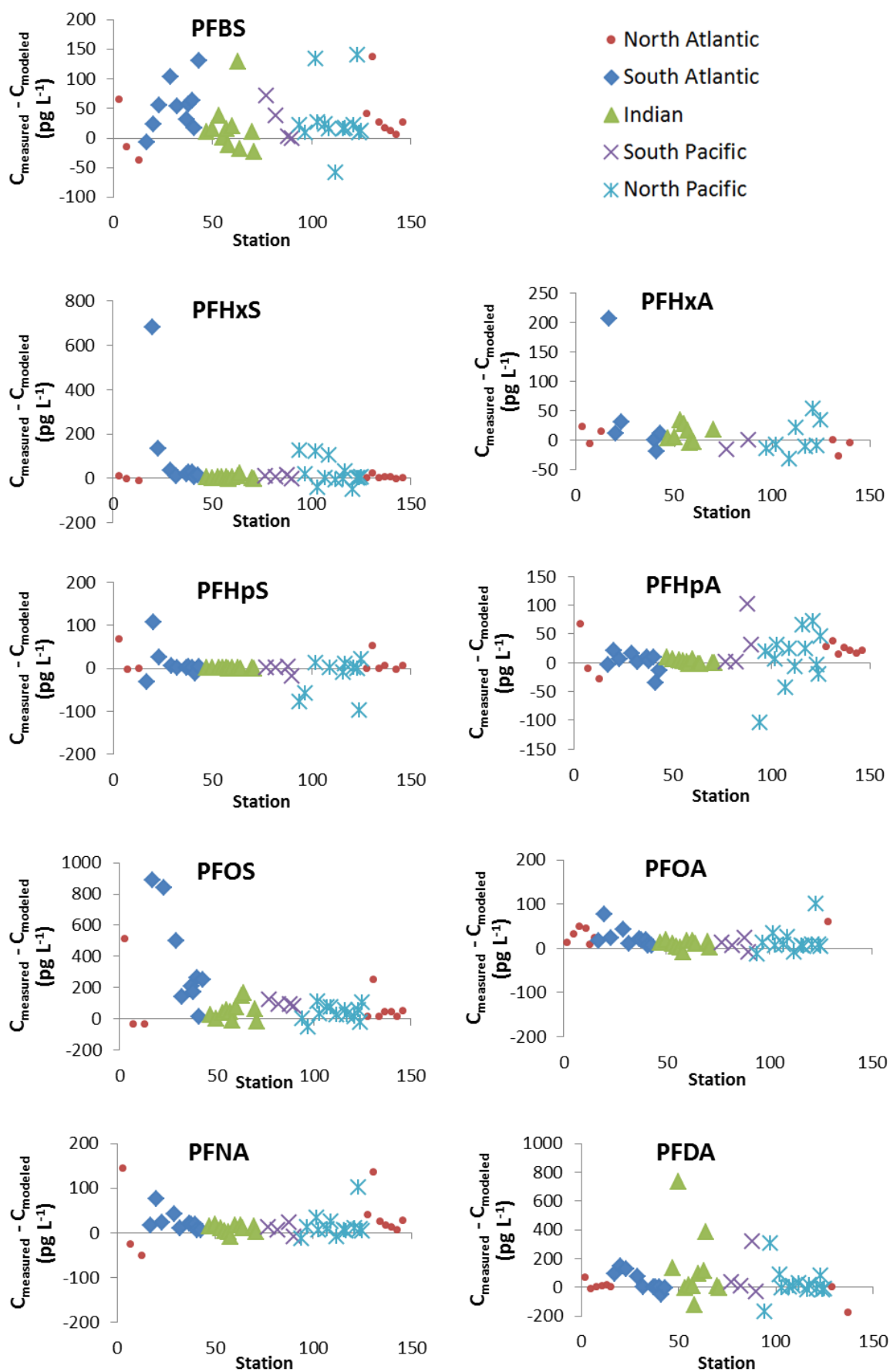


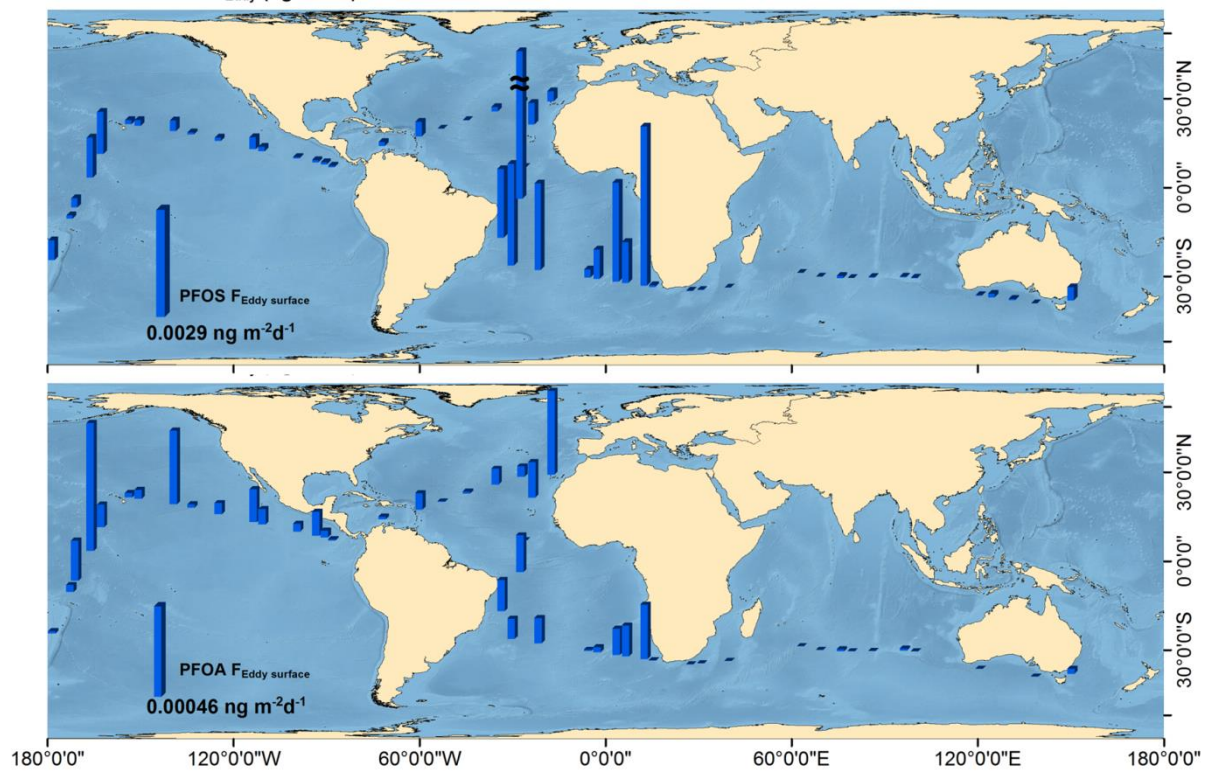
Table S4.7. Turbulent fluxes (F_{Eddy} , ng m⁻²day⁻¹)

Station	Surface Turbulent Fluxes									DCM Turbulent Fluxes								
	PFBS	PFBS	PFHxS	PFHpS	PFOS	PFOA	PFHpA	PFHxA	PFNA	PFBS	PFHxS	PFHpS	PFOS	PFOA	PFHpA	PFHxA	PFNA	PFDA
3	8,85 10 ⁻⁴	8,85 10 ⁻⁴	3,81 10 ⁻⁴	8,62 10 ⁻⁶	3,81 10 ⁻⁴	5,98 10 ⁻⁴	5,98 10 ⁻⁴	2,16 10 ⁻⁴	8,03 10 ⁻⁴	9,67 10 ⁻⁴	2,35 10 ⁻⁴	1,61 10 ⁻⁵	4,16 10 ⁻⁴	1,28 10 ⁻³	6,53 10 ⁻⁴	1,34 10 ⁻³	8,76 10 ⁻⁴	4,16 10 ⁻³
7	3,73 10 ⁻⁴	3,73 10 ⁻⁴	7,95 10 ⁻⁴	1,36 10 ⁻⁵	7,95 10 ⁻⁴	2,55 10 ⁻⁴	2,55 10 ⁻⁴	1,03 10 ⁻⁴	7,60 10 ⁻⁴	1,00 10 ⁻⁴	2,77 10 ⁻⁵	1,59 10 ⁻⁵	2,14 10 ⁻⁴	1,58 10 ⁻⁴	6,85 10 ⁻⁵	4,09 10 ⁻⁵	2,04 10 ⁻⁴	1,13 10 ⁻³
13	5,86 10 ⁻⁷	5,86 10 ⁻⁷	1,08 10 ⁻⁶	1,26 10 ⁻⁶	1,08 10 ⁻⁶	5,53 10 ⁻⁷	5,53 10 ⁻⁷	2,03 10 ⁻⁷	7,39 10 ⁻⁶	2,07 10 ⁻⁴	7,17 10 ⁻⁵	2,01 10 ⁻⁵	3,82 10 ⁻⁴	3,99 10 ⁻⁴	1,95 10 ⁻⁴	5,63 10 ⁻⁵	2,61 10 ⁻³	8,39 10 ⁻³
17	2,22 10 ⁻³	2,22 10 ⁻³	5,42 10 ⁻²	6,40 10 ⁻⁶	5,42 10 ⁻²	2,64 10 ⁻⁴	2,64 10 ⁻⁴	1,17 10 ⁻²	2,49 10 ⁻⁴	8,01 10 ⁻⁴	2,88 10 ⁻³	6,24 10 ⁻⁴	1,96 10 ⁻²	2,68 10 ⁻⁴	9,53 10 ⁻⁵	3,12 10 ⁻⁴	9,00 10 ⁻⁵	3,98 10 ⁻⁴
20	2,04 10 ⁻⁶	2,04 10 ⁻⁶	4,52 10 ⁻⁵	3,44 10 ⁻⁵	4,52 10 ⁻⁵	1,89 10 ⁻⁷	1,89 10 ⁻⁷	4,84 10 ⁻⁶	4,32 10 ⁻⁷	2,75 10 ⁻⁶	6,54 10 ⁻⁶	1,73 10 ⁻⁶	6,10 10 ⁻⁵	1,08 10 ⁻⁶	2,56 10 ⁻⁷	2,53 10 ⁻⁶	5,84 10 ⁻⁷	3,45 10 ⁻⁶
23	3,21 10 ⁻⁴	3,21 10 ⁻⁴	2,54 10 ⁻³	3,94 10 ⁻⁶	2,54 10 ⁻³	2,24 10 ⁻⁴	2,24 10 ⁻⁴	4,00 10 ⁻⁴	3,25 10 ⁻³	7,03 10 ⁻⁶	8,76 10 ⁻⁶	1,26 10 ⁻⁶	5,56 10 ⁻⁵	9,17 10 ⁻⁶	4,90 10 ⁻⁶	2,80 10 ⁻⁶	7,11 10 ⁻⁵	2,77 10 ⁻⁴
29	9,20 10 ⁻⁵	9,20 10 ⁻⁵	3,75 10 ⁻³	3,40 10 ⁻⁶	3,75 10 ⁻³	1,45 10 ⁻⁴	1,45 10 ⁻⁴	3,11 10 ⁻⁴	1,51 10 ⁻⁴	3,49 10 ⁻⁶	1,18 10 ⁻⁵	2,38 10 ⁻⁶	1,42 10 ⁻⁴	8,70 10 ⁻⁶	5,50 10 ⁻⁶	-	5,73 10 ⁻⁶	3,19 10 ⁻⁶
32	4,97 10 ⁻⁴	4,97 10 ⁻⁴	3,19 10 ⁻³	3,31 10 ⁻⁵	3,19 10 ⁻³	1,80 10 ⁻⁴	1,80 10 ⁻⁴	3,12 10 ⁻⁴	2,78 10 ⁻³	5,00 10 ⁻⁵	3,14 10 ⁻⁵	4,60 10 ⁻⁶	3,20 10 ⁻⁴	4,94 10 ⁻⁵	1,81 10 ⁻⁵	-	2,79 10 ⁻⁴	1,50 10 ⁻⁴
37	-	-	3,03 10 ⁻⁴	4,40 10 ⁻⁶	3,03 10 ⁻⁴	8,22 10 ⁻⁶	8,22 10 ⁻⁶	1,97 10 ⁻⁵	7,16 10 ⁻⁶	-	3,00 10 ⁻⁵	4,36 10 ⁻⁶	4,63 10 ⁻⁴	5,67 10 ⁻⁵	1,26 10 ⁻⁵	-	1,09 10 ⁻⁵	1,24 10 ⁻⁵
38	1,56 10 ⁻⁴	1,56 10 ⁻⁴	1,08 10 ⁻³	2,84 10 ⁻⁵	1,08 10 ⁻³	3,77 10 ⁻⁵	3,77 10 ⁻⁵	1,52 10 ⁻⁴	4,56 10 ⁻⁵	2,64 10 ⁻⁴	2,57 10 ⁻⁴	2,89 10 ⁻⁵	1,83 10 ⁻³	1,45 10 ⁻⁴	6,38 10 ⁻⁵	-	7,72 10 ⁻⁵	5,91 10 ⁻⁵
40	1,06 10 ⁻³	1,06 10 ⁻³	3,65 10 ⁻³	8,15 10 ⁻⁷	3,65 10 ⁻³	1,89 10 ⁻⁴	1,89 10 ⁻⁴	7,92 10 ⁻⁴	8,51 10 ⁻⁵	1,48 10 ⁻⁴	1,11 10 ⁻⁴	6,12 10 ⁻⁶	5,10 10 ⁻⁴	4,11 10 ⁻⁵	2,65 10 ⁻⁵	8,32 10 ⁻⁸	1,19 10 ⁻⁵	4,85 10 ⁻⁶
41	1,05 10 ⁻⁴	1,05 10 ⁻⁴	1,51 10 ⁻³	3,54 10 ⁻⁴	1,51 10 ⁻³	2,20 10 ⁻⁴	2,20 10 ⁻⁴	1,79 10 ⁻⁴	9,84 10 ⁻⁵	2,87 10 ⁻⁴	4,90 10 ⁻⁴	2,41 10 ⁻⁴	4,13 10 ⁻³	3,28 10 ⁻⁴	6,00 10 ⁻⁴	3,05 10 ⁻⁴	2,69 10 ⁻⁴	7,16 10 ⁻⁴
43	3,53 10 ⁻⁴	3,53 10 ⁻⁴	5,86 10 ⁻³	4,39 10 ⁻⁶	5,86 10 ⁻³	3,89 10 ⁻⁴	3,89 10 ⁻⁴	1,27 10 ⁻³	2,87 10 ⁻⁴	3,63 10 ⁻⁴	1,30 10 ⁻³	9,38 10 ⁻⁵	6,03 10 ⁻³	5,65 10 ⁻⁴	4,00 10 ⁻⁴	5,16 10 ⁻⁵	2,95 10 ⁻⁴	1,82 10 ⁻⁴
44	1,08 10 ⁻⁵	1,08 10 ⁻⁵	7,77 10 ⁻⁵	8,03 10 ⁻⁶	7,77 10 ⁻⁵	1,55 10 ⁻⁶	1,55 10 ⁻⁶	9,19 10 ⁻⁶	2,18 10 ⁻⁶	2,70 10 ⁻⁴	2,30 10 ⁻⁴	1,33 10 ⁻⁵	1,95 10 ⁻³	1,51 10 ⁻⁴	3,88 10 ⁻⁵	1,06 10 ⁻⁵	5,45 10 ⁻⁵	2,06 10 ⁻⁵
46	1,22 10 ⁻⁶	1,22 10 ⁻⁶	1,40 10 ⁻⁵	1,54 10 ⁻⁵	1,40 10 ⁻⁵	9,52 10 ⁻⁷	9,52 10 ⁻⁷	9,34 10 ⁻⁷	5,27 10 ⁻⁶	3,58 10 ⁻⁵	2,74 10 ⁻⁵	1,79 10 ⁻⁵	4,10 10 ⁻⁴	1,03 10 ⁻⁴	2,79 10 ⁻⁵	1,80 10 ⁻⁵	1,55 10 ⁻⁴	8,12 10 ⁻⁴
47	2,11 10 ⁻⁶	2,11 10 ⁻⁶	1,14 10 ⁻⁵	7,92 10 ⁻⁶	1,14 10 ⁻⁵	1,11 10 ⁻⁶	1,11 10 ⁻⁶	1,18 10 ⁻⁶	8,61 10 ⁻⁶	5,18 10 ⁻⁵	2,89 10 ⁻⁵	1,09 10 ⁻⁵	2,81 10 ⁻⁴	7,66 10 ⁻⁵	2,73 10 ⁻⁵	2,94 10 ⁻⁵	2,12 10 ⁻⁴	1,68 10 ⁻³
50	2,22 10 ⁻⁶	2,22 10 ⁻⁶	7,53 10 ⁻⁶	9,78 10 ⁻⁶	7,53 10 ⁻⁶	8,26 10 ⁻⁷	8,26 10 ⁻⁷	1,21 10 ⁻⁶	1,76 10 ⁻⁶	9,15 10 ⁻⁵	4,97 10 ⁻⁵	8,17 10 ⁻⁶	3,10 10 ⁻⁴	6,55 10 ⁻⁵	3,40 10 ⁻⁵	4,23 10 ⁻⁵	7,27 10 ⁻⁵	2,48 10 ⁻⁴
53	4,49 10 ⁻⁶	4,49 10 ⁻⁶	2,92 10 ⁻⁸	1,75 10 ⁻⁵	8,38 10 ⁻⁶	6,71 10 ⁻⁷	6,71 10 ⁻⁷	1,17 10 ⁻⁶	8,05 10 ⁻⁷	2,30 10 ⁻⁴	6,02 10 ⁻⁵	1,52 10 ⁻⁵	4,29 10 ⁻⁴	1,14 10 ⁻⁴	3,44 10 ⁻⁵	1,10 10 ⁻⁴	4,13 10 ⁻⁵	2,64 10 ⁻⁴
55	1,62 10 ⁻⁶	1,62 10 ⁻⁶	8,38 10 ⁻⁶	5,82 10 ⁻⁶	8,07 10 ⁻⁶	1,17 10 ⁻⁶	1,17 10 ⁻⁶	1,09 10 ⁻⁶	2,48 10 ⁻⁶	3,22 10 ⁻⁵	2,16 10 ⁻⁵	4,62 10 ⁻⁶	1,60 10 ⁻⁴	7,41 10 ⁻⁵	2,32 10 ⁻⁵	9,99 10 ⁻⁵	4,94 10 ⁻⁵	3,33 10 ⁻⁴
57	1,75 10 ⁻⁵	1,75 10 ⁻⁵	8,07 10 ⁻⁶	9,14 10 ⁻⁶	7,88 10 ⁻⁵	1,68 10 ⁻⁵	1,68 10 ⁻⁵	9,52 10 ⁻⁶	1,93 10 ⁻⁴	2,88 10 ⁻⁵	1,57 10 ⁻⁵	6,42 10 ⁻⁶	1,30 10 ⁻⁴	1,12 10 ⁻⁴	2,76 10 ⁻⁵	5,66 10 ⁻⁵	3,17 10 ⁻⁴	1,49 10 ⁻³
58	4,16 10 ⁻⁶	4,16 10 ⁻⁶	7,88 10 ⁻⁵	5,95 10 ⁻⁶	4,71 10 ⁻⁶	8,93 10 ⁻⁷	8,93 10 ⁻⁷	5,88 10 ⁻⁷	1,09 10 ⁻⁵	1,36 10 ⁻⁴	1,93 10 ⁻⁵	4,72 10 ⁻⁶	1,55 10 ⁻⁴	1,01 10 ⁻⁴	2,93 10 ⁻⁵	6,27 10 ⁻⁵	3,59 10 ⁻⁴	1,43 10 ⁻³
60	4,23 10 ⁻⁶	4,23 10 ⁻⁶	4,71 10 ⁻⁶	3,37 10 ⁻⁵	2,49 10 ⁻⁵	6,63 10 ⁻⁷	6,63 10 ⁻⁷	4,45 10 ⁻⁷	8,28 10 ⁻⁶	1,41 10 ⁻⁴	1,48 10 ⁻⁵	2,25 10 ⁻⁵	8,31 10 ⁻⁴	1,30 10 ⁻⁴	2,21 10 ⁻⁵	5,36 10 ⁻⁵	2,76 10 ⁻⁴	7,56 10 ⁻⁴
63	6,69 10 ⁻⁶	6,69 10 ⁻⁶	2,49 10 ⁻⁵	7,00 10 ⁻⁷	2,14 10 ⁻⁵	1,51 10 ⁻⁵	1,51 10 ⁻⁵	3,35 10 ⁻⁶	1,10 10 ⁻⁵	9,82 10 ⁻⁵	4,91 10 ⁻⁵	6,80 10 ⁻⁷	3,14 10 ⁻⁴	5,40 10 ⁻⁵	2,21 10 ⁻⁴	-	1,62 10 ⁻⁴	1,62 10 ⁻³
64	2,50 10 ⁻⁵	2,50 10 ⁻⁵	2,14 10 ⁻⁵	3,97 10 ⁻⁶	2,54 10 ⁻⁵	9,61 10 ⁻⁷	9,61 10 ⁻⁷	1,31 10 ⁻⁶	3,64 10 ⁻⁶	5,66 10 ⁻⁴	2,96 10 ⁻⁵	3,79 10 ⁻⁶	5,75 10 ⁻⁴	9,71 10 ⁻⁵	2,18 10 ⁻⁵	-	8,26 10 ⁻⁵	3,37 10 ⁻⁴
70	3,67 10 ⁻⁶	3,67 10 ⁻⁶	2,54 10 ⁻⁵	3,90 10 ⁻⁵	2,29 10 ⁻⁵	7,20 10 ⁻⁷	7,20 10 ⁻⁷	1,56 10 ⁻⁶	1,92 10 ⁻⁶	2,04 10 ⁻⁴	8,68 10 ⁻⁵	3,93 10 ⁻⁵	1,28 10 ⁻³	2,39 10 ⁻⁴	4,00 10 ⁻⁵	3,01 10 ⁻⁴	1,07 10 ⁻⁴	1,28 10 ⁻⁴
71	3,97 10 ⁻⁵	3,97 10 ⁻⁵	2,29 10 ⁻⁵	1,15 10 ⁻⁶	1,28 10 ⁻⁴	-	-	6,90 10 ⁻⁶	9,22 10 ⁻⁶	4,07 10 ⁻⁴	7,07 10 ⁻⁵	2,15 10 ⁻⁵	1,32 10 ⁻³	1,65 10 ⁻⁴	-	-	9,45 10 ⁻⁵	1,84 10 ⁻⁴
74	9,58 10 ⁻⁷	9,58 10 ⁻⁷	1,28 10 ⁻⁴	2,76 10 ⁻⁵	5,08 10 ⁻⁵	-	-	1,75 10 ⁻⁶	6,82 10 ⁻⁶	4,11 10 ⁻⁵	7,50 10 ⁻⁵	3,65 10 ⁻⁵	2,18 10 ⁻³	2,24 10 ⁻⁴	-	-	2,92 10 ⁻⁴	8,91 10 ⁻⁴

Station	Surface Turbulent Fluxes									DCM Turbulent Fluxes								
	PFBS	PFBS	PFHxS	PFHpS	PFOS	PFOA	PFHpA	PFHxA	PFNA	PFBS	PFHxS	PFHpS	PFOS	PFOA	PFHpA	PFHxA	PFNA	PFDA
75	1,77 10 ⁻⁶	1,77 10 ⁻⁶	5,08 10 ⁻⁵	2,35 10 ⁻⁵	8,72 10 ⁻⁶	1,59 10 ⁻⁶	1,59 10 ⁻⁶	6,71 10 ⁻⁷	1,20 10 ⁻⁵	1,05 10 ⁻⁴	3,99 10 ⁻⁵	3,15 10 ⁻⁵	5,18 10 ⁻⁴	2,68 10 ⁻⁴	9,43 10 ⁻⁵	1,50 10 ⁻⁴	7,13 10 ⁻⁴	2,99 10 ⁻³
77	7,06 10 ⁻⁵	7,06 10 ⁻⁵	8,72 10 ⁻⁶	6,02 10 ⁻⁶	4,94 10 ⁻⁴	3,57 10 ⁻⁵	3,57 10 ⁻⁵	4,32 10 ⁻⁵	1,28 10 ⁻⁴	1,40 10 ⁻⁴	8,54 10 ⁻⁵	2,64 10 ⁻⁵	9,77 10 ⁻⁴	2,37 10 ⁻⁴	7,05 10 ⁻⁵	4,81 10 ⁻⁴	2,52 10 ⁻⁴	3,43 10 ⁻⁴
82	5,54 10 ⁻⁴	5,54 10 ⁻⁴	4,94 10 ⁻⁴	7,48 10 ⁻⁶	7,33 10 ⁻⁴	1,57 10 ⁻⁵	1,57 10 ⁻⁵	6,72 10 ⁻⁵	8,68 10 ⁻⁵	2,33 10 ⁻⁴	2,83 10 ⁻⁵	7,02 10 ⁻⁶	3,08 10 ⁻⁴	7,40 10 ⁻⁵	6,59 10 ⁻⁶	-	3,65 10 ⁻⁵	9,12 10 ⁻⁵
88	-	-	7,33 10 ⁻⁴	8,83 10 ⁻⁶	1,34 10 ⁻⁴	5,15 10 ⁻⁵	5,15 10 ⁻⁵	8,44 10 ⁻⁶	3,88 10 ⁻⁵	-	1,23 10 ⁻⁶	5,95 10 ⁻⁷	1,96 10 ⁻⁵	2,96 10 ⁻⁶	7,52 10 ⁻⁶	1,11 10 ⁻⁶	5,67 10 ⁻⁶	7,85 10 ⁻⁵
90	-	-	1,34 10 ⁻⁴	9,88 10 ⁻⁵	3,34 10 ⁻⁴	2,86 10 ⁻⁴	2,86 10 ⁻⁴	2,11 10 ⁻⁵	2,49 10 ⁻⁵	-	3,13 10 ⁻⁵	2,03 10 ⁻⁴	4,95 10 ⁻⁴	9,96 10 ⁻⁵	4,24 10 ⁻⁴	-	3,70 10 ⁻⁵	2,22 10 ⁻⁴
94	3,06 10 ⁻⁵	3,06 10 ⁻⁵	3,34 10 ⁻⁴	7,58 10 ⁻⁵	1,48 10 ⁻³	9,11 10 ⁻⁴	9,11 10 ⁻⁴	7,48 10 ⁻⁵	4,83 10 ⁻⁴	1,92 10 ⁻⁶	4,70 10 ⁻⁶	4,99 10 ⁻⁵	9,32 10 ⁻⁵	1,92 10 ⁻⁵	5,73 10 ⁻⁵	-	3,03 10 ⁻⁵	9,96 10 ⁻⁵
97	-	-	1,48 10 ⁻³	2,20 10 ⁻⁶	1,55 10 ⁻³	1,61 10 ⁻⁴	1,61 10 ⁻⁴	4,17 10 ⁻⁵	7,74 10 ⁻⁵	-	3,31 10 ⁻⁵	4,54 10 ⁻⁴	1,23 10 ⁻³	1,18 10 ⁻⁴	1,28 10 ⁻⁴	1,13 10 ⁻⁴	6,14 10 ⁻⁵	1,04 10 ⁻⁴
102	3,54 10 ⁻⁵	3,54 10 ⁻⁵	1,55 10 ⁻³	6,06 10 ⁻⁵	1,55 10 ⁻⁴	3,17 10 ⁻⁵	3,17 10 ⁻⁵	8,86 10 ⁻⁶	1,58 10 ⁻⁵	4,37 10 ⁻⁵	1,09 10 ⁻⁵	1,10 10 ⁻⁵	1,91 10 ⁻⁴	2,83 10 ⁻⁵	3,92 10 ⁻⁵	4,93 10 ⁻⁵	1,95 10 ⁻⁵	3,79 10 ⁻⁵
103	5,69 10 ⁻⁵	5,69 10 ⁻⁵	1,55 10 ⁻⁴	-	2,05 10 ⁻⁴	6,48 10 ⁻⁵	6,48 10 ⁻⁵	3,26 10 ⁻⁴	4,15 10 ⁻⁵	3,42 10 ⁻⁴	1,96 10 ⁻³	-	1,23 10 ⁻³	4,53 10 ⁻⁴	3,89 10 ⁻⁴	-	2,49 10 ⁻⁴	4,85 10 ⁻⁴
107	3,02 10 ⁻⁴	3,02 10 ⁻⁴	2,05 10 ⁻⁴	-	3,85 10 ⁻⁴	5,23 10 ⁻⁴	5,23 10 ⁻⁴	1,37 10 ⁻⁴	4,82 10 ⁻⁵	2,24 10 ⁻⁴	1,02 10 ⁻⁴	-	2,86 10 ⁻⁴	6,57 10 ⁻⁵	3,89 10 ⁻⁴	-	3,58 10 ⁻⁵	4,50 10 ⁻⁵
109	3,45 10 ⁻⁵	3,45 10 ⁻⁵	3,85 10 ⁻⁴	1,86 10 ⁻⁴	7,45 10 ⁻⁵	2,56 10 ⁻⁵	2,56 10 ⁻⁵	6,07 10 ⁻⁵	2,65 10 ⁻⁵	3,04 10 ⁻⁵	5,35 10 ⁻⁵	1,01 10 ⁻⁵	6,57 10 ⁻⁵	2,54 10 ⁻⁵	2,25 10 ⁻⁵	7,99 10 ⁻⁵	2,33 10 ⁻⁵	2,81 10 ⁻⁵
112	1,32 10 ⁻⁴	1,32 10 ⁻⁴	7,45 10 ⁻⁵	-	1,19 10 ⁻⁴	7,87 10 ⁻⁵	7,87 10 ⁻⁵	3,68 10 ⁻⁵	1,89 10 ⁻⁵	5,78 10 ⁻⁵	1,61 10 ⁻⁵	-	5,22 10 ⁻⁵	2,02 10 ⁻⁵	3,45 10 ⁻⁵	4,85 10 ⁻⁵	8,29 10 ⁻⁶	5,57 10 ⁻⁶
116	2,33 10 ⁻⁴	2,33 10 ⁻⁴	1,19 10 ⁻⁴	1,33 10 ⁻⁵	4,38 10 ⁻⁴	2,36 10 ⁻⁴	2,36 10 ⁻⁴	9,03 10 ⁻⁴	4,85 10 ⁻⁵	1,55 10 ⁻⁴	6,01 10 ⁻⁴	8,17 10 ⁻⁵	2,91 10 ⁻⁴	9,46 10 ⁻⁵	1,57 10 ⁻⁴	-	3,22 10 ⁻⁵	1,90 10 ⁻⁴
117	5,19 10 ⁻⁵	5,19 10 ⁻⁵	4,38 10 ⁻⁴	2,41 10 ⁻⁶	1,67 10 ⁻⁴	1,09 10 ⁻⁴	1,09 10 ⁻⁴	1,39 10 ⁻⁴	8,58 10 ⁻⁶	1,73 10 ⁻⁵	4,65 10 ⁻⁵	3,86 10 ⁻⁶	5,59 10 ⁻⁵	1,80 10 ⁻⁵	3,63 10 ⁻⁵	1,88 10 ⁻⁴	2,86 10 ⁻⁶	2,78 10 ⁻⁵
121	3,86 10 ⁻⁵	3,86 10 ⁻⁵	1,67 10 ⁻⁴	4,57 10 ⁻⁷	5,79 10 ⁻⁵	5,68 10 ⁻⁵	5,68 10 ⁻⁵	6,41 10 ⁻⁵	-	3,20 10 ⁻⁵	5,30 10 ⁻⁵	3,17 10 ⁻⁶	4,79 10 ⁻⁵	1,36 10 ⁻⁵	4,70 10 ⁻⁵	1,43 10 ⁻⁴	-	1,39 10 ⁻⁵
123	1,60 10 ⁻⁴	1,60 10 ⁻⁴	5,79 10 ⁻⁵	2,01 10 ⁻⁷	9,06 10 ⁻⁵	1,71 10 ⁻⁴	1,71 10 ⁻⁴	7,15 10 ⁻⁵	-	2,70 10 ⁻⁵	1,21 10 ⁻⁵	3,52 10 ⁻⁶	1,53 10 ⁻⁵	7,42 10 ⁻⁶	2,89 10 ⁻⁵	6,86 10 ⁻⁵	-	2,33 10 ⁻⁵
124	7,67 10 ⁻⁵	7,67 10 ⁻⁵	9,06 10 ⁻⁵	1,42 10 ⁻⁵	7,88 10 ⁻⁵	5,08 10 ⁻⁵	5,08 10 ⁻⁵	7,25 10 ⁻⁶	1,04 10 ⁻⁵	2,57 10 ⁻⁴	2,43 10 ⁻⁵	5,58 10 ⁻⁴	2,64 10 ⁻⁴	5,90 10 ⁻⁵	1,70 10 ⁻⁴	-	3,47 10 ⁻⁵	1,53 10 ⁻⁴
125	4,15 10 ⁻⁵	4,15 10 ⁻⁵	7,88 10 ⁻⁵	1,42 10 ⁻⁶	6,11 10 ⁻⁵	9,83 10 ⁻⁶	9,83 10 ⁻⁶	4,37 10 ⁻⁶	1,64 10 ⁻⁶	1,26 10 ⁻⁴	1,33 10 ⁻⁵	1,30 10 ⁻⁴	1,86 10 ⁻⁴	4,65 10 ⁻⁵	2,99 10 ⁻⁵	6,41 10 ⁻⁴	4,98 10 ⁻⁶	4,65 10 ⁻⁵
128	8,75 10 ⁻⁵	8,75 10 ⁻⁵	6,11 10 ⁻⁵	3,83 10 ⁻⁷	1,45 10 ⁻⁴	1,98 10 ⁻⁵	1,98 10 ⁻⁵	8,25 10 ⁻⁶	3,14 10 ⁻⁵	1,27 10 ⁻⁴	1,20 10 ⁻⁵	4,80 10 ⁻⁷	2,10 10 ⁻⁴	6,46 10 ⁻⁵	2,87 10 ⁻⁵	-	4,54 10 ⁻⁵	3,51 10 ⁻⁴
131	4,93 10 ⁻⁴	4,93 10 ⁻⁴	1,45 10 ⁻⁴	1,90 10 ⁻⁸	5,43 10 ⁻⁴	1,16 10 ⁻⁴	1,16 10 ⁻⁴	3,40 10 ⁻⁵	2,55 10 ⁻⁵	2,17 10 ⁻⁵	1,50 10 ⁻⁶	2,50 10 ⁻⁸	2,39 10 ⁻⁵	2,99 10 ⁻⁶	5,12 10 ⁻⁶	1,12 10 ⁻⁶	1,12 10 ⁻⁶	3,83 10 ⁻⁵
134	5,70 10 ⁻⁶	5,70 10 ⁻⁶	5,43 10 ⁻⁴	3,12 10 ⁻⁷	5,36 10 ⁻⁶	5,03 10 ⁻⁶	5,03 10 ⁻⁶	1,34 10 ⁻⁶	-	2,90 10 ⁻⁵	6,82 10 ⁻⁶	3,42 10 ⁻⁷	2,73 10 ⁻⁵	3,41 10 ⁻⁵	2,56 10 ⁻⁵	2,64 10 ⁻⁴	-	5,12 10 ⁻⁶
137	1,08 10 ⁻⁵	1,08 10 ⁻⁵	5,36 10 ⁻⁶	9,16 10 ⁻⁷	2,20 10 ⁻⁵	1,45 10 ⁻⁵	1,45 10 ⁻⁵	7,04 10 ⁻⁶	8,91 10 ⁻⁶	1,38 10 ⁻⁵	9,00 10 ⁻⁶	1,20 10 ⁻⁷	2,82 10 ⁻⁵	2,16 10 ⁻⁵	1,86 10 ⁻⁵	-	1,14 10 ⁻⁵	7,20 10 ⁻⁶
140	5,89 10 ⁻⁵	5,89 10 ⁻⁵	2,20 10 ⁻⁵	-	1,55 10 ⁻⁴	1,13 10 ⁻⁴	1,13 10 ⁻⁴	7,07 10 ⁻⁶	4,71 10 ⁻⁵	1,20 10 ⁻⁵	1,44 10 ⁻⁶	-	3,17 10 ⁻⁵	2,50 10 ⁻⁵	2,31 10 ⁻⁵	3,94 10 ⁻⁵	9,61 10 ⁻⁶	5,29 10 ⁻⁶
143	5,96 10 ⁻⁵	5,96 10 ⁻⁵	1,55 10 ⁻⁴	3,59 10 ⁻⁵	1,10 10 ⁻⁴	7,63 10 ⁻⁵	7,63 10 ⁻⁵	5,58 10 ⁻⁶	2,61 10 ⁻⁵	1,56 10 ⁻⁴	1,46 10 ⁻⁵	3,36 10 ⁻⁵	2,87 10 ⁻⁴	2,14 10 ⁻⁴	1,99 10 ⁻⁴	-	6,80 10 ⁻⁵	8,75 10 ⁻⁵
146	1,11 10 ⁻⁸	1,11 10 ⁻⁸	1,10 10 ⁻⁴	7,99 10 ⁻⁵	2,92 10 ⁻⁸	3,24 10 ⁻⁸	3,24 10 ⁻⁸	7,85 10 ⁻⁹	8,20 10 ⁻⁹	5,51 10 ⁻⁵	3,88 10 ⁻⁵	7,94 10 ⁻⁵	1,45 10 ⁻⁴	1,29 10 ⁻⁴	1,61 10 ⁻⁴	-	4,08 10 ⁻⁵	1,22 10 ⁻⁵

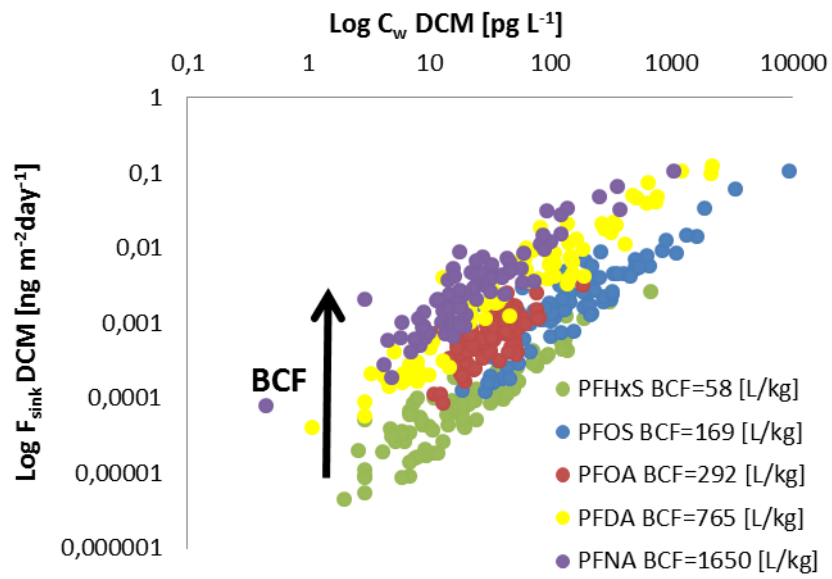
Zero values (-) attend for a null turbulence due to; i) a concentration of the compound under LOD, ii) a depletion of the quantified compound because of the calculated ongoing diffusion iii) a diminution of the measured concentration too low for appreciating a variation and thus quantifying a flux, or iv) to a missing value of the eddy diffusion coefficients.

Figure S4.5. Turbulent fluxes at Surface for PFOS and PFOA (F_{Eddy} , $\text{ng m}^{-2}\text{day}^{-1}$)



Bars with \approx symbol have been manually diminished by a factor of 10 in order to ease the global comparison of all the measurements.

Figure S4.6. Relation between DCM concentrations and $F_{Settling}$ on a logarithmic scale for PFASs with different BCF



BCFs have been taken from Loi et al. ²

Table S4.8. Organic Carbon Sinking fluxes (F_{OC} , mg C m⁻²day⁻¹)

Station	F_{oc Phyto}	F_{oc Fecal}	Total F_{oc}
2	5.24	26.46	31.69
3	2.96	29.67	32.63
5	5.10	44.04	49.14
7	6.33	50.92	57.25
8	6.66	53.92	60.58
9	11.44	79.24	90.67
11	10.97	79.32	90.29
12	8.59	53.54	62.14
13	11.07	62.89	73.96
14	13.67	68.05	81.72
15	9.01	61.34	70.35
17	2.06	55.28	57.34
18	1.18	55.16	56.35
20	0.21	35.79	36.00
21	0.14	28.64	28.78
23	0.27	34.78	35.05
24	0.49	43.92	44.41
26	0.75	43.42	44.16
28	0.38	35.40	35.78
29	0.47	34.28	34.75
30	0.53	34.63	35.16
31	0.24	27.45	27.69
32	0.16	27.52	27.67
33	0.10	24.45	24.55
35	0.10	21.18	21.28
37	0.05	19.25	19.30
38	0.07	22.31	22.38
39	0.09	26.72	26.80
40	0.13	25.39	25.52
41	0.21	24.16	24.36
42	0.31	25.52	25.82
43	0.79	31.31	32.10
44	2.43	41.23	43.65
46	4.19	51.01	55.20
47	2.27	43.36	45.64
49	0.97	38.63	39.60
50	0.60	38.37	38.97
52	0.25	20.81	21.06
53	0.87	31.25	32.13
55	0.21	19.01	19.22
57	0.18	16.96	17.14
58	0.18	16.80	16.99
60	0.19	18.87	19.05

Station	F_{oc} Phyto	F_{oc} Fecal	Total F_{oc}
63	0.19	15.44	15.63
64	0.28	18.69	18.97
66	0.95	29.11	30.06
67	0.98	39.81	40.79
70	3.70	41.98	45.68
71	2.68	39.25	41.93
74	7.24	48.63	55.87
75	9.13	49.80	58.92
77	20.73	88.53	109.26
78	13.10	71.47	84.56
82	1.28	37.85	39.13
84	2.46	43.32	45.79
86	0.50	40.06	40.56
88	0.49	39.62	40.11
90	2.26	54.41	56.67
92	10.59	97.14	107.73
94	9.42	74.90	84.32
97	0.63	34.73	35.36
99	0.68	36.79	37.47
102	0.60	42.10	42.70
103	0.54	40.18	40.72
106	0.53	37.63	38.17
107	0.39	36.94	37.33
109	0.30	32.96	33.26
110	0.79	35.81	36.60
112	0.61	40.84	41.45
113	1.75	44.82	46.57
114	1.20	42.84	44.04
116	2.91	52.96	55.87
117	3.56	56.49	60.04
120	3.53	48.01	51.54
121	5.88	52.70	58.58
123	33.00	127.11	160.11
124	48.62	176.16	224.78
125	21.84	93.34	115.18
128	4.34	52.20	56.54
129	4.77	48.64	53.41
131	3.34	46.50	49.84
132	1.25	32.82	34.06
134	0.37	20.85	21.22
135	0.26	19.01	19.27
137	0.40	18.24	18.64
138	0.24	14.19	14.43
140	0.14	12.17	12.31
141	0.14	13.44	13.58

Station	F_{oc} Phyto	F_{oc} Fecal	Total F_{oc}
143	0.19	14.87	15.07
144	0.26	16.58	16.84
146	0.64	28.07	28.71
147	0.69	26.17	26.86

All the values are extracted from Siegel et al. ³ database at the corresponding locations and month.

Table S4.9. Biological pump fluxes ($F_{Settling}$, $\text{ng m}^{-2}\text{day}^{-1}$)

Station	PFHxS		PFOS		PFOA		PFNA		PFDA	
	Algae	Fecal								
2										
3	$5.80 \cdot 10^{-6}$	$5.82 \cdot 10^{-5}$	$4.72 \cdot 10^{-4}$	$4.74 \cdot 10^{-3}$	$2.88 \cdot 10^{-4}$	$2.89 \cdot 10^{-3}$	$9.24 \cdot 10^{-3}$	$9.27 \cdot 10^{-2}$	$8.62 \cdot 10^{-3}$	$8.65 \cdot 10^{-2}$
5										
7										
8	$5.94 \cdot 10^{-6}$	$4.81 \cdot 10^{-5}$	$2.01 \cdot 10^{-4}$	$1.62 \cdot 10^{-3}$	$2.75 \cdot 10^{-4}$	$2.23 \cdot 10^{-3}$	$7.18 \cdot 10^{-3}$	$5.81 \cdot 10^{-2}$	$1.13 \cdot 10^{-2}$	$9.12 \cdot 10^{-2}$
9	$8.22 \cdot 10^{-6}$	$5.69 \cdot 10^{-5}$	$1.30 \cdot 10^{-4}$	$8.98 \cdot 10^{-4}$	$1.99 \cdot 10^{-4}$	$1.38 \cdot 10^{-3}$	$9.40 \cdot 10^{-4}$	$6.51 \cdot 10^{-3}$	$1.15 \cdot 10^{-3}$	$7.95 \cdot 10^{-3}$
11	$8.18 \cdot 10^{-6}$	$5.91 \cdot 10^{-5}$	$1.14 \cdot 10^{-4}$	$8.24 \cdot 10^{-4}$	$1.85 \cdot 10^{-4}$	$1.34 \cdot 10^{-3}$	$8.13 \cdot 10^{-4}$	$5.88 \cdot 10^{-3}$	$7.63 \cdot 10^{-4}$	$5.51 \cdot 10^{-3}$
12	$4.58 \cdot 10^{-6}$	$2.85 \cdot 10^{-5}$	$1.94 \cdot 10^{-4}$	$1.21 \cdot 10^{-3}$	$2.32 \cdot 10^{-4}$	$1.45 \cdot 10^{-3}$	$6.48 \cdot 10^{-3}$	$4.03 \cdot 10^{-2}$	$6.22 \cdot 10^{-3}$	$3.87 \cdot 10^{-2}$
13	$5.64 \cdot 10^{-6}$	$3.20 \cdot 10^{-5}$	$1.79 \cdot 10^{-4}$	$1.02 \cdot 10^{-3}$	$2.22 \cdot 10^{-4}$	$1.26 \cdot 10^{-3}$	$4.05 \cdot 10^{-3}$	$2.30 \cdot 10^{-2}$	$7.45 \cdot 10^{-3}$	$4.23 \cdot 10^{-2}$
14	$9.82 \cdot 10^{-6}$	$4.89 \cdot 10^{-5}$	$2.29 \cdot 10^{-4}$	$1.14 \cdot 10^{-3}$	$3.16 \cdot 10^{-4}$	$1.58 \cdot 10^{-3}$	$5.65 \cdot 10^{-3}$	$2.81 \cdot 10^{-2}$	$1.21 \cdot 10^{-2}$	$6.02 \cdot 10^{-2}$
15	$2.49 \cdot 10^{-6}$	$1.70 \cdot 10^{-5}$	$4.43 \cdot 10^{-5}$	$3.02 \cdot 10^{-4}$	$1.05 \cdot 10^{-4}$	$7.16 \cdot 10^{-4}$	$6.00 \cdot 10^{-4}$	$4.09 \cdot 10^{-3}$	$1.21 \cdot 10^{-3}$	$8.27 \cdot 10^{-3}$
17	$6.79 \cdot 10^{-5}$	$1.82 \cdot 10^{-3}$	$2.13 \cdot 10^{-3}$	$5.71 \cdot 10^{-2}$	$5.75 \cdot 10^{-5}$	$1.55 \cdot 10^{-3}$	$1.53 \cdot 10^{-4}$	$4.10 \cdot 10^{-3}$	$4.07 \cdot 10^{-4}$	$1.09 \cdot 10^{-2}$
18	$2.38 \cdot 10^{-5}$	$1.11 \cdot 10^{-3}$	$6.86 \cdot 10^{-4}$	$3.20 \cdot 10^{-2}$	$2.17 \cdot 10^{-5}$	$1.01 \cdot 10^{-3}$	$9.74 \cdot 10^{-5}$	$4.54 \cdot 10^{-3}$	$1.05 \cdot 10^{-4}$	$4.90 \cdot 10^{-3}$
20	$1.49 \cdot 10^{-5}$	$2.54 \cdot 10^{-3}$	$6.11 \cdot 10^{-4}$	$1.04 \cdot 10^{-1}$	$8.49 \cdot 10^{-6}$	$1.45 \cdot 10^{-3}$	$2.49 \cdot 10^{-5}$	$4.25 \cdot 10^{-3}$	$4.30 \cdot 10^{-5}$	$7.34 \cdot 10^{-3}$
21	$2.04 \cdot 10^{-6}$	$4.19 \cdot 10^{-4}$	$6.87 \cdot 10^{-5}$	$1.41 \cdot 10^{-2}$	$3.96 \cdot 10^{-6}$	$8.13 \cdot 10^{-4}$	$7.62 \cdot 10^{-6}$	$1.57 \cdot 10^{-3}$	$1.85 \cdot 10^{-5}$	$3.81 \cdot 10^{-3}$
23	$3.80 \cdot 10^{-6}$	$4.88 \cdot 10^{-4}$	$6.96 \cdot 10^{-5}$	$8.93 \cdot 10^{-3}$	$3.33 \cdot 10^{-6}$	$4.28 \cdot 10^{-4}$	$1.21 \cdot 10^{-5}$	$1.55 \cdot 10^{-3}$	$5.53 \cdot 10^{-5}$	$7.10 \cdot 10^{-3}$
24	$7.00 \cdot 10^{-6}$	$6.31 \cdot 10^{-4}$	$1.34 \cdot 10^{-4}$	$1.21 \cdot 10^{-2}$	$1.26 \cdot 10^{-5}$	$1.14 \cdot 10^{-3}$	$1.22 \cdot 10^{-4}$	$1.10 \cdot 10^{-2}$	$4.22 \cdot 10^{-4}$	$3.80 \cdot 10^{-2}$
26	$4.20 \cdot 10^{-6}$	$2.44 \cdot 10^{-4}$	$1.16 \cdot 10^{-4}$	$6.72 \cdot 10^{-3}$	$1.06 \cdot 10^{-5}$	$6.14 \cdot 10^{-4}$	$7.47 \cdot 10^{-5}$	$4.34 \cdot 10^{-3}$	$7.91 \cdot 10^{-4}$	$4.60 \cdot 10^{-2}$
28	$8.37 \cdot 10^{-7}$	$7.86 \cdot 10^{-5}$	$4.64 \cdot 10^{-5}$	$4.36 \cdot 10^{-3}$	$4.01 \cdot 10^{-6}$	$3.77 \cdot 10^{-4}$	$6.62 \cdot 10^{-6}$	$6.21 \cdot 10^{-4}$	$1.96 \cdot 10^{-5}$	$1.84 \cdot 10^{-3}$
29	$1.78 \cdot 10^{-6}$	$1.30 \cdot 10^{-4}$	$7.25 \cdot 10^{-5}$	$5.27 \cdot 10^{-3}$	$1.07 \cdot 10^{-5}$	$7.79 \cdot 10^{-4}$	$1.27 \cdot 10^{-4}$	$9.21 \cdot 10^{-3}$	$5.12 \cdot 10^{-5}$	$3.73 \cdot 10^{-3}$
30	$5.13 \cdot 10^{-6}$	$3.34 \cdot 10^{-4}$	$2.17 \cdot 10^{-4}$	$1.41 \cdot 10^{-2}$	$1.29 \cdot 10^{-5}$	$8.39 \cdot 10^{-4}$	$7.12 \cdot 10^{-5}$	$4.64 \cdot 10^{-3}$	$1.05 \cdot 10^{-5}$	$6.85 \cdot 10^{-4}$
31	$1.36 \cdot 10^{-6}$	$1.59 \cdot 10^{-4}$	$4.77 \cdot 10^{-5}$	$5.57 \cdot 10^{-3}$	$1.01 \cdot 10^{-5}$	$1.17 \cdot 10^{-3}$	$2.68 \cdot 10^{-4}$	$3.13 \cdot 10^{-2}$	$3.56 \cdot 10^{-5}$	$4.16 \cdot 10^{-3}$
32	$2.38 \cdot 10^{-7}$	$4.19 \cdot 10^{-5}$	$9.03 \cdot 10^{-6}$	$1.59 \cdot 10^{-3}$	$1.52 \cdot 10^{-6}$	$2.67 \cdot 10^{-4}$	$1.14 \cdot 10^{-5}$	$2.01 \cdot 10^{-3}$	$6.32 \cdot 10^{-6}$	$1.11 \cdot 10^{-3}$
33	$5.47 \cdot 10^{-7}$	$1.28 \cdot 10^{-4}$	$3.51 \cdot 10^{-5}$	$8.19 \cdot 10^{-3}$	$1.76 \cdot 10^{-6}$	$4.11 \cdot 10^{-4}$	$3.11 \cdot 10^{-6}$	$7.26 \cdot 10^{-4}$	0	0
35	$1.95 \cdot 10^{-7}$	$4.25 \cdot 10^{-5}$	$9.43 \cdot 10^{-6}$	$2.06 \cdot 10^{-3}$	$9.38 \cdot 10^{-7}$	$2.05 \cdot 10^{-4}$	$1.22 \cdot 10^{-6}$	$2.67 \cdot 10^{-4}$	$6.38 \cdot 10^{-7}$	$1.39 \cdot 10^{-4}$

Station	PFHxS		PFOS		PFOA		PFNA		PFDA	
	Algae	Fecal								
37	1.09 10 ⁻⁷	3.97 10 ⁻⁵	3.55 10 ⁻⁶	1.29 10 ⁻³	6.48 10 ⁻⁷	2.36 10 ⁻⁴	1.33 10 ⁻⁶	4.84 10 ⁻⁴	4.78 10 ⁻⁷	1.74 10 ⁻⁴
38	2.88 10 ⁻⁷	9.50 10 ⁻⁵	5.65 10 ⁻⁶	1.87 10 ⁻³	9.88 10 ⁻⁷	3.26 10 ⁻⁴	1.87 10 ⁻⁶	6.18 10 ⁻⁴	7.40 10 ⁻⁷	2.45 10 ⁻⁴
39	1.73 10 ⁻⁷	5.27 10 ⁻⁵	5.58 10 ⁻⁶	1.70 10 ⁻³	9.12 10 ⁻⁷	2.78 10 ⁻⁴	1.98 10 ⁻⁶	6.04 10 ⁻⁴	1.30 10 ⁻⁷	3.97 10 ⁻⁵
40	4.38 10 ⁻⁷	8.48 10 ⁻⁵	1.11 10 ⁻⁵	2.14 10 ⁻³	1.43 10 ⁻⁶	2.77 10 ⁻⁴	3.73 10 ⁻⁶	7.23 10 ⁻⁴	8.29 10 ⁻⁷	1.60 10 ⁻⁴
41	9.48 10 ⁻⁷	1.11 10 ⁻⁴	2.04 10 ⁻⁵	2.39 10 ⁻³	3.42 10 ⁻⁶	4.01 10 ⁻⁴	9.17 10 ⁻⁶	1.08 10 ⁻³	1.75 10 ⁻⁶	2.05 10 ⁻⁴
42	1.11 10 ⁻⁶	9.21 10 ⁻⁵	3.11 10 ⁻⁵	2.57 10 ⁻³	3.20 10 ⁻⁶	2.65 10 ⁻⁴	1.17 10 ⁻⁵	9.70 10 ⁻⁴	2.05 10 ⁻⁶	1.70 10 ⁻⁴
43	6.41 10 ⁻⁶	2.53 10 ⁻⁴	1.32 10 ⁻⁴	5.21 10 ⁻³	1.43 10 ⁻⁵	5.65 10 ⁻⁴	2.17 10 ⁻⁵	8.55 10 ⁻⁴	4.65 10 ⁻⁶	1.83 10 ⁻⁴
44	5.19 10 ⁻⁶	8.81 10 ⁻⁵	2.49 10 ⁻⁴	4.23 10 ⁻³	3.26 10 ⁻⁵	5.53 10 ⁻⁴	9.58 10 ⁻⁵	1.63 10 ⁻³	1.13 10 ⁻⁵	1.92 10 ⁻⁴
46	6.77 10 ⁻⁶	8.24 10 ⁻⁵	9.79 10 ⁻⁵	1.19 10 ⁻³	4.70 10 ⁻⁵	5.72 10 ⁻⁴	5.46 10 ⁻⁴	6.65 10 ⁻³	1.55 10 ⁻³	1.89 10 ⁻²
47	2.11 10 ⁻⁶	4.02 10 ⁻⁵	3.41 10 ⁻⁵	6.51 10 ⁻⁴	2.45 10 ⁻⁵	4.68 10 ⁻⁴	4.11 10 ⁻⁴	7.84 10 ⁻³	8.93 10 ⁻⁴	1.70 10 ⁻²
49	1.02 10 ⁻⁶	4.07 10 ⁻⁵	1.64 10 ⁻⁵	6.54 10 ⁻⁴	9.50 10 ⁻⁶	3.80 10 ⁻⁴	4.44 10 ⁻⁵	1.77 10 ⁻³	8.43 10 ⁻⁵	3.37 10 ⁻³
50	3.93 10 ⁻⁷	2.50 10 ⁻⁵	5.71 10 ⁻⁶	3.63 10 ⁻⁴	7.71 10 ⁻⁶	4.91 10 ⁻⁴	1.83 10 ⁻⁴	1.16 10 ⁻²	6.29 10 ⁻⁴	4.00 10 ⁻²
52	2.46 10 ⁻⁷	2.03 10 ⁻⁵	7.85 10 ⁻⁶	6.46 10 ⁻⁴	2.44 10 ⁻⁶	2.01 10 ⁻⁴	1.52 10 ⁻⁵	1.25 10 ⁻³	5.30 10 ⁻⁵	4.36 10 ⁻³
53	9.79 10 ⁻⁷	3.50 10 ⁻⁵	1.61 10 ⁻⁵	5.76 10 ⁻⁴	7.44 10 ⁻⁶	2.66 10 ⁻⁴	2.30 10 ⁻⁵	8.21 10 ⁻⁴	1.23 10 ⁻⁵	4.39 10 ⁻⁴
55	1.67 10 ⁻⁷	1.51 10 ⁻⁵	4.39 10 ⁻⁶	3.98 10 ⁻⁴	1.21 10 ⁻⁶	1.09 10 ⁻⁴	4.47 10 ⁻⁶	4.05 10 ⁻⁴	1.35 10 ⁻⁵	1.22 10 ⁻³
57	1.79 10 ⁻⁷	1.68 10 ⁻⁵	3.05 10 ⁻⁶	2.85 10 ⁻⁴	1.18 10 ⁻⁶	1.10 10 ⁻⁴	7.39 10 ⁻⁶	6.93 10 ⁻⁴	3.45 10 ⁻⁵	3.23 10 ⁻³
58										
60	1.58 10 ⁻⁷	1.58 10 ⁻⁵	7.13 10 ⁻⁶	7.15 10 ⁻⁴	2.39 10 ⁻⁶	2.40 10 ⁻⁴	2.38 10 ⁻⁵	2.39 10 ⁻³	3.71 10 ⁻⁵	3.72 10 ⁻³
63	2.16 10 ⁻⁷	1.77 10 ⁻⁵	9.15 10 ⁻⁶	7.49 10 ⁻⁴	1.95 10 ⁻⁶	1.59 10 ⁻⁴	4.18 10 ⁻⁵	3.42 10 ⁻³	4.92 10 ⁻⁵	4.03 10 ⁻³
64	7.26 10 ⁻⁷	4.88 10 ⁻⁵	1.82 10 ⁻⁵	1.22 10 ⁻³	2.78 10 ⁻⁶	1.87 10 ⁻⁴	4.87 10 ⁻⁵	3.28 10 ⁻³	1.59 10 ⁻⁴	1.07 10 ⁻²
66	3.26 10 ⁻⁶	1.00 10 ⁻⁴	1.32 10 ⁻⁴	4.06 10 ⁻³	2.17 10 ⁻⁵	6.69 10 ⁻⁴	1.64 10 ⁻⁴	5.05 10 ⁻³	2.01 10 ⁻⁴	6.18 10 ⁻³
67	3.36 10 ⁻⁶	1.37 10 ⁻⁴	1.87 10 ⁻⁴	7.64 10 ⁻³	2.05 10 ⁻⁵	8.37 10 ⁻⁴	3.59 10 ⁻⁴	1.47 10 ⁻²	2.95 10 ⁻³	1.20 10 ⁻¹
70	2.06 10 ⁻⁶	2.34 10 ⁻⁵	9.52 10 ⁻⁵	1.08 10 ⁻³	3.91 10 ⁻⁵	4.44 10 ⁻⁴	9.16 10 ⁻⁵	1.04 10 ⁻³	7.00 10 ⁻⁵	7.95 10 ⁻⁴
71	1.18 10 ⁻⁶	1.73 10 ⁻⁵	6.98 10 ⁻⁵	1.02 10 ⁻³	2.11 10 ⁻⁵	3.08 10 ⁻⁴	3.64 10 ⁻⁵	5.33 10 ⁻⁴	3.87 10 ⁻⁵	5.66 10 ⁻⁴
74	6.48 10 ⁻⁶	4.35 10 ⁻⁵	3.22 10 ⁻⁴	2.16 10 ⁻³	1.30 10 ⁻⁴	8.76 10 ⁻⁴	1.90 10 ⁻³	1.27 10 ⁻²	1.09 10 ⁻³	7.33 10 ⁻³
75	5.02 10 ⁻⁶	2.74 10 ⁻⁵	1.65 10 ⁻⁴	8.99 10 ⁻⁴	1.03 10 ⁻⁴	5.64 10 ⁻⁴	9.07 10 ⁻⁴	4.95 10 ⁻³	1.26 10 ⁻³	6.87 10 ⁻³
77	3.53 10 ⁻⁵	1.51 10 ⁻⁴	1.25 10 ⁻³	5.32 10 ⁻³	3.45 10 ⁻⁴	1.47 10 ⁻³	5.79 10 ⁻³	2.47 10 ⁻²	1.85 10 ⁻³	7.88 10 ⁻³

Station	PFHxS		PFOS		PFOA		PFNA		PFDA	
	Algae	Fecal								
78	1.51 10 ⁻⁵	8.22 10 ⁻⁵	4.86 10 ⁻⁴	2.65 10 ⁻³	2.38 10 ⁻⁴	1.30 10 ⁻³	5.59 10 ⁻⁴	3.05 10 ⁻³	6.29 10 ⁻⁴	3.43 10 ⁻³
82	2.01 10 ⁻⁶	5.94 10 ⁻⁵	7.81 10 ⁻⁵	2.31 10 ⁻³	2.24 10 ⁻⁵	6.62 10 ⁻⁴	6.31 10 ⁻⁵	1.86 10 ⁻³	7.18 10 ⁻⁵	2.12 10 ⁻³
84	1.80 10 ⁻⁶	3.17 10 ⁻⁵	1.39 10 ⁻⁴	2.44 10 ⁻³	3.24 10 ⁻⁵	5.69 10 ⁻⁴	3.44 10 ⁻⁴	6.05 10 ⁻³	1.14 10 ⁻³	2.00 10 ⁻²
86			5.41 10 ⁻⁵	4.35 10 ⁻³	8.12 10 ⁻⁶	6.53 10 ⁻⁴	2.81 10 ⁻⁵	2.26 10 ⁻³	7.48 10 ⁻⁵	6.01 10 ⁻³
88	7.10 10 ⁻⁷	5.79 10 ⁻⁵	1.51 10 ⁻⁵	1.23 10 ⁻³	6.13 10 ⁻⁶	5.00 10 ⁻⁴	4.62 10 ⁻⁵	3.77 10 ⁻³	2.36 10 ⁻⁴	1.93 10 ⁻²
90	1.42 10 ⁻⁶	3.41 10 ⁻⁵	1.56 10 ⁻⁴	3.76 10 ⁻³	2.49 10 ⁻⁵	6.01 10 ⁻⁴	4.03 10 ⁻⁵	9.70 10 ⁻⁴	1.06 10 ⁻⁴	2.55 10 ⁻³
92	8.29 10 ⁻⁶	7.61 10 ⁻⁵	8.50 10 ⁻⁴	7.80 10 ⁻³	2.45 10 ⁻⁴	2.25 10 ⁻³	5.03 10 ⁻⁴	4.62 10 ⁻³	2.04 10 ⁻³	1.87 10 ⁻²
94	1.35 10 ⁻⁴	1.07 10 ⁻³	6.32 10 ⁻⁴	5.02 10 ⁻³	1.62 10 ⁻⁴	1.29 10 ⁻³	4.55 10 ⁻⁴	3.62 10 ⁻³	8.02 10 ⁻⁴	6.37 10 ⁻³
97	1.60 10 ⁻⁶	8.78 10 ⁻⁵	2.10 10 ⁻⁵	1.15 10 ⁻³	9.59 10 ⁻⁶	5.26 10 ⁻⁴	9.09 10 ⁻⁵	4.99 10 ⁻³	2.82 10 ⁻⁴	1.55 10 ⁻²
99	6.84 10 ⁻⁶	3.70 10 ⁻⁴	4.82 10 ⁻⁵	2.61 10 ⁻³	2.12 10 ⁻⁵	1.15 10 ⁻³	5.75 10 ⁻⁵	3.11 10 ⁻³	1.73 10 ⁻⁴	9.39 10 ⁻³
102	7.79 10 ⁻⁶	5.46 10 ⁻⁴	2.66 10 ⁻⁵	1.86 10 ⁻³	1.24 10 ⁻⁵	8.67 10 ⁻⁴	4.44 10 ⁻⁵	3.11 10 ⁻³	8.12 10 ⁻⁵	5.69 10 ⁻³
103	2.73 10 ⁻⁶	2.03 10 ⁻⁴	1.41 10 ⁻⁵	1.05 10 ⁻³	7.89 10 ⁻⁶	5.87 10 ⁻⁴	3.81 10 ⁻⁵	2.83 10 ⁻³	1.68 10 ⁻⁵	1.25 10 ⁻³
106	2.07 10 ⁻⁶	1.46 10 ⁻⁴	1.98 10 ⁻⁵	1.39 10 ⁻³	5.19 10 ⁻⁶	3.66 10 ⁻⁴	2.66 10 ⁻⁵	1.88 10 ⁻³	1.37 10 ⁻⁵	9.67 10 ⁻⁴
107	9.21 10 ⁻⁷	8.70 10 ⁻⁵	1.53 10 ⁻⁵	1.44 10 ⁻³	4.31 10 ⁻⁶	4.07 10 ⁻⁴	2.05 10 ⁻⁵	1.94 10 ⁻³	5.84 10 ⁻⁶	5.51 10 ⁻⁴
109	3.96 10 ⁻⁶	4.33 10 ⁻⁴	9.37 10 ⁻⁶	1.02 10 ⁻³	5.50 10 ⁻⁶	6.00 10 ⁻⁴	3.64 10 ⁻⁵	3.97 10 ⁻³	9.03 10 ⁻⁶	9.87 10 ⁻⁴
110	6.02 10 ⁻⁶	2.73 10 ⁻⁴	3.24 10 ⁻⁵	1.46 10 ⁻³	1.36 10 ⁻⁵	6.17 10 ⁻⁴	3.06 10 ⁻⁵	1.38 10 ⁻³	3.91 10 ⁻⁵	1.77 10 ⁻³
112	1.22 10 ⁻⁶	8.12 10 ⁻⁵	1.92 10 ⁻⁵	1.29 10 ⁻³	7.32 10 ⁻⁶	4.89 10 ⁻⁴	3.62 10 ⁻⁵	2.42 10 ⁻³	3.01 10 ⁻⁵	2.01 10 ⁻³
113			3.63 10 ⁻⁵	9.30 10 ⁻⁴	7.70 10 ⁻⁶	1.97 10 ⁻⁴			1.91 10 ⁻⁵	4.90 10 ⁻⁴
114			3.14 10 ⁻⁵	1.12 10 ⁻³	2.52 10 ⁻⁵	9.01 10 ⁻⁴	6.06 10 ⁻⁵	2.16 10 ⁻³	4.79 10 ⁻⁵	1.71 10 ⁻³
116	2.18 10 ⁻⁵	3.98 10 ⁻⁴	8.13 10 ⁻⁵	1.48 10 ⁻³	2.64 10 ⁻⁵	4.81 10 ⁻⁴	1.00 10 ⁻⁴	1.83 10 ⁻³	2.10 10 ⁻⁵	3.83 10 ⁻⁴
117	1.35 10 ⁻⁵	2.14 10 ⁻⁴	2.87 10 ⁻⁵	4.56 10 ⁻⁴	9.96 10 ⁻⁶	1.58 10 ⁻⁴			7.57 10 ⁻⁵	1.20 10 ⁻³
120	2.21 10 ⁻⁶	3.01 10 ⁻⁵	2.15 10 ⁻⁵	2.92 10 ⁻⁴	3.15 10 ⁻⁵	4.29 10 ⁻⁴	9.43 10 ⁻⁵	1.28 10 ⁻³	1.07 10 ⁻⁴	1.45 10 ⁻³
121			1.07 10 ⁻⁴	9.59 10 ⁻⁴	6.78 10 ⁻⁵	6.07 10 ⁻⁴	7.86 10 ⁻⁶	7.04 10 ⁻⁵		
123	1.03 10 ⁻⁵	3.98 10 ⁻⁵	6.02 10 ⁻⁴	2.32 10 ⁻³	1.77 10 ⁻³	6.81 10 ⁻³	1.76 10 ⁻³	6.80 10 ⁻³	3.82 10 ⁻³	1.47 10 ⁻²
124	4.06 10 ⁻⁵	1.47 10 ⁻⁴	3.55 10 ⁻⁴	1.29 10 ⁻³	4.86 10 ⁻⁴	1.76 10 ⁻³	4.33 10 ⁻⁴	1.57 10 ⁻³	8.70 10 ⁻⁴	3.15 10 ⁻³
125	1.82 10 ⁻⁵	7.80 10 ⁻⁵	9.04 10 ⁻⁴	3.86 10 ⁻³	1.38 10 ⁻⁴	5.89 10 ⁻⁴				
128	2.27 10 ⁻⁶	2.72 10 ⁻⁵	9.12 10 ⁻⁵	1.10 10 ⁻³	6.85 10 ⁻⁵	8.23 10 ⁻⁴	1.55 10 ⁻⁴	1.86 10 ⁻³	9.81 10 ⁻⁴	1.18 10 ⁻²

Station	PFHxS		PFOS		PFOA		PFNA		PFDA	
	Algae	Fecal								
129	6.97 10 ⁻⁶	7.11 10 ⁻⁵	1.83 10 ⁻⁴	1.86 10 ⁻³	1.25 10 ⁻⁴	1.28 10 ⁻³	2.13 10 ⁻⁴	2.17 10 ⁻³	6.96 10 ⁻⁴	7.10 10 ⁻³
131	8.72 10 ⁻⁶	1.21 10 ⁻⁴	2.62 10 ⁻⁴	3.64 10 ⁻³	5.97 10 ⁻⁵	8.31 10 ⁻⁴	1.79 10 ⁻⁴	2.49 10 ⁻³		
132	3.90 10 ⁻⁷	1.03 10 ⁻⁵	1.25 10 ⁻⁵	3.29 10 ⁻⁴	2.81 10 ⁻⁵	7.42 10 ⁻⁴	5.55 10 ⁻⁵	1.46 10 ⁻³		
134	7.64 10 ⁻⁸	4.35 10 ⁻⁶	2.11 10 ⁻⁶	1.21 10 ⁻⁴	1.00 10 ⁻⁵	5.70 10 ⁻⁴	1.63 10 ⁻⁵	9.29 10 ⁻⁴	1.51 10 ⁻⁶	8.61 10 ⁻⁵
135	3.47 10 ⁻⁷	2.58 10 ⁻⁵	2.49 10 ⁻⁶	1.85 10 ⁻⁴	6.86 10 ⁻⁶	5.10 10 ⁻⁴	1.22 10 ⁻⁵	9.03 10 ⁻⁴	2.11 10 ⁻⁶	1.57 10 ⁻⁴
137	2.92 10 ⁻⁷	1.33 10 ⁻⁵	5.35 10 ⁻⁶	2.44 10 ⁻⁴	1.01 10 ⁻⁵	4.60 10 ⁻⁴	2.13 10 ⁻⁵	9.75 10 ⁻⁴	4.40 10 ⁻⁶	2.01 10 ⁻⁴
138	2.95 10 ⁻⁷	1.78 10 ⁻⁵	2.86 10 ⁻⁶	1.73 10 ⁻⁴	6.67 10 ⁻⁶	4.03 10 ⁻⁴	1.12 10 ⁻⁵	6.74 10 ⁻⁴	3.24 10 ⁻⁶	1.95 10 ⁻⁴
140	1.05 10 ⁻⁷	8.89 10 ⁻⁶	2.05 10 ⁻⁶	1.74 10 ⁻⁴	9.78 10 ⁻⁷	8.31 10 ⁻⁵	2.13 10 ⁻⁶	1.81 10 ⁻⁴	2.96 10 ⁻⁶	2.51 10 ⁻⁴
141	8.84 10 ⁻⁸	8.42 10 ⁻⁶	1.25 10 ⁻⁶	1.19 10 ⁻⁴	3.93 10 ⁻⁶	3.74 10 ⁻⁴	6.71 10 ⁻⁶	6.39 10 ⁻⁴	5.83 10 ⁻⁷	5.55 10 ⁻⁵
143			2.01 10 ⁻⁶	1.54 10 ⁻⁴	3.88 10 ⁻⁶	2.97 10 ⁻⁴	1.16 10 ⁻⁵	8.83 10 ⁻⁴	2.14 10 ⁻⁶	1.64 10 ⁻⁴
144	8.11 10 ⁻⁸	5.19 10 ⁻⁶	2.44 10 ⁻⁶	1.56 10 ⁻⁴	6.13 10 ⁻⁶	3.92 10 ⁻⁴	1.39 10 ⁻⁵	8.86 10 ⁻⁴	4.64 10 ⁻⁶	2.97 10 ⁻⁴
146	2.02 10 ⁻⁷	8.79 10 ⁻⁶	1.04 10 ⁻⁵	4.53 10 ⁻⁴	2.13 10 ⁻⁵	9.29 10 ⁻⁴	3.44 10 ⁻⁵	1.50 10 ⁻³	6.21 10 ⁻⁶	2.71 10 ⁻⁴
147	2.16 10 ⁻⁷	8.20 10 ⁻⁶	7.77 10 ⁻⁶	2.95 10 ⁻⁴	2.87 10 ⁻⁵	1.09 10 ⁻³	6.56 10 ⁻⁵	2.49 10 ⁻³	7.61 10 ⁻⁶	2.88 10 ⁻⁴

REFERENCES

1. González-Gaya, B.; Dachs, J.; Roscales, J. L.; Caballero, G.; Jiménez, B., Perfluoroalkylated Substances In The Global Tropical And Subtropical Surface Oceans. *Environmental Science & Technology* **2014**, *48*, (22), 13076-13084.
2. Loi, E. I.; Yeung, L. W.; Taniyasu, S.; Lam, P. K.; Kannan, K.; Yamashita, N., Trophic magnification of poly- and perfluorinated compounds in a subtropical food web. *Environ Sci Technol* **2011**, *45*, (13), 5506-13.
3. Siegel, D. A.; Buesseler, K. O.; Doney, S. C.; Sailley, S. F.; Behrenfeld, M. J.; Boyd, P. W., Global assessment of ocean carbon export by combining satellite observations and food-web models. *Global Biogeochemical Cycles* **2014**, *28*, (3), 2013GB004743.

5. CYCLING OF POLYCYCLIC AROMATIC HYDROCARBONS IN THE SURFACE OPEN OCEAN

Supporting Information

Belén González-Gaya ^{1,2*}, María-Carmen Fernández-Pinos ¹, Cristóbal Galbán-Malagón ¹, Antonio Bode ³, Montserrat Vidal ⁴, Begoña Jiménez ², and Jordi Dachs ¹

*Corresponding Author email: bggqam@idaea.csic.es

INDEX

Table S5.1. Sampling: Ancillary data for water sample's transects

Table S5.2. Sampling: Ancillary data for Plankton samples

Text S5.1. Materials and Methods

Table S5.3. Blanks (total pg per sample) and Surrogate recoveries (%) for particulate phase samples

Table S5.4. Blanks (total pg per sample), Breakthroughs and Surrogate recoveries (%) for plankton samples

Table S5.5. Particulate Organic Carbon (POC, μM) at surface (5 m depth)

Table S5.6. Carbon, Nitrogen and estimated Trophic position for plankton samples

Table S5.7. Organic carbon export from the surface mixed layer due to phytoplankton ($F_{OC-Phyto}$), zooplankton pellets ($F_{OC-Fecal}$) and total fluxes (F_{OC}) ($\text{mgC m}^{-2}\text{day}^{-1}$)

Table S5.8. Dissolved phase measured PAHs concentrations (ng L^{-1})

Table S5.9. Particulate phase measured PAHs concentrations ($\text{ng g}_{\text{dw}}^{-1}$)

Figure S5.1. Relative abundance of PAHs in the particulate phase

Table S5.10. Plankton phase measured PAHs concentrations ($\text{ng g}_{\text{dw}}^{-1}$)

Figure S5.2. Relative occurrence of individual PAHs in plankton per subbasin (%)

Figure S5.3. K_{OC} in surface waters for some representative PAHs

Table S5.11. Slopes fitted to the field data of $C_{Plankton}$ versus biomass

Table S5.12. Biological pump fluxes

Table S5.1. Sampling: Ancillary data for water sample's transects

Station	Volume filtered (L)	Particles dry weight (g)	Initial				Final			
			Date	Time (UTC)	Longitude	Latitude	Date	Time (UTC)	Longitude	Latitude
1	169.50	0.3626	16/12/10	11:45	-9.564	35.195	16/12/10	21:10	-11.173	34.580
0	192.00	0.3115	18/12/10	8:50	-15.158	31.823	18/12/10	22:10	-16.600	30.370
4	165.60	0.3587	20/12/10	10:51	-19.102	28.311	20/12/10	22:13	-20.125	26.452
6	240.88	0.3154	22/12/10	8:41	-22.247	23.255	22/12/10	21:24	-22.658	22.633
8	211.11	0.3522	24/12/10	8:55	-24.316	20.260	24/12/10	18:30	-24.974	19.063
10	345.21	0.6808	26/12/10	8:15	-26.005	14.519	26/12/10	22:08	-25.999	13.660
12	391.30	0.2067	28/12/10	8:46	-25.994	9.563	28/12/10	21:15	-26.014	8.571
14	259.26	0.3246	30/12/10	8:35	-26.033	5.012	30/12/10	20:15	-25.998	3.695
16	277.96	0.4133	01/01/11	9:28	-26.019	0.269	01/01/11	20:05	-26.481	-1.140
18	237.88	0.3146	03/01/11	9:31	-28.168	-4.780	03/01/11	20:45	-28.709	-5.954
20	367.50	0.3023	05/01/11	9:00	-30.187	-9.125	05/01/11	18:20	-30.443	-13.443
22	323.11	0.2686	07/01/11	9:43	-32.378	-13.735	07/01/11	20:40	-32.659	-14.263
24	272.31	0.2502	09/01/11	9:01	-34.671	-18.399	09/01/11	22:12	-35.114	-19.369
26	161.56	0.3467	11/01/11	9:45	-36.980	-23.002	11/01/11	20:50	-38.086	-23.374
27	240.75	0.2512	18/01/11	13:45	-39.661	-23.694	19/01/11	12:28	-37.530	-24.104
28	317.16	0.2969	19/01/11	14:36	-37.522	-24.105	20/01/11	12:00	-33.485	-24.789
29	185.79	-	20/01/11	13:00	-33.443	-24.781	20/01/11	21:45	-31.647	-25.155
30	249.90	0.2746	21/01/11	0:45	-31.070	-25.272	21/01/11	17:45	-30.049	-25.439
34	170.87	0.3394	24/01/11	15:38	-21.148	-26.999	26/01/11	0:12	-16.224	-27.884
37	355.70	0.4088	27/01/11	0:45	-10.446	-28.881	28/01/11	16:45	-7.588	-29.374
41	68.73	0.3001	01/02/11	1:10	2.954	-31.172	01/02/11	19:00	4.913	-31.498
42	148.18	0.2686	01/02/11	20:45	5.304	-31.555	02/02/11	21:37	8.036	-32.020
43	147.93	0.401	02/02/11	23:08	8.349	-32.074	04/02/11	2:00	12.440	-32.754
44	229.95	0.367	04/02/11	2:30	12.520	-32.769	04/02/11	20:00	13.463	-32.919
45	214.25	0.2988	04/02/11	20:45	13.637	-32.951	05/02/11	18:30	16.751	-33.479
0	118.67	0.393	12/02/11	7:58	20.976	-35.167	12/02/11	19:50	23.790	-35.099
46	289.95	0.3184	14/02/11	6:25	27.543	-34.836	14/02/11	18:48	29.637	-34.596
48	251.18	0.3367	16/02/11	5:30	33.709	-34.176	16/02/11	18:14	35.500	-33.998
50	358.00	0.3585	18/02/11	5:25	39.880	-33.532	18/02/11	18:14	41.684	-33.369
0	186.65	0.3491	20/02/11	4:00	54.284	-31.781	20/02/11	17:34	55.536	-31.495
0	154.38	0.3047	22/02/11	6:00	58.943	-30.852	22/02/11	14:14	61.458	-30.053
53	213.96	0.3418	25/02/11	3:00	63.247	-27.979	25/02/11	17:00	65.051	-27.899
55	337.09	0.3422	27/02/11	4:24	69.420	-29.360	27/02/11	16:25	70.811	-29.333
57	177.53	0.3404	01/03/11	3:03	76.079	-29.904	01/03/11	15:19	77.898	-29.879
59	226.99	0.3134	03/03/11	3:07	82.624	-29.810	03/03/11	15:22	84.578	-29.777
61	266.53	0.3278	05/03/11	2:55	89.466	-29.677	05/03/11	16:59	91.679	-29.666
63	343.13	0.3118	07/03/11	1:36	96.400	-29.579	08/03/11	1:40	99.998	-29.905
65	216.90	0.2707	09/03/11	2:00	103.311	-30.332	09/03/11	16:05	105.848	-30.635
67	187.85	0.3392	11/03/11	0:10	110.179	-31.154	11/03/11	13:44	112.038	-31.361
74	219.69	0.4088	24/03/11	0:25	110.180	-31.154	24/03/11	12:02	137.546	-39.648

Station	Volume filtered (L)	Particles dry weight (g)	Initial				Final			
			Date	Time (UTC)	Longitude	Latitude	Date	Time (UTC)	Longitude	Latitude
0	266.09	0.2869	09/04/11	0:30	156.778	-33.911	09/04/11	11:50	159.463	-33.985
80	242.00	0.3548	17/04/11	22:12	177.743	-30.970	18/04/11	8:17	179.143	-28.406
83	222.63	0.2935	21/04/11	19:14	-176.935	-20.602	22/04/11	6:51	-176.364	-19.796
85	256.00	0.3054	23/04/11	20:08	-174.497	-15.889	24/04/11	5:50	-174.102	-15.038
88	269.45	0.309	25/04/11	23:39	-172.736	-11.201	26/04/11	8:25	-172.560	-10.646
92	319.32	0.3518	29/04/11	21:35	-169.462	-3.398	30/04/11	10:32	-168.669	-1.872
95	206.91	0.3427	02/05/11	23:48	-165.403	4.622	03/05/11	9:40	-164.674	6.290
98	242.86	0.3093	05/05/11	22:20	-162.259	11.921	06/05/11	9:40	-161.379	13.758
104	271.17	0.2944	16/05/11	16:00	-150.360	21.066	17/05/11	6:30	-149.556	20.938
106	270.44	0.2942	18/05/11	15:30	-145.208	20.344	19/05/11	4:42	-146.308	20.085
108	207.28	0.2675	20/05/11	15:45	-138.966	19.279	21/05/11	3:11	-138.110	19.079
110	196.26	0.3285	22/05/11	14:55	-133.262	18.053	23/05/11	7:30	-131.486	17.582
112	197.44	0.2908	24/05/11	14:40	-127.569	16.624	25/05/11	4:30	-125.962	16.248
114	300.72	0.2819	26/05/11	14:45	-121.996	15.311	27/05/11	4:37	-120.109	14.845
116	255.68	0.3796	28/05/11	13:30	-115.768	13.771	29/05/11	4:00	-114.664	13.529
118	211.57	0.3135	30/05/11	13:35	-110.393	12.497	31/05/11	3:06	-109.574	12.321
121	283.11	0.3744	02/06/11	12:35	-102.447	10.757	03/06/11	2:10	-100.838	10.428
124	262.15	0.4244	05/06/11	12:50	-93.148	8.760	06/06/11	1:00	-91.917	8.482
126	257.84	0.3702	07/06/11	11:45	-87.960	7.224	08/06/11	1:00	-86.393	6.630
0	219.00	0.2999	11/06/11	15:15	-78.946	9.779	12/06/11	3:35	-76.588	10.160
129	224.57	0.3154	22/06/11	10:13	-69.291	15.075	22/06/11	23:36	-68.229	15.325
0	258.22	0.3278	24/06/11	11:55	-63.363	16.415	25/06/11	1:04	-60.863	17.082
133	198.50	0.3766	27/06/11	10:20	-55.160	19.020	27/06/11	23:40	-53.689	19.720
136	244.82	0.3138	30/06/11	9:05	-47.785	21.731	30/06/11	23:40	-45.908	22.374
138	246.74	0.3178	02/07/11	7:30	-41.908	23.736	02/07/11	22:45	-39.832	24.458
140	290.41	0.3162	04/07/11	7:35	-35.268	26.111	04/07/11	23:00	-34.037	26.532
142	251.45	0.2989	06/07/11	6:35	-29.671	27.981	06/07/11	21:43	-28.192	28.455
144	177.06	0.2584	08/07/11	6:45	-23.691	29.967	08/07/11	21:27	-22.053	30.507
146	249.09	0.2084	10/07/11	5:43	-17.262	32.083	10/07/11	20:20	-16.101	32.453

Table S5.2. Sampling: Ancillary data for Plankton samples

Station	Date	Time (UTC)	Longitude	Latitude	Total dry weight (g)	Biomass (g m ⁻³)
1	16/12/10	11:45	-9.530	35.165	1.07	4.73 10 ⁻³
0	19/12/10	8:50	-17.285	29.686	1.11	5.46 10 ⁻³
6	22/12/10	8:41	-22.244	23.256	1.34	7.89 10 ⁻³
8	24/12/10	8:55	-24.304	20.260	1.96	1.45 10 ⁻²
10	26/12/10	8:15	-26.005	14.519	3.48	3.85 10 ⁻²
12	28/12/10	8:46	-25.994	9.564	2.25	1.47 10 ⁻²
14	30/12/10	8:35	-26.033	5.011	3.42	2.08 10 ⁻²
16	01/01/11	9:28	-26.019	0.270	5.42	4.00 10 ⁻²
18	03/01/11	9:31	-28.174	-4.773	1.94	1.04 10 ⁻²
20	05/01/11	9:00	-30.189	-9.110	1.98	6.50 10 ⁻³
22	07/01/11	9:43	-32.378	-13.729	1.57	5.79 10 ⁻³
24	09/01/11	9:01	-34.675	-18.399	3.14	1.23 10 ⁻²
26	11/01/11	9:45	-35.975	-21.090	0.74	2.35 10 ⁻³
27	19/01/11	13:45	-36.223	-24.314	0.28	1.15 10 ⁻³
28	20/01/11	14:36	-33.095	-24.852	0.17	1.15 10 ⁻³
29	21/01/11	13:00	-30.131	-25.400	3.23	2.04 10 ⁻²
30	22/01/11	0:45	-27.589	-25.863	3.11	1.96 10 ⁻²
0	23/01/11	-	-24.243	-26.424	2.10	1.16 10 ⁻²
34	26/01/11	15:38	-14.789	-28.101	1.74	6.40 10 ⁻³
37	30/01/11	0:45	-5.401	-29.687	0.32	1.81 10 ⁻³
41	02/02/11	1:10	6.786	-31.772	3.73	3.00 10 ⁻²
42	03/02/11	20:45	9.417	-32.104	2.19	1.38 10 ⁻²
43	04/02/11	23:08	12.749	-32.791	2.13	1.05 10 ⁻²
44	05/02/11	2:30	15.474	-33.297	0.27	3.93 10 ⁻³
45	13/02/11	-	25.558	-35.139	2.03	2.00 10 ⁻²
46	14/02/11	6:25	27.546	-34.837	4.01	2.15 10 ⁻²
48	16/02/11	5:30	33.724	-34.172	2.32	1.25 10 ⁻²
50	18/02/11	5:25	39.880	-33.532	0.15	9.73 10 ⁻⁴
52	24/02/11	-	61.458	-30.053	2.21	1.00 10 ⁻²
53	25/02/11	3:00	63.248	-27.976	0.19	8.42 10 ⁻⁴
55	27/02/11	4:24	69.414	-29.363	0.87	5.51 10 ⁻³
57	01/03/11	3:03	76.086	-29.906	1.80	1.06 10 ⁻²
59	03/03/11	3:07	82.624	-29.810	1.82	1.08 10 ⁻²
61	05/03/11	2:55	89.478	-29.681	0.86	6.32 10 ⁻³
63	07/03/11	1:36	96.395	-29.582	1.71	1.16 10 ⁻²
65	09/03/11	2:00	103.309	-30.333	1.82	1.34 10 ⁻²
67	11/03/11	0:10	110.180	-31.154	3.65	1.79 10 ⁻²
74	24/03/11	0:25	135.224	-39.225	1.00	1.04 10 ⁻²
0	09/04/11	0:30	159.057	-33.976	0.41	7.29 10 ⁻³
79	17/04/11	-	176.016	-34.056	1.89	1.12 10 ⁻²
83	21/04/11	19:14	-177.417	-21.442	2.40	1.41 10 ⁻²
85	23/04/11	20:08	-174.488	-15.903	0.60	3.39 10 ⁻³

Station	Date	Time (UTC)	Longitude	Latitude	Total dry weight (g)	Biomass (g m ⁻³)
88	26/04/11	23:39	-172.323	-9.460	0.81	4.54 10 ⁻³
92	30/04/11	21:35	-168.357	-1.304	1.47	9.60 10 ⁻³
95	03/05/11	23:48	-164.427	6.978	3.24	2.94 10 ⁻²
98	06/05/11	22:20	-160.861	15.017	1.43	6.47 10 ⁻³
103	16/05/11	16:00	-150.366	21.067	3.36	1.53 10 ⁻²
105	18/05/11	15:30	-145.212	20.341	4.41	1.86 10 ⁻²
106	19/05/11	-	-141.617	19.902	2.09	9.15 10 ⁻³
107	20/05/11	15:45	-138.966	19.279	3.05	1.28 10 ⁻²
109	22/05/11	14:55	-133.262	18.057	3.35	1.58 10 ⁻²
111	24/05/11	14:40	-127.627	16.617	4.04	1.91 10 ⁻²
113	26/05/11	14:45	-121.995	15.311	4.46	1.95 10 ⁻²
115	28/05/11	13:30	-115.775	13.760	5.76	3.08 10 ⁻²
116	29/05/11	-	-113.270	13.195	3.22	1.52 10 ⁻²
117	30/05/11	13:35	-110.392	12.493	2.27	9.25 10 ⁻³
118	31/05/11	-	-108.046	11.992	4.23	3.11 10 ⁻²
120	02/06/11	12:35	-102.448	10.757	2.23	1.58 10 ⁻²
123	05/06/11	12:50	-93.148	8.764	4.41	3.47 10 ⁻²
125	07/06/11	11:45	-87.947	7.221	4.61	3.88 10 ⁻²
129	22/06/11	10:13	-69.289	15.073	3.43	1.68 10 ⁻²
131	25/06/11	-	-59.829	17.428	4.07	2.18 10 ⁻²
133	27/06/11	10:20	-55.160	19.020	1.60	5.90 10 ⁻³
136	28/06/11	-	-52.629	20.013	1.79	6.81 10 ⁻³
136	30/06/11	9:05	-47.790	21.742	1.02	4.02 10 ⁻³
138	02/07/11	7:30	-41.912	23.736	1.24	7.80 10 ⁻³
140	04/07/11	7:35	-35.274	26.111	0.16	8.79 10 ⁻⁴
142	06/07/11	6:35	-29.673	27.983	0.46	2.71 10 ⁻³
144	08/07/11	6:45	-23.693	29.966	1.75	7.95 10 ⁻³
146	10/07/11	5:43	-17.260	32.088	1.26	6.78 10 ⁻³

Text S5.1. Materials and Methods

Dissolved samples

XAD-2 resin was extracted sequentially with 200 mL of methanol (MeOH) and 300 mL of dichloromethane (DCIM) pumped contrariwise to the sampling direction flux, in order to facilitate the extraction and avoid preferent pathways. Both elutants were kept separated and were surrogate recovery spiked. After a rotary evaporator reduction, the MeOH fraction was liquid-liquid extracted with hexane (Hx, 30 mL) on a decanting funnel three times. Both phases were further purified over a anhydrous sulfate muffled open funnel; first the MeOH phase and the MeOH was discarded and then the Hx phase which was kept and additionally washed with Hx. This elutant was mixed with the DCIM phase, reduced down to Hx and fractioned over an alumina column (3 g, 90% deactivated alumina with a 1 cm sulfate top layer, packed with Hx). Fractioning was set with 5 mL Hx for the the first fraction of alifatic compounds, 12 mL Hx/DCIM (1:2) for the second fraction containing the aromatic compounds, and 15 mL MeOH/DCIM (1:2) for other polar compounds. Fractions 1 and 2 were reduced under a gentle nigrogen stream and solvent changed to isooctane down to 100 uL.

Particulate samples

Filters containing the particulate samples were freeze dried, weighted and soxhlet extracted overnight with DCIM/MeOH (2:1). The extract was concentrated on a rotary evaporator system and solvent changed to isooctane. Then, samples were further purified and fractioned over an alumina column (3 g, 90% deactivated alumina with a 1 cm sulfate top layer, packed with Hx). Fractioning was set with 6 mL Hx for the the first fraction of alifatic compounds, 12 mL Hx/DCIM (3:1) for the second fraction containing the aromatic compounds, 35 mL DCIM for organophosphate esters on a third fraction, and a last fraction of 15 mL DCIM/MeOH (2:1) for other products. Fractions 1, 2 and 3 were reduced under a gentle nitrogen stream and solvent changed to isooctane down to 100 uL.

Plankton samples

Plankton filters were freeze dried, weighted and soxhlet extracted overnight with DCl/Hex (1:1). Plankton samples were purified and fractioned over a combined silica and alumina column (top 1 cm sulphate, intermediate 5 g muffled neutral silica, and bottom 3 g, 90% deactivated alumina, packed with Hx). Fractioning was set with 25 mL Hx for the the first fraction of alifatic compounds, 40 mL Hx/DCIM (3:1) for the second fraction containing the aromatic compounds, 20 mL DCIM/Acetone (70:30) for organophosphate esters on a third fraction and a last fraction of 25 mL DCIM/MeOH (2:1) for other polar compounds. Fractions 1, 2 and 3 were reduced under a gentle nigrogen stream and solvent changed to isooctane down to 100 uL.

Table S5.3. Blanks (total pg per sample) and Surrogate recoveries (%) for particulate phase samples

	Mean laboratory blank (n=7)	Mean field blank (n=4)		Surrogate recovery (n=69)
Naphthalene	0.154	0.165		
Dimethylnaphthalenes	0.057	0.053		
Methylnaphthalenes	0.000	0.000		
Acenaphtylene	0.038	0.045		
Acenaphtene	0.112	0.242		
Fluorene	0.095	0.295		
Dibenzothiophene	0.049	0.098		
Methyldibenzothiophenes	0.174	0.341		
Dimethyldibenzothiopenes	0.214	0.356		
Phenanthrene	0.433	1.016		
Methylphenantrenes	0.303	0.345		
Dimethylphenanthrenes	0.222	0.248		
Anthracene	0.047	0.049		
Fluoranthene	0.336	0.370		
Pyrene	0.130	0.173		
Methylpyrene	0.051	0.068		
Dimethylpyrene	0.000	0.085		
Benzo(ghi)fluoranthene	0.069	0.070		
Benzo(a)anthracene	0.134	0.201		
Chrysene	0.069	0.079		
Methylchrysenes	0.000	0.056		
Benzo(b+k)fluoranthenes	0.164	0.165		
Benzo(e)pyrene	0.076	0.096		
Benzo(a)pyrene	0.011	0.080		
Perylene	0.097	0.101	Perylene D12	76.2
Indeno(1,2,3-cd)pyrene	0.045	0.095		
Dibenzo(a,h)anthracene	0.062	0.089		
Benzo(ghi)perylene	0.058	0.095		

All samples have been surrogate recovery corrected by Perylene D12.

Table S5.4. Blanks (total pg per sample), Breakthroughs and Surrogate recoveries (%) for plankton samples

	Mean laboratory blank (n=7)	Mean field blank (n=4)	Mean 1st Breakthrough extraction (n=5)		Surrogate recovery (n=71)
Naphthalene	0.006	0.185	81.1		
Methylnaphthalenes	0.027	0.838	85.4		
Dimethylnaphthalenes	0.012	0.942	96.0		
Acenaphtylene	0.000	0.030	90.7	Acenaphtene D10	25.1
Acenaphtene	0.013	0.418	99.0		
Fluorene	0.004	0.069	91.7		
Dibenzothiophene	0.000	0.000	100.0		
Methyldibenzothiophenes	0.002	0.000	87.5		
Dimethyldibenzothiopenes	0.000	0.000	93.7		
Phenanthrene	0.015	0.264	97.4	Phenanthrene D10	41.9
Methylphenantrenes	0.004	0.196	97.0		
Dimethylphenanthrenes	0.007	0.000	99.3		
Anthracene	0.000	0.067	85.6		
Fluoranthene	0.036	0.128	97.4		
Pyrene	0.026	0.275	95.6		
Methylpyrenes	0.000	0.000	100.0		
Dimethylpyrenes	0.000	0.000	100.0		
Benzo(ghi)fluoranthene	0.000	0.037	100.0		
Benzo(a)anthracene	0.114	0.120	96.1		
Chrysene	0.021	0.015	95.4	Chrysene D12	70.1
Methylchrysenes	0.000	0.000	100.0		
Benzo(b+k)fluoranthenes	0.120	0.000	94.2		
Benzo(e)pyrene	0.000	0.078	93.3		
Benzo(a)pyrene	0.000	0.000	100.0		
Perylene	0.000	0.000	100.0	Perylene D12	102.4
Indeno(1,2,3-cd)pyrene	0.071	0.000	100.0		
Dibenzo(a,h)anthracene	0.281	0.000	100.0		
Benzo(ghi)perylene	0.148	0.000	99.7		

All samples have been surrogate recovery corrected by the indicated deuterated standard.

Table S5.5. Particulate organic carbon (POC, μM) at surface (5 m depth)

Station	POC	Station	POC
1	1.9	83	3.7
0	1.7	85	2.7
4	1.6	88	1.7
6	1.7	92	1.4
8	1.7	95	2.0
10	2.2	98	1.4
12	2.3	103	4.6
14	2.4	105	1.6
16	2.0	107	2.7
18	2.3	109	2.4
20	2.3	111	1.4
22	1.5	113	1.3
24	2.2	115	2.5
26	2.5	117	1.9
27	2.5	120	2.3
28	2.5	123	4.9
29	1.6	125	9.3
30	3.4	0	2.3
34	3.4	129	2.2
37	1.8	0	1.7
41	1.8	133	-
42	1.7	136	2.0
43	3.3	138	1.6
44	4.3	140	1.7
45	4.3	142	1.3
0	6.1	144	1.8
46	2.2	146	4.5
48	1.6		
50	1.4		
0	1.3		
0	1.2		
53	2.4		
55	0.9		
57	0.9		
59	1.0		
61	0.9		
63	1.1		
65	4.4		
67	2.3		
74	2.4		
0	-		
80	2.2		

Table S5.6. Carbon, Nitrogen and estimated trophic position for plankton samples

Station	N biomass <i>(mg N m⁻³)</i>	C biomass <i>(mg C m⁻³)</i>	C:N <i>(molar)</i>	d¹⁵N <i>(‰)</i>	d¹³C <i>(‰)</i>	Trophic position*
1						
3						
6						
8						
10	1.56	6.43	4.81	4.95	-19.57	1.58
12						
14						
16						
18						
20						
22						
24						
25						
27						
28						
29	2.78	11.66	4.88	1.92	-19.77	
30						
31						
35	1.09	4.30	4.60	5.87	-21.43	1.29
37						
39	2.07	9.86	5.56	8.42	-18.34	1.57
42						
43						
44						
45	2.77	10.89	4.58	6.55	-19.07	1.43
46	2.13	8.46	4.64	4.92	-20.09	1.70
48	1.11	5.65	5.94	4.38	-21.78	1.80
50	0.50	2.46	5.81	4.85	-17.75	1.41
52	1.90	7.19	4.43	4.68	-20.86	1.17
53	2.32	9.09	4.57	3.75	-20.87	1.27
55	1.47	5.50	4.37	4.76	-20.96	1.24
57	1.71	6.64	4.54	5.59	-21.08	1.46
59	1.07	4.39	4.78	8.86	-21.24	1.43
61	1.88	7.42	4.60	6.59	-20.93	1.55
63	1.54	6.14	4.64	8.19	-21.30	1.21
65	1.88	6.96	4.32	3.53	-22.29	1.20
67	1.40	5.86	4.88	3.92	-20.54	1.89
74	2.24	8.72	4.54	12.61	-20.30	1.64
4b1						
79	1.96	7.13	4.25	6.88	-20.69	1.31
83	1.98	8.05	4.76	1.68	-19.88	1.66
85	1.29	5.11	4.61	2.27	-19.08	1.44

Station	N biomass	C biomass	C:N	d¹⁵N	d¹³C	Trophic position*
	<i>(mg N m⁻³)</i>	<i>(mg C m⁻³)</i>	<i>(molar)</i>	<i>(‰)</i>	<i>(‰)</i>	
88	1.65	6.13	4.33	12.65	-19.33	1.72
92	2.13	8.10	4.44	3.57	-19.42	1.57
95	7.36	27.90	4.43	6.26	-19.83	1.70
98	0.86	3.86	5.25	8.11	-19.48	1.88
103	2.08	7.84	4.40	8.12	-20.36	1.42
105	2.04	8.07	4.61	4.45	-20.36	1.60
106	1.39	5.39	4.52	7.92	-20.81	1.45
107	1.79	6.88	4.49	8.76	-20.92	1.52
109	2.47	9.60	4.54	8.16	-20.40	1.65
111	2.56	10.21	4.65	10.25	-20.80	1.91
113	2.43	9.37	4.50	10.48	-20.91	1.68
115	3.13	12.09	4.51	10.38	-21.01	1.45
116	2.03	8.33	4.79	8.68	-21.76	2.12
117	2.30	9.18	4.66	9.68	-20.62	1.50
118	2.50	9.76	4.56	10.43	-20.59	1.76
120	3.54	15.30	5.05	9.49	-19.32	1.50
123	5.42	20.02	4.31	6.75	-21.45	1.63
125	6.28	24.29	4.51	5.10	-21.34	1.80
129	3.10	12.14	4.57	1.11	-18.50	1.73
131	1.38	5.40	4.58	1.87	-18.97	1.66
133	1.70	6.73	4.61	0.39	-19.25	1.49
134	1.99	7.97	4.67	0.30	-18.52	1.56
136	1.56	6.18	4.63	0.69	-19.36	1.32
138	1.48	6.21	4.90	1.04	-19.24	1.77
140	1.12	4.72	4.94	1.52	-20.41	1.64
142	1.08	4.16	4.51	2.59	-21.33	1.44
144	1.92	7.40	4.49	3.36	-21.44	1.66
145	1.97	7.72	4.58	3.21	-21.76	1.70

*Trophic position attends for the estimated TP of the plankton Fraction 500-1000 mm calculated by $(\delta N^{15}_{500-1000} - \delta N^{15}_{40-200}/3.4) - 1.5$.

Table S5.7. Organic carbon export from the surface mixed layer due to phytoplankton ($F_{OC-Phyto}$), zooplankton pellets ($F_{OC-Fecal}$) and total fluxes (F_{OC}) ($\text{mgC m}^{-2}\text{day}^{-1}$)

Station	$F_{OCPhyto}$	$F_{OCFecal}$	F_{OC}
1	5.92	26.61	32.53
3	2.96	29.67	32.63
6	5.36	43.10	48.45
8	6.66	53.92	60.58
10	10.97	79.32	90.29
12	8.59	53.54	62.14
14	13.67	68.05	81.72
16	7.82	60.17	67.99
18	1.18	55.16	56.35
20	0.21	35.79	36.00
22	0.15	30.60	30.75
24	0.49	43.92	44.41
25	0.75	43.42	44.16
27	0.43	42.07	42.50
28	0.38	35.40	35.78
29	0.47	34.28	34.75
30	0.53	34.63	35.16
31	0.24	27.45	27.69
34	0.10	21.18	21.28
37	0.05	19.25	19.30
41	0.21	24.16	24.36
42	0.31	25.52	25.82
43	0.79	31.31	32.10
44	2.43	41.23	43.65
45	54.30	198.96	253.26
46	4.19	51.01	55.20
48	1.17	41.44	42.61
50	0.60	38.37	38.97
52	0.25	20.81	21.06
53	0.87	31.25	32.13
55	0.21	19.01	19.22
57	0.18	16.96	17.14
59	0.15	16.07	16.22
61	0.18	18.28	18.45
63	0.19	15.44	15.63
65	0.34	21.71	22.05
67	0.98	39.81	40.79
74	8.15	49.69	57.83
4b1	6.29	52.28	58.56
79	2.36	37.35	39.71

Station	<i>F_{OCPhyto}</i>	<i>F_{OCFecal}</i>	<i>F_{OC}</i>
83	2.31	41.33	43.65
85	1.00	38.23	39.23
88	0.49	39.62	40.11
92	10.59	97.14	107.73
95	7.46	69.10	76.56
98	0.62	33.67	34.30
103	0.54	40.18	40.72
105	0.36	38.43	38.79
106	0.53	37.63	38.17
107	0.39	36.94	37.33
109	0.30	32.96	33.26
111	0.46	33.09	33.55
113	1.75	44.82	46.57
115	2.02	51.62	53.64
116	2.91	52.96	55.87
117	3.56	56.49	60.04
118	3.95	55.09	59.04
120	3.53	48.01	51.54
123	33.00	127.11	160.11
125	21.84	93.34	115.18
129	4.77	48.64	53.41
131	3.34	46.50	49.84
133	0.74	24.20	24.94
134	0.37	20.85	21.22
136	0.15	16.35	16.50
138	0.24	14.19	14.43
140	0.14	12.17	12.31
142	0.21	15.32	15.53
144	0.26	16.58	16.84
146	0.64	28.07	28.71

Table S5.8. Dissolved phase measured PAHs concentrations (ng L⁻¹)

Station	Naphthalene	Methyl/naphthalenes	Dimethyl/naphthalenes	Acenaphthylene	Acenaphthene	Fluorene	Dibenzothiophene	Methyl/dibenzothiophene s	Dimethyl/dibenzothiophene s	Phenanthrene	Methyl/phenantrenes	Dimethyl/phenanthrene s	Anthracene	Fluoranthene	Pyrene	Methyl/pyrene s	Dimethyl/pyrene s	Benzo(ghi)fluoranthene	Benzo(a)anthracene	Chrysene	Methyl/chrysenes	Benzo(b+k)fluoranthenes	Benzo(e)pyrene	Benzo(a)pyrene	Perylene	Indeno(1,2,3-cd)pyrene	Dibenzo(a,h)anthracene	Benzo(ghi)perylene	Σ ₆₄ PAHs
1	0.132	0.575	1.15	0.016	0.542	0.555	0.132	0.118	0.099	0.888	0.339	0.123	0.088	0.237	0.278	0.035	0.018	0.013	0.019	0.017	0.006	0.006	0.007	0.004	0.000	0.019	0.031	0.023	5.47
0	0.024	0.136	0.428	0.010	0.271	0.426	0.096	0.097	0.085	0.635	0.239	0.103	0.070	0.185	0.218	0.028	0.013	0.014	0.016	0.011	0.004	0.004	0.006	0.002	0.001	0.025	0.036	0.022	3.21
4	0.031	0.117	0.313	0.013	0.189	0.571	0.102	0.106	0.093	0.723	0.312	0.126	0.057	0.247	0.280	0.033	0.013	0.013	0.026	0.013	0.005	0.003	0.006	0.001	0.001	0.025	0.037	0.009	3.47
6	0.154	0.558	1.03	0.046	0.488	0.433	0.095	0.111	0.101	0.541	0.271	0.126	0.049	0.235	0.281	0.062	0.035	0.012	0.140	0.026	0.036	0.005	0.017	0.006	0.003	0.018	0.025	0.010	4.91
8	0.000	0.000	0.017	0.024	0.007	0.000	0.007	0.009	0.012	0.000	0.000	0.000	0.000	0.001	0.001	0.034	0.052	0.000	0.004	0.000	0.007	0.000	0.000	0.000	0.001	0.001	0.001	0.000	0.180
10	0.002	0.000	0.122	0.006	0.067	0.294	0.071	0.100	0.094	0.528	0.303	0.130	0.068	0.306	0.368	0.042	0.018	0.009	0.057	0.014	0.004	0.003	0.006	0.002	0.001	0.013	0.015	0.004	2.65
12	0.001	0.017	0.109	0.042	0.034	0.148	0.094	0.088	0.084	0.316	0.251	0.106	0.062	0.236	0.303	0.040	0.020	0.052	0.008	0.018	0.012	0.002	0.008	0.003	0.001	0.012	0.014	0.006	2.09
14	0.022	0.000	0.000	0.304	0.401	0.000	1.07	0.694	0.108	0.604	0.000	0.115	0.027	0.318	0.352	0.199	0.095	0.000	0.000	0.038	0.013	0.000	0.000	0.000	0.000	0.011	0.012	0.000	4.39
16	0.000	0.000	0.000	0.911	0.090	0.000	1.73	0.629	0.137	0.326	0.000	0.044	0.000	0.000	0.000	0.267	0.000	0.000	0.082	0.021	0.044	0.000	0.000	0.050	0.000	0.000	0.000	4.34	
18	0.000	0.033	0.192	0.060	0.067	0.124	0.122	0.115	0.128	0.238	0.451	0.172	0.058	0.376	0.516	0.067	0.035	0.017	0.052	0.023	0.023	0.005	0.015	0.005	0.001	0.016	0.019	0.008	2.94
20	0.000	0.001	0.008	0.001	0.006	0.048	0.015	0.049	0.061	0.129	0.156	0.089	0.014	0.216	0.276	0.032	0.013	0.010	0.023	0.011	0.003	0.003	0.006	0.001	0.001	0.037	0.048	0.010	1.27
22	0.002	0.007	0.046	0.020	0.019	0.061	0.039	0.059	0.068	0.119	0.182	0.081	0.027	0.202	0.259	0.031	0.011	0.012	0.022	0.009	0.004	0.002	0.004	0.002	0.001	0.009	0.009	0.004	1.31
24	0.000	0.010	0.000	0.000	0.428	0.000	0.301	0.114	0.000	0.000	0.000	0.000	0.109	0.000	0.023	0.198	0.155	0.000	0.000	0.000	0.070	0.000	0.000	0.000	0.000	0.000	0.000	0.000	1.41
26	0.019	0.000	0.000	0.000	0.219	0.000	2.28	1.54	0.301	0.000	0.000	0.000	0.281	0.312	0.209	0.252	0.091	0.000	0.000	0.000	0.145	0.000	0.000	0.005	0.000	0.000	0.026	0.000	5.67
27	0.011	0.130	0.163	0.005	0.028	0.123	0.035	0.100	0.128	0.303	0.347	0.241	0.042	0.414	0.495	0.138	0.138	0.023	0.066	0.080	0.138	0.012	0.060	0.019	0.002	0.021	0.020	0.013	3.29
28	0.003	0.028	0.081	0.004	0.016	0.089	0.038	0.124	0.172	0.313	0.358	0.202	0.042	0.469	0.535	0.083	0.029	0.017	0.061	0.019	0.006	0.004	0.006	0.003	0.002	0.028	0.041	0.007	2.78

Station	Naphthalene	Methylnaphthalenes	Dimethylnaphthalenes	Acenaphylene	Acenaphtene	Fluorene	Dibenzothiophene	Methyldibenzothiophene s	Dimethyldibenzothiophene s	Phenanthrene	Methylphenantrenes	Dimethylphenanthrene s	Anthracene	Fluoranthene	Pyrene	Methylpyrene s	Dimethylpyrene s	Benzo(ghi)fluoranthene	Benzo(a)anthracene	Chrysene	Methylchrysenes	Benzo(b+k)fluoranthenes	Benzo(e)pyrene	Benzo(a)pyrene	Perylene	Indeno(1,2,3-cd)pyrene	Dibenzo(a,h)anthracene	Benzo(ghi)perylene	Σ ₆₄ PAHs
29	0.001	0.000	0.000	0.010	0.000	0.065	0.051	0.099	0.129	0.216	0.338	0.124	0.027	0.347	0.401	0.044	0.021	0.018	0.021	0.014	0.007	0.003	0.006	0.003	0.001	0.024	0.032	0.013	2.02
30	0.008	0.041	0.087	0.004	0.017	0.048	0.018	0.057	0.074	0.147	0.170	0.098	0.027	0.225	0.229	0.041	0.020	0.007	0.025	0.015	0.016	0.003	0.009	0.003	0.001	0.015	0.015	0.004	1.42
34	0.001	0.000	0.036	0.004	0.000	0.029	0.030	0.041	0.059	0.130	0.213	0.101	0.020	0.272	0.305	0.037	0.012	0.019	0.015	0.007	0.005	0.002	0.003	0.002	0.001	0.030	0.032	0.008	1.42
41	0.010	0.052	0.197	0.011	0.016	0.198	0.100	0.214	0.225	0.526	0.568	0.302	0.074	0.699	0.715	0.111	0.082	0.045	0.048	0.043	0.063	0.008	0.032	0.011	0.007	0.085	0.096	0.033	4.57
42	0.217	0.144	0.000	1.307	0.000	1.063	2.02	0.684	0.579	0.481	0.000	0.294	0.000	0.557	0.628	0.859	0.502	0.000	0.413	0.000	0.150	0.067	0.000	0.146	0.128	0.143	0.109	0.097	10.6
43	0.000	1.77	1.19	0.000	0.000	1.15	1.52	0.000	0.000	0.082	0.000	0.298	0.000	0.127	0.127	0.112	0.000	0.000	0.149	0.000	0.048	0.151	0.000	0.187	0.000	0.286	0.255	0.203	7.65
44	0.010	0.024	0.089	0.003	0.019	0.063	0.031	0.085	0.098	0.244	0.241	0.135	0.020	0.291	0.297	0.029	0.009	0.006	0.016	0.008	0.002	0.002	0.003	0.001	0.001	0.006	0.007	0.002	1.74
45	0.003	0.007	0.028	0.000	0.005	0.013	0.007	0.024	0.039	0.054	0.069	0.052	0.005	0.098	0.102	0.013	0.005	0.003	0.003	0.004	0.002	0.001	0.002	0.000	0.001	0.007	0.011	0.002	0.559
0	0.017	0.032	0.067	0.000	0.009	0.032	0.019	0.054	0.066	0.158	0.402	0.075	0.020	0.189	0.210	0.023	0.009	0.010	0.006	0.007	0.004	0.001	0.004	0.003	0.004	0.016	0.023	0.014	1.47
46	0.000	0.054	0.151	0.000	0.000	0.000	0.154	0.160	0.000	0.000	0.000	0.000	0.000	0.055	0.077	0.445	0.142	0.000	0.493	0.000	0.107	0.000	0.000	0.000	0.000	0.014	0.000	0.009	1.86
48	0.021	0.086	0.180	0.000	0.029	0.058	0.029	0.075	0.101	0.227	0.226	0.128	0.022	0.298	0.304	0.035	0.012	0.010	0.008	0.009	0.002	0.002	0.004	0.001	0.001	0.023	0.029	0.014	1.93
50	0.001	0.010	0.026	0.000	0.002	0.027	0.020	0.064	0.079	0.174	0.216	0.109	0.018	0.271	0.275	0.032	0.010	0.006	0.013	0.008	0.002	0.002	0.003	0.001	0.001	0.009	0.014	0.004	1.40
0	0.024	0.078	0.136	0.004	0.024	0.059	0.035	0.078	0.094	0.221	0.205	0.102	0.025	0.270	0.267	0.037	0.013	0.011	0.010	0.006	0.003	0.001	0.002	0.001	0.001	0.018	0.026	0.013	1.76
0	0.012	0.041	0.119	0.005	0.000	0.044	0.041	0.071	0.101	0.161	0.164	0.101	0.025	0.235	0.239	0.039	0.013	0.013	0.009	0.006	0.005	0.001	0.003	0.001	0.002	0.030	0.036	0.009	1.53
53	0.000	0.000	0.000	0.000	0.000	0.037	0.017	0.050	0.077	0.145	0.191	0.106	0.021	0.278	0.275	0.030	0.012	0.012	0.014	0.008	0.003	0.002	0.004	0.002	0.001	0.015	0.020	0.010	1.33
55	0.032	0.095	0.174	0.003	0.039	0.064	0.033	0.075	0.097	0.247	0.229	0.115	0.028	0.292	0.318	0.033	0.010	0.007	0.010	0.009	0.002	0.003	0.004	0.003	0.001	0.008	0.010	0.004	1.94
57	0.042	0.146	0.262	0.002	0.043	0.073	0.036	0.083	0.097	0.270	0.233	0.111	0.033	0.320	0.357	0.030	0.009	0.013	0.005	0.008	0.002	0.002	0.003	0.002	0.001	0.059	0.079	0.017	2.34
59	0.007	0.024	0.069	0.002	0.015	0.064	0.028	0.070	0.079	0.209	0.199	0.104	0.019	0.251	0.285	0.034	0.009	0.020	0.008	0.006	0.002	0.001	0.003	0.001	0.001	0.144	0.170	0.032	1.86

Station	Naphthalene	Methylnaphthalenes	Dimethylnaphthalenes	Acenaphylene	Acenaphtene	Fluorene	Dibenzothiophene	Methylidibenzothiophene s	Dimethyldibenzothiophene s	Phenanthrene	Methylphenantrenes	Dimethylphenanthrene s	Anthracene	Fluoranthene	Pyrene	Methylpyrene s	Dimethylpyrene s	Benzo(ghi)fluoranthene	Benzo(a)anthracene	Chrysene	Methylchrysenes	Benzo(b+k)fluoranthenes	Benzo(e)pyrene	Benzo(a)pyrene	Perylene	Indeno(1,2,3-cd)pyrene	Dibenzo(a,h)anthracene	Benzo(ghi)perylene	Σ ₆₄ PAHs		
61	0.018	0.048	0.108	0.000	0.019	0.038	0.018	0.047	0.067	0.131	0.147	0.086	0.017	0.231	0.261	0.028	0.009	0.010	0.007	0.007	0.002	0.001	0.002	0.001	0.001	0.001	0.001	0.023	0.033	0.007	1.37
63	0.023	0.078	0.173	0.003	0.037	0.087	0.037	0.088	0.103	0.288	0.250	0.131	0.027	0.319	0.348	0.032	0.009	0.010	0.008	0.006	0.002	0.001	0.002	0.001	0.001	0.001	0.020	0.030	0.010	2.12	
65	0.024	0.034	0.108	0.000	0.000	0.105	0.052	0.128	0.142	0.379	0.383	0.172	0.043	0.400	0.428	0.050	0.019	0.019	0.016	0.014	0.005	0.002	0.004	0.002	0.002	0.036	0.052	0.019	2.64		
67	0.129	0.337	0.550	0.000	0.087	0.119	0.062	0.146	0.177	0.454	0.402	0.207	0.056	0.548	0.598	0.051	0.017	0.021	0.008	0.013	0.004	0.003	0.005	0.002	0.002	0.083	0.096	0.033	4.21		
74	0.016	0.050	0.125	0.000	0.020	0.028	0.016	0.035	0.044	0.119	0.106	0.075	0.015	0.149	0.178	0.018	0.006	0.014	0.003	0.004	0.001	0.001	0.001	0.001	0.001	0.041	0.059	0.015	1.14		
0	0.012	0.038	0.098	0.000	0.017	0.026	0.018	0.044	0.063	0.136	0.128	0.075	0.014	0.203	0.276	0.024	0.007	0.007	0.004	0.007	0.002	0.002	0.003	0.001	0.001	0.025	0.033	0.008	1.27		
80	0.068	0.285	0.480	0.004	0.066	0.092	0.044	0.091	0.117	0.309	0.250	0.131	0.034	0.319	0.394	0.030	0.009	0.012	0.005	0.008	0.002	0.002	0.003	0.001	0.001	0.033	0.052	0.019	2.86		
83	0.033	0.090	0.293	0.002	0.046	0.108	0.052	0.131	0.166	0.386	0.359	0.189	0.045	0.484	0.568	0.047	0.013	0.018	0.017	0.012	0.003	0.003	0.005	0.002	0.001	0.032	0.048	0.016	3.17		
85	0.026	0.091	0.263	0.000	0.046	0.100	0.052	0.132	0.173	0.394	0.356	0.184	0.045	0.461	0.583	0.051	0.013	0.016	0.033	0.013	0.003	0.002	0.004	0.002	0.001	0.027	0.041	0.013	3.12		
88	0.030	0.085	0.301	0.000	0.053	0.105	0.055	0.136	0.182	0.408	0.365	0.197	0.043	0.502	0.643	0.055	0.013	0.016	0.049	0.013	0.003	0.003	0.005	0.002	0.001	0.030	0.046	0.014	3.36		
92	0.016	0.067	0.181	0.000	0.028	0.066	0.044	0.118	0.141	0.320	0.301	0.151	0.031	0.391	0.504	0.043	0.011	0.019	0.009	0.012	0.004	0.003	0.004	0.002	0.001	0.030	0.039	0.013	2.55		
95	0.024	0.070	0.171	0.000	0.031	0.065	0.043	0.120	0.148	0.325	0.336	0.176	0.033	0.461	0.574	0.046	0.012	0.023	0.009	0.014	0.003	0.004	0.006	0.002	0.002	0.081	0.100	0.037	2.91		
98	0.045	0.133	0.269	0.005	0.038	0.087	0.060	0.152	0.221	0.457	0.445	0.191	0.029	0.504	0.605	0.068	0.023	0.016	0.009	0.015	0.006	0.003	0.006	0.003	0.003	0.022	0.035	0.015	3.47		
103	0.019	0.057	0.118	0.003	0.047	0.083	0.032	0.068	0.081	0.250	0.202	0.091	0.017	0.232	0.260	0.032	0.010	0.011	0.012	0.007	0.002	0.002	0.003	0.001	0.001	0.022	0.029	0.008	1.70		
105	0.010	0.025	0.071	0.005	0.030	0.073	0.031	0.071	0.108	0.246	0.200	0.117	0.030	0.215	0.243	0.032	0.015	0.013	0.008	0.012	0.004	0.003	0.003	0.001	0.001	0.038	0.046	0.015	1.67		
107	0.013	0.054	0.124	0.003	0.042	0.077	0.029	0.071	0.097	0.235	0.215	0.127	0.027	0.230	0.261	0.033	0.011	0.015	0.007	0.008	0.003	0.001	0.003	0.002	0.001	0.048	0.063	0.020	1.82		
109	0.005	0.027	0.096	0.005	0.035	0.094	0.038	0.084	0.105	0.306	0.237	0.127	0.022	0.280	0.299	0.043	0.011	0.013	0.007	0.008	0.002	0.002	0.003	0.001	0.001	0.047	0.077	0.010	1.98		
111	0.005	0.031	0.089	0.004	0.032	0.081	0.032	0.073	0.085	0.261	0.202	0.106	0.024	0.240	0.268	0.028	0.008	0.018	0.005	0.006	0.002	0.001	0.003	0.001	0.001	0.050	0.068	0.019	1.75		

Station	Naphthalene	Methylnaphthalenes	Dimethylnaphthalenes	Acenaphthylene	Acenaphthene	Fluorene	Dibenzothiophene	Methyldibenzothiophenes	Dimethyldibenzothiophenes	Phenanthrene	Methylphenantrenes	Dimethylphenanthrenes	Anthracene	Fluoranthene	Pyrene	Methylpyrenes	Dimethylpyrenes	Benzo(ghi)fluoranthene	Benzo(a)anthracene	Chrysene	Methylchrysenes	Benzo(b+k)fluoranthenes	Benzo(e)pyrene	Benzo(a)pyrene	Perylene	Indeno(1,2,3-cd)pyrene	Dibenzo(a,h)anthracene	Benzo(ghi)perylene	Σ_{64} PAHs
113	0.005	0.018	0.062	0.002	0.025	0.046	0.027	0.068	0.078	0.231	0.208	0.111	0.027	0.266	0.302	0.038	0.010	0.012	0.005	0.009	0.002	0.001	0.003	0.002	0.001	0.055	0.071	0.012	1.70
115	0.003	0.017	0.075	0.004	0.018	0.083	0.040	0.096	0.110	0.300	0.252	0.129	0.033	0.302	0.341	0.046	0.025	0.015	0.007	0.008	0.003	0.001	0.003	0.001	0.002	0.013	0.037	0.009	1.97
117	0.013	0.035	0.110	0.004	0.047	0.074	0.039	0.096	0.112	0.329	0.275	0.146	0.033	0.372	0.425	0.042	0.012	0.014	0.009	0.010	0.002	0.002	0.004	0.002	0.001	0.045	0.065	0.012	2.33
120	0.016	0.045	0.128	0.003	0.043	0.080	0.046	0.109	0.120	0.361	0.312	0.160	0.042	0.425	0.475	0.045	0.012	0.015	0.007	0.011	0.002	0.003	0.004	0.002	0.001	0.043	0.060	0.011	2.58
123	0.027	0.096	0.248	0.002	0.076	0.107	0.058	0.139	0.152	0.439	0.363	0.188	0.055	0.462	0.534	0.044	0.013	0.015	0.007	0.012	0.003	0.003	0.005	0.002	0.001	0.037	0.054	0.016	3.16
125	0.065	0.197	0.389	0.006	0.100	0.124	0.067	0.173	0.208	0.478	0.462	0.242	0.052	0.603	0.703	0.062	0.017	0.017	0.010	0.015	0.004	0.004	0.006	0.003	0.002	0.048	0.079	0.030	4.17
0	0.025	0.135	0.347	0.007	0.108	0.170	0.092	0.207	0.216	0.631	0.541	0.262	0.057	0.722	0.902	0.068	0.013	0.018	0.078	0.028	0.005	0.005	0.008	0.004	0.002	0.052	0.079	0.024	4.81
129	0.001	0.000	0.000	0.004	0.000	0.080	0.052	0.114	0.084	0.406	0.286	0.151	0.036	0.434	0.540	0.063	0.022	0.019	0.026	0.020	0.004	0.003	0.005	0.002	0.001	0.028	0.035	0.013	2.43
0	0.074	0.263	0.457	0.006	0.098	0.163	0.086	0.220	0.222	0.618	0.588	0.290	0.066	0.737	0.912	0.068	0.022	0.029	0.031	0.029	0.006	0.006	0.010	0.005	0.001	0.075	0.086	0.035	5.20
133	0.005	0.062	0.131	0.008	0.039	0.065	0.035	0.098	0.126	0.275	0.274	0.137	0.030	0.378	0.460	0.039	0.012	0.015	0.012	0.013	0.003	0.004	0.005	0.002	0.001	0.027	0.037	0.011	2.30
136	0.001	0.013	0.054	0.020	0.000	0.128	0.051	0.127	0.157	0.401	0.335	0.165	0.036	0.440	0.463	0.043	0.011	0.016	0.014	0.012	0.005	0.004	0.009	0.001	0.002	0.147	0.199	0.042	2.90
138	0.001	0.011	0.059	0.017	0.000	0.126	0.054	0.132	0.152	0.397	0.339	0.168	0.045	0.468	0.474	0.060	0.013	0.036	0.011	0.013	0.007	0.004	0.007	0.002	0.001	0.305	0.344	0.064	3.31
140	0.003	0.027	0.101	0.001	0.017	0.068	0.038	0.094	0.113	0.289	0.252	0.128	0.026	0.334	0.352	0.036	0.008	0.013	0.012	0.010	0.003	0.002	0.004	0.001	0.001	0.059	0.082	0.017	2.10
142	0.016	0.185	0.348	0.002	0.065	0.098	0.043	0.104	0.116	0.345	0.281	0.130	0.030	0.345	0.360	0.030	0.008	0.014	0.006	0.010	0.002	0.003	0.004	0.001	0.001	0.058	0.082	0.015	2.70
144	0.017	0.081	0.151	0.001	0.030	0.065	0.035	0.082	0.094	0.262	0.247	0.106	0.024	0.302	0.316	0.027	0.007	0.007	0.006	0.007	0.002	0.002	0.003	0.002	0.001	0.005	0.013	0.002	1.90
146	0.019	0.175	0.393	0.004	0.066	0.123	0.049	0.109	0.117	0.376	0.303	0.142	0.041	0.350	0.356	0.027	0.007	0.009	0.006	0.009	0.003	0.002	0.003	0.002	0.001	0.011	0.018	0.003	2.73

Table S5.9. Particulate phase measured PAHs concentrations (ng g_{dw}⁻¹)

Station	Naphthalene	Dimethylnaphthalenes	Methylnaphthalenes	Acenaphthylene	Acenaphthene	Fluorene	Dibenzothiophene	Methyl dibenzothiophenes	Dimethyl dibenzothiophenes	Phenanthrene	Methylphenantrenes	Dimethylphenanthrenes	Anthracene	Fluoranthene	Pyrene	Methylpyrenes	Dimethylpyrenes	Benzo(ghi)fluoranthene	Benzo(a)anthracene	Chrysene	Methylchrysenes	Benzo(b+k)fluoranthenes	Benzo(e)pyrene	Benzo(a)pyrene	Perylene	Indeno(1,2,3-cd)pyrene	Dibenzo(a,h)anthracene	Benzo(ghi)perylene	Σ ₆₄ PAHs
1	2.20	0.666	0.000	0.747	2.40	4.66	3.35	7.37	5.70	8.29	4.82	3.05	0.353	2.07	2.90	0.152	0.680	0.756	1.07	0.908	0.229	2.19	1.79	0.971	0.636	0.339	0.472	1.22	60.0
0	58.6	53.9	0.000	0.269	0.765	0.898	0.366	1.26	1.76	4.16	2.78	2.18	0.380	3.40	3.36	0.500	0.995	0.672	1.45	1.03	0.597	2.74	1.73	1.14	1.01	2.46	0.622	1.67	151
4	1.98	0.082	0.000	0.214	0.520	0.840	0.514	1.71	1.92	3.05	2.18	1.70	0.192	1.89	3.65	0.166	0.799	0.410	0.886	0.665	0.270	1.13	1.00	0.622	0.469	1.31	0.384	0.923	29.5
6	201	185	0.000	0.317	4.57	1.99	0.393	1.39	1.59	3.07	2.91	2.81	0.426	3.42	3.55	0.748	0.966	0.784	1.44	0.934	0.534	2.80	1.42	0.962	1.02	4.26	0.694	2.48	432
8	129	120	0.000	0.560	2.35	2.20	0.725	2.48	2.79	4.13	4.16	3.80	0.436	2.87	3.53	0.682	1.63	0.651	1.09	0.885	0.804	2.82	1.13	0.846	1.03	4.72	0.506	2.36	299
10	1.54	0.332	0.000	0.414	1.60	1.42	1.10	4.54	4.93	4.93	17.7	14.5	3.11	2.51	3.38	0.198	0.995	3.65	0.707	0.712	1.90	1.95	0.953	0.632	0.746	3.00	0.722	3.36	81.5
12	3.48	0.572	0.000	0.599	2.76	5.09	1.45	5.19	6.17	8.09	11.6	16.9	1.07	6.38	7.66	0.729	1.88	10.1	1.71	1.36	12.0	4.17	3.11	1.97	2.84	8.63	0.690	1.70	128
14	11.8	0.411	0.000	0.697	3.99	1.76	0.644	2.60	2.97	4.61	6.45	11.5	0.736	4.78	4.93	0.307	1.56	1.01	1.26	1.03	5.82	2.77	1.85	1.49	1.61	6.20	0.467	1.78	85.0
16	1.44	0.233	0.000	0.353	0.840	1.25	0.545	2.07	8.45	3.46	5.85	14.9	0.651	5.04	5.58	0.156	3.28	0.610	2.27	1.58	4.14	4.91	3.22	2.85	1.68	6.80	0.599	4.34	87.1
18	2.18	0.143	0.000	0.535	1.41	0.862	0.787	2.83	3.70	2.78	5.43	9.74	0.562	2.62	3.25	0.357	0.989	0.540	1.21	0.843	0.771	2.18	1.55	1.27	0.809	1.23	0.641	1.42	50.7
20	0.082	0.061	0.000	0.262	1.03	0.539	0.374	1.38	2.28	2.26	5.53	5.25	0.688	2.78	3.13	0.269	0.900	0.521	1.05	0.731	0.661	2.10	1.43	1.05	0.841	0.693	0.623	1.30	37.8
22	0.919	0.673	0.000	0.404	1.28	1.65	0.505	1.44	3.51	3.73	3.78	3.79	0.446	5.25	6.24	0.594	1.57	0.975	2.18	1.17	2.31	4.05	2.56	2.16	1.51	5.03	1.12	3.68	62.5
24	2.75	0.331	0.000	0.427	1.39	1.03	0.653	1.81	1.77	2.75	2.94	2.76	0.391	2.58	2.26	0.399	0.802	3.52	1.27	0.707	0.473	2.29	1.37	1.12	0.926	1.05	0.597	1.11	39.5
26	1.19	0.366	0.000	0.300	0.441	1.17	0.335	0.594	3.25	12.5	2.99	2.40	0.441	3.32	3.18	0.324	0.519	0.000	0.000	0.000	0.452	1.80	1.18	1.40	1.29	3.24	0.634	4.78	48.0
27	1.40	0.282	0.000	0.734	5.05	1.37	0.597	1.23	1.45	10.6	6.05	8.05	0.987	4.06	3.99	0.427	0.796	0.761	2.03	1.45	0.698	2.96	1.92	1.61	0.969	0.662	0.678	1.28	62.0
28	2.20	0.320	0.000	0.505	8.32	4.77	0.851	2.43	2.71	6.38	4.66	4.49	0.443	2.24	2.90	0.211	0.671	0.644	1.07	0.762	0.557	2.30	1.29	1.04	0.827	0.681	0.565	1.09	54.9

Station	Naphthalene	Dimethylnaphthalenes	Methylnaphthalenes	Acenaphthylene	Acenaphthene	Fluorene	Dibenzothiophene	Methyl dibenzothiophenes	Dimethyl dibenzothiophenes	Phenanthrene	Methylphenantrenes	Dimethylphenanthrenes	Anthracene	Fluoranthene	Pyrene	Methylpyrenes	Dimethylpyrenes	Benzo(ghi)fluoranthene	Benzo(a)anthracene	Chrysene	Methylchrysenes	Benzo(b+k)fluoranthenes	Benzo(e)pyrene	Benzo(a)pyrene	Perylene	Indeno(1,2,3-cd)pyrene	Dibenzo(a,h)anthracene	Benzo(ghi)perylene	Σ ₆₄ PAHs
29	4.57	0.260	0.000	0.637	9.62	3.42	0.713	1.92	2.16	5.44	4.68	6.00	0.676	1.88	3.10	0.216	0.622	0.575	1.09	0.802	0.783	2.11	1.16	0.907	0.752	0.681	0.494	0.783	56.1
30	6.93	0.200	0.000	0.770	10.9	2.07	0.575	1.41	1.62	4.50	4.70	7.50	0.908	1.52	3.31	0.220	0.573	0.505	1.11	0.841	1.01	1.92	1.03	0.779	0.677	0.680	0.423	0.479	57.2
34	11.2	0.454	0.000	0.911	8.63	2.05	1.96	7.07	8.39	6.84	4.43	3.53	1.38	1.63	1.78	0.576	0.534	0.412	0.762	0.449	0.311	0.943	0.639	0.512	0.505	0.439	0.362	0.559	67.2
	1.59	0.252	0.000	0.775	5.31	4.29	6.29	30.2	35.0	14.1	11.5	8.00	1.19	1.93	2.75	0.162	0.598	0.294	0.844	0.388	0.544	1.03	1.02	0.325	0.328	1.59	0.447	2.29	133
37	7.30	0.243	0.000	0.989	8.46	2.06	0.800	2.49	2.25	3.46	1.61	1.87	0.846	0.708	1.32	0.000	0.337	0.315	0.684	0.299	0.401	1.16	1.78	0.283	0.475	0.675	0.235	0.247	41.3
41	0.503	0.554	0.000	0.180	1.17	0.139	0.000	0.547	0.319	0.124	0.000	0.511	0.186	0.000	0.000	0.000	0.104	0.000	0.000	0.000	0.000	1.70	0.000	0.282	0.000	1.07	0.000	0.367	7.75
42	14.8	37.5	0.000	6.54	10.2	117	12.2	39.2	42.4	22.7	7.90	15.0	4.16	2.20	2.30	6.86	23.7	19.4	0.000	0.000	0.000	3.57	5.08	1.15	10.3	0.000	1.92	1.52	408
43	2.57	0.284	0.000	0.204	1.91	5.35	0.243	0.654	0.764	3.24	2.67	2.41	0.229	1.62	1.42	0.229	0.435	0.294	0.703	0.516	0.322	1.32	0.763	0.592	0.466	0.355	0.374	0.679	30.6
44	0.357	0.124	0.000	0.196	1.18	5.33	0.202	0.771	1.29	4.27	16.0	8.31	1.89	2.69	2.21	0.265	0.517	0.389	0.991	0.703	0.578	1.71	1.16	0.924	0.640	0.397	0.468	1.03	54.5
45	1.13	0.365	0.000	0.321	0.817	7.59	0.975	3.25	4.92	5.23	6.16	5.97	0.779	2.34	2.26	0.206	0.781	0.000	0.000	0.000	0.756	1.58	1.34	1.33	1.20	1.69	0.519	1.66	53.2
0	0.415	1.02	0.000	0.454	0.860	2.78	5.18	32.6	48.7	9.98	57.89	17.5	2.10	4.81	5.20	0.324	2.07	0.465	1.26	0.962	2.03	4.50	1.50	1.06	1.56	5.56	0.414	4.65	216
46	29.9	13.0	0.000	49.3	170	187	191	668	635	350	397	260	23.3	226	192	10.0	41.6	33.2	114	94.3	35.5	273	179	1534	95.1	43.4	55.7	165	4690
48	0.433	1.08	0.000	0.848	2.40	3.61	3.09	8.62	6.04	5.07	8.65	9.58	0.875	3.65	2.76	0.154	0.923	0.532	1.80	1.22	1.30	4.79	2.33	1.76	1.79	2.54	0.978	4.80	81.6
50	40.8	333	0.000	8.42	22.3	36.31	29.2	70.7	78.4	18.8	14.0	0.000	6.05	0.000	0.000	0.000	0.000	0.000	0.000	7.24	0.000	2.97	0.000	4.42	5.35	3.08	0.000	4.73	686
0	0.935	0.141	0.000	0.690	1.27	0.838	0.724	2.17	2.23	2.25	8.47	8.69	1.40	1.74	1.04	0.175	0.427	0.348	0.731	0.534	0.900	1.32	0.650	0.543	0.542	1.18	0.369	0.492	40.8
0	36.7	33.3	0.000	0.482	0.491	11.8	2.64	15.6	15.5	1.02	1.98	0.000	0.488	5.42	5.12	0.000	13.2	0.000	13.5	7.08	0.000	6.65	4.57	3.96	5.35	0.711	1.21	4.19	191
53	65.4	860	0.000	8.86	49.9	51.5	120	56.6	14.6	15.3	0.000	52.5	21.2	0.000	6.96	35.0	25.6	19.8	46.2	27.5	0.000	3.72	0.000	3.09	5.94	2.03	0.000	4.59	1500
55	3.00	3.86	0.000	2.20	5.49	8.54	16.8	92.7	158	32.8	68.9	70.1	3.31	10.3	17.1	0.478	2.89	1.54	3.43	2.52	1.86	7.52	3.62	3.10	2.32	2.61	1.55	2.84	529

Station	Naphthalene	Dimethylnaphthalenes	Methylnaphthalenes	Acenaphthylene	Acenaphthene	Fluorene	Dibenzothiophene	Methyl dibenzothiophenes	Dimethyl dibenzothiophenes	Phenanthrene	Methylphenantrenes	Dimethylphenanthrenes	Anthracene	Fluoranthene	Pyrene	Methylpyrenes	Dimethylpyrenes	Benzo(ghi)fluoranthene	Benzo(a)anthracene	Chrysene	Methylchrysenes	Benzo(b+k)fluoranthenes	Benzo(e)pyrene	Benzo(a)pyrene	Perylene	Indeno(1,2,3-cd)pyrene	Dibenzo(a,h)anthracene	Benzo(ghi)perylene	Σ ₆₄ PAHs
57	6.41	112	0.000	3.26	20.7	26.6	51.7	21.2	41.8	6.38	13.3	83.1	29.0	0.000	18.7	165	26.3	24.5	11.7	0.000	29.0	1.78	2.84	3.67	1.41	0.796	0.000	0.000	701
59	474	96.7	0.000	18.5	0.000	40.1	383	136	66.3	91.2	97.6	201	64.3	0.000	11.1	4.36	0.000	25.3	7.40	7.29	0.000	8.94	0.000	3.73	0.000	3.16	2.75	0.000	1740
61	26.0	30.8	0.000	0.390	0.000	2.10	6.35	6.44	5.94	6.69	14.0	7.01	2.20	2.06	1.58	0.000	1.33	0.382	0.763	1.06	0.950	1.57	0.414	0.468	1.08	3.12	0.429	1.39	125
63	0.443	1.17	0.000	0.295	3.74	2.55	1.26	2.87	3.55	13.4	8.86	3.68	0.407	2.51	1.90	0.196	0.505	0.402	0.862	0.567	0.462	2.00	0.670	0.548	0.691	2.04	0.392	0.480	56.4
65	0.260	1.36	0.000	0.217	1.87	2.11	2.21	7.14	11.8	30.0	26.3	14.8	0.547	6.65	5.65	0.297	0.708	0.475	0.905	0.548	0.539	1.11	0.648	0.502	0.672	1.14	0.454	0.543	119
67	0.347	0.783	0.000	0.196	1.12	2.08	1.21	3.41	4.68	12.2	9.14	4.82	0.336	2.48	1.83	0.199	0.675	0.340	0.811	0.378	0.520	2.46	0.804	0.721	0.878	3.58	0.371	2.40	58.8
74	0.652	0.428	0.000	0.143	0.404	0.967	0.327	1.13	2.10	2.62	1.71	1.31	0.755	1.51	1.09	0.141	0.583	0.239	0.522	0.295	0.445	1.29	0.764	0.744	0.747	2.33	0.271	1.95	25.5
0	0.578	0.513	0.000	0.207	0.591	1.36	0.423	1.44	2.94	3.60	4.32	2.95	0.470	3.10	2.64	0.218	1.12	0.431	0.928	1.04	0.682	1.05	1.13	0.607	1.21	2.69	0.756	2.95	39.9
80	0.679	0.673	0.000	0.181	0.277	1.57	0.501	2.03	3.61	4.32	3.17	2.02	0.369	2.44	1.88	0.183	0.672	0.325	0.877	0.501	0.512	6.22	2.17	0.546	1.05	2.02	0.399	1.79	41.0
83	0.453	1.32	0.000	0.185	1.35	4.03	9.37	72.9	140	37.7	47.7	43.1	5.94	5.18	10.2	0.142	1.86	0.433	1.03	0.718	0.918	4.76	1.64	0.817	1.23	2.83	0.826	2.85	400
85	0.364	0.578	0.000	0.371	0.367	2.58	3.51	16.4	21.4	19.6	8.66	5.51	0.515	2.54	2.67	0.149	0.907	0.351	0.696	0.506	0.443	5.22	1.96	0.397	1.27	1.86	0.804	4.03	104
88	0.308	1.18	0.000	0.563	0.855	2.57	6.18	32.9	48.1	24.1	16.8	12.2	0.665	2.65	3.32	0.158	0.615	0.369	0.624	0.387	0.476	1.53	0.489	0.356	0.528	1.56	0.306	0.349	160
92	0.092	0.528	0.000	0.452	0.478	2.30	2.92	9.59	10.5	13.0	5.53	4.13	0.399	2.04	2.31	0.154	0.526	0.361	0.744	0.518	0.869	1.81	0.632	0.516	0.632	1.05	0.283	0.438	62.7
95	0.213	0.240	0.000	0.426	1.211	1.57	3.21	16.3	21.6	12.5	13.7	7.35	0.577	1.91	2.13	0.162	0.459	0.292	0.560	0.388	0.960	7.00	0.400	0.352	0.565	1.07	0.280	0.371	95.7
98	0.204	0.284	0.000	0.275	0.404	2.49	9.65	61.1	107	27.6	33.4	30.7	0.688	3.81	7.91	0.149	1.35	0.401	0.789	0.580	0.534	1.53	0.624	0.552	0.651	0.990	0.394	0.550	295
103	0.724	0.825	0.000	0.380	1.382	3.28	4.19	20.9	30.8	19.7	20.6	16.5	1.79	3.48	2.67	0.000	1.21	0.554	0.758	0.659	0.979	1.52	0.563	0.528	1.44	2.22	0.846	1.93	141
105	0.755	0.598	0.000	0.375	0.742	4.40	10.5	54.4	71.7	23.0	21.2	13.8	0.766	2.99	3.51	0.193	1.21	0.499	0.930	0.658	0.533	1.57	0.663	0.535	0.939	2.10	0.764	1.89	221
109	3.10	0.000	0.000	0.322	0.000	1.26	0.255	0.787	1.19	40.3	2.29	0.742	37.4	0.940	0.148	0.527	1.10	1.04	0.290	0.256	0.316	0.295	0.000	0.553	1.51	1.24	0.000	2.14	97.4

Station	Naphthalene	Dimethylnaphthalenes	Methylnaphthalenes	Acenaphthylene	Acenaphthene	Fluorene	Dibenzothiophene	Methyl dibenzothiophenes	Dimethyl dibenzothiophenes	Phenanthrene	Methylphenantrenes	Dimethylphenanthrenes	Anthracene	Fluoranthene	Pyrene	Methylpyrenes	Dimethylpyrenes	Benzo(ghi)fluoranthene	Benzo(a)anthracene	Chrysene	Methylchrysenes	Benzo(b+k)fluoranthenes	Benzo(e)pyrene	Benzo(a)pyrene	Perylene	Indeno(1,2,3-cd)pyrene	Dibenzo(a,h)anthracene	Benzo(ghi)perylene	Σ ₆₄ PAHs
111	0.021	0.187	0.000	0.165	0.290	0.377	0.400	1.99	2.45	1.41	3.04	1.76	0.254	2.08	1.36	0.202	0.536	0.353	0.801	0.456	0.420	0.790	0.618	0.480	0.956	1.91	0.396	1.36	25.1
113	0.367	0.123	0.000	0.211	0.913	1.72	4.76	46.6	118	18.3	43.5	54.8	1.20	7.38	15.3	0.000	4.34	0.637	0.808	0.911	1.32	1.23	0.964	0.481	2.33	2.10	0.378	0.710	330
115	0.415	0.341	0.000	0.155	0.453	0.461	0.619	3.85	6.01	1.77	5.25	3.76	0.246	2.35	1.75	0.143	0.722	0.618	0.650	0.427	0.481	2.08	0.714	0.623	1.06	0.819	0.537	1.32	37.6
117	0.211	0.250	0.000	0.179	0.429	0.609	2.64	25.8	66.8	7.64	21.9	29.6	0.545	5.80	8.36	0.190	2.77	0.556	1.01	0.823	0.715	1.78	0.841	0.825	0.800	1.63	0.000	0.509	183
120	0.425	0.393	0.000	0.200	0.564	1.20	0.680	2.36	2.23	4.42	5.38	3.17	0.400	2.19	1.80	0.143	0.486	0.321	0.785	0.481	0.557	1.96	1.19	0.586	1.20	0.820	0.641	2.88	37.4
125	0.111	2.61	0.000	0.000	0.000	2.17	3.81	38.7	50.1	24.0	39.7	20.9	0.874	5.05	8.71	0.122	7.00	0.329	0.776	0.628	3.07	1.77	1.37	1.06	1.67	0.644	0.000	3.93	219
129	0.130	0.706	0.000	0.000	0.672	3.49	2.44	17.3	18.3	18.6	15.3	9.53	0.605	2.69	2.23	0.198	0.667	0.000	0.679	0.870	0.809	1.43	1.04	0.556	1.78	1.42	0.607	2.03	104
0	0.166	0.438	0.000	0.285	0.822	1.25	5.05	49.7	112	27.5	32.9	38.5	0.645	3.72	9.31	0.271	2.93	0.000	0.000	0.477	0.350	0.697	0.530	0.297	0.434	0.658	0.000	0.297	289
133	0.384	0.147	0.000	0.313	1.57	1.24	3.06	16.3	20.9	13.6	15.9	11.7	0.732	2.54	2.18	0.182	0.553	1.13	0.893	0.893	0.620	1.12	0.605	0.616	0.693	0.484	0.301	0.398	98.9
	1.25	0.651	0.000	0.196	1.62	2.22	4.16	47.4	120	20.7	35.0	43.2	0.315	6.46	13.4	0.329	1.93	7.64	0.744	1.01	0.968	7.16	4.50	0.946	1.48	0.823	0.834	3.32	328
136	0.924	0.063	0.000	0.328	1.31	1.34	5.44	49.6	110	25.4	49.0	48.7	1.79	6.54	10.0	0.249	1.61	0.000	1.04	0.495	0.939	1.37	0.608	0.638	0.645	0.612	0.367	0.573	319
138	0.715	0.157	0.000	0.435	1.95	2.00	8.64	69.6	139	38.9	58.4	48.4	1.59	8.20	10.56	0.325	1.32	0.509	1.29	0.771	1.20	1.63	0.852	0.825	0.919	0.745	0.445	0.656	400
140	0.329	0.150	0.000	0.416	2.29	1.79	3.77	23.8	36.7	17.8	29.4	20.6	1.65	3.681	4.19	0.244	0.531	0.471	1.38	0.854	1.10	2.00	1.11	0.969	1.03	0.631	0.367	0.686	158
142	0.681	0.086	0.000	0.311	0.947	1.28	3.05	18.5	27.4	11.9	29.1	18.0	1.55	2.77	2.98	0.261	0.530	0.468	1.33	0.553	1.23	1.89	1.18	0.969	1.10	0.543	0.371	0.800	130
144	0.496	0.833	0.000	0.327	1.44	2.48	3.35	17.8	22.1	11.0	15.6	8.48	1.14	2.62	2.39	0.176	0.748	0.580	0.982	1.44	0.788	1.53	0.785	0.500	0.000	1.30	0.953	1.25	101
146	0.160	0.191	0.000	0.271	0.906	1.56	8.94	92.8	198	39.3	70.5	64.4	2.05	8.14	15.8	0.387	3.52	0.740	2.02	1.28	1.33	2.76	1.91	1.66	1.22	1.35	0.510	1.74	523

Figure S5.1. Relative abundance of PAHs in the particulate phase

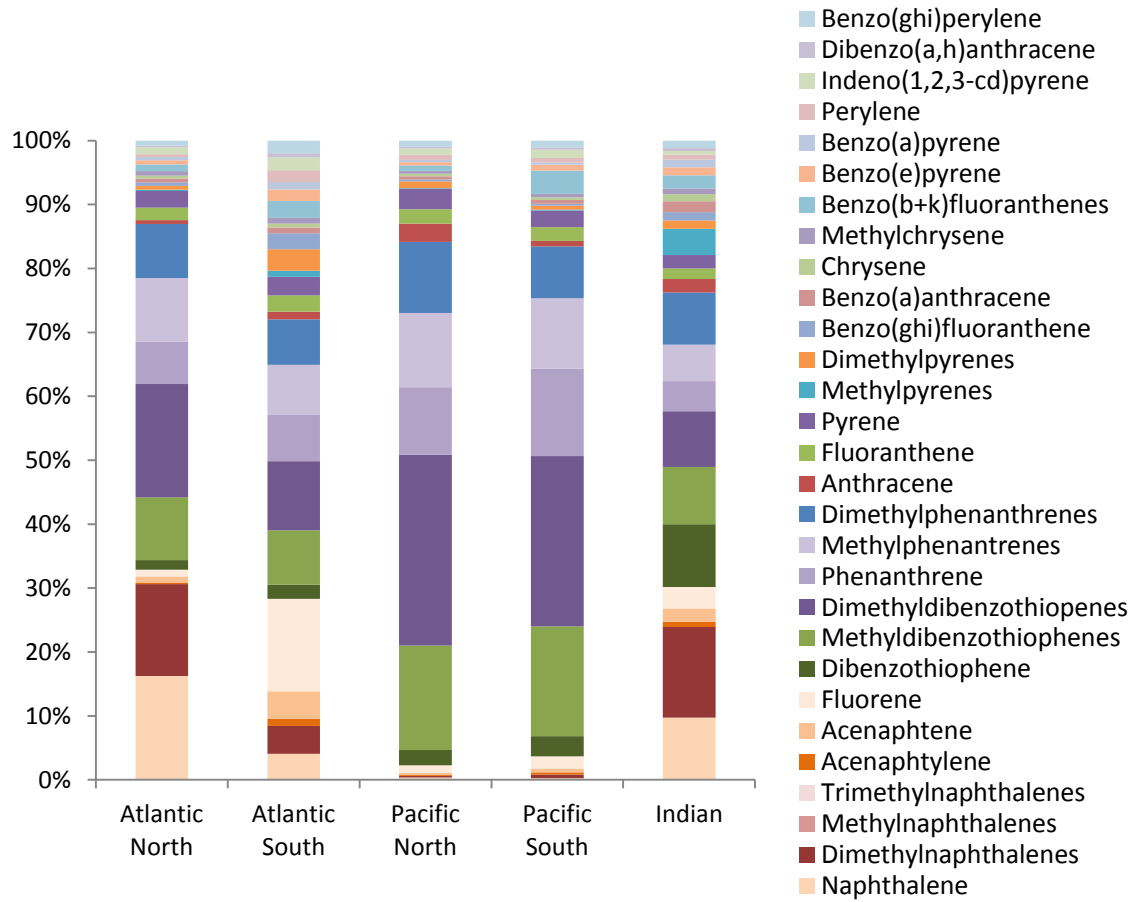


Table S5.10. Plankton phase measured PAHs concentrations (ng g_{dw}⁻¹)

Station	Naphthalene	Methylnaphthalenes	Dimethylnaphthalenes	Acenaphthylene	Acenaphthene	Fluorene	Dibenzothiophene	Methyldibenzothiophenes	Dimethyldibenzothiophenes	Phenanthrene	Methylphenantrenes	Dimethylphenanthrenes	Anthracene	Fluoranthene	Pyrene	Methylpyrenes	Dimethylpyrenes	Benzo(ghi)fluoranthene	Benzo(a)anthracene	Chrysene	Methylchrysene	Benzo(b+k)fluoranthenes	Benzo(e)pyrene	Benzo(a)pyrene	Perylene	Indeno(1,2,3-cd)pyrene	Dibenzo(a,h)anthracene	Benzo(ghi)perylene	Σ ₆₄ PAHs
1	1.77	3.63	9.42	0.958	11.6	5.51	3.76	29.2	76.6	37.0	111	190	2.91	19.0	17.2	9.73	19.3	1.77	4.54	8.42	10.4	7.59	4.55	2.77	2.59	3.87	1.21	5.08	602
3	0.818	1.31	4.12	0.389	8.97	4.60	2.34	14.2	21.4	19.8	29.1	28.4	1.46	8.53	6.61	1.67	3.19	0.526	1.84	2.57	2.21	4.12	2.20	1.35	0.839	1.41	0.677	1.97	177
6	16.7	87.2	65.1	0.350	6.02	2.21	0.070	0.369	0.874	5.70	7.84	14.2	0.424	50.9	40.8	1.31	2.50	0.623	50.5	52.1	2.58	30.1	4.74	2.56	1.23	4.58	1.30	4.50	459
8	34.6	26.0	40.3	0.707	19.5	5.58	0.000	32.6	10.8	72.5	98.0	32.9	0.342	33.7	15.8	0.262	0.753	0.163	0.261	12.3	0.505	9.66	0.441	0.222	0.165	0.216	0.244	2.72	451
10	6.56	20.2	16.3	8.96	21.6	30.0	0.000	25.0	26.0	117	264	79.7	68.5	35.3	9.92	0.300	0.599	0.106	11.0	11.1	0.548	8.52	9.74	0.266	0.156	0.218	0.189	0.342	789
12	14.1	27.3	49.1	6.21	25.3	26.7	0.000	0.179	0.226	95.3	97.3	22.0	20.0	10.1	8.02	0.334	0.451	0.125	0.219	0.225	0.237	9.76	0.325	0.248	0.253	0.000	0.272	0.088	434
14	5.23	22.2	10.6	50.5	2.99	28.8	0.000	0.078	0.032	3.17	5.78	7.34	0.177	10.1	8.23	0.355	0.684	0.110	11.0	10.4	0.461	6.64	9.78	0.171	0.148	0.178	0.172	0.345	213
16	0.283	0.397	1.69	0.214	3.09	0.614	0.000	0.029	0.000	0.984	0.879	1.10	0.119	0.768	0.213	0.092	0.246	0.051	0.108	0.204	0.250	0.628	0.276	0.119	0.103	0.107	0.137	0.197	13.1
18	3.06	4.24	8.32	0.475	7.22	1.96	0.266	1.25	1.84	4.18	4.49	5.00	0.374	4.52	1.10	0.322	0.649	0.137	0.355	0.551	0.614	1.18	0.450	0.248	0.232	0.250	0.239	0.355	56.4
20	0.500	0.598	1.47	0.102	0.987	0.793	0.281	1.71	2.35	3.83	5.00	4.30	0.330	7.86	0.861	0.194	0.427	0.134	0.378	0.479	0.413	1.47	0.589	0.329	0.320	0.329	0.295	0.420	37.2
22	0.319	0.618	3.39	0.216	6.95	2.39	0.385	1.64	1.97	9.23	16.0	19.0	0.533	8.78	3.77	1.43	1.93	0.330	1.64	2.66	1.68	3.78	1.93	0.767	0.690	1.28	0.536	1.41	95.5
24	0.205	0.436	2.22	0.201	4.08	1.10	1.10	11.3	108	7.34	38.9	284	2.23	4.34	8.84	14.7	44.1	1.95	2.63	9.14	21.3	3.82	3.15	0.926	0.421	1.69	0.467	3.96	583
25	2.24	3.03	7.96	0.517	9.59	3.08	0.390	2.31	3.71	8.10	8.367	10.3	0.847	8.57	2.46	0.571	1.07	0.311	0.552	0.906	0.984	2.72	0.887	0.575	0.436	0.230	0.570	0.573	83.6
27	57.7	117	96.6	2.94	90.7	28.9	1.55	6.13	6.30	32.0	25.1	14.3	3.72	9.64	5.92	2.00	3.45	1.30	2.00	3.35	3.83	7.57	3.99	1.92	1.39	0.196	0.000	1.17	574
28	141	177	136	3.86	120	90.5	8.57	40.2	46.5	119	93.7	67.7	7.60	17.0	19.4	4.40	8.86	1.83	3.90	5.96	9.48	16.0	8.23	4.16	2.62	2.96	3.54	6.42	1270
29	0.147	0.221	0.976	0.149	2.67	0.921	0.000	0.070	0.016	3.17	2.98	3.33	0.312	6.38	1.68	0.342	0.473	0.238	0.379	0.514	0.376	0.961	0.418	0.220	0.323	0.183	0.184	0.485	28.3
30	1.65	3.50	6.50	0.107	1.98	1.16	0.147	0.879	1.39	2.86	3.36	2.68	0.328	9.51	0.721	0.206	0.247	0.076	0.226	0.233	0.219	0.636	0.214	0.211	0.154	0.086	0.132	0.150	40.8

Station	Naphthalene	Methylnaphthalenes	Dimethylnaphthalenes	Acenaphthylene	Acenaphthene	Fluorene	Dibenzothiophene	Methyldibenzothiophenes	Dimethyldibenzothiophenes	Phenanthrene	Methylphenantrenes	Dimethylphenanthrenes	Anthracene	Fluoranthene	Pyrene	Methylpyrenes	Dimethylpyrenes	Benzo(ghi)fluoranthene	Benzo(a)anthracene	Chrysene	Methylchrysene	Benzo(b+k)fluoranthenes	Benzo(e)pyrene	Benzo(a)pyrene	Perylene	Indeno(1,2,3-cd)pyrene	Dibenzo(a,h)anthracene	Benzo(ghi)perylene	Σ ₆₄ PAHs
31	1.64	4.83	8.59	0.079	2.22	1.82	0.000	0.032	0.029	4.26	5.37	6.97	0.435	7.63	5.70	0.805	1.37	0.535	0.601	1.14	2.54	1.19	0.786	0.350	0.303	0.303	0.281	1.35	62.4
34	3.55	11.5	18.7	0.528	5.41	2.40	0.000	0.083	0.039	3.89	5.45	5.93	0.720	3.91	3.52	1.34	1.12	0.470	1.97	2.14	1.40	3.55	1.94	1.49	0.653	1.42	0.544	1.59	87.9
37	176	128	63.2	1.00	58.1	17.4	1.047	4.66	5.80	29.4	26.2	24.2	2.50	11.7	8.26	1.86	3.46	1.05	2.90	5.82	4.43	11.2	4.79	2.23	1.66	2.90	1.95	3.42	744
41	0.875	1.15	1.67	0.121	5.69	2.24	0.075	0.133	0.062	25.2	7.71	5.03	3.37	32.4	23.4	5.84	1.84	2.31	16.0	14.7	3.93	20.3	10.5	9.67	2.79	11.8	3.30	8.66	221
42	7.53	23.3	47.1	0.319	8.42	18.3	0.089	0.740	1.11	23.8	16.3	40.8	1.92	8.59	9.57	3.44	8.33	1.72	2.98	6.75	9.06	6.30	3.39	1.52	0.472	2.95	0.840	4.44	266
43	2.27	9.55	20.5	0.135	2.79	6.73	0.000	0.092	0.099	2.17	2.08	2.48	0.335	4.48	1.70	0.336	0.394	0.226	0.341	1.36	0.676	1.73	0.588	0.232	0.412	0.528	0.282	0.557	64.8
44	117	72.6	30.9	0.766	20.8	9.05	0.527	3.78	5.90	24.1	20.9	22.3	2.83	12.2	8.51	1.58	4.69	1.12	1.65	3.06	4.64	8.95	3.05	1.89	1.41	0.464	1.88	2.06	473
45	11.1	9.18	8.55	0.624	6.88	4.83	1.00	5.05	7.06	19.0	28.3	48.6	2.15	9.26	10.77	3.72	6.62	2.31	3.49	6.68	6.11	7.08	4.48	2.60	0.721	3.63	0.931	6.38	235
46	1.14	1.38	2.60	0.124	4.45	0.960	0.105	0.576	1.04	2.75	2.94	6.31	0.386	1.33	0.936	0.360	1.04	0.168	0.396	0.995	0.819	1.22	0.519	0.273	0.240	0.468	0.150	0.498	35.2
48	1.78	4.49	15.2	0.505	11.9	5.86	0.856	5.40	8.09	23.6	88.2	185	11.1	4.72	9.43	7.87	20.6	1.55	1.75	4.93	10.7	2.74	1.88	0.749	0.257	1.12	0.331	2.60	435
50	14.9	24.4	33.2	1.31	20.4	3.69	0.000	2.76	1.72	18.3	12.7	9.64	6.00	9.41	3.77	0.940	1.24	1.43	2.13	2.19	2.35	19.5	7.17	6.04	3.89	0.000	5.19	4.12	231
52	0.128	0.249	1.13	0.191	3.99	1.22	0.000	0.177	0.150	2.48	1.49	1.66	0.535	1.32	0.350	0.095	0.234	0.093	0.162	0.176	0.254	1.15	0.414	0.328	0.227	0.000	0.280	0.189	18.8
53	1.95	6.35	25.9	2.25	39.1	18.8	1.76	10.1	11.8	59.3	50.0	32.2	5.53	7.48	6.86	1.43	1.80	0.970	1.98	2.01	1.73	10.6	2.87	2.27	1.92	0.000	2.42	1.16	313
55	0.236	1.01	2.95	0.174	2.17	0.901	0.000	0.065	0.158	5.33	4.28	4.04	0.529	1.41	0.865	0.257	0.478	0.247	0.412	0.507	0.663	2.34	0.771	0.530	0.431	0.049	0.535	0.520	32.1
57	0.254	0.306	1.33	0.115	3.15	0.705	0.000	0.027	0.058	1.85	1.51	1.13	0.261	0.467	0.304	0.134	0.154	0.092	0.149	0.186	0.250	1.12	0.327	0.200	0.210	0.000	0.254	0.076	14.9
59	1.21	0.948	1.49	0.151	3.78	0.809	0.000	0.125	0.192	2.41	2.13	1.68	0.310	0.675	0.393	0.093	0.169	0.097	0.157	0.241	0.336	1.07	0.307	0.207	0.198	0.000	0.251	0.083	20.5
61	2.23	7.52	28.2	0.829	40.7	8.60	0.000	0.412	0.189	13.8	15.3	21.6	2.52	2.20	2.10	1.49	5.25	0.504	0.988	1.79	4.43	3.94	2.08	0.713	0.537	0.592	0.680	1.39	172
63	2.96	4.00	5.86	0.255	9.08	1.43	0.000	0.126	0.039	6.63	5.46	5.37	0.474	1.75	1.45	0.316	0.662	0.295	0.517	0.782	1.07	1.68	0.799	0.337	0.246	0.211	0.334	0.572	55.0

Station	Naphthalene	Methylnaphthalenes	Dimethylnaphthalenes	Acenaphthylene	Acenaphthene	Fluorene	Dibenzothiophene	Methyl dibenzothiophenes	Dimethyl dibenzothiophenes	Phenanthrene	Methylphenantrenes	Dimethylphenanthrenes	Anthracene	Fluoranthene	Pyrene	Methylpyrenes	Dimethylpyrenes	Benzo(ghi)fluoranthene	Benzo(a)anthracene	Chrysene	Methylchrysene	Benzo(b+k)fluoranthenes	Benzo(e)pyrene	Benzo(a)pyrene	Perylene	Indeno(1,2,3-cd)pyrene	Dibenzo(a,h)anthracene	Benzo(ghi)perylene	Σ ₆₄ PAHs
65	0.780	1.08	1.85	0.126	2.23	1.23	0.000	0.057	0.065	5.89	2.67	2.52	0.233	1.35	0.739	0.152	0.150	0.135	0.235	0.395	0.313	1.18	0.384	0.209	0.168	0.060	0.231	0.127	25.2
67	0.577	1.26	4.87	0.395	3.17	4.61	0.000	0.104	0.141	1.81	1.48	1.34	0.333	0.948	0.206	0.135	0.123	0.051	0.127	0.127	0.164	0.644	0.182	0.416	0.468	0.301	0.279	0.067	24.8
74	1.33	4.38	16.9	1.35	43.2	12.0	0.000	0.706	0.563	18.0	18.1	9.52	2.63	1.00	0.703	0.447	0.273	0.149	0.264	0.275	0.320	2.44	0.633	0.426	0.469	0.000	0.581	0.127	138
4b1	0.102	2.00	8.98	0.705	10.7	5.38	0.171	0.866	1.65	32.6	28.4	39.4	1.54	13.4	8.95	2.19	4.42	2.01	3.19	7.97	4.92	8.17	4.26	2.40	1.12	2.25	1.34	3.19	202
79	0.022	0.317	2.68	0.324	6.41	3.59	0.139	0.686	1.14	7.55	5.80	7.11	0.646	2.30	2.08	0.401	0.798	0.372	0.921	1.34	0.905	2.28	1.25	0.976	0.441	1.02	0.389	1.21	53.2
83	0.683	0.824	1.63	0.161	2.83	0.627	0.166	0.604	0.797	4.82	1.71	1.92	0.268	6.23	11.9	0.091	0.235	0.991	0.171	0.266	0.226	0.850	0.396	0.232	0.157	0.023	0.175	0.349	40.0
85	1.66	0.000	0.000	51.4	0.000	40.6	0.000	0.000	0.000	0.000	0.000	0.000	0.000	2.40	2.61	0.000	0.000	5.57	0.000	0.000	0.000	26.2	0.000	0.000	5.07	0.000	0.000	2.95	138
88	0.308	1.49	5.49	0.494	18.4	4.06	0.000	0.565	0.284	19.5	67.4	160	9.48	4.12	8.92	7.57	21.9	1.93	2.08	4.72	12.1	4.44	2.73	0.913	0.585	0.549	0.707	2.98	364
92	1.44	2.80	7.66	0.490	13.4	4.49	0.583	2.84	4.38	10.6	9.29	16.8	1.45	5.00	2.62	1.03	2.93	0.836	1.96	3.01	6.21	4.37	2.25	1.12	0.516	1.58	0.687	2.37	114
95	0.005	0.064	0.944	0.999	8.27	1.80	0.000	0.130	0.000	4.86	6.50	12.8	0.619	3.16	1.66	0.786	1.97	0.242	0.875	1.19	1.57	2.71	0.829	0.890	0.282	1.45	1.13	1.58	57.3
98*	12.4	27.2	41.8	4.68	443	419	37.1	54.6	27.6	1040	238	144	119	1250	850	159	52.4	69.9	517	486	103	463	254	253	69.4	270	83.6	219	7710
103	0.350	0.62	1.66	0.153	4.19	0.583	0.065	0.355	0.684	4.15	4.19	5.70	0.271	2.11	2.36	0.750	1.41	0.428	0.432	0.752	0.841	0.887	0.538	0.255	0.095	0.355	0.218	0.738	35.4
105	0.000	0.000	0.000	0.000	0.000	0.000	0.000	0.000	0.000	0.000	0.000	0.000	0.000	0.000	0.000	0.000	0.000	0.000	0.000	0.000	0.000	0.000	0.000	0.000	0.000	0.000	0.000	0.000	0.000
106	3.84	4.05	7.03	0.484	13.5	3.39	0.136	0.843	1.13	9.70	8.25	9.89	0.743	3.58	2.36	0.494	1.13	0.318	0.567	1.11	1.73	1.92	0.840	0.403	0.448	0.157	0.440	0.468	82.0
107	1.13	1.75	3.95	0.261	8.27	1.52	0.292	1.23	4.22	8.81	9.04	30.0	1.42	4.58	4.75	2.28	8.62	0.958	1.45	2.81	6.96	2.29	1.60	0.556	0.508	1.11	0.378	2.40	114
109	0.174	1.01	3.74	0.164	6.45	0.916	0.121	0.574	0.733	3.90	3.92	5.95	0.418	4.55	1.10	0.290	0.784	0.134	0.214	0.632	0.912	0.809	0.348	0.217	0.097	0.107	0.182	0.260	38.9
111	0.625	0.830	1.41	0.335	2.88	0.400	0.019	0.186	0.011	4.90	4.53	5.11	0.517	6.52	4.69	0.677	0.986	0.497	1.67	2.40	1.44	1.89	0.923	0.354	0.346	0.509	0.223	0.558	45.9
113	0.234	0.262	0.645	0.052	1.60	0.249	0.008	0.153	0.026	1.16	0.950	1.22	0.216	9.35	0.233	0.054	0.167	0.055	0.094	0.151	0.258	0.431	0.136	0.108	0.068	0.000	0.124	0.064	18.3

Station	Naphthalene	Methylnaphthalenes	Dimethylnaphthalenes	Acenaphthylene	Acenaphthene	Fluorene	Dibenzothiophene	Methyl dibenzothiophenes	Dimethyl dibenzothiophenes	Phenanthrene	Methylphenantrenes	Dimethylphenanthrenes	Anthracene	Fluoranthene	Pyrene	Methylpyrenes	Dimethylpyrenes	Benzo(ghi)fluoranthene	Benzo(a)anthracene	Chrysene	Methylchrysene	Benzo(b+k)fluoranthenes	Benzo(e)pyrene	Benzo(a)pyrene	Perylene	Indeno(1,2,3-cd)pyrene	Dibenzo(a,h)anthracene	Benzo(ghi)perylene	Σ ₆₄ PAHs
115	0.258	0.415	0.884	0.080	2.08	0.377	0.000	0.088	0.184	0.657	0.664	0.967	0.098	2.69	0.169	0.042	0.126	0.042	0.053	0.080	0.171	0.320	0.093	0.060	0.058	0.000	0.081	0.045	11.0
116	1.62	1.35	3.25	0.183	5.62	1.20	0.156	0.870	1.01	2.85	1.95	1.88	0.375	6.99	0.293	0.077	0.184	0.050	0.085	0.118	0.236	0.441	0.132	0.090	0.082	0.005	0.121	0.065	32.5
117	0.408	0.552	1.01	0.067	1.53	0.163	0.000	0.275	0.393	1.03	1.33	2.29	0.257	4.42	0.520	0.108	0.376	0.081	0.156	0.218	0.462	0.611	0.216	0.217	0.119	0.007	0.162	0.113	17.4
118	2.64	3.54	4.99	0.261	8.59	1.43	0.025	0.174	0.169	2.57	1.81	2.17	0.271	2.51	3.12	0.135	0.357	0.349	0.148	0.254	0.571	0.471	0.267	0.119	0.178	0.063	0.109	0.234	39.6
120	0.563	1.06	2.19	0.066	1.85	0.368	0.037	0.213	0.220	9.21	7.16	6.56	0.191	4.78	1.24	0.184	0.372	0.172	0.177	0.848	0.515	0.962	0.317	0.182	0.160	0.064	0.234	0.140	40.5
123	0.192	0.274	0.689	0.100	1.05	0.364	0.000	0.031	0.036	6.18	1.85	2.05	0.086	1.26	0.378	0.108	0.292	0.063	0.169	0.311	0.410	0.522	0.216	0.127	0.132	0.058	0.123	0.118	17.3
125	0.569	0.529	0.750	0.075	1.40	0.312	0.000	0.070	0.109	2.15	3.43	7.41	0.400	0.810	0.913	0.538	2.20	0.202	0.391	0.628	1.85	0.729	0.494	0.235	0.114	0.132	0.130	0.434	27.5
129	0.000	0.000	0.154	23.6	137	49.9	0.000	1.04	0.349	5.72	41.0	23.8	1.04	1.24	1.17	0.605	0.189	0.124	0.509	1.42	0.796	1.13	0.714	0.334	0.148	0.597	0.467	0.700	294
131	0.181	0.801	3.37	0.146	4.85	1.55	0.154	0.761	1.13	10.6	3.68	4.19	0.378	2.43	1.52	0.217	0.623	0.200	0.547	1.17	0.886	1.13	0.661	0.197	0.133	0.272	0.184	0.381	42.5
133	0.000	0.285	2.15	0.238	6.59	1.70	0.000	0.327	0.490	3.80	4.06	4.70	0.494	7.04	0.785	0.179	0.334	0.138	0.379	0.494	0.348	1.32	0.395	0.266	0.234	0.000	0.267	0.141	37.3
134	2.50	5.78	13.0	0.259	10.7	1.82	0.419	2.30	1.71	7.94	4.63	4.53	0.903	7.99	0.806	0.179	0.370	0.115	0.171	0.283	0.389	0.855	0.229	0.167	0.183	0.000	0.363	0.084	70.6
136	0.585	2.66	6.83	0.461	10.0	2.28	0.131	0.424	0.597	4.45	3.16	3.41	0.640	2.40	0.600	0.000	0.000	0.000	0.250	0.279	0.000	1.43	0.000	0.260	0.000	0.000	0.000	0.051	41.3
138	3.86	3.23	4.64	0.332	10.2	2.01	0.026	0.514	0.835	6.44	4.72	3.66	0.697	2.17	0.851	0.224	0.550	0.144	0.293	0.310	1.15	1.57	0.365	0.325	0.280	0.618	0.443	0.555	53.9
140	15.3	13.6	25.9	2.12	71.8	15.1	0.000	1.76	1.14	99.0	34.4	27.2	3.03	10.2	5.94	1.35	1.03	1.18	1.85	5.53	2.10	11.7	3.15	0.000	2.25	0.000	0.000	0.164	368
142	2.42	2.48	4.87	0.413	11.1	3.37	0.000	0.798	0.579	15.6	9.34	9.01	1.10	4.99	2.24	0.689	0.367	0.281	0.705	0.748	0.576	3.73	0.853	0.644	0.753	0.000	0.000	0.000	79.7
144	0.398	0.621	1.60	0.315	2.91	1.45	0.512	3.52	10.5	7.49	11.4	25.78	0.675	6.57	6.95	1.97	10.2	1.29	4.23	6.38	13.3	6.69	6.28	4.09	1.05	4.87	2.03	6.50	150
145	0.273	0.599	1.58	0.116	2.17	1.00	0.000	0.108	0.160	2.16	1.19	1.31	0.214	0.963	0.393	0.183	0.387	0.135	0.324	0.514	0.808	1.52	0.592	0.330	0.276	0.000	0.000	0.137	17.8

*Sample 98 has been diminished by 10 fold in graphics.

Figure S5.2. Relative occurrence of individual PAHs in plankton per oceanic subbasin (%)

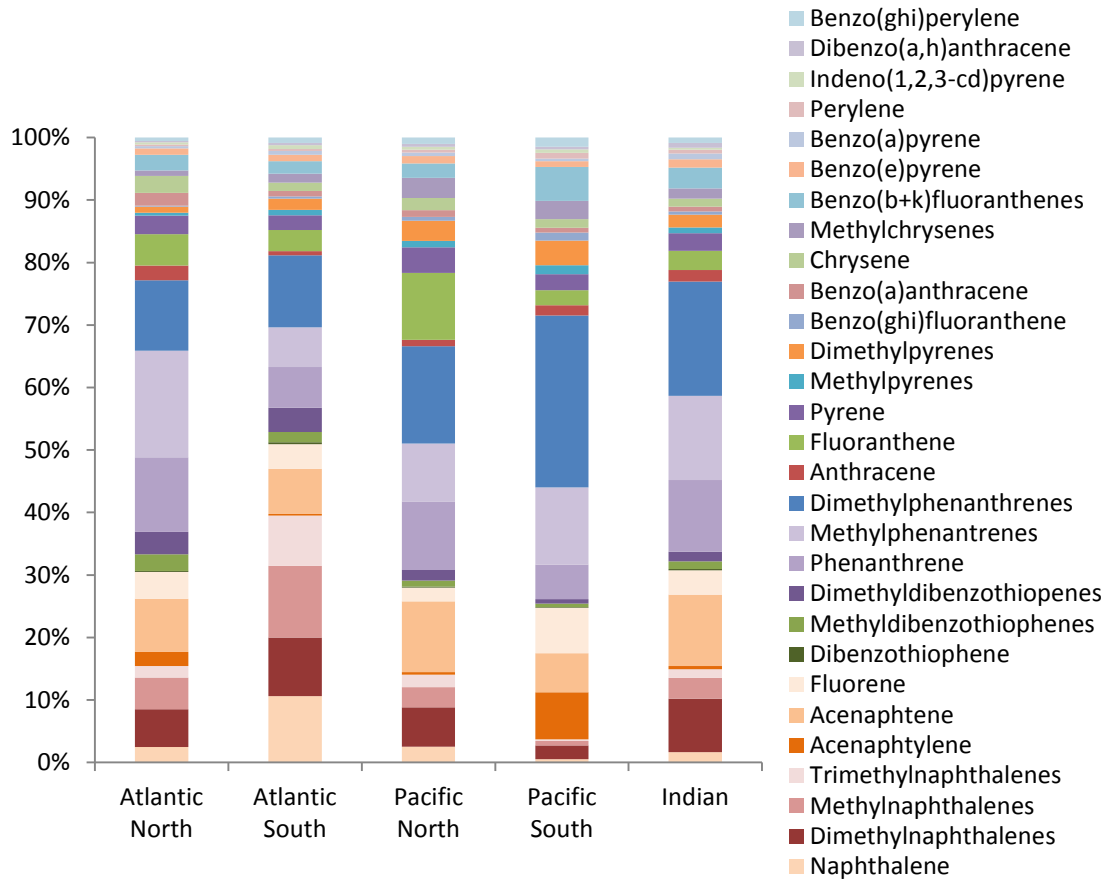


Figure S5.3. K_{oc} in surface waters for some representative PAHs

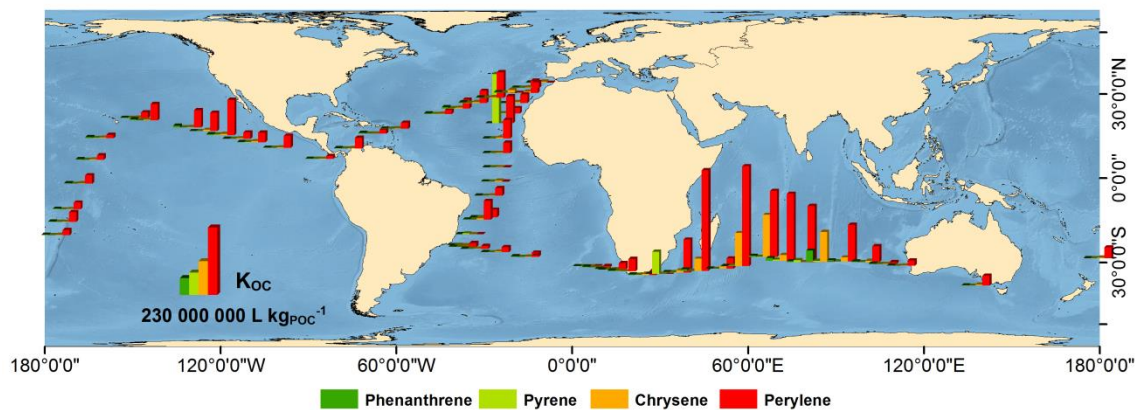


Table S5.11. Slopes fitted to the field data of $C_{Plankton}$ versus Biomass

	m
Naphthalene	-1.59
Dimethylnaphthalenes	-1.32
Methylnaphthalene	-1.48
Acenaphtylene	-0.87
Acenaphtene	-0.88
Fluorene	-1.10
Dibenzothiophene	-1.46
Methyldibenzothiophenes	-1.26
Dimethyldibenzothiophenes	-1.29
Phenanthrene	-1.02
Methylphenantrenes	-1.11
Dimethylphenanthrenes	-1.03
Anthracene	-0.96
Fluoranthene	-1.20
Pyrene	-1.25
Methylpyrenes	-1.14
Dimethylpyrenes	-1.04
Benzo(ghi)fluoranthene	-0.98
Benzo(a)anthracene	-1.16
Chrysene	-1.19
Methylchrysenes	-0.94
Benzo(b+k)fluoranthenes	-1.15
Benzo(e)pyrene	-1.09
Benzo(a)pyrene	-1.08
Perylene	-1.11
Indeno(1,2,3-cd)pyrene	-1.10
Dibenzo(a,h)anthracene	-0.97
Benzo(ghi)perylene	-1.23

Table S5.12. Biological pump fluxes

Station	F_{Phyto} (ng m ⁻² day ⁻¹)																											
	Naphthalene	Dimethylnaphthalenes	Methylnaphthalenes	Acenaphthylene	Acenaphthene	Fluorene	Dibenzothiophene	Methyl dibenzothiophenes	Dimethyl dibenzothiophenes	Phenanthrene	Methylphenantrenes	Dimethylphenanthrenes	Anthracene	Fluoranthene	Pyrene	Methylpyrene	Dimethylpyrene	Benzo (ghi) fluoranthene	Benzo (a)anthracene	Chrysene	Methylchrysene	Benzo (b+k) fluoranthenes	Benzo (e)pyrene	Benzo (a)pyrene	Perylene	Indeno (1,2,3-cd)pyrene	Dibenzo (ah)anthracene	Benzo (ghi) perylene
1	0.134	0.713	0.275	0.073	0.875	0.417	0.285	2.21	5.79	2.80	8.36	14.4	0.221	1.44	1.30	0.736	1.46	0.134	0.344	0.637	0.784	0.574	0.344	0.210	0.196	0.293	0.091	0.385
3	0.036	0.180	0.057	0.017	0.391	0.201	0.102	0.620	0.932	0.861	1.27	1.24	0.063	0.372	0.288	0.073	0.139	0.023	0.080	0.112	0.096	0.180	0.096	0.059	0.037	0.061	0.030	0.086
6	0.964	3.76	5.04	0.020	0.348	0.128	0.004	0.021	0.050	0.329	0.453	0.823	0.025	2.94	2.36	0.076	0.144	0.036	2.92	3.01	0.149	1.74	0.274	0.148	0.071	0.264	0.075	0.260
8	7.733	9.01	5.79	0.158	4.36	1.25	0.000	7.28	2.41	16.2	21.9	7.34	0.076	7.52	3.52	0.059	0.168	0.036	0.058	2.75	0.113	2.16	0.099	0.050	0.037	0.048	0.055	0.606
10	0.776	1.93	2.39	1.06	2.55	3.55	0.000	2.95	3.07	13.8	31.3	9.43	8.09	4.17	1.17	0.035	0.071	0.012	1.30	1.31	0.065	1.01	1.15	0.031	0.018	0.026	0.022	0.040
12	1.97	6.85	3.82	0.867	3.53	3.72	0.000	0.025	0.032	13.3	13.6	3.06	2.79	1.41	1.12	0.047	0.063	0.017	0.031	0.031	0.033	1.36	0.045	0.035	0.035	0.000	0.038	0.012
14	0.943	1.92	4.01	9.11	0.539	5.19	0.000	0.014	0.006	0.571	1.04	1.32	0.032	1.83	1.48	0.064	0.123	0.020	1.99	1.87	0.083	1.20	1.76	0.031	0.027	0.032	0.031	0.062
16	0.048	0.286	0.067	0.036	0.525	0.104	0.000	0.005	0.000	0.167	0.149	0.187	0.020	0.130	0.036	0.016	0.042	0.009	0.018	0.035	0.043	0.107	0.047	0.020	0.017	0.018	0.023	0.033
18	0.065	0.177	0.090	0.010	0.154	0.042	0.006	0.026	0.039	0.089	0.096	0.106	0.008	0.096	0.023	0.007	0.014	0.003	0.008	0.012	0.013	0.025	0.010	0.005	0.005	0.005	0.005	0.008
20	0.001	0.004	0.001	0.000	0.002	0.002	0.001	0.004	0.006	0.009	0.012	0.010	0.001	0.019	0.002	0.000	0.001	0.000	0.001	0.001	0.001	0.004	0.001	0.001	0.001	0.001	0.001	0.001
22	0.000	0.005	0.001	0.000	0.010	0.003	0.001	0.002	0.003	0.013	0.023	0.027	0.001	0.013	0.005	0.002	0.003	0.000	0.002	0.004	0.002	0.005	0.003	0.001	0.001	0.002	0.001	0.002
24	0.002	0.019	0.004	0.002	0.035	0.010	0.010	0.098	0.937	0.064	0.337	2.462	0.019	0.038	0.077	0.128	0.383	0.017	0.023	0.079	0.185	0.033	0.027	0.008	0.004	0.015	0.004	0.034
25	0.006	0.023	0.009	0.001	0.027	0.009	0.001	0.007	0.011	0.023	0.024	0.029	0.002	0.024	0.007	0.002	0.003	0.001	0.002	0.003	0.003	0.008	0.003	0.002	0.001	0.001	0.002	0.002
27	0.014	0.023	0.028	0.001	0.022	0.007	0.000	0.001	0.002	0.008	0.006	0.003	0.001	0.002	0.001	0.000	0.001	0.000	0.000	0.001	0.001	0.002	0.001	0.000	0.000	0.000	0.000	0.000
28	0.132	0.127	0.166	0.004	0.113	0.085	0.008	0.038	0.044	0.112	0.088	0.063	0.007	0.016	0.018	0.004	0.008	0.002	0.004	0.006	0.009	0.015	0.008	0.004	0.002	0.003	0.003	0.006
29	0.003	0.020	0.005	0.003	0.055	0.019	0.000	0.001	0.000	0.066	0.062	0.069	0.006	0.133	0.035	0.007	0.010	0.005	0.008	0.011	0.008	0.020	0.009	0.005	0.007	0.004	0.004	0.010
30	0.037	0.147	0.079	0.002	0.045	0.026	0.003	0.020	0.031	0.064	0.076	0.060	0.007	0.214	0.016	0.005	0.006	0.002	0.005	0.005	0.005	0.014	0.005	0.005	0.003	0.002	0.003	0.003
31	0.007	0.038	0.021	0.000	0.010	0.008	0.000	0.000	0.000	0.019	0.024	0.031	0.002	0.034	0.025	0.004	0.006	0.002	0.003	0.005	0.011	0.005	0.003	0.002	0.001	0.001	0.001	0.006
34	0.012	0.064	0.039	0.002	0.018	0.008	0.000	0.000	0.000	0.013	0.019	0.020	0.002	0.013	0.012	0.005	0.004	0.002	0.007	0.007	0.005	0.012	0.007	0.005	0.002	0.005	0.002	0.005

37	0.062	0.022	0.045	0.000	0.020	0.006	0.000	0.002	0.002	0.010	0.009	0.008	0.001	0.004	0.003	0.001	0.001	0.000	0.001	0.002	0.002	0.004	0.002	0.001	0.001	0.001	0.001	0.001
41	0.008	0.015	0.010	0.001	0.052	0.020	0.001	0.001	0.001	0.231	0.070	0.046	0.031	0.296	0.214	0.053	0.017	0.021	0.146	0.134	0.036	0.185	0.096	0.088	0.026	0.108	0.030	0.079
42	0.014	0.085	0.042	0.001	0.015	0.033	0.000	0.001	0.002	0.043	0.029	0.074	0.003	0.015	0.017	0.006	0.015	0.003	0.005	0.012	0.016	0.011	0.006	0.003	0.001	0.005	0.002	0.008
43	0.017	0.158	0.073	0.001	0.021	0.052	0.000	0.001	0.001	0.017	0.016	0.019	0.003	0.034	0.013	0.003	0.003	0.002	0.003	0.010	0.005	0.013	0.005	0.002	0.003	0.004	0.002	0.004
44	4.50	1.19	2.80	0.030	0.802	0.350	0.020	0.146	0.228	0.930	0.807	0.862	0.109	0.469	0.329	0.061	0.181	0.043	0.064	0.118	0.179	0.345	0.118	0.073	0.055	0.018	0.073	0.080
45	1.99	1.53	1.65	0.112	1.23	0.866	0.180	0.906	1.27	3.41	5.07	8.73	0.386	1.66	1.93	0.668	1.19	0.414	0.626	1.20	1.10	1.27	0.804	0.467	0.129	0.651	0.167	1.14
46	0.022	0.050	0.026	0.002	0.085	0.018	0.002	0.011	0.020	0.053	0.056	0.121	0.007	0.025	0.018	0.007	0.020	0.003	0.008	0.019	0.016	0.023	0.010	0.005	0.005	0.009	0.003	0.010
48	0.008	0.070	0.021	0.002	0.055	0.027	0.004	0.025	0.038	0.109	0.409	0.859	0.051	0.022	0.044	0.036	0.095	0.007	0.008	0.023	0.050	0.013	0.009	0.003	0.001	0.005	0.002	0.012
50	0.006	0.014	0.010	0.001	0.009	0.002	0.000	0.001	0.001	0.008	0.005	0.004	0.003	0.004	0.002	0.000	0.001	0.001	0.001	0.001	0.001	0.008	0.003	0.003	0.002	0.000	0.002	0.002
52	0.000	0.001	0.000	0.000	0.003	0.001	0.000	0.000	0.000	0.002	0.001	0.001	0.000	0.001	0.000	0.000	0.000	0.000	0.000	0.000	0.000	0.001	0.000	0.000	0.000	0.000	0.000	0.000
53	0.000	0.004	0.001	0.000	0.006	0.003	0.000	0.001	0.002	0.009	0.007	0.005	0.001	0.001	0.001	0.000	0.000	0.000	0.000	0.000	0.000	0.002	0.000	0.000	0.000	0.000	0.000	0.000
55	0.000	0.001	0.000	0.000	0.001	0.000	0.000	0.000	0.000	0.002	0.002	0.002	0.000	0.001	0.000	0.000	0.000	0.000	0.000	0.000	0.000	0.001	0.000	0.000	0.000	0.000	0.000	0.000
57	0.000	0.001	0.000	0.000	0.002	0.000	0.000	0.000	0.000	0.001	0.001	0.001	0.000	0.000	0.000	0.000	0.000	0.000	0.000	0.000	0.000	0.001	0.000	0.000	0.000	0.000	0.000	0.000
59	0.001	0.001	0.001	0.000	0.003	0.001	0.000	0.000	0.000	0.002	0.001	0.001	0.000	0.000	0.000	0.000	0.000	0.000	0.000	0.000	0.000	0.001	0.000	0.000	0.000	0.000	0.000	0.000
61	0.001	0.008	0.002	0.000	0.011	0.002	0.000	0.000	0.000	0.004	0.004	0.006	0.001	0.001	0.001	0.000	0.001	0.000	0.000	0.000	0.001	0.001	0.001	0.000	0.000	0.000	0.000	0.000
63	0.002	0.004	0.003	0.000	0.006	0.001	0.000	0.000	0.000	0.004	0.004	0.003	0.000	0.001	0.001	0.000	0.000	0.000	0.000	0.001	0.001	0.001	0.001	0.000	0.000	0.000	0.000	0.000
65	0.001	0.002	0.001	0.000	0.003	0.001	0.000	0.000	0.000	0.007	0.003	0.003	0.000	0.002	0.001	0.000	0.000	0.000	0.000	0.000	0.000	0.001	0.000	0.000	0.000	0.000	0.000	0.000
67	0.003	0.026	0.007	0.002	0.017	0.025	0.000	0.001	0.001	0.010	0.008	0.007	0.002	0.005	0.001	0.001	0.001	0.000	0.001	0.001	0.001	0.003	0.001	0.002	0.003	0.002	0.001	0.000
74	0.023	0.294	0.076	0.024	0.753	0.210	0.000	0.012	0.010	0.313	0.315	0.166	0.046	0.017	0.012	0.008	0.005	0.003	0.005	0.005	0.006	0.042	0.011	0.007	0.008	0.000	0.010	0.002
4b1	0.001	0.094	0.021	0.007	0.112	0.056	0.002	0.009	0.017	0.341	0.297	0.412	0.016	0.140	0.094	0.023	0.046	0.021	0.033	0.083	0.051	0.085	0.045	0.025	0.012	0.024	0.014	0.033
79	0.000	0.018	0.002	0.002	0.043	0.024	0.001	0.005	0.008	0.050	0.039	0.047	0.004	0.015	0.014	0.003	0.005	0.002	0.006	0.009	0.006	0.015	0.008	0.006	0.003	0.007	0.003	0.008
83	0.005	0.012	0.006	0.001	0.021	0.005	0.001	0.004	0.006	0.035	0.013	0.014	0.002	0.045	0.087	0.001	0.002	0.007	0.001	0.002	0.002	0.006	0.003	0.002	0.001	0.000	0.001	0.003
85	0.002	0.000	0.000	0.061	0.000	0.048	0.000	0.000	0.000	0.000	0.000	0.000	0.000	0.003	0.003	0.000	0.000	0.007	0.000	0.000	0.000	0.031	0.000	0.000	0.006	0.000	0.000	0.004
88	0.000	0.004	0.001	0.000	0.012	0.003	0.000	0.000	0.000	0.013	0.044	0.104	0.006	0.003	0.006	0.005	0.014	0.001	0.001	0.003	0.008	0.003	0.002	0.001	0.000	0.000	0.000	0.002
92	0.033	0.173	0.063	0.011	0.303	0.101	0.013	0.064	0.099	0.239	0.210	0.379	0.033	0.113	0.059	0.023	0.066	0.019	0.044	0.068	0.140	0.099	0.051	0.025	0.012	0.036	0.016	0.054
95	0.000	0.013	0.001	0.014	0.117	0.025	0.000	0.002	0.000	0.069	0.092	0.181	0.009	0.045	0.023	0.011	0.028	0.003	0.012	0.017	0.022	0.038	0.012	0.013	0.004	0.020	0.016	0.022
98	0.023	0.078	0.051	0.009	0.829	0.785	0.069	0.102	0.052	1.94	0.446	0.269	0.223	2.33	1.59	0.297	0.098	0.131	0.967	0.910	0.193	0.866	0.475	0.474	0.130	0.505	0.157	0.410
103	0.001	0.003	0.001	0.000	0.008	0.001	0.000	0.001	0.001	0.008	0.008	0.011	0.001	0.004	0.004	0.001	0.003	0.001	0.001	0.001	0.002	0.002	0.001	0.000	0.000	0.001	0.000	0.001
105	0.000	0.000	0.000	0.000	0.000	0.000	0.000	0.000	0.000	0.000	0.000	0.000	0.000	0.000	0.000	0.000	0.000	0.000	0.000	0.000	0.000	0.000	0.000	0.000	0.000	0.000	0.000	0.000
106	0.006	0.011	0.007	0.001	0.022	0.006	0.000	0.001	0.002	0.016	0.013	0.016	0.001	0.006	0.004	0.001	0.002	0.001	0.001	0.002	0.003	0.003	0.001	0.001	0.001	0.000	0.001	0.001

107	0.001	0.005	0.002	0.000	0.011	0.002	0.000	0.002	0.006	0.012	0.012	0.039	0.002	0.006	0.006	0.003	0.011	0.001	0.002	0.004	0.009	0.003	0.002	0.001	0.001	0.001	0.000	0.003
109	0.000	0.003	0.001	0.000	0.006	0.001	0.000	0.001	0.001	0.003	0.003	0.005	0.000	0.004	0.001	0.000	0.001	0.000	0.000	0.001	0.001	0.001	0.000	0.000	0.000	0.000	0.000	0.000
111	0.001	0.002	0.001	0.001	0.004	0.001	0.000	0.000	0.000	0.008	0.007	0.008	0.001	0.010	0.007	0.001	0.002	0.001	0.003	0.004	0.002	0.003	0.001	0.001	0.001	0.001	0.000	0.001
113	0.002	0.004	0.002	0.000	0.010	0.002	0.000	0.001	0.000	0.008	0.006	0.008	0.001	0.061	0.002	0.000	0.001	0.000	0.001	0.001	0.002	0.003	0.001	0.001	0.000	0.000	0.001	0.000
115	0.002	0.008	0.004	0.001	0.019	0.003	0.000	0.001	0.002	0.006	0.006	0.009	0.001	0.025	0.002	0.000	0.001	0.000	0.000	0.001	0.002	0.003	0.001	0.001	0.001	0.000	0.001	0.000
116	0.015	0.031	0.013	0.002	0.054	0.012	0.001	0.008	0.010	0.027	0.019	0.018	0.004	0.067	0.003	0.001	0.002	0.000	0.001	0.001	0.002	0.004	0.001	0.001	0.001	0.000	0.001	0.001
117	0.003	0.007	0.004	0.000	0.010	0.001	0.000	0.002	0.003	0.007	0.009	0.015	0.002	0.029	0.003	0.001	0.002	0.001	0.001	0.001	0.003	0.004	0.001	0.001	0.001	0.000	0.001	0.001
118	0.060	0.113	0.080	0.006	0.195	0.032	0.001	0.004	0.004	0.058	0.041	0.049	0.006	0.057	0.071	0.003	0.008	0.008	0.003	0.006	0.013	0.011	0.006	0.003	0.004	0.001	0.002	0.005
120	0.004	0.014	0.007	0.000	0.012	0.002	0.000	0.001	0.001	0.060	0.047	0.043	0.001	0.031	0.008	0.001	0.002	0.001	0.001	0.006	0.003	0.006	0.002	0.001	0.001	0.000	0.002	0.001
123	0.020	0.071	0.028	0.010	0.108	0.037	0.000	0.003	0.004	0.636	0.191	0.211	0.009	0.129	0.039	0.011	0.030	0.007	0.017	0.032	0.042	0.054	0.022	0.013	0.014	0.006	0.013	0.012
125	0.036	0.047	0.033	0.005	0.088	0.020	0.000	0.004	0.007	0.135	0.215	0.465	0.025	0.051	0.057	0.034	0.139	0.013	0.025	0.039	0.116	0.046	0.031	0.015	0.007	0.008	0.008	0.027
129	0.000	0.002	0.000	0.281	1.64	0.595	0.000	0.012	0.004	0.068	0.488	0.283	0.012	0.015	0.014	0.007	0.002	0.001	0.006	0.017	0.009	0.013	0.009	0.004	0.002	0.007	0.006	0.008
131	0.004	0.082	0.019	0.004	0.118	0.038	0.004	0.018	0.027	0.257	0.089	0.102	0.009	0.059	0.037	0.005	0.015	0.005	0.013	0.029	0.022	0.028	0.016	0.005	0.003	0.007	0.004	0.009
133	0.000	0.003	0.000	0.000	0.008	0.002	0.000	0.000	0.001	0.004	0.005	0.005	0.001	0.008	0.001	0.000	0.000	0.000	0.000	0.001	0.000	0.002	0.000	0.000	0.000	0.000	0.000	0.000
134	0.001	0.007	0.003	0.000	0.006	0.001	0.000	0.001	0.001	0.004	0.003	0.003	0.001	0.004	0.000	0.000	0.000	0.000	0.000	0.000	0.000	0.000	0.000	0.000	0.000	0.000	0.000	0.000
136	0.000	0.001	0.000	0.000	0.002	0.000	0.000	0.000	0.000	0.001	0.001	0.001	0.000	0.000	0.000	0.000	0.000	0.000	0.000	0.000	0.000	0.000	0.000	0.000	0.000	0.000	0.000	0.000
138	0.002	0.002	0.002	0.000	0.005	0.001	0.000	0.000	0.000	0.003	0.003	0.002	0.000	0.001	0.000	0.000	0.000	0.000	0.000	0.000	0.001	0.001	0.000	0.000	0.000	0.000	0.000	0.000
140	0.001	0.001	0.001	0.000	0.003	0.001	0.000	0.000	0.000	0.005	0.002	0.001	0.000	0.000	0.000	0.000	0.000	0.000	0.000	0.000	0.000	0.000	0.000	0.000	0.000	0.000	0.000	0.000
142	0.001	0.001	0.001	0.000	0.003	0.001	0.000	0.000	0.000	0.004	0.002	0.002	0.000	0.001	0.001	0.000	0.000	0.000	0.000	0.000	0.000	0.000	0.000	0.000	0.000	0.000	0.000	0.000
144	0.000	0.001	0.000	0.000	0.001	0.001	0.000	0.002	0.005	0.004	0.006	0.013	0.000	0.003	0.003	0.001	0.005	0.001	0.002	0.003	0.007	0.003	0.003	0.002	0.001	0.002	0.001	0.003
146	0.000	0.002	0.001	0.000	0.002	0.001	0.000	0.000	0.000	0.002	0.001	0.001	0.000	0.001	0.000	0.000	0.000	0.000	0.000	0.001	0.001	0.002	0.001	0.000	0.000	0.000	0.000	0.000

F_{Fecal} (ng m⁻²day⁻¹)

Station	Naphthalene	Dimethylnaphthalenes_	Methylnaphthalenes	Acenaphthylene	Acenaphthene	Fluorene	Dibenzothiophene	Methyl dibenzothiophenes	Dimethyl dibenzothiophenes	Phenanthrene	Methylphenantrenes	Dimethylphenanthrenes	Anthracene	Fluoranthene	Pyrene	Methylpyrene	Dimethylpyrene	Benzo(ghi)fluoranthene	Benzo(a)anthracene	Chrysene	Methylchrysene	Benzo(b+k)fluoranthenes	Benzo(e)pyrene	Benzo(a)pyrene	Perylene	Indeno(1.2.3-cd)pyrene	Dibenzo(ah)anthracene	Benzo(ghi)perylene
1	0.600	3.20	1.24	0.326	3.93	1.87	1.28	9.92	26.2	12.6	37.6	64.6	0.991	6.45	5.85	3.31	6.57	0.601	1.54	2.86	3.52	2.58	1.55	0.942	0.881	1.31	0.410	1.73
3	0.358	1.80	0.571	0.170	3.92	2.01	1.03	6.22	9.34	8.64	12.7	12.4	0.636	3.73	2.89	0.729	1.39	0.230	0.806	1.13	0.967	1.80	0.961	0.590	0.367	0.615	0.296	0.860
6	7.76	30.3	40.5	0.163	2.80	1.03	0.033	0.172	0.406	2.65	3.65	6.62	0.197	23.7	19.0	0.611	1.16	0.290	23.5	24.2	1.20	14.0	2.203	1.19	0.570	2.13	0.606	2.09
8	62.6	72.9	46.9	1.28	35.3	10.1	0.000	58.9	19.5	131	177	59.4	0.618	60.9	28.5	0.474	1.36	0.294	0.471	22.3	0.913	17.5	0.797	0.401	0.298	0.390	0.442	4.91
10	5.61	13.9	17.2	7.66	18.5	25.6	0.000	21.4	22.2	100	226	68.2	58.5	30.1	8.48	0.256	0.512	0.090	9.37	9.46	0.468	7.28	8.33	0.227	0.134	0.187	0.162	0.292
12	12.2	42.7	23.8	5.40	22.0	23.2	0.000	0.155	0.197	82.9	84.7	19.1	17.4	8.81	6.97	0.290	0.393	0.109	0.191	0.195	0.206	8.49	0.283	0.216	0.220	0.000	0.237	0.077
14	4.69	9.54	20.0	45.4	2.69	25.8	0.000	0.070	0.029	2.84	5.19	6.59	0.159	9.08	7.38	0.319	0.614	0.099	9.89	9.32	0.413	5.96	8.774	0.154	0.132	0.160	0.154	0.310
16	0.370	2.20	0.518	0.279	4.04	0.803	0.000	0.038	0.000	1.29	1.15	1.44	0.156	1.00	0.279	0.120	0.321	0.067	0.141	0.267	0.327	0.820	0.360	0.156	0.134	0.139	0.179	0.257
18	3.04	8.26	4.21	0.471	7.17	1.95	0.264	1.24	1.82	4.15	4.46	4.96	0.372	4.49	1.10	0.319	0.644	0.135	0.352	0.547	0.609	1.17	0.447	0.246	0.230	0.248	0.237	0.352
20	0.206	0.605	0.247	0.042	0.407	0.327	0.116	0.706	0.968	1.58	2.06	1.77	0.136	3.24	0.355	0.080	0.176	0.055	0.156	0.197	0.171	0.605	0.243	0.136	0.132	0.136	0.122	0.173
22	0.092	0.977	0.178	0.062	2.00	0.689	0.111	0.472	0.567	2.66	4.59	5.46	0.154	2.53	1.09	0.412	0.554	0.095	0.471	0.764	0.485	1.09	0.555	0.221	0.199	0.368	0.154	0.407
24	0.160	1.73	0.341	0.157	3.19	0.859	0.859	8.84	84.5	5.74	30.4	222	1.75	3.40	6.91	11.5	34.5	1.52	2.06	7.15	16.7	2.99	2.46	0.724	0.329	1.33	0.365	3.10
25	0.372	1.32	0.503	0.086	1.59	0.511	0.065	0.383	0.615	1.34	1.39	1.70	0.141	1.42	0.408	0.095	0.178	0.052	0.092	0.150	0.163	0.452	0.147	0.095	0.072	0.038	0.095	0.095
27	1.34	2.24	2.72	0.068	2.11	0.671	0.036	0.142	0.146	0.744	0.584	0.331	0.087	0.224	0.138	0.046	0.080	0.030	0.046	0.078	0.089	0.176	0.093	0.045	0.032	0.005	0.000	0.027
28	12.4	11.9	15.6	0.340	10.6	7.97	0.755	3.54	4.10	10.5	8.25	5.96	0.670	1.49	1.71	0.388	0.780	0.161	0.343	0.525	0.835	1.41	0.724	0.366	0.231	0.261	0.312	0.565
29	0.222	1.48	0.334	0.225	4.04	1.39	0.000	0.106	0.024	4.80	4.50	5.04	0.472	9.66	2.54	0.518	0.715	0.360	0.573	0.778	0.569	1.45	0.632	0.333	0.488	0.278	0.278	0.733
30	2.42	9.55	5.14	0.157	2.91	1.70	0.215	1.29	2.03	4.20	4.94	3.94	0.482	14.0	1.06	0.303	0.362	0.112	0.332	0.341	0.321	0.933	0.315	0.309	0.226	0.126	0.194	0.220
31	0.849	4.438	2.50	0.041	1.14	0.941	0.000	0.017	0.015	2.20	2.77	3.60	0.225	3.94	2.94	0.416	0.706	0.277	0.310	0.589	1.31	0.616	0.406	0.181	0.156	0.156	0.145	0.697
34	2.63	13.9	8.54	0.391	4.01	1.78	0.000	0.061	0.029	2.88	4.04	4.39	0.534	2.90	2.61	0.995	0.833	0.348	1.46	1.59	1.04	2.63	1.44	1.11	0.484	1.05	0.404	1.18
37	22.4	8.04	16.2	0.128	7.39	2.22	0.133	0.593	0.737	3.73	3.34	3.08	0.318	1.49	1.05	0.236	0.440	0.133	0.368	0.740	0.563	1.42	0.609	0.284	0.211	0.369	0.247	0.435

41	0.939	1.79	1.23	0.130	6.10	2.40	0.080	0.142	0.066	27.1	8.26	5.39	3.61	34.72	25.1	6.26	1.98	2.48	17.1	15.7	4.22	21.7	11.2	10.4	2.99	12.6	3.53	9.28
42	1.13	7.03	3.49	0.048	1.26	2.74	0.013	0.111	0.166	3.56	2.44	6.09	0.287	1.28	1.43	0.514	1.25	0.256	0.445	1.01	1.35	0.941	0.506	0.227	0.071	0.441	0.125	0.663
43	0.689	6.21	2.90	0.041	0.846	2.04	0.000	0.028	0.030	0.659	0.630	0.751	0.102	1.36	0.517	0.102	0.120	0.069	0.104	0.413	0.205	0.526	0.178	0.070	0.125	0.160	0.085	0.169
44	76.4	20.3	47.6	0.502	13.6	5.93	0.346	2.48	3.86	15.8	13.7	14.6	1.86	7.96	5.58	1.04	3.07	0.735	1.08	2.01	3.04	5.86	2.00	1.24	0.926	0.304	1.23	1.35
45	7.29	5.62	6.04	0.410	4.52	3.18	0.658	3.32	4.64	12.5	18.6	32.0	1.42	6.08	7.08	2.45	4.35	1.52	2.29	4.39	4.01	4.66	2.95	1.71	0.474	2.39	0.612	4.19
46	0.267	0.608	0.322	0.029	1.04	0.224	0.025	0.134	0.243	0.640	0.685	1.47	0.090	0.309	0.218	0.084	0.243	0.039	0.092	0.232	0.191	0.285	0.121	0.064	0.056	0.109	0.035	0.116
48	0.293	2.50	0.737	0.083	1.95	0.963	0.141	0.887	1.33	3.88	14.5	30.5	1.82	0.777	1.55	1.29	3.38	0.254	0.288	0.810	1.759	0.451	0.309	0.123	0.042	0.183	0.054	0.428
50	0.407	0.906	0.665	0.036	0.558	0.101	0.000	0.075	0.047	0.499	0.345	0.263	0.164	0.257	0.103	0.026	0.034	0.039	0.058	0.060	0.064	0.532	0.196	0.165	0.106	0.000	0.141	0.113
52	0.007	0.059	0.013	0.010	0.209	0.064	0.000	0.009	0.008	0.130	0.078	0.087	0.028	0.069	0.018	0.005	0.012	0.005	0.008	0.009	0.013	0.060	0.022	0.017	0.012	0.000	0.015	0.010
53	0.010	0.135	0.033	0.012	0.204	0.098	0.009	0.053	0.061	0.309	0.260	0.168	0.029	0.039	0.036	0.007	0.009	0.005	0.010	0.010	0.009	0.055	0.015	0.012	0.010	0.000	0.013	0.006
55	0.008	0.102	0.034	0.006	0.075	0.031	0.000	0.002	0.005	0.183	0.147	0.139	0.018	0.049	0.030	0.009	0.016	0.008	0.014	0.017	0.023	0.080	0.026	0.018	0.015	0.002	0.018	0.018
57	0.012	0.065	0.015	0.006	0.154	0.034	0.000	0.001	0.003	0.090	0.073	0.055	0.013	0.023	0.015	0.007	0.008	0.004	0.007	0.009	0.012	0.054	0.016	0.010	0.010	0.000	0.012	0.004
59	0.086	0.106	0.067	0.011	0.268	0.057	0.000	0.009	0.014	0.171	0.151	0.119	0.022	0.048	0.028	0.007	0.012	0.007	0.011	0.017	0.024	0.076	0.022	0.015	0.014	0.000	0.018	0.006
61	0.063	0.792	0.211	0.023	1.14	0.241	0.000	0.012	0.005	0.386	0.429	0.605	0.071	0.062	0.059	0.042	0.147	0.014	0.028	0.050	0.124	0.110	0.058	0.020	0.015	0.017	0.019	0.039
63	0.156	0.308	0.210	0.013	0.478	0.075	0.000	0.007	0.002	0.349	0.287	0.283	0.025	0.092	0.076	0.017	0.035	0.016	0.027	0.041	0.056	0.088	0.042	0.018	0.013	0.011	0.018	0.030
65	0.059	0.139	0.081	0.010	0.168	0.093	0.000	0.004	0.005	0.444	0.202	0.190	0.018	0.102	0.056	0.011	0.011	0.010	0.018	0.030	0.024	0.089	0.029	0.016	0.013	0.005	0.017	0.010
67	0.126	1.07	0.277	0.087	0.694	1.01	0.000	0.023	0.031	0.396	0.325	0.294	0.073	0.208	0.045	0.030	0.027	0.011	0.028	0.028	0.036	0.141	0.040	0.091	0.103	0.066	0.061	0.015
74	0.141	1.79	0.465	0.143	4.59	1.28	0.000	0.075	0.060	1.91	1.92	1.01	0.279	0.106	0.075	0.048	0.029	0.016	0.028	0.029	0.034	0.259	0.067	0.045	0.050	0.000	0.062	0.013
4b1	0.009	0.781	0.174	0.061	0.927	0.468	0.015	0.075	0.143	2.84	2.47	3.43	0.134	1.16	0.779	0.190	0.384	0.175	0.277	0.693	0.428	0.711	0.370	0.209	0.098	0.196	0.116	0.277
79	0.002	0.283	0.033	0.034	0.676	0.379	0.015	0.072	0.120	0.796	0.611	0.749	0.068	0.243	0.219	0.042	0.084	0.039	0.097	0.141	0.095	0.240	0.132	0.103	0.046	0.107	0.041	0.128
83	0.089	0.213	0.108	0.021	0.370	0.082	0.022	0.079	0.104	0.630	0.224	0.250	0.035	0.813	1.56	0.012	0.031	0.129	0.022	0.035	0.029	0.111	0.052	0.030	0.020	0.003	0.023	0.046
85	0.076	0.000	0.000	2.34	0.000	1.85	0.000	0.000	0.000	0.000	0.000	0.000	0.000	0.110	0.119	0.000	0.000	0.254	0.000	0.000	0.000	1.19	0.000	0.000	0.231	0.000	0.000	0.135
88	0.016	0.290	0.079	0.026	0.974	0.215	0.000	0.030	0.015	1.03	3.57	8.46	0.501	0.218	0.472	0.400	1.16	0.102	0.110	0.250	0.642	0.235	0.144	0.048	0.031	0.029	0.037	0.158
92	0.299	1.59	0.580	0.101	2.78	0.930	0.121	0.588	0.906	2.19	1.93	3.48	0.300	1.04	0.542	0.214	0.606	0.173	0.407	0.624	1.29	0.906	0.467	0.231	0.107	0.327	0.142	0.491
95	0.001	0.124	0.008	0.131	1.08	0.236	0.000	0.017	0.000	0.637	0.852	1.68	0.081	0.413	0.218	0.103	0.258	0.032	0.115	0.156	0.206	0.354	0.109	0.117	0.037	0.189	0.148	0.207
98	1.25	4.24	2.76	0.475	45.0	42.6	3.77	5.54	2.80	105	24.2	14.6	12.1	126	86.4	16.1	5.32	7.09	52.5	49.4	10.5	47.0	25.8	25.7	7.05	27.4	8.49	22.2
103	0.049	0.233	0.087	0.022	0.590	0.082	0.009	0.050	0.096	0.584	0.589	0.803	0.038	0.297	0.332	0.106	0.198	0.060	0.061	0.106	0.118	0.125	0.076	0.036	0.013	0.050	0.031	0.104
105	0.000	0.000	0.000	0.000	0.000	0.000	0.000	0.000	0.000	0.000	0.000	0.000	0.000	0.000	0.000	0.000	0.000	0.000	0.000	0.000	0.000	0.000	0.000	0.000	0.000	0.000	0.000	0.000
106	0.442	0.808	0.466	0.056	1.54	0.390	0.016	0.097	0.130	1.12	0.948	1.14	0.085	0.411	0.272	0.057	0.129	0.037	0.065	0.128	0.198	0.221	0.097	0.046	0.052	0.018	0.051	0.054
107	0.140	0.490	0.216	0.032	1.03	0.188	0.036	0.153	0.523	1.09	1.12	3.72	0.176	0.568	0.589	0.282	1.07	0.119	0.180	0.348	0.862	0.284	0.198	0.069	0.063	0.137	0.047	0.298

109	0.017	0.365	0.098	0.016	0.629	0.089	0.012	0.056	0.072	0.380	0.382	0.580	0.041	0.444	0.107	0.028	0.076	0.013	0.021	0.062	0.089	0.079	0.034	0.021	0.009	0.010	0.018	0.025
111	0.069	0.157	0.092	0.037	0.320	0.044	0.002	0.021	0.001	0.544	0.503	0.568	0.057	0.725	0.521	0.075	0.110	0.055	0.186	0.267	0.160	0.210	0.103	0.039	0.038	0.057	0.025	0.062
113	0.039	0.108	0.044	0.009	0.268	0.042	0.001	0.026	0.004	0.194	0.159	0.204	0.036	1.57	0.039	0.009	0.028	0.009	0.016	0.025	0.043	0.072	0.023	0.018	0.011	0.000	0.021	0.011
115	0.061	0.210	0.098	0.019	0.492	0.089	0.000	0.021	0.044	0.156	0.157	0.229	0.023	0.637	0.040	0.010	0.030	0.010	0.012	0.019	0.041	0.076	0.022	0.014	0.014	0.000	0.019	0.011
116	0.282	0.565	0.235	0.032	0.978	0.210	0.027	0.151	0.175	0.496	0.340	0.328	0.065	1.22	0.051	0.013	0.032	0.009	0.015	0.021	0.041	0.077	0.023	0.016	0.014	0.001	0.021	0.011
117	0.042	0.104	0.056	0.007	0.157	0.017	0.000	0.028	0.040	0.106	0.136	0.235	0.026	0.453	0.053	0.011	0.038	0.008	0.016	0.022	0.047	0.063	0.022	0.022	0.012	0.001	0.017	0.012
118	0.834	1.58	1.12	0.082	2.72	0.452	0.008	0.055	0.053	0.812	0.572	0.686	0.086	0.793	0.986	0.043	0.113	0.110	0.047	0.080	0.181	0.149	0.085	0.038	0.056	0.020	0.035	0.074
120	0.050	0.195	0.094	0.006	0.165	0.033	0.003	0.019	0.020	0.821	0.638	0.585	0.017	0.426	0.110	0.016	0.033	0.015	0.016	0.076	0.046	0.086	0.028	0.016	0.014	0.006	0.021	0.013
123	0.076	0.273	0.109	0.040	0.417	0.144	0.000	0.012	0.014	2.45	0.734	0.813	0.034	0.498	0.150	0.043	0.116	0.025	0.067	0.123	0.163	0.207	0.086	0.050	0.052	0.023	0.049	0.047
125	0.153	0.201	0.142	0.020	0.375	0.084	0.000	0.019	0.029	0.578	0.920	1.99	0.107	0.218	0.245	0.145	0.592	0.054	0.105	0.169	0.496	0.196	0.133	0.063	0.031	0.035	0.035	0.116
129	0.000	0.019	0.000	2.87	16.7	6.06	0.000	0.127	0.042	0.695	4.98	2.89	0.126	0.150	0.142	0.073	0.023	0.015	0.062	0.173	0.097	0.138	0.087	0.041	0.018	0.072	0.057	0.085
131	0.061	1.14	0.271	0.050	1.639	0.523	0.052	0.258	0.381	3.58	1.25	1.42	0.128	0.821	0.513	0.074	0.211	0.068	0.185	0.397	0.300	0.384	0.224	0.067	0.045	0.092	0.062	0.129
133	0.000	0.082	0.011	0.009	0.252	0.065	0.000	0.013	0.019	0.145	0.155	0.180	0.019	0.269	0.030	0.007	0.013	0.005	0.014	0.019	0.013	0.051	0.015	0.010	0.009	0.000	0.010	0.005
134	0.080	0.418	0.185	0.008	0.343	0.058	0.013	0.074	0.055	0.255	0.148	0.145	0.029	0.256	0.026	0.006	0.012	0.004	0.005	0.009	0.012	0.027	0.007	0.005	0.006	0.000	0.012	0.003
136	0.011	0.131	0.051	0.009	0.191	0.044	0.003	0.008	0.011	0.085	0.060	0.065	0.012	0.046	0.011	0.000	0.000	0.000	0.005	0.005	0.000	0.027	0.000	0.005	0.000	0.000	0.000	0.001
138	0.124	0.149	0.104	0.011	0.327	0.065	0.001	0.016	0.027	0.207	0.151	0.117	0.022	0.070	0.027	0.007	0.018	0.005	0.009	0.010	0.037	0.050	0.012	0.010	0.009	0.020	0.014	0.018
140	0.062	0.105	0.055	0.009	0.292	0.062	0.000	0.007	0.005	0.403	0.140	0.111	0.012	0.042	0.024	0.005	0.004	0.005	0.008	0.023	0.009	0.048	0.013	0.000	0.009	0.000	0.000	0.001
142	0.044	0.088	0.045	0.007	0.199	0.061	0.000	0.014	0.010	0.280	0.168	0.162	0.020	0.090	0.040	0.012	0.007	0.005	0.013	0.013	0.010	0.067	0.015	0.012	0.014	0.000	0.000	0.000
144	0.013	0.051	0.020	0.010	0.093	0.046	0.016	0.113	0.335	0.240	0.364	0.826	0.022	0.211	0.223	0.063	0.327	0.041	0.136	0.204	0.426	0.214	0.201	0.131	0.034	0.156	0.065	0.208
146	0.012	0.070	0.027	0.005	0.096	0.044	0.000	0.005	0.007	0.096	0.053	0.058	0.010	0.043	0.017	0.008	0.017	0.006	0.014	0.023	0.036	0.067	0.026	0.015	0.012	0.000	0.000	0.006

F_{Settling} (ng m⁻²day⁻¹)

Station	Naphthalene	Dimethylnaphthalenes	Methylnaphthalenes	Acenaphthylene	Acenaphthene	Fluorene	Dibenzothiophene	Methyl dibenzothiophenes	Dimethyl dibenzothiophenes	Phenanthrene	Methylphenantrenes	Dimethylphenanthrenes	Anthracene	Fluoranthene	Pyrene	Methylpyrenes	Dimethylpyrenes	Benzo(ghi)fluoranthene	Benzo(a)anthracene	Chrysene	Methylchrysene	Benzo(b+k)fluoranthenes	Benzo(e)pyrene	Benzo(a)pyrene	Perylene	Indeno(1.2.3-cd)pyrene	Dibenzo(ah)anthracene	Benzo(ghi)perylene
1	0.734	3.92	1.51	0.398	4.80	2.29	1.56	12.1	31.8	15.4	45.9	79.0	1.21	7.89	7.15	4.04	8.03	0.734	1.89	3.50	4.31	3.15	1.89	1.15	1.08	1.61	0.502	2.11
3	0.393	1.98	0.628	0.187	4.32	2.21	1.13	6.84	10.3	9.50	14.0	13.7	0.700	4.10	3.18	0.801	1.53	0.253	0.886	1.24	1.06	1.98	1.06	0.649	0.403	0.676	0.326	0.946
6	8.72	34.0	45.6	0.183	3.15	1.16	0.037	0.193	0.457	2.98	4.10	7.45	0.222	26.6	21.3	0.687	1.31	0.326	26.4	27.3	1.35	15.7	2.48	1.34	0.641	2.39	0.681	2.35
8	70.3	81.9	52.6	1.44	39.6	11.3	0.000	66.2	21.9	147	199	66.8	0.694	68.4	32.0	0.533	1.53	0.331	0.530	25.0	1.03	19.6	0.896	0.451	0.335	0.438	0.496	5.52
10	6.38	15.9	19.6	8.72	21.0	29.2	0.000	24.3	25.3	114	257	77.6	66.6	34.3	9.65	0.292	0.583	0.103	10.7	10.8	0.533	8.29	9.48	0.259	0.152	0.213	0.184	0.332
12	14.2	49.5	27.6	6.27	25.5	26.9	0.000	0.180	0.228	96.2	98.3	22.2	20.2	10.2	8.09	0.337	0.456	0.126	0.221	0.227	0.239	9.85	0.328	0.250	0.256	0.000	0.275	0.089
14	5.64	11.5	24.0	54.5	3.23	31.0	0.000	0.084	0.035	3.41	6.23	7.92	0.191	10.9	8.87	0.383	0.738	0.119	11.9	11.2	0.496	7.15	10.5	0.185	0.159	0.192	0.185	0.372
16	0.418	2.49	0.586	0.315	4.57	0.907	0.000	0.043	0.000	1.45	1.30	1.63	0.176	1.13	0.315	0.136	0.363	0.076	0.159	0.302	0.370	0.927	0.407	0.176	0.151	0.158	0.203	0.290
18	3.10	8.43	4.30	0.481	7.32	1.99	0.270	1.26	1.86	4.24	4.56	5.06	0.380	4.59	1.12	0.326	0.658	0.138	0.360	0.559	0.622	1.19	0.456	0.252	0.235	0.254	0.242	0.359
20	0.208	0.608	0.248	0.042	0.410	0.329	0.116	0.710	0.974	1.59	2.08	1.78	0.137	3.26	0.357	0.080	0.177	0.056	0.157	0.199	0.171	0.608	0.244	0.136	0.133	0.136	0.122	0.174
22	0.092	0.982	0.179	0.062	2.01	0.693	0.111	0.474	0.570	2.67	4.62	5.49	0.154	2.54	1.09	0.414	0.557	0.095	0.473	0.768	0.487	1.09	0.557	0.222	0.200	0.370	0.155	0.409
24	0.162	1.75	0.344	0.159	3.23	0.869	0.869	8.94	85.4	5.81	30.7	225	1.77	3.43	6.99	11.7	34.9	1.54	2.08	7.23	16.8	3.02	2.49	0.732	0.333	1.34	0.369	3.13
25	0.378	1.34	0.512	0.087	1.62	0.519	0.066	0.389	0.626	1.37	1.41	1.73	0.143	1.45	0.415	0.096	0.181	0.052	0.093	0.153	0.166	0.460	0.150	0.097	0.074	0.039	0.096	0.097
27	1.36	2.27	2.75	0.069	2.13	0.678	0.036	0.144	0.148	0.751	0.590	0.335	0.087	0.226	0.139	0.047	0.081	0.031	0.047	0.079	0.090	0.178	0.094	0.045	0.033	0.005	0.000	0.028
28	12.5	12.1	15.8	0.343	10.7	8.06	0.763	3.58	4.14	10.6	8.34	6.02	0.677	1.51	1.73	0.392	0.788	0.163	0.347	0.531	0.844	1.43	0.732	0.370	0.233	0.263	0.315	0.572
29	0.225	1.50	0.339	0.229	4.09	1.41	0.000	0.107	0.024	4.86	4.56	5.11	0.478	9.79	2.57	0.525	0.725	0.365	0.581	0.789	0.577	1.47	0.641	0.337	0.495	0.281	0.282	0.743
30	2.456	9.693	5.22	0.159	2.96	1.72	0.219	1.31	2.07	4.26	5.01	4.00	0.489	14.2	1.08	0.308	0.368	0.113	0.337	0.347	0.326	0.948	0.320	0.314	0.230	0.128	0.197	0.223
31	0.856	4.476	2.52	0.041	1.15	0.949	0.000	0.017	0.015	2.22	2.80	3.63	0.227	3.97	2.97	0.419	0.712	0.279	0.313	0.594	1.32	0.621	0.409	0.182	0.158	0.158	0.146	0.703
34	2.64	13.9	8.58	0.393	4.03	1.79	0.000	0.061	0.029	2.90	4.06	4.41	0.537	2.91	2.62	0.999	0.837	0.350	1.47	1.59	1.04	2.64	1.45	1.11	0.487	1.06	0.405	1.186
37	22.5	8.06	16.3	0.128	7.41	2.22	0.134	0.594	0.739	3.74	3.35	3.09	0.319	1.49	1.05	0.237	0.441	0.134	0.369	0.742	0.564	1.42	0.610	0.284	0.212	0.370	0.248	0.436

41	0.947	1.80	1.24	0.131	6.15	2.42	0.081	0.144	0.067	27.3	8.33	5.44	3.64	35.0	25.3	6.31	1.99	2.50	17.3	15.9	4.25	21.9	11.3	10.5	3.02	12.8	3.56	9.36
42	1.14	7.11	3.53	0.048	1.27	2.77	0.013	0.112	0.168	3.60	2.47	6.17	0.291	1.30	1.45	0.520	1.26	0.259	0.450	1.02	1.37	0.952	0.512	0.230	0.071	0.446	0.127	0.671
43	0.706	6.37	2.97	0.042	0.868	2.09	0.000	0.028	0.031	0.676	0.646	0.770	0.104	1.39	0.530	0.104	0.123	0.070	0.106	0.423	0.210	0.539	0.183	0.072	0.128	0.164	0.088	0.173
44	80.9	21.5	50.4	0.532	14.4	6.28	0.366	2.63	4.09	16.7	14.5	15.9	1.96	8.43	5.90	1.10	3.25	0.778	1.14	2.13	3.22	6.21	2.12	1.31	0.981	0.322	1.31	1.43
45	9.28	7.15	7.69	0.522	5.76	4.04	0.838	4.23	5.91	15.9	23.7	40.7	1.80	7.75	9.01	3.12	5.54	1.93	2.92	5.59	5.11	5.93	3.75	2.18	0.603	3.04	0.779	5.34
46	0.289	0.658	0.348	0.031	1.12	0.242	0.027	0.145	0.263	0.693	0.742	1.59	0.097	0.335	0.236	0.091	0.263	0.042	0.100	0.251	0.207	0.309	0.131	0.069	0.060	0.118	0.038	0.126
48	0.301	2.57	0.758	0.085	2.01	0.990	0.145	0.912	1.37	3.99	14.9	31.3	1.87	0.798	1.59	1.33	3.47	0.262	0.296	0.833	1.81	0.463	0.317	0.127	0.044	0.188	0.056	0.440
50	0.413	0.920	0.675	0.036	0.567	0.102	0.000	0.077	0.048	0.506	0.351	0.267	0.166	0.261	0.104	0.026	0.034	0.040	0.059	0.061	0.065	0.540	0.199	0.167	0.108	0.000	0.144	0.114
52	0.007	0.060	0.013	0.010	0.211	0.064	0.000	0.009	0.008	0.131	0.079	0.088	0.028	0.070	0.019	0.005	0.012	0.005	0.009	0.009	0.013	0.061	0.022	0.017	0.012	0.000	0.015	0.010
53	0.010	0.139	0.034	0.012	0.209	0.101	0.009	0.054	0.063	0.318	0.268	0.172	0.030	0.040	0.037	0.008	0.010	0.005	0.011	0.011	0.009	0.057	0.015	0.012	0.010	0.000	0.013	0.006
55	0.008	0.103	0.035	0.006	0.075	0.031	0.000	0.002	0.005	0.185	0.148	0.140	0.018	0.049	0.030	0.009	0.017	0.009	0.014	0.018	0.023	0.081	0.027	0.018	0.015	0.002	0.019	0.018
57	0.013	0.065	0.015	0.006	0.155	0.035	0.000	0.001	0.003	0.091	0.074	0.056	0.013	0.023	0.015	0.007	0.008	0.005	0.007	0.009	0.012	0.055	0.016	0.010	0.010	0.000	0.013	0.004
59	0.087	0.107	0.068	0.011	0.271	0.058	0.000	0.009	0.014	0.173	0.152	0.120	0.022	0.048	0.028	0.007	0.012	0.007	0.011	0.017	0.024	0.076	0.022	0.015	0.014	0.000	0.018	0.006
61	0.063	0.800	0.213	0.023	1.15	0.243	0.000	0.012	0.005	0.390	0.433	0.611	0.071	0.062	0.059	0.042	0.149	0.014	0.028	0.051	0.126	0.112	0.059	0.020	0.015	0.017	0.019	0.039
63	0.158	0.312	0.213	0.014	0.484	0.076	0.000	0.007	0.002	0.353	0.291	0.286	0.025	0.093	0.077	0.017	0.035	0.016	0.028	0.042	0.057	0.089	0.043	0.018	0.013	0.011	0.018	0.030
65	0.060	0.142	0.082	0.010	0.171	0.094	0.000	0.004	0.005	0.451	0.205	0.193	0.018	0.103	0.057	0.012	0.011	0.010	0.018	0.030	0.024	0.091	0.029	0.016	0.013	0.005	0.018	0.010
67	0.130	1.09	0.284	0.089	0.711	1.04	0.000	0.023	0.032	0.405	0.333	0.301	0.075	0.213	0.046	0.030	0.028	0.012	0.029	0.029	0.037	0.145	0.041	0.093	0.105	0.068	0.063	0.015
74	0.164	2.09	0.541	0.167	5.35	1.49	0.000	0.087	0.070	2.22	2.23	1.18	0.325	0.124	0.087	0.055	0.034	0.018	0.033	0.034	0.040	0.301	0.078	0.053	0.058	0.000	0.072	0.016
4b1	0.010	0.875	0.195	0.069	1.04	0.524	0.017	0.084	0.161	3.18	2.77	3.84	0.150	1.30	0.873	0.213	0.431	0.196	0.310	0.777	0.479	0.796	0.415	0.234	0.109	0.219	0.130	0.311
79	0.002	0.300	0.036	0.036	0.719	0.402	0.016	0.077	0.128	0.846	0.650	0.796	0.072	0.258	0.233	0.045	0.089	0.042	0.103	0.150	0.101	0.255	0.140	0.109	0.049	0.114	0.044	0.136
83	0.094	0.225	0.114	0.022	0.390	0.086	0.023	0.083	0.110	0.665	0.236	0.264	0.037	0.858	1.65	0.013	0.032	0.137	0.024	0.037	0.031	0.117	0.055	0.032	0.022	0.003	0.024	0.048
85	0.078	0.000	0.000	2.40	0.000	1.90	0.000	0.000	0.000	0.000	0.000	0.000	0.000	0.113	0.122	0.000	0.000	0.261	0.000	0.000	0.000	1.226	0.000	0.000	0.238	0.000	0.000	0.138
88	0.017	0.294	0.080	0.026	0.986	0.217	0.000	0.030	0.015	1.04	3.61	8.56	0.507	0.221	0.477	0.405	1.18	0.103	0.111	0.253	0.650	0.238	0.146	0.049	0.031	0.029	0.038	0.160
92	0.332	1.76	0.643	0.112	3.09	1.03	0.134	0.652	1.01	2.43	2.14	3.86	0.333	1.15	0.601	0.237	0.672	0.192	0.451	0.692	1.43	1.005	0.518	0.257	0.119	0.362	0.158	0.544
95	0.001	0.137	0.009	0.145	1.20	0.261	0.000	0.019	0.000	0.706	0.944	1.86	0.090	0.458	0.241	0.114	0.286	0.035	0.127	0.173	0.228	0.393	0.120	0.129	0.041	0.210	0.163	0.229
98	1.28	4.32	2.81	0.484	45.8	43.4	3.84	5.64	2.85	107	24.6	14.9	12.3	129	87.9	16.4	5.42	7.22	53.4	50.3	10.7	47.9	26.3	26.2	7.18	27.9	8.65	22.6
103	0.050	0.236	0.088	0.022	0.598	0.083	0.009	0.051	0.098	0.591	0.597	0.814	0.039	0.301	0.336	0.107	0.201	0.061	0.062	0.107	0.120	0.127	0.077	0.036	0.014	0.051	0.031	0.105
105	0.000	0.000	0.000	0.000	0.000	0.000	0.000	0.000	0.000	0.000	0.000	0.000	0.000	0.000	0.000	0.000	0.000	0.000	0.000	0.000	0.000	0.000	0.000	0.000	0.000	0.000	0.000	0.000
106	0.448	0.819	0.472	0.056	1.57	0.395	0.016	0.098	0.132	1.13	0.961	1.15	0.087	0.417	0.276	0.058	0.131	0.037	0.066	0.130	0.201	0.224	0.098	0.047	0.052	0.018	0.051	0.055
107	0.141	0.495	0.219	0.033	1.04	0.190	0.037	0.155	0.529	1.10	1.13	3.76	0.178	0.574	0.595	0.285	1.08	0.120	0.181	0.352	0.871	0.287	0.201	0.070	0.064	0.139	0.047	0.301

109	0.017	0.368	0.099	0.016	0.635	0.090	0.012	0.056	0.072	0.383	0.386	0.585	0.041	0.448	0.108	0.029	0.077	0.013	0.021	0.062	0.090	0.080	0.034	0.021	0.010	0.011	0.018	0.026
111	0.070	0.159	0.094	0.038	0.324	0.045	0.002	0.021	0.001	0.552	0.510	0.576	0.058	0.735	0.528	0.076	0.111	0.056	0.188	0.271	0.162	0.213	0.104	0.040	0.039	0.057	0.025	0.063
113	0.041	0.112	0.046	0.009	0.278	0.043	0.001	0.027	0.005	0.201	0.166	0.212	0.038	1.63	0.041	0.009	0.029	0.010	0.016	0.026	0.045	0.075	0.024	0.019	0.012	0.000	0.022	0.011
115	0.063	0.218	0.102	0.020	0.511	0.093	0.000	0.022	0.045	0.162	0.164	0.238	0.024	0.662	0.042	0.010	0.031	0.010	0.013	0.020	0.042	0.079	0.023	0.015	0.014	0.000	0.020	0.011
116	0.297	0.596	0.248	0.034	1.03	0.221	0.029	0.160	0.185	0.523	0.359	0.346	0.069	1.28	0.054	0.014	0.034	0.009	0.016	0.022	0.043	0.081	0.024	0.017	0.015	0.001	0.022	0.012
117	0.044	0.110	0.060	0.007	0.167	0.018	0.000	0.030	0.043	0.112	0.145	0.249	0.028	0.481	0.057	0.012	0.041	0.009	0.017	0.024	0.050	0.067	0.024	0.024	0.013	0.001	0.018	0.012
118	0.893	1.69	1.20	0.088	2.91	0.484	0.009	0.059	0.057	0.870	0.613	0.735	0.092	0.850	1.06	0.046	0.121	0.118	0.050	0.086	0.193	0.160	0.091	0.040	0.060	0.021	0.037	0.079
120	0.054	0.210	0.101	0.006	0.177	0.035	0.004	0.020	0.021	0.881	0.684	0.628	0.018	0.458	0.118	0.018	0.036	0.016	0.017	0.081	0.049	0.092	0.030	0.017	0.015	0.006	0.022	0.013
123	0.096	0.344	0.137	0.050	0.525	0.182	0.000	0.016	0.018	3.09	0.924	1.02	0.043	0.627	0.189	0.054	0.146	0.032	0.084	0.156	0.205	0.261	0.108	0.063	0.066	0.029	0.061	0.059
125	0.189	0.249	0.175	0.025	0.462	0.103	0.000	0.023	0.036	0.713	1.14	2.45	0.133	0.268	0.303	0.178	0.731	0.067	0.129	0.208	0.612	0.242	0.164	0.078	0.038	0.044	0.043	0.144
129	0.000	0.021	0.000	3.15	18.3	6.66	0.000	0.139	0.047	0.763	5.46	3.17	0.139	0.165	0.155	0.081	0.025	0.016	0.068	0.190	0.106	0.151	0.095	0.045	0.020	0.080	0.062	0.093
131	0.066	1.22	0.290	0.053	1.76	0.561	0.056	0.276	0.408	3.83	1.33	1.52	0.137	0.880	0.550	0.079	0.226	0.073	0.198	0.426	0.321	0.411	0.240	0.071	0.048	0.099	0.067	0.138
133	0.000	0.085	0.011	0.009	0.260	0.067	0.000	0.013	0.019	0.150	0.160	0.185	0.019	0.277	0.031	0.007	0.013	0.005	0.015	0.019	0.014	0.052	0.016	0.010	0.009	0.000	0.011	0.006
134	0.082	0.425	0.189	0.008	0.349	0.059	0.014	0.075	0.056	0.259	0.151	0.148	0.029	0.261	0.026	0.006	0.012	0.004	0.006	0.009	0.013	0.028	0.007	0.005	0.006	0.000	0.012	0.003
136	0.011	0.132	0.051	0.009	0.193	0.044	0.003	0.008	0.012	0.086	0.061	0.066	0.012	0.046	0.012	0.000	0.000	0.000	0.005	0.005	0.000	0.028	0.000	0.005	0.000	0.000	0.000	0.001
138	0.126	0.151	0.105	0.011	0.332	0.066	0.001	0.017	0.027	0.210	0.154	0.119	0.023	0.071	0.028	0.007	0.018	0.005	0.010	0.010	0.038	0.051	0.012	0.011	0.009	0.020	0.014	0.018
140	0.063	0.107	0.056	0.009	0.296	0.062	0.000	0.007	0.005	0.408	0.142	0.112	0.012	0.042	0.024	0.006	0.004	0.005	0.008	0.023	0.009	0.048	0.013	0.000	0.009	0.000	0.000	0.001
142	0.044	0.089	0.045	0.008	0.202	0.061	0.000	0.015	0.011	0.284	0.170	0.164	0.020	0.091	0.041	0.013	0.007	0.005	0.013	0.014	0.011	0.068	0.016	0.012	0.014	0.000	0.000	0.000
144	0.013	0.052	0.020	0.010	0.095	0.047	0.017	0.114	0.341	0.244	0.370	0.839	0.022	0.214	0.226	0.064	0.333	0.042	0.138	0.208	0.433	0.218	0.204	0.133	0.034	0.159	0.066	0.211
146	0.012	0.072	0.027	0.005	0.098	0.045	0.000	0.005	0.007	0.098	0.054	0.059	0.010	0.044	0.018	0.008	0.018	0.006	0.015	0.023	0.037	0.069	0.027	0.015	0.013	0.000	0.000	0.006